P

67P

► 67P/Churyumov–Gerasimenko

PAH

► Polycyclic Aromatic Hydrocarbon

Paleomagnetism

Nicholas Arndt
ISTerre, Université Grenoble Alpes, France

Definition

Paleomagnetism is the record of the Earth's past magnetic field preserved in rocks. The orientation of the magnetic field, retained in ferromagnetic minerals (Fe-Ti oxides and sulfides), mirrors the Earth's magnetic field at the time the minerals passed through their Curie point (i.e., the temperature at which certain magnetic materials undergo a sharp change in their magnetic properties). By measuring the orientation (inclination and declination) and the intensity of this magnetism, it is possible to establish the paleo-latitude of the sample at the time of its cooling or recrystallization. Apparent polar wander curves determined using such data record the displacement of continents and provide evidence of past ► plate tectonics. Variations in intensity of the remnant field record changes in the strength of the Earth's ► magnetic field and the start of crystallization of the inner core. Paleomagnetism has also been measured on ► Mars and shown that natural remnant magnetism is concentrated in the southern hemisphere, suggesting a single-hemisphere dynamo generator.

See Also

► Magnetic Anomaly
► Magnetic Field
► Magnetic Pole
► Magnetite
► Mars
► Oceanic Crust
► Plate Tectonics

Paleoproterozoic Carbon Isotope Excursion

► Lomagundi Carbon Isotope Excursion

M. Gargaud et al. (eds.), *Encyclopedia of Astrobiology*,
DOI 10.1007/978-3-662-44185-5

Paleoproterozoic Ice Ages

► Huronian Glaciation

Paleoproterozoic Snowball Earth

► Huronian Glaciation

Paleosols

Kosei E. Yamaguchi
Geochemical Laboratory, Department of Chemistry, Toho University, Funabashi, Chiba, Japan

Keywords

Atmosphere; Rock alteration (mechanical, chemical); Weathering profile

Definition

A paleosol is a layer of lithified ancient ► weathering profile or paleoweathering profile (not necessarily a lithified "soil") that formed in place by alteration of its parent geologic materials by physical, chemical, and in many cases, biological ► weathering processes. In the astrobiological context, Precambrian paleosols have been targets of intensive research, and also hot debate, in attempts to constrain the redox state of the coeval atmosphere. Paleosols, especially their uppermost parts, were in direct contact with the overlying atmosphere during their formation and were affected by its chemistry. However, in many cases, the uppermost parts of paleosols were eroded away before deposition of the overlying sedimentary materials.

Overview

General overviews of paleosols are given in Kraus (1999) and Retallack (2001). "Paleosols" are not necessarily fossil "soils"; they are, in a broad sense, paleoweathering profiles to variable degrees. Hereafter, we focus on the astrobiological aspects of paleosols as important materials that potentially record atmospheric evolution in the distant past. Continental weathering and its elemental fluxes into the oceans should have been very different under an oxic atmosphere and an anoxic atmosphere, because (bio)geochemical behaviors of what we call "redox-sensitive elements," such as iron, are very different (e.g., Ohmoto 1996; Rye and Holland 1998). (Bio)geochemical reactions that mobilize or stabilize elements in weathering profiles are influenced by (1) the redox state of weathering fluids, which is in turn affected by atmospheric chemistry and (2) development of terrestrial biota as a source of organic acids that would accelerate rock weathering. Because of such potentials, Precambrian paleosols have been targets of intensive research, and at the same time, of controversies (e.g., Ohmoto 1996).

The biggest problem is probably to unambiguously identify a complete section of paleosol. Misidentification of a middle (or deeper) part with an uppermost part (because it was eroded away) leads to serious misinterpretation of geochemical data of the profile (e.g., Rye and Holland 1998; Beukes et al. 2002; Yang and Holland 2003; Yamaguchi et al. 2007). Middle or deeper weathering horizons of modern weathering profiles typically show a signature of reducing conditions (e.g., leaching of Fe), even when an oxic atmosphere overlies the uppermost part of the paleosol. Therefore, discovering reducing horizons in paleosols developed before the inferred GOE (e.g., Rye and Holland 1998; Yang and Holland 2003) does not necessarily indicate that the coeval atmosphere was reducing/anoxic.

Paleosols have been used to constrain not only O_2 but also CO_2 or CH_4 concentrations in the ancient atmosphere (e.g., Rye et al. 1995; Sheldon 2006). Rye et al. (1995) proposed that the concentration of CO_2 as a greenhouse gas in the 2.2 Ga

old atmosphere was not high enough to sustain warm climate under the faint young sun, and that CH_4, an additional greenhouse gas, was required. This suggestion indicates that the atmosphere was not oxic, because substantial amounts of CH_4 and O_2 do not usually coexist. Remnants of arguably the oldest terrestrial life have been reported from a 2.6 Ga paleosol in South Africa (Watanabe et al. 2000). More studies with older samples may extend such records further back in time.

See Also

- ▶ Oxygenation of the Earth's Atmosphere
- ▶ Red Beds
- ▶ Weathering
- ▶ Weathering Profile

References and Further Reading

Beukes NJ, Dorland H, Gutzmer J, Nedachi M, Ohmoto H (2002) Tropical laterites, life on land, and the history of atmospheric oxygen in the Paleoproterozoic. Geology 30:491–494

Kraus MJ (1999) Paleosols in clastic sedimentary rocks: their geologic applications. Earth Sci Rev 47:41–70

Ohmoto H (1996) Evidence in pre-2.2 Ga paleosols for the early evolution of atmospheric oxygen and terrestrial biota. Geology 24:1135–1138

Retallack GJ (2001) Soils of the past, 2nd edn. Blackwell, New York

Rye R, Holland HD (1998) Paleosols and the evolution of atmospheric oxygen; a critical review. Am J Sci 298:621–672

Rye R, Kuo PH, Holland HD (1995) Atmospheric carbon dioxide concentrations before 2.2 billion years ago. Nature 378:603–605

Sheldon ND (2006) Precambrian paleosols and atmospheric CO_2 levels. Precambrian Res 147:148–155

Watanabe Y, Martini JE, Ohmoto H (2000) Geochemical evidence for terrestrial ecosystems 2.6 billion years ago. Nature 408:574–578

Yamaguchi KE, Johnson CM, Beard BL, Beukes NJ, Gutzmer J, Ohmoto H (2007) Isotopic evidence for iron mobilization during paleoproterozoic lateritization of the Hekpoort paleosol profile from Gaborone, Botswana. Earth Planet Sci Lett 256:577–587

Yang W, Holland HD (2003) The Hekpoort paleosol profile in Strata 1 at Gaborone, Botswana: soil formation during the Great Oxidation Event. Am J Sci 303:187–220

Pallas

Carmen Tornow
Institute of Planetary Research, German Aerospace Center, Berlin, Germany

Definition

(2) Pallas named after Greek goddess Pallas Athena is located in the main asteroid belt between 2.13 AU and 3.41 AU (http://ssd.jpl.nasa.gov/sbdb.cgi). Its inclination is higher than the one of the majority of numbered asteroids. Pallas revolves in 4.61 years around the sun and rotates in 7.81 h around itself. With a radiometric diameter of 545 km, it is the second largest asteroid after (1) Ceres. However, due to its lower density (2,762 kg/m^3) it has only 81 % of the mass contained in (4) Vesta. As a B-type asteroid its chemical composition can be related to the one of carbonaceous chondrites subjected to some thermal processing.

History

The discovery of Pallas on March 28, 1802, by astronomer Heinrich W. M. Olbers was a lucky coincidence since it passed Ceres during this time. Olbers tried to verify the positions of Ceres predicted by Carl F. Gauss, 1801. At that time astronomers thought that a planet would orbit between Mars and Jupiter according to the Titus–Bode hypothesis. This conjecture seemed to be confirmed by the detection of Ceres. However, the discovery of Pallas has put serious doubts on this assumption. The point-like appearance of Ceres and Pallas has motivated William Herschel in 1802 to recommend a separate category for these objects called asteroids (http://dictionary.reference.com/browse/asteroid), which was finally accepted by the community. However, both notations (asteroid and planet) were used over many decades of years. Continuing his study of asteroid families Kiyotsugu Hirayama 1928 has identified a small set of

objects linked with Pallas and sharing its orbital and spectral characteristic parameters within some range of variability. Today, the existence of the Pallas asteroid family with a clearly larger set of members is well accepted.

See Also

- ▶ Asteroid
- ▶ Asteroid Belt, Main
- ▶ Carbonaceous Chondrite
- ▶ Ceres
- ▶ Keplerian Orbits
- ▶ Vesta

Palus, Paludes

Stephan van Gasselt
Planetary Sciences and Remote Sensing, Institute of Geological Sciences, Freie Universität Berlin, Berlin, Germany

Synonyms

Marsh

Definition

Paludes are lunar low-albedo surface features considered to be small (150–300 km in diameter) and isolated lunar Mare patches. They are situated near larger lunar maria.

The three named lunar paludes are Palus Epidemiarum (marsh of epidemics), Palus Putredinis (marsh of decay), and Palus Somni (marsh of sleep).

See Also

- ▶ Mare, Maria

Pangea

Nicholas Arndt
ISTerre, Université Grenoble Alpes, France

Definition

Pangea is the name of the supercontinent that existed through most of the Paleozoic, from about 480 to 180 Ma. It comprised the older portions of all present landmasses. The single enormous ocean surrounding Pangea was accordingly named Panthalassa. The reasons for the formation of the Pangea supercontinent are poorly understood. Around 180 Ma, it started to split apart, initially into the supercontinents ▶ Laurasia and ▶ Gondwana, subsequently into the present continents. The ponding of mantle plumes below the pangean continental lithosphere may have weakened it and favored large-scale continental rifting and breakup.

History

In his book *Die Entstehung der Kontinente und Ozeane*, the German astronomer and meteorologist Alfred Wegener postulated that all the continents had at one time formed a single supercontinent which he called the "Urkontinent," before later breaking up and drifting. The term Pangaea appeared in 1928 during a symposium in Tulsa, Oklahoma, to discuss Alfred Wegener's theory of continental drift.

See Also

- ▶ Gondwana
- ▶ Laurasia
- ▶ Plate Tectonics
- ▶ Rodinia
- ▶ Supercontinent

Pan-Glacial

► Snowball Earth

Panorama Formation

► North Pole Dome (Pilbara, Western Australia)

Panspermia

Jean-Pierre de Vera
DLR, Institut für Planetenforschung, Berlin, Germany

Keywords

Habitable planets; Impact; Interplanetary transfer of life; Origins of life; Space exposure experiments

Synonyms

Interplanetary transfer of life

Definition

Panspermia (Greek: πανσπερμία from πᾶς/πᾶν (*pas*/pan) "all" and σπέρμα (*sperma*) "seed") is the hypothesis that "seeds" or "spores" of life can survive space travel and spread throughout the Universe. Consequences of this hypothesis are that life on Earth may have originated at some other place in the Universe and its evolution on Earth is due to a fertilization of the planet through such interplanetary or interstellar transfer of "seeds." Consequently, life could be delivered to and start a new evolution on all habitable planets, moons, and satellites.

History

The term *Panspermia* is known to have been mentioned in the fifth century BC for the first time by the Greek philosopher Anaxagoras. He might have influenced scientists in the Middle Ages, as, for example, Giordano Bruno (1548–1600). Giordano had access to old Greek scriptures in the libraries of the medieval monasteries and universities and he proposed the existence of multiple worlds. However, he did not propose interplanetary transfer of life between these worlds. The idea of Panspermia was revived in the nineteenth and twentieth centuries by scientists like J. J. Berzelius (1834), W. T. Kelvin (1871), H. von Helmholtz (1879), S. Arrhenius (1903), and F. Hoyle (1915–2001). During that time the main idea originated that if life once started at some place, it may be able to spread to other environments suitable for replication. Some controversial theories even proposed that diseases may originate in space with space-borne viruses causing, for example, influenza (Hoyle and Wickramasinghe 1979, 1984, 1986). But according to Henderson et al. (1989) the likelihood of this theory to hold true is very low.

Overview

Panspermia can occur in three different ways. (1) The classical Panspermia hypothesis postulates the transfer of uncovered "seeds" by radiation pressure through space (Arrhenius 1903, 1908). (2) The so-called Lithopanspermia (Greek: litho = stone) hypothesis assumes that a ► rock hosts the organisms during interplanetary transfer. (3) The Chemical Panspermia hypothesis is based on the presumed formation of chemical compounds in interstellar molecular clouds and assumes that the first prebiotic molecules also formed there. The interstellar molecular clouds are formed after the explosions of the first generations of ► stars in ► supernovae. This prebiotic complex organic material can be transported by solar or ► stellar winds into deep space and may have "seeded" a planet that may then be host to the resulting

formation and evolution of life. The seeds are assumed to be interstellar dust grains, ▶ meteorites, and ▶ comets (Chyba and Sagan 1992; Martins et al. 2008). Francis Crick also intriguingly postulated a "directed Panspermia" where intelligent beings would be deliberately "seeding" the Universe (Crick and Orgel 1973). In 1998 scientists started to systematically analyze the likelihood of Lithopanspermia by performing suitable experiments. The Mars-Earth System served as a model system in these studies. Because ▶ Mars is similar to Earth in many aspects and may have had a similar early evolution and because of its proximity to Earth, it is conceivable that life may have originated on Mars and spread to the Earth. The discussion was furthered by the albeit controversial discovery of fossil nanostructures in the Martian meteorite ▶ ALH 84001 in 1996. In general, Panspermia could occur if: (1) rock hosting microorganisms from an inhabited "home" or "donor" planet was ejected into space; (2) the ejected material traveled a potentially long time (about thousands to millions of years) through space without disintegration of the life forms; and (3) the host rock entered into the atmosphere of a habitable "acceptor" planet where the ▶ microorganisms would come back to life and replicate. All three elements of the scenario have been thoroughly tested and additional tests are still in progress. Crater impact researchers have provided data on shockwave pressures that will be reached in the spallation zone during an impact event. Studies of craters on Mars are the basis of this data and have helped to get the most realistic conditions for impact simulation experiments. The shockwave experiments were run by shooting into (Mastrapa et al. 2001), or by the use of explosive devices on rocky material hosting microorganisms, creating realistic simulation of asteroid impacts, which are reaching according to calculations of shockwave pressures up to 50 GPa (Stöffler et al. 2007; Horneck et al. 2008). The results of these experiments showed that the tested microorganisms such as ▶ bacteria and ▶ lichen spores survived. The second step of the Panspermia scenario was tested by ground-based space simulations and by space exposure experiments on ESA or NASA space hardware devices like ▶ BIOPAN mounted on the satellite FOTON and launched by Soyuz rockets, or by the exposure platforms ▶ EXPOSE-E and EXPOSE-R on the ▶ International Space Station launched by Space Shuttles. The results of these experiments support the Lithopanspermia hypothesis. But tests of the entry part of the hypothesis in an experiment named ▶ STONE using the reentry devices of the FOTON satellite were negative because the tested organisms failed to survive. New tests using satellite reentry devices are planned for the near future. To better design realistic experiments it is important to consider that various models of Panspermia exist.

Basic Methodology

The three elements of (Litho-)Panspermia can be studied by using ▶ asteroid impact simulation devices and space exposure platforms. Asteroid impact events producing shockwaves are achieved by experiments using explosive devices or projectile experiments. Further steps of Panspermia are checked by space exposure tests on space exposure platforms like ISS or FOTON and by reentry experiments that are performed on reentry devices of satellites like the FOTON capsule.

Key Research Findings

The performed Panspermia experiments have shown that besides very resistant prokaryotic microorganisms (bacteria and archaea), even eukaryotic microorganisms (lichens and spores of fungi) are able to survive asteroid impact events and space travel, whereas the reentry process seems to be the most harmful for both of these groups of microorganisms.

Applications/Future Directions

Experiments on verification or falsification of the Panspermia hypothesis are ongoing using various

organisms and species. Especially the reentry experiments are not completed, and new sets of tests are still in progress.

See Also

- ALH 84001
- Asteroid
- Bacteria
- BIOPAN
- Comet
- Crater, Impact
- Eukarya
- EXPOSE
- Foton Capsule, Spacecraft
- International Space Station
- Lichens
- Mars
- Meteorites
- Microorganism
- Origin of Life
- Planet
- Prebiotic Chemistry
- Prokaryote
- Replication (Genetics)
- Rock
- Satellite or Moon
- Star
- Stellar Winds
- STONE
- Supernova

References and Further Reading

Arrhenius S (1903) Die Verbreitung des Lebens im Weltraum. Umschau 7:481–485
Arrhenius S (1908) Worlds in the making: the evolution of the universe. Harper & Row, New York
Chyba C, Sagan C (1992) Endogenous production, exogenous delivery and impact-shock synthesis of organic molecules: an inventory for the origins of life. Nature 355:125–132
Crick FHC, Orgel LE (1973) Directed panspermia. Icarus 19:341–346
Henderson IM, Hendy MD, Penny D (1989) Influenza viruses, comets and the science of evolutionary trees. J Theor Biol 140(3):289–303
Horneck G, Stöffler D, Ott S, Hornemann U, Cockell CS, Möller R, Meyer C, de Vera JP, Fritz J, Schade S, Artemieva N (2008) Microbial rock inhabitants survive hypervelocity impacts on Mars-like host planets: first phase of lithopanspermia experimentally tested. Astrobiology 8(1):17–44
Hoyle F, Wickramasinghe NC (1979) Diseases from space. J.M. Dent, London
Hoyle F, Wickramasinghe NC (1984) Living comets. University Cardiff College Press, Cardiff
Hoyle F, Wickramasinghe NC (1986) The case for life as a cosmic phenomenon. Nature (Lond) 322:509–511
Martins Z, Botta O, Fogel ML, Sephton MA, Glavin DP, Watson JS, Dworkin JP, Schwartz AW, Eherenfreund P (2008) Extraterrestrial nucleobases in the Murchison meteorite. Earth Planet Sci Lett 270:130–136
Mastrapa RME, Glanzberg H, Head JN, Melosh HJ, Nicholson WL (2001) Survival of bacteria exposed to extreme acceleration: implications for panspermia. Earth Planet Sci Lett 189(1–2):1–8
Stöffler D, Horneck G, Ott S, Hornemann U, Cockell CS, Möller R, Meyer C, de Vera JP, Fritz J, Artemieva NA (2007) Experimental evidence for the impact ejection of viable microorganisms from Mars-like planets. Icarus 186:585–588

Paraformaldehyde

- Formaldehyde
- Polyoxymethylene

Parallax

Daniel Rouan
LESIA, Observatoire Paris-Site de Meudon, Meudon, France

Definition

In astronomy, parallax is the apparent difference in angular position of a celestial object with respect to background stars, as seen from different positions as the Earth travels along its orbit

around the Sun (and in recent times, as the Sun moves in its orbit around the center of our Galaxy). As a tabulated quantity for stars (the annual parallax), it is equal to the angle subtended from a star by the mean radius of the Earth's orbit. The farther the star, the smaller the parallax. The inverse of the parallax is thus a direct measurement of the distance of a star, which is usually expressed in ▶ parsecs. A parsec is the distance for which the annual parallax is 1 arc sec. Historically, parallax was the first reliable way to determine distances to nearby stars, and it remains a key technique today, with the use of spacecraft such as ▶ Hipparcos. Radio astronomers have used VLBI techniques to accurately measure parallax and hence distances, for example, to the center of the Milky Way. Units: arc second.

See Also

▶ AU
▶ Gaia Mission
▶ Hipparcos
▶ Parsec

Paralog

▶ Paralogous Gene

Paralogous Gene

David Moreira and Purificación López-García
Unité d'Ecologie, Systématique et Evolution
CNRS UMR8079, Université Paris-Sud 11, Paris, Orsay Cedex, France

Synonyms

Paralog

Definition

Paralogous genes (or paralogs) are a particular class of homologous genes. They are the result of gene duplication and the gene copies resulting from the duplication are called paralogous of each other. After duplication, the paralogous genes can keep the same function (for example, the multiple copies of ribosomal RNA genes found in many genomes), but they often diverge and develop different functions (for example, the translation elongation factors Tu and G). Paralogous genes can be retained in the genome after their duplication, but some copies can also be lost. This can generate complex patterns of presence/absence of the different paralogues that may render very difficult the interpretation of ▶ phylogenetic trees, leading sometimes to erroneous inferences about the relationships between species. This is usually called the "hidden paralogy" problem.

See Also

▶ Gene
▶ Homology
▶ Orthologous Gene
▶ Phylogenetic Tree
▶ Phylogeny

Parametric Release

Catharine A. Conley
NASA Headquarters, Washington, DC, USA

Definition

Parametric release is an operational alternative to end-product testing. In general to authorize the release of a product, a manufacturer performs

tests and analysis on the final product. For parametric release instead of testing the end-product, checking the parameters of the various processes used during the production is sufficient if those processes have been certified. For instance, parametric release is accepted in some case by the US food and drug administration for release of drug products for injection. The parametric release is based on evidence that the process has been performed successfully: this includes monitoring of the process, documentation, and in-process data to match the pre-defined specifications.

Parent Body

Jacques Crovisier
LESIA, Observatoire de Paris, Meudon, France

Keywords

Asteroid; Comet; Meteor; Meteorite; Meteoroid; Planet

Definition

A parent body is the object from which a given ▶ meteorite or meteoroid was ejected. Most meteorites come from the fragmentation of asteroids following collisions. Meteor showers are due to sizable dust particles shed by ▶ comets.

Overview

With the exception of lunar and Martian meteorites, it is believed that most meteorites are derived from parent bodies in the ▶ asteroid belt. This idea progressively emerged in the mid-nineteenth century from the works of Robert P. Greg (1826–1906), Auguste Daubrée (1814–1896), and Adolphe Boisse (1810–1896) (see Marvin 2006).

There is a large diversity among both meteorites and asteroids. However, few specific asteroids are firmly identified as parent bodies. The comparison of spectral and mineralogical characteristics is basically hampered by the alteration of the asteroid surfaces by space weathering. The problem is further complicated because present asteroids may not be primordial, but the product of collisions themselves.

Could some meteorites, such as carbonaceous chondrites, be coming from comet nuclei? As was discussed by Campins and Swindle (1998) the question is still open. The specific case for the Orgueil meteorite, which could have come on a comet-like orbit, was studied by Gounelle et al. (2006).

The connections between comets and meteor showers, based upon orbital considerations, are easier to establish. The first link was obtained by Giovanni Schiaparelli (1835–1910) who related 109P/Swift-Tuttle and the Perseid meteors. This is now well-documented for most meteor showers (Jenniskens 2006), which are related to present or extinct comets, or near-Earth asteroids.

A cheap way to study extraterrestrial matter, in contrast to costly sample return space missions, is to analyze this matter provided in the form of meteorites on the Earth's surface or of meteoroids or stratospheric dust particles in the Earth's atmosphere. It is therefore of paramount importance to relate this material to its parent bodies.

See Also

- ▶ Asteroid
- ▶ Comet
- ▶ Fragmentation of Interstellar Clouds
- ▶ Interplanetary Dust Particle
- ▶ Meteorites
- ▶ Micrometeorites
- ▶ Minor Planet
- ▶ NEO
- ▶ Planet

References and Further Reading

Bottke WF, Cellino A, Paolicchi P, Binzel RP (2002) Asteroids III. University of Arizona Press, Tucson
Burbine TH, McCoy TJ, Meibom A, Gladman B, Keil K (2002) Meteoritic parent bodies: their number and identification. In: Bottke WF, Cellino A, Paolicchi P, Binzel RP (eds) Asteroids III. University of Arizona Press, Tucson, pp 653–667
Campins H, Swindle TD (1998) Expected characteristics of cometary meteorites. Meteorit Planet Sci 33:1201–1211
Gounelle M, Spurny P, Bland PA (2006) The orbit and atmospheric trajectory of the Orgueil meteorite from historical records. Meteorit Planet Sci 41:135–150
Jenniskens P (2006) Meteor showers and their parent comets. Cambridge University Press, Cambridge
Lauretta DS, McSween HY (2006) Meteorites and the early solar system II. University of Arizona Press, Tucson
Marvin UB (2006) Meteorites in history: an overview from the renaissance to the 20th century. In: McCall GJH, Bowden AJ, Howarth RJ (eds) The history of meteoritics and key meteorite collections: fireballs, falls and finds, vol 256, Geological society special publications., pp 15–71
McSween HY (1999) Meteorites and their parent planets, 2nd edn. Cambridge University Press, Cambridge
Schiaparelli GV (1867) Sur la relation qui existe entre les comètes et les étoiles filantes. Astron Nachr 68:331–332

Parent Molecule (Ion, Species)

► Precursor

Parent Molecule, Comet

Jacques Crovisier
LESIA, Observatoire de Paris, Meudon, France

Definition

A parent molecule is a molecule directly released from cometary material, e.g., by ► sublimation of cometary ices. It contrasts with daughter molecules, which are their degradation products. Historically, daughter molecules (CN, C_2, C_3, CH, OH, NH...) were first observed in cometary spectra from their electronic bands in the visible and the nature of their parents was the subject of speculations. Parent molecules (H_2O, CO, CO_2, NH_3, HCN, hydrocarbons...) were definitely identified more recently from their vibrational bands and rotational lines in the infrared and radio spectral domains, as well as from in situ mass spectroscopy.

See Also

► Comet
► Daughter Molecule, Comet

Parity Nonconservative Energy Difference

► PVED

Parity Violation Energy Difference

► PVED

Parsec

Daniel Rouan
LESIA, Observatoire Paris-Site de Meudon, Meudon, France

Synonyms

pc

Definition

The parsec is the distance from which the average Earth–Sun distance (149.6 10^6 km 1 AU) subtends an angle of 1 arc sec. This is one of the basic units of astronomy, and was originally based on the measurement of the ▶ parallax effect. Other distance units (kpc, Mpc, etc.) derive from it. The name derives from the French "par seconde" (per second).

See Also

▶ AU
▶ Parallax

Partial Antigen

▶ Hapten

Partitioning

▶ Fractionation

Pasteurization

Catharine A. Conley
NASA Headquarters, Washington, DC, USA

Definition

Pasteurization is the name of a particular heat-treatment process that reduces the number of viable microorganisms by a factor of 10^5 but does not necessarily bring that number to zero. This process applies mainly to food products using moderate temperatures (under 100 °C). It could be used for planetary protection to reduce the bioburden on thermosensitive components.

See Also

▶ Bioburden Reduction
▶ Disinfection
▶ Inactivation
▶ Planetary Protection
▶ Sterilization

Patera, Paterae

Ernst Hauber
Deutsches Zentrum für Luft- und Raumfahrt (DLR) e.V., Institut für Planetenforschung, Berlin, Germany

Definition

Patera is an irregular crater or a complex one with scalloped edges (definition by the International Astronomical Union, http://planetarynames.wr.usgs.gov/jsp/append5.jsp) and is used as a descriptor term for naming surface features on ▶ Mars, ▶ Venus, and the Jovian satellite, ▶ Io.

See Also

▶ Crater, Impact
▶ Io
▶ Mars
▶ Satellite or Moon
▶ Venus

pc

► Parsec

PCR

► Polymerase Chain Reaction

PDR

► Photodissociation Region

67P/Churyumov–Gerasimenko

Hervé Cottin
Laboratoire Interuniversitaire des Systèmes Atmosphériques, Université Paris Est-Créteil, Créteil, France

67P/Churyumov–Gerasimenko, Fig. 1 Picture of the nucleus of comet 67P/Churyumov–Gerasimenko seen from the ROSETTA spacecraft on September 19, 2014, from a distance of about 30 km. The two lobes can be seen as well as the irregular terrains made of pits, cliffs, boulders, and rather smooth areas (Credit: ESA/Rosetta/NAVCAM)

Keywords

Comet; ROSETTA

Synonyms

67P

Definition

Comet 67P/Churyumov–Gerasimenko is the target of the ESA ROSETTA mission. This comet was selected because its orbit allowed its exploration by the European spacecraft for a launch scheduled in 2004 and an encounter in 2014. It was also of particular interest since it is thought that the comet has not a long history in the inner Solar System and therefore could contain primitive material kept at low temperature and far from the Sun since the formation of the Solar System.

Overview

Comet 67P/Churyumov–Gerasimenko is the target of the ESA ROSETTA mission. ROSETTA has reached the comet in August 2014 and delivered on the nucleus a lander called PHILAE on November 12, 2014, after a global mapping of the surface in order to choose the best landing site. The comet was discovered by Klim Ivanovich Churyumov and Svetlana Ivanovna Gerasimenko in September 1969. Its current orbital period is 6.44 years, with an aphelion at 5.7 AU and a perihelion at 1.24 AU. Observations of the nucleus with ROSETTA have revealed a stunning unexpected irregular shape with two lobes. This could be the sign that the comet is made of

two distinct objects that came into contact or that the primary nucleus was asymmetrically eroded. Comet 67P nucleus (Fig. 1) is about 4.1 × 3.3 × 1.8 km in size for the larger lobe and 2.6 × 2.3 × 1.8 km for the smaller one. Its mass is 1.0×10^{13} kg and density about 0.5 g.cm^3. It rotates in about 12.4 h.

It has been calculated that before 1840, the comet perihelion was about 4 AU and that successive dynamical interactions with Jupiter progressively shifted it to its current position.

Comet Churyumov–Gerasimenko is the first cometary nucleus so closely scrutinized by a spacecraft, for such a long period of time (about 2 years) and on which an automated module has landed.

See Also

- ▶ Comet (Nucleus)
- ▶ Philae Lander
- ▶ Rosetta Spacecraft

51 Pegasi B

David W. Latham[1] and Nader Haghighipour[2]
[1]Harvard-Smithsonian Center for Astrophysics, Cambridge, MA, USA
[2]Institute for Astronomy, University of Hawaii-Manoa, Honolulu, Hawaii, HI, USA

Keywords

Radial-velocity planet; Exoplanet; Hot Jupiters

Definition

51 Pegasi b is an extrasolar planet orbiting the solar-type star 51 Pegasi.

History

51 Pegasi b is the first Jupiter-type planet, with a minimum mass slightly smaller than half of that of Jupiter, discovered around a Sunlike star. It was detected by ▶ radial-velocity observations obtained with the Elodie ▶ spectrometer on the 1.93-m telescope at the Observatoire de Haute Provence in France (Mayor and Queloz 1995). The extraordinarily short ▶ period of 4.230785 ± 0.000036 days was completely unexpected for a planet with a mass close to that of Jupiter and led to some initial skepticism that the unseen companion of 51 Pegasi could be a gas ▶ giant planet (e.g., Gray 1997). However, the subsequent announcement of several other ▶ radial-velocity planet candidates soon convinced most people of the reality of ▶ extrasolar planets.

Overview

51 Pegasi is classified as a G dwarf similar to the Sun but slightly cooler, at a distance of 15.6 parsecs (50.9 light years). A periodic variation in the ▶ radial velocity of the star indicates an unseen companion with minimum mass of 0.472 ± 0.039 Jupiter masses, if the orbit is viewed edge-on, but the actual orbital inclination is not well established. The ▶ orbit is nearly circular, with an ▶ eccentricity of 0.013 ± 0.012, presumably the result of circularization by tidal forces. The proximity of the planet to its star, 20 times closer than the Earth to the Sun, implies a temperature on the order of 1,200 K. 51 Pegasi b is the prototype for a population of ▶ hot Jupiters that probably formed much farther from their parent stars, where conditions were cool enough for a gas giant planet to form, followed by migration into a much tighter orbit around the host star.

See Also

- ▶ Dwarf Star
- ▶ Eccentricity

- ▶ Extrasolar Planets
- ▶ Giant Planets
- ▶ Hot Jupiters
- ▶ Inclination (Astronomy)
- ▶ Planetary Migration
- ▶ Radial-Velocity Planets

References and Further Reading

Gray D (1997) Nature 385:795
Mayor M, Queloz D (1995) Nature 378:355

Pelite

- ▶ Shale

Pentopyranosyl-RNA

- ▶ p-RNA

Peptide

- ▶ Oligopeptide
- ▶ Protein

Peptide Nucleic Acids

- ▶ PNA

Peptidoglycan

Felipe Gomez
Centro de Astrobiología (CSIC/INTA), Instituto Nacional de Técnica Aeroespacial, Torrejón de Ardoz, Madrid, Spain

Definition

Peptidoglycan is a polymer with a structural role in the bacterial ▶ cell wall. It is a barrier that provides structural strength to the ▶ bacteria. It is made of polysaccharides attached to oligopeptides in linear chains (*N*-acetylglucosamine and *N*-acetylmuramic acid alternating with cross-linked oligopeptides (no more than five amino acids)). The oligopeptides are attached to *N*-acetylmuramic acid. Due to the cross-linked oligopeptide, it constitutes a 3D structural layer, which is thicker in the case of ▶ Gram-positive bacteria (Fig. 1).

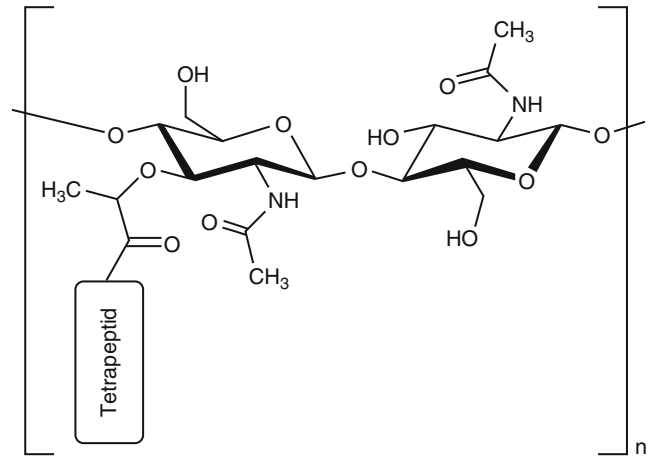

Peptidoglycan, Fig. 1 Peptidoglycan basic monomer with two elements (*N*-acetylglucosamine and *N*-acetylmuramic acid). Cross-linked oligopeptide constitutes a 3D network with structural role in the bacterial cell wall

See Also

- ▶ Bacteria
- ▶ Cell Wall
- ▶ Gram-Negative Bacteria
- ▶ Gram-Positive Bacteria
- ▶ Periplasm

Perchlorates on Mars

Daniela Tirsch[1] and Alessandro Airo[2]
[1]German Aerospace Center DLR, Institute of Planetary Research, Berlin, Germany
[2]Institut für Geologische Wissenschaften Tektonik und Sedimentäre Geologie, Freie Universität Berlin, Fachbereich Geowissenschaften, Berlin, Germany

Definition

Perchlorates are salts derived from the perchlorate acid ($HClO_4$). They form through oxidative processes in the atmosphere and accumulate with the dust (Smith et al. 2014). In 2008 perchlorates were detected by the Phoenix lander in the Martian soil. Sample analysis by the NASA rover "Curiosity" at Gale crater suggest the presence of perchlorates in an aeolian dune at the location called "Rocknest". Perchlorates are of particular relevance in terms of ▶ Habitability on Mars because they could oxidize and therefore decompose possible organic compounds. Furthermore, on Earth perchlorates found in the Atacama Desert have been shown to serve as Nutrients for microbes.

See Also

- ▶ Habitability on Mars
- ▶ Nutrients

Reference

Smith ML, Claire MW, Catling DC, Zahnle KJ (2014) The formation of sulfate, nitrate and perchlorate salts in the martian atmosphere. Icarus 231:51–64

Perennial Heat Source

Catharine A. Conley
NASA Headquarters, Washington, DC, USA

Definition

For planetary protection, a perennial heat source is a device, usually containing radioactive materials, like radioisotopic thermoelectric generator (RTG) or radioisotopic heating unit (RHU), that will continue to produce heat for a significant length of time after a spacecraft has ceased operation.

Perennially Frozen Ground

- ▶ Permafrost

Periapsis

- ▶ Periastron

Periastron

David W. Latham
Harvard-Smithsonian Center for Astrophysics, Cambridge, MA, USA

Synonyms

Periapsis; Pericenter

Definition

For an object in an elliptical Keplerian orbit around a star, periastron is the point of closest approach of the object to the star (and to the center of mass of the system). The terms *perihelion* and *perigee* are used for the same concept when orbits are around the Sun or Earth, respectively. Apastron, aphelion, and apogee are the corresponding points of largest separation.

See Also

► Aphelion

Pericenter

► Periastron

Peridot

► Olivine

Peridotite

Nicholas Arndt
ISTerre, Université Grenoble Alpes, France

Definition

Peridotite is an ultramafic (silica-poor, magnesium-rich) intrusive rock. It is coarse-grained and pale to dark green and is composed of >90 % mafic (ferromagnesian) minerals: typically ► olivine, orthopyroxene, and clinopyroxene. Minor phases include plagioclase, spinel or garnet, amphibole or biotite, and Fe-Cr-Ti oxides. Peridotite is the dominant component of the upper ► mantle of the Earth and other planets and is thus the most common rock in the Solar System. Peridotite is also found as main component of some shergottites, one of the classes of Martian ► SNC meteorites.

See Also

► Archean Mantle
► Asthenosphere
► Mantle
► SNC Meteorites

Period

David W. Latham
Harvard-Smithsonian Center for Astrophysics, Cambridge, MA, USA

Definition

The period is the length of time between two successive realizations of a well-defined physical state of a system that appears repeatedly on a fully regular basis. The phenomenon is then said to be periodic. For instance, a planet at a given position along its ► orbit around a star will be at exactly the same position after a time equal to one period of revolution. Spin, waves, oscillations are other examples of periodic phenomena. The period, whose unit is the second, is the inverse of the frequency, which is expressed in Hertz (Hz).

See Also

► Orbit

Period (Half-Life Period)

► Half-Life

Periphyton

► Biofilm

Periplasm

Felipe Gomez
Centro de Astrobiología (CSIC/INTA), Instituto Nacional de Técnica Aeroespacial, Torrejón de Ardoz, Madrid, Spain

Definition

Periplasm is the inner space located between the cell plasma membrane and the outer cell wall, or peptidoglycan in ▶ Gram-negative bacteria. Periplasm is easily recognized by electron microscopy. Periplasm is a gel-like structure that contains fluids with hydrolytic enzymes and binding proteins involved in the transport of material into the cell. The existence of similar functions associated with ▶ Gram-positive bacteria allows the existence of an equivalent structure in this type of microorganism to be postulated.

See Also

- ▶ Bacteria
- ▶ Chemotaxis
- ▶ Gram-Negative Bacteria
- ▶ Gram-Positive Bacteria
- ▶ Transport, Biological

Permafrost

Daniele L. Pinti
GEOTOP Research Center for Geochemistry and Geodynamics, Université du Québec à Montréal, Montréal, QC, Canada

Synonyms

Perennially frozen ground

Definition

Permafrost is soil that remains below the freezing point of water (0 °C) throughout the year. It is mainly located at high latitudes (24 % of the exposed land in the Earth's northern hemisphere) and high altitude (alpine permafrost). ▶ Mars is the other rocky planet in the Solar System that could have a permafrost layer. Asteroid 25143-Itokawa and Eros show surface morphologies that suggest the occurrence of a permafrost and occasionally meltwater. Earth's permafrost is a site of microbial activity within thin films of liquid water between ice and soil particles. The occurrence and distribution of these microbial communities are studied as possible analogues of life forms on icy planets and satellites in the Solar System and for exoplanets.

See Also

- ▶ Antarctica
- ▶ Exoplanets, Discovery
- ▶ Itokawa Asteroid
- ▶ Mars

Permeability

David Deamer
Department of Chemistry, University of California, Santa Cruz, Santa Cruz, CA, USA

Keywords

Bilayer; Concentration gradient

Definition

Permeability is a measure of the ability of a fluid or gas to pass through porous solids or aggregates. In the biological sense, it also refers to the relative ability of solutes to diffuse through the ▶ lipid bilayer barrier of ▶ membranes. Biological membranes and lipid vesicles are relatively permeable

to small, uncharged molecules such as water, carbon dioxide, and oxygen, and relatively impermeable to ionized solutes like sodium, potassium, chloride, and ▶ amino acids.

Overview

All cellular life is defined by boundary membranes that provide a selective barrier to the free diffusion of solutes such as ions (sodium, potassium, chloride, phosphate, protons) and nutrients (glucose, amino acids). The permeability barrier is the lipid bilayer, and cells have evolved a variety of ▶ proteins that act as channels and transporters to select which solutes can enter or leave a cell. The rate at which a given solute crosses the bilayer barrier is usually expressed in terms of a permeability coefficient (P), which by convention is defined as the amount of solute crossing a square centimeter of membrane in 1 s down a unit concentration gradient. A simplified equation for the permeability coefficient is $P = J/\Delta C$, where J is the flux in mol cm^{-2} s^{-1}, and ΔC is the difference in concentration driving the flux in mol cm^{-3}. The units are then cm s^{-1}. A typical measurement of the permeability coefficient of water is 10^{-3} s^{-1}, whereas the permeability of an ion such as potassium is 10^{-11} cm s^{-1}, which is eight orders of magnitude lower. A more intuitive way to think about permeability is in terms of the half-time of decay of a gradient. For instance, water permeation across liposome membranes has a half-time measured in milliseconds, while the decay of a potassium gradient in the same system is measured in hours.

Solutes have two mechanisms for crossing a lipid bilayer barrier. The simplest mechanism is referred to as solubility-diffusion, in which the solute dissolves in the hydrocarbon phase and diffuses to the other side where it dissolves in the opposite bulk phase. Small neutral molecules, like water and gas molecules, pass through the membrane barrier by this process. The other mechanism involves transient or permanent transmembrane defects. For instance, membranes would be virtually impermeable to ionized solutes such as potassium ions due to the Born energy required for an ion to move from a high dielectric polar solvent like water to a low dielectric phase such as the nonpolar interior of a lipid bilayer, which is composed of hydrocarbon chains. However, ions can penetrate the lipid bilayer by passing through transient defects that constantly appear and disappear in the bilayer. The protein channels in biological membranes overcome the Born energy barrier by providing a permanent high dielectric pathway through the hydrocarbon chains.

Selective permeability to solutes is an essential property of cell membranes today, and must also have been important to the first forms of cellular life. It is likely that primitive cell membranes were composed of short chain amphiphilic molecules available in the prebiotic environment, which would be much more permeable than the evolved membranes of cells today. Therefore, the function of membranes in the first forms of life would be to maintain large polymers within a compartment so that they could interact, while allowing access to nutrient solute molecules such as amino acids.

See Also

- ▶ Amino Acid
- ▶ Lipid Bilayer
- ▶ Membrane

References and Further Reading

Deamer D, Kleinzeller A, Fambrough DW (eds) (1999) Membrane permeability: 100 years since Ernest Overton. Current topics in membranes, vol 48. Academic, New York

Peroxisome

Ricardo Amils
Departamento de Biologia Molecular, Universidad Autónoma de Madrid, Madrid, Spain

Definition

A peroxisome is a membrane-enclosed ▶ organelle present in almost all eukaryotic cells, whose

function is to produce hydrogen peroxide (H_2O_2) from the reduction of O_2 by various hydrogen donors. They participate in the metabolism of fatty acids and many other metabolites. The hydrogen peroxide produced in the peroxisome is degraded to H_2O and O_2 by the enzyme catalase. Peroxisomes are bound by a single membrane that separates their contents from the cytosol and contains membrane proteins involved in different functions (transport, proliferation). Peroxisomes originate in the cell by incorporating their proteins and lipids from the cytoplasm, eventually becoming a membrane-enclosed entity that can enlarge and divide in synchrony with the cell. Peroxisomes are absent in prokaryotic organisms.

See Also

- ▶ Eukaryote
- ▶ Organelle

PGE

- ▶ Platinum Group Elements

pH

Kensei Kobayashi
Yokohama National University, Tokiwadai, Hodogaya-ku, Yokohama, Japan

Synonyms

Hydrogen ion concentration index

Definition

pH describes the activity of hydronium ions (H_3O^+, or more precisely the hydrated form of the proton H^+ in solution) in aqueous solution. pH characterizes the acidity or basicity of aqueous solutions. It is formally defined by the relation:

$$\mathrm{pH} = -\log_{10} a_{\mathrm{H}}$$

in which a_{H} is the activity of the solvated hydronium ion. The pH of an acidic solution is less than 7, and the pH of basic solution is greater than 7 at 25 °C, but pH values change as a function of temperature.

See Also

- ▶ Hydrogen

Phase Transition

Henderson James (Jim) Cleaves II
Earth–Life Science Institute (ELSI), Tokyo Institute of Technology, Meguro–ku, Tokyo, Japan
Institute for Advanced Study, Princeton, NJ, USA
Blue Marble Space Institute of Science, Washington, DC, USA
Center for Chemical Evolution, Georgia Institute of Technology, Atlanta, GA, USA

Definition

Matter in the universe generally exists in one of four phases (states in which matter has essentially uniform physical properties): plasma, gas, liquid, and solid. The transition between each phase has an associated name (Fig. 1). Transitions can also occur within the solid phase.

The transition of matter between phases may be exergonic or endergonic. The change in energy is due to the change in interactions and ordering of the atoms or molecules and the associated changes of entropy and/or enthalpy (e.g., upon the freezing of a liquid phase, in which the

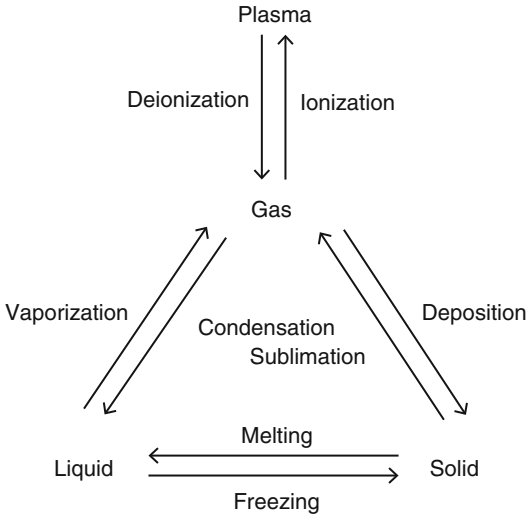

Phase Transition, Fig. 1 The four phases of matter and the transitions between them

components are highly mobile (with higher entropy), to a solid phase in which the components are in relatively fixed positions (with lower entropy)).

When a phase change occurs at a constant temperature, the energy required to cause the phase change (in the case where such a change is not spontaneous or energetically favorable) or the energy liberated (in the case where a phase change is spontaneous) is referred to as the latent heat. The value of this quantity is specific to the type of material in question (i.e., the latent heat of water is different than the latent heat of lead).

See Also

- ▶ Endergonic
- ▶ Enthalpy
- ▶ Entropy
- ▶ Exergonic
- ▶ Free Energy
- ▶ Latent Heat
- ▶ Triple Point
- ▶ Water
- ▶ Water in the Solar System
- ▶ Water in the Universe
- ▶ Water, Solvent of Life

References and Further Reading

McQuarrie DA, Simon JD (1997) Physical chemistry: a molecular approach. University Science, Sausalito

Phase, Orbital

David W. Latham
Harvard-Smithsonian Center for Astrophysics, Cambridge, MA, USA

Definition

For an object in a periodic orbit, the phase is the fraction of period that has passed since the time $t = 0$. Mathematically, the location of $t = 0$ can be any arbitrary point on an orbit; however, in Keplerian orbits, the point of ▶ periastron is considered as the location of $t = 0$. Usually, the phase is measured from the most recent periastron passage, but sometimes the phase will include an integer count for the number of orbital cycles since a fiducial periastron passage. For a circular orbit, the usual convention is to define phase zero as the time of maximum radial velocity of recession for the more massive component.

See Also

- ▶ Periastron

Phenetics

Carlos Briones
Centro de Astrobiología (CSIC/INTA), Consejo Superior de Investigaciones Científicas, Madrid, Spain

Synonyms

Numerical taxonomy

Definition

Taxonomical analysis aimed at classifying organisms with respect to their ▶ phenotype. It considers the overall similarities in observable/measurable characters – such as morphology or metabolic traits – among organisms or biological taxa regardless of their phylogenetic or evolutionary relationships. Phenetic techniques include various forms of clustering. They measure a – usually large – number of variables, analyze them by mathematical and statistical means to reduce them to a manageable level, and generally produce two- or three-dimensional graphs where different clusters of phenotypes are located.

See Also

▶ Phenotype
▶ Phylogeny
▶ Taxonomy

Phenotype

Susanna Manrubia
Systems Biology Program, Centro Nacional de Biotecnología (CSIC), Madrid, Spain

Keywords

Adaptation; Environment; Genotype; Morphology; Natural selection; Survival

Definition

The phenotype of an organism is the collection of all its observable characteristics, such as morphological traits, physiology, or behavioral properties. The phenotype arises from the interaction of the total genetic inheritance of each organism with the ▶ environment where it develops and grows, and might change during its life due to aging processes or environmental changes. In its turn, the phenotype determines how suited an organism is to survive and reproduce in a given environment. In the case of a virus, the phenotype refers mainly to the effects it causes in the infected host. The phenotype of a molecule consists of its structure and chemical function.

Overview

The relationship between ▶ genotype and phenotype is essential to understand how biological evolution proceeds. The distinction between the hereditary and developmental pathways as causally separated processes dates back to 1911 (Johannsen 1911): the genome is inherited, while the phenotype is its final expression under the environmental conditions specific to an organism. While innovations in biological evolution result from unintentional changes (▶ mutations) at the genomic level, ▶ natural selection can only act on the phenotype. Therefore, phenotypic variation is a prerequisite for evolution by natural selection.

The genotype-phenotype map is a many-to-many relationship, and as such it is only partly deterministic. One genotype might produce different phenotypes, since not all inherited possibilities are expressed. Plants growing in different watering conditions, for instance, are able to adjust their size and the shape of their leaves. Another example is that of certain proteins – fully functional in their native folded state – that become infectious agents (▶ prions) when mis-folded. Even identical human twins differ in their fingerprints, and behave distinctly as a result of nurture. The environment-dependent expression of genotype (a one-to-many relationship) is called phenotypic plasticity (De Witt and Scheiner 2004). On the other hand, the construction of an organism from genotype to phenotype displays a great amount of redundancy (a many-to-one relationship). Redundancy is an essential property conferring robustness when organisms face endogenous or exogenous change, fluctuations, or randomness. The neutral theory of molecular evolution (Kimura 1983)

analyzes the important role of a huge number of mutations present in the genotype that do not have an effect on phenotype (beyond changing the genomic sequence) but strongly affect the population structure and its intrinsic diversity, and thus its ability to adapt to new environments. The extent to which changes in genotype do not affect phenotype is called genetic canalization (Rendel 1967; Jen 2005).

The concept of extended phenotype (Dawkins 1982) refers to all the effects a gene can have upon the world which influence its chances of ▶ survival, thus extending beyond the genome-carrying individual organism. Examples are dams constructed by beavers, the elaborately woven nests of weaver birds, or the behavior a parasite can induce upon an infected host.

See Also

- ▶ Adaptation
- ▶ Environment
- ▶ Evolution, Biological
- ▶ Evolution, In Vitro
- ▶ Genotype
- ▶ Mutation
- ▶ Natural Selection
- ▶ Prion
- ▶ Selection
- ▶ Species
- ▶ Survival

References and Further Reading

Dawkins R (1982) The extended phenotype. Oxford University Press, New York
De Witt TJ, Scheiner SM (2004) Phenotypic plasticity. Functional and conceptual approaches. Oxford University Press, New York
Jen E (2005) Robust design. A repertoire of biological, ecological, and engineering case studies. Oxford University Press, New York
Johannsen W (1911) The genotype conception of heredity. Am Nat 45:129–159
Kimura M (1983) The neutral theory of molecular evolution. Cambridge University Press, Cambridge
Rendel JM (1967) Canalisation and gene control. Logos Press/Academic Press, London/New York

Phenylalanine

Kensei Kobayashi
Yokohama National University, Tokiwadai, Hodogaya-ku, Yokohama, Japan

Definition

Phenylalanine is one of the 20 protein ▶ amino acids whose chemical structure is NH_2—CH($CH_2C_6H_5$)—COOH. Its three-letter symbol is Phe, and one-letter symbol is F. Its molecular weight of 165.19, and its isoelectric point (p*I*) is 5.48. It shows poorer water solubility than most of the other amino acids. Since its side chain is a benzyl group (—$CH_2C_6H_5$), it is grouped as an aromatic amino acid together with tyrosine and tryptophan. ▶ Proteins present a UV absorbance at 280 nm because of the UV-absorbing aromatic rings present in these amino acids. Phenylalamine has recently been detected in extracts from Antarctic carbonaceous chondrites.

See Also

- ▶ Amino Acid
- ▶ Protein

Philae Lander

Hervé Cottin
Laboratoire Interuniversitaire des Systèmes Atmosphériques, Université Paris Est-Créteil, Créteil, France

Keywords

Lander; Rosetta; Comet; 67P/Churyumov-Gerasimenko

Definition

Philae is the lander of the ▶ ESA ▶ Rosetta mission which successfully landed on the nucleus of comet 67P/Churyumov-Gerasimenko on November 12, 2014.

Overview

Philae is the first automated vehicle that successfully landed on the nucleus of a comet. It is part of the European mission ROSETTA. Its overall mass is 98 kg including a scientific payload of 27 kg. The name of the lander follows the name of a Nile island where an obelisk was found, whose association with the Rosetta stone helped Champollion to understand the meaning of hieroglyphs.

On November 12, 2014, the Philae lander was released from its mother spacecraft at a distance of about 3 AU from the Sun and 20 km from the surface of comet 67P/Churyumov-Gerasimenko to land after 7 h of free fall. The landing site (called Agilkia) was meant to be a relatively smooth terrain on the smaller lobe of comet 67P. Contact with the nucleus was reported at 15:34 UTC, but it turned out that the lander did not anchor at the surface and bounced twice on the comet before making it to its final landing site after 2 h hovering above the nucleus in its low gravity environment. There, not sufficiently illuminated by the Sun, it could rely only on its primary battery to achieve its first science measurements sequence. After 64 h of operations at the surface of the comet, Philae went into safe mode due to lack of power. Philae woke up again and communicated with the Rosetta spacecraft on June 13, 2015, while the comet was approaching the Perihelion.

At the beginning, communication did not last more than few minutes or few seconds. The link was not stable enough to upload the data stored or to download new commands from the mother ship. Hopes were remaining to improve the link before the end of the extended mission, end of September

See Also

- ▶ 67P/Churyumov–Gerasimenko
- ▶ Comet (Nucleus)
- ▶ Rosetta Spacecraft

Phobos

Harald Hoffmann
DLR, Institute of Planetary Research, Berlin, Germany

Definition

Phobos is the inner of the two Martian satellites that were discovered by Asaph Hall in 1877. It is in nearly circular synchronous (Phobos's; length of day and orbital period are identical) orbit around ▶ Mars with an average distance of 9,375 km to the center of the ▶ planet and an orbital period of 0.32 days (Jacobson 2010). Phobos measures 26.8 × 22.4 × 18.4 km; it has a bulk density of about 1.9 g/cm^3. The heavily cratered surface indicates an old formation age. Two hypotheses are actually discussed to explain the origin of Phobos: capture of a D-type ▶ Asteroid or reaccretion of Martian ejecta.

See Also

- ▶ Asteroid
- ▶ Deimos
- ▶ Mars
- ▶ Phobos-Grunt
- ▶ Planet
- ▶ Satellite or Moon

References and Further Reading

Jacobson RA (2010) Astronomical J 139(668). doi:10.1088/0004-6256/139/2/668

Phobos Soil

► Phobos-Grunt

Phobos-Grunt

Michel Cabane
LATMOS/IPSL B102/T45-46, Université Pierre et Marie Curie UPMC-Paris 6, Paris, France

Keywords

Asteroid; Carbonaceous chondrite; In situ; Mars; Mars Express; Phobos; Satellite

Synonyms

Phobos soil

Definition

Phobos-Grunt is a mission to ► Phobos, one of the two small satellites of ► Mars; it was developed by the Russian agency ► Roskosmos, with the participation of other countries to the science payload. Launch occured in Baikonur, on November 8, 2011, for an arrival end-2012, and a landing on Phobos mid-2013; the payload consisted in Phobos-Grunt and ► YingHuo-1, a Chinese satellite, intended to study Mars and Phobos. One of the goals of Phobos-Grunt was to proceed to in situ soil analyses, to help understand the composition of Phobos (structure, mineralogy, organic matter), hence its origin. About 200 g of soil samples should have been sent from Phobos to Earth, for a; landing in 2014. Unfortunately, due to some concerns in the cruise stage, the probe was unable to leave its elliptical orbit around the Earth, and to begin its cruise to Mars and Phobos. After orbiting for 2 months, it desintegrated while entering Earth dense layers of the atmosphere, and the debris felt in Pacific Ocean. The idea of a return to Phobos exists, this reflight should mainly utilize spare models of the experiments that were on the previous probe.

Overview

Due to its low ► albedo and spectral characteristics (Murchie and Erard 1996; Simonelli et al. 1997), Phobos could be identified as a captured ► asteroid, with a composition close to the organic-bearing carboneous chondrites (Rivkin et al. 2002); nevertheless, its low apparent density (1.9 g/cm^3) (Avanesov et al. 1991) leads to think that it could contain water ice (Christensen et al. 1977) or have a "rubble pile" structure (Murchie and Erard 1996). This possible porosity (25–35 %) could also be explained by an origin at the moment of Mars' formation, or as the result of an asteroidal impact on Mars. Phobos's surface is covered by impact craters: near the rim of the huge crater Stickney, for example, "blue" material indicates material that possibly originates at depth (Fig. 1).

Twenty years after the USSR's Phobos 1 and 2 missions, Roskosmos developed Phobos-Grunt (P-G), to be launched in 2011 (Zelenyi et al. 2010). It will carry the Chinese satellite Yinghuo-1, devoted to Mars study, and it will land on Phobos in April 2013 (Figs. 2 and 3).

The in situ science payload of the P-G lander (Zelenyi et al. 2010) resembles those of MSL and ► Exomars. Its 40 kg includes, among others, cameras, radar, and seismometer to understand Phobos structure, and classical in situ instruments searching for elementary and mineralogical composition (Mossbauer, APX, IR, γ and n spectrometers, laser ablation mass spectrometer). The Gas Analytical Package will proceed to analyze soil samples, delivered by the P-G manipulator arm, possibly using a drill. Heating and pyrolysis of these samples, followed by analysis of evolved gases (► GC-Ms and IR laser spectroscopy), will detect the presence of any water ice (Christensen et al. 1977) and the structural gases of the minerals (H_2O, CO_2, etc.). Using the same techniques, this instrument will be able to search for ► noble gases, ► organic molecules (nature, ► isotopic ratios) present in the

Phobos-Grunt, Fig. 1 Crater Stickney, at right, as observed from 5,800 km by NASA probe Mars Reconnaissance Orbiter (March 2008; resolution: 5.8 m/pixel) (Credit: NASA/JPL/ University of Arizona http://hirise.lpl.arizona.edu/phobos.php)

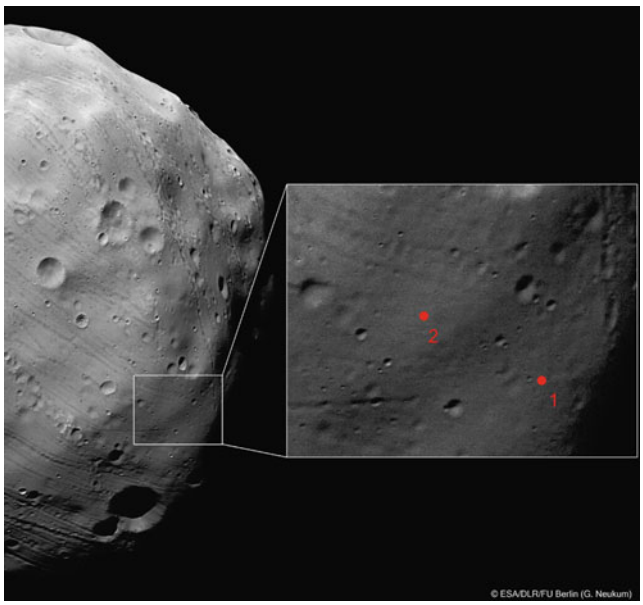

Phobos-Grunt, Fig. 2 Possible landing sites for Phobos-Grunt, as observed by ESA probe Mars Express (March 2010; resolution 4.4 m/pixel) (Credit ESA/DLR/FU Berlin – G. Neukum http://www.esa.int/images/5_h7915__Phobos_LandingSites_H.jpg)

ground, to be compared to the ones present in ▶ meteorites (Rivkin et al. 2002), to give clues on the origin and history of Phobos. Once landed, P-G will also sample the ground and bring to Earth (arrival July 2014; Galimov 2010) about 200 g of material, in a devoted container (see Fig. 3: small brown sphere on top of P-G) for further analyses.

The experiment Living Interplanetary Fight Experiment (LIFE) proposed by a US nonprofit association (the Planetary Society) will sit in the Phobos sample return capsule. Two titanium containers specially designed by the Russian Institute for Medico-Biological Problems will house terrestrial organisms (like seeds) and

Phobos-Grunt, Fig. 3 Mock-up (scale 1/1) of Phobos-Grunt lander (Moscow, November 2006) (Credit: CNES photo http://smsc.cnes.fr/PHOBOS/Fr/)

microorganisms. Pure culture of known resistant microorganisms strains from the three domains of life (Archaea, Bacteria, and Eukarya) will sit along a sample of a terrestrial natural soil. All this samples will be tested for survival upon their recovery with the Phobos samples and subsequently analyzed. The containers will mimic rock and this will be an attempt to evaluate the possibility of panspermia while those organisms will experience a 34-month round trip to Mars.

See Also

- ▶ Albedo
- ▶ Asteroid
- ▶ Carbonaceous Chondrite
- ▶ ExoMars
- ▶ GC/MS
- ▶ Mars Express
- ▶ Mars Science Laboratory
- ▶ Panspermia
- ▶ Phobos

References and Further Reading

Avanesov G et al (1991) Results of TV imaging of Phobos (experiment VSK-Fregat). Planet Space Sci 39:281–295

Christensen EJ, Born GH, Hildebrand CE, Williams BG (1977) The mass of Phobos from Viking flybys. Icarus 4:555–557

Galimov EM (2010) Phobos sample return: scientific substantiation. Sol Syst Res 44:7–16

Murchie S, Erard S (1996) Spectral properties and heterogeneity of Phobos from measurements by Phobos 2. Icarus 123:63–86

Rivkin AS, Brown RH, Trilling DE, Bell JF III, Plassmann JH (2002) Near-infrared spectrophotometry of Phobos and Deimos. Icarus 156:64–75

Simonelli DP, Wisz M, Switala A, Adinolfi D, Veverka J, Thomas PC, Helfenstein P (1997) Photometric properties of Phobos surface materials from Viking images. Icarus 131:52–77

Zelenyi LM, Zakharov AV, Polischnik GM, Martynov MB (2010) Project of the mission to Phobos. Sol Syst Res 44:17–28

Phoebe

Therese Encrenaz
LESIA, Observatoire de Paris - Section de Meudon, Meudon, France

Definition

Saturn's satellite Phoebe was discovered in 1899 by William Henry Pickering; it has been for a

century the outermost known satellite of ► Saturn. It orbits at about 13 million kilometers (or 215 Saturnian radii) from Saturn; its orbit is highly inclined and is retrograde, which suggests that Phoebe was captured, rather than having been formed together with Saturn. It may have originated as a Kuiper Belt Object. Phoebe was first observed by Voyager 2 in 1981 and then extensively explored by the ► Cassini orbiter. Its diameter is 220 km and its density is 1.6 g/cm^3. Phoebe might be the source of a tenuous external Saturnian ring, and might also be responsible for feeding the dark side of ► Iapetus with dark material.

See Also

► Iapetus
► Kuiper Belt
► Saturn
► Voyager, Spacecraft

Phoenix

Michel Viso
CNES/DSP/SME, Vétérinaire/DVM, Astro/Exobiology, Paris Cedex 1, France

Definition

Phoenix was launched for its cruise to Mars from Cape Canaveral by a Delta II rocket on August 4, 2007. The soft landing in the north polar region occurred on May 25, 2008. The five science instruments, provided by US institutions with contributions from the Max Plank Institute (Germany) and the Canadian Space Agency (Canada), examined water ice under the surface, checking if this place could support life. A meteorological station provided data on the atmosphere and the water cycle. After 5 months of operation, the power declined as the illumination by the sun decreased. The last brief signal was received on November 2, 2008. In early 2010, attempts to communicate with Phoenix failed. The hardware was not designed to survive the cold and ice-coating load of an arctic Martian winter. One of the main results is the hypothesis of the presence of carbonate and perchlorate as well as the evidence of subsurface ► ice.

Phosphaethyne

Didier Despois
Laboratoire d'Astrophysique de Bordeaux, CNRS-Universite de Bordeaux, France

Synonyms

HCP; Methinophosphide

Definition

Phosphaethyne is, with PN, PH_3, and the radical CP, one of the few molecules detected outside the Earth that contain phosphorus, an element that plays a crucial role in biochemistry (being part of the structural framework of DNA and RNA and being used to transport cellular energy). HCP is similar in many ways to hydrogen cyanide, HCN, as phosphorus is below nitrogen in the Periodic Table. In the laboratory, phosphaethyne is a reactive species that spontaneously and rapidly polymerizes.

History

Phosphaethyne has been detected by Agúndez et al. (2007) in the carbon-rich circumstellar envelope of the evolved star IRC +10216 (CW Leo).

See Also

- ▶ Molecules in Space
- ▶ Phosphorus Monoxide

References and Further Reading

Agúndez M, Cernicharo J, Guélin M (2007) Discovery of phosphaethyne (HCP) in space: phosphorus chemistry in circumstellar envelopes. Astrophys J Lett 662: L91–L94

Phosphates

Francis Albarède
Ecole Normale Supérieure de Lyon, Lyon, France

Definition

▶ Phosphates are minerals containing the tetraheadral PO_4^{3-} group, the most abundant of which is apatite $Ca_{10}(PO_4)_6(X)_2$, where X is OH, F, Cl, or CO_3. Apatite is the main repository of phosphate in the Earth's mantle and the crust, and is used by both vertebrates and invertebrates to build solid parts (skeletons). In natural waters, the phosphate anion is an essential nutrient entering nucleic acids, phospholipids, and the universal energy currency adenosine triphosphate (ATP). Surface waters are depleted in phosphate by organic productivity. At depth, phosphate strongly correlates with nitrate and the remarkably constant C:N:P proportions of phytoplankton (105:15:1) are known as the Redfield ratio. ▶ Mid-ocean ridges and sediments are net P sinks, whereas continents are the dominant source of oceanic phosphate.

See Also

- ▶ Mid-Ocean Ridges
- ▶ Nucleic Acids
- ▶ Phosphates on Mars

Phosphates on Mars

Daniela Tirsch[1] and Alessandro Airo[2]
[1]German Aerospace Center DLR, Institute of Planetary Research, Berlin, Germany
[2]Institut für Geologische Wissenschaften Tektonik und Sedimentäre Geologie, Freie Universität Berlin, Fachbereich Geowissenschaften, Berlin, Germany

Definition

Phosphates are the salts and esters of phosphoric acid (H_3PO_4). Since phosphate is a essential nutrient for life on Earth and part of the backbone of DNA, its occurrence is important for estimating the ▶ habitability on Mars. Phosphates can be derived from minerals (e.g., apatite $Ca_5[(PO_4)_3(OH, F, Cl)]$) through the weathering of igneous rocks. Calcium-phosphate minerals have a high solubility in acidic water. Measurements done by the Mars Pathfinder Rover and the Mars Exploration Rover indicate that the Martian soil is enriched in phosphorus relative to the rock.

See Also

- ▶ Habitability of the Solar System
- ▶ Mars
- ▶ Mineral
- ▶ Sulfates, Extraterrestrial

Phosphine

Matthew A. Pasek
University of South Florida, Tampa, FL, USA

Synonyms

Hydrogen phosphide; Phosphorus hydride

Definition

Phosphine, PH_3, is a toxic, phosphorus gas at standard temperature and pressure, boiling at 185 K and freezing below 135 K. Relative to phosphate, the redox state of the phosphorus atom in phosphine is reduced to −3. Phosphine is the most abundant, naturally occurring volatile phosphorus species, and has been detected in the atmospheres of the gas giants Jupiter and Saturn, in the atmospheric envelopes of giant stars, and as a trace constituent in the atmosphere of the Earth. Its terrestrial origin may be linked to microbial activity or to anthropogenic sources; hence, phosphine plays a small role in the phosphorus biogeochemical cycle. At low temperatures (below 70–80 K), it can be trapped as a clathrate in water ice.

reduction of phosphate by lightning strikes or other high-energy events, and may have comprised some portion of the total phosphorus in the early Archean oceans.

See Also

- ▶ Phosphates
- ▶ Phosphoric Acid
- ▶ Pyrophosphate

Phosphonate

- ▶ Phosphite

Phosphite

Matthew A. Pasek
University of South Florida, Tampa, FL, USA

Synonyms

H-phosphonate; Phosphonate

Definition

Phosphite (HPO_3^{2-}) is the anion of phosphorous acid (H_3PO_3), an oxide of phosphorus in which the phosphorus has a +3 valence state. In contrast to orthophosphate dissolved in solution, in phosphite one hydrogen atom is directly bound to the central P atom, instead of being bound through an O atom. Phosphite is more soluble in ocean water than phosphate. Oxidation of phosphite yields phosphate and, under certain conditions, also pyrophosphate and larger polyphosphates. Phosphite on the Earth may have originated from corrosion of iron-rich meteorites or from

Phosphoric Acid

Matthew A. Pasek
University of South Florida, Tampa, FL, USA

Synonyms

Orthophosphate

Definition

Phosphoric acid is a triprotic acid with a formula of H_3PO_4. Its pK_as are about 2, 7, and 12.5 at 25 C. Heating of phosphoric acid results in dehydration leading to pyrophosphoric acid and larger polyphosphoric acid polymers.

See Also

- ▶ Diphosphate
- ▶ Phosphine
- ▶ Phosphite

Phosphorus Hydride

► Phosphine

Phosphorus Monoxide

Didier Despois
Laboratoire d'Astrophysique de Bordeaux, CNRS-Universite de Bordeaux, France

Synonyms

PO

Definition

Phosphorus monoxide is an unusual oxidized form of phosphorus, recently detected in the envelope expelled by an evolved star (the most common phosphorus oxides on Earth are P_4O_6 and P_4O_{10}). PO is, with HCP, PN, PH_3, and CP, one of the few molecular species outside the Earth containing phosphorus, an element that plays a central role in biochemistry. The P—O bond is present in adenosine diphosphate (ADP) and adenosine triphosphate (► ATP).

History

Tenenbaum et al. (2007) detected phosphorus monoxide in the circumstellar shell of the oxygen-rich supergiant star VY Canis Majoris.

See Also

► ATP
► Molecules in Space

References and Further Reading

Tenenbaum ED, Woolf NJ, Ziurys LM (2007) Identification of phosphorus monoxide ($X^2\Pi_r$) in VY Canis Majoris: detection of the first P—O bond in space. Astrophys J Lett 666:L29–L32

Photoattachment

► Radiative Attachment

Photoautotroph

Ricardo Amils
Departamento de Biologia Molecular, Universidad Autónoma de Madrid, Madrid, Spain

Synonyms

Photosynthetic organism

Definition

Photoautotrophs are organisms that obtain cellular ► energy from radiation and assimilate CO_2 as a source of carbon. They differ from photoheterotrophs that produce ATP using solar energy but obtain carbon for biosynthesis from reduced organic compounds. The ► photosynthesis reaction center of photoautotrophic organisms contains chlorophyll, a pigment responsible for the transduction of radiation into cellular energy. Photoautotrophs can be divided in two groups, anoxygenic and oxygenic, depending on the number of reaction centers in their photosynthetic apparatus and on their ability to use water as a source of reducing power and generating oxygen as a by-product. Anoxygenic photoautotrophs are dependent on environmental reducing power to assimilate

CO_2. From an ecological point of view, life on Earth has been considered to be dependent on photoautotrophy; however, the recent discovery of underground strict chemolithoautotrophs is challenging this concept.

See Also

- ▶ Anoxygenic Photosynthesis
- ▶ Bioenergetics
- ▶ Carbon Dioxide
- ▶ Chlorophylls
- ▶ Cyanobacteria
- ▶ Energy
- ▶ Energy Conservation
- ▶ Green Bacteria
- ▶ Photosynthesis
- ▶ Photosynthesis, Oxygenic
- ▶ Photosynthetic Pigments

Photobiology

Petra Rettberg
German Aerospace Center (DLR), Institute of Aerospace Medicine, Cologne, Germany

Keywords

Bioluminescence; Chronobiology; Environmental photobiology; Infrared radiation; Nonionizing radiation; Photosynthesis; Photocarcinogenesis; Photomedicine; Ultraviolet radiation; Visible radiation

Definition

Photobiology is the branch of biology concerned with the biological and bioenvironmental effects of ultraviolet, visible, or infrared radiation.

Overview

Photobiological responses are the result of chemical and/or physical changes induced in biological systems by nonionizing radiation. The radiation spectrum covered by the discipline photobiology ranges from ultraviolet radiation with wavelengths from 10 to 400 nm to visible light from 400 to 750 nm to the infrared radiation from 750 nm to 300 μm.

The research topics in photobiology are very broad: *Photobiology at the molecular and cellular level* deals with photochemical reactions after the absorption of nonionizing radiation and the following biological responses in cells, e.g., enzymatic repair of UV radiation-induced ▶ DNA damage or the induction of the synthesis of photoprotecting compounds. Another research field is the investigation of *bioluminescence*, the production of light by biochemical cellular reactions in some bacteria, invertebrates, and vertebrates. Organisms had developed it for signaling and communication purposes. In biotechnology, bioluminescence is used as a reporter signal for genetic engineering. ▶ *Photosynthesis*, the process of utilizing solar radiation and carbon dioxide for the synthesis of organic compounds in plants, algae, and some species of bacteria, is another important field of photobiological research. At the organism level, *chronobiology* examines periodic phenomena in living organisms and their adaptation to solar-related rhythms. *Photocarcinogenesis* research aims at the discovery of the complex simultaneous and sequential biochemical events in higher organisms that ultimately lead to the occurrence of skin cancer, in many cases several years after exposure. In *photomedicine*, the application of light with respect to health and disease is studied and used for therapy. Photomedical aspects can be found in various fields of medicine including dermatology, surgery, dentistry, optical diagnostics, cardiology, and oncology. Effects of solar radiation on ecosystem level are monitored and examined in *environmental photobiology*. In *astrobiology*, the early Earth's ▶ UV climate

with wavelengths down to 200 nm penetrating the atmosphere to the Earth's surface was found to be a major driving force for biological evolution. Based on photobiological laboratory experiments in planetary and space simulation facilities and on space experiments in low Earth orbit like ADAPT on the EXPOSE-E facility on the ▶ International Space Station (ISS) in 2008/2009, the hability of other planets, e.g., Mars, with respect to a UV climate different from today's Earth is estimated.

See Also

- ▶ Biological Evolution
- ▶ Darwin's Conception of the Origins of Life
- ▶ DNA Damage
- ▶ Expose
- ▶ Extreme Ultraviolet Light
- ▶ Faint Young Sun Paradox
- ▶ International Space Station
- ▶ Ionizing Radiation, Biological Effects
- ▶ Life in the Solar System (History)
- ▶ Photochemistry
- ▶ Photochemistry, Atmospheric
- ▶ Photosynthesis
- ▶ Radiation Biology
- ▶ Solar UV Radiation, Biological Effects
- ▶ UV Climate
- ▶ UV Radiation
- ▶ UV Radiation, Biological Effects
- ▶ VUV

References and Further Reading

Hockberger PE (2002) A History of ultraviolet photobiology for humans, animals and microorganisms. Photochem Photobiol 76(6):561–579

IUPAC (1997) Compendium of chemical terminology, 2nd edn. Compiled by McNaught AD, Wilkinson A. Blackwell Scientific Publications, Oxford. XML on-line corrected version: http://goldbook.iupac.org (2006) created by Nic M, Jirat J, Kosata B; updates compiled by Jenkins A. ISBN 0-9678550-9-8. doi:10.1351/goldbook

Photochemistry

John H. Black
Department of Earth and Space Sciences, Chalmers University of Technology, Onsala Space Observatory, Onsala, Sweden

Keywords

Cosmic rays; Interstellar medium; Photodissociation

Definition

Photochemistry refers to the processes by which energy is transferred from electromagnetic radiation (in practice mainly ultraviolet and visible light) into chemical activity in gases, solid particles, and living matter. Photochemical processes partly control the initial conditions for the formation of stars and planets, they may leave traces of the early chemical evolution of planetary systems in the abundances of isotopes, they regulate the input of stellar energy into atmospheres of planets, and they play important roles in the chemistry of living organisms on Earth.

Overview

Photochemical processes are very effective in driving a system away from thermodynamic equilibrium. Consider complex systems where no single temperature characterizes the physical and chemical state. For example, visible and near-infrared radiation from the surface of the Sun at an effective temperature of 5,800 K reaches the atmosphere, oceans, and solid surface of the Earth, which achieves a balance between absorbed and reradiated energy at an average temperature (<300 K) very conducive to the chemistry of life. The corona of the Sun radiates an intensity of ultraviolet (UV) light that greatly

exceeds what is expected from a 5,800-K blackbody. The ultraviolet sunlight penetrates only the upper layers of our atmosphere, where it interacts with molecules through various quantum processes. The physical and chemical states of these upper layers must then be analyzed kinetically (in terms of the rates of individual microscopic processes), in contrast to the troposphere, which is well mixed and close to local thermodynamic equilibrium. For example, photodissociation of an oxygen molecule by a quantum (γ) of UV light produces free atoms $O_2 + \gamma \rightarrow O + O$, some of which then associate with a molecule to form ozone O_3. Occasionally an ozone molecule meets a free hydrogen atom (typically a daughter born of the photodissociation of water): the result is a reaction $O_3 + H \rightarrow OH^* + O_2$ in which the product hydroxyl, OH, is formed preferentially in highly excited vibrational states. The internal energy of excited OH is so far out of equilibrium with its surroundings that it is likely to produce several infrared photons rather than to share its excess energy with neighboring molecules. These photons produce an airglow that would illuminate our way at night if we had infrared-sensitive eyes. This infrared airglow nearly blinds sensitive infrared detectors on astronomical telescopes. If this airglow radiation had been excited by thermal processes instead of by photochemistry, it would be characterized by temperatures of 1,000 K or more, in contrast to the 200-K temperature actually prevailing at 90-km altitude where the ozone-plus-hydrogen source maximizes.

The study of photochemistry in astrophysics and planetary science is severely dependent upon theory and experiment in molecular physics and physical chemistry, owing to the need for vast amounts of data on fundamental processes like photodissociation, photoionization, and two-body chemical reactions. In the interstellar clouds that collapse to form stars, protoplanetary disks, and eventually planets, the most abundant gaseous molecules are H_2 and CO, yet the heating and cooling processes are partly controlled by other minor species, like atomic C, C^+, and O, which arise directly from the photochemistry of CO. The surfaces of interstellar clouds (and some layers of planet-forming disks) are exposed to ultraviolet starlight that typically has an abrupt cutoff at the wavelength of the Lyman limit of atomic hydrogen, 91.2 nm, because of absorption by hydrogen atoms. These surface layers, called photon-dominated or photodissociation regions (PDRs), exhibit a rich photochemistry far out of equilibrium. Both H_2 and CO are special in that they are photodissociated via line absorptions that easily become self-shielding (optically thick) in the interior of the cloud, whereas most other molecules are photodissociated in continuous absorption processes and shielded mainly by the absorption and scattering by dust particles. In CO, the photodissociation can be isotope-selective in the sense that the less abundant isotopologues $^{13}C^{16}O$ and $^{12}C^{18}O$ are more readily broken apart than the most common form $^{12}C^{16}O$. At low temperatures, <50 K, this effect competes with a temperature-sensitive ion-exchange reaction $^{13}C^+ + {}^{12}CO \rightleftarrows {}^{12}C^+ + {}^{13}CO$, which tends to enhance the abundance of the rarer species. It has been suggested that isotope-selective photodissociation of CO in the protoplanetary disk of the immature solar system might account for abundance anomalies in oxygen isotopes that have persisted in meteorites to the present time. This effect is unlikely to be important, however, unless carbon monoxide is the primary reservoir of oxygen in the first place.

The initial conditions for star formation may be set in gas and dust at temperatures of 10 K where the density is of the order of 10,000 hydrogen molecules cm^{-3}. In the centers of these dark clouds where no starlight penetrates, one might expect no photochemistry; however, the cosmic rays (mainly protons with energies greater than 10 MeV) ionize hydrogen, and the resulting fast electrons lose significant energy by exciting other hydrogen molecules to radiate ultraviolet photons. This internal source of radiation, known as the ▶ Prasad-Tarafdar mechanism, adds significant photochemical activity to what is driven

directly by cosmic-ray ionizations. Cosmic rays are perhaps the most extreme example of a non-thermal, disequilibrating agent. Photochemistry regulates the abundances of ions and free electrons in the mostly neutral material of star-forming clouds and planet-forming disks. These charged particles in turn couple the magnetic field to the gas and thus mediate the effects of magnetic forces, rotation, and gas flows in the early evolution of stars and planets.

Once a planetary system has formed, photochemistry operates in many ways. For example, Saturn's largest satellite, ▶ Titan, has a thick nitrogen-methane atmosphere (surface pressure 1.5 bar) with a rich organic photochemistry. Photoionization of N_2 by extreme-ultraviolet sunlight is more effective than photodissociation, so that $N_2^+ + CH_4 \rightarrow CH_3^+ + H + N_2$ initiates an ion-driven photochemistry. As a result, the ionosphere must be considered together with the neutral atmosphere, and transport mechanisms complement the basic microscopic chemical processes.

In the coming years, as atmospheres of extrasolar planets become better observed, there will be increasing recognition of the role of photochemistry in their structures and evolution. There are already indications that the abundances of stable molecules like CH_4, CO_2, CO, and H_2O depart from equilibrium at pressures above 1 bar in the atmosphere of exoplanet HD 189733b. Photochemistry can affect atmospheric dynamics and evolution through photodissociation processes that yield kinetically hot product atoms and molecules.

It is widely thought that photochemistry has played an important role in the origin of life on Earth and in the subsequent impact of living organisms on the physical evolution of the terrestrial atmosphere. An oxygen-rich atmosphere is one consequence of our inhabited planet, where photosynthesis in plants has been operating. Strategies for astronomical searches for evidence of life elsewhere can be evaluated in relation to the spectrum and photometric variability of earthshine, the reflected light of Earth as seen from outside. The reflectance spectrum of terrestrial vegetation has a sharp edge at 700-nm wavelength, although this may be neither a universal nor a unique signature of life on planets.

See Also

- ▶ Absorption Cross Section
- ▶ Biomarkers, Spectral
- ▶ Comet
- ▶ Exoplanets, Discovery
- ▶ Interstellar Chemistry
- ▶ Isotopic Fractionation (Interstellar Medium)
- ▶ Magnetic Field
- ▶ Magnetic Fields and Planetary Systems Formation
- ▶ Photodissociation Region
- ▶ Prasad-Tarafdar Mechanism
- ▶ Protoplanetary Disk
- ▶ Star Formation, Theory
- ▶ Titan

References and Further Reading

Arnold L (2008) Earthshine observation of vegetation and implication for life detection on other planets. Space Sci Rev 135:323

de Pater I, Lissauer JJ (2010) Planetary sciences, 2nd edn. Cambridge University Press, Cambridge

Gredel R, Lepp S, Dalgarno A, Herbst E (1989) Cosmic ray-induced photodissociation and photoionization rates of interstellar molecules. Astrophys J 347:289

Grenfell JL, Rauer H, Selsis F et al (2010) Co-evolution of atmospheres, life, and climate. Astrobiology 10:77

Krasnolposky VA (2009) A photochemical model of Titan's atmosphere and ionosphere. Icarus 201:226

Lequeux J (2005) The interstellar medium. Springer, Berlin

Line MR, Liang MC, Yung YL (2010) High-temperature photochemistry in the atmosphere of HD 189733b. Astrophys J 717:496

Röllig M, Abel NP, Bell T et al (2007) A photon dominated region code comparison study. Astron Astrophys 467:187

Visser R, van Dishoeck EF, Black JH (2009) The photodissociation and chemistry of CO isotopologues: applications to interstellar clouds and circumstellar disks. Astron Astrophys 503:323

Photochemistry, Atmospheric

Melissa G. Trainer
NASA Goddard Space Flight Center Code 699, Greenbelt, MD, USA

Definition

Atmospheric photochemistry is the study of light initiated chemical reactions which occur in the atmospheres of planetary bodies. These reactions play an important role in climate, and likely contributed to prebiotic organic synthesis.

Overview

Planetary atmospheric photochemistry occurs when incident radiation contains enough energy to dissociate bonds within the atmospheric molecules. Bond energies in atmospheric molecules are on the order of 10^2–10^3 kJ mol^{-1}, and thus bond dissociation requires photons in the ultraviolet and visible region of the electromagnetic spectrum. A photochemical reaction occurs when the absorption of light triggers an electronic transition within the molecule, activating the reaction. Products of photo dissociation are typically highly reactive radicals.

A photochemical reaction is represented by the following general equation:

$$AB + h\nu \rightarrow A + B$$

where $h\nu$ represents the energy of the photon. This reaction is characterized by a first-order rate constant (known as a "J-value"), and the rate of photochemical dissociation is expressed as:

$$\text{Rate}\left(\text{molecules cm}^{-3}\text{s}^{-1}\right) = -\text{J}(\text{AB}).$$

The J-value is dependent upon the absorption spectrum of the molecule, the available light in the atmosphere, and the quantum yield for dissociation once the molecule is electronically excited by light absorption. The quantum yield is the ratio of the number of molecules dissociated to the number of photons absorbed, a dimensionless parameter ranging from 0 to 1. The lifetime (τ) of a particular molecule with respect to photolysis loss is given by 1/J, and this value allows for comparison between photolysis and other possible loss processes, such as transport.

To calculate a J-value at any point in the atmosphere for any particular molecule, the following summation is used over the wavelength (λ) range of interest:

$$\text{J}\ (\text{s}-1) = \Sigma_i \text{I}(\lambda)\sigma(\lambda)\varphi(\lambda)\text{d}\lambda$$

where $I(\lambda)$ is the available light (photons cm^{-2} s^{-1}), $\sigma(\lambda)$ is the absorption cross section of the molecule (cm^2 $molecule^{-1}$), and $\varphi(\lambda)$ is the quantum yield. The photon flux is a property of the planet, determined by the incident angle of sunlight, flux at the top of the atmosphere, and the amount of light absorbed above the point of interest. Both the absorption cross section and quantum yield are properties of the molecule.

The dependence on the photon flux leads to a strong dependence on altitude, which contributes to the vertical distribution of gases within an atmosphere and serves to attenuate the light that reaches the planet's surface. Figure 1 shows the penetration depth of ultraviolet solar radiation into the Earth's atmosphere and relevant absorbing molecules. On Earth, the highest energy ultraviolet radiation is effectively absorbed by O_2 and O_3 before reaching the surface, protecting life from this damaging radiation.

Atmospheric photochemistry on the current Earth, early Earth, and other planets is of interest because of the effects photochemical processes can have on planetary environments. These include the chemical composition of the atmosphere, the attenuation of sunlight reaching the surface, the radiative balance of the planet, the oxidative capacity of the atmosphere, the

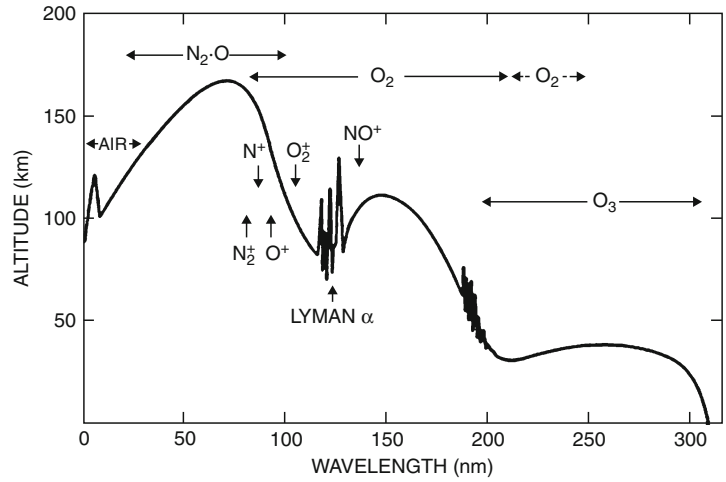

Photochemistry, Atmospheric, Fig. 1 Depth of penetration of ultraviolet radiation in the Earth's atmosphere. The altitudes correspond to an attenuation of 1/e. The principle absorbers are indicated (Adapted from Brasseur and Solomon 2005)

production and delivery of organic molecules to the surface, and the generation of radiatively shielding hazes and pollution.

See Also

- ▶ Atmosphere, Organic Synthesis
- ▶ VUV

References and Further Reading

Brasseur GP, Solomon S (2005) Aeronomy of the middle atmosphere: chemistry and physics of the stratosphere and mesosphere, 3rd edn. Springer, Dordrecht

Seinfeld JH, Pandis SN (1998) Atmospheric chemistry and physics. Wiley, New York

Photodesorption

Karin I. Öberg
Harvard-Smithsonian Center for Astrophysics, Cambridge, MA, USA

Keywords

Interstellar dust; Snow line

Synonyms

Photoevaporation; Photosputtering

Definition

The absorption of a UV (or X-ray) photon by a molecule condensed on a surface can result in its desorption (direct photodesorption) or in the "kick-out" of a nearby molecule (indirect photodesorption). In space, photodesorption can regulate the locations of "snow-lines," the transition regions where the dominant phase of volatiles changes from gas to ice (particularly in protoplanetary disks). Photodesorption, from ices and other surfaces that mimic interstellar grain compositions, is characterized experimentally to determine molecule-specific desorption efficiencies and mechanisms.

Overview

In dense and cold regions in space, atoms and molecules freeze out on interstellar grains, forming icy mantles that continue to evolve chemically. Photodesorption connects the surface/ice chemistry with the gas phase in regions that are too cold for efficient thermal ice evaporation. In the presence of strong radiation fields,

photodesorption will affect the location of "snow-lines," i.e., the molecule-specific transition regions where ice desorption overtakes freeze-out. In less exposed regions, where the ice phase dominates, low-level photodesorption can maintain a small fraction of molecules in the gas phase. This is important because it potentially enables the use of gas-phase spectroscopic observations as a probe of ice compositions.

Ice photodesorption efficiencies are measured experimentally in ultra-high-vacuum chambers, where interstellar ice equivalents are irradiated with broadband or monochromatic UV/X-ray sources and desorption rates are measured using a quartz balance, infrared spectroscopy, or mass spectrometry, or a combination of two or more of these techniques. These experiments can also be used to characterize the desorption process based on how the photodesorption rate responds to radiation at different fluxes and frequencies, and based on the effects of ice thickness, temperature, and morphology on the desorption efficiency. Experiments on photodesorption off metal surfaces have a long history (Avouris and Walkup 1989), while investigations of ice photodesorption date back to the mid 1990s (Westley et al. 1995).

Measured photodesorption efficiencies are generally high, of the order 10^{-2}–10^{-3} desorbed molecules per incident photon for species with electric-dipole-allowed transitions within the frequency range of the UV source. Derived desorption mechanisms are ice specific. Ices that only present nondissociative excitations mainly desorb through the excitation of a subsurface molecule, followed by the kick-out of a surface molecule. CO and N_2 are in this category when exposed to a typical interstellar radiation field. In contrast, two other astrophysically important molecules, H_2O and CO_2, only have strong dissociative transitions in the far-UV and photodesorption proceeds differently: following absorption of a photon, the dissociation fragments either desorb directly, or recombine and desorb, or kick-out a surface molecule. The number of active layers is generally larger for dissociative photodesorption because of the dynamics involved. Extreme UV and X-ray photons may ionize as well as dissociate molecules resulting in the photodesorption of molecular ions.

Photodesorption efficiencies are included in astrochemical models of clouds, protostars, and protoplanetary disks to determine the division of molecules between the gas phase and the grain surfaces. Since the gas phase and grain surface chemical reactions are different, this is important to predict the chemical evolution during most stages of star and planet formation.

See Also

- ▶ Interstellar Ices
- ▶ Snow Line
- ▶ Solar Nebula

References and Further Reading

Andersson S, van Dishoeck EF (2008) Photodesorption of water ice. A molecular dynamics study. J Astron Astrophys 491:907–916

Andrade DPP, Rocco MLM, Boechat-Roberty HM (2010) X-ray photodesorption from methanol ice. Mon Not R Astron Soc 409:1289–1296

Avouris P, Walkup RE (1989) Fundamental mechanisms and desorption and fragmentation induced by electronic transitions at surfaces. Annu Rev Phys Chem 40:173–206

Bertin M, Fayolle EC, Romanzin C, Öberg KI, Michaut X, Moudens A, Philippe L, Jeseck P, Linnartz H, Fillion J-H (2012) UV photodesorption of interstellar CO ice analogues: from excitation to surface desorption. Phys Chem Chem Phys 14:9929–9935

Hama T, Yokoyama M, Yabushita A, Kawasaki M, Andersson S, Western CM, Ashfold MNR, Dixon RN, Watanabe N (2010) A desorption mechanism of water following vacuum-ultraviolet irradiation on amorphous solid water at 90 K. J Chem Phys 132:164508–164616

Öberg KI, Visser R, van Dishoeck EF, Linnartz H (2009a) Photodesorption of ices. II. H_2O and D_2O. Astrophys J 93:1209–1218

Öberg KI, van Dishoeck EF, Linnartz H (2009b) Photodesorption of ices. I. CO, N_2 and CO_2. J Astron Astrophys 496:281–293

Westley MS, Baragiola RA, Johnson RE, Baratta GA (1995) Photodesorption from low-temperature water ice in interstellar and circumsolar grains. Nature 373:405–407

Photodestruction

► Photodissociation

Photodetachment

Steven B. Charnley
Solar System Exploration Division, Code 691, Astrochemistry Laboratory, NASA Goddard Space Flight Center, Greenbelt, MD, USA

Definition

Photodetachment is the chemical process whereby an electron is removed from an ► anion (e.g., CN^-) by absorption of a photon.

See Also

► Anion

Photodissociation

Steven B. Charnley
Solar System Exploration Division, Code 691, Astrochemistry Laboratory, NASA Goddard Space Flight Center, Greenbelt, MD, USA

Synonyms

Photodestruction

Definition

Photodissociation is the chemical process whereby a molecule is broken apart by absorption of a photon. Specific processes include direct photodissociation, ► predissociation, coupled-states photodissociation, and spontaneous radiative photodissociation.

See Also

► Photolysis

References and Further Reading

Duley WW, Williams DA (1984) Interstellar chemistry. Academic, London

Photodissociation Region

Mark G. Wolfire[1] and Michael J. Kaufman[2]
[1]Astronomy Department, University of Maryland, College Park, MD, USA
[2]Department of Physics and Astronomy, San José State University, San Jose, CA, USA

Keywords

Interstellar medium (ISM); Molecular cloud; Star formation; Thermal process

Synonyms

PDR; Photon dominated region

Definition

A photodissociation region (PDR) is an interstellar gas phase in which far-ultraviolet (FUV; 6 eV $< h\nu <$ 13.6 eV, where eV is the energy of the radiation in electron volts) radiation plays a role in the heating and/or chemistry (Tielens and Hollenbach 1985a). These regions include the diffuse atomic ► interstellar medium, and the surfaces of interstellar molecular clouds exposed to the interstellar radiation field and to intense

radiation from nearby OB stars. Note that in the following article we use the standard astronomical notation of square brackets (e.g., [CII]) indicating "forbidden" transitions, that is, transitions from a metastable state. Likewise, the ionization state of an atom is indicated by a Roman numeral, so that I indicates the neutral atom, II is once ionized, and so on (e.g., HII for ionized hydrogen).

Overview

The FUV range of energies is responsible for dissociating molecules and dominates the heating process in photodissociation regions (PDRs). The upper bound of this range is the energy required to ionize hydrogen, and thus PDRs are neutral hydrogen regions (in contrast, astronomers refer to plasmas of electrons and ionized hydrogen as ▶ HII regions). The FUV field is often measured in units of the Draine (Draine 1978) interstellar radiation field, equal to ∼1.7 times the Habing (Habing 1968) local interstellar FUV field (1.6×10^{-3} erg cm^{-2} s^{-1} or $\sim 10^{8}$ photons cm^{-2} s^{-1}). A common notation is that G_0 is the radiation field in units of the Habing field, and field strengths that are typically encountered range between $G_0 \sim 1.7$ for the interstellar field and $G_0 \sim 10^5$ for the Orion nebular PDR.

PDRs are found where FUV radiation from OB stars or the general interstellar radiation field shines on molecular clouds. The FUV radiation can affect the chemistry for visual extinctions up to $A_V \sim 8$ by maintaining in atomic form that oxygen that is not tied up in CO. The relation between extinction and hydrogen nucleus ▶ column density is $N = 1.9 \times 10^{21} A_V/Z'$ cm^{-2} where Z' is the dust abundance relative to the abundance in the local galaxy. The mean extinction in giant ▶ molecular clouds is also $A_V \sim 8$ (Solomon et al. 1987), so much of the mass in molecular gas is in PDRs. PDRs are also found in the diffuse medium in cold ($T \sim 100$ K) and warm ($T \sim 8{,}000$ K) neutral hydrogen clouds (see ▶ Interstellar Medium). The same physics that applies in the molecular cloud surfaces (Kaufman et al. 2006; Abel et al. 2005; Le Petit et al. 2006) also applies in the diffuse atomic interstellar medium (Wolfire et al. 2003; Shaw et al. 2006; Wolfire et al. 2008) but with weaker FUV field ($G_0 \sim 1$–10) and lower hydrogen nucleus column densities ($N \sim 10^{19}$–10^{21} cm^{-2}). PDRs are also present in the neutral interstellar medium in starburst galaxies (Kaufman et al. 1999) and in galaxies with active galactic nuclei (Meijerink et al. 2007).

Structure

A PDR can be divided into various chemical regimes as a function of ▶ optical depth from the cloud surface (Sternberg and Dalgarno 1995). In the outer portions, the gas is mainly neutral atomic H, He, O, and C^+ (see Fig. 1, where ISRF is the interstellar radiation field and transition regions are indicated in color). Incident FUV radiation is absorbed by dust and large carbon molecules – ▶ polycyclic aromatic hydrocarbons (PAHs) – and mostly results in excitation of PAHs and grain heating. However, as much as 0.1–1 % of the absorbed FUV is converted to energetic photoelectrons that are ejected from PAHs and grains and heat the gas. The gas generally attains a higher temperature ($T \sim 100$–$5{,}000$ K) than the grains ($T \sim 10$–50 K) because of the much less effective cooling of the gas (predominantly via [CII] 158 μm and [OI] 63 μm ▶ line emission) relative to the dust continuum cooling. On the surfaces of molecular clouds, the warm gas leads to intense emission of the [CII] 158 μm line and the [OI] 63 and 145 μm lines, as well as infrared (IR) dust continuum and near-infrared emission features (at 3.3, 6.2, 7.7, 8.6, and 11.3 μm) believed to arise from PAHs. Additional diagnostic line emission is provided by [SiII] 35 μm and [FeII] 26 μm (Si^+ and Fe^+), which can be used to estimate elemental abundances (Kaufman et al. 2006).

At extinctions $A_V > 1$ atomic hydrogen is converted to molecular hydrogen on grain surfaces and molecular H_2 vibrational transitions are produced. The grain photoelectric heating

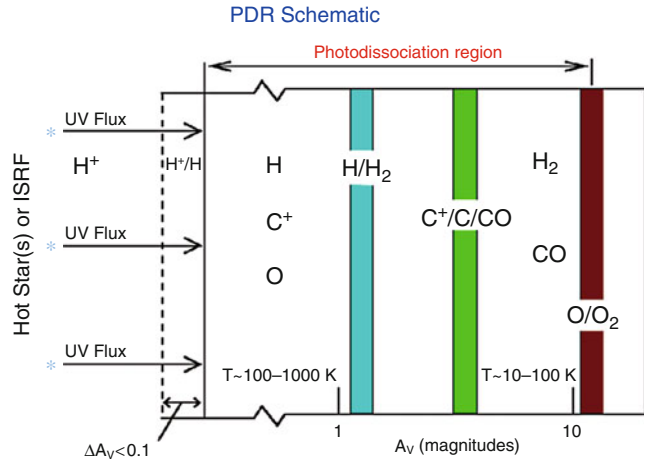

Photodissociation Region, Fig. 1 Typical structure of PDR chemical zones as a function of extinction A_V into a cloud illuminated by an FUV radiation field

process still dominates, balanced by C^+ and O^0 fine-structure line cooling. In this region, the gas is mainly H_2, but the carbon is in the form of C^+ and not CO. Since CO is often used as a tracer of molecular gas, this regime has been called "dark gas" (i.e., no CO emission; Grenier et al. 2005; Wolfire et al. 2010; this has nothing to do with dark matter or dark energy). The dark gas may increase the molecular mass of galactic clouds by ~30 % relative to estimates based on the CO emission alone and could increase the molecular mass by a factor of ~30 in low-metallicity (low abundance of elements heavier than helium) galaxies such as the Small Magellanic Cloud (Leroy et al. 2007). Deeper in PDRs ($A_V > 2$–3), the transition of C^+ to C to CO occurs, and the CO rotational and [CI] 370 and 609 μm lines originate. In the deepest layers, grain photoelectric heating or cosmic-ray heating dominates depending on the strength of the incident field, balanced by cooling from rotational transitions of CO. The chemistry of oxygen and carbon not locked in CO is affected by the FUV radiation to cloud depths of $A_V \sim 5$–10.

Heating

Detailed investigations of the grain photoelectric heating process have been presented by Bakes and Tielens (1994) and Weingartner and Draine (2001). An FUV photon is absorbed by a dust grain that can eject a hot electron into the gas. The electron kinetic energy is a function of the accumulated charge on the grain since the electron must overcome the Coulomb barrier of the accumulated charges. The grain charge is found by balancing the ▶ photoionization rate with the recombination rate. The calculated heating efficiency from Bakes and Tielens (1994) is shown in Fig. 2.

Figure 2 shows that as grains become positively charged and hence the electron density n_e in the gas increases, the heating efficiency drops. For typical conditions in the neutral diffuse ISM (Wolfire et al. 2003) ($G_0 \sim 1.7$, $n_e/n \sim 1.6 \times 10^{-4}$, $n \sim 30$ cm^{-3}, $T \sim 85$ K, where n is the hydrogen nucleus volume density; i.e., n includes both atomic and molecular hydrogen), grains are mainly neutral, and the photoelectric heating efficiency is near maximum. In contrast, for the photodissociation region in Orion (Tielens and Hollenbach 1985b) ($n \sim 2 \times 10^5$ cm^{-3}, $G_0 \sim 1 \times 10^5$, and $T \sim 550$ K), grains are highly charged, and the heating efficiency is a factor of 10 lower.

Note, however, that the efficiency shown in Fig. 2 is integrated over the grain size distribution from large grains, ~0.1 μm, to large molecules, ~5 Å, with a distribution in radius $n(a) \propto a^{-3.5}$. Bakes and Tielens (1994) found that ~1/2 of the heating comes from the smallest grain sizes. The efficient heating from small grains is mainly for two reasons. First, the yield increases as the grain

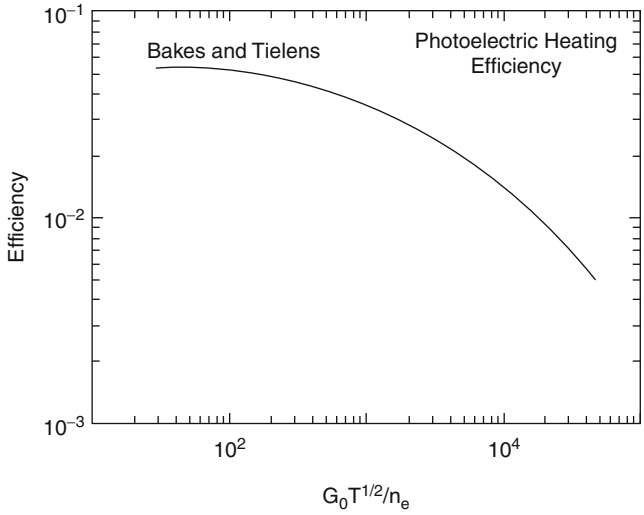

Photodissociation Region, Fig. 2 Grain photoelectric heating efficiency from Bakes and Tielens (1994), where T is temperature, n_e is electron density and G_0 measures the radiation field (see text)

size decreases. The yield is the fraction of electrons that reach the grain surface that are ejected from the grain. In a large grain, the electron energy is lost to infrared continuum radiation, but in a small grain, a greater fraction can reach the surface to be ejected.

Second, the ionization-to-recombination ratio is proportional to a^2 so that larger grains become charged and their heating efficiency drops. The smallest population of grains is almost certainly PAHs (polycyclic aromatic hydrocarbons; Allamandola et al. 1985; Leger and Puget 1984). The simplest PAH is benzene with six carbon atoms in a ring; larger PAHs are composed of multiple rings.

In addition to photoelectric heating from grains, various other heating processes could contribute depending on the incident field strength and depth into the cloud. At large ▶ optical depth, heating from cosmic-ray ionization could become important. The primary ionization rate per hydrogen nucleus is approximately $\zeta_{xp} \sim 1.8 \times 10^{-17}$ s^{-1} with each ionization producing a primary electron of mean energy 35 eV. The primary electrons can produce secondary ionizations, molecular dissociation, atomic and molecular excitation, or gas heating, with yields depending on the electron and molecular abundances (Dalgarno et al. 1999). Additional heating processes at large optical depth may include IR dust continuum pumping of [OI] 63 μm followed by collisional de-excitation and gas-dust interactions (Tielens and Hollenbach 1985a).

At small ▶ optical depth, the heating is dominated by grain photoelectric heating, while photoionization of CI and photodissociation of H_2 contributes about 1 % to the heating (Tielens and Hollenbach 1985a).

Cooling

At $A_V < 3$, the gas cools mainly by collisional excitation by H and H_2 of fine-structure transitions, followed by radiative de-excitation. Dominant cooling lines include [CII] 158 μm, [OI] 63 μm, and [CI] 610 μm. Along with the cooling transitions, weaker lines can be used as diagnostics of the gas density, temperature, and incident FUV fields. These include [OI] 145 μm, [CI] 370 μm, [SiII] 35 μm, [FeII] 26 μm, and the H_2 rotational transitions 0–0 S(0) 28 μm, 0–0 S(1) 17 μm, and 0–0 S(2) 12 μm. Deeper into the cloud, CO rotational transitions dominate the gas cooling.

Chemistry

Formation and Destruction of H_2

In steady state, photodissociation of molecular hydrogen is balanced by formation on dust grains. An H_2 molecule in the ground state can

absorb an FUV photon ($\lambda < 1{,}108$ Å) and be excited to the first or second electronic level. About 10 % of the pumped molecules de-excite to the vibrational continuum thereby dissociating the molecule. The remainder land in bound excited states resulting in a UV emission line and an IR vibrational cascade. PDR computational codes have been constructed including detailed H_2 models that account for self-shielding in individual pumping lines as well as the infrared line emission produced in the fluorescent cascade (Draine and Bertoldi 1996; Sternberg and Dalgarno 1989; Black and van Dishoeck 1987). For $G_0/n < 0.025$, H_2 self-shielding dominates over dust shielding, and the H/H_2 transition is drawn to the cloud surface (Burton et al. 1990).

Formation and Destruction of CO

The formation of CO follows that of H_2 and OH as one goes deeper into the cloud. In the gas phase, the formation of OH is initiated by the cosmic-ray ionization of H_2 (van Dishoeck and Black 1986; see also ▶ Interstellar Chemical Processes). Reactions with H_2 and O lead to

$$H_2^+ + H_2 \rightarrow H_3^+$$

$$H_3^+ + O \rightarrow OH^+$$

$$OH^+ + H_2 \rightarrow H_2O^+$$

$$H_2O^+ + H_2 \rightarrow H_3O^+$$

Dissociative recombination of H_3O^+ leads directly to OH or to H_2O (which is then photodissociated to form OH).

Hollenbach et al. (2009) has suggested that for typical cosmic-ray ionization rates, formation of OH on grain surfaces can exceed the gas phase production. In this case, the OH abundance is determined by equating the formation of OH on grain surfaces

$$O + \text{Grain} \rightarrow OH$$

to the FUV photodissociation of OH

$$OH + h\nu \rightarrow O + H$$

where hν represents a photon.

Once OH is formed, the chemistry proceeds as follows (van Dishoeck and Black 1988):

$$OH + C^+ \rightarrow CO^+ + H$$

$$CO^+ + H_2 \rightarrow HCO^+ + H$$

$$HCO^+ + e \rightarrow CO + H$$

$$CO + h\nu \rightarrow C + O$$

The first reaction dominates the formation of CO^+; the second reaction dominates the destruction of CO^+ and the formation of HCO^+; the third reaction dominates the destruction of HCO^+ and the formation of CO; the last reaction dominates the destruction of CO. As a result, every CO^+ that is formed by the first reaction results in a formation of a CO by the third reaction. The H_2 absorption lines in the FUV overlap with several of the CO dissociating transitions, and thus the H_2 can shield the CO at larger optical depth. The shielding factor is tabulated for a range of H_2 and CO columns in Visser et al. (2009). An expression for the depth at which the CO ($J = 1$–0) line becomes optically thick, N(CO) $\sim 2 \times 10^{16}$ cm^{-2}, is given by Wolfire et al. (2010).

Since the heating rates and the depth to the transition regions depend on G_0/n, we expect regions with the same ratio of G_0/n to have similar structure.

Electron Abundance

The electron abundance is important in setting the grain photoelectric heating rate and in setting the abundance of various atomic and molecular ions that are neutralized or destroyed by recombination. At low Av (<2–3), electrons are mainly provided by the photoionization of C to C^+ and by photoionization of He by soft X-rays. Essentially, all the C is in the form of C^+ yielding an electron abundance $n_e/n \sim n_{C+}/n \sim 1.6 \times 10^{-4}$, the

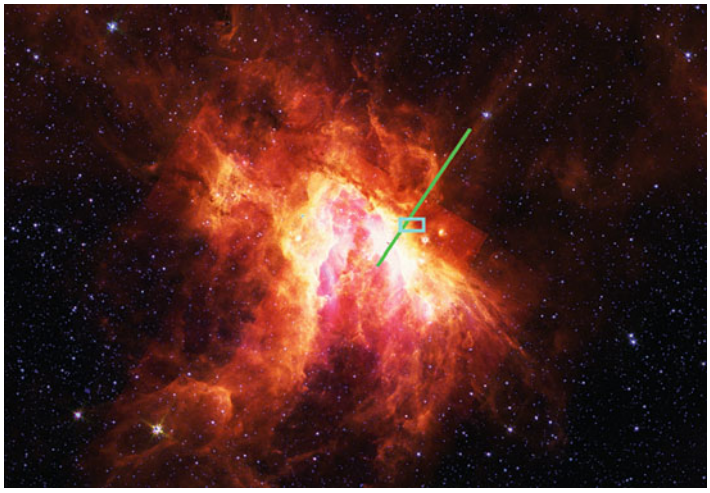

Photodissociation Region, Fig. 3 Spitzer IRAC observations of the M17 HII region and PDR. The *green line* is about 10 arcmin in length and crosses the M17SW PDR, and shows the direction of the [CII] strip map shown in Fig. 4. The *box* shows the location of the Spitzer IRS spectrum shown in Fig. 5

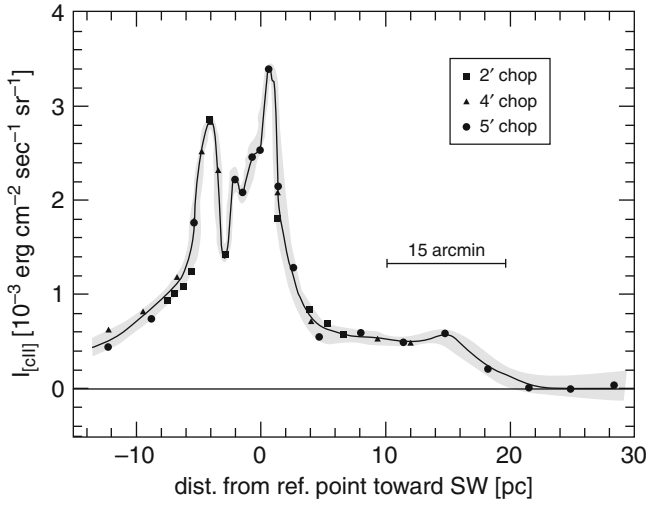

Photodissociation Region, Fig. 4 Strip map of [CII] 158 μm emission in M17SW PDR from Stutzki et al. (1988)

value of the gas phase carbon abundance in the ▶ interstellar medium (Sofia et al. 2004). The charge exchange of metal cations with PAH^- can effectively compete with gas phase recombination, and the inclusion of PAHs in the chemical network can significantly decrease the optical depth to the C^+/C transition and increase the neutral abundances of species such as C^0, Si^0, Mg^0, Fe^0, and S^0 (Wolfire et al. 2008; Bakes and Tielens 1998). Deeper into the cloud, electrons are provided mainly by cosmic-ray ionization of H and He.

Model Example

A sample model calculation is presented in Wolfire et al. (2010).

Observations

The bright HII region M17 and associated PDR are shown in Fig. 3. The image is taken with the Spitzer IRAC instrument and is dominated by PAH emission. The PAH emission lies between the ionized gas at the center and molecular gas to the upper left and right. Shown in Fig. 4 is a strip map in [CII] 158 μm emission taken along the

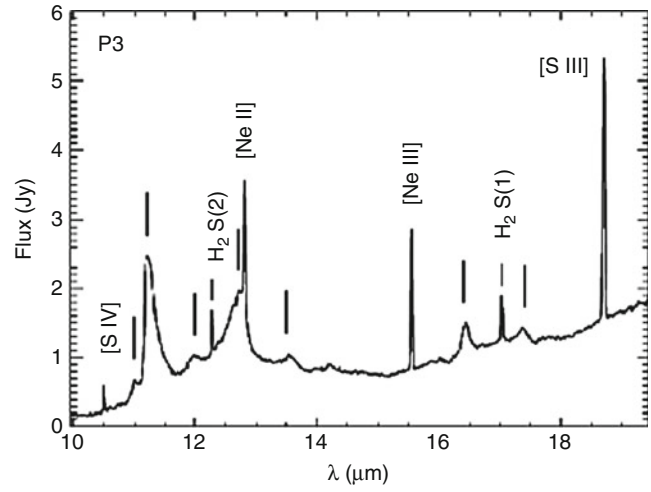

Photodissociation Region, Fig. 5 Spitzer IRS observations of the PDR M17SW showing flux versus wavelength, from Povich et al. (2007). *Vertical solid lines* show the location of the PAH features

line shown in Fig. 3. The [CII] line emission peaks at the PDR but also seems to have a tail of emission in the molecular gas, perhaps indicating FUV penetration in a clumpy medium. We also show in Fig. 5 a Spitzer IRS spectrum near the ionized/neutral interface showing bright PAH emission but also H_2 pure rotational lines and fine-structure lines from ionized gas.

Future Directions

The basic PDR model seems to provide good fits to many observations, especially for bright PDRs. There are, however, a few emerging problems in which more detailed modeling is required or laboratory measurements are needed to constrain the theory.

Turbulence

We know that atomic and molecular clouds are turbulent with a log-normal probability density distribution (Goodman et al. 2009; Vazquez-Semadeni 1994). The chemical rates are proportional to the gas density squared, and thus the rates can be quite different in the extreme densities. In general, the dynamic time to transport molecular material out of the cloud interior to the atomic surface, or to transport atomic material from the surface inward, is longer than the chemical equilibrium times (Wolfire et al. 2010), but there are cases for low G_0 or strong H_2 self-shielding when the time-dependent chemistry can be important (Glover and Mac Low 2007). An additional problem is that the FUV penetration depends on column density that can be different in the high-density and low-density regions. Some initial work has been done to investigate turbulent PDRs, but much more can be done in the areas of time-dependent chemistry, turbulent structure, and line emission.

XDRs

Another type of region that is of increasing importance is called an XDR (Meijerink et al. 2007), in which hard X-ray radiation ($h\nu > 1$ keV) dominates the heating and chemistry. The most luminous XDRs are associated with black holes in galactic nuclei in which the X-ray emission penetrates the surrounding molecular clouds. XDRs are expected to have large hydrogen nucleus column densities ($N > 10^{22}$ cm^{-2}) and high volume densities ($n > 10^5$ cm^{-3}), and we expect to see highly excited molecules such as CO with rotational transitions up to $J = 30$–29 (~87 μm; Spaans and Meijerink 2008). Spectrometers on board Herschel and the aircraft SOFIA will open new spectral windows in order to observe the highly excited molecular gas in XDRs.

See Also

- ▶ Column Density
- ▶ Extinction, Interstellar or Atmospheric
- ▶ Herschel, William
- ▶ HII Region
- ▶ Interstellar Dust
- ▶ Molecular Cloud
- ▶ Optical Depth
- ▶ Photodissociation
- ▶ Photoionization
- ▶ Polycyclic Aromatic Hydrocarbon
- ▶ Turbulence, Interstellar

References and Further Reading

Abel NP, Ferland GJ, Shaw G, van Hoof PAM (2005) The H II region/PDR connection: self-consistent calculations of physical conditions in star-forming regions. Astrophys J Suppl 161:65

Abgrall H et al (1992) Photodissociation of H2 and the H/H2 transition in interstellar clouds. Astron Astrophys 253:525

Allamandola LJ, Tielens AGGM, Barker JR (1985) Polycyclic aromatic hydrocarbons and the unidentified infrared emission bands – auto exhaust along the Milky Way. Astrophys J 290:L25

Bakes ELO, Tielens AGGM (1994) The photoelectric heating mechanism for very small graphitic grains and polycyclic aromatic hydrocarbons. Astrophys J 427:822

Bakes ELO, Tielens AGGM (1998) The effects of polycyclic aromatic hydrocarbons on the chemistry of photodissociation regions. Astrophys J 499:258

Black JH, van Dishoeck EF (1987) Fluorescent excitation of interstellar H2. Astrophys J 322:412

Burton MG, Hollenbach DJ, Tielens AGGM (1990) Line emission from clumpy photodissociation regions. Astrophys J 365:620

Dalgarno A, Yan M, Liu W (1999) Electron energy deposition in a gas mixture of atomic and molecular hydrogen and helium. Astrophys J Suppl 125:237

Draine BT (1978) Photoelectric heating of interstellar gas. Astrophys J Suppl 36:595

Draine BT, Bertoldi F (1996) Structure of stationary photodissociation fronts. Astrophys J 468:269

Dubernet ML, Gargaund M, McCarroll R (1992) Reaction rates of C(+) with OH at low interstellar temperatures. Astron Astrophys 259:373

Glover SCO, Mac Low M-M (2007) Simulating the formation of molecular clouds. II. Rapid formation from turbulent initial conditions. Astrophys J 659:1317

Goodman AA, Pineda JE, Schnee SL (2009) The "true" column density distribution in star-forming molecular clouds. Astrophys J 692:91

Grenier IA, Casandjian J-M, Terrier R (2005) Unveiling extensive clouds of dark gas in the solar neighborhood. Science 307:1292

Habing HJ (1968) The interstellar radiation density between 912 A and 2400 A. Bull Astron Inst Neth 19:421

Hollenbach D, Kaufman MJ, Bergin EA, Melnick GJ (2009) Water, O_2, and ice in molecular clouds. Astrophys J 690:1497

Kaufman MJ, Wolfire MG, Hollenbach DJ, Luhman ML (1999) Far-infrared and submillimeter emission from galactic and extragalactic photodissociation regions. Astrophys J 527:795

Kaufman MJ, Wolfire MG, Hollenbach DJ (2006) [Si II], [Fe II], [C II], and H_2 emission from massive star-forming regions. Astrophys J 644:283

Le Petit F, Nehmé C, Le Bourlot J, Roueff E (2006) A model for atomic and molecular interstellar gas: the meudon PDR code. Astrophys J Suppl 164:506

Leger A, Puget JL (1984) Identification of the 'unidentified' IR emission features of interstellar dust? Astron Astrophys 137:L5

Leroy A et al (2007) The spitzer survey of the small magellanic cloud: far-infrared emission and cold gas in the small magellanic cloud. Astrophys J 658:1027

Meijerink R, Spaans M, Israel FP (2007) Diagnostics of irradiated dense gas in galaxy muclei. II. A grid of XDR and PDR models. Astron Astrophys 461:793

Povich MS et al (2007) A multiwavelength study of M17: the spectral energy distribution and PAH emission morphology of a massive star formation region. Astrophys J 660:346

Shaw G, Ferland GJ, Srianand R, Abel NP (2006) Physical conditions in the interstellar medium toward HD 185418. Astrophys J 639:941

Sofia UJ et al (2004) Interstellar carbon in translucent sight lines. Astrophys J 605:272

Solomon PM, Rivolo AR, Barrett J, Yahil A (1987) Mass, luminosity, and line width relations of galactic molecular clouds. Astrophys J 319:730

Spaans M, Meijerink R (2008) On the detection of high-redshift black holes with ALMA through CO and H_2 emission. Astrophys J 678:L5

Sternberg A, Dalgarno A (1989) The infrared response of molecular budrogen gas to ultraviolet radiation – high-density regions. Astrophys J 338:197

Sternberg A, Dalgarno A (1995) Chemistry in dense photon-dominated regions. Astrophys J Suppl 99:565

Stutzki J et al (1988) Submillimeter and far-infrared line observations of M17 SW – a clumpy molecular cloud penetrated by ultraviolet radiation. Astrophys J 322:379

Tielens AGGM, Hollenbach D (1985a) Photodissociation regions. I. Basic model. Astrophys J 291:722

Tielens AGGM, Hollenbach D (1985b) Photodissociation regions. II. A model for the Orion photodissociation region. Astrophys J 291:747

van Dishoeck EF, Black JH (1986) Comprehensive models of diffuse interstellar clouds – physical

conditions and molecular abundances. Astrophys J Suppl 62:109
van Dishoeck EF, Black JH (1988) The photodissociation and chemistry of interstellar CO. Astrophys J 334:771
Vazquez-Semadeni E (1994) Hierarchical structure in nearly pressureless flows as a consequence of self-similar statistics. Astrophys J 423:681
Visser R, van Dishoeck EF, Black JH (2009) The photodissociation and chemistry of CO isotopologues: applications to interstellar clouds and circumstellar disks. Astron Astrophys 503:323
Weingartner JC, Draine BT (2001) Photoelectric emission from interstellar dust: grain charging and gas heating. Astrophys J Suppl 134:263
Wolfire MG, McKee CF, Hollenbach D, Tielens AGGM (2003) Neutral atomic phases of the interstellar medium in the galaxy. Astrophys J 587:278
Wolfire MG, Tielens AGGM, Hollenbach D, Kaufman MJ (2008) Chemical rates on small grains PAHs: C+ recombination and H_2 formation. Astrophys J 680:384
Wolfire MG, Hollenbach DJ, McKee CF (2010) The dark molecular gas. Astrophys J 716:1191

Photoevaporation

► Photodesorption

Photoevaporation of Protoplanetary Disks

Steven B. Charnley
Solar System Exploration Division, Code 691, Astrochemistry Laboratory, NASA Goddard Space Flight Center, Greenbelt, MD, USA

Definition

The physical process in which radiation from a young ► protostar causes the removal of gas from its circumstellar disk is called photoevaporation. Energetic stellar radiation, comprising mainly extreme ultraviolet (EUV; wavelengths from 121 nm down to 10 nm) and far ultraviolet (FUV; 200–122 nm) photons and X-rays, heats the surface layers of the gaseous disk, producing thermal pressure gradients that permit the gas to escape the gravitational potential of the disk in an expanding ► hydrodynamic flow.

See Also

► Protostars

Photoionization

Steven B. Charnley
Solar System Exploration Division, Code 691, Astrochemistry Laboratory, NASA Goddard Space Flight Center, Greenbelt, MD, USA

Definition

Photoionization is the chemical process in which absorption of a photon by a neutral molecule produces a positive ion (cation) and a free electron.

Photolysis

Steven B. Charnley
Solar System Exploration Division, Code 691, Astrochemistry Laboratory, NASA Goddard Space Flight Center, Greenbelt, MD, USA

Synonyms

Photodissociation

Definition

Photolysis is a chemical reaction in which a chemical compound is broken down (dissociated) by the absorption of electromagnetic radiation (photons).

See Also

- ▶ Interstellar Chemical Processes
- ▶ Photodissociation Region

Photon

Daniel Rouan
LESIA, Observatoire Paris-Site de Meudon, Meudon, France

Definition

A photon is an elementary particle that is the basic unit (quantum) of light and of all other forms of ▶ electromagnetic radiation. The photon has no rest mass and no charge and by definition travels at the speed of light. It is characterized by very few parameters: its energy and its polarization state. Its energy E is directly related to the frequency ν of the electromagnetic wave it is associated with, through the relation $E = h\nu$, where h is the Planck constant.

As regards fundamental interactions, the photon is the quantum of the electromagnetic field. This means that it mediates the interaction between charged particles, that is, the electromagnetic force.

Photons belong to the broad family of bosons, which are described as the carriers of the various fundamental interactions and are a necessary consequence of physical laws having particular symmetries at every point in space-time. Because it is made of bosons, a collection of photons can present very specific properties, one of the best known being the laser or ▶ maser effect.

Photons exhibit wave-particle duality. In other words, they exhibit properties of both waves and particles. For example, a single photon follows the same path as the optical beam and can be refracted or reflected just as the electromagnetic waves which are solutions of Maxwell's equations, but it can also act as a particle, for instance, when extracting an electron from a metal (photoelectric effect).

See Also

- ▶ Electromagnetic Radiation
- ▶ Electromagnetic Spectrum

Photon Dominated Region

- ▶ Photodissociation Region

Photosphere

Daniel Rouan
LESIA, Observatoire Paris-Site de Meudon, Meudon, France

Definition

The photosphere corresponds to the apparent visible surface of a star and especially of the Sun. It is a very thin shell where most of the light a star radiates is produced. Its thickness is less than one thousandth of the star's radius. Its temperature, which is typically between 3,000 and 40,000 K, is one of the fundamental parameters characterizing a stellar type.

See Also

- ▶ Effective Temperature
- ▶ Hertzsprung-Russell Diagram
- ▶ Star

Photosputtering

- ▶ Photodesorption

Photosynthesis

Francisco Montero
Department of Biochemistry and Molecular Biology I, Facultad de Ciencias Químicas, Universidad Complutense de Madrid, Madrid, Spain

Keywords

Photobiology; Photosynthetic antennae; Photosynthetic generation of protonmotive force; Photosynthetic pigments; Reaction center

Definition

Photosynthesis is the metabolic process by means of which organisms capture light in order to carry out an ▶ endergonic synthesis of organic molecules. In a general sense, photosynthesis can be considered as the primary event in the process of converting the energy associated to photons into a gradient of electrochemical potential of protons across some biological membranes, that is to say, into a ▶ protonmotive force.

Overview

Although initially photosynthesis was used to describe the events by means of which the energy of visible light was transduced in the synthesis of sugars from carbonic anhydride in plants and cyanobacteria, the phenomenon is more general, and in all the cases the primary events are not associated with such a synthesis, but with the translocation of protons across biological membranes as the thylakoid membrane of the chloroplast in plants or the cytoplasmic membrane in photosynthetic bacteria. The different photosynthetic mechanisms can be classified into three classes:

1. Direct coupling between absorption of photons and translocation of protons, the simplest mechanism of phototransduction. One example is bacteriorhodopsin, a family of monomeric membrane proteins with a prosthetic group (retinal) that suffers a conformational change as a consequence of the absorption of light. This causes a change in the pK of several residues of the protein amino acids, leading to the exclusion of protons and then to the origination of a protonmotive force. The reentry of protons through the ▶ ATP synthase yields ATP. In 1971, bacteriorhodopsin from halophilic archaea was shown to function as a light-driven ▶ proton pump. In 2000, a new type of rhodopsins, proteorhodopsins, was found in marine bacteria. These proteins are present in most of the phototrophic microorganisms living in ocean surface waters.
2. Cyclic ▶ electron transport. This is the case of many purple bacteria as *Rhodobacter sphaeroides* (see Fig. 1a). A dimmer of bacteriochlorophyll whose maximum of absorption is at 870 nm (P_{870}) absorbs electromagnetic radiation and, in its excited state, has a very negative ▶ redox potential. As a consequence, an electron from the dimmer can be transferred to another spatial closed molecule, as bacteriopheophytin. Eventually, the electron comes back to the dimmer of bacteriochlorophyll through a non-hemo Fe and a ubiquinone (UQ) molecule. In the transport of electrons, a bc_1 complex, similar to complex III in the respiratory chain, is also implicated. As a consequence of this cyclic electron transport, a net exclusion of protons from the cytoplasm of the bacteria takes place, and a protonmotive force is generated. In this kind of photosynthesis, no direct reducing power is produced. In order to get this, a reverse transport of electrons coupled with the reentry of protons is needed. Moreover, the reentry of protons drives the synthesis of ATP by means of an ATP synthase. A main conclusion of these facts is the universality of mechanisms of the transduction processes in bioenergetics and a closely related evolutionary history of these mechanisms.
3. Noncyclic electron transport. In these systems electrons flow from an initial donor to a final

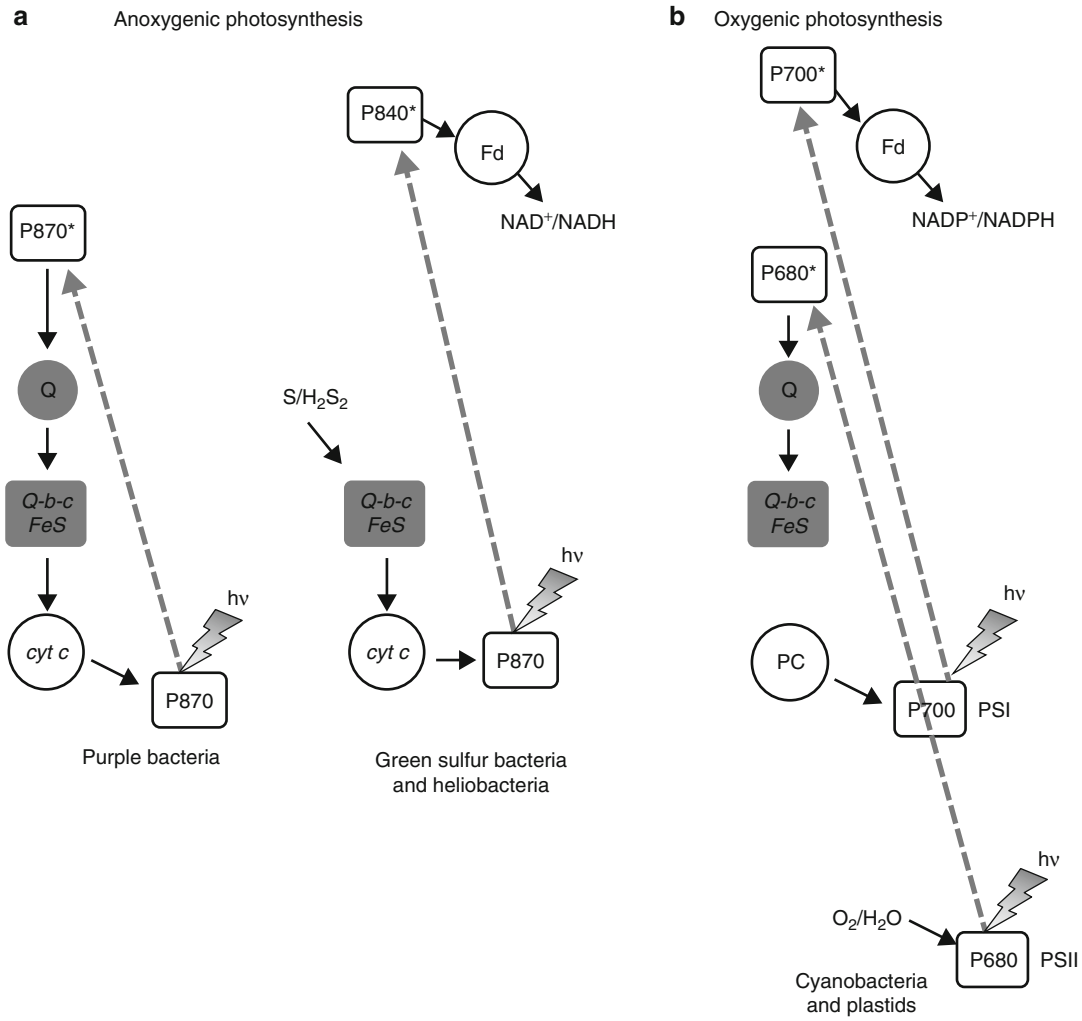

Photosynthesis, Fig. 1 Examples of anoxygenic and oxygenic photosynthetic electron transport chains. (**a**) In purple bacteria (*left*) and green sulfur bacteria and heliobacteria (*right*), only one photosystem is operative. After excitation by photons, the bacteriochlorophyll of the reaction center (P870 or P840) releases an electron to a cyclic (*left*) or a linear (right) transport chain. In the second case, an external electron donor (usually H_2S) reestablishes the fundamental state in P840. (**b**) In cyanobacteria and plastids, two photosystems act in series allowing the transport of electrons from water to $NADP^+$. The position of the different components is approximate to their reduction potential. *Arrows* indicate electron transfer and *broken arrows*, excitation by photons; *boxes* indicate the bacteriochlorophyll (or the chlorophyll) of the reaction centers; *gray boxes* indicate a multimeric electron transport complex; *circles* indicate small electron carriers; *gray circles* indicate the quinone pool. *PS I* photosystem I, *PS II* photosystem II, *cyt* cytochrome, *Fd* ferredoxin, *PC* plastocyanin

acceptor, eventually producing reduction power, usually NAD(P)H. In plants and cyanobacteria, the initial donor of electrons is a water molecule (see Fig. 1b). The water-splitting reaction (water photolysis) as a consequence of the absorption of electromagnetic radiation is one of the most intriguing mechanisms in the biosphere. The releasing of molecular oxygen as a consequence of water oxidation (i.e., ▶ oxygenic photosynthesis) has had a dramatic effect on the evolution of the chemical composition of the Earth atmosphere, from an early anoxic planet to the current oxygen-rich atmosphere. A molecule

of chlorophyll (named as P_{680}) in the excited state reaches a very negative oxidoreduction potential, leading one electron to a molecule of pheophytin, resulting in a chlorophyll with a positive charge. The pair chl^+/chl has a very positive redox potential (~+1,200 mV), being able to accept one electron from the water molecules. All these processes take place in the named Photosystem II, a purple bacteria-like photosynthetic center. On the other hand, other chlorophyll (P_{700}), integrated in the Photosystem I (green sulfur bacteria-like photosynthetic center), in its excited state as a consequence of absorption of light, releases one electron that through a successive transport across different molecules, including ferredoxin, eventually reduces a molecule of $NADP^+$. The P_{700}^+ so produced captures the electron originated in the Photosystem II, which is transported sequentially through plastoquinones, *bf* complex (very similar in molecular organization to complex III in mitochondria), and plastocyanin. The main contribution to the protonmotrive force is originated in the *bf* complex. Thus, in these organisms, two different photosystems are working in series.

While in cyanobacteria the photosynthetic systems are localized in the cytoplasmic membrane, in plants all the processes take place in the chloroplast, in a highly organized internal membrane named thylakoid. As a consequence of the photosynthetic processes, protons are released to the interior of the thylakoid generating the protonmotive force, and by means of an ATP synthase, the transit of the internal protons to the stroma (space between the external membrane of the chloroplast and the thylakoid) yields ATP. Both the ATP so produced and the NADPH resulting from the noncyclic transport of electrons are necessary for the fixation of the carbonic dioxide and its conversion in different metabolites. These processes classically, and incorrectly, have been known as *light-independent reactions*.

Other microorganisms, as green sulfur bacteria and heliobacteria, also show a noncyclic electron transfer in their photosystems (Fig. 1a). However, there are two main differences with respect to the photosynthetic chains of cyanobacteria (and chloroplasts): they posses only one photosystem, and the initial electron donor usually is hydrogen sulfide instead of water. Oxygen is not a by-product of these photosynthetic chains, hence the name of anoxygenic photosynthesis. The organization of the photosystems of green sulfur bacteria is closely related to Photosystem I of cyanobacteria and chloroplasts. In the same way, Photosystem II is related to photosystems of purple bacteria.

Although the mechanism described above takes place in the reaction centers, the excitation of these centers does not occur by a direct absorption of light by such centers, but by the transfer of the excitation from other molecules grouped in complexes known as antennae, and is composed of many molecules of chlorophylls and carotenoids. Except haloarchaea, all the other photosynthetic systems have antennae. The existence of these complexes of antennae has several advantages. On one hand, the turnover time of the photosynthetic center is about 100 s^{-1}, whereas the capacity of absorption of light for this center, even under very bright sunlight, is only one ▶ photon every second. This means that without other source of excitation, the photosynthetic center will be for most of the time not working. Antennae supplies continuously excitation to the reaction center, and so the kinetic impediment mentioned above is overcome. On the other hand, the molecule components of the reaction center only absorb radiation of certain ▶ wavelength, usually near the red. That means that photons with less wavelength would be discarded. The existence of the antennae avoids this problem, harvesting photons of lower wavelength and transferring the excitation to the reaction center by means of several mechanisms, mainly by resonance and by excitons. The structural organization of the antennae around the reaction center is very precise in order to get the optimization of the excitation transfer processes.

Regarding the origin and evolution of photosynthetic electron transport chains, several models have been proposed. Since oxygenic photosynthesis is the main source of molecular

oxygen known, the study of the changes in atmospheric composition throughout the geological time is a key evidence to date the origin of Photosystem II, most probably by molecular evolution from an ancestral form similar to purple bacteria photosystems. In any case, the origin of the water-oxidizing ability remains obscure. Some authors propose that the two photosystem chains arose by fusion of gene repertoires from anoxygenic photosynthetic bacteria and the late emergence of a water-splitting enzyme. On the other hand, others postulate the existence of an ancestral cyanobacteria-like microorganism encoding both photosystem types and with the ability of expressing them differentially. This model postulates the loss of the switching ability or one or the other photosystem to explain the origin of the oxygenic or the anoxygenic photosynthesis, respectively.

Basic Methodology

Spectroscopic techniques, mainly absorption and fluorescence spectra, have been one of the main methodologies in the study of photosynthetic mechanisms. For example, a loss of absorbance (bleaching) at a certain wavelength indicates the loss of an electron of a molecule absorbing at this wavelength. On the other hand, fluorescence has been a very useful technique for evaluating the order of the transmission of the excitation as well as the kinetic details of the processes.

Details about the chain of reaction involved in the transfer of electrons have been obtained by using similar techniques as those used for the respiratory chains, for example, using some specific inhibitors of the electron transport complexes.

The structural determination of photosynthetic systems, mainly through X-ray diffraction, has been decisive in order to know precisely the mechanism of the different events that take place in the photosystems. Unfortunately, many of them have a very large size, and the preparation of crystals is difficult. At present, only a few reaction centers and antennae of some bacteria are known at atomic resolution.

Key Research Findings

- The influence of light in the consume of CO_2 and in the liberation of O_2 by the plant was first described by Jean Senebier in 1796.
- In the middle of the twentieth century, Cornelius Bernardus van Niel demonstrated that photosynthesis is a light-dependent redox reaction. In this reaction an oxidable compound (not necessarily water) reduces CO_2 to yield sugars.
- The existence of two photosynthetic systems working in parallel was derived from the so-called *red drop* or Emerson effect. This author studied the evolution of O_2 by algae illuminated at different wavelengths. In the range from 400 to 680 nm, O_2 evolved very effectively, but at higher wavelength, the production of O_2 decreased sharply, but this production was reestablished if the system was illuminating with a non-saturating light at 650 nm.
- Determination of the structure of the reaction center of photosystems, as well as of the antennae, by X-ray diffraction. The seminal works were developed on purple bacteria photosystems by several authors (Johann Deisenhofer, Robert Huber, and Hartmut Michel).

Applications

- Artificial photosynthesis
- Agriculture and the new challenges for photosynthesis research

Future Directions

- Structural determination at atomic resolution of reaction centers and antennae systems of cyanobacteria and plants. Although some details of this are known, further studies are necessary in order to understand completely the mechanisms of actuation.
- Artificial photosynthesis. This tries to merge some aspects of photosynthesis, as the conversion of sunlight, water, and CO_2 into sugars and O_2, or to produce a protonmotive force, by using artificial membranes.

See Also

- ▶ Anoxygenic Photosynthesis
- ▶ ATP Synthase
- ▶ Bioenergetics
- ▶ Electron Transport
- ▶ Endergonic
- ▶ Oxidizing Atmosphere
- ▶ Oxygenation of the Earth's Atmosphere
- ▶ Photoautotroph
- ▶ Photobiology
- ▶ Photochemistry
- ▶ Photosynthesis, Oxygenic
- ▶ Photosynthetic Pigments
- ▶ Phototroph
- ▶ Proton Motive Force
- ▶ Proton Pump
- ▶ Redox Potential
- ▶ Wavelength

References and Further Reading

Allen JF, Martin W (2007) Evolutionary biology: out of thin air. Nature 445:610–612
Bryant DA, Frigaard NU (2006) Prokaryotic photosynthesis and phototrophy illuminated. Trends Microbiol 14:488–496
Codgell RS, Isaac NW, Oward TD, McLuskey K, Fraser NJ, Prince SM (1999) How photosynthetic bacteria harvest solar energy. J Bacteriol 181:3869–3879
Heathcote P, Fyfe PK, Jones MR (2002) Reaction centers: the structure and evolution of solar power. Trends Biochem Sci 27:79–87
Heinnickel M, Golbeck JH (2007) Heliobacterial photosynthesis. Photosynth Res 92:35–53
Kiang NY, Siefert J, Govindjee BRE (2007a) Spectral signatures of photosynthesis. I. Review of earth organisms. Astrobiology 7:222–251
Kiang NY, Segura A, Tinetti G, Govindjee BRE, Cohen M, Siefert J, Crisp D, Meadows VS (2007b) Spectral signatures of photosynthesis. II. Coevolution with other stars and the atmosphere on extrasolar worlds. Astrobiology 7:252–274
Long SP, Zhu XG, Naidu SL, Donald R (2006) Can improvement in photosynthesis increase crop yields? Plant Cell Environ 29:315–330
Murchie EH, Pinto M, Horton P (2009) Agriculture and the new challenges for photosynthesis research. New Phytol 181:532–552
Nicholls DG, Ferguson SJ (2001) Photosynthetic generators of protonmotive force, in Bioenergetics 3. Academic, London
Pennazio S (2008) Photosynthesis: the years of light. Riv Biol 101:443–462
Peterhansel C, Niessen M, Kebeish RM (2008) Metabolic engineering towards the enhancement of photosynthesis. Photochem Photobiol 84:1317–1323
Renger G, Kuhn P (2007) Reaction pattern and mechanism of light induced oxidative water splitting in photosynthesis. Biochim Biophys Acta 1767:458–471
Schlodder E (2009) Introduction to optical methods in photosynthesis. Photosynth Res 101:93–104
Stephan E, Giovanni F, Francis-André W (2008) The dynamics of photosynthesis. Annu Rev Genet 42:463–515
Vacha F, Bumba L, Kaftan D, Vacha M (2005) Microscopy and single molecule detection in photosynthesis. Micron 6:483–502
van Brederode ME, Jones MR (2000) Reaction centres of purple bacteria. Subcell Biochem 35:621–676
Xion J, Bauer CE (2002) Complex evolution of photosynthesis. Annu Rev Plant Biol 53:503–521
Xiong J (2006) Photosynthesis: what color was its origin? Genome Biol 206:1465–6914

Photosynthesis, Oxygenic

Juli Peretó
Institut Cavanilles de Biodiversitat i Biologia Evolutiva, Universitat de València, València, Spain

Definition

Oxygenic photosynthesis is a noncyclic photosynthetic electron chain where the initial electron donor is water and, as a consequence, molecular oxygen is liberated as a by-product. The use of water as an ▶ electron donor requires a photosynthetic apparatus with two reaction centers. It is present in ▶ cyanobacteria and its evolutionary related eukaryotic organelles, the ▶ chloroplast. Oxygenic ▶ photosynthesis was responsible for the transformation of the Earth's primitive anoxygenic atmosphere to one with molecular oxygen.

See Also

- ▶ Chlorophylls
- ▶ Chloroplast
- ▶ Cyanobacteria
- ▶ Electron Donor
- ▶ Photosynthesis

Photosynthetic Eukaryotes

► Algae

Photosynthetic Organism

► Photoautotroph
► Phototroph

Photosynthetic Pigments

Francisco Montero
Department of Biochemistry and Molecular Biology I, Facultad de Ciencias Químicas, Universidad Complutense de Madrid, Madrid, Spain

Keywords

Carotenoids; Chlorophyll; Photosynthesis

Synonyms

Pigment molecules

Definition

Photosynthetic pigments are the molecules responsible for absorbing electromagnetic radiation, for transferring the energy of the absorbed photons to the reaction center, and for photochemical conversion in the photosynthetic systems of organisms capable of photosynthesis.

Overview

Photosynthetic pigments derive their name from the fact they can absorb visible light (from Lat. pi(n)g(ere) – to paint + ment(um)). The molecules of photosynthetic pigments are quite ubiquitous and are always composed of chlorophylls and carotenoids. Chlorophylls consist of a porphyrin ring, which is bounded to an ion Mg^{2+}, attached to a phytol chain. Chlorophylls form part of reaction centers – where the photochemical conversion takes place – and antennas, or light-harvesting complexes, i.e., collectors of electromagnetic radiation, whereas carotenoids are found only in the antennas. Both types of molecules are found in "quasi-crystalline" structures in photosynthetic systems, associated with protein molecules that form part of biological membranes, either the cytoplasmic membranes of photosynthetic bacteria or thylakoid membranes inside plant chloroplasts. Chlorophylls found in bacteria are called bacteriochlorophylls. Photosynthetic systems also contain another pigment, pheophytin (bacteriopheophytin in bacteria), which plays a crucial role in the transfer of electrons in photosynthetic systems. Moreover, other pigments can be found in particular photosynthetic systems, such as xanthophylls in plants.

The oxidation-reduction potential of reaction center chlorophylls in an excited state as a consequence of the absorption of a photon can become very negative, which promotes the transfer of electrons to neighboring molecules, usually pheophytins. This is the primary photochemical reaction that takes place in reaction centers.

There is one class of pigment that exists only in halobacteria, called bacteriorhodopsin. It is composed of a protein attached to a retinal prosthetic group, which is responsible for the absorption of light photons, leading to a conformational change in the protein, which results in the expulsion of the protons from the cell.

See Also

► Bacteriochlorophyll
► Chlorophylls
► Chloroplast
► Photochemistry
► Photosynthesis

References and Further Reading

Cogdell RJ, Isaac NW, Howard TD, McLuskey K, Fraser NJ, Prince SM (1999) How photosynthetic bacteria harvest solar energy. J Bacteriol 181:3869–3879

Speer BR (1997) Photosynthetic pigments. In: UCMP Glossary (online). University of California, Berkeley Museum of Paleontology. (http://www.ucmp.berkeley.edu/glossary/gloss3/pigments.html). Accessed 12 Mar 2007

Phototroph

Juli Peretó
Institut Cavanilles de Biodiversitat i Biologia Evolutiva, Universitat de València, València, Spain

Synonyms

Photosynthetic organism

Definition

Phototroph is an organism that can use visible light as a primary ▶ energy source for metabolism, a process known as ▶ photosynthesis. Phototrophs contrast with ▶ chemotrophs, which obtain energy from the oxidation of organic compounds. Most phototrophs are autotrophs, also known as photoautotrophs, making use of the energy obtained from photosynthesis to assimilate carbon dioxide (CO_2). Photoheterotrophs produce ATP using solar energy, but their source of carbon for biosynthesis is reduced organic compounds. From an ecological point of view, it has been considered that life on Earth is dependent on photoautotrophy, although the recent discovery of submarine strict chemolithoautotrophs is challenging this concept. Phototrophic organisms contain pigments that allow the use of light as an energy source.

See Also

- ▶ Anoxygenic Photosynthesis
- ▶ Bioenergetics
- ▶ Carbon Dioxide
- ▶ Chemotroph
- ▶ Chlorophylls
- ▶ Chloroplast
- ▶ Cyanobacteria
- ▶ Energy
- ▶ Energy Conservation
- ▶ Halophile
- ▶ Photosynthesis
- ▶ Photosynthesis, Oxygenic

Phyllosilicates, Extraterrestrial

Daniela Tirsch
German Aerospace Center DLR, Institute of Planetary Research, Berlin, Germany

Keywords

Hydrated minerals; Mars

Synonyms

Clay minerals; Micas; Sheet silica

Definition

Term for hydrated minerals that consist of parallel sheets of silicate SiO_4 tetrahedra.

Overview

Phyllosilicates are usually built as alteration products of olivine- or magnesium-rich ▶ rocks, often associated with hydrothermal weathering. They can also result from the transformation of primary ▶ minerals (e.g., feldspar). Their

formation is controlled by bedrock composition, climate factors (temperature, pH-value, accessibility of liquid ▶ water), topography, time, and kinetics of mineral reaction. During the weathering process, OH groups are incorporated into the crystal lattice, leading to the hydration of these minerals. Thus, their existence is an indicator for the long-term availability of liquid water at the time of mineralization. Depending on their tetrahedral structure, phyllosilicates are grouped in dual- and triple-layer phyllosilicates. The silicate sheets are interleaved with layers of other elements. A typical characteristic of clay minerals, which constitute a subgroup of phyllosilicates, is their ability to expand and shrink in response to the reversible adsorption of water molecules.

Extraterrestrial phyllosilicates do not differ from terrestrial ones except for the abundance of individual mineral types. Typical phyllosilicates found on ▶ Mars are, for example, ▶ kaolinite ($Al_2Si_2O_5(OH)_4$), smectite (e.g., montmorillonite ($(Na, Ca)_{0.33}(Al, Mg)_2(Si_4O_{10})(OH)_2 \cdot nH_2O$)), and chlorite (e.g., chamosite ($(Fe^{2+}, Mg, Fe^{3+})_5Al(Si_3Al)O_{10}(OH, O)_8$)). The bulk of the Martian phyllosilicates were probably built in a nonacidic aqueous alteration regime in ▶ Noachian times, which has been proposed to be termed the phyllosian period (Bibring et al. 2006). The various formation hypotheses include sedimentation and aqueous alteration in fluvial channels and standing bodies of water (e.g., Story et al. 2010), impact-induced hydrothermalism (e.g., Schwenzer and Kring 2009; Marzo et al. 2010), subsurface alteration by hydrothermal groundwater circulation (Ehlmann et al. 2011), and pedogenesis (e.g., Le Deit et al. 2012).

See Also

- ▶ Carbonate, Extraterrestrial
- ▶ Mars
- ▶ Mineral
- ▶ Noachian
- ▶ Rock
- ▶ Sulfates, Extraterrestrial
- ▶ Water

References and Further Reading

Anthony JW, Bideaux RA, Bladh KW, Nichols MC (1995) Handbook of mineralogy, vol 2(1). Mineral Data Publishing, Tucson

Bibring J-P, Langevin Y, Gendrin A, Gondet B, Poulet F, Berthé M, Soufflot A, Arvidson R, Mangold N, Mustard J, Drossart P, The OMEGA Team (2006) Global mineralogical and aqueous mars history derived from OMEGA/Mars express data. Science 312:400–404

Deer WA, Howie RA, Zussman J (1992) An introduction to the rock-forming minerals, 2nd edn. Longman Group UK Limited, Essex

Ehlmann BL, Mustard JF, Murchie SL, Bibring J-P, Meunier A, Fraeman AA, Langevin Y (2011) Subsurface water and clay mineral formation during the early history of Mars. Nature 479:53–60

http://www.handbookofmineralogy.com

Le Deit L, Flahaut J, Quantin C, Hauber E, Mège D, Bourgeois O, Gurgurewicz J, Massé M, Jaumann R (2012) Extensive surface pedogenic alteration of the Martian Noachian crust suggested by plateau phyllosilicates around Valles Marineris. J Geophysic Res Planets 117(E3), doi:10.1029/2011je003983

Marzo GA, Davila AF, Tornabende LL, Dohm JM, Fairén AG, Gross C, Kneissl T, Bishop JL, Roush TL, McKay CP (2010) Evidence for Hesperian impact-induced hydrothermalism on Mars. Icarus 208:667–683

Poulet F, Bibring JP, Mustard JF, Gendrin A, Mangold N, Langevin Y, Arvidson RE, Gondet B, Gomez C (2005) Phyllosilicates on Mars and implications for early Martian climate. Nature 438:623–627

Schwenzer SP, Kring DA (2009) Impact-generated hydrothermal systems capable of forming phyllosilicates on Noachian Mars. Geology 37:1091–1094

Story S, Bowen BB, Benison KC, Schulze DG (2010) Authigenic phyllosilicates in modern acid saline lake sediments and implications for Mars. J Geophys Res 115(E12012), doi:10.1029/2010JE003687

P

Phylogenetic Tree

David Moreira
Unité d'Ecologie, Systématique et Evolution
CNRS UMR8079, Université Paris-Sud 11,
Paris, Orsay Cedex, France

Keywords

Chronogram; Cladogram; Homology; Phylogram

Synonyms

Evolutionary tree; Tree of life; Universal tree of life

Definition

Phylogenetic trees, often called evolutionary trees, are tree-like diagrams depicting the evolutionary relationships among organisms or other entities (such as gene sequences) that derive from a ▶ common ancestor. Phylogenetic trees are usually drawn as bifurcating diagrams, so that technically they can be defined as noncircular connected graphs. They are composed of nodes and branches (or edges). Both branches and nodes can be internal or external. An internal node corresponds to the last common ancestor of all branches and nodes arising from it (therefore, internal nodes are also called ancestral nodes). External or terminal nodes, also called leaves, represent the entities from which the tree was inferred. Phylogenetic trees can be rooted or unrooted (Fig. 1). In general, rooting a tree requires the use of an outgroup organism or sequence, which allows constructing directed or polarized trees (i.e., trees in which the order of changes occurring in the species or sequences can be inferred).

Overview

Phylogenetic trees are inferred using different kinds of information, in particular morphological and molecular characters. The aim of these trees is to provide an accurate representation of the evolutionary relationship between organisms or sequences using the evolutionary information contained in the characters. This information can be treated using different methods (such as distance, maximum parsimony, and maximum likelihood ones) to estimate the degree of relatedness of the units (e.g., organisms or sequences) for which the phylogenetic tree is constructed. Once the tree is constructed, it can be represented in different ways, which include: (1) cladograms, which only represent the branching pattern without drawing branch lengths proportional to the divergence between organisms or sequences; (2) phylograms, which show branch lengths proportional to the divergence (number of changes in the characters used) between organisms or sequences; and (3) chronograms, which have branch lengths that are proportional to the time of divergence between organisms or sequences. In addition, all these representations can be rooted or unrooted. Rooted phylogenetic trees are directed or polarized trees containing a node that corresponds to the most recent ancestor of all the leaves of the tree. This node is usually identified by using an outgroup, namely, an organism or sequence (or a set of them)

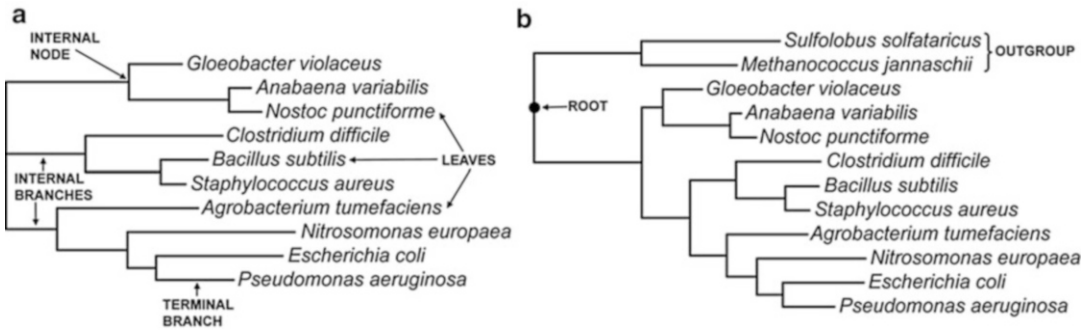

Phylogenetic Tree, Fig. 1 Phylogenetic tree of bacterial species based on ribosomal RNA sequence comparison. (**a**) Unrooted tree showing different elements of the tree; (**b**) the same tree but rooted using two sequences of archaeal species as outgroup

that is known not to be part of the group for which the phylogenetic tree is constructed (i.e., the ingroup) but that have characters that are homologous to those used for the tree construction. Rooting the tree allows inferring the order of emergence of the different branches in the tree, as well as the order of evolutionary change in the states of the characters used to construct the tree. In contrast, unrooted trees do not specify the ancestry but just provide information about the relatedness among the branches.

The universal tree of life, also known as "the tree of life," depicts the phylogenetic relationships among all living beings. It can be reconstructed using markers that are present in all species. The most famous version of the tree of life is based on the analysis of small subunit ribosomal RNA sequences which led to the classification of living beings into the three domains of life: Bacteria, Archaea, and Eucarya.

See Also

- ▶ Common Ancestor
- ▶ Domain (Taxonomy)
- ▶ Evolution, Biological
- ▶ Homology
- ▶ Last Common Ancestor
- ▶ Phylogeny
- ▶ Prokaryote
- ▶ Sequence

References and Further Reading

Brinkmann H, Philippe H (2005) The universal tree of life: from simple to complex or from complex to simple. In: Gargaud M, Barbier B, Martin H, Reisse J (eds) Lectures in astrobiology, series: advances in astrobiology and biogeophysics, vol II. Springer, Berlin, pp 617–656

Felsenstein J (2004) Inferring phylogenies. Sinauer Associates, Sunderland

Phylogenetics

- ▶ Phylogeny

Phylogeny

David Moreira
Unité d'Ecologie, Systématique et Evolution
CNRS UMR8079, Université Paris-Sud 11,
Paris, Orsay Cedex, France

Keywords

Distance methods; Homology; Maximum likelihood; Maximum parsimony

Synonyms

Phylogenetics

Definition

Phylogeny concerns the study of the evolutionary relationships among organisms or among ▶ sequences of biological macromolecules (DNA, RNA, or proteins) using information from morphological, structural, developmental, or molecular markers (the latter commonly called molecular phylogeny). Phylogeny implies that the organisms or sequences analyzed derive from a ▶ common ancestor (i.e., the common descent principle) and that evolution proceeds through a branching process. This means that species evolve and separate into different branches or disappear (extinction). The representation of this process can be done using ▶ phylogenetic trees. Phylogeny has become the basis of modern ▶ taxonomy, commonly called "phylogenetic systematics," so that the different taxa should represent monophyletic groups inferred by phylogenetic analysis.

Overview

Phylogenetic analysis is based on the comparison of characters found in the different entities (e.g., species or gene sequences) for which a

phylogenetic tree is constructed. An essential requisite for a proper phylogenetic reconstruction is that those characters have to be homologous (namely, to have been inherited from a common ancestor) and they have to be variable. This means that they can exist in different forms, which are called character states (e.g., the four nucleotides A, T, C, and G for a site in a DNA sequence or the different morphologies of organisms). The information (called "phylogenetic signal") that is analyzed by the phylogenetic approach is contained in the particular configuration of states of the characters examined. These characters are compared among the different organisms or sequences in order to estimate their degree of relatedness, which can be measured in different ways (see the section "Basic Methodology" below).

Basic Methodology

The simplest method of phylogenetic inference is the ▶ phenetic approach based on the construction of distance matrices based on overall similarity between the entities studied compared two by two (the simplest distance is the p-distance or the number of characters with different character states divided by the total number of characters, and it can be expressed as a percentage of similarity). More sophisticated methods include maximum parsimony, maximum likelihood, and Bayesian inference. These are called discrete data methods because they examine each character separately and look for the phylogenetic tree that best accommodates the corresponding information. Maximum parsimony, a method inspired by the cladistic approach, is intended to find the phylogenetic tree that minimizes the number of changes required to explain the distribution of character states found in the set of organisms or sequences studied. Maximum likelihood and Bayesian inference require a model of character evolution (or substitution model), that is, a series of rules about the probabilities of change from a given character state to the other possible states. Using this kind of models, maximum likelihood estimates the probability for each character of the distribution of character states found in the set of organisms or sequences studied and tries to find the phylogenetic tree with maximum global probability for the entire set of characters analyzed. Bayesian inference has a similar basis, but it also evaluates the probability of the character data set for a given phylogenetic tree.

Distance methods are much faster than discrete data methods but they are much less informative: Their outcome is only a phylogenetic tree whereas the other methods also provide information about the evolution of the different characters along the tree. The only way to assure that the best phylogenetic tree has been found using the discrete data methods is to test all the possible trees to choose the most parsimonious or the most likely one. However, this is possible in practice only for data sets containing a very small amount of species or sequences. In fact, for a data set of size 10, there are 2,027,025 possible different bifurcating trees, and the number is of $\sim 2 \times 10^{20}$ different trees for 20 species. The latter are impossible to treat in a reasonable time using the complex parsimony or likelihood calculations. Therefore, different techniques of non-exhaustive exploration, called heuristic search methods, have been developed to search the tree space of all possible trees. Nevertheless, they do not assure retrieving the best tree.

Phylogenetic analysis can be biased by a series of data and methodological problems that have been characterized in the last decades. Stochastic errors arise when all character states have not changed following the same evolutionary pattern. This problem is particularly critical when a small number of characters are used for phylogenetic analysis. Therefore, there is a tendency to utilize as much characters as possible (the "total evidence" approach), though this can induce other types of problems (the systematic biases) which can be exacerbated by the addition of increasing number of characters, especially when they are analyzed using models that do not describe correctly the evolutionary process. Convergent evolution is a well-known source of error that can lead to the inference of incorrect phylogenies. For example, parasitic species often have simple morphologies because they lose organs that are

unnecessary since many functions are provided by their hosts. Therefore, parasites of different evolutionary origins may be artificially grouped together in phylogenies because of their convergent similarity. Molecular phylogeny can also be affected by convergence problems. For example, hyperthermophilic prokaryotes tend to have ribosomal RNA (rRNA) sequences rich in G and C nucleobases because they are more stable at high temperatures. Phylogenetic trees reconstructed using rRNA sequences analyzed with inadequate models can group hyperthermophiles of different origins just because their sequences may appear to be similar due to their high GC content. This type of compositional bias is a clear example of systematic error in molecular phylogeny because the artefactual result becomes stronger as more and more sequence data are used. This is also the case with fast-evolving species or sequences, which are affected by the so-called long-branch attraction artifact: the tendency to group fast-evolving entities irrespective of their true evolutionary relationships.

Key Research Findings

The findings of the application of phylogenetic analysis to the study of biological evolution and diversity have been numerous and very important, beginning with the recognition during the eighteenth and nineteenth centuries that many animal and plant fossils could be affiliated to groups still existing, or the discovery that contemporary birds are the descendants of an ancient dinosaur ancestor. However, it is thanks to the development of molecular phylogeny based on the analysis of DNA and protein sequences that the most radical changes in our view of biological evolution have been possible. In particular, the first phylogenies based on the comparison of the rRNA gene sequences led to the discovery in the late 1970s that all living beings can be classified into three major groups or domains, Eukaryotes, Bacteria, and Archaea, the latter being unknown to the scientific community until then (Woese and Fox 1977). Molecular phylogeny has also demonstrated the endosymbiotic origin of mitochondria and chloroplasts from bacterial ancestors (alphaproteobacteria and cyanobacteria, respectively), as well as the importance of horizontal or ▶ lateral gene transfer in microbial evolution.

Applications

The applications of phylogenetic analysis are extremely diverse, from very basic to applied ones. It is the tool of choice to address a variety of evolutionary questions, not only the inference of the evolutionary relationships between species but also the evolution of genes (including gene duplications, horizontal gene transfer, etc.) and biogeography. Phylogeny has also a large spectrum of medical applications, including epidemiology studies and forensic medicine.

Future Directions

Phylogeny is a very active field of research in evolutionary biology. Particular effort is now devoted to take advantage of the huge amount of molecular data that are made available by the sequencing of complete genomes or large scale metagenome projects. This has launched a new field called phylogenomics, which is promoting active investigation to improve algorithms and models to cope with very big data sets.

See Also

- ▶ Biodiversity
- ▶ Bioinformatics
- ▶ Common Ancestor
- ▶ Domain (Taxonomy)
- ▶ Evolution, Biological
- ▶ Homology
- ▶ Lateral Gene Transfer
- ▶ Phenetics
- ▶ Phylogenetic Tree
- ▶ Sequence
- ▶ Taxonomy

References and Further Reading

Avise JC (1994) Molecular markers, natural history and evolution. Chapman & Hall, New York
Felsenstein J (2004) Inferring phylogenies. Sinauer Associates, Sunderland
Woese CR, Fox GE (1977) Phylogenetic structure of the prokaryotic domain: the primary kingdoms. Proc Natl Acad Sci U S A 74:5088–5090

Phylotype

David Moreira and Purificación López-García
Unité d'Ecologie, Systématique et Evolution
CNRS UMR8079, Université Paris-Sud 11, Paris, Orsay Cedex, France

Synonyms

Environmental sequence; Operational taxonomic unit; OTU

Definition

In microbiology, a phylotype is an environmental DNA sequence or group of sequences sharing more than an arbitrarily chosen level of similarity of a particular gene marker. The most widely used phylogenetic marker is the small subunit ribosomal RNA gene. Two prokaryotic sequences are generally considered as belonging to the same phylotype when they are more than 97–98 % identical (for eukaryotes, the values generally used are in the 98–99 % nucleotide identity range). In prokaryotic microbiology, phylotypes, often referred to as Operational Taxonomic Units (OTUs), are a proxy for ► species.

See Also

► Phylogeny
► Species
► Taxonomy

Phylum

David Moreira and Purificación López-García
Unité d'Ecologie, Systématique et Evolution
CNRS UMR8079, Université Paris-Sud 11, Paris, Orsay Cedex, France

Synonyms

Division

Definition

Plural, phyla. A phylum is a high-order taxonomic category in the hierarchical biological classification system. Situated below the domain and kingdom levels, it is above the taxonomic level of class. The term Division is used as synonym, particularly in botany. In prokaryotic microbiology, although the term phylum is preferred for taxa including cultivated members, the expression "Candidate Division" is used for clusters of environmental sequences that, phylogenetically, constitute groups equivalent to phyla for described species.

History

The term was coined in 1876 to mean a "division of the plant or animal kingdom" by the French naturalist Georges Dagobert, Baron Cuvier (1769–1832), from the Greek phylon "race, stock," related to phyle "tribe, clan," and phylein "bring forth."

See Also

► Taxonomy

Physical Adsorption

► Physisorption

Physicalism

Physicalism Malaterre
Institut d'Histoire et Philosophie des Sciences et Techniques (IHPST), Université Paris 1-Panthéon Sorbonne, Paris, France

Keywords

Materialism; Metaphysics; Physical theory; Physicalism; Supervenience

Synonyms

Materialism

Definition

Physicalism is the metaphysical thesis that everything is physical. According to this thesis, everything in the world, including chemical, biological, mental, and social entities and processes, is constituted by or results from physical entities and processes. In analytic philosophy, one might say that physicalism is the claim that everything supervenes on, or is necessitated by, the physical.

Overview

Physicalism is sometimes taken as synonymous to "► materialism." Historically though, the word had a different meaning as it used to be associated with a particular linguistic thesis of positivist philosophers of the Vienna Circle. It is now generally understood as a metaphysical claim about the nature of the world emphasizing a connection to physics and the physical sciences (and no longer solely to matter, as was initially the case with "materialism"). According to physicalism then, everything that exists is physical.

As such, this claim blends three types of questions, each of which is controversial on its own: What does it mean to say that *everything* satisfies a given condition? What does it mean for something to say that it satisfies the condition of being *physical*? And, is it *true* that everything is physical?

One answer to the first question is to appeal to the notion of supervenience. Accordingly, "everything is physical" is taken to mean that "everything supervenes on the physical," or, in other words with the language of modal logic, that "no two possible worlds can be identical in their physical properties yet differ in some of their other properties such as their chemical, biological, mental or social properties" (e.g., Davidson 1970; Lewis 1986; Stalnaker 1996).

One way to answer the second question is to link the notion of a physical property to that of a physical theory. Accordingly, a "property is physical" is taken to mean that this property belongs to (or supervenes on) the type of properties that physical theory tells us about (e.g., Smart 1978; Chalmers 1996; Stoljar 2001).

Different answers to both questions are possible as they remain much controversial (as exemplified by the debate about nonreductive physicalism and emergence).

As to the truth question of physicalism, much debate arises in philosophy of mind: in particular, the existence of qualia (i.e., the felt qualities of experience) that would be distinct from the physical is considered as one of the most serious challenges to physicalism (e.g., Chalmers 1996), whereas the argument of the causal closure of the world (i.e., intuitively the idea that every cause is a physical cause) is usually taken as establishing physicalism (e.g., Kim 1993).

See Also

► Chance and Randomness
► Materialism
► Reductionism
► Vitalism

References and Further Reading

Chalmers D (1996) The conscious mind. Oxford University Press, New York

Davidson D (1970) Mental events. In: Davidson D - (ed) Essays on actions and events. Oxford University Press, Oxford, pp 207–223
Kim J (1993) Mind and supervenience. Cambridge University Press, Cambridge
Lewis D (1986) On the plurality of Worlds. Blackwell, Oxford
Smart JJC (1978) The content of physicalism. Philos Q 28:239–41
Stalnaker R (1996) Varieties of supervenience. Philos Perspect 10:221–241
Stoljar D (2001) Two conceptions of the physical. Philos Phenomenol Res 62:253–281

Physisorption

Steven B. Charnley
Solar System Exploration Division, Code 691, Astrochemistry Laboratory, NASA Goddard Space Flight Center, Greenbelt, MD, USA

Synonyms

Physical adsorption

Definition

Physisorption involves van der Waals interactions between an adsorbed atom or molecule and the molecules present in a solid surface, such as that of an interstellar grain. This weak bonding contrasts with the strong, covalent bonding of ▶ chemisorption.

See Also

▶ Chemisorption
▶ Interstellar Dust

pI

▶ Isoelectric Point

Piezophile

Daniel Prieur
Université de Bretagne Occidentale (University of Western Britanny), Brest, France
Institut Universitaire Européen de la Mer (IUEM), Technopôle Brest–Iroise, Plouzané, France

Keywords

Deep biosphere; Deep-sea; Extremophile; Hydrostatic pressure

Synonyms

Barophile

Definition

A piezophile (adjective – piezophilic) is an organism that lives under elevated hydrostatic pressure. While piezotolerant organisms only tolerate high pressures, piezophiles grow better under high pressures, and strict or obligate piezophiles require pressures above atmospheric pressure for growth. Piezophiles are known among vertebrates and invertebrates but prokaryotic piezophiles (Bacteria and ▶ Archaea) are the most extensively studied. They live in various habitats that are exposed to elevated hydrostatic pressure (deep aquifers, deep oil reservoirs, etc.), but the best known are from the deep ocean floor.

Overview

Hydrostatic pressure is a function of the weight of liquid above a given surface. Hydrostatic pressure is expressed in different units: 1 kg cm^{-2} = 1 atm = 1 bar = 0.103 MegaPascal (MPa).

Hydrostatic pressure increases 0.103 MPa every 10 m of water. At the seafloor in the Marianna Trench (10,790 m), hydrostatic pressure is about 110 MPa. Study of piezophilic organisms requires the use of bioreactors that simulate high pressure conditions. After many years of research on this topic, microbiologist A. Yayanos (Scripps Institution of Oceanography, San Diego, USA) concluded that piezophily is a common property for bacteria isolated from cold deep oceans at depths from 1,957 to 10,476 m. He observed that in cold oceans, there is a piezophily threshold at about 1,800–2,000 m, and that piezophily increases with the depth of capture. A. Yayanos was the first to isolate, from a dead amphipod collected at the Marianna Trench, the first strict piezophile, strain MT 41, that grows optimally at 2 °C and 69 MPa, with a generation time of 25 h. This organism was unable to grow at pressures below 39 MPa, and died when exposed at atmospheric pressures. Only known for ▶ psychrophiles for many years, piezophilic organisms have recently been discovered for hyperthermophilic Archaea living at deep-sea hydrothermal vents. D. Prieur's laboratory (University of Brest, France) isolated the archaeon *Pyrococcus yayanosii* strain CH1 from samples collected at 4,100 m from the mid-Atlantic Ridge. This strictly anaerobic organism grows optimally at 95 °C and 52 MPa, with a generation time of 51 min, and requires more than 15 MPa for growth. For bacteria, the cellular membrane and cell wall are involved in mechanisms of adaptation to elevated hydrostatic pressure. When grown at increasing pressures, piezophiles showed an increase in long chain polyunsaturated fatty acids located in the cell membrane. Also, it was found that specific porins located in the outer membrane of Gram-negative organisms were expressed with increasing pressures. Further studies on piezophiles will require the development of innovative techniques, such as diamond anvil cells, that allow microorganisms living under pressure to be imaged and Raman spectroscopy among other techniques to analyze their metabolism.

See Also

- ▶ Black Smoker
- ▶ Deep-Sea Microbiology
- ▶ Deep Subsurface Microbiology
- ▶ Early Archean
- ▶ Extremophiles
- ▶ Hot Vent Microbiology
- ▶ Hydrothermal Vent Origin of Life Models
- ▶ Hyperthermophile
- ▶ Psychrophile

References and Further Reading

Alain K et al (2002) *Marinitoga piezophila* sp. Nov., a rod-shaped, thermo-piezophilic bacterium isolated under high hydrostatic pressure from a deep-sea hydrothermal vent. Int J Syst Evol Microbiol 52:1331–1339

Deming JW, Baross JA (1993) Deep-sea smokers: windows to a subsurface biosphere? Geochim Cosmochim Acta 57:3219–3230

Ishii A et al (2004) Effects of high hydrostatic pressure on bacterial cytoskeleton FtsZ polymers in vivo and in vitro. Microbiology 150:1965–1972

Kato C (1999) Barophiles (piezophiles). In: Horikoshi K, Tsujii K (eds) Extremophiles in deep-sea environments. Springer, Tokyo, pp 91–111

Marteinsson VT et al (1999) *Thermococcus barophilus* sp. Nov., a new barophilic and hyperthermophilic archaeon isolated under high hydrostatic pressure from a deep-sea hydrothermal vent. Int J Syst Bacteriol 49:351–359

Miller JF et al (1988) Pressure and temperature effects on growth and methane production of the extreme thermophile *Mehanococcus jannaschii*. Appl Environ Microbiol 54:3039–3042

Prieur D, Marteinsson VT (1998) Prokaryotes living under elevated hydrostatic pressure. Adv Biochem Eng Biotechnol 61:23–35

Prieur D et al (2010) Piezophilic prokaryotes. In: Sebert P (ed) Comparative high pressure biology. Science, Enfield/Jersey/Plymouth, pp 285–322

Roussel E et al (2008) Extending the sub sea-floor Biosphere. Science 320:1046

Xiang Z et al (2009) Pyrococcus CH1, an obligate piezophilic hyperthermophile isolated from a deep-sea hydrothermal vent. ISME J 1:4

Yayanos AA (1986) Evolutional and ecological implications of the properties of deep-sea barophilic bacteria. Proc Natl Acad Sci U S A 83:9542–9546

Pigment Molecules

► Photosynthetic Pigments

Pilbara

► Pilbara Craton

Pilbara Craton

Martin J. Van Kranendonk
School of Biological, Earth and Environmental Sciences, University of New South Wales, Australia

Keywords

Archean; Greenstone belt; Granite; Australia; Astrobiology sites; Stromatolites

Synonyms

Pilbara

Definition

The Archean Pilbara Craton in northwestern Australia is a nearly circular piece of generally low-grade granite-greenstone crust, whose boundaries are defined by aeromagnetic and gravity anomalies and by flanking Proterozoic orogenic belts. The northern part of the craton is well exposed over an area of 530 × 230 km and is divided into several discrete terranes with distinct geological histories from 3.52 to 3.11 Ga that were stitched together by granites and overlain by late sedimentary basins during accretion and subsequent crustal relaxation from 3.07 to 2.83 Ga. The Pilbara Craton is famous for containing some of the Earth's oldest well-preserved rocks and fossil ► stromatolites and is a location for several astrobiology analogue sites and ► Archean drilling projects (see single entries listed below for a detailed description of those Pilbara's localities of astrobiology interest).

Overview

The Archean Pilbara Craton consists of five terranes, five late-tectonic, dominantly clastic sedimentary basins, a variety of granite suites, and a suite of large layered mafic-ultramafic igneous complexes (Fig. 1: Van Kranendonk et al. 2007). Terranes include the 3.53–3.17 Ga East Pilbara Terrane, representing the ancient nucleus of the craton; the ≥3.18 Ga Kurrana and ≥3.27 Ga Karratha terranes, which have older Nd-model ages and may represent rifted fragments of the ancient nucleus; c. 3.20 Ga Regal Terrane of ► komatiites and basaltic rocks; and juvenile volcanic rocks of the c. 3.12 Ga Sholl Terrane, interpreted as a rifted oceanic arc complex (Smithies et al. 2005).

The East Pilbara Terrane is underlain by the 3.53–3.17 Ga Pilbara Supergroup, which consists of four thick, autochthonous volcano-sedimentary groups deposited on granitic crust up to 3.82 Ga old (Fig. 2). The lower three groups were erupted episodically to 3.24 Ga from melts derived from both fertile mantle and progressively depleted subcontinental mantle, leading to a thick mantle root. The stratigraphically highest Soanesville Group was deposited during rifting of East Pilbara Terrane margins at c. 3.18 Ga, followed by ocean closure at

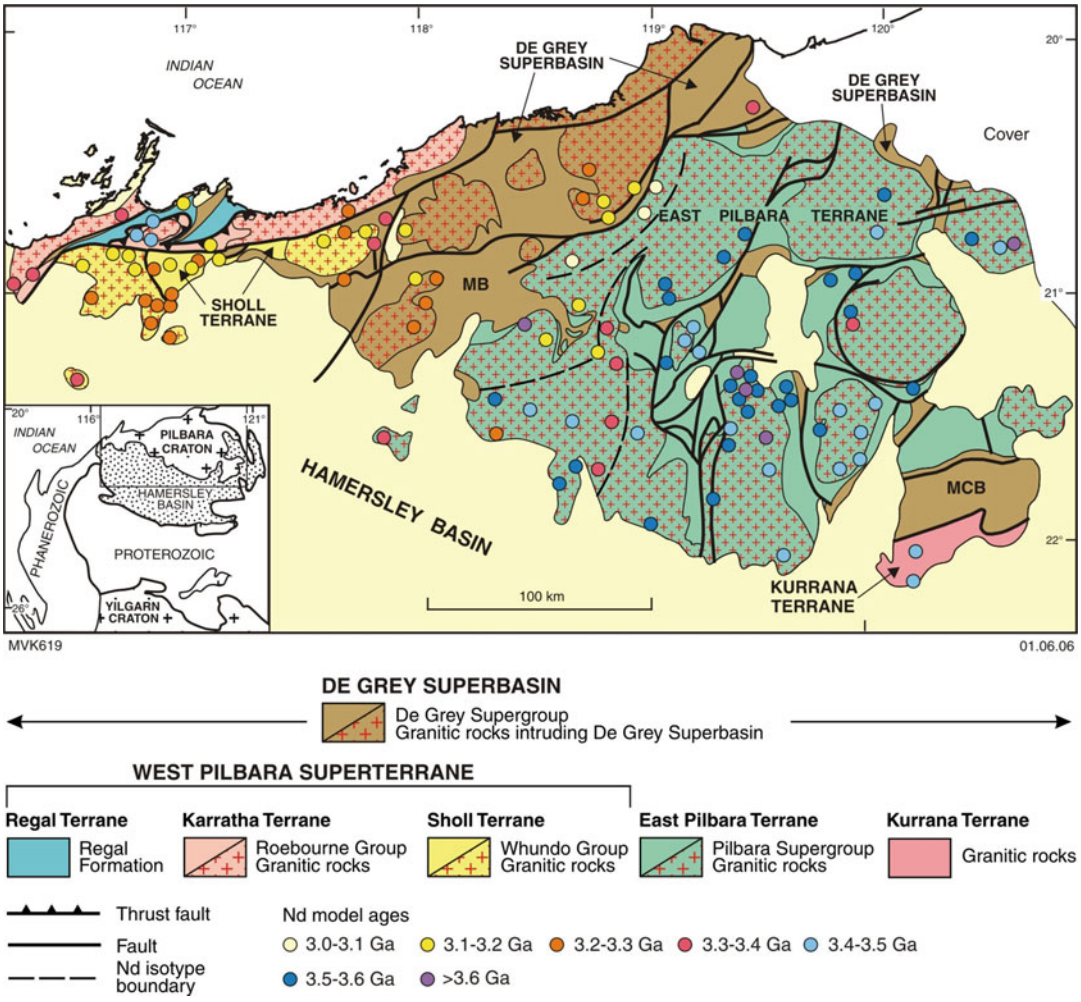

Pilbara Craton, Fig. 1 Simplified geological map of the northern Pilbara Craton, showing the East Pilbara Terrane, West Pilbara Superterrane, Kurrana Terrane, and the distribution of the c. 3.02–2.93 Ga De Grey Supergroup in the Mallina Belt (*MB*), Mosquito Creek Belt (*MCB*), and areas in between. *Colored* or *gray dots* denote whole-rock Nd model ages

3.12 Ga and terrane accretion at 3.07 Ga. Diverse evidence for life is preserved at a variety of levels throughout the supergroup and elsewhere through the craton (Van Kranendonk et al. 2007).

The dominantly coarse clastic De Grey Supergroup was deposited across the whole of the craton during post-orogenic collapse (3.01–2.99 Ga) and subsequent regional orogeny (2.97–2.91 Ga). Major depositional basins include the c. 3.02 Ga Gorge Creek Basin across the whole of the craton, and the 2.97–2.94 Ga Mallina and Mosquito Creek basins (Fig. 1). Lithospheric extension occurred at c. 3.02 Ga and 2.97–2.95 Ga, followed by compressional deformation at 2.94–2.905 Ga during accretion of Kurrana Terrane (Van Kranendonk et al. 2007).

Pilbara Craton,

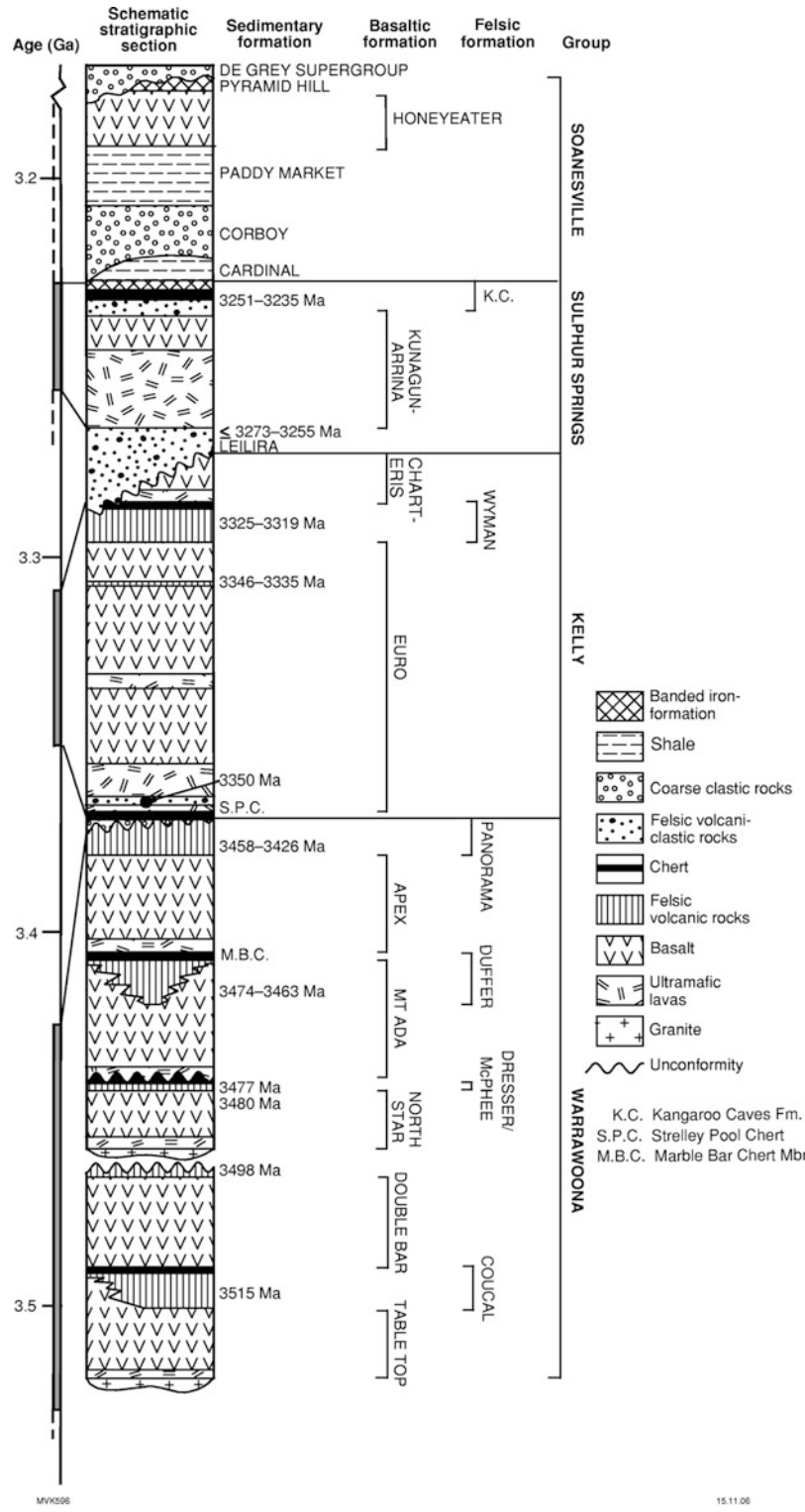

Fig. 2 Simplified stratigraphic column of the Pilbara Supergroup in the East Pilbara Terrane, showing available age dates. Unconformity at the top of the Coonterunah Subgroup is with the base of the Kelly Group. Unconformably overlying, topmost coarse clastic unit represents the De Grey Supergroup in the Lalla Rookh Basin

See Also

- ▶ Apex Basalt, Australia
- ▶ Apex Chert
- ▶ Apex Chert, Microfossils
- ▶ Archean Drilling Projects
- ▶ Archean Tectonics
- ▶ Archean Traces of Life
- ▶ Banded Iron Formation
- ▶ Barberton Greenstone Belt
- ▶ Earth, Formation and Early Evolution
- ▶ Komatiite
- ▶ North Pole Dome (Pilbara, Western Australia)
- ▶ Stromatolites

References and Further Reading

Smithies RH, Champion DC, Van Kranendonk MJ, Howard HM, Hickman AH (2005) Modern-style subduction processes in the Mesoarchaean: geochemical evidence from the 3.12 Ga Whundo intraoceanic arc. Earth Planet Sci Lett 231:221–237

Van Kranendonk MJ, Smithies RH, Bennet V (2007) Earth's oldest rocks, vol 15, Developments in Precambrian geology. Elsevier, Amsterdam, pp 855–896

Pili

Ricardo Amils
Departamento de Biologia Molecular, Universidad Autónoma de Madrid, Madrid, Spain

Definition

Pili are short filamentous structures composed of protein that extend from the surface of the cell. Pili are similar to fimbriae, but in general are longer and only one or a few pili are present on the cell surface. A pilus is typically 6–7 nm in diameter and is primarily composed of oligomeric pilin proteins. Although possibly involved in cell attachment, as are fimbriae, pili are clearly involved in the process of ▶ conjugation. The process of conjugation involves a donor cell, which contains a particular type of ▶ plasmid, a conjugative plasmid, and a receptor cell. Several plasmid genes are involved in the synthesis of sex pili. Only donor cells produce pili. Pili allow specific pairing between the donor cell and the recipient cell. The pili make specific contact with a receptor of the recipient cell and then retract, pulling the two cells together. When the contact between the donor and the recipient cells becomes stable, the plasmidic DNA is then transferred from one cell to the other. Through this mechanism, advantageous genetic traits can be disseminated among a population of bacteria. Not all bacteria have the ability to create sex pili; however, sex pili can interchange genetic information between bacteria of different species.

See Also

- ▶ Conjugation
- ▶ Lateral Gene Transfer
- ▶ Plasmid

Pillars

Vincent Minier and Pascal Tremblin
CEA, Saclay, France

Keywords

HII region; Ionisation; Interstellar medium; Star formation; Comet-tail; Cometary globules

Synonyms

Elephant trunks

Definition

Pillars are elongated structures made of molecular gas and interstellar dust. Observed at the border of

HII regions around massive star clusters, pillars are mainly shaped by the ionization due to the strong UV radiation from the massive stars. Pillars are composed of a head facing the UV radiation, a tail elongated by ionization pressure, and a base where the initial clumpy structure within the parent molecular cloud was hit and transformed.

History

The use of the word "pillars" in astronomy to describe an astronomical feature probably started in 1995. No clear occurrence in scientific paper abstracts (via ADS search) is retrieved before 1996, except for "pillars of cosmology," with the meaning of foundation, or "sun pillar" in a rainbow. *Pillars of Creation* were first mentioned as the title of an image release aiming at publicizing observations of the Hubble space telescope in November 1995. The image exhibits three columns of interstellar matter and the text introduced them as "Undersea corral" "Enchanted castles" "Space serpents" and then "incubators of new stars." The overwhole title of the press release, including images and texts, clearly referred to the scientific paper: *Embryonic stars emerge from interstellar "Eggs."* Seven months later, the scientific publication by Hester et al. (1996) resumed the observations with the title: *Hubble Space Telescope WFPC2 Imaging of M16: Photoevaporation and Emerging Young Stellar Objects*. No mention of the pillars is present in the whole paper. Hester et al. preferred "elephant trunks" and focused the study on the evaporating gas globules (EGGs) at the tip of the trunks. Since, "pillars" or "elephant trunks" were put forward in various publications, from scientific papers to press releases on results from infrared space telescopes like Herschel, Spitzer, or WISE. The suggestive comparison of these elongated ionized gas objects and massive megaliths was studied by Kessler (2006). It was proposed that the Hubble images were produced with a romantic landscape iconography inspired from American painters in late nineteeth century like Thomas Moran and his *Chasm of Colorado*. The *Pillars of Creation* image symbolizes the ambivalent attitude and difficult choice to adopt between disseminating a valuable scientific result and making a pretty picture, the balance between scientific research and art powerful suggestiveness.

Overview

In star-forming regions within giant molecular clouds, the ionizing radiation from OB stars forms elongated gas structures at the interface between the ionized gas (HII region) and molecular clouds. Early examples of such structures can be found in Minkowski (1949) and Frieman (1954). Since, they were named as "comet-tail," "elephant trunk," "speck," "teardrop" and somehow connected to cometary globules. These globules are bubbles of cold gas that are inside the HII region and disconnected from the molecular cloud. Elephant trunks are cometary globules with tails that connect them to the molecular cloud. With the Hubble Space Telescope image of the Eagle Nebula released in 1995, but published in 1996 (M16, Hester et al. 1996), the term "pillar" was introduced to describe the features of a precise structure: a column-like shape and a physical connection to the gas reservoir of the molecular cloud. Note that pillar term was not used in the scientific paper but imposed by the title of an image release. Typical characteristics of the pillars include: a long head-tail structure pointing toward the illuminating source; a bright rim at the edge of the head; a concentration of mass at the head, which might form stars; and a complex velocity structure with rotation with period of 1–7 Myr, helical motion and an intrinsic velocity gradient (e.g., Gahm et al. 2006). Pillars are typically 1–4 pc long and a width between 0.1 and 0.7 pc. Star formation might be observed in the dense head of the pillars (e.g., Sugitani et al. 1989) and can lead to spectacular jets from

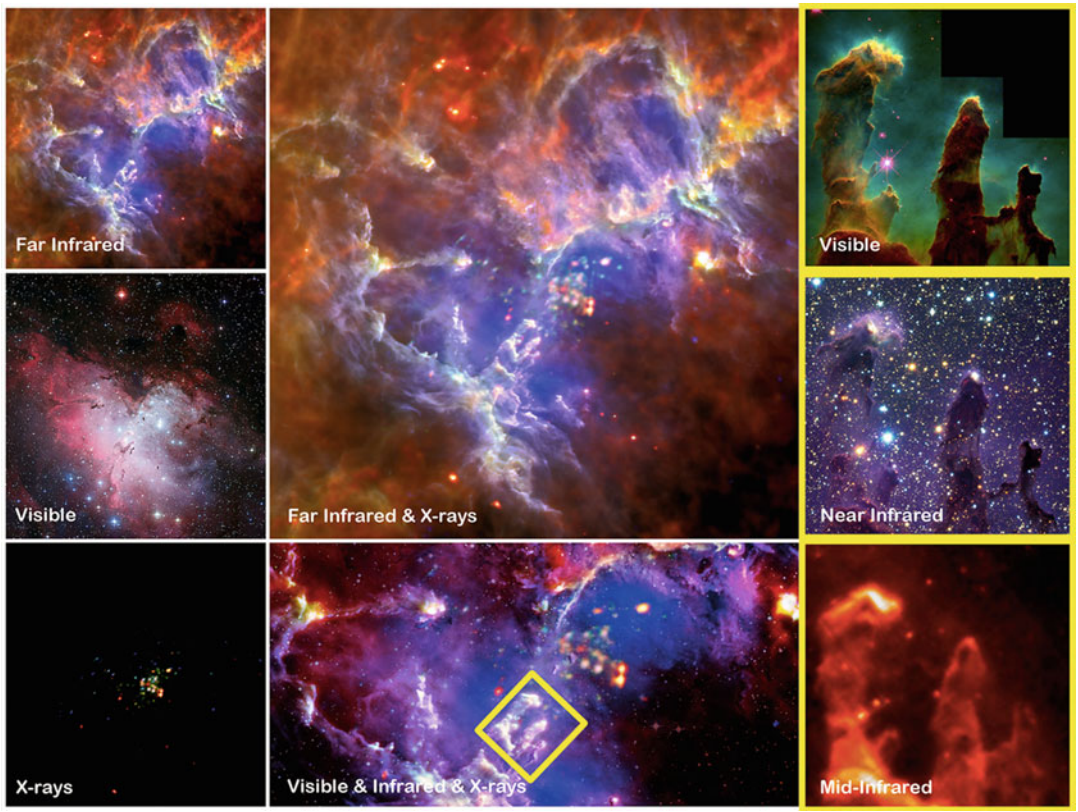

Pillars, Fig. 1 Images showing the Eagle nebula (M16) and its pillars in various wavelengths, from far-infrared to X-rays. The iconic image of the Hubble space telescope is at the top right of this montage, with their image in near and mid-infrared below. The centre images propose a global view of the ionizing massive stars detected in X-rays and the interstellar matter reshaped by ionization observed with Herschel (Credit: ESA, ESO, NASA)

proto-stars escaping of the head (e.g., HH901/902 in the Carina nebula). Despite these signatures, it is often unclear whether the star formation is triggered by ionization in these structures.

Basic Methodology

Infrared observations with the Herschel space observatory and the Spitzer space telescope revealed many more pillars in HII regions where OB stars have already formed, indicating that the UV radiation from massive stars plays a key role in their formation and possibly to stars inside. HII regions can have very complex shapes depending on the distribution of the ionizing sources and the initial structures in the surrounding gas. They range from spherical bubbles (e.g., RCW120, Zavagno et al. 2010), bipolar nebulae (e.g., RCW 36, Minier et al. 2013) to complex and large regions like Cygnus X OB2 and OB9. Dense layers of gas and dust are observed at the interface between the HII regions and their parent molecular clouds (e.g., Thompson et al. 2012; Zavagno et al. 2010). All around the inner shell of HII regions, elongated columns/pillars of gas are observed pointing toward the ionizing sources and usually connected to the molecular cloud

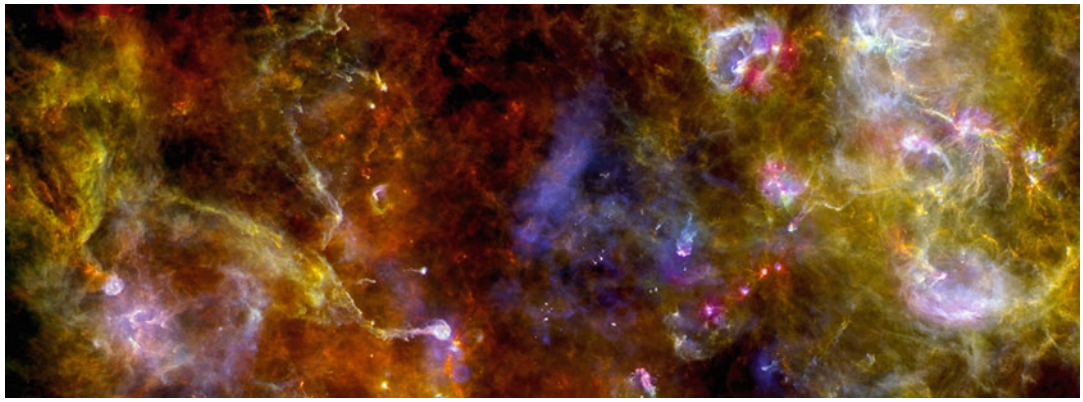

Pillars, Fig. 2 Other examples of pillars observed by Herschel at the interface between molecular clouds and HII regions in Cygnus X. (Credit: ESA/Herschel)

(e.g., M16, Fig. 1). Various scenarios have investigated the physical connection between the formation of these clumpy structures and the appearance of pillars and globules. The collect and collapse scenario (see Elmegreen and Lada 1977) proposed that the shell could become sufficiently dense enough thanks to cooling of the swept-up gas, to reach the gravitational instability and therefore form dense condensations. Bertoldi (1989) proposed that cometary globules could be the result of the radiative implosion of an isolated gravitationally stable condensation. Mackey and Lim (2010) explained pillar formation by the shadowing effect of clumps in the density field. Parsec scale simulations showed that most of clumps and pillars could be formed from the interaction between the turbulence of the molecular cloud and the ionization (e.g., Gritschneder et al. 2010). Tremblin et al. (2013) proposed that the important parameter for the formation of pillars and clumps at the interface is the degree of curvature of the dense shell perturbed by pre-existing structures. A high curvature triggers the collapse of the shell on itself to form pillars whereas low curvature only triggers the formation of dense clumps that are accelerated with and remain in the shell. The level of turbulence compared to the pressure of the HII region and the initial morphology of the molecular cloud would be key ingredients for the formation of clumps, pillars and cometary globules.

Key Research Findings

With the infrared and submillimeter wave data provided by Herschel and Spitzer, understanding pillar formation was possible thanks to comparison between continuum and spectral line emission on one hand and numerical simulations on the other hand. The prototypical examples of pillars are the molecular gas features observed in M16 (Fig. 1). Other pillars can be observed in the Rosette Nebula, Cygnus X, and W5-E for instance (Fig. 2, e.g., Schneider et al. 2012; Deharveng et al. 2012). The Eagle Nebula (M16) is located in the constellation of Serpens at 1.8 kpc from the Sun. A young stellar cluster NGC 6611 is ionizing the molecular gas of this star-forming region (Fig. 1). The principal ionizing sources are O4 and O5 stars whose combined ionizing flux is of order $2 \times 10^{50} s^{-1}$. The region is chemically rich and spectral line studies of the region are numerous (e.g., White et al. 1999; Schuller et al. 2006; and many others). Flagey et al. (2011) studied the dust spectral energy distribution (SED) using Spitzer data. They

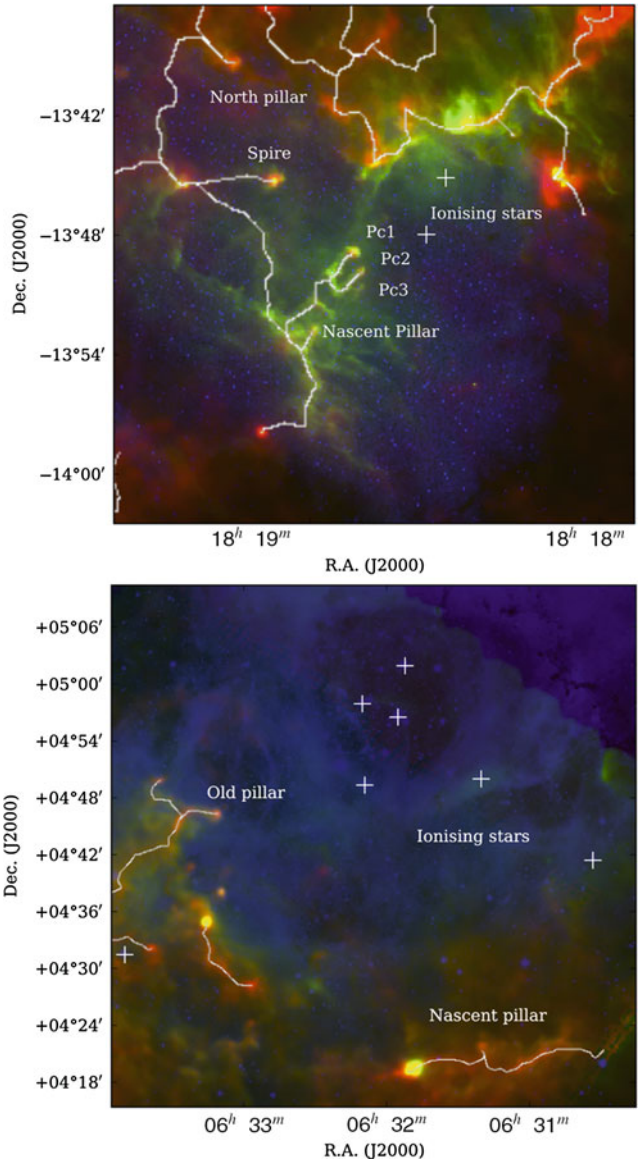

Pillars, Fig. 3 (**Top**) Three-color image of the interface between the Eagle Nebula and the HII region around NGC 6611 (*red*: Herschel column density map, *green*: PACS 70 μm, *blue*: Hα). The *white crosses* indicate the O stars. The *white lines* indicate the filamentary structure skeleton of the molecular cloud. (**Bottom**) Three-color image of the interface between the Rosette molecular cloud and the HII region around NGC 2244 (*red*: Herschel column density map, *green*: PACS 70 μm, *blue*: Hα). The *white crosses* indicate the O stars

showed that the SED could not be accounted for by interstellar dust heating by UV radiation but an additional source of heating was needed to match the mid IR flux. They proposed two possible origins: stellar winds or a supernova remnant. Herschel provided new observations on the region, and Hill et al. (2012) studied in detail the impact of the ionizing source on the initial temperature of prestellar cores located at the edge or deep into the molecular gas and did not find evidence for an extra source of heating.

Tremblin et al. (2013) revisited the Herschel data and confronted them to numerical simulations of pillar formation. Using a crest-detection algorithm to outline pillars in the column density maps, pillars appear as disconnected filaments pointing toward the ionizing sources and connected at the base to the rest of the molecular

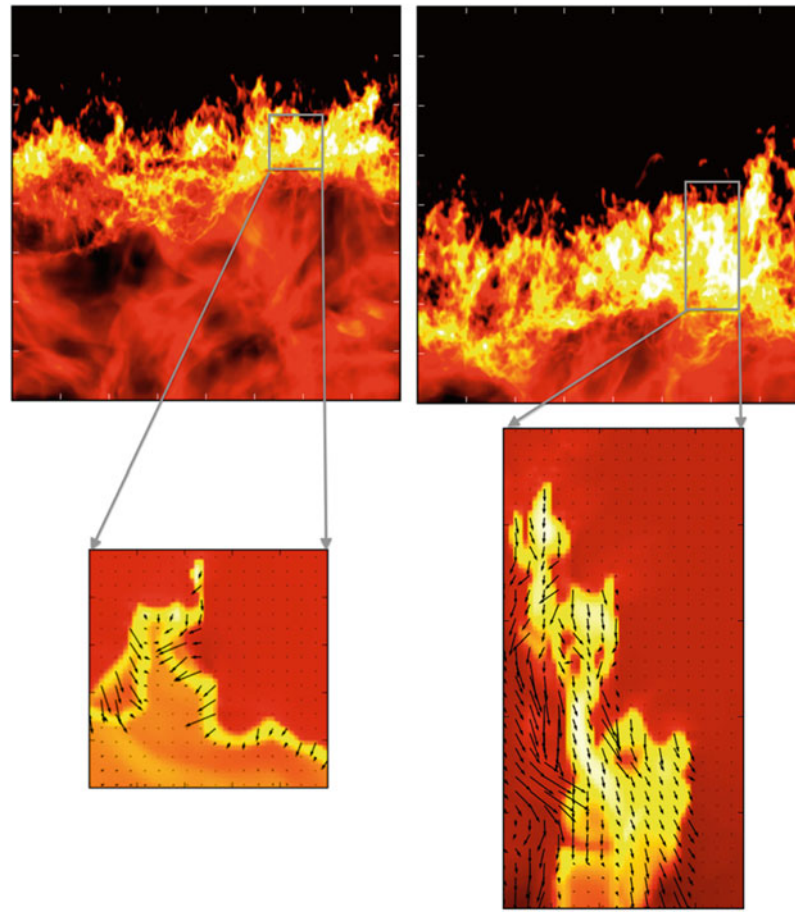

Pillars, Fig. 4 Pillar formation during the ionization of a turbulent molecular cloud. The *top panels* are two global column density snapshops of the simulation during the expansion of the ionized gas, the ionization is coming from the top of the box. The *bottom panels* are local density cuts with the velocity field represented by the *black arrows*. The *left panel* is a cut before the curved compressed layer (dense layer in *yellow*) collapses in on itself. The velocity field (*black arrows*) shows that the two sides of the curved layer are going to collide at the centre. The *right panel* is a cut after the collapse, when the pillar is formed. After the collapse the pillar is connected to the rest of the compressed layer and moves down as shown by the velocity field (Credit: P. Tremblin)

cloud by a triple point in the interstellar filament skeleton (Fig. 3). A nascent pillar was detected at the south of the Pillars of Creation and another one in the Rosette Nebula whose velocity structure is consistent with numerical simulations (Fig. 3). The velocity field has a characteristic pattern predicted by numerical simulations, showing that the compressed shell of gas is curved and collapsing in on itself to form the elongated structure (Fig. 4).

The observations deduced from Herschel data converged with previous numerical works to give a clear picture of the formation of pillars and globules around HII regions: (1) Pillars are formed when the shell is sufficiently curved to collapse in on itself. (2) If not sufficiently curved, formation of clumpy condensations is triggered inside the shell. (3) Globules can detach themselves from the parent molecular when the turbulent ram pressure of the gas is bigger than the pressure of the ionized gas. Gravity-based scenarios such as the Rayleigh Taylor instability or more recently the remains of an accretion flow are ruled out by the velocity field structure in the case of the Pillars of Creation. All previous models do not predict a collapsing shell that is observed in the case of the nascent pillar in the Rosette Nebula. The structures both in M16 and Rosette are consistent with the interaction between ionization and turbulence, although other scenarios might still happen in other regions.

Applications

A direct consequence of this pillar formation scenario is that a pre-existing dense clump will curve the shell around it, trigger the collapse and the

formation of a pillar while a low-density perturbation will not sufficiently curve the shell to trigger the pillar formation. Instead, a dense clump is subsequently formed in the shell by the accumulation of matter triggered by the perturbation. This effect has been simulated in Tremblin et al. (2013) and also in Minier et al. (2013) in the special case of RCW36. Therefore, star formation happening at the tip of pillars is likely to happen even without ionization, while star formation in dense clumps in the shell is likely to be triggered by the feedback.

Future Directions

With the recent statistics of YSOs located at the edge of ionized bubbles (e.g., Thompson et al. 2012), it becomes clear that star formation triggered by the feedback of massive stars is indeed frequent and an important ingredient for the understanding of galactic star formation. Pillars, globules and clumpy condensations, and more generally HII region morphology are tools to disentangle physical phenomena responsible for star formation in a molecular cloud under the influence of high-mass star radiative feedback.

See Also

- ▶ Interstellar Filaments
- ▶ Interstellar Medium
- ▶ Molecular Cloud
- ▶ Photoionization

References and Further Reading

Bertoldi F (1989) The photoevaporation of interstellar clouds. I – Radiation-driven implosion. Astrophys J 346:735–755

Deharveng L, Zavagno A, Anderson LD, Motte F, Abergel A, André P, Bontemps S, Leleu G, Roussel H, Russeil D (2012) Interstellar matter and star formation in W5-E. A Herschel view. Astron Astrophys 546:74

Elmegreen BG, Lada CJ (1977) Sequential formation of subgroups in OB associations. Astrophys J 214:725. doi:10.1086/155302

Flagey N, Boulanger F, Noriega-Crespo A, Paladini R, Montmerle T, Carey SJ, Gagné M, Shenoy S (2011) Tracing the energetics and evolution of dust with Spitzer: a chapter in the history of the Eagle Nebula. Astron Astrophys 531:51

Frieman EA (1954) On elephant-trunk structures in the region of O associations. Astrophys J 120:18, 29

Gahm GF, Carlqvist P, Johansson LEB, Nikolić S (2006) Rotating elephant trunks. Astron Astrophys 454(1):201–212, 33

Gritschneder M, Burkert A, Naab T, Walch S (2010) Detailed numerical simulations on the formation of pillars around H ii regions. Astrophys J 723(2):971–984. doi:10.1088/0004-637X/723/2/971, 60, 68

Hester JJ et al (1996) Hubble space telescope WFPC2 imaging of M16: photoevaporation and emerging young stellar objects. Astron J 111:2349

Hill T et al (2012) The M 16 molecular complex under the influence of NGC 6611. Herschel's perspective of the heating effect on the Eagle Nebula. Astron Astrophys 542:114, 105

Kessler EA (2006) Spacescapes: romatic aesthetics and the Hubble space telescope images. PhD thesis, University of Chicago

Mackey J, Lim AJ (2010) Dynamical models for the formation of elephant trunks in HII regions. MNRAS 403(2):714–730, 30

Minier V, Tremblin P, Hill T et al (2013) Ionisation impact of high-mass stars on interstellar filaments. A Herschel study of the RCW 36 bipolar nebula in Vela C. Astron Astrophys 550:50

Minkowski R (1949) The diffuse nebula in Monoceros. PASP 61:151, 33

Schneider N et al (2012) Cluster-formation in the Rosette molecular cloud at the junctions of filaments. Astron Astrophys 540:L11, 35

Schuller F, Leurini S, Hieret C, Menten KM, Philipp SD, Güsten R, Schilke P, Nyman LA (2006) Molecular excitation in the eagle nebula's fingers. Astron Astrophys 454(2):L87–L90, 33

Sugitani K, Fukui Y, Mizuni A, Ohashi N (1989) Star formation in bright-rimmed globules – evidence for radiation-driven implosion. Astrophys J 342: L87–L90, 33

Thompson MA, Urquhart JS, Moore TJT, Morgan LK (2011) The statistics of triggered star formation: an overdensity of massive YSOs around Spitzer bubbles, Monthly Notices of the Royal Astronomical Society 421(1):408–418

Tremblin P, Minier V, Schneider N, Audit E et al. (2013) Pillars and globules at the edges of H ii regions. Confronting Herschel observations and numerical simulations. Astron Astrophys 560:11

White G et al (1999) The Eagle Nebula's fingers – pointers to the earliest stages of star formation? Astron Astrophys 342:233–256

Zavagno A et al (2010) Star formation triggered by the galactic H II region RCW 120. First results from the Herschel space observatory. Astron Astrophys 518: L81, 35

Pillow Lava

Nicholas Arndt
ISTerre, Université Grenoble Alpes, France

Definition

Pillow lava is a form of volcanic rock that results when low-viscosity magma such as ▶ basalt erupts under water. Pillows are irregular tube-like structures, circular to elliptical in cross-section, typically 30 cm to about a meter in diameter. They form when the crust of a lava flow, or of another pillow, fractures to allow the extrusion of a spurt of lava. A thin elastic crust forms at the surface so that lava continues to flow into the interior of the tube or pillow. Pillow lavas are common in all types of modern submarine volcanic settings – mid-ocean ridges, oceanic islands, and island arcs – and also are the most common volcanic feature in well-preserved Archean ▶ greenstone belts. Recently, pillow basalt has received much attention by astrobiologists for the occurrence of tubular microscopic structures in pillow lava of Archean age that could be related to biological activity (Archean, Traces of Life).

See Also

- ▶ Archean Traces of Life
- ▶ Basalt
- ▶ MORB
- ▶ Oceanic Crust

Pioneer F for Pioneer 11

▶ Pioneer Spacecraft

Pioneer G for Pioneer 10

▶ Pioneer Spacecraft

Pioneer Spacecraft

Michel Viso
CNES/DSP/SME, Vétérinaire/DVM, Astro/Exobiology, Paris Cedex 1, France

Synonyms

Pioneer F for Pioneer 11; Pioneer G for Pioneer 10

Definition

These two NASA Pioneer probes were part of the Pioneer program to explore the Solar System. Pioneer 10 and 11 were aimed to visit the ▶ Jupiter and ▶ Saturn, the two Giant planets of the outer Solar System. Pioneer 10 was launched from Cape Canaveral on March 2, 1972. It flew by Jupiter on December 3, 1973 and then continued its trip having gained sufficient momentum to escape the Solar System. The last contact with the probe was on January 23, 2003 while it was heading toward the Aldebaran constellation that it will reach in about two million years. Pioneer 11 was launched as schedule almost 13 month after it sister spacecraft on April 5, 1973. The spacecraft arrived at Jupiter and observed the planet's red spot on December 2, 1974 before heading toward Saturn. The spacecraft reached Saturn on September 1, 1979. The last contact with Pioneer 11 occurred on November 1, 1995.

The two identical spacecrafts were equipped with radioisotopic thermo generators and have a dry mass of about 257 kg. Pioneer 10 carried a payload of 11 scientific instruments; Pioneer 11 carried one instrument more. The sister probes were designed to study the target ▶ planets and their satellites as well as the ▶ space environment, the solar wind, the cosmic rays, and the planetary and cosmic ▶ magnetic fields. Pioneer probes are recognized for their achievements (first photos from Jupiter, Saturn, Saturn's moons, ...). Both spacecrafts carry a gold

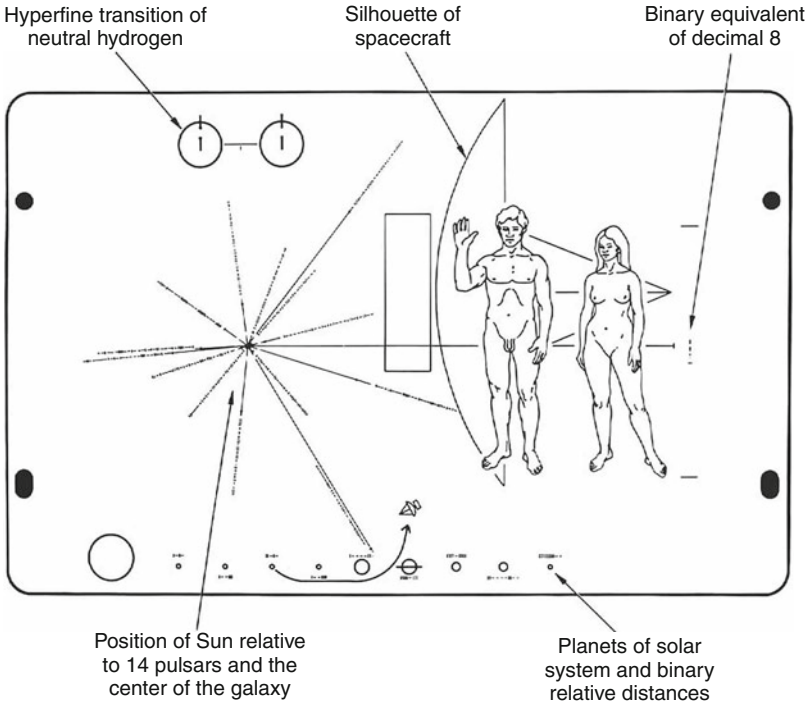

Pioneer Spacecraft, Fig. 1 The drawing of the pioneer plate with explanations (Photo NASA)

anodized plate (Fig. 1) designed by Carl Sagan, Linda Salzman-Sagan, and Frank Drake with a message to extraterrestrial civilizations that they may encounter about the origin of the spacecrafts. They are also known for the detection of the so-called Pioneer anomaly. A Doppler drift in the radio signal demonstrated a slight unexpected change in the acceleration of the probes. The finding remains unexplained to the present day and is of great interest to theoretical physics and cosmology.

References and Further Reading

http://www.nasa.gov/centers/ames/missions/archive/pioneer.html#.UyLbNO-AGko

α Piscis Austrinus b

► Fomalhaut b

Pitchblende

► Uraninite

PIXE

Jun-Ichi Takahashi
NTT Microsystem Integration Laboratories, Atsugi, Japan

Synonyms

Proton-induced x-ray emission

Definition

Proton-induced x-ray emission (PIXE) is a technique used in the determination of the elemental makeup of a material or sample. Bombardment with MeV protons produced by an ion accelerator causes inner shell ionization of atoms, and outer

shell electrons drop down to replace inner shell vacancies with certain allowed transitions. X-rays of a characteristic energy of the element are emitted and provide information about the composition of the sample. PIXE is a powerful yet nondestructive elemental analysis technique now used routinely. Recent extensions of PIXE using tightly focused beams (down to 1 μm) give the additional capability of microscopic analysis. This technique, called microPIXE, can be used to determine the distribution of trace elements with high spatial resolution in a wide range of samples.

Planet

Tilman Spohn
Deutsches Zentrum für Luft- und Raumfahrt (DLR), Institut für Planetenforschung, Berlin, Germany

Definition

The IAU (International Astronomical Union) General Assembly officially defined the term planet in resolution 5A (Resolution_GA26-5-6) in 2006. According to this definition a planet is an object that orbits the Sun, has cleared the neighborhood around its orbit from pre-planetary debris, and has sufficient mass for its self-gravity to maintain a nearly round shape.

See Also

- ▶ Debris Disk
- ▶ Dynamo, Planetary
- ▶ Jupiter
- ▶ Mars
- ▶ Mercury
- ▶ Neptune
- ▶ Planet Formation
- ▶ Planetary Migration
- ▶ Planetary Nebula
- ▶ Plate Tectonics
- ▶ Probing Lensing Anomalies Network
- ▶ Protoplanetary Disk
- ▶ Saturn
- ▶ Solar System, Inner
- ▶ Sun (and Young Sun)
- ▶ Uranus
- ▶ Venus

Planet Detection: Transit Timing Variation

Nader Haghighipour
Institute for Astronomy, University of Hawaii-Manoa, Honolulu, Hawaii, HI, USA

Definition

Planet detection from transit timing variations is a method for determining the existence and properties of a planet from the gravitational perturbations it induces on the orbit of another transiting planet. In an unperturbed planetary system consisting of a star and a planet, the two bodies revolve around their center of mass in a ▶ Keplerian orbit. If in this system, the planet transits the star, it will cross the disk of the star at same time during each transit. As a result, the time of the middle of the transit will be identical every time the planet completes one orbit. If because of some external perturbation (e.g., a second planet) the motion of the transiting planet deviates from purely Keplerian, the time of the mid-transit will be different from one orbit to another. This is known as the transit timing variation (TTV). Figure 1 shows this schematically.

Overview

The difference between the observed time of mid-transit and its theoretically expected

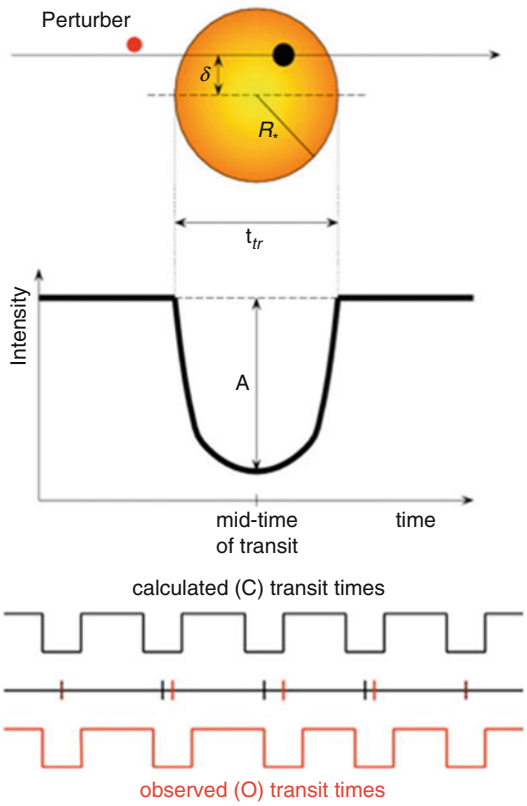

Planet Detection: Transit Timing Variation, Fig. 1 Schematic view of transit timing variation

(i.e., calculated) value, known as O−C, when determined for different transit numbers (or cycles) can be used to extract information about the mass and orbital properties of the perturber. This is known as the transit timing variation method of planetary detection. As expected, when the orbital periods of the two planets are commensurate (in the ratio of small integers), the perturbing effect of one planet on the orbital motion of the other is enhanced. This causes the measured value of the time of mid-transit of the transiting planet to show large variations from its expected value. As a result, the amplitude of the O−C diagram is amplified when the two planets are in a ▶ mean-motion resonance (Agol et al. 2005; Steffen and Agol 2005; Agol and Steffen 2007). Figure 2 shows this for a three-body system with a 0.367 solar-mass star, a Jupiter-mass transiting planet in a 10-day orbit, and an Earth-mass perturber. The top panel shows the TTVs when the perturber is in a 16.11-day orbit. The bottom panel corresponds to near an interior 1:2 resonance of the two planets (Haghighipour and Kirste 2011). As expected, the amplitude of TTV is enhanced by an order of magnitude. The enhancement of the O−C amplitude when the two planets are in a resonance (i.e., with commensurate orbits) increases the possibility of the detection of these variations. The two outer planets of the Kepler 9 system (Kepler-9b and c) are the first to have been confirmed using the TTV method. These two planets are in a near 2:1 mean-motion resonance (Holman et al. 2010).

Because different combinations of the mass and orbital elements of the transiting planet and perturber can produce similar values of O−C, the TTV method suffers from strong degeneracies when used as a mechanism for detecting planets. Several efforts have been made to analyze the O−C diagram and determine the relevant planetary candidates quickly (Nesvorný and Morbidelli 2008; Nesvorný 2009; Nesvorný and Beaugé 2010; Borkovits et al. 2011). Once a region of the parameter space is identified which can produce the O−C values, other detection techniques need to be employed in order to break this degeneracy. In cases when the free eccentricities of the planets are sufficiently small, TTVs can be used to determine the mass and eccentricity of each planet (Lithwick et al. 2012).

The transit timing variation method has been used to assess the detectability of a variety of systems including extrasolar satellites (Kipping 2009a, b; Schneider 2014), Trojan and co-orbital planets (Ford and Gaudi 2006; Haghighipour et al. 2013), as well as habitable terrestrial planets and super-Earths around a low-mass star (Haghighipour and Kirste 2011).

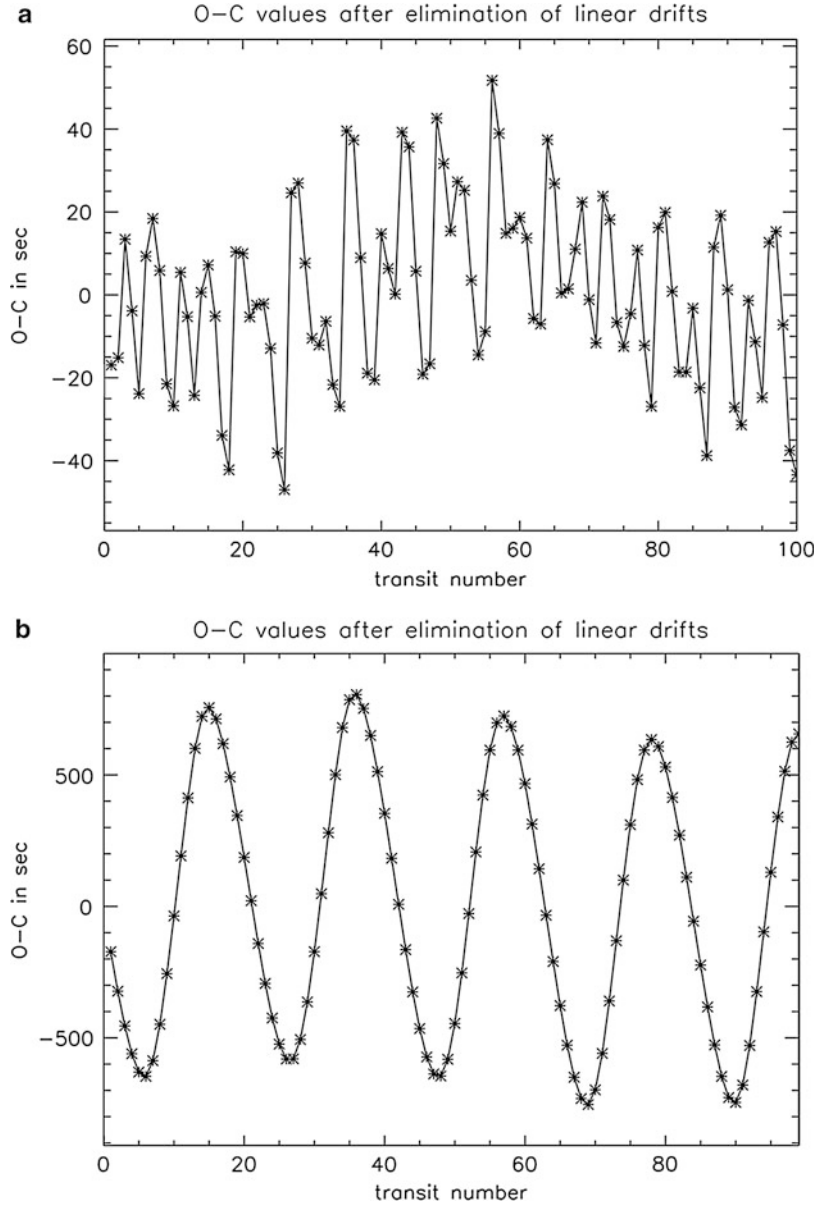

Planet Detection: Transit Timing Variation, Fig. 2 A system with a 0.367 solar-mass star, a Jupiter-mass transiting planet in a 10-day orbit, and an Earth-mass perturber. The *top* panel shows the TTVs when the perturber is in a 16.11-day orbit. The *bottom* panel corresponds to near an interior 1:2 resonance (Haghighipour and Kirste 2011). The amplification of the O−C amplitude is by an order of magnitude

See Also

► Transiting Planets

References and Further Reading

Agol E, Steffen JH (2007) A limit on the presence of Earth-mass planets around a Sun-like star. MNRAS 374:941

Agol E, Steffen J, Sari R, Clarkson W (2005) On detecting terrestrial planets with timing of giant planet transits. MNRAS 359:567

Ford EB, Gaudi BS (2006) Observational constraints on Trojans of transiting extrasolar planets. Astrophys J 652:L137

Haghighipour N, Kirste S (2011) On the detection of (habitable) super-Earths around low-mass stars using Kepler and transit timing variation method. Celest Mech Dyn Astron 111:267

Haghighipour N, Capen S, Hinse TC (2013) Detection of Earth-mass and super-Earth Trojan planets using

transit timing variation method. Celest Mech Dyn Astron 117:75
Holman MJ et al (2010) Kepler-9: a system of multiple planets transiting a Sun-like star, confirmed by timing variations. Science 330:51
Kipping DM (2009a) Transit timing effects due to an exomoon. MNRAS 392:181
Kipping DM (2009b) Transsit timing effects due to an exomoon-II. MNRAS 396:1797
Lithwick Y, Xie J-W, Wu Y (2012) Extracting planet mass and eccentricity from TTV data. Astrophys J 761, article id. 122
Schneider J, Lainy V, Cabrera J (2014) The next step in exoplanetology: exomoons. Int J Astrobiol 14:191–199
Simon A, Szatmáry K, Szabó GM (2007) Determination of the size, mass, and density of "exomoons" from photometric transit timing variations. Astron Astrophys 470:727
Steffen JH, Agol E (2005) An analysis of the transit times of TrES-1b. MNRAS 364:L96

Planet Detection; Eclipse Timing Variation

Nader Haghighipour
Institute for Astronomy, University of Hawaii-Manoa, Honolulu, Hawaii, HI, USA

Definition

Planet detection from eclipse timing variations is a method for determining the existence and properties of a planet in an eclipsing binary star system from the gravitational perturbations the planet induces in the orbit of the binary.

Overview

The mutual orbit of an isolated, unperturbed binary star system is purely Keplerian. That is, the two stars of the binary revolve around their center of mass in Keplerian orbits. In such systems, the orbital evolution of the system can be predicted precisely. If the two stars eclipse each other (in which case the system is known as an eclipsing binary), the eclipses will happen at the same time and will have the same durations. However, if the orbit of the binary is perturbed, changes will appear in the period of the binary eclipses. This is known as Eclipse Timing Variation or ETV.

Eclipse timing variations may be induced by several processes (Conroy et al. 2014):

1. Light travel time effect (LITE): a third body perturbing the center of mass of the binary system creates a light-time delay along the line of sight which can cause eclipses to appear earlier or later than expected
2. Non-hierarchical third body: the presence of a third body actually changes the period of the binary over time
3. Mass transfer: mass transfer between the components in the binary changes the period
4. Gravitational quadrupole coupling (Applegate effect): spin–orbit transfer of angular momentum in a close binary due to one of the stars being active produces period changes up to 10–5 times the binary period (Applegate 1992)
5. Apsidal motion: the rotation of the line of apsides causes a change in the time between primary and secondary eclipses even though the period remains unchanged (requires an eccentric orbit; see Apsidal Angle)
6. Spurious signals: due to spots and other effects that distort the eclipsing binary light curve

Figure 1 shows a gallery of ETVs caused by the LITE.

Using eclipse timing variations to find exoplanets is a well-known method (Schwarz et al. 2011). The idea of photometric detection of extrasolar planets around eclipsing binaries was first presented by Schneider and Chevreton (1990). This idea was later developed by many authors (Schneider and Doyle 1995; Doyle et al. 1998; Doyle and Deeg 2004; Deeg et al. 2008; Muterspaugh et al. 2010) and is based on the fact that a circumprimary/circumbinary planet can perturb the orbit of the two stars and create variations in the timing and duration of their eclipses. The measurement of these variations, when compared with theoretical models, can reveal information about the mass and orbital elements of the perturbing planet.

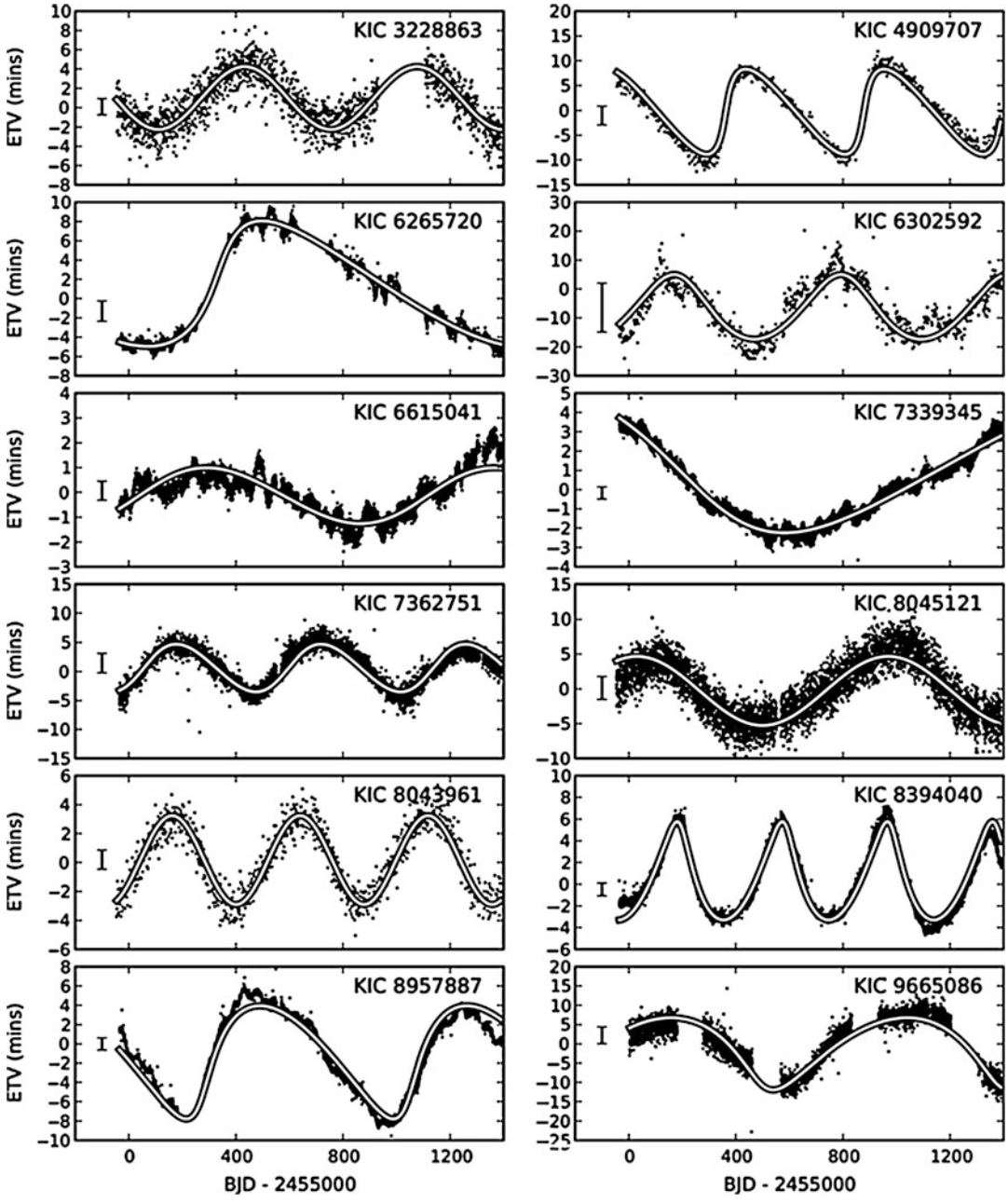

Planet Detection; Eclipse Timing Variation, Fig. 1 Gallery of ETV signals due to the LITE found in close binaries KIC 3228863, 4909707, 6265720, 6302592, 6615041, 7339345, 7362751, 8045121, 8043961, 8394040, 8957887, and 9665086. Horizontal axis in days. Typical errors for ETV measurements are shown to the left of the data (Conroy et al. 2014)

Similar to transit timing variations (TTVs) in close eclipsing binaries, variations in a binary's eclipse timing may be due to a circumbinary planet. The difference between the observed time of mid-eclipse and its theoretically expected (i.e., calculated) value, known as O-C, when determined for different eclipse numbers (or cycles) can be used to extract information

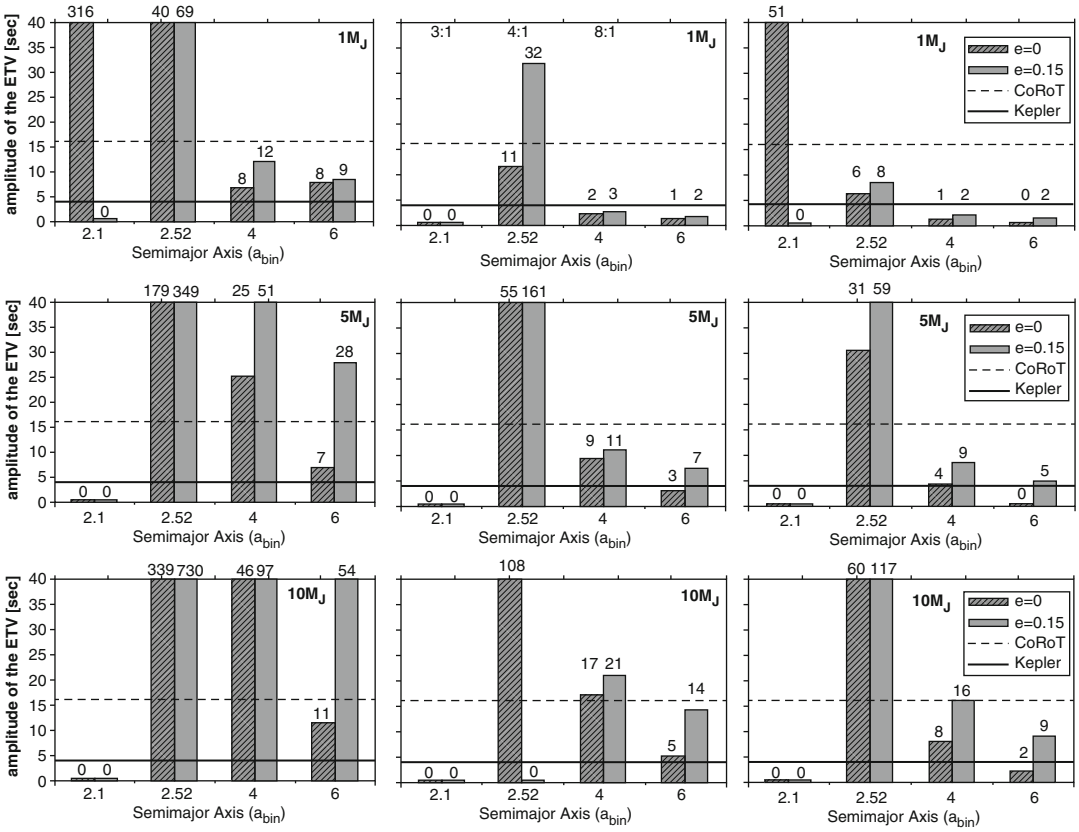

Planet Detection; Eclipse Timing Variation, Fig. 2 Graphs of the maximum amplitude of ETVs for three binary models with zero orbital eccentricity. The locations of the bars on the horizontal axis correspond to mean motion resonances (MMR) of 3:1 MMR at 2.1 a_{bin}, 4:1 MMR at 2.52 a_{bin}, 8:1 MMR at 4 a_{bin} and a non-resonant case at 6 a_{bin}, where a_{bin} is the semi-major axis of the binary orbit. Graphs are shown for two values of the planet's orbital eccentricity (0 and 0.15). As a point of comparison, the maximum values of detectable timing amplitudes (sensitivity limits) for *CoRoT* and *Kepler* (Sybilski et al. 2011) are also shown (Schwarz et al. 2011)

about the mass and orbital properties of the perturber (i.e., the circumbinary planet). As expected, when the orbital periods of the planet and binary are commensurate (in the ratio of small integers), the perturbing effect of the planet on the motion of the binary is enhanced. This causes the measured value of the time of mid-eclipse to show large variations from its expected value. As a result, the amplitude of the O-C diagram is amplified when the planet and binary are in a mean motion resonance, making the detection of such planets more practical (Schwarz et al. 2011). Figure 2 shows the maximum values of O-C for different eclipsing binaries with circumbinary planets in different mean-motion resonances.

See Also

- ▶ Planet Detection: Transit Timing Variation
- ▶ Transiting Planets

References and Further Reading

Applegate JH (1992) A mechanism for orbital period modulation in close binaries. Astrophys J 385:621

Conroy KE, Prsa A, Stassun KG, Orosz JA, Fabrycky DA, Welsh WF (2014) Kepler eclipsing binary stars. IV. Precise eclipse times for close binaries and identification of candidate three-body systems. Astron J 147:45

Deeg HJ, Ocana B, Kozhevnikov VP, Charbonneau D, O'Donovan FT, Doyle LR (2008) Extrasolar planet detection by binary stellar eclipse timing: evidence

for a third body around CM Draconis. Astron Astrophys 480:563
Doyle LR, Deeg H-J (2004) Timing detection of eclipsing binary planets and transiting extrasolar moons. In: Norris R, Stootman F (eds) Bioastronomy 2002: life among the stars. Proceedings of IAU symposium, vol 213. Astronomical Society of the Pacific, San Francisco, p 80
Doyle LR et al (1998) Detectability of Jupiter-to-Brown-Dwarf-Mass companions around small eclipsing binary systems. In: Rebolo R, Martin EL, Zapatero-Osorio MR (eds) Detectability of Jupiter-to-brown-dwarf-mass companions around small eclipsing binary system, brown dwarfs & extrasolar planets. ASP conference series vol 134. Astronomical Society of the Pacific, San Francisco, p 224
Muterspaugh MW, Konacki M, Lane BF, Pfahl E (2010) Observational techniques for detecting planets in binary systems. In: Haghighipour N (ed) Planets in binary star systems. Astrophysics and space science library, vol 366. Springer, Berlin, p 77
Schneider J, Chevreton M (1990) The photometric search for earth-sized extrasolar planets by occultation in binary systems. Astron Astrophys 232:251
Schneider J, Doyle LR (1995) Ground-based detection of terrestrial extrasolar planets by photometry: the case for CM Draconis. Earth Moon Planet 71:153
Schwarz R, Haghighipour N, Eggl S, Pilat-Lohinger E, Funk B (2011) Prospects of the detection of circumbinary planets with Kepler and CoRoT using the variations of eclipse timing. Mon Not R Astron Soc 414:2763
Sybilski P, Konacki M, Kozlowski S (2011) Detecting circumbinary planets using eclipse timing of binary stars – numerical simulations. Mon Not R Astron Soc 405:657

Planet Formation

Alessandro Morbidelli
Observatoire de la Cote d'Azur, Nice, France

Keywords

Planetesimals; Protoplanetary disk; Accretion disks

Synonyms

Accretion; Planetary

Definition

Planet formation is the process by which planetary bodies are formed from a disk of gas and dust around a protostar. Planets can form in two ways. In the regions far from the central star, where the disk can cool efficiently, giant gaseous planets might form as a result of the gravitational instability of the disk; alternatively, these planets may form from the protoplanetary cores discussed below. In the inner regions, planets are expected to form in a more complex, multistage process: first, the dust settles onto the disk's midplane and coagulates to form asteroid- or comet-like bodies called ▶ *planetesimals*. Then, the planetesimals accrete with each other during low-velocity collisions to form *planetary embryos* or *protoplanetary cores*. The former are rocky bodies with masses of the order of the lunar to Martian mass, which form in the hottest region of the disk, where water is not in solid form. The protoplanetary cores, which form beyond the ▶ snow line, are a mixture of rock and ice and are expected to have multiple Earth masses. These protoplanetary cores then accrete a massive hydrogen and helium atmosphere before the disappearance of the gaseous component of the disk and become ▶ giant planets. ▶ Planetary embryos collide with each other at moderate velocities giving rise to terrestrial-like planets.

Overview

In the ▶ protoplanetary disk, the most refractory materials condense first, gradually followed – while the local temperature drops – by more and more volatile elements. The dust grains thus formed float in the gas. Collisions stick the grains together, forming fractal aggregates, possibly helped by electrostatic and magnetic forces. Other collisions then rearrange the aggregates and compact them. When the grains reach a size of about a centimeter, they begin to rapidly sediment onto the median plane of the disk, in a time of the order of 10^3 years. This timescale, however, could be longer if the nebula is strongly turbulent.

The growth from centimeter-size grains to kilometer-size planetesimals is still unexplained. Particles of centimeter size are too small for gravity to be effective in particle-particle collisions but are too big to stick through electrostatic forces. Moreover, grains are subject to ▶ gas drag, which makes them drift toward the central star (Weidenschilling 1977). The drift speed is size dependent; thus, particles of different sizes must collide with non-negligible relative velocities (of the order of several cm/s). At these velocities, particles should break, rather than coagulate. Because the drift speed toward the central star is maximal for meter-size boulders, this issue is known as the "▶ meter-size catastrophe," though it is likely that this bottleneck for accretion starts already at much smaller sizes (cm or dm).

One possible solution of this problem is that planetesimals form thanks to the collective gravity of massive swarms of small particles, concentrated at some locations (vortices or intervortex regions, depending on particle sizes) by the turbulence of the disk (Johansen et al. 2007; Cuzzi et al. 2008). This model can explain the formation of large planetesimals (100 km or larger) and the internal structure of these bodies as revealed by the petrology of undifferentiated meteorites.

Once the protoplanetary disk contains a substantial population of planetesimals, the second stage of planet formation starts. The dynamics of accretion is first dominated by the effect of the gravitational attraction between pairs of planetesimals, which increases the collisional cross sections. A ▶ *runaway growth* phase starts, during which the big bodies grow faster than the small ones, hence increasing their relative difference in mass (Greenberg et al. 1978). This process can be summarized by the equation

$$\mathrm{d}/\mathrm{d}t(M_1/M_2) > 0,$$

where M_1 and M_2 are, respectively, the characteristic masses of the "big" and of the "small" bodies, and can be explained as follows.

Generally speaking, accretion is favored by a high collision rate, which occurs when the relative velocities are large, but also by large collisional cross sections and gentle impacts, which occur when the relative velocities are low. Therefore, the relative velocities between the different planetesimal populations govern the growth regime.

At the beginning of the runaway growth phase, the largest planetesimals represent only a small fraction of the total mass. Hence, the dynamics is governed by the small bodies, in the sense that the relative velocities among the bodies are of the order of the escape velocity of the small bodies, $V_{\mathrm{esc}(2)}$.

This velocity is independent of the mass M_1 of the big bodies and is smaller than the escape velocity of the large bodies, $V_{\mathrm{esc}(1)}$.

For a given body, the collisional cross section is enhanced with respect to the geometric cross section by the so-called gravitational focusing factor:

$$F_{\mathrm{g}} = 1 + {V_{\mathrm{esc}}}^2/{V_{\mathrm{rel}}}^2$$

where V_{esc} is the body's escape velocity and V_{rel} is the relative velocity of the other particles in its environment. Because $V_{\mathrm{rel}} \sim V_{\mathrm{esc}(2)}$, the gravitational focusing factor of the small bodies ($V_{\mathrm{esc}} = V_{\mathrm{esc}(2)}$) is of order unity, while that of the large bodies ($V_{\mathrm{esc}} = V_{\mathrm{esc}(1)} >> V_{\mathrm{esc}(2)}$) is much larger. In this situation, one can show that the relative growth rate (Ida and Makino 1993) is an increasing function of the body's mass, which is the condition for the runaway growth.

The runaway growth stops when the mass of the large bodies becomes important (Ida and Makino 1993) and the latter start to govern the dynamics. The condition for this to occur is

$$n_1{M_1}^2 > n_2{M_2}^2,$$

where n_1 (respectively n_2) is the number of big bodies (respectively small bodies).

In this case, the growth rate of the embryos gets slower and slower as the bodies grow and the relative differences in mass among the embryos are also slowly reduced. In principle, one could expect that the small bodies catch up, narrowing their mass difference with the embryos. But in reality, the now large relative velocities prevent

the small bodies from accreting with each other. The small bodies can only participate in the growth of the embryos. This phase is called ▶ *oligarchic growth*.

The runaway growth phase happens all through the disk, with timescales that depend on the local dynamical time (Keplerian time) and on the local density of available solid material. This density will also determine the maximum size of the embryos and/or planets when the runaway growth ends (Lissauer 1987). Assuming a reasonable surface density of solid materials, the runaway growth process forms planetary embryos of lunar to martian mass at 1 AU in 10^5–10^6 years, separated by a few 10^{-2} AU. Beyond the so-called snow line at about 4 AU for a solar luminosity star, where condensation of water ice occurred thanks to the low temperature, enhancing the surface density of solid material, runaway growth could produce objects as large as several Earth masses, called protoplanetary cores, in a few million years (Thommes et al. 2003). Then, the last stage can lead to the formation of the planets.

Giant Planet Formation

When the protoplanetary cores reach a mass of 5–10 Earth masses, they start to accrete a significant amount of gas from the protoplanetary disk. The gas accretion continues at a roughly constant rate over a few million years, until a total mass of 20–30 Earth masses is reached; then, the gas gravitationally collapses onto the planet: the mass of the planet grows exponentially and reaches hundreds of Earth masses in ∼10,000 years (Pollack et al. 1996). A giant planet is formed.

This model explains well the structure of Jupiter and Saturn, gaseous planets with solid cores of 5–15 Earth masses. It also explains the nature of Uranus and Neptune, ∼15 Earth-mass planets with only a few Earth masses of gas: these cores would have formed more slowly, given the larger distances to the Sun, so that the gas was removed from the protoplanetary disk before the conditions for the gas gravitational collapse could be met.

There are, however, many conceptual problems with this model. First, although analytic theories predict the formation of 10 Earth-mass cores beyond the snow line, numerical simulations show that the cores have problems to grow above ∼1 Earth mass (Levison et al. 2010) for various dynamical reasons. Second, planetary cores should undergo a fast orbital migration toward the central star, as a result of their gravitational interactions with the disk of gas (known as "Type I migration"; Ward 1997). Consequently, they should be lost before having a chance to accrete a massive atmosphere and become giant planets. Third, according to theoretical estimates, the conditions for the onset of the gravitational collapse of the gas might not be met before several millions of years (Podolak 2003), a time longer than the typical lifetime of protoplanetary disks (Haisch et al. 2001). Finally, if the gas gravitational collapse takes place, the planet should grow to 5–10 Jupiter masses in a very short time, which makes it difficult to explain the much smaller terminal masses of Jupiter and Saturn.

To circumvent some of these problems, particularly those related to the formation of the cores and their survival in the disk, it has been proposed that giant planets might form directly from concentrations of gas, like a star, without the need of the prior formation of massive solid cores (Boss 2000). In fact, it has been shown that a cold, massive protoplanetary disk can break into a number of self-gravitating gas clumps, which then contract forming giant gaseous planets (Durisen et al. 2007). The key issue is the temperature: as the concentration of gas increases, the temperature rises, which tends to prevent the further accumulation of gas. Thus, the formation of self-gravitating clumps and their subsequent contraction requires an efficient cooling of the gas. For this reason, new hydrodynamical simulations that model more accurately the thermodynamics in the protoplanetary disk find that formation of long-lived self-gravitating clumps of gas is likely only at large distances from the central star (more than 50–100 AU;

Boley 2009). It is still unclear, though, whether the end products of these clumps can be giant planets or must be ▶ brown-dwarf-mass objects (Stamatellos and Whitworth 2008). For all these reasons, the gravitational instability model is now less favored than the core accretion model for the formation of the giant planets of the solar system as well as most extrasolar planets, while it might be an explanation for the origin of massive distant extrasolar "planets" such as those of the HR 8,799 system.

The core accretion scenario, on the other hand, has been recently strenghtened by the proposal of a new mechanism for the growth of the solid cores that overcomes the 1 Earth-mass barrier discussed in Levison et al. (2010). According to this new mechanism, dubbed "pebble accretion," the largest planetesimals which formed from self-gravitating clumps of small pebbles continue to accrete pebbles from the protoplanetary disk (Lambrechts and Johansen 2012). In fact, due to gas drag, most of pebbles passing through the Hill sphere of a growing planet would spiral down to the planetary surface and deliver their mass. Pebble accretion is extremely efficient and fast and potentially can lead to the formation of a 10 Earth-mass core well within the gas disk lifetime.

Terrestrial Planet Formation

The terrestrial planets form from the collisions of the planetary embryos that accreted during the runaway and oligarchic growth phases, in the inner part of the disk. In our solar system, given the presence of Jupiter at ∼5 AU, the typical result of this highly chaotic collisional phase – simulated with several numerical N-body integrations – is the elimination of all the embryos originally situated in the asteroid belt (2–4 AU) and the formation of a small number of terrestrial planets on stable orbits in the 0.5–2 AU region in a timescale of ∼50–100 My (Chambers and Wetherill 1998; O'Brien et al. 2006; Raymond et al. 2007). This scenario explains the small number of terrestrial planets existing in our system, their orbital eccentricities and inclinations, their accretion timescales determined from the analysis of the radioactive chronometers (Kleine et al. 2009), and their enrichment in volatile elements (including water; Morbidelli et al. 2000) relative to what is expected for planetesimals formed well inside of the snow line.

The main problem of this scenario is that the mass of the synthetic planet formed in the simulations at the location of Mars is typically ∼5 times too massive (Raymond et al. 2009). Hansen (2009) proposed an original solution to this problem, showing that if the disk of planetesimals and embryos, out of which the terrestrial planets formed, had an outer edge at 1 AU, the large mass ratio between the Earth and Mars is systematically reproduced in the simulations. Mars in this case is an embryo which is rapidly ejected out of the annulus of material by a close encounter with the proto-Earth. Consequently, the accretion of Mars is aborted and the planet can preserve its small initial mass.

The existence of the outer edge of the disk at 1 AU was just an ad hoc assumption in Hansen's work, but its origin was later explained in Walsh et al (2011), by invoking the migration of Jupiter during the gas-disk phase. More specifically, hydrodynamical simulations have shown that Jupiter migrates inward while it is "alone" in the disk, but when Saturn reaches its current mass, the presence of this second planet is capable of reversing the migration direction of Jupiter, forcing the latter to move outward. The inward-then-outward migration of Jupiter severely depletes the portion of the disk crossed by the planet. Thus if Jupiter reversed migration (or "tacked") around 1.5 AU, the disk of embryos and planetesimals would have been truncated at ∼1 AU, just as required in Hansen's model. This scenario is now called "Grand Tack scenario."

See Also

- ▶ Core Accretion, Model for Giant Planet Formation
- ▶ Giant Planets

- ▶ Gravitational Collapse, Planetary
- ▶ HR 8799: The First Directly Imaged Multi-planet System
- ▶ Late-Stage Accretion
- ▶ Meter-Size Catastrophe
- ▶ Oligarchic Growth
- ▶ Planetary Migration
- ▶ Planetesimals
- ▶ Protoplanetary Disk
- ▶ Protoplanetary Disk Instability
- ▶ Runaway Growth
- ▶ Snow Line
- ▶ Terrestrial Planet

References and Further Reading

Boley AC (2009) The two modes of gas giant planet formation. Astrophys J 695:L53–L57

Boss AP (2000) Possible rapid gas giant planet formation in the solar nebula and other protoplanetary disks. Astrophys J 536:L101–L104

Chambers JE, Wetherill GW (1998) Making the terrestrial planets: N-body integrations of planetary embryos in three dimensions. Icarus 136:304–327

Cuzzi JN, Hogan RC, Shariff K (2008) Toward planetesimals: dense chondrule clumps in the protoplanetary nebula. Astrophys J 687:1432–1447

Durisen RH, Boss AP, Mayer L, Nelson AF, Quinn T, Rice WKM (2007) Gravitational instabilities in gaseous protoplanetary disks and implications for giant planet formation. In: Reipurth B, Jewitt D, Keil K (eds) Protostars and planets V. University of Arizona Press, Tucson, pp 607–622

Greenberg R, Hartmann WK, Chapman CR, Wacker JF (1978) Planetesimals to planets – numerical simulation of collisional evolution. Icarus 35:1–26

Haisch KE Jr, Lada EA, Lada CJ (2001) Disk frequencies and lifetimes in young clusters. Astrophys J 553: L153–L156

Hansen BMS (2009) Formation of the terrestrial planets from a narrow annulus. Astrophys J 703:1131–1140

Ida S, Makino J (1993) Scattering of planetesimals by a protoplanet – slowing down of runaway growth. Icarus 106:210

Johansen A, Oishi JS, Mac Low MM, Klahr H, Henning T, Youdin A (2007) Rapid planetesimal formation in turbulent circumstellar disks. Nature 448:1022–1025

Kleine T, Touboul M, Bourdon B, Nimmo F, Mezger K, Palme H, Jacobsen SB, Yin Q-Z, Halliday AN (2009) Hf-W chronology of the accretion and early evolution of asteroids and terrestrial planets. Geochim Cosmochim Acta 73:5150–5188

Lambrechts M, Johansen A (2012) Rapid growth of gas-giant cores by pebble accretion. Astron Astrophys 544:A32

Levison HF, Thommes E, Duncan MJ (2010) Modeling the formation of giant planet cores. I. Evaluating key processes. Astron J 139:1297–1314

Lissauer JJ (1987) Timescales for planetary accretion and the structure of the protoplanetary disk. Icarus 69:249–265

Marois C, Zuckerman B, Konopacky QM, Macintosh B, Barman T (2010) Images of a fourth planet orbiting HR 8799. Nature 468:1080–1083

Morbidelli A, Chambers J, Lunine JI, Petit JM, Robert F, Valsecchi GB, Cyr KE (2000) Source regions and time scales for the delivery of water to Earth. Meteorit Planet Sci 35:1309–1320

O'Brien DP, Morbidelli A, Levison HF (2006) Terrestrial planet formation with strong dynamical friction. Icarus 184:39–58

Podolak M (2003) The contribution of small grains to the opacity of protoplanetary atmospheres. Icarus 165:428–437

Pollack JB, Hubickyj O, Bodenheimer P, Lissauer JJ, Podolak M, Greenzweig Y (1996) Formation of the giant planets by concurrent accretion of solids and gas. Icarus 124:62–85

Raymond SN, Quinn T, Lunine JI (2007) High-resolution simulations of the final assembly of earth-like planets. 2. Water delivery and planetary habitability. Astrobiology 7:66–84

Raymond SN, O'Brien DP, Morbidelli A, Kaib NA (2009) Building the terrestrial planets: constrained accretion in the inner solar system. Icarus 203:644–662

Stamatellos D, Whitworth AP (2008) Can giant planets form by gravitational fragmentation of discs? Astron Astrophys 480:879–887

Thommes EW, Duncan MJ, Levison HF (2003) Oligarchic growth of giant planets. Icarus 161:431–455

Walsh KJ, Morbidelli A, Raymond SN, O'Brien DP, Mandell AM (2011) A low mass for Mars from Jupiter's early gas-driven migration. Nature 475:206–209

Ward WR (1997) Protoplanet migration by nebula tides. Icarus 126:261–281

Weidenschilling SJ (1977) Aerodynamics of solid bodies in the solar nebula. Mon Not R Astron Soc 180:57–70

Planet V Hypothesis

Sean N. Raymond
Laboratoire d'Astrophysique de Bordeaux, CNRS, Universite de Bordeaux, France

Definition

The Planet V hypothesis proposes that a fifth terrestrial planet (named "planet V") formed exterior

to Mars' orbit and became dynamically unstable several hundred million years after its formation. This instability could have led to the impact of a large number of asteroids on the Earth-Moon system. The Planet V hypothesis is the main alternate mechanism to the ▶ Nice model for the origin of the ▶ Late Heavy Bombardment.

See Also

▶ Late Heavy Bombardment
▶ Nice Model

References and Further Reading

Chambers JE (2007) On the stability of a planet between Mars and the asteroid belt: implications for the planet V hypothesis. Icarus 189:386–400

Planetary

▶ Planet Formation

Planetary and Space Simulation Facilities

Corinna Panitz
German Aerospace Center (DLR), Institute of Aerospace Medicine, Cologne, Germany

Keywords

Microgravity; Simulation facility; Space environment; Temperature; UV; Vacuum; VUV; X-ray

Definition

Planetary and space simulation facilities are laboratory devices aimed at mimicking extraterrestrial conditions, for example, the conditions of outer space (vacuum, temperature, radiation), of spaceflight, or those of other planets (atmospheric composition and pressure, temperature fluctuations, radiation for ▶ Mars) or moons (gas mixture, pressure, low temperature for Saturn's moon Titan). They are valuable instruments in the preparation of flight experiments (selection of suitable biological candidates, chemical compounds, and hardware material for astrobiological and space biological experiments in Earth orbit), for assessing the habitability of other planets (e.g., of Mars), or for studying different physical or chemical processes (e.g., for Titan).

Overview

Planetary and space simulation facilities allow a broad range of tests of biological and chemical as well as physical material individually or integrated into space hardware. The results of these experiments support the design optimization and verification of spacecraft devices, the selection of the most promising biological and chemical material for flight experiments, and the selection of search for life experiments for planetary missions. The following extraterrestrial conditions have been simulated for astrobiology purposes:

- *Simulation of outer space conditions*: Space simulation facilities have been first developed for testing and qualifying space hardware. Test parameters were ultrahigh vacuum, low temperature, extraterrestrial solar ▶ UV radiation, and X-rays for the simulation of the ionizing component in space. With the increasing interest in astrobiology, these facilities were adapted to exposures of organics and biological organisms to simulated space (Horneck 1999; Rabbow et al. 2005). Space simulation facilities have the common construction principle of stainless steel cylinders of different sizes equipped with numerous flanges and ports for instrumentation and observation. The main vacuum chamber is connected to different high-performance pumping systems to generate a lowest possible

vacuum for the simulation of representative space conditions. A solar simulator, consisting of an array of powerful lamps, reproduces the extraterrestrial solar electromagnetic radiation (from ultraviolet to infrared radiation) at high intensities. Optical filter system allows the selection of desired wavelength bands and controlled intensities of the radiation. Furthermore, cryogenic systems provide controlled temperatures. Space simulation facilities were intensely used in preparation of the astrobiology exposure experiments in space, such as those using the space ▶ exposure facilities on Spacelab 1 and D2, ▶ ERA on ▶ EURECA, Exostack on LDEF, ▶ BIOPAN on Foton, and ▶ EXPOSE on the ISS (Cockell et al. 2005; Fekete et al. 2005; de la Torre et al. 2007; Rabbow et al. 2009). They were used as test systems in the preparation of the flight experiments, as well as for the simultaneous ground control experiments (Fig. 1).

- *Simulation of spaceflight (microgravity) conditions*: Various ground-based methodologies have been employed to simulate microgravity for studying its effects on microorganisms, cells, and small biological objects. One of the most common devices used to provide a functional weightlessness is the clinostat. Sedimentation is compensated by fast rotating a small sample centered on a horizontally positioned axis perpendicular to the direction of the gravity vector. Another device is a rotating wall vessel (RWV) bioreactor. While maintaining cells in suspension as they continuously fall through the medium under $1 \times g$ conditions, the RWV bioreactor can also induce a perfusion of nutrients to and waste from the cell environment. Other approaches for exploring the effect of altered gravity conditions on living systems while still on Earth are free fall, neutral buoyancy, and diamagnetic levitation (Clément and Slenska 2006; Horneck et al. 2010)
- *Simulation of planetary surface conditions*: The evolution of facilities for simulating Mars conditions has progressed over time from very simple anoxic systems to highly sophisticated simulation chambers (reviewed by Hansen 2007). They generally consist of a stainless steel chamber with control of gas composition, pressure, temperature, and humidity as well as provision of a UV radiation source with optical filters simulating the UV radiation climate of Mars (Schuerger et al. 2003, 2006; Tauscher et al. 2006; Jensen et al. 2008; Osman et al. 2008; de Vera et al. 2010).

Planetary and Space Simulation Facilities, Fig. 1 Ground tests of the astrobiology experiments accommodated in the exposure tray of the Exobiology Radiation Assembly (ERA) of the European EURECA mission. Tests were performed within the planetary and space simulation facilities at the DLR (Photo courtesy DLR)

See Also

- ▶ BIOPAN
- ▶ Cosmic Rays in the Heliosphere
- ▶ Desiccation
- ▶ Environment
- ▶ ERA
- ▶ EURECA

- ▶ Expose
- ▶ Exposure Facilities
- ▶ Extreme Ultraviolet Light
- ▶ Foton Capsule, Spacecraft
- ▶ Gravitational Biology
- ▶ Habitat
- ▶ International Space Station
- ▶ Ionizing Radiation, Biological Effects
- ▶ Mars
- ▶ Microgravity
- ▶ Radiation Biology
- ▶ Solar UV Radiation, Biological Effects
- ▶ Space Biology
- ▶ Space Environment
- ▶ Space Vacuum Effects
- ▶ UV Climate
- ▶ UV Radiation
- ▶ UV Radiation, Biological Effects
- ▶ UV Radiation Dose

References and Further Reading

Clément G, Slenska K (eds) (2006) Fundamentals of space biology – research on cells, animals, and plants in space. Space Technology Library with Microcosm Press and Springer, El Segundo

Cockell CS, Schuerger AC, Billi D, Friedmann EI, Panitz C (2005) Effects of a simulated Martian UV flux on the cyanobacterium, *Chroococcidiopsis* sp. 029. Astrobiology 5:127–140

de la Torre NR, Sancho LG, Pintado A, Rettberg P, Rabbow E, Panitz C, Deutschmann U, Reina M, Horneck G (2007) BIOPAN experiment LICHENS on the Foton M2 mission pre-flight verification tests of the *Rhizocarpon geographicum*-granite ecosystem. Adv Space Res 40:1665–1671

de Vera J-P, Möhlmann D, Butina F, Lorek A, Wernecke R, Ott S (2010) Survival potential and photosynthetic activity of lichens under Mars-like conditions: a laboratory study. Astrobiology 10:215–227

Fekete A, Modos K, Hegedüs M, Kovacs G, Gy R, Peter A, Lammer H, Panitz C (2005) DNA damage under simulated extraterrestrial conditions in bacteriophage T7. Adv Space Res 36:305–310

Häder D-P, Hemmersbach R, Lebert M (2005) Gravity and the behavior of unicellular organisms. Cambridge University Press, Cambridge

Hansen AA (2007) Mars simulations – past studies on the biological response to simulated Martian conditions. In: Cockell CS, Horneck G (eds) Response of organisms to the Martian environment. ESA SP-1299. ESA/ESTEC, Noordwijk

Horneck G (1999) Astrobiological studies of microbes in simulated interplanetary space. In: Ehrenfreund P, Kraft C, Kochan H, Pironello V (eds) Laboratory astrophysics and space research. Kluwer, Dordrecht, pp 667–685

Horneck G, Klaus D, Mancinelli RL (2010) Space microbiology. Mol Microbiol Rev 74:121–156

Jensen LL, Merrison J, Hansen AA, Mikkelsen KA, Kristoffersen T, Nørnberg P, Lomstein BA, Finster K (2008) A facility for long-term Mars simulation experiments: the Mars environmental simulation chamber (MESCH). Astrobiology 8:537–548

Osman S, Peeters Z, La Duc MT, Mancinelli R, Ehrenfreund P, Venkateswaran K (2008) Effect of shadowing on survival of bacteria under conditions simulating the Martian atmosphere and UV radiation. Appl Environ Microbiol 74:959–970

Rabbow E, Rettberg P, Panitz C, Drescher J, Horneck G, Reitz G (2005) SSIOUX – space simulation for investigating organics, evolution and exobiology. Adv Space Res 36:297–302

Rabbow E, Horneck G, Rettberg P, Schott J-U, Panitz C, L'Afflitto A, von Heise-Rotenburg R, Willnecker R, Baglioni P, Hatton J, Dettmann J, Demets R, Reitz G (2009) EXPOSE, an astrobiological exposure facility on the international space station – from proposal to flight. Orig Life Evol Biosph 39:581–598

Schuerger AC, Mancinelli RL, Kern RG, Rothschild LJ, McKay CP (2003) Survival of endospores of *Bacillus subtilis* on spacecraft surfaces under simulated Martian environments: implications for the forward contamination of Mars. Icarus 165:253–276

Schuerger AC, Richards JT, Newcombe DA, Venkateswaran KJ (2006) Rapid inactivation of seven *Bacillus* spp. under simulated Mars UV irradiation suggests minimum forward contamination around landing sites. Icarus 181:52–62

Tauscher C, Schuerger AC, Nicholson WL (2006) Survival and germinability of *Bacillus subtilis* spores exposed to simulated Mars solar radiation: Implications for life detection and planetary protection. Astrobiology 6:592–605

Planetary Chronostratigraphy

- ▶ Chronostratigraphy

Planetary Core

- ▶ Core, Planetary

Planetary Debris Disks

► Debris Disk

Planetary Ecosynthesis

Christopher P. McKay
NASA Ames Research Center, Moffett Field, CA, USA

Keywords

Biospheres; Global ecology; Life; Mars; Terraforming

Synonyms

Ecopoesis; Terraforming

Definition

Planetary Ecosynthesis: The purposeful alteration of another planetary environment so as to improve the chances of survival of an indigenous biology or, in the absence of any native life-forms, to allow for habitation of most, if not all, terrestrial life-forms.

History

Terraforming was first used as a word in a science fiction short story in 1942 by Jack Williamson. The first scientific discussion was a suggestion by Carl Sagan, as part of a paper in *Science*, to remove the thick carbon dioxide atmosphere of ► Venus by seeding the planet with algae. The seminal suggestion to use supergreenhouse gases to warm ► Mars was made by Lovelock and Allaby (1984) in their science fiction book *The Greening of Mars*. The first technical paper dealing entirely with terraforming was in *Nature* in 1991 by Chris McKay, Brian Toon, and James Kasting, entitled *Making Mars Habitable* The first discussion of the environmental ethics issues appeared in 1990 in the book *Moral Expertise* in chapters written by Robert Haynes and by Chris McKay. In 1997, the NASA Astrobiology Institute included as one of its six founding questions "What is the potential for survival and biological evolution beyond the planet of origin?" The two international journals *Astrobiology* and the *International Journal of Astrobiology* both include terraforming studies in the scope of papers they publish.

Overview

Terraforming has been discussed for the Moon, Venus, Mars, and Titan (the moon of Saturn). Only for Mars does planetary ecosynthesis appear feasible in the near term. Mars appears to have had habitable conditions in the past, and the fundamental challenge of restoring habitable conditions to Mars is to warm the planet from its current −60 °C to somewhat over 10 °C. Humans have demonstrated the technology to warm the Earth by a few degrees using greenhouse gases. On Mars, the warming needed would be tens of degrees – many times larger than on Earth. The materials needed to construct a biosphere are water, carbon dioxide, and nitrogen. These are likely to be present on Mars in adequate supply, although there is uncertainty in the total nitrogen available. The fundamental physical aspects of Mars that would be virtually impossible to alter, such as axial tilt, rotation rate, and eccentricity, are similar to the corresponding values for Earth, except for surface gravity, which is 0.38 of the Earth value. If the sunlight incident on Mars was captured with 100 % efficiency, it would take only ∼10 years to warm that planet. Greenhouse gas efficiencies of 10 % are plausible, and thus,

the timescale for warming Mars is ~100 years. In contrast, it would take over 100,000 years to produce enough oxygen on Mars to support humans, and this is based on the optimistic assumption that the efficiency for oxygen production of Mars' biosphere would be the same as Earth's current biosphere. Thus, warming Mars and recreating a thick carbon dioxide atmosphere is within current technology and human timeframes, but creating an oxygen-rich atmosphere is not. Humans would require a source of oxygen, but many microorganisms, some plants, and even a few animals could survive despite the low oxygen content. The practical method to warm Mars involves low levels of supergreenhouse gases composed only of the elements F, S, C, and H. Supergreenhouse gases containing Cl and Br are not used because of the effect these gases have on ozone. If there is enough carbon dioxide ice present in the polar regions of Mars, then a warming of 20 °C caused by artificially produced greenhouse gases would cause the complete evaporation of that ice through a positive feedback mechanism. The first ecosystems on Mars would probably resemble alpine ecosystems. A key biological threshold would be the first growth of trees – treeline.

See Also

- ▶ Mars
- ▶ Venus

References and Further Reading

Averner MM, MacElroy RD (1976) On the habitability of Mars: an approach to planetary ecosynthesis. NASA SP-414

Fogg MJ (1995) Terraforming: engineering planetary environments. SAE International, Warrendale

Lovelock J, Allaby M (1984) The greening of Mars. St. Martin's Press and Warner Books, New York

Marinova MM, McKay CP, Hashimoto H (2005) Radiative-convective model of warming Mars with artificial greenhouse gases. J Geophys Res 110, E03002. doi:10.1029/2004JE002306

McKay CP (2009) Planetary ecosynthesis on Mars: restoration ecology and environmental ethics. In: Bertka C (ed) Exploring the origin, extent, and future of life: philosophical, ethical, and theological perspectives. Cambridge Astrobiology, New York, pp 245–260

McKay CP, Haynes RH (1990) Should we implant life on Mars? Sci Am 263(6):144

McKay CP, Toon OB, Kasting JF (1991) Making Mars habitable. Nature 352:489–496

Planetary Embryo

Yann Alibert[1] and Ravit Helled[2]
[1]Space Research and Planetary Sciences, Physics Institute, University of Bern, Bern, Swiss
[2]Geophysical, Atmospheric and Planetary Sciences, Tel Aviv University, Raymond and Beverly Sackler Faculty of Exact Sciences, Tel Aviv, Israel

Keywords

Planet formation; Solar nebula

Definition

In ▶ Planet Formation theory, planetary embryos are solid bodies that dominate gravitationally in their ▶ Feeding Zone. Planetary embryos form from ▶ planetesimals, with the formation process leading to a bifurcated mass distribution as a result of ▶ oligarchic growth; they typically have masses of fractions of an Earth mass.

See Also

- ▶ Feeding Zone
- ▶ Oligarchic Growth
- ▶ Planetesimals
- ▶ Planet Formation

Planetary Evolution

Jean-Pierre Bibring
Institut d'Astrophysique Spatiale, Université Paris Sud, Orsay, France

Keywords

Planets; Solar system evolution

Definition

All solar system bodies (planets, satellites) show an extraordinary diversity in their physical aspect and properties. This entry describes the different physicochemical processes involved in the evolution of a planet, which may be responsible for changes in its internal structure, surface, atmosphere, or magnetosphere, and eventually account for such a diversity.

Overview

From Motion to Evolution

Planets (*vagabonds*, in Greek) have first been recognized and characterized by their apparent movements in space, traveling among the fixed frame of stars. Their motion was proposed as heliocentric by Copernicus and then formalized by Newton; this ended a long, complex, and tough quest, over centuries, with more and more accurate measurements contradicting the dogma of a centrally located Earth. A critical outcome has been that the Earth and the planets belong to the same family. As a consequence, the fact that the Earth has a History and thus evolves implies that all planets do, possibly in a manner similar to the Earth: worlds' plurality has long been a concept of reference.

However, the prime role of the Sun in controlling the planetary motion and their illumination has erroneously been extrapolated to most, if not all planetary properties: that they would be primarily influenced by the solar gravitational and electromagnetic fields. The planets would thus differ from stars in their lack of energetic means to evolve by themselves: they would essentially simply respond to solar inputs.

Space exploration has dramatically modified this view, in enabling close and in situ analyses of the planets and satellites, which had long remained poorly resolved objects in ground telescopic observations. All these objects exhibit a degree of diversity totally unexpected, and far beyond what could be achieved if the Sun was solely responsible of their evolution.

The state of the four Jovian Galilean satellites, revealed by the NASA/Voyager flybys in 1979, is exemplary of this diversity: these bodies, of similar mass, location, and age, have followed totally distinct evolutionary pathways. Io has been discovered to be a world of extreme volcanic activity, the most intense of the entire solar system: its surface is entirely reprocessed on a timescale of some thousands of years. The surface of ▶ Callisto is still saturated with impact craters acquired just after it formed, during the heavy bombardment period; no global resetting seems to have erased this ancient record. ▶ Europa is entirely covered with a thick layer of fresh water ice, with a number of crevasses and no craters nor volcanoes. ▶ Ganymede is a mixture of rocks and ices, with faults and other features recording past tectonic activity.

The inner planets exhibit similar contrasts. ▶ Mars has a few but giant volcanoes, all having ceased to outflow; none are observed on ▶ Mercury, but thousands on ▶ Venus. The atmospheric pressure varies from 90 bars at Venus, down to 10 mbars at Mars, and almost zero at Mercury. The cloud coverage varies from none, for Mercury and the Moon, to full, for Venus; the Earth is somewhat in between Venus and Mars, for both its atmospheric pressure and cloud cover. Apart from the Earth, no object, within the solar system, has been found sustaining liquid water at its surface.

This high degree of diversity strikingly contrasts with the large commonalities in their origin that all solar system objects share: the catastrophic origin of the planets has been definitely abandoned in favor of their being accreted in a single

collapsing molecular cloud, formed at the same time (some 4.57 billions of years ago), at the same location in our Galaxy, from essentially the same material. How to account for their differences? What triggers and drives planetary evolution?

It is one of the prime goals of planetary exploration to characterize the specificities of each planet and to derive the clues of their distinct evolution. A central focus is on the Earth, with particular still unresolved questions such as what are the unique conditions that prevailed and still do, which harbored life and maintained its adaptive evolution, up to now? What are the subtle processes at work that sustain the biosphere, with a highly specific ocean and cloud cover? These questions are not of mere curiosity, as our environment changes with an increasingly shortening timescale, now only decades.

To address these questions, as for any dynamical system, one needs to decipher both the *initial conditions* that shaped the planetary evolution, and the *energies* at work all along their history.

Initial Conditions

The initial conditions of planetary formation consist actually in a sequence of processes, over millions to tens and hundreds millions of years.

During its collapse, the protosolar cloud has been subjected to a very specific chemical evolution, ending with a highly complex molecular mixture dominated by H_2, with abundant H_2O and a wide variety of C-rich species. In particular, large carbon chains were built, giving rise to refractory organics – possibly with chirality trapped in. The cloud was first heated by the energy released while the central core was collapsing, until it reached thermodynamic equilibrium. The p-p thermonuclear chain then started; the Sun, as a star, was born. The emitted radiation blocked further collapse. The cloud started cooling, and minerals condensed through a sequence primarily dictated by the elemental and molecular composition of the gas. At distances far enough for H_2O ice to become stable, it constituted the most abundant solid phase: the growing bodies accreted predominantly water ice, as a matrix in which most other grains and species, including the organics, were trapped.

The composition of the material subjected to collisions did thus strongly vary with heliocentric distance. Within the inner solar system, minerals were the only solid grains. Slow enough collisions (typically less than hundreds of meters per second) led to accretion of ▶ planetesimals, some of which accreted further to become planetary embryos; they were essentially anhydrous. At larger distances, water ice started to be stable, first as a minor constituent (>2 astronomical units, AU), then as a major one for >4 AU, typically. Large ice-rich bodies of ~10 terrestrial masses grew fast enough to trap and bind gravitationally the surrounding nebula, ending as "giant" gaseous planets. The rapid formation of ▶ Jupiter, and to a lesser extent of ▶ Saturn, had a major impact on the further evolution of the entire nebula by the gravitational perturbations they induced, both in the inner and outer parts of the system.

Although this is not fully confirmed yet, Jupiter and Saturn did actually migrate, in a very specific pattern that severely modeled the further evolution of most solar system objects. In this scenario referred to as the "Nice model", Jupiter migrated inward first, emptying most of the disk from their planetesimals, down about 1.5 astronomical units (AU). Saturn then arrived, at a distance corresponding to a 2/3 resonance with Jupiter. The mass ratio of these two large bodies prevent them to pursue their inward migration, and made them migrating outward, blocked in this resonance, leaving most of the inner disk confined within 1 AU: its further evolution led to the accretion of the inner planets with their proper mass distribution, characterized by Mars being much smaller than Earth. This accretion was accompanied with inner grains ejected outward, and outer materials injected to the growing inner protoplanets, which led to both repopulating the asteroidal belt, and feeding the inner planets with water and other volatile compounds. When stabilized close to their present orbit, Jupiter and Saturn gravitational perturbations to objects forming closer and beyond, resulted in stopping their growth, as "small bodies", which preserve, up to now, the records of these early times. Some of the later,

predominantly formed of ices and volatile species, were eventually re-ejected into the inner solar system by later (planetary or stellar) perturbations: their partial sublimation when passing close to the Sun (a few astronomical units apart at most) produces "comae" of gases surroundings their nucleus, thus they are being called ► *comets*.

Thus, the growth of Jupiter and other ► giant planets has preserved bodies small enough to have avoided further differentiation, maintaining their pristine composition, in particular in volatile (e.g., H_2O) and organic species. During the early phases of the dynamical evolution of the solar system, collisions played a critical role, in particular when the inner planets, depleted in volatile compounds, were impacted by small bodies formed at larger distances that were thus loaded with low temperature constituents such as ices: this fed the inner planets with large amounts of organics and of water. The terrestrial oceans thus seem to have an extraterrestrial origin. Their seeding with refractory organics might have favored the emergence of biochemistry.

The same process – collisions – which led to planetary accretion for small relative velocities also triggered destruction for large impact velocities (in the kilometer per second range). This explains that the planets and satellites which have, at least partially, preserved the surface structures acquired during the first hundreds of millions of years after they formed are heavily cratered. Actually, some 4 billion years ago, all planets were similarly cratered and looked as most of the Moon and Mercury surface still does. What has differed for planets like the Earth, which no longer exhibits cratered terrains, is their further activity, which erased the records of this ancient bombardment.

The Earth has preserved a key record of its primordial bombardment: its Moon. It is now generally accepted that the formation of the Moon results from a giant impact of a large embryo, with mass of about 1/10 of that of the Earth, on the proto-Earth. This impact deeply modified the further evolution of the Earth. It melted most, if not all of it, and ejected in a disk a large fraction of the impacting embryo, as well as Earth's mantle material. Re-accretion within the disk formed the Moon, whose presence still induces important gravitational (tidal) effects. In particular, it prevented the Earth's obliquity from oscillating around its mean value of 23° by more than 1.5°, which is totally unique in the solar system. Earth has maintained rather steady climatic conditions over its entire history, and this may constitute a key ingredient to the survival of habitable conditions on the Earth, at least for complex organisms. Most of the volatile constituents of the disk fell rapidly back to the Earth. Water in particular was mixed to the outer part of the magma, whose hydration may have eased its convection and contributed to initiating ► plate tectonics.

Other planets might have also been subjected to giant impacts. For example, it has been suggested that the present Mars dichotomy, with its northern hemisphere some 15 km below the altitude of the southern terrains, might have been formed in this way; the two small moons of Mars, Phobos and Deimos, could have re-accreted within the circumplanetary disk. However, their very small mass is insufficient to block the chaotic oscillation of Mars's obliquity, which has driven part of Mars's climatic evolution.

Did the heavy bombardment steadily decrease over the first half billion years, or was it made of more than one episode? No definite answer is available yet, although several lines of evidences seem to favor the second scenario, exhibiting at least two phases of bombardment. The first one, coupled to the planetary accretion, lasted some tens of millions of years; for the Earth, it included, and possibly ended with the giant impact from which the Moon formed. This bombardment dropped with the decline in the number of potential impactors. Some hundreds of millions of years later, the impact rate suddenly increased, giving rise to a "► late heavy bombardment" (LHB) phase. Its possible trigger is the following: During their rapid inward, then outward migration, according to the Nice model, Saturn and Jupiter remained in their 2/3 resonance. However, their gravitational interaction with the outer solar system objects, Uranus and Neptune primarily, broke this resonance

some hundreds of millions years later, leading to a massive inward ejection of grains and bodies (the LHB), giving rise to a violent bombardment of the inner planets, during tens of millions of years, some 4 billion years ago. A large fraction of the craters, still visible on the Moon, Mercury, and Mars, results from this LHB.

It happens that the migration of Jupiter and Saturn stopped at heliocentric distances larger than 1 AU. This is in striking contrast with the situation found in many other stellar systems, in which giant exoplanets are located much closer to their star, as a result of a much longer migration. The evolution of the Earth and other inner planets would likely have been deeply disturbed if Jupiter had spiraled over them rather than staying at significant distances.

The diversity of our present solar system does not merely originate from the early dynamical history. The composition – elemental, isotopic, molecular, and mineralogical – acquired during the accretion also played a key role. It is remarkable that bodies having preserved records of this primordial composition still exist, enabling its deciphering. This is mainly a result of the specific dynamical history of the protosolar nebula, with the rapid growth of the giant planets inhibiting further growth of comets and asteroids, which remain "small bodies": with limited energetic content precluding their thermal modification, they still preserve the composition and properties acquired at the time they formed. They constitute objects of utmost importance to trace back the initial conditions of the solar system, from a compositional standpoint. Their characterization can be performed in two ways: by in situ space exploration and, in the laboratory, by analyses of samples either collected and returned from them, or impact ejected from these parent bodies, as meteorites and micrometeorites.

With the highly sophisticated tools nowadays available, most analyses can be performed down to the scale of individual grains. These methods point out the effects of the isotopic and molecular composition, acquired during the final stages of protoplanetary accretion, on the evolution of the growing bodies. As examples, the "short-lived" radioactive species such as ^{26}Al, trapped together with ^{27}Al in minerals during the condensation sequence, have constituted the dominant energy input at a protoplanetary scale, eventually triggering early mineralogical differentiation of these bodies. Icy grains and hydrated phases, condensed at large heliocentric distances, brought most of the volatile molecules to the inner bodies, including in particular water and complex macromolecules of potential astrobiological relevance.

A fundamental contribution of the isotopic analyses is their enabling of a precise dating of the events that paved the early history of the solar system, within the first tens to hundreds of millions of years following its birth, some 4.57 billion years ago. Some of them are now determined with an accuracy of 1 Ma. One can both identify the processes that were operating within the early solar system and time tag them in a global and accurate cosmo-chronology.

Energy Sources

The sources of energy that sustain activity fundamentally differ between planets and stars. Stellar evolution is essentially driven by the strong interaction, through nuclear reactions triggered by the temperature and pressure produced by the gravitational collapse. At a given point in their life cycle only a few nuclear reactions are enabled, and the stars maintain almost steady global conditions, which allow classifying them in families according to their evolutionary stage. By contrast, all the physical interactions operate for planets, with distinct intensities and time constants, building distinct evolutionary paths and leading to a wide diversity.

The electromagnetic interaction acts predominantly through the solar irradiation. However, photons only penetrate into liquids and solids down to very shallow depths: the solar flux does not contribute to the internal activity. Other electromagnetic effects can operate deep in the planet's interiors, such as phase changes. Whenever gaseous species condense, liquid freezes or solidifies, energy is released. As examples, the formation of helium rain deep in the atmosphere of giant planets might constitute an important energy input for their evolution. Similarly, the

progressive solidification of the outer liquid core within planets releases energy that slows down their transformation.

The gravitational interaction acts through self-collapsing for individual gaseous bodies and through remote interactions for all of them. Tidal effects play specific roles, such as synchronizing rotation and revolution for corotating bodies (planets and satellites). In a few cases, tides may constitute the dominant driver of internal activity. This happens with Io, the closest Galilean satellite, whose strong gravitational lock by Jupiter varies along its ellipcal orbit, and is perturbed by Ganymede and Callisto: the energy dissipated deep within Io's mantle produces the highest degree of volcanism within the entire solar system, with plumes some hundreds of kilometers in altitude. Io's surface is entirely remodeled by volcanic outflows on a timescale of a few thousand years.

The weak nuclear interaction is a key provider of energy, through the radioactive decay of isotopes with time constants similar to the age of the planets (10^9–10^{10} years typically). Actually, only very few such nuclei exist, and those playing the dominant role are ^{238}U, ^{235}U, ^{232}Th, and ^{40}K. Their relative abundance is low, leading to power release in the order of 10^{-8} W/m^3. However, they are present in the bulk of the planetary interior, which makes their input dominate the internal evolution of a variety of planets, in particular of the inner planets, including the Earth.

A specific feature associated with the radioactive energy is its time dependence: as the release is coupled to the transformation of parent nuclei, it necessarily decreases with time. A planet cannot remain in a steady state, as stars do; its activity declines with time. Since the energetic load varies as the volume in which the radioactive species are distributed, while the energy loss operates by surface radiation, the thermal balance depends on the radius. The larger the body, the higher the volume/surface ratio and thus the energy gain/loss ratio, therefore the temperature onset before declining: the later the geological death will occur. This explains why it happened for the Moon some 3 billion years ago, for Mars some tens of millions of years at most, while the Earth is still active. On the other hand, objects small enough (tens of kilometers in size at most) to efficiently radiate their internal energy have escaped major heating and preserved their primitiveness.

Internal Activity

The internal activity depends both on the available energy and on its transportation throughout the object. For example, the initial gravitational energy load produced during accretion is still partially present in most planets, at least in their core: for the Earth, up to half of the total available energy today might still originate from this early input.

A key feature must be outlined. When the temperature gradient enables convection to operate, sustained motions of matter take place, possibly up to the surface: the object is active.

Mineralogical differentiation under gravity precipitates the denser materials downward, leaving the lightest ones toward the surface. A high density (∼8) solid core forms, constituted of metal-rich compounds, dominated by Fe/Ni alloys; it is possibly surrounded by a liquid envelope of similar elemental (metallic) composition. If turbulent convection in this outer liquid core occurs, a dynamo is generated: the planet develops a global magnetic field.

Above the core, a mantle of fused rocks exists, covered by a light crust. As the temperature decreases toward the surface, both the upper part of the mantle and the crust are cold enough to be solid, constituting a *lithosphere* (Greek for "sphere of stones"); the inner part of the mantle down to the core is sufficiently warmed to be fluid, thus it is called an ▶ asthenosphere, swept by convection movements. Upwelling flows of magma slowly solidify as rigid plates as they approach the surface, and then drift horizontally at a velocity of some centimeters per year. They thicken by cooling, until their mass forces them to sink back to the mantle, at *subduction* zones. This latter movement is severely constrained and proceeds by pulses capable of generating earthquakes and tsunamis.

These convective cells drive the global planetary internal activity, known as *plate tectonics*. In

the case of the Earth, most of these plates are covered with oceans. The remaining ~30 % are covered with continents, which are thus carried in the drift of the plates. As the continents are made of material less dense than the underlying floor, they remain at the surface and stay blocked over the subduction zones, where they eventually collide with a continent moving counterward: the shock results in mountains and faults.

This geological evolution typically operates over timescales of tens to hundreds of millions years. With the slow decrease of internal energetic resources, and the correlated thickening of the outer rigid layer, the planet approaches its geological death: it occurs when its surface becomes no longer affected by the internal activity. Only exogenous and atmospheric processes may further drive their evolution.

Atmospheric Evolution

The planetary atmospheres evolve both in composition and density, with timescales ranging from long-term variations to seasonal changes. As an example, the present-day terrestrial atmosphere, with a pressure of one bar dominated by N_2 (78.9 %) and O_2 (20.1 %), differs from the early one in at least two respects: most of the CO_2, whose pressure amounted to tens of bars (as is still the case for Venus), have been dissolved and trapped into carbonates, thanks to the sustained presence of stable oceans, leaving N_2 the most abundant species; on the contrary, most of the present O_2 appeared long after the planet formed. It results from the photosynthetic activity of living organisms, as an outcome of their building C-rich molecules from CO_2. Both these changes operated over hundreds of millions of years. By contrast, a huge enrichment of the amount of CO_2 is observed nowadays, with timescales of decades, most likely as a result of human activity – most energy is produced through the combustion of C-rich molecules (oil, coal, wood).

Importantly, the atmospheric content in major, minor, and trace elements does depend on the planet's internal activity, in at least two ways: through outgassing mostly coupled to volcanic activity and through plate tectonics. For example, a fraction of the CO_2 originates from the dissociation of carbonates within continents reaching subduction zones. As such, the radioactive energy plays a key atmospheric – and thus climatic – role in sustaining the recycling of key species, as discussed below for greenhouse gases.

However, by far the dominant energy source that drives atmospheric processes originates from the solar irradiation. The radiation transfer is highly dependent on the composition of the atmospheric constituents: gases, clouds, ices, aerosols, and grains. A complex photochemistry takes place, thermodynamically constrained, resulting both in a layering of the atmosphere and in its movement, with circulation loops at different scales.

These interactions translate into a specific thermal profile of the atmosphere, well described in the case of the Earth. The temperature profile exhibits three *inversion* layers (inversion of the sign of temperature vertical gradient). From the surface upward, the temperature slowly decreases within the *troposphere*, mostly heated by contact with the surface. At some 20 km in altitude, the thermal gradient becomes positive: in the overlying *stratosphere*, the temperature increases, through the absorption of ultraviolet (UV) solar photons. O_2 is dissociated and the freed O atoms, reacting primarily with O_2 and N_2, form ozone (O_3) and a variety of N-rich molecules, blocking all the UV solar photons. The stratosphere thus shields the troposphere against the lethal effects of these high-energy photons. The upper limit of the stratosphere (~40 km) is defined by the pressure above which the cross section for the O_2 photodissociation becomes marginal (the pressure is too low): in the absence of photon absorption, the temperature thus decreases with altitude in the *mesosphere*, as it does in the troposphere. At still higher altitudes (~80 km), solar X-rays are absorbed and ionize the atoms: the top atmospheric layer above the mesosphere is accordingly named the *ionosphere*.

Consequently, the incoming solar flux is progressively depleted in its high-energy photons (X, UV), in the ionosphere and then the stratosphere, before entering the troposphere, where the visible wavelengths (0.4–0.8 μm) dominate.

The photons that are not reflected (mostly by the clouds and the surface ice) are absorbed on the ground. They are then reemitted with a distinct energy distribution, imposed by the surface temperature, which is some 20 times lower than that of the solar photosphere: their spectrum covers primarily the infrared (IR) range, according to Planck's law. Minor constituents of the terrestrial atmosphere, such as H_2O and CO_2, have no transition in the visible, but strong vibration modes in the IR: they are transparent to the incoming solar flux, but highly absorbing for the radiation emitted by the surface at longer wavelength. They constitute very efficient *greenhouse* gases responsible for an increase in the Earth's surface temperature of $\sim 33°$. More generally, the surface temperature of a planet, in particular with respect to water stability, does not merely depend on the solar influx, but also on its atmospheric composition, in particular with respect to its content in greenhouse gases.

The orbital evolution of the planets has strong effects on their level of insulation. Over the year, the total amount of solar energy received varies with the distance to the Sun, with larger variations for more eccentric orbits. In addition, the insulation depends on the obliquity, defined as the angle between the planetary axis of rotation and the orbit plane – known as the ecliptic. The Earth is closer to the Sun in early January; it receives some 6 % more energy in northern winters than in northern summers which, given the distribution of continents and oceans, contributes to damping the global annual temperature variations. This configuration changes over time, as the axis of rotation spins with a period of some 25,000 years (precession of the equinoxes). Actually, all orbital parameters vary with time, which induces variations of most climatic parameters, primarily of the temperature distribution with average amplitude changes of some degrees. This is the major driver of the recurrent glaciations, as first demonstrated by Milutin Milanković.

An important factor that dictates the temperature of the lower atmosphere is the cloud coverage, which strongly differs from one planet to the next. The cloud ▶ albedo is high enough to reflect a large fraction of the incident solar flux: terrestrial cumulus clouds block up to 50 % of the incoming energy. Has their coverage changed with time, which would have led to significant variations of the global averaged temperature? Actually, a definite answer cannot be given yet, since cloud formation results from a rather complex suite of processes, involving still unknown nucleation sites on which water or other molecules condense, if enabled by thermodynamics. This microphysics remains an era of deep studies, with potential major outcomes for the present climatic change operating on Earth: clouds, which have a greenhouse effect given their composition, are also cooling agents by reflecting a fraction of the incident solar input, thus decreasing the energy available at lower altitudes. The potential for part of the water, which increasingly evaporates from the oceans as the temperature rises, to condense as clouds might thus constitute an efficient retroactive means to control the global temperature.

Altogether, the evolution of planets result from a highly complex coupling of processes involving all forces, with often key roles played by minor or trace species, such as long-lived radioactive isotopes for the internal activity, greenhouse gases for surface temperatures, and nucleation sites for cloud formation. The early dynamical evolution has paved the entire solar system history with unique properties.

The more we observe and decipher this complexity, the more we realize that the diversity we discover does not result from observational biases, but rather constitutes a key feature of planetary evolution.

See Also

- ▶ Chronological History of Life on Earth
- ▶ Cratering Chronology
- ▶ Differentiation, Planetary
- ▶ Giant Planets
- ▶ Late Heavy Bombardment
- ▶ Lithosphere, Planetary
- ▶ Planetesimals
- ▶ Plate Tectonics
- ▶ Protosolar Nebula, Minimum Mass

Planetary Migration

Avi M. Mandell
NASA Goddard Space Flight Center, Greenbelt, MD, USA

Keywords

Type I migration; Type II migration; Type III migration

Synonyms

Tidal migration

Definition

Planetary migration is the decrease or increase in the orbital radius of a planet embedded in a ▶ protoplanetary disk due to interactions with the surrounding gas and/or solid material. Migration occurs when a planetary body loses or gains orbital angular momentum due to either friction (either through aerodynamic drag with the surrounding gas or dynamical friction with surrounding smaller planetesimals) or the imbalance of momentum transfer between the planetary body and the nearby disk material. Planetary migration is thought to account for the position of giant extrasolar planets discovered orbiting at very small orbital radii and may be an important dynamical process in the evolution of protoplanetary bodies of all sizes.

Overview

Prior to the discovery of the first extrasolar planets orbiting very close to their parent stars, planets were thought to form and evolve in the same general region of a planetary system over their whole lifetime (unless a planet's orbit was dramatically altered due to scattering from a close encounter with another planetary body). Small planetesimals would grow into larger bodies by accreting nearby material, and accretion would stop when a planet had depleted its local orbital region of material. In this relatively quiescent picture of ▶ planet formation, a mature planet found at a specific orbital radius could be assumed to have formed in situ from a collection of smaller bodies with similar compositional properties.

However, the existence of giant planets at small orbital radii immediately confounded the idea that all planets form and remain in their initial orbital locations. Giant planets are composed primarily of a massive gaseous atmosphere and for the atmosphere to gravitationally contract the planet must form in a relatively cold region of the disk (beyond ~3 AU; Bodenheimer et al. 2000). The first extrasolar planet, a Jupiter-mass planet orbiting at 0.04 AU, therefore, suggested that some mechanism must have transferred the planet from the outer regions of the system to its current location.

The theory of planetary migration had been postulated prior to the discovery of close-in extrasolar planets; in fact, dynamical theorists might have predicted the existence of these planets if they had correctly interpreted their results on the evolution of giant planets embedded in viscously evolving protoplanetary disks. Papaloizou and Lin (1984), and Lin and Papaloizou (1986), first showed that a planet with a mass significantly large with respect to a surrounding gaseous nebula could open a gap in the disk, leading to angular momentum transfer between the inner and outer regions of the disk and the planet. They correctly showed that this would lead to orbital migration of the planet if the difference in mass between the two regions of the disk was significant; the authors, therefore, concluded that the amount of nebular gas interior and exterior to Jupiter's formation region in our own Solar System must have been equal to 0.1 M_{Sun} in order to avoid the rapid migration of Jupiter either inward or outward. This mechanism for planetary migration, eventually codified as "type II" gas-driven migration by Ward (1997), was immediately posited as the process responsible for transporting extrasolar giant planets to very small orbital radii (Lin et al. 1996).

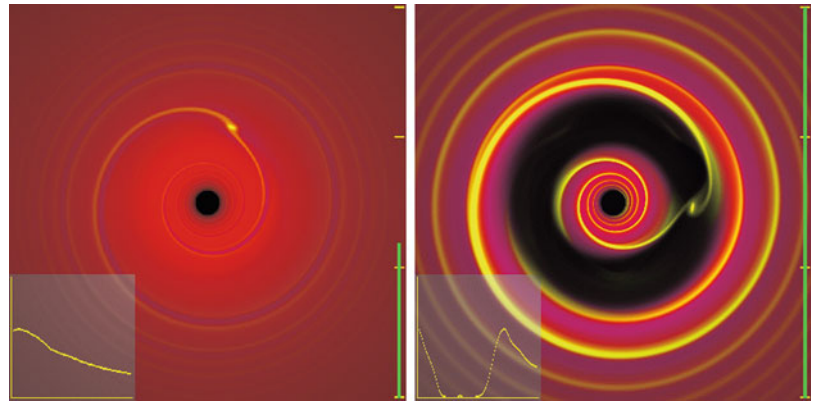

Planetary Migration, Fig. 1 Results from simulations of gas-driven migration, showing the disk density for a planet that is unable to open a gap and therefore experiences "type I" migration (*left*) compared with a high-mass planet that clears a gap and experiences "type II" migration (*right*) (Source: Armitage and Rice 2005)

In the next paragraph, we will discuss the various theoretical mechanisms for orbital migration in a circumstellar disk of planetary and protoplanetary bodies, ranging from giant planets down to micron-size dust particles, and the current evidence for the role that each process plays in the evolution of a planetary system. Please note that there exists another type of orbital migartin due to tidal interactions between a star and planet (see Tides).

Migration Mechanism

Gas-Driven Migration

Gas-driven migration refers to a loss of orbital angular momentum from a planet due to gravitational interactions with the gaseous disk. This mechanism is the most common process referred to when discussing planetary migration, due to the early adoption of gas-driven migration as the most likely scenario to explain the existence of close-in extrasolar planets. As the name suggests, type II gas-driven migration was not actually the original form of gas-driven migration proposed. "Type I" gas-driven migration, first theorized by Goldreich and Tremaine (1980) and discussed in more detail by Ward (1986), operates on planets whose mass is low enough (thought to be close to the mass of Saturn for a disk around a solar-type star) to avoid perturbing the disk enough to open a gap. Type II gas-driven migration describes a similar mechanism for higher-mass planets which perturb the disk enough to block the infall of gas toward the star and create a gap, leading to the locking of the planet with the viscous evolution of the disk (i.e., the spiralling in of the disk material onto the central star) (Fig. 1).

Type I Gas-Driven Migration

Type I gas-driven migration relies on the torques exerted on a planet from density waves that are excited in the gaseous material close to the planet's Lindblad resonances (the orbital locations relative to a planet where the orbital period of a satellite around the planet equals the orbital period of the planet around the star, leading to a resonant orbital motion). These density waves remove energy from the planet, which can lead to a decrease in the orbital velocity and an inward migration. The originally calculated timescale for an Earth-mass body to fall into the central star from 5 AU due to type I gas-driven migration was $\sim 10^4$ years, making this process the most rapid migration mechanism acting in protoplanetary disks and a huge problem for the survival of planets, since the lifetime of a gaseous protoplanetary disk is $\sim 5 \times 10^6$ years. The rate of type I migration increases with increasing planet mass until the planet reaches the gap-opening threshold.

Research is ongoing to determine how type I gas-driven migration is slowed (it must be slowed since we observe planets the size of Earth and larger in both our own Solar System and other planetary systems, so they must survive). Initial models for calculating the migration efficiency assumed a very simplistic version of a

protoplanetary disk: no turbulence, no temperature variations, constant viscosity throughout the disk, etc. Many different theories are being explored that rely on more realistic details of the disk conditions and structure to decrease the migration rate, and it is currently unclear which slowing mechanisms are dominant in different disk conditions. The most promising theories focus on non-isothermal conditions near the planet and the resulting effects on energy transfer (Jang-Condell and Sasselov 2005; Paardekooper and Mellema 2008), and inclusion of turbulence (e.g., Laughlin et al. 2004) and investigations of "dead zones" in the disk where the disk viscosity drops to near zero, leading to a dramatic decrease in the energy transfer rate between the planet and the disk (Oishi et al. 2007). In recent years, large progress has been made in the determination of the planetary migration rate, for different thermoynamical properties regimes in the protoplanetary disk (Paardekooper et al. 2011).

Type II Gas-Driven Migration

As stated above, the mechanism known as type II gas-driven migration becomes important when a planet becomes large enough to be comparable with the scale height of the disk, causing all the material in an annulus around the star to either be accreted onto the planet or transferred out of the orbital region by mass transfer to the outer disk. Once the annulus is cleared, no material is transferred across the boundary, but the planet is still gravitationally pulled toward a faster orbital velocity by material from the inner disk, while losing angular momentum to material in the outer disk. If the outer disk is more massive, this transfer of angular momentum is imbalanced and the planet loses energy and spirals inward. Since the planet is locked to the viscous evolution of the disk, it migrates at a rate unrelated to the mass of the planet; two-dimensional and three-dimensional simulations suggest timescales of $\sim 10^5$ years for the migration time from 5 AU (D'Angelo et al. 2003).

This timescale is still shorter than the dissipation of the disk, and therefore a stopping mechanism must be invoked to stop planets from falling into the central star. Initial stopping mechanisms invoked interactions with the central star to explain the origin of close-in giant planets – either a removal of disk material by some process such as magnetospheric clearing or photoevaporation, or tidal interactions with a rapidly rotating star (Lin et al. 1996). However, these mechanisms are only applicable at very small distances from the parent star. For planets from 0.1 AU out to 3 AU, there must be either a different stopping mechanism or a different migration mechanism at work. The explanation of last resort has always been the "last of the Mohicans" argument, which suggests that the only planets we see are the last ones to migrate in and become stranded when the disk finally dissipates (Trilling et al. 1998). However, the currently favored explanation is that when two or more planets form in relative proximity in time and orbital radius, they can quickly migrate into a resonant relationship (such as the 3:2 ▶ mean-motion resonance), at which point their gaps can overlap and cause them to cease migrating or even reverse their migration direction (Morbidelli and Crida 2007; Morbidelli et al. 2007). This explains the lack of a close-in extrasolar planet in the Solar System, while leaving considerable parameter space for a wide range of planetary configurations. In addition, planetary systems with more than one planet can become unstable after the gas disk dissipates, scattering one planet out of the system and leaving only a single remaining giant planet in an eccentric orbit – a scenario observed frequently in extrasolar planetary systems.

Migration Due to Aerodynamic Drag

Gas-driven migration is effective for both giant planets (type II) and Earth-mass planets down to km-sized bodies (type I), but the gaseous disk also leads to migration of very small planetsimals ($r < 1$ m) due to aerodynamic drag. First analyzed with respect to protoplanetary disks by Adachi et al. (1976), frictional drag due to a particle's motion through the gaseous disk can lead to eccentricity and inclination damping and inward radial migration on timescales as short at 100 years from 1 AU for cm-sized particles. For smaller particles, the grains become entrained with the gas and their differential velocity decreases; for larger particles, the aerodynamic

drag force is too small to affect the angular momentum of the body significantly.

Drag forces can help to enhance the growth of bodies as a result of accretion, by damping collisional velocities between particles, but this would be of no consequence if particles were quickly lost into the central star on 100-year timescales. This problem is called the "cm-sized barrier," connoting the difficulty of growing planetesimals beyond this limit, since traditional collisional accretion timescales for expected particle densities are much longer than 100 years. Possible solutions to this problem include rapid planetesimal growth due to gravitational instabilities, which have recently been shown to form km-sized bodies from pebbles over the course of 5–10 orbital timescales (Johansen et al. 2009), as well as phenomena that could cause pileups of inwardly drifting material in the disk, such as condensation fronts (Stevenson and Lunine 1988). Radial migration of small bodies due to aerodynamic drag may also have had a beneficial effect on planet formation and habitability by delivering volatile-rich bodies from the outer solar system into the dry inner disk, leading to increased water contents for the terrestrial planets (e.g., Ciesla and Cuzzi 2006).

Planetesimal-Driven Migration

Planetary migration can also be achieved without the need for a gaseous disk. Loss of angular momentum from a planet can be achieved by transferring it to smaller nearby solid bodies during a scattering event. First suggested by Safronov (1972), the mechanism was first modeled numerically by Fernandez and Ip (1984) for giant planets in the Solar System, and the outward migration of Neptune due to the scattering of outer-disk planetesimals can be traced by mapping the scattered and resonant ▶ Kuiper Belt objects (e.g., Malhotra 1993). More recently, inward migration of the giant planets in the Solar System due to planetsimal scattering was invoked to explain the Late Heavy Bombardment as a critical aspect of the "▶ Nice model" (Gomes et al. 2005). According to the Nice model, Jupiter and Saturn would slowly have migrated inward due to the migration instability, eventually crossing into a mean-motion resonance which pumped up their eccentricities dramatically, leading to a chaotic reshuffling of the outer Solar System.

The planetesimal-driven migration instability has also been suggested as an important migration mechanism in extrasolar planetary systems (Murray et al. 1998). However, in order to move a Jupiter-mass planet from the outer system all the way to within 0.1 AU of the star, a disk with approximately 1 Jupiter mass of planetesimals would be required interior to the planet's original orbit. This would require a massive disk ($\sim$0.1 M_{Sun}), and while this is not impossible, it would be unlikely to be responsible for the bulk of migration in extrasolar planetary systems.

See Also

- ▶ Exoplanets, Discovery
- ▶ Gas Drag
- ▶ Hot Jupiters
- ▶ Mean Motion Resonance
- ▶ Nice Model
- ▶ Planetesimals
- ▶ Planet Formation
- ▶ Protoplanetary Disk
- ▶ Tides, Planetary
- ▶ Water, Delivery to Earth

References and Further Reading

Adachi I, Hayashi C, Nakazawa K (1976) The gas drag effect on the elliptical motion of a solid body in the primordial solar nebula. Prog Theor Phys 56:1756

Armitage P, Rice WKM (2005) A decade of extrasolar planets around normal stars. STScI May symposium 2005, astro-ph/0507492

Bodenheimer P, Hubickyj O, Lissauer JJ (2000) Models of the in situ formation of detected extrasolar giant planets. Icarus 143:2

Ciesla FJ, Cuzzi JN (2006) The evolution of the water distribution in a viscous protoplanetary disk. Icarus 181:178

D'Angelo G, Kley W, Henning T (2003) Orbital migration and mass accretion of protoplanets in three-dimensional global computations with nested grids. Astrophys J 586:540

Fernandez JA, Ip W (1984) Some dynamical aspects of the accretion of uranus and neptune – the exchange of

orbital angular momentum with planetesimals. Icarus 58:109
Goldreich P, Tremaine S (1980) Disk-satellite interactions. Astrophys J 241:425
Gomes R, Levison HF, Tsiganis K, Morbidelli A (2005) Origin of the cataclysmic late heavy bombardment period of the terrestrial planets. Nature 435:466
Jang-Condell H, Sasselov DD (2005) Type I migration in a nonisothermal protoplanetary disk. Astrophys J 619:1123
Johansen A, Youdin A, Mac Low M (2009) Particle clumping and planetesimal formation depend strongly on metallicity. Astrophys J 704:L75
Laughlin G, Steinacker A, Adams FC (2004) Type I planetary migration with MHD turbulence. Astrophys J 608:489
Lin DNC, Papaloizou J (1986) On the tidal interaction between protoplanets and the protoplanetary disk. III – orbital migration of protoplanets. Astrophys J 309:846
Lin DNC, Bodenheimer P, Richardson DC (1996) Orbital migration of the planetary companion of 51 Pegasi to its present location. Nature 380:606
Malhotra R (1993) The origin of Pluto's peculiar orbit. Nature 365:819
Morbidelli A, Crida A (2007) The dynamics of jupiter and saturn in the gaseous protoplanetary disk. Icarus 191:158
Morbidelli A, Tsiganis K, Crida A, Levison HF, Gomes R (2007) Dynamics of the giant planets of the solar system in the gaseous protoplanetary disk and their relationship to the current orbital architecture. Astron J 134:1790–1798
Murray N, Hansen B, Holman M, Tremaine S (1998) Migrating planets. Science 279:69
Oishi J, Mac Low M, Menou K (2007) Turbulent torques on protoplanets in a dead zone. Astrophys J 670:805
Paardekooper S-J, Mellema G (2008) Growing and moving low-mass planets in non-isothermal disks. Astron Astrophys 478:245
Paardekooper S-J, Baruteau C, Kley W (2011) A torque formula for non-isothermal type I planetary migration – II effects of diffusion. MNRAS 410:293
Papaloizou J, Lin DNC (1984) On the tidal interaction between protoplanets and the primordial solar nebula. I – linear calculation of the role of angular momentum exchange. Astrophys J 285:818
Safronov VS (1972) The motion, evolution of orbits, and origin of comets. In: Chebotarev GA, Kazimirchak-Polonskaia EI, Marsden BG (eds) IAU symposium. Reidel, Dordrecht, p 329, IAU symposium no 45
Stevenson DJ, Lunine JI (1988) Rapid formation of Jupiter by diffuse redistribution of water vapor in the solar nebula. Icarus 75:146
Trilling DE, Benz W, Guillot T, Lunine JI, Hubbard WB, Burrows A (1998) Orbital evolution and migration of giant planets: modeling extrasolar planets. Astrophys J 500:428
Ward WR (1986) Density waves in the solar nebula – differential Lindblad torque. Icarus 67:164
Ward WR (1997) Protoplanet migration by nebula tides. Icarus 126:261

Planetary Nebula

Nikos Prantzos
Institut d'Astrophysique de Paris, Paris, France

Definition

A planetary nebula is the glowing shell of gas, typically one light-year across, ejected during the late AGB phase of intermediate and low mass stars. The name derives from the appearance in a small telescope, similar to that of a planet. It surrounds the hot, luminous core of the star, which emits ultraviolet radiation and ionizes the gas. The planetary nebula phase lasts for only a few 10^4 years, after that the star (the future ▶ white dwarf) is no longer hot enough to ionize the gas. This material eventually dissolves in the interstellar medium, enriching it with the nucleosynthesis products of the parent star (He-4, C-12, N-14, and ▶ s-process elements). The number of planetary nebulae in the Galaxy is estimated at 3,000.

See Also

▶ Asymptotic Giant Branch Star
▶ S-Process
▶ White Dwarf

Planetary Protection

Catharine A. Conley
NASA Headquarters, Washington, DC, USA

Keywords

Backward contamination; Contamination control; Forward contamination; Life detection; Sample return

Synonyms

Planetary quarantine

Definition

Planetary Protection is the process of preventing contamination of planetary environments by living organisms from other planets, in accordance with Article IX of the 1967 Outer Space Treaty and policies maintained by the Committee on Space Research (▶ COSPAR). Nations sending missions to other planets must ensure that Earth life does not contaminate them (forward contamination), and that any samples brought to Earth do not release harmful organisms into our environment (backward contamination). Protecting the Earth is the highest priority for planetary protection. Protecting other planets from Earth life preserves our investments in scientific exploration and the search for life elsewhere.

Overview

Planetary protection requirements are based on the type of planetary mission and target location (s), according to Categories defined in COSPAR policy. The lead agency for a mission is responsible for ensuring compliance by all participants with planetary protection requirements, and reporting to COSPAR on mission activities.

▶ Mars, ▶ Europa, and ▶ Enceladus are Solar System objects considered to have the highest probability for hosting indigenous life, and for contamination by transported Earth life. The probability of contaminating these objects with Earth life must be less than 1×10^{-4} per mission. Missions to Mars are allowed to meet this requirement by limiting the number of "▶ spores" contaminating the spacecraft at launch, based on calculations performed by ▶ NASA's ▶ Viking project in the 1970s. Missions that search for life, either in situ or in samples returned to Earth, must ensure that samples being analyzed are not contaminated by ▶ biomarkers from Earth life. A high-confidence life detection event would impose more strict cleanliness requirements on subsequent missions, so minimizing "false positive" results is required by planetary protection. To protect the environment of the Earth, any samples that are returned to Earth from objects that might host indigenous life (e.g., ▶ Mars Sample Return) must be contained similarly to the most infectious human pathogens, until they have been demonstrated to be nonhazardous.

Missions encountering only targets that cannot host Earth life are not required to limit ▶ bioburden, but mission operations and disposition of hardware must be documented. Missions encountering objects of interest for understanding prebiotic chemistry and the origins of life (e.g., Venus, the Moon) must retain samples of all organic materials carried on the spacecraft in quantities that might be detectable by future missions.

Planetary protection requirements for human missions are still being developed, but must meet the same goals of preventing forward and backward contamination. However, it will not be possible to prevent astronauts from being exposed to planetary materials, nor is it possible to ensure that no Earth life is released into a planetary environment. Thus, constraints on human missions focus on understanding what Earth organisms are present on the mission and how they change over time to affect astronaut health, as well as minimizing and documenting cross-contamination between terrestrial and other planetary materials.

See Also

- ▶ Bioburden
- ▶ Bioburden Reduction
- ▶ Biomarkers
- ▶ COSPAR
- ▶ Mars Sample Return Mission
- ▶ Panspermia

- ▶ Sample Receiving Facility
- ▶ Spore
- ▶ Sterilization
- ▶ Viking

References and Further Reading

COSPAR (2008) Panel on planetary protection and planetary protection policy
Meltzer M (2008) When biospheres collide: a history of NASA's planetary protection programs, NASA SP – 2008-4233. NASA Aeronautics and Space Administration. Washington, DC

Planetary Protection Category

Catharine A. Conley
NASA Headquarters, Washington, DC, USA

Definition

Individual missions are assigned a ▶ planetary protection category based on the type of mission (flyby, orbiting spacecraft, landing probes) and the target object that the spacecraft will investigate. The categorization system is used to set requirements based on the level of concern regarding the possibility of contaminating a target object by Earth life, as well as the possibility that returned samples might contain extraterrestrial life, as specified in ▶ COSPAR planetary protection policy. The possible assignments include missions that target locations of no concern for contamination by Earth life (Category I), missions to locations where Earth life could not survive but there is interest in studying possible prebiotic organic chemistry (Category II), and missions that target locations where Earth life could survive and reproduce (Category III for flybys and orbiting spacecraft, Category IV for landing probes). All missions that return samples to Earth are assigned to Category V, but only missions returning samples from locations that might host indigenous life (e.g., ▶ Mars, ▶ Europa, ▶ Enceladus) have additional restrictions beyond those imposed on the outbound portion of the mission.

Planetary Quarantine

- ▶ Planetary Protection

Planetary Rings

Françoise Roques
Laboratoire d'Etudes Spatiales et d'Instrumentation en Astrophysique (LESIA), Observatoire de Paris, Meudon, France

Keywords

Accretion; Collisions; Giant planets; Particles; Resonance; Tide; Waves

Synonyms

Circumplanetary disk

Definition

Planetary rings are systems of dust, particles, and small satellites orbiting around the ▶ giant planets of the solar system, in the nearby vicinity of a planet, where large satellites cannot form because of tidal effects.

Overview

Before observations were possible, the ancients imagined that stars were similar to the Sun and were surrounded by exoplanets, but no one imagined the possibility of planets surrounded by

rings. In fact, all the giant planets are surrounded by a ring system located close to the planet. Giant planets own also large and regular satellites with prograde and circular orbits and, farther away, irregular satellites with orbits possibly retrograde and/or inclined.

The first telescope allowed Galileo Galilei to observe in 1610 that ▶ *Saturn* has a strange shape, which changed in course of time. It was only 46 years later that Huyguens (1656) proposed that "Saturn is surrounded by a thin flat ring, nowhere touching and inclined to the ecliptic." This correct interpretation of poor-quality observations was based on the philosophical model of Descartes that a vortex is a natural shape in the Universe. It was only in 1857 that theoretical considerations led JC Maxwell to conclude that the ring is composed of small orbiting particles and not a solid ring, as initially thought.

In 1977, the ▶ occultation of a bright star by ▶ *Uranus* was observed by Elliot and his colleagues to study the planet's atmosphere. The star disappeared very briefly nine times before and after the occultation by the planet, revealing Uranus' ring system. This was the discovery that Saturn was not the only planet to be surrounded by rings and that narrow planetary rings can be stable. Subsequently, Goldreich and Tremaine (1982) showed that gravitational interactions between ring particles and nearby satellites can account for narrow and eccentric rings. This shepherding mechanism is one of the numerous and complex phenomena due to ring-satellite interactions.

The next ring was discovered around ▶ *Jupiter* by a space mission, Voyager 1, in 1979. This third ring system is very different from the first two; it is broad and ethereal, a million times less opaque than the dense Saturn rings. The dust particles, governed by nongravitational forces, have short lifetimes and must be permanently resupplied by moons. Dusty rings exist in the four planetary systems and are associated with satellites.

The last giant planet hid its ring system until 1984. Again, it was a stellar occultation that revealed a ring structure around ▶ *Neptune* (Hubbard et al. 1986). This discovery included another surprise, as the ring was detected on one side of the planet but not on the other side, showing an incomplete ring. An intensive campaign of stellar occultation observations revealed that one-tenth of the ring length is denser than the rest. This was confirmed when Voyager 2 imaged, in 1989, three dense arcs embedded in dusty ethereal rings. From this time, the three arcs have evolved to four arcs, two of which have partially vanished, showing the short lifetime of these structures. Resonances with moons on eccentric and/or inclined orbits explain the stability of incomplete rings. However, recent observations found that the arcs are not at the position predicted by the theory, leaving a puzzling situation.

The four ring systems and embedded satellites are described in Fig. 1. Particle characteristics are summarized in Table 1. The Saturn system is composed of five rings, with most edges confined by observed satellite resonances. In the ethereal Jupiter system, a 1,000-km wide region between the Adrastea and Metis orbits could be the location of invisible (smaller than 0.5 km) bodies, "parents" of dusty rings. Shepherding by satellites of the narrow Uranus rings and the Neptune arcs is not yet completely explained.

Basic Methodology

Observations from ground and from space (survey and orbiter missions) of the last 50 years have led to a good knowledge of the ring systems. After Pioneer surveys of Jupiter and Saturn, Voyagers I and II in the 1980s explored the four systems and led us to the current conception of young and dynamic rings. The Cassini orbiter is now in orbit around Saturn after having flown by Jupiter. Evolution in ring structures can also be monitored from the ground, thanks to high-angular-resolution observations. Special events such as stellar occultations and ring-plane crossings provide unique information on the ring structures and particle sizes.

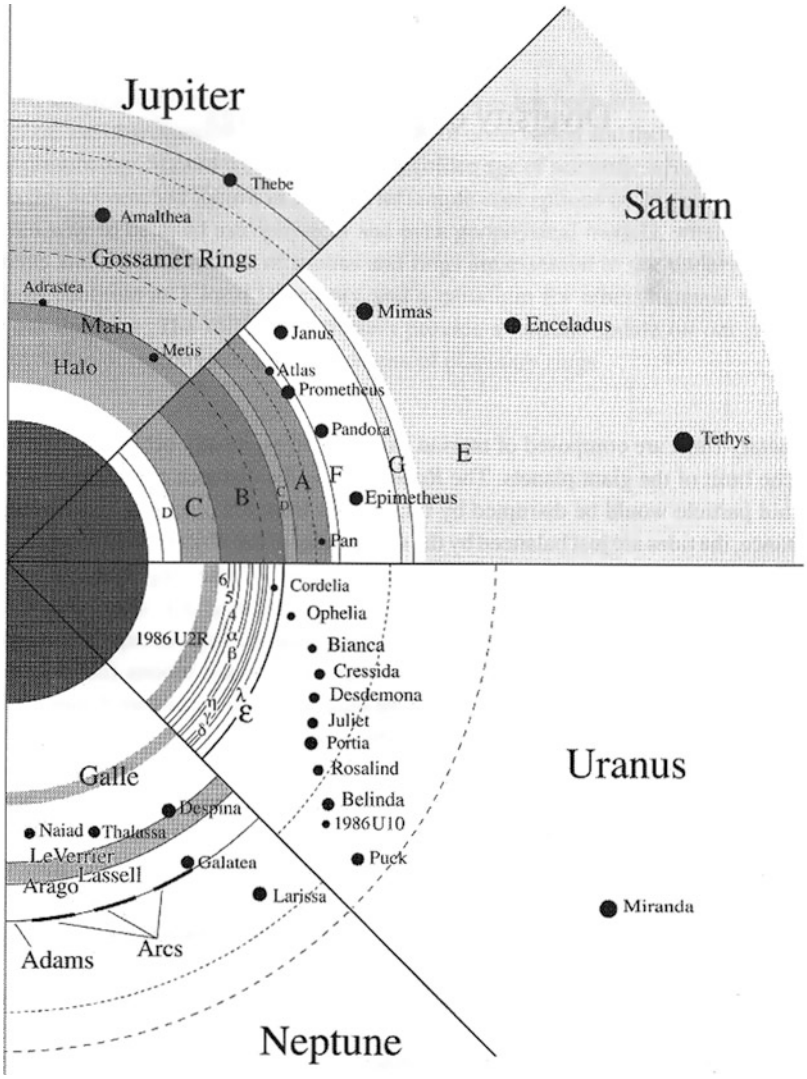

Planetary Rings, Fig. 1 A comparison of the four planetary ring systems, including the nearby satellites, scaled to a common planetary equatorial radius. Density of cross-hatching indicates the relative optical depth of the different ring components. Synchronous orbit is indicated by a *dashed line*, the Roche limit for a density of 1 g cm^{-3} by a *dotted line* (From Esposito 2006)

N-body simulations with tens of thousands of particles, taking into account mutual gravitational forces, can simulate formation of viscous instability, collective wakes, and accretion phenomena (Salo 2001). The rings and their evolution can also be fruitfully simulated as fluid (hydrodynamics) or gas (kinetic theory).

Planetary rings are a laboratory where dynamic mechanisms including waves, wakes, braids, clumps, confinement, or migration are observed and studied at all scales (Fig. 2). These mechanisms are certainly involved in other astrophysical disks, such as occur in galaxies, accretion disks, protoplanetary disks, disks of second generation, etc.

The natural evolution of colliding particles orbiting around a planet is to aggregate into a satellite because of inelastic collisions. However, within the Roche limit (D_R) of

$$D_R = 2.456 * R \left(\frac{\rho_P}{\rho} \right)^{1/3}$$

where R is the planet radius, ρ is the particle density, and ρ_P is the planet density, differential gravity (tides) caused by the planet can overcome

Planetary Rings, Table 1 Planetary rings characteristics (From Esposito 2006)

	Planetocentric distance (width) (km)	Optical depth	Dust fraction (%)	Power-law index (particle size distribution)	Notes
Jupiter					
Halo	92,000–122,500	10^{-6}	100	?	12,500 km thick
Main ring	122,000–12,980	3×10^{-6}	~50(?)	$q < 2.5$	Bounded by Adrastea
Amalthea Gossamer	129,000–182,000	10^{-7}	100(?)	?	2,000 km thick
Thebe Gossamer	129,000–226,000	3×10^{-8}	100(?)	?	4,400 km thick
Saturn					
D ring	66,000–74,000	10^{-3}	5–100	?	Internal structure
C ring	74,490–91,983		<3	3.1	Some isolated ringlets
B ring	91,983–117,516	<2.5	<3	2.75	Abundant structure
Cassini division	117,516–122,053	0.05–0.15	<3		Several plateaus
A ring	122,053–136,774		<3	2.75–2.90	Many density waves
F ring	140,200 ($W \cong 50$ km)	09.1–0.5	>98	2–3	Narrow, broad components
G ring	166,000–173,000	10^{-6}	>99	1.5–3.5	
E ring	180,000–450,000	10^{-5}	100		Peak near Enceladus
Uranus					
1986 U2R	37,000–39,500	$10^{-4} - 10^{-3}$	?	?	Still unnamed
Dust belts	41,000–50,000	10^{-5}	?	?	Fine internal structure
6	41,837	0.3	<1	$q > 3.5$	
5	42,234	0.5	<1	$q > 3.5$	
4	42,570	0.3	<1	$q > 3.5$	
α	44,718	0.3	<1	$q > 3.5$	
β	45,661	0.2	<1	$q > 3.5$	
η	47,175	0.3	<1	?	
γ	47,627	2	<1	?	
δ	48,300	0.4	<1	?	
λ	50,023	10^{-3}	>95	?	
ε	51,149	0.5–2.3	<1	$2.5 < q < 3.0$	Adjacent to Cordelia
Neptune					
Galle	41,000–43,000	$4–10 \times 10^{-5}$	?	?	
LeVerrier	53,000 ($W = 10$ km)	10^{-2}	4–70	?	Adjacent to Despina
Lasell	53,000–58,000	$1–3 \times 10^{-4}$	?	?	
Adams	62,930 ($W = 50$ km)	10^{-2}	2–50	?	Adjacent to Galatea
Adams arcs	62,930 ($W = 10$ km)	10^{-1}	4–70	?	

the gravitational attraction between the particles. As a result, satellites can orbit inside the Roche limit only if they are small enough to be held together by their tensile strength, rather than by their own gravitation.

As inelastic collisions dissipate energy but overall angular momentum is conserved, the initial particle orbits flatten within a short timescale into the equilibrium plane, that is, the equatorial plane of the planet.

The spreading timescale is longer than the flattening one. The relative motion between particles is dominated by Keplerian shear (i.e., particles closer to the planet move faster than more distant ones). Collisions between a more rapid inner particle and a slower outer particle make the inner particle slow down and lose angular momentum and the outer particle accelerate and win angular momentum.

Most images of rings, and in particular of dense rings, show very small structures, down to the limit of definition of the images. They are caused by different-size particles gravitationally interacting. Perturbations of a satellite create visible structures in the ring at locations of resonance. At these locations, successive gravitational perturbations are cumulative. Resonance effects are complex, because they concern three parameters for each orbit: mean motion, apsidal precession of an eccentric orbit, and node of an inclined orbit. The mean motion of the satellite orbit is $n_S = \frac{2\pi}{P} = \left(\frac{GM}{a^3}\right)^{1/2}$, where P is the revolution period, G is the gravitation constant, M is the planet mass, and a is the semimajor axis of the orbit. The epicyclic frequency, κ_S, is connected to the motion of the elliptical orbit apsidal line and the vertical frequency, μ_S, to the motion of the node of an inclined orbit. If the planet is oblate, $\mu_s > n_S > \kappa_S$, the apsidal line regresses and the node precesses. Resonance occurs when the forcing satellite frequency, $W_f = m.n_s + p\kappa_S + k\mu_S$, where m, p, and k are integers, matches one of the three particle natural frequencies (Fig. 2).

The most spectacular effect of resonances is the shepherding of a narrow ringlet by two satellites as observed for the ε ring of Uranus or the F ring of Saturn. The resonances accumulate near the satellite orbit, and the cumulative torque of a satellite on a ringlet of width w, at a distance d is

$$T \approx \frac{G^2 m_S{}^2 \sigma a r}{n_S{}^2 d^4},$$

where m_S is the satellite mass and σ is the ring surface density. Note that dissipation is essential even if the torque intensity does not depend on the dissipation mechanism.

Dusty ring particles are sensitive to nongravitational forces. Solar radiation pressure, plasma effects, and magnetic perturbations limit the lifetimes of particles. Consequently, these rings must be replenished continuously by micrometeoroidal bombardment or collisions of

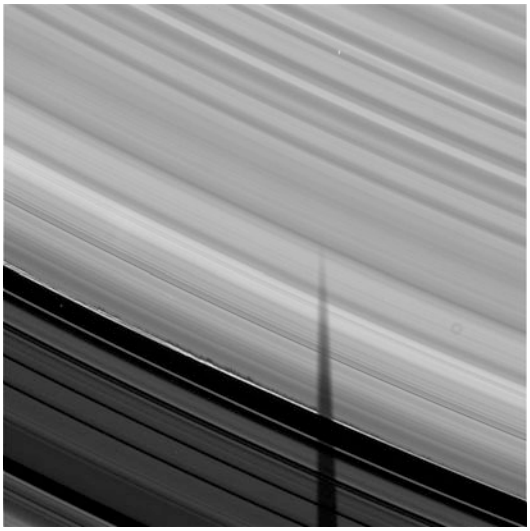

Planetary Rings, Fig. 2 Shadows on the Saturn rings: bright upper part is the outer part of the B ring showing several wave patterns. The outer B ring is confined by the 2:1 resonance with Mimas. The lower dark region is the Cassini division. The bright structures along the B ring edge are 3 km in height above the ring and throw laced shadows on the ring. The longest shadows are 100 km long. The Sun is 1.9° above the ring plane. The long shadow is caused by Mimas, which is 70,000 km away from this image (© NASA/JPL/SSI)

"parent" bodies. Dusty radial structures, called "spokes," have been observed in the Saturn rings but remain partially unexplained.

Key Research Findings

Rings orbit in the sense of the planet's rotation, as do most of the satellites. This makes one think that they are formed in the same protoplanetary disk. However, the short timescale of involved mechanisms favors a recent creation from a disrupted satellite. Moreover, the very short lifetimes of observed structures require active processes for maintaining them.

Modeling shows that dense ring material is subject to very rapid (week timescale) growing mechanisms, with smooth collisions and sticking of small particles, until house-sized objects are formed and disrupted. These structures are called DEBs (dynamic ephemeral bodies) or rubble piles.

The origin of the Saturn rings is still controversial. It is difficult to give a scenario explaining at the same time the spreading timescales, which are smaller than the age of the solar system, and the large mass of Saturn's rings, as capture and/or disruption of a satellite sufficiently massive to make the rings is very unlikely after the end of the planet formation period.

The ethereal Jupiter rings are clearly the by-product of small satellites. If the Saturn ring is coeval with the planet, the question is why Jupiter has not a similarly large ring system.

The Uranus and the Neptune rings are more easily explained by a captured object. The disruption inside the Roche limit would have left a mixture of small satellites and particles reorganized in the observed configuration.

Future Directions

The next generation of high-contrast imaging instruments will provide the first unresolved image of an extrasolar planet. While the emitted infrared light from the planet in thermal equilibrium should show almost no phase effect, the reflected visible light will vary with the orbital phase angle. A ring around an extrasolar planet, both obviously unresolved, can be detected by its specific photometric signature (Arnold and Schneider 2004).

See Also

- ▶ Giant Planets
- ▶ Jupiter
- ▶ Neptune
- ▶ Occultation
- ▶ Roche Limit
- ▶ Saturn
- ▶ Uranus
- ▶ Voyager, Spacecraft

References and Further Reading

Arnold L, Schneider J (2004) The detectability of extrasolar planet surroundings. I. Reflected-light photometry of unresolved rings. Astron Astrophys 420:1153–1162

Charnoz S et al (2009) Origin and evolution of Saturn's ring system. In: Dougherty MK, Esposito LW, Krimigis SM (eds) Saturn from Cassini-Huygens. Springer, The Netherlands

Colwell JE (2009) The structure of Saturn's ring. In: Dougherty MK, Esposito LW, Krimigis SM (eds) Saturn from Cassini-Huygens. Springer, The Netherlands

Goldreich P, Tremaine S (1982) The dynamics of planetary rings. Annu Rev Astron Astrophys 20:249–283

Elliot JL, Dunham EW, Mink DJ (1977) The rings of Uranus. Nature 267:328–330

Esposito L (2006) Planetary rings. Cambridge Planetary Science, Cambridge

Hubbard W, Brahic A, Sicardy B et al (1986) Occultation detection of a Neptunian ring-like arc. Nature 319:636–640

Huyguens C (1656) De Saturni luna observatio nova in Oeuvres Complètes de Christiaan Huyguens, vol XV. The Hague, 1925, pp 172–177

Salo H (2001) Viscous overstability in Saturn B ring. IIcarus 153:295–315

Planetary Surface Ages

- ▶ Chronostratigraphy

Planetary Theories and Cosmology, Islamic Theories

Ahmed Ragab
Harvard Divinity School, Cambridge, MA, USA

Keywords

Islam; Islamic astronomy; Andalus; Iberia; Medieval; Tusi; Averroes; Maragha; Observatory; Zij; Kindi; Avicenna; Tusi couple; al-Haytham

Overview

Following Ptolemy's instructions in the Almagest that "he who comes after us throughout the epochs take measurements as we have done, and if they find an imperfection, they should correct," Islamic works of astronomy were motivated in part with this process of minor rectifications, along with two other lines of inquiry: creation of astronomical tables (zij) and timekeeping, on the one hand, and planetary theories on the other.

Ptolemy's Almagest remained the more influential text in medieval Islamic astronomy, along with Aristotle's De Caelo. The Almagest provided astronomers with important tools to solve their different practical problems, and its explanations of planetary movement were sufficiently viable to allow for its continual usage. De Caelo presented a robust philosophical system explaining planetary movement but without a viable practical model. The first class of Islamic authors included al-Kindi (d. 873; explained Almagest's first book and wrote on Platonic cosmological theories), Thābit ibn Qurra (d. 901; addressed transfer of motion across orbs), and al-Battānī (d. 929; composed one of the earliest zijs). The contradictions between Ptolemy and Aristotle motivated a number of responses through history, such as those of Ibn Tufayl and his students in al-Andalus, and of the "Maragha School."

Ibn Sīnā (Avicenna; d. 1037) and his student al-Juzjānī (d. 1070) objected to Ptolemy's eccentrics, as they violated Earth's centrality. Avicenna claimed to have reached a solution to this problem, but only after so much effort that he was not willing to share it. Juzjānī proposed an alternative to the Ptolemaic model that proved unsuccessful. In Andalusia, Ibn Tufayl (d. 1185), sharing the same objections, claimed to have found an alternative solution, but never wrote it. His more famous student, Ibn Rushd (Averroes; d. 1189) proposed that Aristotle's solutions were lost and should be rediscovered but left the task of rediscovery to his younger students. Another student of Ibn Tufayl, al-Bitruji (Alpetragius; d. 1204), proposed a solution that avoided eccentrics by employing only concentric orbits around the earth and suggesting the possibility of the orbs' poles circling other orbs. The contributions of these Andalusian scholars had little influence on other Islamic astronomers. However, these views carried more influence with renowned Jewish astronomers such as Yosef Nahmias and Levi Ben Greson.

The Maragha School, led by al-Ṭūsī (d. 1274), al-Shīrāzī (d. 1311) and al-ʿUrdī (d. 1266), took to rectifying Ptolemaic models without attempting to overrule them as did their Andalusian predecessors. One of the more famous accomplishments of this school is the Tusi couple, which was a geometrical device that transformed circular movement into linear one. The goal of al-Tūsī's work was to explain orbital movements in relation to the different physical principles. The Maragha scholars were rooted in a tradition of criticizing Ptolemy and uncovering the problems with his model that started with Ibn al-Haytham's (Alhazen; d. 1040) "Doubts on Ptolemy," where the latter showed how a number of Ptolemy's propositions violated laws of Aristotelian physics. However, probably similar to Ibn al-Haytham, who did not reject Ptolemy entirely, the Maragha astronomers seemed to remain invested in the Ptolemaic model, with all its practical possibilities, and did not reject it in favor of Aristotle's more elegant, yet less practical, model of planetary and orbital movement.

See Also

- ▶ Al-Andalus, Cosmological Ideas
- ▶ Al-Tūsī, Nasir al-Dīn

References and Further Reading

Kennedy ES (1966) Late medieval planetary theory. Isis 57:365–378
King DA (1984) The astronomy of the mamluks: a brief overview. Muqarnas 2:73–84
King DA (1993) Astronomy in the service of Islam. Variorum, Aldershot
Langermann YT (1997) Arabic cosmology. Early Sci Med 2:185–213
Sabra AI (1984) The Andalusian revolt against ptolemaic astronomy: averroes and Al-Bitruji. In: Transformation and tradition in the sciences. pp 133–153
Sabra AI (1998) Configuring the universe: aporetic, problem solving, and kinematic modeling as themes of Arabic astronomy. Perspect Sci 6(3):288–330
Saliba G (1994) Early Arabic critique of Ptolemaic cosmology: a ninth-century text on the motion of celestial spheres. J Hist Astron 25:115
Saliba G (1995) A history of Arabic astronomy: planetary theories during the golden Age of Islam. NYU Press, New York
Saliba G (2002) Greek astronomy and the medieval Arabic tradition the medieval Islamic astronomers were not merely translators. They may also have played a key role in the Copernican revolution. Am Sci 90:360–67

PLAnetary Transits and Oscillations of Stars

- ▶ PLATO 2.0 Satellite

Planetesimals

Rory Barnes
Astronomy Department, University of Washington, Seattle, WA, USA

Definition

In models of planetary formation, planetesimals are small bodies in orbit around a star that can be accreted by forming planets. The formation process and the mass function of these objects are subject to active research and are not well known. Planetesimals are usually assumed to be significantly larger than 1 m, e.g., 100 m to 100 km in radius.

See Also

- ▶ Dynamical Friction
- ▶ Gas Drag
- ▶ Gravitational Collapse, Planetary
- ▶ Late-Stage Accretion
- ▶ Meteorites
- ▶ Planet Formation
- ▶ Planetary Migration
- ▶ Viscous Stirring

Planet-Forming Disk

- ▶ Protoplanetary Disk

Planetoid

- ▶ Asteroid

Planets in Binary Star Systems

Nader Haghighipour
Institute for Astronomy, University of Hawaii-Manoa, Honolulu, Hawaii, HI, USA

Definition

A survey of currently known planet-hosting stars indicates that approximately 10 % of extrasolar planetary systems are within dual-star environments. Several of these systems contain stellar companions on orbits moderately close to one of

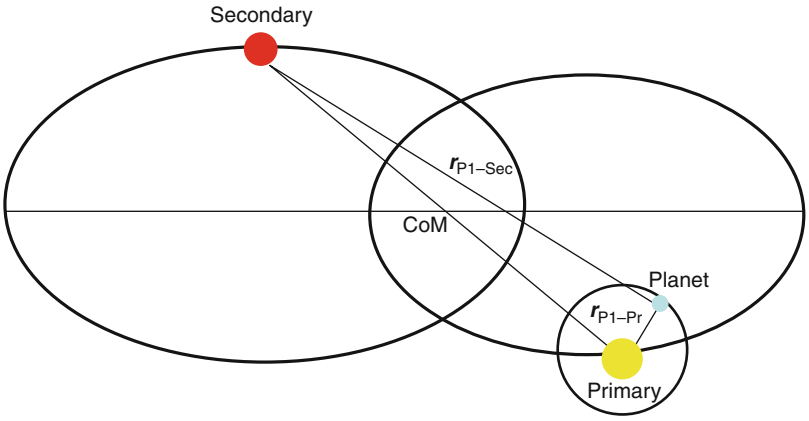

Planets in Binary Star Systems, Fig. 1 Schematic presentation of an S-type system

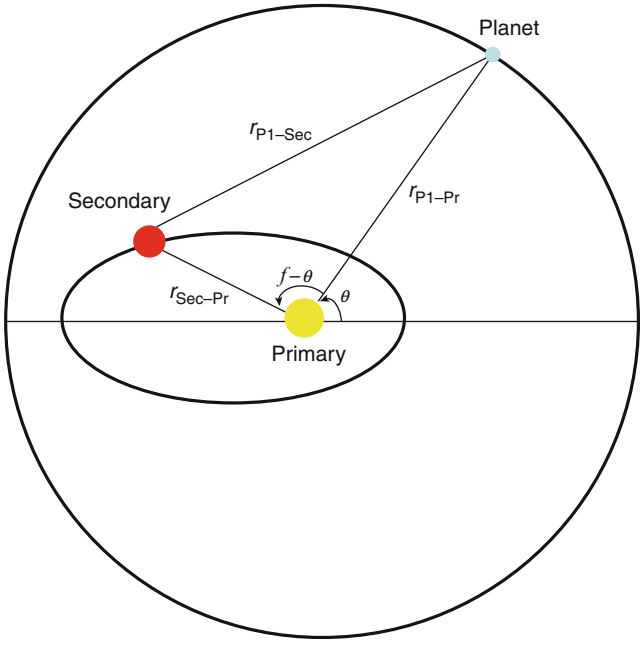

Planets in Binary Star Systems, Fig. 2 General schematic presentation of a P-type system

the stars, or have planets in circumbinary orbits. The following website presents an up to date list of all of these systems: http://www.univie.ac.at/adg/schwarz/binary.html

From a dynamical point of view, three types of orbits are recognized for the motion of a planet in a binary star system. These orbits have been historically labeled as:

1. The S-type (or Satellite-type) orbit where the planet revolves around one of the stars of the binary (see ▶ circumprimary planet, Fig. 1).
2. The P-type (or Planetary-type) orbit where the planet revolves around the entire binary system (see ▶ circumbinary planet, Fig. 2), and
3. The L-type (or Libration-type) where the planet moves in the same orbit as the secondary star, but 60° ahead or behind it (analogous to the position of the ▶ Trojan asteroids relative to ▶ Jupiter).

For more details see the book entitled Planets in Binary Star Systems (Haghighipour 2010).

References and Further Reading

Haghighipour N (2010) Planets in binary star systems, astrophysics and space science library, vol 366. Springer, Dordrecht/New York

Schwartz R (2014 & regularly updated) http://www.univie.ac.at/adg/schwarz/binary.html. Accessed 16 Oct 2014

Planitia

Roland J. Wagner
German Aerospace Center (DLR), Institute of Planetary Research, Berlin, Germany

Definition

A planitia designates a low-lying plain on the ▶ terrestrial planets ▶ Mercury, ▶ Venus, Moon, and ▶ Mars, on the Saturnian satellites ▶ Enceladus and ▶ Titan, and on ▶ Triton (▶ Neptune). A planitia can extend from a few ten thousands to several millions of square kilometers across a planetary surface. Guinevere Planitia on Venus is the largest one known with a diameter of 7,520 km. Tectonism or impacts are the primary processes that can create vast low-lying plains. On ▶ planets or satellites with an atmosphere (Venus, Mars, Titan), planitiae can be subsequently modified by material deposited in the plain by wind or fluid flow.

See Also

- ▶ Enceladus
- ▶ Mars
- ▶ Mercury
- ▶ Moon, The
- ▶ Neptune
- ▶ Planet
- ▶ Planum
- ▶ Satellite or Moon
- ▶ Terrestrial Planet
- ▶ Titan
- ▶ Triton
- ▶ Venus

Planck, Max

Fernando B. Figueiredo
CITEUC, University of Coimbra, Coimbra, Portugal

History

Max Karl Ernst Ludwig Planck (1858–1947) was a German physicist Nobel laureate in 1918 by his discovery of energy quanta. He postulates that the energy did not flow in a steady continuum but in discrete packets or quanta. He established a relationship between the energy (E) radiated from a heated body and the frequency of that radiation (ν): $E = h\nu$ (where h is known as Planck's constant and has the value $6.62606957 \times 10^{-34}$ Js).

The NASA/ESA partnership space mission, which was launched on May 14, 2009, was designed to measure the Cosmic Microwave Background (CMB) over a broad range of far-infrared wavelengths.

See Also

- ▶ Line Emission

Plankton

Felipe Gomez
Centro de Astrobiología (CSIC/INTA), Instituto Nacional de Técnica Aeroespacial, Torrejón de Ardoz, Madrid, Spain

Definition

Plankton refers to the microscopic organisms, mainly ▶ algae and protozoa, which are present

in oceans and freshwater bodies. These microorganisms float and drift passively and support a significant part of the food chain for larger organisms in bodies of water.

See Also

- ▶ Algae
- ▶ Eukarya
- ▶ Photosynthesis
- ▶ Photosynthesis, Oxygenic
- ▶ Protists

Planum

Roland J. Wagner
German Aerospace Center (DLR), Institute of Planetary Research, Berlin, Germany

Definition

A feature termed planum is a topographically high-standing plain or plateau. These features are found on the terrestrial planets ▶ Mercury, ▶ Venus, Moon, and ▶ Mars, on Jupiter's satellite ▶ Io, and on Neptune's satellite ▶ Triton. The spatial extent (diameter) of a planum is a few hundred kilometers up to approximately 2,400 km (Lakshmi Planum, Venus). High-standing plains were created by (cryo-)volcanism and/or tectonism.

See Also

- ▶ Cryovolcanism
- ▶ Io
- ▶ Jupiter
- ▶ Mars
- ▶ Mercury
- ▶ Moon, The
- ▶ Neptune
- ▶ Planitia
- ▶ Satellite or Moon
- ▶ Terrestrial Planet
- ▶ Triton
- ▶ Venus

Plasma

Daniel Rouan
LESIA, Observatoire Paris-Site de Meudon, Meudon, France

Definition

A plasma is a gaseous medium principally made of charged particles: ions and electrons. A plasma is globally neutral as it contains balanced charges of positive and negative types. Since a plasma is electrically conductive, it responds strongly to electromagnetic fields. For instance, a plasma is the medium where Alfvén waves can develop and propagate. Plasmas are found everywhere: in stars, in the upper atmospheres of planets, in the interstellar medium (HII regions), in stellar envelopes (planetary nebulae), at the center of clusters of galaxies, etc. It is generally admitted that more than 99 % of the baryonic matter in the universe is in the form of plasma.

See Also

- ▶ HII Region

Plasma Membrane

- ▶ Cell Membrane
- ▶ Membrane

Plasmid

Carlos Briones
Centro de Astrobiología (CSIC/INTA),
Consejo Superior de Investigaciones Científicas,
Madrid, Spain

Synonyms

Episome; Extrachromosomal genetic element

Definition

A plasmid is a genetic element with autonomous replication within a suitable host. Plasmids are extrachromosomal elements frequent in ▶ bacteria and ▶ archaea, and they are also found in certain yeasts. Plasmids are, together with viruses, the main mobile genetic elements involved in ▶ lateral gene transfer throughout evolution. They are circular or linear double-stranded ▶ DNA molecules of 10^3 to 10^6 nucleotides in length, maintained within the cell either in single copy or in multicopy format. In general, they are not essential for the organism but they may confer a selective advantage. For example, bacterial plasmids may carry genes that code for proteins able to degrade naturally occurring antibiotics – therefore producing antibiotic-resistant phenotypes – or to metabolize a wide range of organic compounds. Plasmids used in genetic engineering and biotechnology, called vectors, allow the biological amplification of exogenous genetic material, the insert, through ▶ cloning the recombinant plasmid – vector + insert – in a culturable host organism.

See Also

- ▶ Amplification (Genetics)
- ▶ Bacteria
- ▶ Cloning
- ▶ Conjugation
- ▶ DNA
- ▶ Genome
- ▶ Lateral Gene Transfer
- ▶ Replication (Genetics)
- ▶ Yeast

Plate Tectonics

Karel Schulmann and Hubert Whitechurch
Ecole et Observatoire de Science de la Terre,
Institute de Physique de Globe, Université de
Strasbourg, Strasbourg, France

Keywords

Earthquake; Hot spot; Lithospheric plate; Mantle convection; Mid-ocean ridge; Orogeny; Plate boundary; Plate tectonics; Subduction; Volcano

Definition

"Plate tectonics" (*from the Greek* |έ||Ƙ = builder) refers to the theory describing the motion of the plates, 100–200 km thick, which form Earth's ▶ lithosphere. These rigid plates, which consist of continental or oceanic crust underlain by lithospheric ▶ mantle, are displaced above the higher-density and lower-strength ▶ asthenosphere. They move with respect to each other along one of three possible plate boundaries: convergent (or subduction/collisional) boundaries; divergent (or spreading), and transform boundaries (where plates move parallel to each other). Earthquakes and magmas produced by mantle melting characterize most plate boundaries.

Convergent boundaries are expressed by topographic lows called trenches, which coincide with sites of subduction of oceanic plates. Also involved are orogenic processes leading to the formation of mountain chains, with subsequent regional metamorphism and continental partial melting. Spreading centers coincide with topographic highs, called ▶ mid-ocean ridges, where upwelling asthenosphere partially melts and

produces new oceanic crust. Movement along transform boundaries accumulates shear stress that is discharged through earthquakes, a common phenomenon along these boundaries (the San Andreas fault, California, is the best-known example). Lithospheric plates are driven by thermal or compositional density variations in the underlying mantle which causes large-scale convection. These movements are transferred to overlying rigid plates through gravitation forces from high-standing ridges (ridge-push) or the downward drag of dense subducting slabs (slab pull).

This review starts with some history: the hypothesis of continental drift and the evolution of ideas that led to the plate tectonics theory. Methods used to investigate plate tectonics are briefly reviewed. The lithospheric plates are then defined, together with the nature of plate boundaries, plate kinematics, and the driving forces of plate movements. The theory is completed with a discussion of the concepts of hot spots and mantle convection and some comments about the growth of the crust and construction of the continents.

History

The Theory of the Continental Drift

The German geophysicist and meteorologist Alfred Wegener proposed the theory of continental drift in 1915 in his book *Die Entstehung der Kontinente und Ozeane* (The Origin of Continents and Oceans). One of the main arguments for continental drift was the similarity between the east coast of South America and the west coast of Africa. The British philosopher Francis Bacon (1620) and subsequently many others had already proposed the possible attachment of these two continents. Wegener was the first who used isostasy and paleobotanical and paleofacies data compiled by the South African geologist A. du Toit, in particular traces of Carboniferous glaciation in Australia, India, and Africa, combined with geodetic measurements to confirm a simple observation – that the continents are moving. However, Wegener failed to explain the forces driving the continental drift. Since Wegener, geologists have compared rock strata at the edges of separate continents to verify whether they once formed a continuous sequence and were initially joined. One good example is the Variscan belt in Europe and the Appalachians in North America which formed a continuous mountain belt before being split by the Atlantic Ocean.

Confirmation of the Wegener theory came initially from the "mobilistic" approach of the Swiss geologist Emile Argand, who in 1924 wrote the book *La Tectonique de l'Asie* (The Tectonics of Asia) using Wegener's idea of tectonic indentation (the penetration of one continent into another) and mountain building to explain the collision of India with Eurasia by closure of the Tethyan ocean (Tethys). He also used the notion of indentation to explain the collision of Africa with Europe. Argand was thus the pioneer of tectonics of convergent boundaries.

The mechanism behind continental drift was proposed by British geologist Arthur Holmes who studied the concentration of radioactive elements in some minerals to estimate the age of the Earth, proposing first 1.6 Ga in 1911 and later 3.4 Ga (Holmes 1928). He concluded that the amount of radiogenic elements decreased with the depth and that in order to evacuate heat from the interior of the Earth, convection currents are needed. He proposed that continental drift was an inevitable consequence of thermal convection. Later, the Dutch geophysicist Vening-Meinesz confirmed the hypothesis of mantle convection by gravity field studies and attributed the mass deficiency underneath deep ocean trenches to downward drag of the subducting oceanic plate.

The Birth of the Modern Plate Tectonics

The most important findings that shaped the theory of plate tectonics came from oceanographic studies. In 1947, the American geophysicist and oceanographer Maurice Ewing and his coworkers confirmed the existence of a topographic rise in the central Atlantic Ocean. These workers found that the oceanic crust is basaltic in composition and significantly thinner than granitic continental crust. The American geologist Harry Hess

provided decisive input in the understanding of plate tectonics in the beginning of 1950 when he used a magnetometer to record magnetic variations across the ocean floor. These magnetic variations are associated with the magnetite contained in oceanic basalts, which records the orientation and intensity of the Earth's magnetic field at the time of basalt extrusion. Most importantly, magnetic studies revealed the existence of alternating stripes of normal and reverse polarity which are symmetrically distributed on either side of the mid-ocean ridge (Vine and Matthews 1963). The alternation of normally and reversely polarized bands, called magnetic striping, led to the theory of sea-floor spreading. In the 1960s, it was suggested that the mid-ocean ridges mark structurally weak zones where the ocean floor was split in two along the ridge crest. It was suggested that pulses of magma rise along the ridge and create new oceanic crust which then migrate laterally away from the ridge – the process called sea-floor spreading. The alternation of direct and inverse magnetic polarity is related to periodical changes in the polarity of the Earth's magnetic field, which is recorded in the basaltic rocks. The explanation of the magnetic striping led to the rapid acceptance of sea-floor spreading as a key element of plate tectonics theory.

A consequence of sea-floor spreading is that new crust is continuously formed. Carey (1958) used this concept to propose a model of Earth expansion, then Hess (1962) suggested that if the ocean floor is expanding along ridges, it must be removed at oceanic trenches, the deep valleys rimming the Pacific Ocean. In other words, as new crust forms at oceanic ridges by magma accretion, old crust is destroyed along trenches – in oceanic subduction zones. The modern theory of plate tectonics proposes that the continents are not moving through oceanic crust (as in the continental drift concept of Wegener) but that oceanic crust and in some cases attached continents move together on the same crustal unit called a "plate." Soon after, plate tectonics evolved significantly with the recognition of transform faults by the Canadian geologist Tuzo Wilson (1965). In his model, the oceans are created, grow, and disappear; and the continents are fragmented, separated, and reassembled in what are now called "Wilson cycles."

Further understanding of plate kinematics came from the work of the American geophysicist William Jason Morgan (1968), who explained relative displacements of two adjacent plates. He showed that the movements are parallel to transform faults and centered on a pole of rotation (the Euler pole), and that variations of sea-floor expansion are a function of the distance from the pole of rotation. Xavier Le Pichon (1968) built on Morgan's concept and proposed a kinematic reconstruction of the formation of the Atlantic and Indian oceans within the frame of six rigid plates including continental masses. Geological aspects of the theory of plate tectonics were developed by Dewey and Bird (1970), who showed that the structure of active continental margins is dependent on the geometry and kinematics of subduction zones. This seminal paper showed geologists how the orogenic belts are linked to movements of the oceanic lithosphere, and explained the relationship between plate tectonics and both the complex three-dimensional movements at continental margins and the magmatic and metamorphic processes of mountain building.

Basic Methodology

Three methods had a decisive impact on the development and further understanding of plate boundaries: seismology, ▶ paleomagnetism, and modern paleoclimatic and paleobiogeographic studies.

Seismology

Seismology developed rapidly in the twentieth century with the construction of seismographs that enabled geophysicists to understand the Earth's internal structure, the composition of continental and oceanic crust, and the boundary between the crust and mantle – the so-called Mohorovičić discontinuity or "▶ Moho," named after its discoverer, the Croatian seismologist Andrija Mohorovičić. The second major discovery was that earthquakes tend to be located along plate boundaries, from the oceanic trenches downwards,

as well as along the spreading ridges and transform faults. The seismologists Hugo Benioff of the California Institute of Technology and Kiyoo Wadati of the Japan Meteorological Agency independently identified earthquake zones that were several hundred kilometers long, oriented parallel to the trenches, and dipping at 40°–60° – the so-called Wadati-Benioff or subduction zones.

Paleomagnetism

Paleomagnetism is the study of the record of the Earth's past magnetic field as preserved in magnetic minerals in rocks. The principle is based on the fossilization of the magnetic field direction at the time of cooling of lavas or deposition of sediments. It is possible to measure the orientation, the polarity, and sometimes even the intensity of the magnetic field. Knowing the magnetic field at the given time allows us to reconstruct the apparent position of the pole and consequently the latitude and orientation of the studied region at a given time. This method has played a decisive role in obtaining a better understanding of the movement and rotation of plates, and the migration of continents over long periods of time. Further, the discovery of magnetic stripes on the ocean floor was decisive for understanding the opening of the oceans and helpful for formulating the new theory of plate tectonics.

Tectonic and Paleobiogeographic Reconstructions

Paleomagnetic studies are intimately connected with tectonic, paleobiogeographic, and paleoclimatologic syntheses. It was shown that the drift of continents across paleo-latitudes was responsible for deposition of climatically sensitive sediments such as evaporites or tillites. In addition, continental drift played a decisive role in the distribution, diversity, and extinction of past life. Continents may break up, separate, and subsequently collide, thereby changing the disposition of faunal provinces and barriers to faunal migration. Paleobiogeographic studies bring key information about the isolation or connection of continents, the position of suture zones and ancient oceans, and the paleogeographic position of lithospheric plates.

Structure of Lithospheric Plates

The outer layers of the Earth are divided into the ▶ lithosphere and ▶ asthenosphere. The distinction is based on differences in mechanical properties and in the process of heat transfer. The concept of lithosphere was introduced by Barell (1914) on the basis of geological and physical evidence suggesting the existence of a strong superficial layer (the lithosphere) floating above a weak zone (the asthenosphere). The lithosphere is defined as a mobile, near-surface, strong layer with a viscosity of about 10^{24} Pa s^{-1} (Isacks et al. 1968) that supports high differential stress. The asthenosphere, in contrast, already flows under low stresses and has a disproportionally lower viscosity of 10^{20}–10^{21} Pa s^{-1}. Consequently, earthquakes occur within the lithosphere but not in the asthenosphere, except where lithospheric slabs sink into the asthenosphere in subduction or collisional zones. As a first approximation, the lithospheric plate can be considered to be an elastic or viscoelastic sheet. The thickness of a plate is also the thickness of the lithosphere, which, at any location, is composed of continental (granitic to granodioritic) or oceanic (basaltic) crust and the subcrustal (peridotitic) mantle. The lithosphere loses heat by conduction, whereas the asthenosphere transfers heat mainly by convection and has a nearly adiabatic temperature gradient. Therefore, the contact between the lithosphere and the asthenosphere is not to a chemical or mineralogical boundary but a strong contrast of rheological behavior dependent on temperature. Two isotherms define this contact. The first, at 1,270–1,340 °C, corresponds to the temperature of the beginning of partial melting of the mantle peridotite as a function of lithostatic pressure. Partial melting of peridotite has been invoked to explain a layer with reduced seismic velocities – the low-velocity zone or LVZ – at the base of the lithosphere. The second isotherm, at 1,100–1,200 °C, corresponds to the temperature at which the deformation mechanism of mantle olivine changes from dislocation creep to diffusional creep.

In the oceans, the lithosphere thickens from the mid-ocean ridge (<20 km) to up to 100 km beneath older oceanic basins. It is even thicker

beneath the continents, ranging from 120 to 250 km underneath old, cold, rigid Archean cratonic crust. The lithosphere under continents is thinner in tectonic regions such as active margins and intracontinental rifts where hot material may exist at shallow depth, and is thicker underneath orogenic belts where the lithosphere-asthenosphere boundary is depressed by thickening of the crust and mantle lithosphere.

Plate Boundaries and Hot Spots

Three main types of plate boundaries exist, each characterized by different relative motions of adjacent plates. Plate boundaries are marked by different tectonic processes and are associated with seismic and magmatic activities. The sites of localized mantle melting, called hot spots, are marked by chains of volcanoes aligned within plates in a direction parallel to plate movement.

Divergent Boundaries

Divergent boundaries occur where two plates move apart from one another. These boundaries, called mid-ocean ridges, are marked by bathymetric highs over the 4,000 m isobath within all the oceans. Here, new oceanic crust is formed by the eruption and crystallization of tholeiitic magmas (MORB, Mid Ocean Ridge Basalt), issued from 10 % to 20 % partial melting of mantle peridotite.

The thickness of the oceanic crust, as determined by seismic experiments (away from the fracture zones and from hot spot influence), varies between 2 and 8 km. With the exception of ultraslow-spreading ridges, the mean thickness of the oceanic crust is 6 km (White et al. 2001). Seismic activity on the ridges is superficial (the depth of earthquake hypocenters is 9 km, close to the brittle-ductile transition), with low magnitude (<6 M) and characterized by extensional focal mechanism. The ridge segments are truncated by transform faults that may reach tens to hundreds of kilometers long (see below). The larger transform faults exhibit high relief and intense seismic activity, with mainly strike-slip focal mechanisms between the ridge segments.

The spreading rate is calculated using magnetic anomalies. These originate from thermo-remnant magnetization of the basaltic crust, registered by Fe-oxides. Magnetic anomalies produce a striped pattern in the oceanic crust that results from changes from normal (in the same direction as the present magnetic field) to inverse (in the opposite direction compared to the present) polarity of the Earth's field at the time of crystallization. The ages of these anomalies have been established by dating of sediments deposited on magnetized blocks and collected during ocean drilling programs (DSDP, ODP, and IODP) or by dating of the volcanic rocks themselves. The anomalies are numbered from 1 to 34, corresponding to the period from the present to the Cretaceous normal quiet period from 84 to 118 Ma. For the older periods, the anomalies have been denoted M0 (118 Ma) to M41 (166 Ma). The anomalies are identified and modeled by measuring the direction of the regional magnetic field, its depth, and the thickness and direction of magnetization of the magnetic layer. Anomalies are present on both sides of the spreading zone but are not always symmetrical. The full spreading rate is calculated using the distance between isochrons of the same age on opposing sides of the ridge and the half spreading rate is defined using the isochrons on only one side (Hellinger 1981).

The spreading rate is variable from one ridge to another. Mid-ocean ridges are classified as ultraslow (0.8–1.5 cm $year^{-1}$), slow (1.5–5 cm $year^{-1}$), intermediate (5–9 cm $year^{-1}$), and fast (9–20 cm $year^{-1}$) (Fig. 1; plate velocities, from Westphal et al. 2002). Spreading rates increase along the ridge away from the position of the Euler pole to the equator. Spreading rates vary through time due to changes in plate motions (e.g., at 17–12 cm $year^{-1}$ during the period 70–45 Ma, to 4 cm $year^{-1}$ during the period 45 Ma to Recent on the SE Indian ridge as a result of the India-Eurasia collision).

Away from the influence of hot spots, the physical parameters of ridges depend on the spreading rate (MacDonald 1982). Slow-spreading ridges exhibit a narrow axial relief (below the 3,000 m isobath) with a pronounced axial valley and rugged transverse and along-axis segmented morphologies with large variations in height (Fig. 2a; slow-spreading ridge from

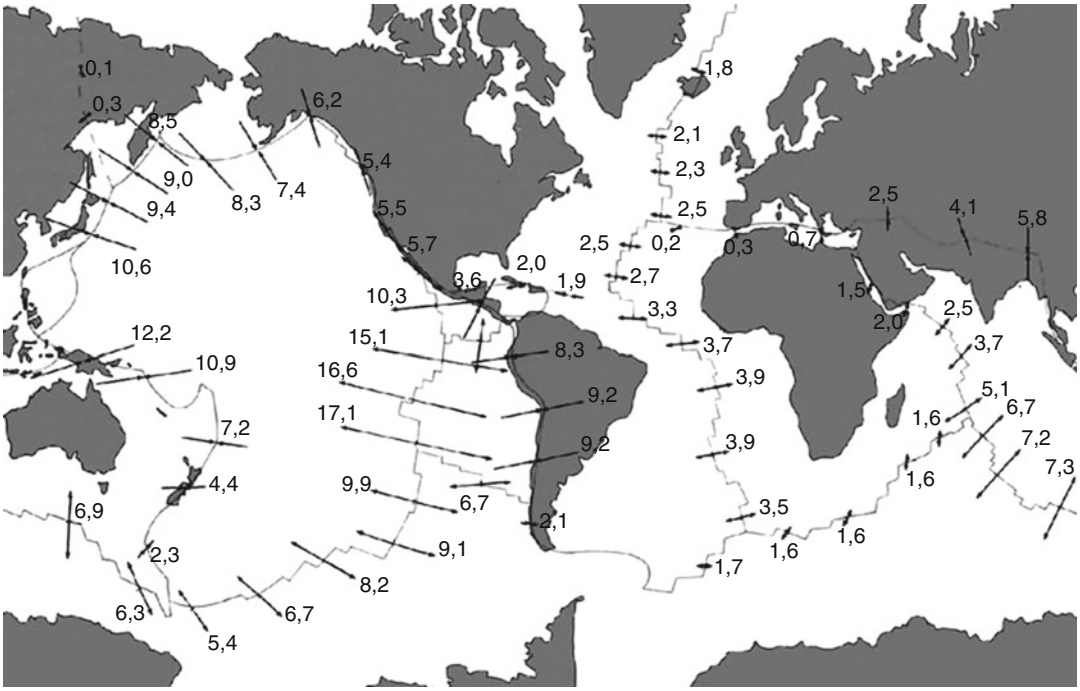

Plate Tectonics, Fig. 1 Directions and full spreading rates (cm year^{-1}) for ridges and direction and shortening rates for subduction zones (Westphal et al. 2002)

Pomerol et al. 2005). Their magma budget is low and mantle peridotite is frequently exposed at the surface. Axial magma chambers have not been detected. Large amplitude mantle gravity anomalies beneath slow-spreading ridges are of "bull eyes" shape. In contrast, fast-spreading ridges exhibit a large axial relief with an axial dome and smoother transverse and along-axis morphologies (Fig. 2b; fast-spreading ridges from Pomerol et al. 2005). Their magma flux is high and an axial magma chamber may be seismically detected. The lithosphere remains thin beneath the flanks of the ridge up to a distance corresponding to 40 Ma. Low-amplitude mantle gravity anomalies beneath fast-spreading ridges are parallel to the ridge. The differences between amplitudes of gravity anomalies indicate either variations in crustal thickness, or the presence of focused hot uprising mantle beneath slow-spreading ridges or along the ridge axis in the case of fast-spreading ridges. Slow-spreading ridges near hot spots (e.g., Reykjanes ridge near Iceland) may have characteristics similar to fast-spreading ridges. This indicates that mantle temperature can also control the physical parameters of divergent boundaries.

Convergent Boundaries

A convergent plate boundary forms when a lithospheric plate, denser than the mantle, slides (subducts) beneath another plate. The oceanic lithosphere plunges beneath other oceanic lithosphere or beneath a continent. When two continents collide, some continental lithosphere may subduct and a mountain range is built (e.g., Himalaya). Broad and almost continuous zones of shallow seismicity, ductile deformation, and metamorphism characterize such zones. The distributed deformation of continents is due to the relatively low strength and low density of continental crust. Subduction zones are characterized by strong and localized seismic activity located within the plunging slab. Friction at the top of the plate causes earthquakes to form the so-called Wadati-Benioff zone. Intraplate compressional and extensional focal mechanisms are the

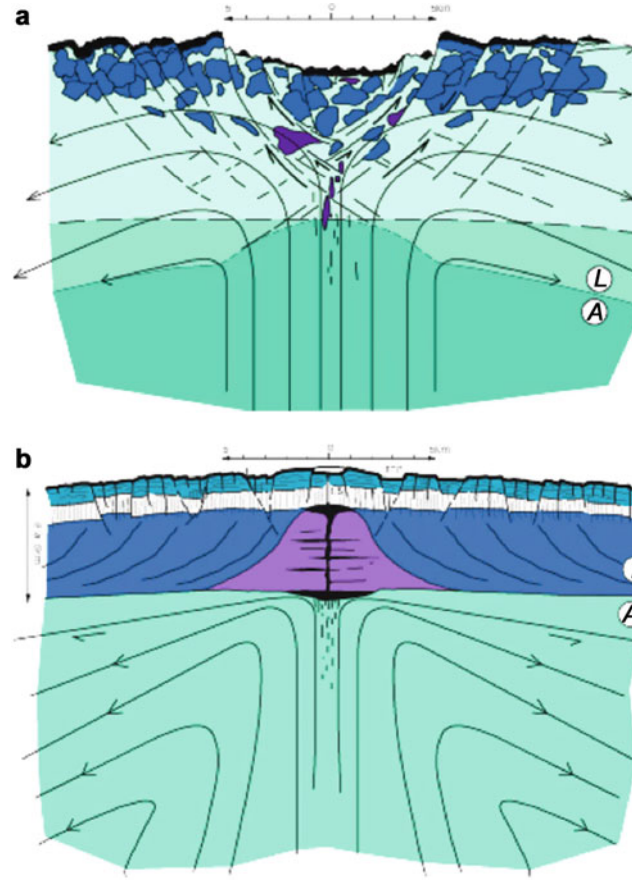

Plate Tectonics, Fig. 2 Ideal cross sections of: (**a**) slow-spreading ridge showing discontinuous small magma chambers (in *violet*) producing discontinuous oceanic crust (serpentinites in *light blue* containing gabbroic pockets in *dark blue*) and (**b**) fast-spreading ridge showing magma chamber, crystal mush (in *violet*), and magma sills and lenses (in *black*) producing a gabbroic (*dark blue*), sheeted dykes (*white*), and basaltic (*dark green*) crust. Flow directions and lithosphere/asthenosphere boundary are indicated in both diagrams (After Pomerol et al. 2005)

responses to stresses generated by the subducting plate. This plate is separated from the overriding plate by deep trenches filled mainly by turbiditic sediments, pelagic sediments, cherts, and fragments of oceanic lithosphere that are internally imbricated in tectonic slices to form an accretionary prism.

Partial melting of the mantle overlying the subducting plate produces calc-alkaline magmas. Those magmas migrate upward and form archipelagos called volcanic arcs (chains of volcanic islands parallel to the subduction zone, f.i.: the "ring of fire" around the Pacific ocean). Two types of volcanic arcs are generally recognized: oceanic (island) arcs are formed by subduction of oceanic plate under another oceanic plate; continental magmatic arcs are formed by subduction of oceanic plate underneath the continent. Arc magma forms when fluids expelled from the subducting slab (pore fluids at shallow depth or metamorphic dehydration of altered oceanic crust at greater depth) induce partial melting of the overlying mantle (the so-called mantle wedge). The magmas of continental arcs exhibit a wide range of calc-alkaline compositions (andesite and diorite, dacite and granodiorite, rhyolite and granite) due to fractional crystallization, continental contamination, and magma mixing in superposed magma chambers.

The distance of island arc volcanism from the trench is dictated by the inclination of the subduction zone, because appropriate temperature-pressure conditions for flux-induced melting occur at the same depth (about 100 km). Continental magmatic arcs are sites of high-temperature, low-pressure metamorphism, and extensive crustal melting due to advection of heat by continuously intruding magmas.

Two types of subduction have been distinguished, depending on the age of the subducting

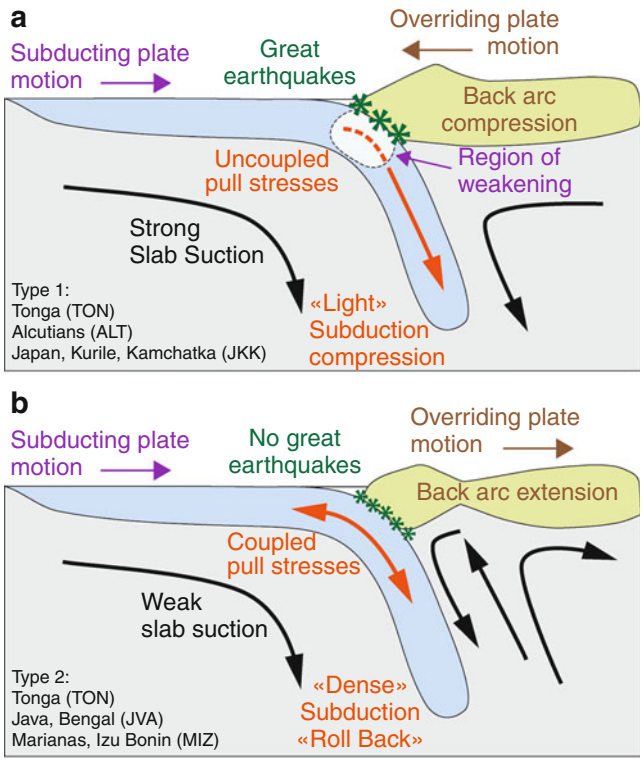

Plate Tectonics, Fig. 3 Two principal architectures of Pacific subduction zones

lithosphere: (a) old, cold, and dense slabs subduct at a high angle or dip (e.g., Mariana subduction); and (b) young, hot, and less dense slabs subduct at a low angle (e.g., Chile subduction) (Fig. 3, from Internet). Mariana-type subduction exhibits deep trenches, short arc-trench distances, deep seismic activity (down to 670 km), and low-magnitude shallow seismicity indicating decoupling between the subducting and overriding plates. Retreat of the subducted plate and accompanying mantle flow (called "roll-over") induces an extension in back-arc basins with eventual creation of new oceanic crust. Chile-type subduction is characterized as a seismic activity which does not exceed 200 km depth, shallow trenches, and long distance between the trench and the volcanic arc. The shallow inverse seismic activity is of high magnitude, indicating a high friction between the two plates that induces arc and back-arc compression.

Subduction zones are the sites of high-pressure, low-temperature metamorphism that develops at the base of the sedimentary prism and within the subduction channel. Thermal modeling shows variable depression of isotherms depending on the age of the lithosphere and rate of subduction. The subducting oceanic crust is metamorphosed progressively from blueschist (low-temperature, moderate-pressure) to eclogite (moderate-temperature, high-pressure) facies. Phase transformations within the subducting lithosphere induce intraplate seismicity and a large increase of density (by the transformation in eclogite of the subducting crust) which provides a major driving force for subduction.

Seismic tomography (two- or three-dimensional imaging of the Earth's interior) shows that high-seismic-velocity, cold mantle from the subducting plate accumulates at the 670-km discontinuity when Mariana-type (steep-dip) subduction occurs. Tomographic imagery shows that cold material sinks episodically into the lower mantle, in some cases down to the core-mantle boundary.

Transform Boundaries

A transform boundary (also known as conservative plate boundary) separates plates that move

parallel to one another with no convergence and divergence, thereby conserving the areas of adjacent plates. The San Andreas Fault (California) or the North- and East-Anatolian faults (Turkey) and the Levant fault (Middle East) are good examples. These boundaries penetrate most of the lithosphere and generally are long-lived structures. They form deep valleys and pull-apart basins at the surface of the Earth. Transform boundaries link other plate boundaries, and can thus "transform" one type of tectonic boundary to another (e.g., from divergent to convergent boundary). Therefore, the stresses generated along the transforms originate from the relative motion of the two plates. Seismic activity can be intense with high magnitude (up to 7).

Ophiolites

An ▶ ophiolite is a slice of oceanic crust and underlying mantle thrust onto a continent by a process called obduction. Obducted ophiolites represent on-land relicts of oceanic lithosphere that escaped the subduction processes. Investigation of these structures has contributed greatly to our understanding of processes at divergent boundaries and tectonic processes related to transform faults. Two types of ophiolites have been described (e.g., Beccaluva et al. 2004): "Tethyan complexes," which comprise complete mantle and crustal sequences (cumulates, dykes and basalts with mid-ocean ridge or island arc affinities) and "Cordilleran complexes" comprising dismembered calc-alkaline arc volcanic and plutonic suites.

The movement of oceanic plates away from the ridge toward the trench is associated with the development of ocean floor stratigraphy which consists, from base to top, or oldest to youngest, of pillow lavas overlain by bedded cherts, deep ocean pelagic sediments, and finally clastic sediments of the accretionary wedge. The interpretation of ocean floor stratigraphy has influenced significantly our understanding of the structure and age of oceanic lithosphere preserved in ophiolite sequences and accretionary orogens.

Hot Spots

Hot Spots are alignments of fossil to recent volcanoes (e.g., Hawaii and Louisville in the Pacific; La Réunion and Kerguelen in the Indian Ocean; Iceland, Azores, and Tristan da Cuhna in the Atlantic Ocean) produced by the passage of a plate over a mantle plume (Fig. 4; position of hot spots from Westphal et al. 2002). These alignments of volcanic chains may exhibit a correlation between the age of the volcanoes and the distance from the active mantle plume. The duration of hot spot tracks varies from negligible to 90 Ma. Active volcanoes on the axis of the mantle plume can be situated near or on divergent plate boundaries, like Iceland on the Atlantic Ridge. Hot spots located near divergent plate boundaries influence the bathymetry and basalt chemistry for distances up to 800 km along the ridge axis. Large hot spots like Hawaii are situated over up-doming or swelling (100 km) of the lithosphere. The Polynesian Archipelagoes in the central Pacific are made up of numerous hot spot volcanoes and overlie a large positive 1,000-km-wide bulge called a "superswell." Analysis of the main hot spot tracks leads to the conclusion that the deep-mantle source hot spots are fixed or move slowly relative to plate velocities. Tomographic images show that low seismic velocity hot mantle columns exist beneath hot spots and in some cases extend down to the core-mantle boundary, suggesting that mantle plumes may originate in the D″ seismic layer. These observations are at the origin of the mantle-plume concept.

Driving Forces of Plate Tectonics

It is generally accepted that plates move because of variations in the density of oceanic lithosphere and the weakness of the asthenosphere. Since more than 50 years, it is acknowledged that dissipation of heat from the mantle drives convection and implicitly also plate tectonics. Modern geophysical methods based on seismic tomography show large lateral variations in density throughout the mantle. These density variations are due in part to differences in rock chemistry and mineral structure, but mainly to changes of temperature that lead to the upwelling of hot regions and the descent of cold regions. It is not entirely understood how plate tectonics is related to these motions. A major problem addressed by researchers since the 1960s is whether the driving

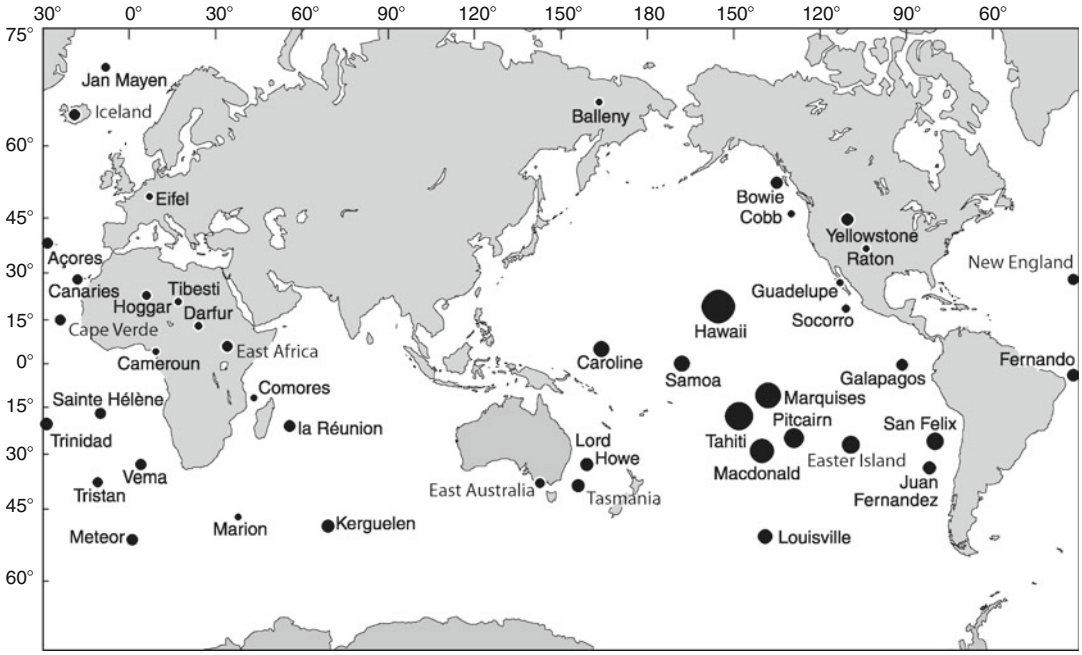

Plate Tectonics, Fig. 4 Position of recent hot spots. The diameter of *black circles* is proportional to the quantity of erupted magma

force of plate tectonics is the mantle convection and/or the activity of mantle plumes, or whether plate tectonics is driven by surface boundary and plate forces such as slab pull and ridge push (see Gravitational Forces; Forsyth and Uyeda 1975). Any valid model has to reproduce the rigid behavior of plates, provide enough energy to produce stresses at the limits of plates, and produce continuous plate motion. Currently, two main types of forces are thought to drive plate tectonics: the friction (localized forces) and gravity (distributed forces) (Fig. 5, driving forces).

Frictional Forces

Basal drag results from friction between the asthenosphere and the lithosphere. It is supposed that the convection movement is transmitted through the asthenosphere and drags the overlying lithosphere. Trench suction occurs in subduction zones where the convection currents exert a frictional pull on the subducting plate. This force results from small-scale convection in the mantle wedge which is driven by a subducting plate.

Gravitational Forces

Gravitational sliding (ridge push) is a distributed gravitational force produced by the higher elevation of oceanic plates due to upwelling of hot material at spreading ridges. Newly formed oceanic lithosphere at mid-ocean ridges is less dense than the underlying asthenosphere, but as the oceanic lithosphere moves away from the ridge it becomes colder, denser, and thicker (McKenzie 1969). Ridge push can be considered as a body force because the increasing thickness of the cold oceanic lithosphere creates a horizontal pressure gradient. However, lithosphere older than 90 Ma undergoes no further cooling and therefore does not contribute to ridge push. In other words, ridge push can be also regarded as a boundary force generated by the upwelling of young warm mantle beneath the ridge crest which causes a topography-driven horizontal pressure gradient that acts at the edge of lithospheric plate. If a hot spot is positioned at the spreading ridge axis, ridge push is amplified at least by a factor two (Ziegler 1993).

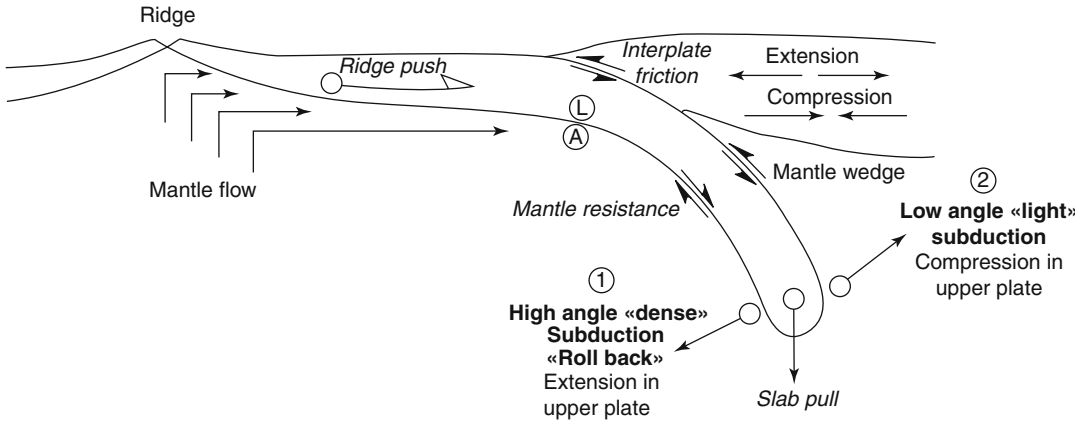

Plate Tectonics, Fig. 5 Schematic diagram for tectonic plate forces

Slab pull results from the weight of the cold and dense subducting lithosphere. This force is dependent on the angle, age, and volume of this lithosphere, as well as the length of the trench (Chapple and Tullis 1977). The lateral distribution of dense and light masses deduced from seismic tomography led Davies (Vigny et al. 1991) to propose a model in which the excess density of the oceanic lithosphere in subduction zones is the most powerful source of plate motion. This hypothesis is supported by studies that show a positive correlation between plate velocities and age of subducting lithosphere. Collisional resistance, a force produced in high-viscosity ductile upper mantle material, is related to slab pull force.

Even if the slab pull is the most important force, it cannot be the only plate tectonic force, because some plates move without subducting boundaries, and other forces like basal drag are locally important. Therefore, plate movement results from the sum of forces acting upon the plate. A significant observation is that lithospheric plates attached to downgoing (subducting) plates move much faster than plates without subducting boundaries. The Pacific plate, which is surrounded by subduction zones, moves much faster than the plates of the Atlantic basin, which are continuous with the flanking continents.

Crustal Growth and Continental Construction

On the modern Earth, continental crust is created mainly at subduction zones. Here, release of aqueous fluid from dehydrating oceanic crust causes melting in the mantle wedge and generates the calc-alkaline magmas that evolve into granitoid continental crust. In other words, on the modern Earth, the formation of continental crust is linked directly to plate tectonics.

Two distinct processes are grouped under the term "continent growth." To a geochemist or petrologist, it refers to the transfer of silicate material from the mantle into the continental crust. To a geodynamicist, the term refers to the construction of a continent, the process that assembles crustal segments of various types, compositions, and origins. This process combines the lateral accretion of island arcs, oceanic crust and oceanic plateaux, and microcontinents, with magmatic addition at convergent margins, to build a continent or ▶ supercontinent. The term "continental crustal growth" or simply "crustal growth" is used for the first process and "continent construction" for the second.

The sites of both crustal growth and continent construction coincide with major accretionary orogens. The accretionary orogens comprise: (1) accretionary wedges, containing material accreted from the downgoing plate and eroded from the upper plate; (2) island arcs, back-arcs, dismembered ophiolites, oceanic plateaux, and old continental blocks; (3) post-accretion granitic rocks and metamorphic products up to the granulite facies, exhumed high- or ultrahigh-pressure metamorphic rocks, and clastic sedimentary

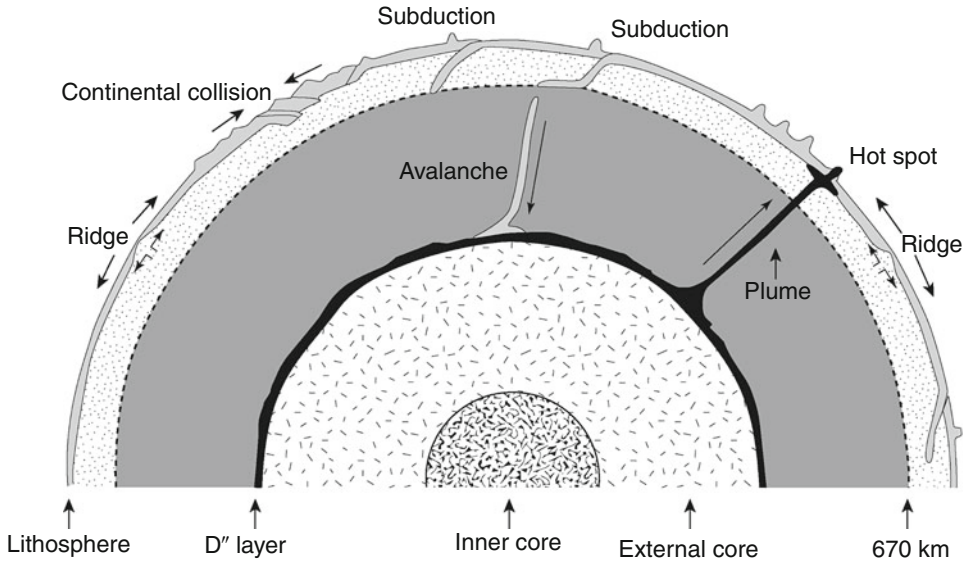

Plate Tectonics, Fig. 6 Schematic cross section of the Earth showing cold subducting plates down to D″ layer and upwelling mantle plumes from D″ layer

basins (e.g., Cawood et al. 2009). The concept of accretionary orogens is associated with the discovery of ocean-floor stratigraphy.

Crustal growth is linked directly to subduction and thus to the formation of oceanic lithosphere at spreading centers: if sea-floor spreading is a continuous process, continental crustal growth should also be continuous. According to many authors, the assembly of continents was an episodic process superimposed on quasi-continuous growth of the continental crust, at least through most of the Phanerozoic. The continental construction processes are commonly associated with large-scale plate reorganization that results from changes in the kinematics of plate motion and/or with superplume activity, which may account for the episodic character of lateral accretion (Vaughan and Scarrow 2003). The fundamental cause of episodes of accelerated growth and construction of the continents can probably be related to changes in the activity of the mantle.

Mantle Convection

Mantle convection has been invoked as a fundamental process controlling plate tectonics (Davies 1999). Heat loss at the surface of the Earth and calculations of heat dissipation in the mantle show that convection is an effective means of evacuating heat from the Earth's interior.

Experiments show that the mantle flows as a solid through two principal deformation mechanisms: diffusion and dislocation creep. The experimental laws of crystal deformation show that the mantle viscosity is a function of activation energy (activation enthalpy and volume), pressure, temperature, and differential stress. Many authors accept that diffusion creep is the major deformation mechanism in the mantle, in which case the viscosity is almost a linear function of depth, except at boundary layers (phase transitions). Reference viscosities of the upper mantle have been estimated using isostatic glacial rebound and subduction zone geoids. Viscosities of the order of 10^{20} Pa s are estimated for the asthenosphere and 10^{21} Pa s for the lower mantle.

The accepted model today describes the internal movement in the mantle as follows: active plunging of cold material in subduction zones, hot uprising mantle currents beneath hot spots, and discontinuous narrow passive upwelling of hot mantle beneath the ocean ridges (Fig. 6; from Westphal et al. 2002). Whether convection occurs in one cell or two depends on the properties at the 670 km depth discontinuity

(Brunet and Machetel 1998). This limit corresponds to a phase transition (spinel-perovskite) which corresponds to a downward increase of density of 0.4 g cm^{-3}, or about 10 %. This density change is greater than the density difference between a cold plunging slab and the surrounding mantle, which means that the slab does not penetrate the discontinuity until all the phases have been transformed.

See Also

- Asthenosphere
- Continental Crust
- Continents
- Lithosphere, Planetary
- Mantle
- Mantle Plume, Planetary
- Mid-Ocean Ridges
- Plate, Lithosphere
- Supercontinent
- Volcano

References and Further Reading

Barell J (1914) The strength of the earth's crust. J Geol 22:441–468

Beccaluva L, Coltorti M, Giunta G, Siena F (2004) Tethyan vs Cordilleran ophiolites: a reappraisal of distinctive tectono-magmatic features of supra-subduction complexes in relation to subduction mode. Tectonophysics 393:163–174

Brunet D, Machetel P (1998) Large scale tectonic feature induced by mantle avalanche with phase, temperature and pressure lateral variations of viscosity. J Geophys Res 103:4929–4945

Carey SW (1958) The tectonic approach to continental drift. In: Carey SW (ed) Continental drift – a symposium. University of Tasmania, Hobart, pp 177–363 (expanding Earth from p 311 to p 349)

Cawood PA, Kröner A, Collins WJ, Kusky TM, Mooney WD, Windley BF (2009) Accretionary orogens through Earth history. Geol Soc Lond Spec Publ 318:1–36

Chapple WM, Tullis TE (1977) Evaluation of the forces that drive the plates. J Geophys Res 82:1967–1984

Davies GF (1999) Dynamic Earth: plates, plumes and mantle convections. Cambridge University Press, Cambridge, 458 pp

Dewey JF, Bird JM (1970) Mountain belts and the new global tectonics. J Geophys Res 74:2625–2647

Forsyth D, Uyeda S (1975) On relative importance of the driving forces of plate motion. Geophys J R Astron Soc 43:163–200

Hellinger SJ (1981) The uncertainties of finite rotations in plate tectonics. J Geophys Res 86:9312–9318

Hess HH (1962) History of ocean basins. In: Engel AEJ, James HL, Leonard BF (eds) Petrologic studies: a volume in honor of A. F. Buddington. Geological Society of America, Denver, pp 599–620

Holmes A (1928) Radioactivity and Earth movements. Trans Geol Soc Glasgow 18:559–606

Isacks B, Oliver J, Sykes LR (1968) Seismology and the new global tectonics. J Geophys Res 73:5855–5900

Le Pichon X (1968) Sea-floor spreading and continental drift. J Geophys Res 73:3661–3696

MacDonald KC (1982) Mid-ocean ridges: fine scale tectonic, volcanic and hydrothermal processes within the plate boundary zone. Annu Rev Earth Planet Sci 10:178–179

McKenzie DP (1969) Speculations on the consequences and causes of plate motions. Geophys J 18:1–32

Morgan JP (1968) Rises, trenches, great faults, and crustal blocks. J Geophys Res 73:1959–1982

Pomerol C, Lagabrielle Y, Renard M (2005) Eléments de Géologie. Dunod, Paris

Vaughan APM, Scarrow JH (2003) Ophiolite obduction pulses as a proxy indicator of superplume events? Earth Planet Sci Lett 213:407–416

Vigny C, Ricard Y, Froidevaux C (1991) The driving mechanism of plate tectonics. Tectonophysics 187:345–360

Vine FJ, Matthews DH (1963) Magnetic anomalies over oceanic ridges. Nature 199:947–949

Westphal M, Whitechurch H, Munschy M (2002) La tectonique des plaques. GB Science, Paris, 307 pp

White RS, Minshull TA, Bickle MJ, Robinson CJ (2001) Melt generation at very slow-spreading oceanic ridges: constraints from geochemical and geophysical data. J Petrol 42:1171–1196

Wilson JT (1965) A new class of faults and their bearing on continental drift. Nature 207:343–347

Ziegler PA (1993) Plate-moving mechanisms: their relative importance. J Geol Soc Lond 150:927–940

Plate Tectonics, History of

Pierre Savaton
Université de Caen Basse-Normandie, Caen, France

Keywords

Continental drift; Isostasy; Mantle convection; Permanence theory; Polar wandering; Seafloor spreading

History

Plate tectonics is the paradigmatic theory of the modern geology since 40 years. It established that the major features of the Earth's surface depend on the dynamics of lithospheric plates, created from the ▶ mantle at the oceanic ridges and absorbed into the mantle at the oceanic trenches, except continental crust that can never sink and, thus, is condemned to be recycled in new mountain ranges. If moving plates are clear scientific evidence today, it was not at the beginning of the twentieth century when German meteorologist and geophysicist Alfred Wegener proposed his theory of continental translation (later translated with derisive sense in continental drift) against the leading theory on mountain formation.

In 1912, Alfred Wegener (1880–1930) proposed to consider that all continents might once have formed a single continent (today called a supercontinent) he named Pangaea that might have been broken. Then, these continental masses might have drifted over oceanic crust. Their front margins (like a ship's bow), compressed and folded by the resistance of the ocean floor, might have formed mountain ranges (like Andes or the Rocky Mountains), and on the opposite, fragments of continents might have been detached in their wake as string of islands. Continents and ocean basins would not be permanent features of the Earth. Horizontal motions were more important than vertical motions defended by the theory of a cooling earth.

The model of mountains by contraction of a cooling Earth was suggested and developed in France by geologist Léonce Elie de Beaumont (1829) and defended in Great Britain by Henry De la Bêche. It found its best formalization at the end of the century in the work of the Austrian geologist Eduard Suess. According to Suess's theory, vertical motions of its crust explained the features of the Earth. As the globe cooled and began to sink, outer crust collapsed creating ocean basins and continents. Successive collapses changed the face of the Earth: ocean basins elevated into continents and continents collapsed to form ocean basins. Suess's theory was centered on "the breaking up of terrestrial globe." But this model of "the shriveling apple" could not explain longer the compression rate calculated to unfold folding strata of the Alps or of the Himalayas. In the Alps, the horizontal extent of strata has been shortened to one quarter to one eighth of its original length, which would have required a shrinking of the circumference of the Earth by 3 %, which means that Earth has cooled of about 2,400 °C.

At the end of the nineteenth century, geological views of Eduard Suess and of the European geologists were not shared by the American scientific community, which widely accepted the "permanence theory" developed by James Hall and James Dana. Oceans and continents were permanent features of the Earth's surface and change confined to limited areas on continental margins (*geosyncline*).

Wegener broke up with the secular cooling theory, collapsed by the discovery of natural radioactivity in 1896, and the assumption of a heating Earth. In contrast, he used the theory of isostasy, suggested by John H. Pratt and George B. Airy and named by Clarence E. Dutton in 1892, to interpret the Earth's crust in two layers. A light continental crust would float and drift on heavy oceanic crust and would never sink. The horizontal motions and deformations of the continents would cause the major geological features. Wegener's theory tried to unify data from paleontology, biogeography, geophysics, stratigraphy, geological mapping, and paleoclimatology to propose a synthetic model. He tried to unify European and American opposite views. The explanation of the rejection of his continental drift by most of the geologists of the 1920s and 1930s is complex and could not be justified only by the lack of a causal explanation of drift. The death of Wegener in 1930 and the inability to prove or disprove his theory closed the controversy. Debate was put aside in spite of the causal models proposed in the end of the 1920s by the Canadian geologist Reginald Daly and the British geologist Arthur Holmes. Daly in *Our Mobile Earth* published in 1926 proposed a gravity sliding as drift mechanism. Holmes in his paper of 1929 about *Radioactivity and Earth movements* proposed subcrustal convection currents to

evacuate heat from the interior of the Earth. He proposed continental drift as consequence of thermal convection. But the question of continental drift was not settled.

Because of his studies about earthquake waves, Sir Harold Jeffreys was persuaded that the Earth possessed a considerable strength, incompatible with models of drifting continents. The transmission of seismic waves could be imagined only within a stiff Earth. The study of the earthquake of Kupa of October 8, 1909, allowed Serbian geophysicist Andrija Mohorovicic to bring to light a brutal acceleration of the speed of propagation of the waves toward 50 km deep and to establish a seismic boundary between the crust and the mantle. Five years later, German seismologist Beno Gutenberg determined a major discontinuity at the depth of 2,900 km: the seismic boundary between mantle and core was discovered. In the 1920s, Gutenberg, through his works about deep-focus earthquakes and identification of a low-velocity zone, concluded to a weak crustal substrate and joined those who defended the possibility of subcrustal currents. In 1934, Gutenberg and an American seismologist Charles Francis Richter published new travel-time curves, which contributed to specify a seismic model of the globe. The discovery of an inner core's discontinuity by Inge Lehman, in 1936, and its interpretation by Beno Gutenberg and Richter as a separation between a fluid outer core and a solid inner core conduced in few years to establish a structural model of Earth's interior. The model of Harold Jeffreys and Keith E. Bullen little changed since 1940. In the 1950s, David Griggs, Harry Hess, and Félix Venig-Meinesz proposed convection models. Like that of Arthur Holmes, their models offered finally a physical reliable cause to the drifting continents of Wegener.

After the Second World War, the development of paleomagnetic studies was going to shake the trust in the continental permanence and revive the idea of drifting continents. The work of Bernard Brunhes in the early 1900s showed that old basaltic lavas are magnetized in directions making sometimes large angles with the present Earth's magnetic field. Basalt acquires its magnetization from the geomagnetic field when it crystallizes and passes under the Curie point of their magnetic minerals (580 °C for magnetite). Considering that the mean geomagnetic field can be compared with an axial dipole situated at the Earth's center, the magnetic field's characteristics, recorded in the rocks, should be those of their geographic localization. Patrick Blackett, Stanley K. Runcorn, Edward Irving, and K. Creer, by the mid-1950s, observed that the geographic North Pole fossilized in lavas changed with geological time. The angle of polar difference increasing with time, a migration either of the poles or of the continents was clearly suggested. Wegener's hypothesis of polar wandering based on paleoclimatic data seemed to be confirmed. Polar wandering paths were determined for North America and Europe by Stanley Runcorn. A systematic difference appeared between the polar wanders of the two continents since the Triassic. But putting side by side North America and Europe, it disappeared. Paleomagnetic arguments strongly supported the idea of moving continents and the possibility of existence of supercontinents in the past, as Pangaea, the old supercontinent imagined by Wegener, 30 years ahead. In the beginning of 1950, the American geologist Harry Hess used a magnetometer to record magnetic variations across the ocean floor. These magnetic variations are associated with the magnetite contained in oceanic basalts, which records the orientation and intensity of the Earth's magnetic field at the time of basalt extrusion. In the 1960s, magnetic studies revealed the existence of alternating stripes of normal and reverse polarity, which are symmetrically distributed on either side of the mid-ocean ridge. The alternation of direct and inverse magnetic polarity is related to periodic changes in the polarity of the Earth's magnetic field, which is recorded in the basaltic rocks. The marine geologists and geophysicists Frederick Vine and Drummond Matthews suggested in 1963 that the ▶ mid-ocean ridges mark structurally weak zones

where the ocean floor was split in two along the ridge crest. It was suggested that pulses of magma rise along the ridge and create new oceanic crust, which then migrate laterally away from the ridge – the process called seafloor spreading. The explanation of the magnetic striping led to the rapid acceptance of seafloor spreading as a key element of plate tectonics theory.

In the 1950s, geological and geophysical oceanographic explorations established a new physiography of the ocean floors. The ocean floor showed a world embracing mid-oceanic ridge system, cut by transverse faults, showed arc-trench system with extinct and active volcanoes, and revealed numerous seamounts, interpreted by Harry H. Hess as subsiding volcanoes. In 1959, Bruce Heezen, Marie Tharp, and Maurice Ewing published the first detailed bathymetric map of the North Atlantic Ocean. Campaigns of coring deep-sea sediment and dredging of rock samples from exposed scarps on the oceanic ridges revealed a great petrographic homogeneity of the seafloor (only basic and ultrabasic rock types) and lack of sedimentary rocks older than Cretaceous. In 1961, Robert S. Dietz expressed his hypothesis of a seafloor spreading, and a year later, Harry Hess, independently, published a paper where he proposed equally that the seafloor was created at mid-ocean ridges, then spread out toward the trenches where it sank into the mantle, driven by convection currents of the mantle. Canadian geophysicist Tuzo Wilson, studying transverse faults of the ridges, suggested in 1965 that they would limit several large, rigid crust areas that he called *plates*. The Earth's surface would be divided into plates limited by ocean ridges, ocean trenches, and transverse faults (such as the St Andreas fault in California) that would transform the one to the other one. Earthquakes and volcanic activity would characterize plate boundaries. In his model, the oceans are created, grow, and disappear; and the continents are fragmented, separated, and reassembled in what are now called "Wilson cycles." But Earth's crust was too thin to be stiff enough and required to extend about 100 km down that meant to the low-velocity zone of the mantle. Plates are lithospheric ones composed of what is called crust and the upper, rigid part of the mantle, the so-called lithospheric mantle. Further understanding of plate kinematics came from the work of the geophysicists William Jason Morgan and Dan McKenzie, who explained in 1968 relative displacements of adjacent plates. He showed that the movements are parallel to transform faults and centered on a pole of rotation (the Euler pole) and that variations of seafloor expansion are a function of the distance from the pole of rotation. Using Jason Morgan's model of plates and Euler's theorem about translation of an area on a sphere, French geophysicist Xavier Le Pichon proposed the same year to divide Earth's surface into six major plates. Plate tectonics break with continental drift, because if continents move, they do not drift over ocean.

Geological aspects of the theory of plate tectonics were developed by the geologists John Dewey and John Bird, who showed in 1970 that the structure of active continental margins is dependent on the geometry and kinematics of subduction zones. This seminal paper showed geologists how the orogenic belts are linked to movements of the oceanic lithosphere and explained the relationship between plate tectonics and both the complex 3D movements at continental margins and the magmatic and metamorphic processes of mountain building. In 1977, the submersible vehicle Alvin observed hydrothermal vents on the east pacific ridge. Geologists were looking for deep-sea hot springs, which they predicted to exist along rifts. They discovered them, and in the same time, they made a greater discovery: vents were jammed with animals. Plate tectonics gave a new breath to understand the early beginning of the life on our Earth.

The early establishment of the theory of plate tectonics in the 1960s represented a revolution in Earth sciences, like British paleontologist Anthony Hallam wrote in 1972. For the first time, data from all of the branches of Earth sciences gathered in a unifying theory, which could explain past and present geological time and can also predict what will happen in the future.

See Also

- ▶ Mantle
- ▶ Mantle Plume, Planetary
- ▶ Mid-Ocean Ridges
- ▶ Plate Tectonics

References and Further Reading

Le Grand H (1988) Drifting continents and shifting theories: the modern revolution in geology and shifting theories. Cambridge University Press, Cambridge

Marvin U (1973) Continental drift. The evolution of a concept. Smithsonian Institution Press, Washington, DC

Oreskes N (1999) The rejection of continental drift. Oxford University Press, New York

Oreskes N (ed) (2003) Plate tectonics: an insider's history of the modern theory of the Earth. Westview Press, Boulder

Plate, Lithospheric

Nicholas Arndt
ISTerre, Université Grenoble Alpes, France

Definition

A plate is a large cohesive mass of oceanic or continental lithosphere which moves as a single element in the process of plate tectonics. The outer layer of the solid Earth is composed of nine major lithospheric or tectonic plates and a large number of minor plates. They are relatively rigid, and they float on and move atop the more deformable ▶ asthenosphere at speeds relative to each other varying from 2 to 10 cm/year. The largest, Pacific, plate is ~4,000 km long and wide and up to 100 km thick. It is the fastest plate, moving at about 10 cm/year. The upper part of the lithosphere plates may consists of either oceanic or of continental crust and are then called "continental" and "oceanic lithosphere", respectively. Oceanic plates are created at mid-ocean ridges and are destroyed at subduction zones. The Pacific and Nazca plates and several smaller plates consist entirely of oceanic lithosphere but most others contain both continental and oceanic lithosphere. Because of thick roots beneath Archean ▶ cratons, the maximum thickness of continental plates reaches several hundred kilometers. The creation, displacement, and destruction of lithospheric plates define ▶ plate tectonics, the dominant geodynamic process at the Earth's surface. Plate movement represents the uppermost element of large-scale convection that affects most of the ▶ mantle.

See Also

- ▶ Asthenosphere
- ▶ Continental Crust
- ▶ Craton
- ▶ Crust
- ▶ Lithosphere, Planetary
- ▶ Mantle
- ▶ Oceanic Crust
- ▶ Plate Tectonics

Platinum Group Elements

Nicholas Arndt
ISTerre, Université Grenoble Alpes, France

Synonyms

PGE

Definition

The platinum group elements (PGE) or metals (PGM) – ruthenium, rhodium, palladium, osmium, iridium, and platinum – have similar

chemical characteristics and behave as a group during geochemical processes. They are strongly siderophile (iron-loving) and chalcophile (sulfur-loving) and are therefore concentrated in the core of the Earth and in iron meteorites, in sulfide ore deposits, and to a lesser extent in the Earth's mantle. An important geological application of the PGE is the use of iridium as a tracer of meteoritic material, most famously in the development of the meteorite impact hypothesis for the origin of the Cretaceous-Tertiary mass extinction. The isotopic system rhenium-osmium is used to date mafic-ultramafic rocks and as a tracer of processes in the Earth's mantle. The occurrence of small excesses of PGE in the mantle has been often indicated as evidence of a late contribution of chondritic material to the Earth (► Late Veneer hypothesis).

See Also

- ► Chalcophile Elements
- ► Chondrite
- ► Iridium
- ► Late Veneer
- ► Radiogenic Isotopes
- ► Siderophile Elements

PLATO 2.0 Satellite

Heike Rauer[1] and Malcolm Fridlund[2]
[1]German Aerospace Center (DLR), Berlin, Germany
[2]Max-Planck-Institut für Astronomie, Heidelberg, Germany

Keywords

Exoplanet; Transit; Asteroseismology; Stars

Synonyms

PLAnetary Transits and Oscillations of stars

Definition

PLATO 2.0 (PLAnetary Transits and Oscillations of stars) is a mission for the detection and characterization (radius, mass, age) of transiting exoplanets at orbital distances up to the habitable zone of solar-like stars. In addition, PLATO 2.0 will study the stellar structure through asteroseismology.

Overview

PLATO 2.0 is the first space mission designed for the simultaneous search for transiting exoplanets and study of their host stars through ► asteroseismology (Rauer et al. 2014). Selected as the 3rd mission of the cosmic vision science programe of ESA, it is planned for a launch in 2024, PLATO 2.0 will be developed in a partnership between ► ESA (providing the spacecraft, launch, and elements of the operation) and a scientific consortium (providing the payload, including the telescopes, elements of the operations, and scientific planning), led by Germany (DLR) and consisting of elements from essentially all of the ESA member states.

Basic Methodology

When an exoplanet travels between its host star and the Earth, it induces a weak drop of the star's brightness (a mini eclipse). The detection of this periodic ► transit in the star's light curve, together with its careful analysis (e.g., discerning the transit signature from, e.g., star spots), reveals the existence of the exoplanet and provides important characteristics such as the planet's radius, its orbit parameters, and the rotation period of the star. By also studying the properties

of the star, such as its radial velocity, its radius, and its age, the absolute values of the mass, radius, and age of the planet can be determined.

Stars, acted on by gravity, pressure, and Coriolis forces, behave as oscillators with many specific modes. These oscillations are detectable through tiny variations in the stellar brightness, and their analysis provides important parameters on the stars' internal structure. Most importantly, parameters such as mass, radius, and age can be determined with significantly higher precision in this way than with classical methods such as spectroscopy.

If the stellar parameters of the planet's host star have been determined through asteroseismology, the planetary values can be determined with unprecedented accuracy.

PLATO 2.0 is designed to have an ultrawide field of 2,250 square degrees that enables it to monitor the flux from hundreds of thousands of stars for uninterrupted periods of up to several years. This allows users of the spacecraft to detect and measure the tiny variations in the stellar flux that are caused either by stellar activity, stellar internal oscillations, and/or the possible transit signature of an orbiting exoplanet. The satellite carries thirty-four (34) six-lens visible telescopes each with a clear aperture of 12 cm and each focusing the stars' light on an individual focal unit hosting four frame-transfer ▶ CCD matrices of 4,510 × 4,510 18 Micron Pixels. The detectors, whose temperature is cooled passively, have a high quantum efficiency in the visible wavelengths. Each telescope is equipped with an individual baffle to reduce the parasitic straylight, as well as the whole assemblage being sheltered by an efficient sun shield. In order to remain shielded from the scattered Sunlight, as the satellite travels around the Sun in its L2 Lissajou (Lagrange points) orbit, it is necessary to rotate the spacecraft 90° around its optical axis every 90 days. Thirty-two of the telescopes (referred to as "normal cameras") observe with a cadence of 25s and monitor objects fainter than visual magnitude 8. The two remaining telescopes (referred to as "fast cameras"), equipped with colored filters, observe with a cadence of 2.5s and observe stars between visual magnitudes 4 and 8.

Key Research Objectives

Exoplanets and Asteroseismology

PLATO 2.0 will monitor about 1,000,000 solar-like stars, during periods of between a few months and ~3 years, searching for the signature of the transit of a planet with the same size as the Earth.

While PLATO 2.0 will be able to detect quite easily super-Earths in short (less than 2 months) orbits, its major breakthrough will be for planets down to Earth size orbiting within the habitable zone (HZ) of large numbers of solar-like stars (which requires the detection capability of periods larger than approximately 6 months). This is a parameter range not explored by any past, current, or planned space mission.

PLATO 2.0 will determine albedo and atmospheric properties for a large number of objects by performing the bulk observation of secondary transits (Alonso et al. 2009a, b), as well as by measuring the changes in illumination of exoplanets as their phases change.

For about 85,000 bright stars with magnitudes smaller than 11.3, the stellar light curve will be recovered with a precision accurate enough to obtain the mass and size of the star with an error of a few percent through asteroseismology. This will allow the detailed characterization of any planet found orbiting those stars. Their ages will also be determined with unprecedented precision (~10 %) and with information about orbital distributions, and from some of the atmospheric parameters we will get the first information about the evolution of exoplanets.

PLATO 2.0 and Stellar Physics

Through asteroseismology solar-like stars, stars hotter than the Sun, and red giants can be studied in detail through solar-like oscillations. Data from the CoRoT and Kepler space missions have demonstrated that the much more capable

PLATO 2.0 will be able to open a new chapter in stellar physics, as well as carry out detailed galactic archeology for our part of the Milky Way galaxy.

Applications

PLATO 2.0 will be the next order-of-magnitude step, beyond CoRoT (Baglin et al. 2007), Kepler (Basri et al. 2005), ▶ TESS, and ▶ CHEOPS, in our search for exoplanets, enabling us to further our understanding of the distribution of sizes and masses of large numbers of small and "rocky" planets. This will enable progress in theories for the formation and evolution of stellar systems and also their host stars. The improvement in physical parameters of large numbers and kinds of stars will allow stellar physics to evolve and will impact on large areas of astrophysics.

PLATO 2.0 will bring together the European exoplanetary community and drive the evolution of ground-based follow-up which will itself impact many areas.

Future Directions

PLATO 2.0, together with the preceeding missions TESS and CHEOPS, will constitute the main steps in preparing for the spectroscopic missions that will follow. ▶ JWST will of course carry out spectroscopy at roughly the same time as PLATO 2.0, but it is equipped with only simple coronographic capability. PLATO 2.0 results will map out the direction that the astronomical community will have to move toward in order to make progress in the search for extraterrestrial life.

See Also

- ▶ Asteroseismology
- ▶ Atmosphere, Temperature Inversion
- ▶ Brown Dwarf
- ▶ CoRoT Satellite
- ▶ Habitability, Effect of Eccentricity
- ▶ Habitable Zone, Effect of Tidal Locking
- ▶ Hot Jupiters
- ▶ Hot Neptunes
- ▶ Kepler Mission
- ▶ Microlensing Planets
- ▶ Planetary Migration
- ▶ Radial Velocity
- ▶ Red Giant
- ▶ Spectroscopy
- ▶ Stellar Pulsation
- ▶ Stellar Rotation
- ▶ Super-Earths
- ▶ Transit
- ▶ Transiting Planets
- ▶ VLT

References and Further Reading

Alonso R, Guillot T, Mazeh T et al (2009a) The secondary eclipse of the transiting exoplanet CoRoT-2b. Astron Astrophys 501:23–26

Alonso R, Alapini A, Aigrain S et al (2009b) The secondary eclipse of CoRoT-1b. Astron Astrophys 506:331–336

Baglin A et al (2007) The CoRoT mission and its scientific objectives. AIP Conf Proc 895:201–209

Basri G, Borucki WJ, Koch D (2005) The Kepler mission: a wide-field transit search for terrestrial planets. New Astron Rev 49(7–9 Special Issue):478–485

Rauer H, Catala C, Aerts C et al (2014) The PLATO 2.0 mission. Exp Astron. 38, 249–330, doi:10.1007/s10686-014-9383-4

P

Ploidy

Ricardo Amils
Departamento de Biologia Molecular, Universidad Autónoma de Madrid, Madrid, Spain

Definition

Ploidy refers to the number of sets of chromosomes in a biological ▶ cell. Sex cells, also called

gametes, combine to produce somatic cells. The haploid number is the number of chromosomes in a gamete. A somatic cell has twice that many chromosomes. However, many organisms have more than two sets of homologous chromosomes and are called polyploidy.

See Also

- ▶ Cell
- ▶ Chromosome
- ▶ Fungi

Plug-Flow Reactor

- ▶ Flow Reactor

Plume

Doris Breuer and Ralf Jaumann
German Aerospace Center (DLR), Institute of Planetary Research, Berlin, Germany

Definition

A plume is a column of one type of matter moving through another one, driven by momentum, diffusion, and buoyancy. The flow can be driven by buoyancy derived from differences in temperature or chemistry between the plume and the surrounding medium. ▶ Mantle plumes are upwelling hot rocks within a planetary mantle driven by a temperature difference of a few hundred Kelvin. Mantle plumes are thought to feed volcanic centers known as hotspots. Plumes also form in planetary atmospheres, e.g., above volcanic eruptions. Umbrella-shaped plumes are eruption columns that eject gas and dust from volcanic vents into space. The most impressive eruption plumes in the ▶ solar system occur on the Jovian satellite Io, reaching more than 400-km height before falling back. The mechanism of plume eruptions is similar to that of geysers.

See Also

- ▶ Heat Flow, Planetary
- ▶ Interior Structure, Planetary
- ▶ Io
- ▶ Mantle
- ▶ Mantle Plume, Planetary
- ▶ Plate Tectonics
- ▶ Rock
- ▶ Solar System

Plurality of Worlds

Florence Raulin-Cerceau
Maître de Conférences, Centre Alexandre Koyré (UMR 8560-CNRS/EHESS/MNHN/CSI)
Muséum National d'Histoire Naturelle, Brunoy, France

The plurality of worlds, regarded as other inhabited worlds in the universe, is a debated question since Antiquity. The Greek philosopher Anaximander considered that countless worlds succeeding one another could be born from an infinite universe. The atomist Democritus, as well as Epicurus and later Lucretius, maintained that worlds in infinite number have emerged from atoms and infinite void, a materialistic view of the universe. Following the heliocentric Copernican theory, new speculations were formulated. Inquisition rejected the infinity of worlds proposed by the dissident Dominican friar Giordano Bruno. However, famous personalities expounded this idea (Kepler, Huygens, Fontenelle) which finally became a scientific topic during the nineteenth century (Flammarion, Proctor). Astrobiology revisits today this concept through space exploration and the continuous discoveries of exoplanets.

See Also

► Bruno, Giordano

Pluricellular Organisms

► Multicellular Organisms

Pluto

Emmanuel Lellouch
Laboratoire d'Etudes Spatiales et d'Instrumentation en Astrophysique (LESIA), Observatoire de Paris, Meudon, France

Keywords

Dwarf planet; Resonant orbit; Satellite system; Trans-Neptunian object

Definition

Pluto (formal designation (134340) Pluto) is the second-most massive and probably the largest known trans-Neptunian object. From its discovery in 1930 to 2006, it was considered the Solar System's ninth planet. However, the International Astronomical Union's (IAU) reclassification of Solar System objects in 2006 puts Pluto in the category of ► dwarf planets, that is, objects large enough to satisfy the condition of hydrostatic equilibrium but that do not dynamically dominate their surrounding population. Pluto is being visited in 2015 by the space mission *New Horizons*.

History

Pluto was discovered on February 18, 1930, by a 23-year-old farmer and amateur astronomer Clyde Tombaugh. Tombaugh was employed at Lowell Observatory with the task of searching for a putative massive (several Earth masses) object, known as "planet X." Planet X had been predicted by Percival Lowell (and independently by others) on the basis of analyses of Uranus' motion, in much the same manner Neptune had been discovered in 1846. After about 1 year of search, Tombaugh spotted a moving object on plates recorded on January 23 and 28, 1930. The discovery was announced on March 13 (for the 75th anniversary of Lowell's birth) in the form of an observation circular cautiously entitled "The Discovery of a Solar System Body Apparently Trans-Neptunian." Inspection of archive observations of the world's major observatories confirmed the detection of the object on no less than 136 plates, the earliest of these "prediscovery" images dating from January 1914. This allowed an accurate ► orbit to be quickly established, confirming that the object, then at 41.3 AU from the Sun, was indeed trans-Neptunian. However, Pluto was immediately realized not to be the object that was looked for. With its faint magnitude (about 15 at discovery) and unresolved appearance, Pluto must have been very small. Initial estimates showed it to be less massive than the Earth (and measurements in subsequent decades only aggravated the problem), indicating that the new object was unable to perturb the motion of Uranus. Tombaugh continued his quest for another 10 years, without success. The mystery was not solved until 1993, when updated calculations of Uranus' motion, using the accurate mass of Neptune provided by Voyager 2, made the perturbations vanish, and with them the need for a planet.

Overview

Orbit

With a semimajor axis of 39.5 AU, Pluto orbits the Sun in a mean 248.1-year period. Its highly elliptical (eccentricity = 0.249) and inclined ($i = 17.1°$ over the ecliptic) orbit is distinctly different from those of the planets. The large

eccentricity brings Pluto to 29.7 AU from the Sun at perihelion and 49.7 AU at perihelion. Pluto is therefore occasionally closer to the Sun than Neptune (lastly between February 1979 and February 1999), but the inclination of Pluto's orbit is such that the two orbits do not intersect; when Pluto is near perihelion, it is also far above the ecliptic plane. Moreover, Pluto and Neptune appear to be in 3:2 mean motion resonance, that is, the mean orbital period of Pluto is equal to 1½ orbits of Neptune (period 165.4 years). Neptune travels faster than Pluto along its orbital path but "overtakes" it only when Pluto is near its aphelion; conversely when Pluto is near perihelion, Neptune is nowhere near, and the two bodies are rather close to quadrature. The consequence of this synchronism is that the minimum distance between Pluto and Neptune is 17 AU. Ironically, Pluto can come closer to Uranus (12 AU). More fundamentally, these large distances imply that Pluto's orbit cannot be destabilized by the giant planets. In spite of this, Pluto's argument of perihelion (one of the elements describing the orbit; see ▶ orbit) is not fixed over timescales of millions of years and librates by $\pm 38^\circ$ about a mean value of 90° with a period of about 10,000 years.

Satellite System

Pluto possesses five sateliites, by order of increasing distance to Pluto: Charon, discovered in 1978 by J. Christy, Styx, Nix, Kerberos, and Hydra, detected over 2005-2012 in Hubble Space Telescope (HST) images. The five satellites have orbital periods of 6.387, 20.2, 24.9, 32.2, and 38.2 days, forming a 1:3:4:5:6 sequence of near (but not exact) mean motion resonances with Charon. Charon and Pluto form a remarkably "balanced" pair, with Charon's radius and mass being approximately one-half and one-eighth of Pluto's (the latter being equal to 0.002 Earth masses), respectively. Ironically, the radius of Charon (604 km), determined from stellar occultation, is more precisely known than that of Pluto (1,160–1,200 km), for which the atmosphere (see below) introduces ambiguity. The barycenter of the Pluto-Charon system lies outside Pluto, justifying the use of the wording "binary system." Strictly speaking, Charon does not orbit Pluto; rather, the two bodies orbit their common barycenter. The period of mutual revolution is exactly equal to Pluto's and Charon's rotation periods on their axes, measured from the observation of their optical light curves (see below). This synchronous motion is the consequence of mutual tidal forces. The plane of Charon's orbit, which can be identified as the equatorial plane of the two bodies, is inclined by 120° to the plane of the system's heliocentric orbit. This large value indicates extreme seasonal effects. The radii of the other four moons are unknown but on the order of 5-25 km for Styx and Kerberos and 20-75 km for Nix and Hydra, based on their magnitudes.

Physical Properties

Appearance

Until the Pluto system will be visited by the New Horizons space mission in July 2015, little can be said about the visual appearance of its members. Information comes from three methods: (1) optical ▶ light curves, which indicate that Pluto's geometric albedo varies from ~ 0.49 to 0.66, and Charon's from ~ 0.37 to 0.41, (2) direct imaging from the Hubble Space Telescope (HST) affording a spatial resolution of about 600 km, and (3) mutual events (Pluto passing in front of Charon or vice versa), which occurred between 1985 and 1990 and provided an indirect means to spatially resolve Pluto's surface. Overall, observations indicate large albedo contrasts (about 5:1) and color variations on Pluto. In general, low latitudes appear darker than high latitudes, but albedo variations occur on all scales. Furthermore, the comparison of HST images taken in 1993–1994 and in 2003–2004 indicates brightness changes in the North Polar and southern hemisphere regions. Little information is available about Charon, except for a hint for a latitudinal albedo trend.

Composition and Thermal Properties

Near-infrared spectroscopy clearly proves that Pluto's surface is covered by a variety of ices: N_2, CO, CH_4, H_2O, and perhaps C_2H_6. N_2 dominates the surface, comprising some 98 % of the molecules, and most of the CO and CH_4 occur in dissolved form in N_2. However, there are regions covered by essentially pure CH_4, and evidence for vertical segregation of methane in the surface. Although it is difficult to correlate the visual appearance of the surface with its chemical composition, it is generally thought that the brightest regions are covered with "fresh" nitrogen ice resulting from atmospheric cycles. Regions of intermediate brightness would represent methane ice, while the darkest areas may contain a mixture of water ice with more or less complex hydrocarbons produced by the long-term irradiation of methane ice.

Charon's surface is covered by H_2O ice, and perhaps with ammonia hydrate crystals. The bulk densities of Pluto and Charon are 2.0 and 1.7, respectively, indicating a mixture of rocks and ices in approximately equal proportions. Thermal measurements indicate that Pluto's surface temperature varies from $\sim$ 35 K in the bright regions to $\sim$ 60 K for the darkest areas when illuminated, with a low surface thermal inertia.

Atmosphere

Since 1985, stellar occultation observations have indicated that Pluto possesses a tenuous and time-variable atmosphere. Due to its high volatility and dominance on Pluto's surface, N_2 must be the major atmospheric compound. Occultation measurements do not probe the atmosphere down to the surface, but the current atmospheric pressure is at least 5 μbar and is estimated to be $\sim$ 15-25 μbar. The surface pressure is determined by sublimation equilibrium of N_2 ice. Occultations indicate a pressure increase by a factor of $\sim$ 2 in the last 20 years. This is a probable consequence of seasonal effects, with regions covered by N_2 ice moving into summer and warming. Nonetheless, in the long term, the atmosphere might ultimately freeze out as Pluto recedes from the Sun toward aphelion and cools. Near-infrared spectroscopy shows CH_4 to be present in Pluto's atmosphere, with a mixing ratio of about 0.5 % of N_2 and CO to be most probably present as well. Methane is much less volatile than N_2, and its relatively elevated abundance probably reflects sublimation from the pure methane patches that are warmer than N_2 ice.

Origin and Relation to Other Kuiper Belt Objects

Once thought to be an escaped satellite of Neptune (we now know, it is impossible for Pluto to originate in a planet that it never approaches), the true place of Pluto in the Solar System was revealed by the discovery of the ▶ Kuiper Belt from 1992 onward. Many resonant objects have been discovered (about 30 % of the trans-Neptunian population); those located in the 3:2 resonance have been termed "Plutinos." According to a popular model known as the "Nice model," the overall structure of the Kuiper Belt results from mutual interactions between an initially massive and "cold" disk (i.e., bodies with low eccentricity and low inclination orbits) of planetesimals and the migrating giant planets. Neptune's outward migration may have involved a brief chaotic phase that expelled most of the planetesimals from the disk, leaving a Kuiper Belt of only $\sim$ 0.03 Earth masses. Subsequent and gentler migration of Neptune would then have captured "cold" objects into mean motion resonances.

Multiple systems are common ($\sim$15 %) in the Kuiper Belt. As for the Moon, the most likely origin of Charon is a giant impact, and computer simulations show this to be a plausible scenario. After the collision, which may well have formed Charon intact, tidal forces over timescales of only a few tens of millions of years would have led to Charon's current circular and synchronous orbit. The other four moons may also be remnants of this collision.

Finally, it should be noted that, for both its atmosphere and surface, Pluto shows a clear similarity with Neptune's satellite ▶ Triton. Triton's

atmosphere, as revealed by Voyager 2, is also very tenuous, nitrogen dominated with some traces of methane. Near-infrared spectra of Triton show that the ice composition, at its surface, is very similar to that of Pluto. This goes along with dynamical arguments that indicate that Triton is a Kuiper Belt object captured by Neptune.

See Also

- ▶ Charon
- ▶ Dwarf Planet
- ▶ IAU
- ▶ Kuiper Belt
- ▶ Lightcurve
- ▶ Orbit
- ▶ Trans-Neptunian Object
- ▶ Triton

References and Further Reading

Barucci MA, Boehnhardt H, Cruikshank DP, Morbidelli A (eds) (2008) The solar system beyond Neptune. University of Arizona Press, Tucson

Doressoundiram A, Lellouch E (2010) At the edge of the solar system. Icy new worlds unveiled. Springer, Berlin

Stern A, Mitton J (1997) Pluto and Charon, ice worlds on the ragged edge of the solar system. Hardcover, Wiley Interscience, New York

Stern SA, Tholen DJ (eds) (1995) Pluto and Charon. University of Arizona Space, Tucson

PNA

Peter E. Nielsen
The Panum Institute, ICMM, University of Copenhagen, Copenhagen, Denmark

Keywords

Genetic material; Nucleic acids; Peptides; Replication

Synonyms

Peptide nucleic acids

Definition

Peptide nucleic acid (PNA) is a DNA mimic that was first described in 1991. Although it is chemically remote from natural ▶ nucleic acids like DNA, being based on a pseudo peptide backbone with pendant nucleobases, it is an effective structural DNA mimic capable of forming stable Watson-Crick sequence complementary duplexes with DNA, RNA, or itself. Furthermore, its chemical structure is uncharged, achiral, and based on "simple" chemistry being compatible with primordial (Earth and meteorite) conditions. Thus, it may be speculated that PNA type of (genetic) informational molecules could have preceded ▶ RNA in prebiotic evolution of life.

Overview

It is often hypothesized that our contemporary life based on DNA, RNA, and protein through the "central dogma" was preceded by a primordial life-form based solely on RNA being both the genetic material and providing enzymatic (catalytic) activity (the "▶ RNA world"), and that this RNA world subsequently evolved into contemporary life by introduction of proteins and DNA. However, due to the very limited stability of RNA as well as lack of robust prebiotic synthesis routes for RNA precursors (in particular ▶ ribose), it is difficult to imagine how RNA molecules could have formed on the primitive Earth and how they would have survived long enough to allow creation of life. Thus, the idea of a pre-RNA life based on a more stable and prebiotically compatible genetic material has been entertained by many researchers. PNA is an example of one such material. It is extremely stable, precursors have been found in "prebiotic

soup" experiments as well as in meteorites, and PNA is able to communicate genetic information with both RNA and DNA via Watson-Crick duplex formation. Furthermore, simple model experiments have demonstrated that chemical PNA replication as well as PNA to RNA transcription type processes may take place. So far, we are lacking evidence that a PNA world and a PNA to RNA world transition did take or even could have taken place at the early stages of the origin of life, but the data should encourage further experiments to investigate the (chemical) feasibility such a scenario. Indeed, a prerequisite for a "PNA world" – in analogy to the RNA world hypothesis – would be the discovery of catalytically active PNA oligomers ("PNazymes"), which might have driven metabolic and replication life processes, and upon which evolutionary selection could have operated.

See Also

- ▶ Nucleic Acids
- ▶ Origin of Life
- ▶ Ribose
- ▶ RNA World
- ▶ Prebiotic Chemistry

References and Further Reading

Böhler C, Nielsen PE, Orgel LE (1995) Template switching between PNA and RNA oligonucleotides. Nature 376:578–581

Meierhenrich UJ, Caro GMM, Bredehöft JH, Jessberger EK, Thiemann WHP (2004) Identification of diamino acids in the Murchison meteorite. Proc Natl Acad Sci U S A 101:9182–9186

Nelson KE, Levy M, Miller SL (2000) Peptide nucleic acids rather than RNA may have been the first genetic molecule. Proc Natl Acad Sci U S A 97:3868–3871

Nielsen PE (1993) Peptide nucleic acid (PNA): a model structure for the primordial genetic material? Orig Life Evol Biosph 23:323–327

Nielsen PE (2007) Peptide nucleic acids and the origin of life. Chem Biodivers 4:1996–2002

Nielsen PE (2008) A new molecule of life? Sci Am 299:64–71

Nielsen PE, Egholm M, Berg RH, Buchardt O (1991) Sequence-selective recognition of DNA by strand displacement with a thymine-substituted polyamide. Science 254:1497–1500

Rasmussen H, Kastrup JS, Nielsen JN, Nielsen JM, Nielsen PE (1997) Crystal structure of a peptide nucleic acid (PNA) duplex at 1.7 Å resolution. Nat Struct Biol 4:98–101

Wittung P, Nielsen PE, Buchardt O, Egholm M, Nordén B (1994) DNA-like double helix formed by peptide nucleic acid. Nature 368:561–563

PO

▶ Phosphorus Monoxide

Polar Axis

Daniel Rouan
LESIA, Observatoire Paris-Site de Meudon, Meudon, France

Synonyms

Rotational axis

Definition

The polar axis of a planet is its axis of rotation. It is perpendicular to the planet's equatorial plane. The inclination of the Earth's polar axis with respect to the plane of its orbit about the Sun is responsible for the phenomenon of seasonal variations. Telescopes with an equatorial mount have one axis, also called the polar axis, which is parallel to the Earth's rotation axis. The slow (26,000 year period) conical motion of the Earth's polar axis is responsible for the ▶ precession of the equinoxes.

See Also

- ▶ Precession
- ▶ Rotation Planet
- ▶ Rotational Velocity

Polar Caps (Mars)

François Forget
Institut Pierre Simon Laplace, Laboratoire de Météorologie Dynamique, UMR 8539, Université Paris 6, Paris, France

Definition

The Martian polar caps are layers of water ice or ▶ carbon dioxide ice accumulated in the Martian polar regions because of the cold polar temperatures. Several distinct objects may be labeled "polar caps" on ▶ Mars. (1) The ▶ polar layered deposits, made of ice and sediments, accumulated at both poles to a depth of several thousand meters and about 1,000 km in diameter. (2) The northern water frost, a layer of relatively pure water ice interacting with the atmosphere and covering the northern layered deposits. (3) The perennial southern ice cap, about 400 km across near the south pole and composed of carbon dioxide ice several meters thick sitting upon a substrate of water ice (the rest of the southern polar deposits is covered by dry sediments). (4) The seasonal polar caps, a layer of carbon dioxide ice a few tens of centimeters thick covering both Mars high latitude in fall, winter, and spring.

See Also

- ▶ Carbon Dioxide
- ▶ Mars
- ▶ Polar Layered Deposits (Mars)

Polar Layered Deposits (Mars)

François Forget
Institut Pierre Simon Laplace, Laboratoire de Météorologie Dynamique, UMR 8539, Université Paris 6, Paris, France

Definition

The polar layered deposits are landforms made of thousands of layers of ice mixed with a few percent of mineral sediments that have accumulated over more than 3,000 m in thickness and 1,000 km in diameter at both poles of ▶ Mars. These deposits are thought to preserve a record of the seasonal and climatic cycling of atmospheric CO_2, H_2O, and dust over millions of years. It has been speculated that a liquid water ▶ Habitat could form at high pressure and temperature at the base of the deposits. However, radar sounding has not confirmed this hypothesis.

See Also

- ▶ Habitat
- ▶ Mars
- ▶ Polar Caps (Mars)

Polar Molecule

William M. Irvine
University of Massachusetts, Amherst, MA, USA

Definition

A Polar Molecule possesses a permanent electric dipole moment and, therefore, in the gas phase has allowed electric dipole transitions between its rotational energy states. Most molecules

observed in space have their rotational transitions in the millimeter and submillimeter domains.

See Also

► Apolar Molecule

Polarized Electron

Jun-Ichi Takahashi
NTT Microsystem Integration Laboratories, Atsugi, Japan

Synonyms

Spin-polarized electron beam

Definition

Polarized electrons can be defined as an electron ensemble in which the average of the spin angular momenta of the electrons is distributed in a specified direction (spin-polarized electrons). The typical spin-polarized electrons existing in nature are beta ray electrons from radioactivity decay of elements. The spin of electrons in beta rays is longitudinally polarized due to parity nonconservation in the weak interaction mediated by charged W particles.

In general, the helical behavior of energetic quantum beams can be characterized with "helicity," that is, the spin angular momentum projection onto the kinetic momentum direction. The spin of beta ray electrons is polarized to the opposite direction of the beam propagation; that is, the helicity of beta electrons is $-1/2$. Expressing positive spin vector as a right-hand helix, positive helicity electrons correspond to right-handed and negative helicity to left-handed symmetries, by analogy to right- and left-handed circularly polarized light.

From the standpoint of astrobiology, one of the hypotheses for the origin of biomolecular chirality is called the "cosmic scenario." In this scenario Asymmetric energy sources in space, such as ► beta rays, induced asymmetric chemical reactions of precursors in interstellar dust, resulting in the enantiomeric excess of terrestrial bio-organic compounds.

See Also

► Beta Rays
► Enantiomeric Excess

Polarized Light and Homochirality

Louis d'Hendecourt
Institut d'Astrophysique Spatiale, Université Paris-Sud 11, Orsay Cedex, France

Keywords

Circular dichroism; Enantioselectivity; Linearly and circularly polarized light; Optical activity

Definition

Natural light is composed of an oscillating electromagnetic field traveling in vacuum at a speed of c. It can thus be represented by a wave vector k indicating its direction of propagation, to which are associated two perpendicular vectors, the electric (E) and magnetic (B) fields, each oscillating at the frequency of the wave, and both at right angles from k. Natural light is not polarized, that is the E vector orientation and amplitude are random. If the electric vector is always in the same plane, the light is said to be linearly polarized. If it rotates around its axis of propagation, with constant amplitude, the light is said to be circularly polarized with two possible helicities, right or left, compared to the direction of the

wave vector k. Ultraviolet circularly polarized light (UV-CPL) is suspected by some to be at the origin of enantioselectivity of chiral molecules, an idea originally proposed by Louis Pasteur as early as 1848.

History

Although the proper description presented above dates back to Maxwell with his theory of electromagnetism (1864), the idea that light behaves as a wave, as opposed to a collection of particles (Newton and later Einstein) had been discussed at length by Huygens. Following the famous interference fringes and diffraction experiments from Fresnel and later Young, most if not all the physicists of the nineteenth century admitted the theory of light waves. Polarization was well known at the time of Pasteur, especially linear polarization, a relatively easy to observe phenomenon. It was noted that some substances are able to rotate the plane of polarization when they are traversed by linearly polarized light. Schematically, Pasteur discovered that some "living" substances, molecules extracted from living organisms, systematically deflect the plane of polarization to the left. Abiotic substances of the same nature do not deviate at all this plane. In physics, this is explained by the symmetry of the chiral molecule responsible for the effect, where the term chiral refers here to organic molecules containing an asymmetric carbon, a carbon whose four valences are bonded to different molecular subgroups. Most amino acids are chiral. Abiotically synthesized amino acids are generally racemic (composed equally of left and right handed molecules). In living systems, they are mostly homochiral, and left-handed, a property noted by Pasteur that he attributed at the time to "unknown forces at work in the cosmos," somehow linked to the origin of life.

Overview

Although many ideas have been proposed to explain ► homochirality with a deterministic origin (Bonner 1991), the most commonly cited is the interaction of UV-CPL with asymmetric (chiral) organic molecules (Bailey 2001). Indeed, this can be simply understood by considering the reverse effect observed by Pasteur. If polarized light can turn its polarization plane while passing through a homochiral assembly of molecules, an action called optical activity, the reverse, obtaining an enantiomeric excess while passing UV-CPL through a racemic mixture must be true. This refers to Curie's Principle (Curie 1894) who was the first to coin this term "chiral photons" or "racemic light." At a molecular level, asymmetric molecules are known to possess a property called circular dichroism, which ensures that a given molecule (e.g., a left or right enantiomer) reacts differently when submitted to UV-CPL with L or with R helicities. Thus, interaction of UV-CPL with chiral molecules may help enantioselective processes to obtain non-racemic molecular materials. To be meaningful for prebiotic chemistry, a scenario has been proposed in which interstellar organic molecules are illuminated by UV-CPL radiation that exists in some places in space (Cronin and Reisse 2006; Meierhenrich 2008). Selection of one enantiomer (L) over the other (D) is certainly possible in astrophysical environments, since some amino acids in meteorites display slight enantiomeric excesses (e.e.) only of the L form. Amplification to homochirality (Soai et al. 1995) is considered as a viable and common phenomenon, as even a slight enantiomeric excess (around 1 %) is able to start this amplification. Thus, UV-CPL experiments on amino acids have shown since 1974 (Balavoine et al. 1974) that asymmetric photolysis can create some excesses, and more recently this effect has been confirmed in the solid state (Meierhenrich et al. 2005). For a valid astrophysical application, these experiments have been transposed to photochemical simulations on interstellar "dirty" ices using UV-CPL from a synchrotron radiation beam to obtain non-racemic amino acids. These difficult experiments, up to now inconclusive, are still under development (Nuevo et al. 2006). Recently, these experiments on analogues of dirty

interstellar ices have succeeded tp produce a significant enatiomeric excess in one amino acid, alanine, the sign of which (L or D) cahnging with the helicity of the UV-CPL used at the beamline DESIRS of the SOLEIL syncrotron (France). This resulte, descibed by de Marcellus et al. (2011) give some support to the idea that interstellar molecules such as amino acids of a given enatiomeric excesses (L, such as the ones found in meteorites) may have seeded the Earth, prior to the onset of homochirality. This scenario is still in the making with running experiments now dedicated to sugars.

See Also

- ▶ Asymmetric Reaction, Absolute
- ▶ Amino Acid
- ▶ D/L-Ratio
- ▶ Homochirality
- ▶ Polarized Electron

References and Further Reading

Bailey J (2001) Astronomical sources of circularly polarized light and the origin of homochirality. Orig Life Evol Biosph 31:167

Balavoine G, Moradpour A, Kagan HB (1974) Preparation of chiral compounds with high optical purity by irradiation with circularly polarized light, a model reaction for the prebiotic generation of optical activity. J Am Chem Soc 96:5152

Bonner WA (1991) The origin and amplification of biomolecular chirality. Orig Life Evol Biosph 21:59

Cronin J, Reisse J (2006) Chirality and the origin of homochirality, in lectures in astrobiology, vol I. Springer, Berlin/Heidelberg, pp 73–115

Curie P (1894) Sur la symétrie dans les phénomènes physiques, symétrie d'un champ électrique et d'un champ magnétique. J Phys Theor Appl 3:393

de Marcellus P, Meinert C, Nuevo M, Filippi JJ, Danger G, Deboffle D, Nahon L, Sergeant L, d'Hendecourt L, Meierhenrich UJ (2011) Non racemic amino acid production by ultraviolet irradiation of achiral interstellar ice analogs with circularly polarized light. Astrophys J Lett 727:L27–L33

Meierhenrich UJ (2008) Amino acids and the asymmetry of life. Springer, Berlin/Heidelberg

Meierhenrich UJ, Nahon L, Alcaraz C et al (2005) Asymmmetric photolysis of amino acids using UV CPL from a synchrotron source. Ange Chem Int Ed 44:5630

Nuevo M, Meierhenrich UJ, Muñoz Caro GM, Dartois E, d'Hendecourt L, Deboffle D, Auger G, Blanot D, Bredehöft J-H, Nahon L (2006) The effects of circularly polarized light on amino acid enantiomers produced by the UV irradiation of interstellar ice analogs. Astron Astrophys 457:741

Soai K, Shibata T, Morioka H, Choji K (1995) Asymmetric autocatalysis and amplification of enantiomeric excess of a chiral molecule. Nature 378:767–768

Polimictic Breccia

Daniele L. Pinti
GEOTOP Research Center for Geochemistry and Geodynamics, Université du Québec à Montréal, Montréal, QC, Canada

Synonyms

Polygenetic breccia; Polylithologic breccia

Definition

A polymictic ▶ breccia is a clastic ▶ sedimentary rock composed of angular clasts from different origins intermixed in a consolidated matrix. The clasts can be formed during tectonic events or meteoric impacts.

See Also

- ▶ Breccia
- ▶ Crater, Impact
- ▶ Impact Melt Rock
- ▶ Impactite

Polycistronic Transcript

- ▶ Operon

Polycyclic Aromatic Hydrocarbon

Els Peeters and Jan Cami
Department of Physics and Astronomy,
The University of Western Ontario, London,
ON, Canada
SETI Institute, 189 Bernardo Avenue, Suite 100,
Mountain View, CA, USA

Keywords

Infrared emission features; Infrared; Ultraviolet; Radio; Spectroscopy; Interstellar chemistry; Interstellar medium; Molecules in space; DIBs

Synonyms

PAH

Definition

Polycyclic aromatic hydrocarbons (PAHs) are organic molecules containing two or more fused ▶ benzene rings that are arranged in a honeycomb structure with hydrogen attached to the edges of the molecule. When used in the context of astrophysical research, the term "PAHs" often refers to a broader class of related molecules, including fully or partially hydrogenated or dehydrogenated PAHs and chemically modified PAHs where one or more hydrogen or carbon atom is replaced by another element (e.g., nitrogen) or metallocomplexes.

Overview

Polycyclic aromatic hydrocarbons (PAHs) are a large class of organic molecules containing – strictly speaking – only carbon and hydrogen. On Earth, they are found as tarry materials that are naturally present in, for example, coal and crude oil. They are formed in combustion processes of many carbonaceous substances and are thus also found in auto exhaust, candle soot, and tobacco smoke. Although some PAHs are used in medicine, public awareness of PAHs is most often raised because of their known carcinogenic properties and their long-term stability, which thus implies a persistent detrimental effect on their environment, for example, when present in soil.

In space, PAHs are observed at high abundances in our ▶ Milky Way galaxy wherever ultraviolet radiation is present and pervade the universe far beyond, as is clear from their detection in galaxies at high ▶ redshifts. PAHs are observed through their emission features at infrared wavelengths – the so-called unidentified infrared (UIR) bands – that dominate the infrared (IR) spectra of almost all environments including the ▶ interstellar medium (ISM), ▶ reflection nebulae, star-forming regions, evolved stars, and entire galaxies. No less than 20–30 % of the galactic IR radiation is emitted in these PAH bands, and it is estimated that 10–15 % of the cosmic carbon is locked up in these molecules. Although not a single specific PAH species has been identified in space, PAHs thus represent a large class of complex ▶ molecules in space.

PAHs form in the outflows of evolved and dying carbon-rich stars and are further processed as they voyage out to the ISM and become part of protostellar environments. In addition, PAHs possibly form in the ISM through destruction of larger dust particles. Given their large abundance, their stability, and their presence in these diverse environments, it is clear that they play a crucial role in many physical and chemical processes in circumstellar and interstellar media. Furthermore, their strong IR emission features are easily observed and show subtle variations in their spectral appearance that depend on various parameters. PAHs are thus ideal tools to probe the environmental conditions in a wide range of astronomical objects.

There is an extensive body of literature about PAHs in astrophysical environments; we refer in particular to the reviews by Allamandola et al. (1989), Puget and Léger (1989), Tielens (2005, 2008), and the proceedings: "PAHs in the Universe" (2011).

Structure

The ability of carbon atoms to have four chemical bonds allows them to form complex structures. Carbon atoms can be configured in planar hexagonal rings – benzene rings – where each carbon atom is bound to three neighboring atoms (either C or H) by covalent σ-bonds (Fig. 1). These bonds result from overlapping sp^2 hybridized orbitals in the same plane, and thus, a planar molecular structure results. The remaining six electrons (one belonging to each carbon atom) in a benzene ring correspond to p orbitals that have lobes perpendicular to this plane. Overlap of these orbitals then results in a delocalized π-bond with molecular orbitals above and below the plane of the molecule. Such a configuration is called an aromatic bond. Hydrocarbon molecules that do not contain aromatic bonds are called aliphatic compounds.

Benzene rings are then the basis for much larger molecules that are composed of several fused rings and therefore called polycyclic. If these polycyclic molecules contain only carbon and hydrogen, they are called polycyclic aromatic hydrocarbons (PAHs, chemical definition). Some chemical modifications might be common in astrophysical environments and change the molecular and spectral properties. For example, when a hydrogen atom is replaced by deuterium, the deuterated PAHs are sometimes called PADs. A PAH molecule where one or more carbon atoms is replaced by nitrogen is a polycyclic aromatic nitrogen heterocycle (PANH).

PAHs are thus a large family of different molecular species with a similar (honeycomb-like) structure. The PAH molecules themselves can be used for even larger structures. PAH platelets are stacks of PAH molecules ordered in parallel layers; PAH clusters contain several PAHs in various ordered configurations. ▶ Amorphous carbon is then a random combination of PAH platelets and PAH clusters.

Note that in an astrophysical context, the term 'PAHs' is not only used to refer to the strict chemical definition of PAHs but also includes PAH-like species such as, for example, PAHs in which an H is substituted by D or a functional group and PAHs in which an atom is replaced by another atom, metallocomplexes, etc. Also, there are many other molecular species made of carbon, such as carbon chains, ▶ fullerenes, nanotubes, diamond, etc. (see Fig. 1), and many of those exist in space.

Detecting PAHs in Space

At astronomical distances, we can only study PAHs through their interaction with electromagnetic radiation. PAHs exhibit electronic transitions in the ultraviolet (UV) and at optical wavelengths and vibrational transitions at IR wavelengths, and some PAHs have pure rotational transitions at radio wavelengths. While there is some observational evidence for PAHs at UV and optical wavelengths, the presence of PAHs in space is thus far primarily established through their bright emission at IR wavelengths.

Infrared Spectroscopy of PAHs

Given the emphasis on the IR characteristics of PAHs, a good understanding of the fundamentals of infrared molecular spectroscopy is in place here.

The energies associated with the vibrational motions between the atoms that make up a molecule are quantized and are such that the transitions between two vibrational levels occur at IR wavelengths. A molecule composed of N atoms is characterized by a unique set of 3 N−6 allowed vibrational modes (and thus a unique IR spectrum), which allows astronomers – at least in principle – to identify specific molecules by means of IR spectroscopy. Moreover, the bandwidths and intensity ratios between different vibrational bands depend on various parameters (e.g., temperature, density); thus, the IR spectrum of molecules contains information on the physical properties of the environment in which they reside. This makes IR molecular spectroscopy a very powerful tool.

However, there is a complicating factor when dealing with collections of large molecules that have a similar structure, such as PAHs. In that case, certain vibrational modes are present in each species. This is typically the case for stretching modes (where the vibrations correspond to changes in bond length between two atoms) and bending modes (where the bond

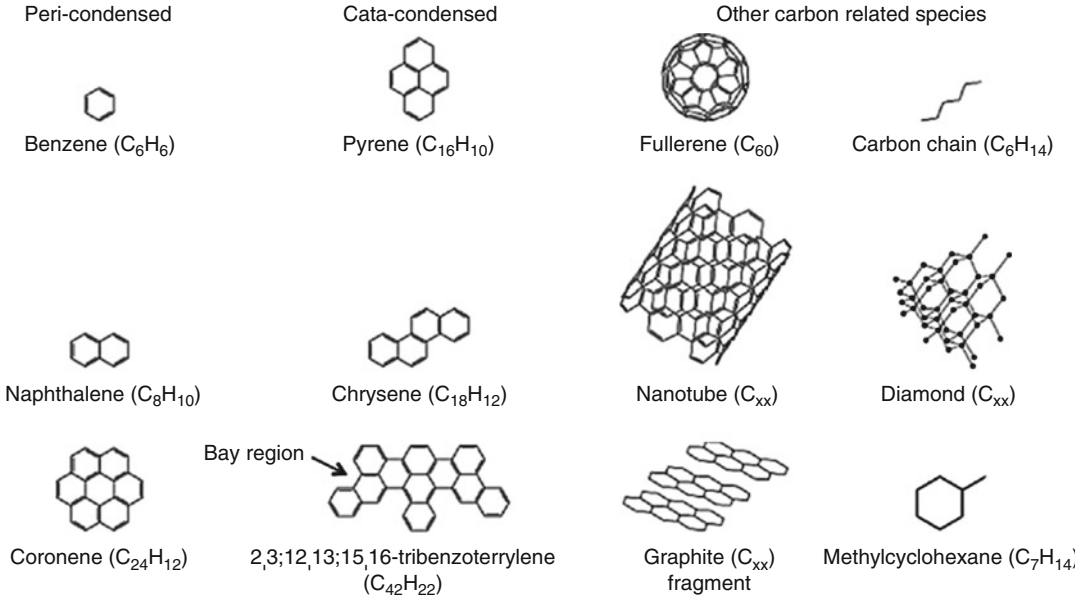

Polycyclic Aromatic Hydrocarbon, Fig. 1 Chemical structure of benzene, some cata- and peri-condensed PAHs, and other forms of carbon and PAH-related species. A bay region is indicated, and irregular PAHs are exemplified by 2,3;12,13;15,16-tribenzoterrylene ($C_{42}H_{22}$) (Adapted from Boersma 2009)

angle between two atoms changes) involving only C and H atoms. The energy required to excite, for example, the C-H stretching mode is similar in all PAH molecules, and thus all PAHs will have a C-H stretching transition at nearly the same wavelength. Although each species in the set will still have its own unique vibrational spectrum, the features due to the common modes will overlap. Typically, a combined spectrum then has strong features where these common modes overlap, but the weaker features that are specific to individual molecules are washed out.

The Unidentified Infrared (UIR) Bands

In the early 1970s, new IR instruments on ground-based and airborne telescopes revealed broad emission features at 3.3, 6.2, 7.7, 8.6, and 11.2 μm in ▶ planetary nebulae, star-forming regions, and ▶ reflection nebulae (Fig. 2). Since the carriers of these features remained unknown for almost a decade, they were dubbed the unidentified infrared (UIR) bands, a name still in use today.

In the past two decades, the unprecedented views of the IR universe offered by the ▶ Infrared Space Observatory (ISO) and the ▶ Spitzer Space Telescope showcased the spectral richness of the UIR spectrum. Observations with these facilities and ground-based telescopes revealed additional weaker bands (at 3.4, 3.5, 5.25, 5.75, 6.0, 6.6, 6.9, 7.2–7.4, 8.2, 10.5, 10.8, 11.0, 12.0, 13.5, 14.2, 15.8, 16.4, 16.6, 17.0, 17.4, and 17.8 μm) perched on top of broad emission plateaus (at roughly 3.2–3.6 μm, 6–9 μm, 11–14 μm, and sometimes 15–20 μm); these weaker features are apparent in some – but not all – astronomical objects. A band at 19 μm was at one point considered to be part of the PAH spectrum; however, it shows a different spatial distribution than the PAH bands in the reflection nebula NGC 7023 (Sellgren et al. 2007) and is now firmly assigned to C_{60} (Cami et al. 2010; Sellgren et al. 2010; see entry on ▶ Fullerene). The 17.4 emission feature is due to both PAHs and C_{60}.

The UIR bands have now been observed in almost all astrophysical environments where UV radiation is present, including the diffuse ▶ interstellar medium (ISM), the edges of ▶ molecular clouds, ▶ reflection nebulae, young stellar objects, star-forming regions, C-rich Wolf-Rayet stars,

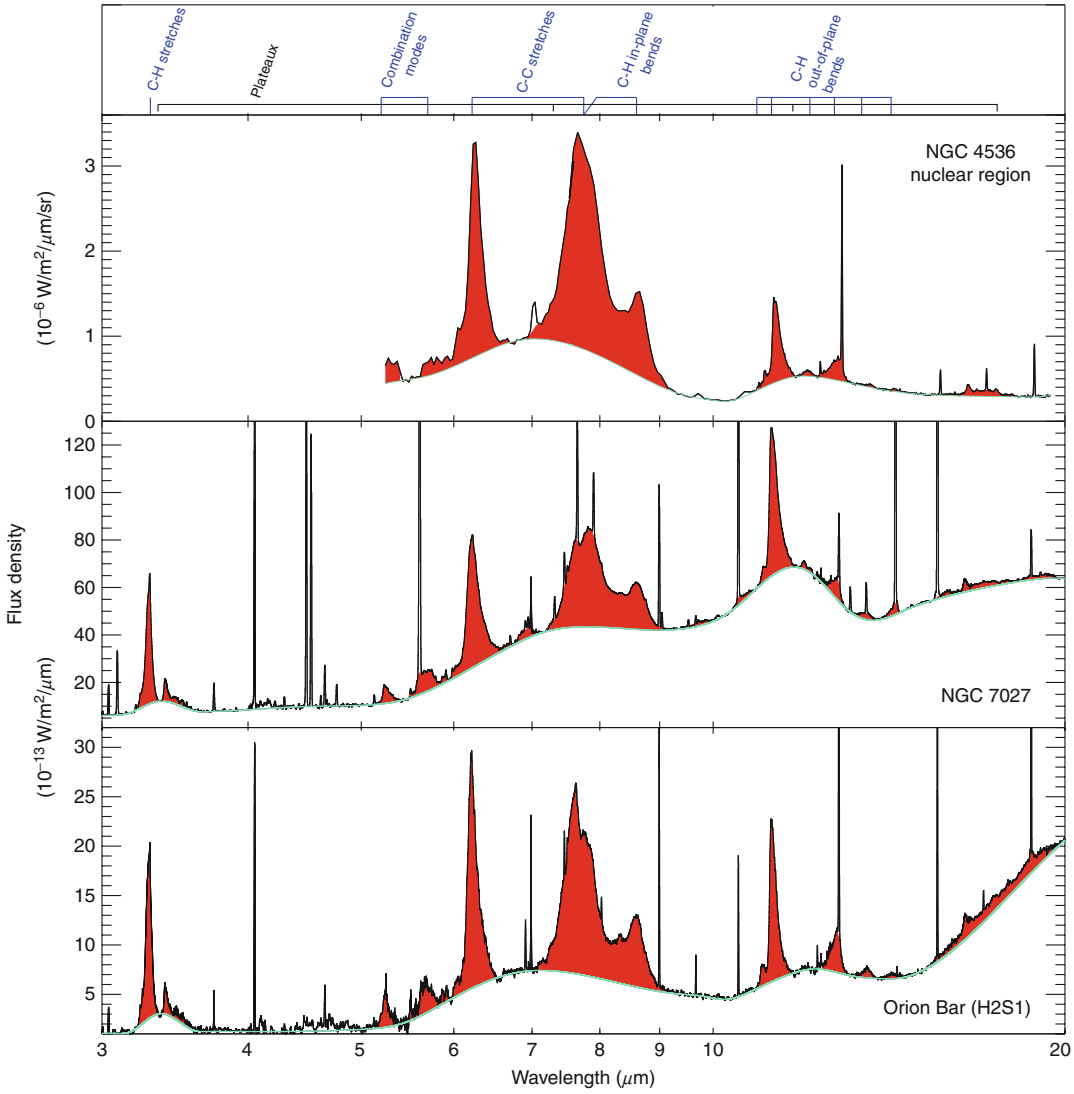

Polycyclic Aromatic Hydrocarbon, Fig. 2 The ISO-SWS spectra of the planetary nebula NGC7027 and the photodissociation region (*PDR*) at the Orion bar and the Spitzer-IRS spectrum of the nuclear region of the galaxy NGC4536 illustrate the richness and variety of the PAH spectra (shown in *red*). Also indicated are the aromatic mode identifications of the major PAH bands and the broad plateaux emission on which the PAH bands are located. Other spectral features (not labeled) are atomic and H_2 emission lines (Reproduced from Peeters in JTPAHs with permission from EDP Sciences)

C-rich post-AGB stars, C-rich ▶ planetary nebulae, ▶ novae, nuclei of galaxies, normal galaxies, starburst galaxies, and ultraluminous IR galaxies (ULIRGs) out to redshifts of ~ 4. The carriers of the UIR bands are thus ubiquitously present throughout the universe, must be stable, and represent an important cosmic component in the astronomical mixtures of gas and dust.

The UIR Bands and PAHs

In the early 1980s, it was recognized that the UIR features coincide with the vibrational modes characteristic of aromatic materials (Duley and Williams 1981). Since then, many different carriers have been proposed, such as ▶ hydrogenated amorphous carbon (HAC), quenched carbon composites (QCC), PAHs

(e.g., Allamandola et al. 1989; Puget and Léger 1989) and coal, and more recently ▶ nanodiamonds, locally aromatic polycyclic hydrocarbons, mixed aromatic-aliphatic organic nanoparticles (MAONs; Kwok and Zhang 2011), and PAH clusters (Peeters et al. 2004a; Tielens 2008 and references therein). Indeed, the vibrational spectrum of almost any (purely) aromatic material can provide a global fit to the observed UIR bands since – at the smallest scales – they have the same aromatic structure as PAHs.

However, the UIR bands are generally attributed to free aromatic molecules in the gas phase rather than to aromatic dust grains (such as HAC and QCC). This is primarily because emission at mid-infrared wavelengths requires excitation temperatures of at least several hundred K, yet the UIR bands have been detected in "cold" environments such as in ▶ reflection nebulae far away from the illuminating stars and in the diffuse ISM where dust temperatures are of the order of only tens of K. Furthermore, it is seen, for example, in reflection nebulae that the UIR band ratios show little variation with distance from the star. That indicates that the carriers of the UIR features can be excited to very high "temperatures" in such cold environments upon absorption of a single far-ultraviolet (FUV) photon (Sellgren 1984). This, in turn, requires the emitting species to be fairly small. Indeed, classical 0.1 μm size grains are too large and do not become hot enough to emit at mid-infrared wavelengths in these environments; typically, sizes of the order of 10 Å are inferred (Sellgren 1984). A molecular origin is further supported by the anharmonic band profiles of several of the main UIR features and the high feature-to-continuum ratio. However, spectral variations have been observed in various environments (see below) that are not compatible with a single molecular species as carrier for the UIR bands. Thus, the general consensus is that the UIR bands originate from a family of aromatic molecules with sizes of $\sim$ 50–100 carbon atoms (e.g., Tielens 2005, 2008).

The physical processes that cause PAH molecules to produce the IR emission bands are relatively well understood qualitatively. Absorption of a far-ultraviolet (FUV) photon by a PAH molecule that is originally in the electronic and vibrational ground state induces a transition to an excited electronic state. The excited molecule then makes rapid isoenergetic transitions to a lower-lying electronic state leaving most of the initial excitation energy in the form of vibrational energy. Subsequently, this highly vibrationally excited molecule cools down, mainly by IR emission in its vibrational modes. After it has cooled down, it will remain cold ($\sim$10 K) for a long time until it absorbs another FUV photon. For a typical interstellar (IS) PAH with 50 carbon atoms ($N_C = 50$; throughout this text, we will use N_C to denote the number of carbon atoms.), photon absorption occurs once a year in the diffuse interstellar medium (ISM) and every 10 min in typical ▶ photodissociation regions (PDRs) such as the Orion bar (Tielens 2005).

The main UIR bands at 3.3, 6.2, 7.7, 8.6, and 11.2 μm are then attributed to various stretching and bending vibrations involving the C-H and C-C bonds in PAH molecules with $N_C \approx 50$–100. In particular, the 3.3 μm band is due to C-H stretching modes and the 6.2 μm band to C-C stretching modes. C-H in-plane bending modes are responsible for the 8.6 μm band and coupled C-C stretching and C-H in-plane bending modes for the 7.7 μm complex. The 11.2 μm band is caused by C-H out-of-plane bending modes. Vibrational transitions at wavelengths longward of 15 μm involve motions of the entire molecular skeleton and hence are more specific to each molecule.

Laboratory measurements and theoretical calculations indicate that the PAH molecules have low-frequency vibrational modes at far-IR wavelengths (Boersma, Joblin in JTPAHs). These low-frequency vibrational modes of PAHs are skeleton or drumhead modes sensitive to the entire structure of the molecule. Detecting these modes would further constrain the PAH population and could possibly lead to the identification of a single molecule. However, little is known observationally about the properties of these far-IR PAH bands, largely because of the lack of sensitive far-IR spectroscopy instruments. Indeed, the recent Herschel Space Observatory (2009–2013) allows for the first time a systematic

study of these far-IR modes. However, these observations are very challenging and require accurate flux calibrations; we are thus still awaiting the first reports on FIR emission from PAHs.

It is important to realize that the carriers of the UIR bands may not all be "pure" PAHs (following the strict chemical definition). Stable PAH-like structures can be made, for example, by substituting one or more C atoms by N, O, or Si. Similarly, H atoms could be replaced by deuterium, by aliphatic carbon chains, or by molecular side groups. However, such substitutions leave a clear spectral imprint (see below), and spectroscopic analyses of the UIR bands show that at most 2 % of the aromatic H can be substituted by methyl groups ($-CH_3$), the most abundant of the functional groups (Tielens 2005), while at most 15 % of the carbon can be in aliphatic form (as opposed to aromatic form) based on the aliphatic bands at 3.4 and 6.85 μm (Li and Draine 2012).

Although the assignment of the UIR bands to vibrational modes from a collection of PAH molecules is now generally accepted, specifics of the emitting population remain elusive. This is due to the fact that the clear spectral signatures of the vibrational modes of PAHs are primarily governed by the physical conditions of the environment (which is the same for all PAHs) and show only a weak dependence on size and structure.

Electronic Transitions of PAHs

The electronic transitions of PAHs occur at UV and optical wavelengths, where the precise transition properties depend primarily on size (and somewhat on charge). Given their large abundance in the interstellar medium inferred from their infrared emission, PAHs are thus often suggested to play a role in various observational phenomena related to interstellar extinction. In particular, PAHs are at least a contributing species to the 217.5 nm extinction hump (see ► UV Absorption Bump) and are also considered as possible carriers of the ► diffuse interstellar bands (DIBs). They might furthermore also be responsible for the ► extended red emission (ERE) and the blue luminescence.

The 217.5 nm band is by far the strongest feature in the interstellar extinction curve and exhibits a fairly constant wavelength but a variable width in different lines of sight. Many individual species have been proposed as carriers for this feature, but the consensus is that this extinction hump is due to a plasmon resonance in carbonaceous material. PAHs must thus contribute to this feature. Laboratory experiments have shown that mixtures of PAHs with sizes larger than 22 carbon atoms result in a 217.5 nm hump that is as smooth as the observed interstellar hump, while mixtures of smaller PAHs exhibit many narrow features. The exact wavelength of the hump depends on the average size of the PAHs, and calculations show that an average interstellar PAH size of 50–60 carbon atoms is required to reproduce the observed peak wavelength of the 217.5 nm hump.

The DIBs are a set of hundreds of absorption lines observed from the near-UV to the near-IR in the spectra of reddened stars (Herbig 1995; Sarre 2006). Their interstellar origin is now well established, but their carriers remain unidentified to date despite many decades of DIB research. Many observational studies point to abundant gas-phase molecules that are able to survive the interstellar radiation field. PAHs (and especially PAH cations) are thus very promising candidates, although the same arguments could favor carbon chains and fullerene compounds. Some consensus is now growing that 'normal'; pure PAHs cannot be the carriers of the strong DIBs (Cami and Cox, 2013). Note that this does not exclude PAH radicals and PAH-metal complexes as DIB carriers.

Rotational Spectroscopy

Neutral PAHs have generally no permanent dipole moment, and thus, they exhibit no allowed rotational transitions. Exceptions are open-shell species (e.g., the polycyclic aromatic nitrogen heterocycles or PANHs) and nonplanar molecules (e.g., the bowl-shaped corannulene, $C_{20}H_{10}$). Also, PAH cations exhibit rotational transitions. Rotational properties have been reported for a few molecules (Tielens 2008 and reference therein, Pilleri et al. 2009) facilitating dedicated searches for these species. Searches for

simple one- and two-ring PANHs have been unsuccessful (Charnley et al. 2005) as was a dedicated search for corannulene in the ▶ Red Rectangle (Pilleri et al. 2009).

PAHs might also contribute to the galactic anomalous foreground emission. This excess microwave emission at frequencies from 10 to 100 GHz has an interstellar origin and is strongly correlated with the dust IR emission. Its origin is still somewhat debated, but is generally attributed to emission from spinning ▶ interstellar dust grains (Draine and Lazarian 1998). The anomalous emission can be well reproduced by theoretical models of spinning PAHs that adopt PAH properties that are in good agreement with those derived from their mid-IR emission (Ysard et al. 2010).

PAHs in the Solar System

For completeness, we note that PAHs have also been observed and found in situ in various objects in the Solar System (e.g., ▶ meteorites, interplanetary dust particles, ▶ comets, ▶ Titan).

Characteristics of the Astronomical PAH Family

We have learned most of what we know about PAHs in space from detailed analyses of their IR emission features – the UIR bands. Such observational studies have revealed a great deal of information on the properties of the astronomical PAHs; more recent work is based on a comparison with databases of theoretically calculated spectral properties of PAHs, confirming these observational results.

The UIR bands observed in a large variety of environments are remarkably similar, and to first order, a generic UIR spectrum emerges. Detailed observational studies, however, have revealed a multitude of spectral variations in peak positions, shapes, and (relative) intensities from source to source, and also spatially within extended sources. The interpretation of the UIR bands and these spectral variations is strongly based upon theoretical and experimental spectroscopy of PAHs and related species. Laboratory experiments and theoretical models reveal how PAH spectra change as a function of parameters such as temperature, charge, size, and the precise molecular (edge) structure. This information can then be used to determine the cause of the observed spectral characteristics in astronomical observations. This comparison uncovers some properties of the astronomical PAH family, as well as their relation to specific environmental parameters.

Distribution and Abundance

As is unequivocally evident from the observations, PAHs pervade the universe: they are found in almost all sources with associated gas and dust within our ▶ Milky Way and in many galaxies near and far (up to a redshift of $\sim$ 3–4). Exceptions are regions with extreme radiation fields or fast shocks, since PAH molecules cannot survive in these environments, and regions well shielded from UV radiation, as in the dense interiors of molecular clouds where PAHs get frozen into the ice mantles on the grain surfaces. Furthermore, the UIR bands generally dominate the IR spectra of these sources. The total emitted power in all the UIR bands combined ranges from a few percent to about 10 % of the total power budget of galaxies. Hence, PAHs are very abundant in space: for a typical PAH size of 50 carbon atoms, the total PAH abundance by number is $\sim 3 \times 10^{-7}$ relative to the number of hydrogen atoms (Tielens 2005).

Charge State

One of the early pivotal results of the laboratory and theoretical studies on PAHs is the remarkable effect of ionization on the infrared spectra (Oomens in JTPAHs [2011]). While peak positions are only modestly affected, the influence on intensity is striking: the C-C bands in the 5–10 μm region grow from the smallest features to become the dominant bands upon ionization. Although anions and multiply charged large PAHs are less studied, they exhibit a similar increase of emission in the C-C modes in the 5–10 μm region relative to the C-H modes at 3.3 and 11.2 μm.

The corresponding C-C and C-H modes of the UIR bands do show strong variations in their relative strengths from source to source, and even within extended sources, suggestive of changes in the charge state of the astronomical

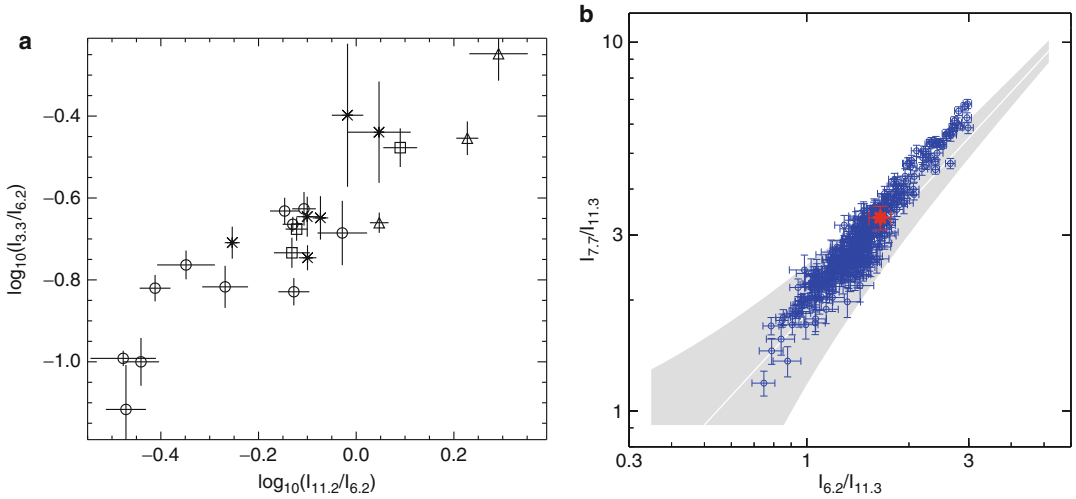

Polycyclic Aromatic Hydrocarbon, Fig. 3 (*Left*) The correlation of the 3.3 and 11.2 μm band strengths normalized to the 6.2 μm band strength. Circles are HII regions, stars intermediate mass star-forming regions, squares are reflection nebulae, and triangles are planetary nebulae (Hony et al. 2001; Credit: Hony et al. A&A, 370, 1030, 2001, reproduced with permission © ESO). (*Right*) The variation in the C-C/C-H band ratios (see Fig. 2) within the starburst galaxy M82. The gray-filled area represents the correlation obtained for the integrated spectra of a large sample of galactic and extragalactic sources. The *red* symbol is the value of the global measurement over the entire galaxy (Galliano et al. 2008, reproduced by permission of the AAS)

PAHs (Fig. 3). The CH out-of-plane bending modes, however (in the 10–15 μm region), do not behave consistently: the 12.7 μm PAH band correlates well with the 6–9 μm modes and not with the 11.2 μm PAH.

Note that several other parameters may influence the observed C-C/C-H intensity ratio; however, several studies indicate that changes in the degree of ionization of the PAHs are the main factor in these different environments (e.g. Hony et al. 2001; Galliano et al. 2008).

Chemical Composition

The PAH band profiles show pronounced variability, in particular for the C-C modes (6.2 and 7.7 μm bands). These variations define three classes, A, B, and C (Fig. 4; Peeters et al. 2002; van Diedenhoven et al. 2004), each having different band profile characteristics. Classes A and B sources show the "classical" UIR features at 6.2, 7.7, and 8.6 μm, but class B profiles are slightly redshifted compared to class A. Moreover, the 7.7 μm complex has a dominant 7.6 μm component in class A sources, but class B sources show a dominant component in this complex peaking between 7.8 and 8 μm. Class C band profiles are significantly different from classes A and B: they show a very broad band peaking at ∼ 8.2 μm. Classes A and C sources show little variation in their profiles at these wavelengths, while large differences are present within class B. The observed variations in the UIR spectra seem to span a continuous distribution going from class A via class B to class C.

Although several properties could in principle determine the precise peak positions of the C-C stretching bands, a strong constraint is offered by the fact that the position of the 6.2 UIR band in class A sources cannot be reproduced by the C-C stretching mode of pure PAHs (Peeters et al. 2002; Hudgins et al. 2005) using the currently available laboratory and theoretical data. The observed variations in the band profiles thus seem to reflect a (chemical) modification of the PAHs. Various PAH-related species have been proposed; in particular see articles by Peeters, Rapacioli, and Simon in JTPAHs (2011) and references therein:

- PANHs: substitution of a C atom by an N atom in a PAH systematically shifts the position of

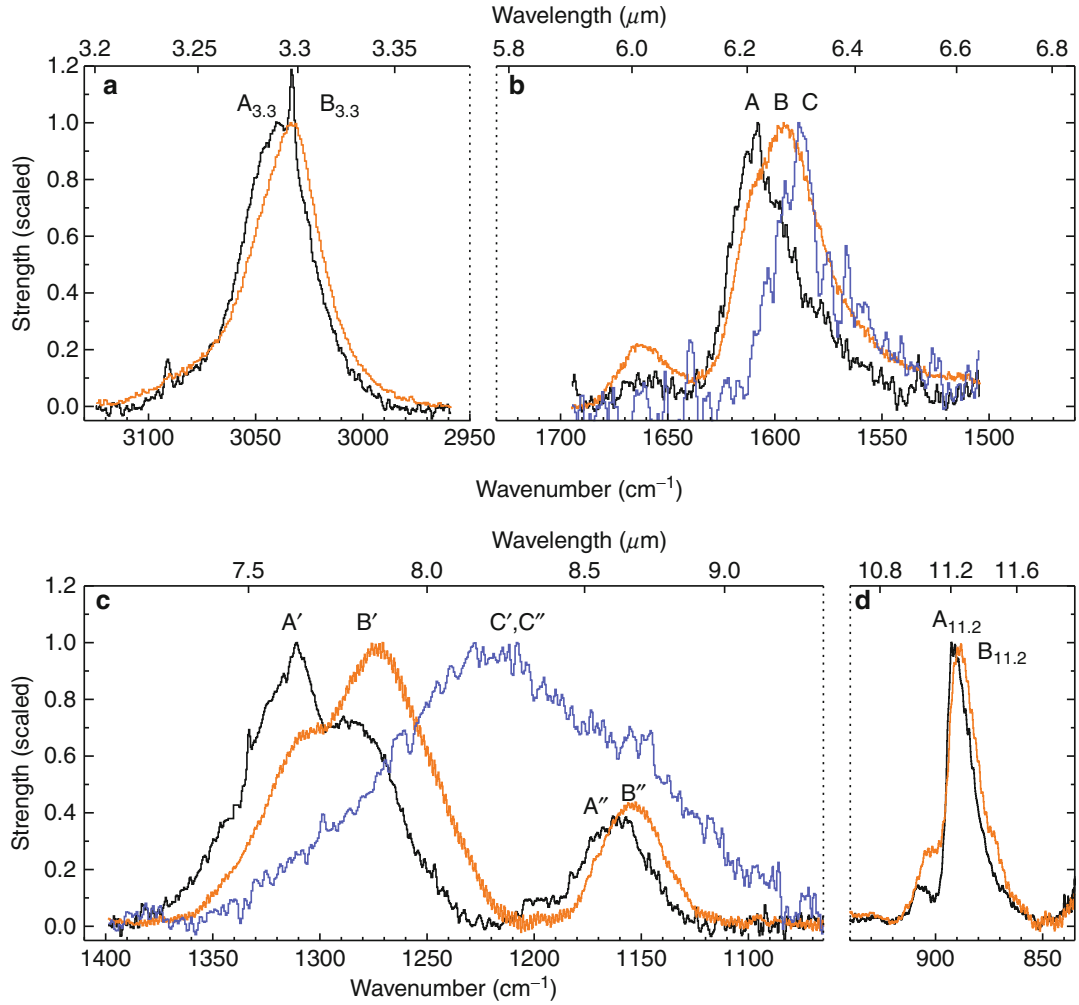

Polycyclic Aromatic Hydrocarbon, Fig. 4 An overview of the source-to-source variations in the position and profile of the main UIR bands in four wavelength bands. In particular large variations are evident in the 6–9 μm regions. Class A peaks at the shortest wavelengths and class B at longer wavelengths. The C-C modes of class C peak at even longer wavelengths (Peeters et al. 2002; van Diedenhoven et al. 2004, reproduced by permission of the AAS)

the strongest C-C stretching mode toward shorter wavelengths while having no systematic effects or shifts on the position of other vibrational modes.

- PAH-metal complexes: these are species in which a metal atom is located either below or above the carbon skeleton.
- PAH clusters: for example, PAH dimers and trimers.
- Aromatic-aliphatic carbonaceous species with different degree of aromaticity (see below).

Additionally, structural modifications to PAHs may also involve the H atoms and include:

- Superhydrogenated and protonated PAHs: These PAHs contain peripheral C atoms bonded to two hydrogen atoms. Hence, these species have aliphatic CH bonds which emit near 3.4 μm (Fig. 2). This band is observed in many sources but is generally weak. Also, emission at this wavelength may be due to methyl side groups attached to PAHs.

- Deuterated PAHs: Toward two star-forming regions, Peeters et al. (2004c) tentatively detected weak emission bands at 4.4 and 4.65 μm, characteristics of the C-D stretching mode in PADs. While the aromatic C-D stretch is very weak, the derived D/H ratio for the aliphatic bands is very large compared to simple molecular species. If confirmed, this suggests that deuterium fractionation is very specific. Moreover, the high D/H ratio is consistent with a current model explaining the observed variations in the gas-phase D/H ratios for different lines of sight. Deuterated PAHs may, therefore, represent a large reservoir of deuterium-enriched species.
- Side groups: Hydrogen can be replaced by chemical side groups. The most important one is methyl group ($-CH_3$), which causes a spectral signature at 3.4 μm (Fig. 2).
- Molecular edge structure (see below).

Size

When a PAH molecule absorbs a UV photon, the absorbed energy is distributed over the vibrational modes. Since larger PAHs have many more available modes, the average energy per mode is lower. As a consequence, smaller PAHs will reach much higher levels of vibrational excitation and thus will be more conducive to emitting at shorter (more energetic) wavelengths.

Thus, the size distribution of molecules that contribute to an observed UIR band will depend on the wavelength of the band. For example, the majority of the 3 μm UIR emission is due to PAHs made up from 30 to 70 carbon atoms, while emission in the 10–15 μm region originates from much larger PAHs, with sizes between 80 and several hundred carbon atoms (Schutte et al. 1993). Clearly, the astronomical PAH family must represent a size distribution.

Laboratory and theoretical studies of PAHs also show clear spectral differences between small and larger PAHs (Bauschlicher et al. 2008, 2009). The spectra of small PAHs are rather diverse, while larger PAHs emit at more consistent wavelengths. However, very large PAHs ($N_C > 150$) exhibit complex spectra unlike those observed in space (Ricca et al. 2012). In addition, small PAHs ($N_C \leq 48$) do emit at ~ 7.6 μm but do not reproduce the 7.8 μm component (e.g., Peeters et al. 2002), while larger PAHs ($54 \leq N_C \leq 130$) emit at 7.8 μm and not at 7.6 μm. Thus, both small and large PAHs are required to reproduce the 7.7 μm complex, and the variable strength of the two components (class A vs. class B) can indicate differing size distributions. Since also the broad class C component can be reproduced by a mixture of small PAHs, the PAH classes may reflect a change of the PAH size distribution in different environments.

At the same time though, the astronomical PAH family is most likely somewhat limited, since the astronomical observations are very similar to first order and do not show the numerous variations that could be expected for millions of PAHs with all possible sorts of structures. This is also clear from the emission in the 15–20 μm region, which is due to carbon skeleton modes and hence more molecule-specific. However, the astronomical spectra only exhibit a limited number of bands and/or a broad emission feature.

Molecular (Edge) Structure

Laboratory studies show that the peak wavelength of the C-H out-of-plane bending mode depends strongly on how much the bond is influenced by the presence of neighboring hydrogen atoms and more specifically to the number of adjacent peripheral C-atoms bonded to an H-atom (Bellamy 1958). While the details depend slightly on the charge state of the carrier, it is clear that the 11.0 and 11.2 μm features are due to solo C-H groups (i.e., there is no adjacent C atom that is bonded to an H atom) while both duos and trios (respectively two and three adjacent C-atoms each with an H attached to them) contribute to the 12.7 μm feature. Variations in the relative strength of these out-of-plane bending modes are thus indicative of variations in the molecular edge structure of the emitting PAHs. Indeed, the solo CH groups decorate long, straight, and smooth edges, while duos and trios are characteristic of corners and irregular edge structures.

Circumstellar PAHs associated with planetary nebulae have a very strong 11.2 μm band and a

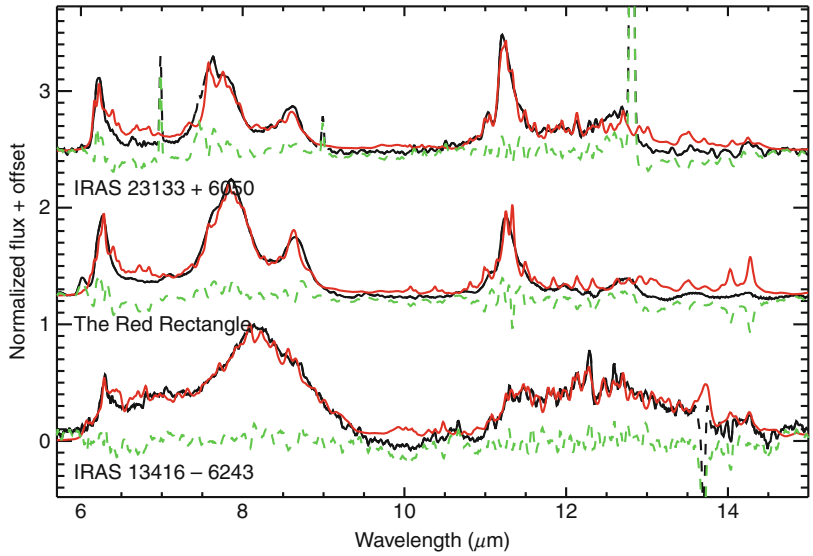

Polycyclic Aromatic Hydrocarbon, Fig. 5 The astronomical UIR spectra (*black*) and the best fit PAH model spectra (*red*) for three types of PAH sources. Residuals are shown in *green*. This PAH model is able to fit all three classes. The HII region IRAS 23133 + 6050 (*black*) is a class A source; the Red Rectangle (*red*) a class B source; and the protoplanetary nebula IRAS 13416-6243 (*blue*) a class C object (Cami in JTPAHs & Cami et al. in preparation) (Reproduced from Cami in JTPAHs with permission from EDP Sciences)

much weaker 12.7 μm band (Fig. 2) and are therefore characterized by very compact molecular structures. On the other hand, the 11.2 μm band in interstellar PAHs is about as strong as the 12.7 μm band (Fig. 2), indicating that interstellar PAHs have more corners, either because they are (on average) smaller or they are more irregular larger species (Fig. 1, Hony et al. 2001; Bauschlicher et al. 2008, 2009).

Laboratory and theoretical studies also reveal that H atoms located in a bay of the edge structure (see Fig. 1) have emission at slightly shorter wavelengths compared to that of non-bay Hs. This difference can be used to estimate the smoothness of the edge structure (Bauschlicher et al. 2009). In addition, a varying degree of bay Hs has been put forward to explain variations in the 3.3 μm band profile (Candian et al. 2012).

Astronomical Observations Versus PAH Databases

One of the strongest criticisms against the PAH hypothesis (i.e., the identification of the UIR bands with emission from PAHs and PAH-like species) has been the lack of a good match between a combination of experimental and/or theoretical PAH spectra and the astronomical UIR spectra. This has been largely due to the limited availability of spectral properties for a large number of PAH species. The NASA Ames infrared spectroscopic database (Bauschlicher et al. 2010; http://www.astrochem.org/pahdb/) now contains theoretically calculated data for hundreds of PAHs and related molecules and has resulted in good fits to astronomical observations of all three classes (Fig. 5, Cami in JTPAHs [2011] and Cami et al. in preparation). The NASA Ames PAH spectral database is highly biased toward small, neutral, and pure PAHs. However, a spectral decomposition of the fits can be used to reveal the contribution of PAHs of different sizes, charge states, and differing compositions. Such work confirms many of the conclusions discussed above.

The PAH Life Cycle

Carbon stardust is formed in the outflow of C-rich AGB stars and is believed to be comparable to terrestrial soot formation in flames – where PAHs are formed. Carbon star outflows are thus believed to be the birthplace of astronomical

PAHs. Most of the carbon in these outflows is tied up in CO and C_2H_2 (▶ acetylene); chemical models then predict the formation of ▶ benzene, PAHs, and ultimately soot (Tielens 2008 and reference therein). There is little direct evidence of PAHs in the outflow of C-rich AGB stars though, possibly as a result of the absence of UV radiation from these stars. Indirect evidence, however, is provided by the ample detection of PAHs in the next evolutionary stages characterized by much stronger UV radiation, the C-rich post-AGB stars and C-rich ▶ planetary nebulae. Eventually, the material in these outflows becomes part of the ▶ interstellar medium and conglomerates in ▶ diffuse clouds that grow in size and evolve into ▶ molecular clouds. In the dense cores of molecular clouds, PAHs get frozen into the ice mantles covering grain surfaces. The cores of molecular clouds will eventually become protostars, at which point the PAH molecules are released into the gas phase and may be incorporated into a planetary system.

PAHs may undergo dramatic changes due to UV and collisional processing, coagulation, accretion, shattering, etc., that are associated with different phases of this life cycle. In addition, shattering of grains by shocks or UV processing of PAH clusters may form PAHs in the interstellar medium (ISM).

There is ample observational evidence for these processes:

- The specific profiles of the UIR bands depend directly on the type of object (Peeters et al. 2002; van Diedenhoven et al. 2004, Peeters in JTPAHs): class A profiles represent the ▶ HII regions, non-isolated Herbig AeBe stars, ▶ reflection nebulae, (diffuse) ISM, and entire galaxies; class B contains most ▶ planetary nebulae, isolated Herbig AeBe stars, and a few post-AGB stars; and class C is mainly comprised of post-AGB stars. Thus, class A profiles are associated with interstellar material, while classes B and C profiles correspond to circumstellar material; the differences between the classes are due to PAH processing. These spectral variations are also seen within spatially extended objects such as reflection nebulae and evolved stars (e.g., Peeters in JTPAHs, Candian et al. 2012, Rosenberg et al. 2011).
- In a sample of post-AGB stars and isolated HAeBe stars (all of PAH class B or C), Sloan et al. (2007) found a remarkable anticorrelation of the peak positions of several of the UIRs with the effective temperature of the exciting star (Fig. 6), suggesting that the components of the PAH family are susceptible to UV processing. This has been interpreted as a varying importance of aliphatics versus aromatics (e.g., Sloan et al. 2007; Boersma et al. 2008, Acke in JTPAHs, Kwok & Zhang 2012) instead of a change in size distribution of the PAH family. Aliphatic carbonaceous species are known to produce broader emission bands compared to PAHs and hence are put forward as the carrier of the class C 7.7 μm complex. An evolution to class B and then to class A is then the result of more UV processing (e.g., due to an increase in effective temperature) of these aliphatic carbonaceous species destroying the aliphatic bonds and hence increasing the aromaticity of species. Such a mechanism could explain the evolution from post-AGB stars to the ISM, but it is hard to think of a plausible process that morphs the aromatic material into more fragile aliphatic material when going from the ISM to protoplanetary environments. Boersma et al. (2008) therefore proposed an active chemical equilibrium between aromatic and aliphatic species in all environments through hydrogenation, carbon reactions building (aliphatic) ▶ hydrocarbons, and UV processing. However, the observational relation does not hold in general. Indeed, several planetary nebulae and class A objects do not follow the correlation; moreover, the PAH bands of Herbig AeBe stars with the same effective temperature can belong to both classes A and B (Boersma et al. 2008). These exceptions seem to suggest that in addition to or in contrast with a dependence on effective temperature, other parameters may play a role.
- Analysis of the spatial behavior of PAHs within extended sources reveals PAHs toward the edge of PDRs, but shows that further

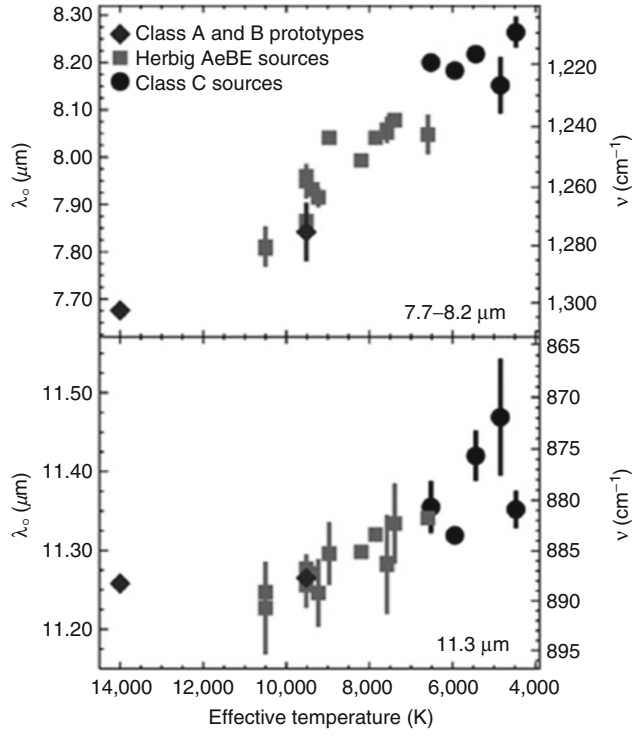

Polycyclic Aromatic Hydrocarbon, Fig. 6 The central wavelengths of the 7.7–8.2 and 11.3 μm UIR features plotted versus the effective temperature of the host star (Sloan et al. 2007; Keller et al. 2008, reproduced by permission of the AAS)

inward the PDR (characterized by less UV radiation), larger species (such as PAH clusters) are found. These studies suggest that the destruction of the PAH clusters by UV photons results in the formation of PAHs. These PAH clusters themselves may be reformed in the denser and more shielded environments of molecular clouds. Similarly, in regions of high UV radiation, small PAHs are destroyed (e.g., Berné, Rapacioli in JTPAHs).

- For galaxies harboring an active galactic nucleus (AGN), the 7.7/11.2 PAH ratio correlates with the hardness of the radiation field (i.e., the proportion of high-energy photons; Calzetti in JTPAHs [2011]). This is unlike the galaxies with HII regions or starburst-like characteristics where the 7.7/11.2 PAH ratio is largely insensitive to the hardness of the radiation field. Since the latter include low ▶ metallicity (for astronomers, low abundances of elements heavier than helium) systems which typically have a harder radiation field, both samples cover the same range in hardness of the radiation field. The PAH family thus seems changed by the presence of an AGN (AGNs are thought to indicate the presence of a supermassive black hole).
- For galaxies, the relative importance of PAHs with respect to dust grains in the spectra depends on the hardness of the radiation field and the ▶ metallicity (Calzetti in JTPAHs [2011]). These two parameters are related, and it is thus difficult to distinguish between an origin in a less efficient PAH formation process (since less carbon is available at lower metallicities) and an increased PAH processing (modification and/or destruction of PAHs by the hard radiation field).

The Role of PAHs in Astronomical Environments

PAH Chemistry

Several chemical processes involve PAHs in the ISM. UV processing (▶ photochemistry) and collisional processing can significantly alter the PAH distribution (in terms of charge and size). PAHs can furthermore chemically react with

abundant atoms such as H, C, N, and O. In ▶ dense clouds, PAHs condense out onto ice mantles and can subsequently undergo UV processing. The photoproducts are later released into the gas phase by thermal heating in the star-forming environment or in the PDRs and by shocks or cosmic-ray ▶ sputtering. For a detailed account of PAH chemistry, see Tielens (2005), ▶ Cosmochemistry, ▶ Interstellar chemical processes, and ▶ Interstellar Ices.

Photochemistry involves photoionization and photodissociation. The ionization potential of PAHs is around 6–7 eV (electron volts) and depends on the PAH size and geometry. PAHs can be multiply ionized, but for a typical 50 C-atom PAH, the fourth positive ionization potential is larger than 13.6 eV, which limits the ionization stage in neutral hydrogen regions. Alternatively, absorption of a UV photon may lead to the loss of an H atom (dehydrogenation) or a side group. The rates for such reactions are highly dependent on the PAH size and the side group in question: for example, hydrogen loss from a methyl group is faster than aromatic hydrogen loss which in turn is much faster than carbon loss (i.e., C_2H_2 ejection). The size below which PAHs may lose all H (because the rehydrogenation rate is lower than the dehydrogenation rate) is estimated to be $\sim$ 35 C-atoms. Following complete dehydrogenation, PAHs may isomerize into carbon chains, rings, or fullerenes. This process removes small PAHs from the PAH family.

As important as UV processing is collisional processing. This results from collisions with high velocity electrons and ions originating in shocks, hot gas, and cosmic rays (Micelotta 2009). Interstellar PAHs ($\sim$50 C-atoms) are destroyed in shocks with velocities greater than 100 km/s. For lower velocity shocks, PAHs survive, but their structures and thus characteristics are severely altered by the loss of carbon atoms (20–40 %). In a hot gas ($T \sim 10^3 - 10^8$ K), PAHs are destroyed through consecutive C_2 loss on the periphery of the structure primarily by He collisions in low temperature gas ($T < 3\ 10^4$ K) and by electronic collisions in high temperature gas ($T > 3\ 10^4$ K). Finally, PAHs are destroyed by cosmic rays on various timescales (depending, e.g., on the collisional particle). Depending on the environment considered (and its physical conditions), different collisional processes dominate.

Gas-phase chemistry involves the following reaction types: electron recombination ($PAH^+ + e \rightarrow PAH$), electron attachment to PAHs ($PAH + e \rightarrow PAH^-$), charge-exchange reactions involving neutral PAHs ($PAH + M^+ \rightarrow PAH^+ + M$ with M a metal), mutual neutralization reaction of PAH anions with atomic or molecular cations ($PAH^- + M^+ \rightarrow PAH + M$), and reactions involving PAH cations and H, N, and O atoms.

Laboratory studies of UV processing of PAHs trapped in ices show that the processing is confined to the peripheral aromatic hydrogen and leaves the carbon skeleton intact. The aromatic hydrogen may be substituted by side groups (e.g., OH, CH_3, COOH, CO, and CN) to form more complex organic compounds such as, for example, quinones (Bernstein et al. 1999). Some of these photoproducts are thus prebiotic molecules and may have relevance for the organic content in space. However, the importance of PAH processing in ices in actual molecular clouds is not yet established.

Shattering of solid carbon in shocks modifies the interstellar grain size distribution (Jones et al. 1996). Typical interstellar shocks may transform 10 % of the solid carbon into small carbon clusters and hence provide a pathway for PAH formation in the ISM. However, faster shocks will destroy the PAHs. Currently, little observational evidence exists for PAH formation in shocks, although Rho (in JTPAHs [2011]) discerned 15–20 μm PAH emission in supernova remnant SNR N132D in the Magellanic Clouds while Engelbracht et al. (2006) detected PAH emission associated with the superwind of the galaxy M82 and entrained by hot shocked gas.

PAH Physics

PAHs play an important role in the physics of the ISM, primarily through their influence on the charge balance and in the heating of the ISM.

The ionization balance of PAHs is set by the ratio of the ionization rate to the recombination rate, which is equal to $G_0 T^{1/2}/n_e$ in which G_0 is

the far-ultraviolet (FUV; 6 eV < photon energy < 13.6 eV) radiation field in units of the Habing field (see ▶ Photodissociation Region), T the gas temperature, and n_e the electron density (for detailed physics, see Tielens 2005; PDRs). At typical interstellar conditions, several charge stages are present simultaneously, as is also indicated by the spectra attributed to PAHs. These include neutral PAHs and ionic PAHs (either cations or anions). PAH anions provide an alternative and effective recombination path for atomic and molecular cations compared to gas-phase recombination in ▶ photodissociation regions and ▶ molecular clouds. PAHs thus influence the charge balance and in this way – through their influence on the equilibrium state of chemical reactions – gas-phase abundances (Tielens 2005, PDRs and references therein).

In addition, PAHs and very small grains dominate the photoelectric heating of the ISM (Tielens 2005, PDRs and references therein). This photoelectric heating couples the gas energy budget with the radiation field of stars in PDRs and hence determines the physical conditions in PDRs.

Applications: PAHs as Diagnostic Tools

The intensity ratios of the CC/CH modes of the UIR bands are determined by the charge balance of the PAHs. If variations in the physical conditions are known (e.g., derived from PDR models), the observed variations of the PAH bands can be used to establish an "empirical" calibration that relates the PAH bands to the local physical conditions. Once such a calibration is known, the physical conditions can be determined based upon the omnipresent PAH bands. This can serve as a diagnostic tool for regions where, for example, the main PDR coolants are not easily observable, such as galaxies at large distances. Such an approach has been tested for a sample of three well-studied objects and has been proven to be very promising (Fig. 7, Galliano et al. 2008). Similarly, physical conditions can be derived from combining the observed PAH ionization ratio and H_2 line ratios in dense, highly irradiated PDRs (Berné et al. 2009).

UIR emission bands are particularly bright in massive star-forming regions since they are excited by strong UV radiation. Combined with their ubiquitous appearance, this makes PAHs a powerful tracer of star formation throughout the universe. PAHs are indeed widely used to derive star formation rates of galaxies (Calzetti in JTPAHs), one of the key indicators for understanding galaxy formation and evolution. In combination with emission lines, they serve as diagnostics for the ultimate physical processes powering galactic nuclei (Calzetti in JTPAHs [2011]).

Finally, the presence of PAHs is used to distinguish between shocked gas and PDRs (van den Ancker et al. 2000) and to determine redshifts in distant galaxies (e.g., Yan et al. 2007).

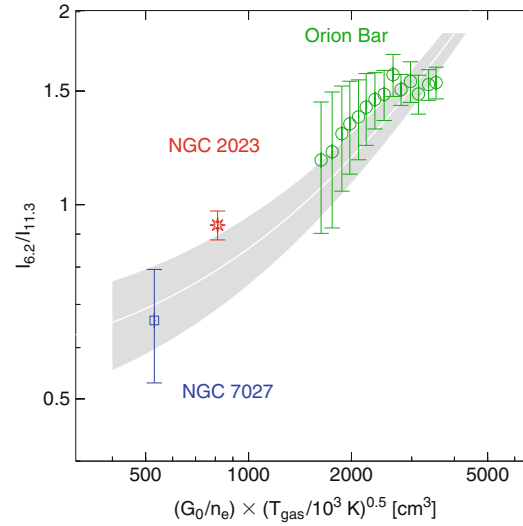

Polycyclic Aromatic Hydrocarbon, Fig. 7 Empirical calibration of the 6.2/11.2 UIR band ratio as a function of the ionization parameter, $G_0T^{1/2}/n_e$ (Galliano et al. 2008, reproduced by permission of the AAS)

Future Directions

Several key questions regarding astronomical PAHs remain and require further investigations. In particular:

1. How exactly do PAH characteristics (e.g., size, charge state, chemical structure) interact with and reflect the physical conditions of

their environment (e.g., density, radiation field, temperature, ▶ metallicity)?
2. How can we use the UIR bands as a probe of the physical conditions in regions near and far?
3. Do we observe long wavelength counterparts to the well-known mid-IR PAH bands? What are their characteristics?
4. What are the spectroscopic signatures of large PAH molecules, PAH clusters, and PAH complexes?
5. Which specific molecules make up the astronomical PAH family?
6. What can we learn from the electronic transitions of PAHs, and what is their relation to the ▶ diffuse interstellar bands (DIBs)?

With the wealth of data obtained with the Herschel Space Observatory and with SOFIA becoming fully operational, we are fortunate to obtain the necessary observations to explore the far-IR modes of the PAHs and to couple the PAH band characteristics to the physical conditions of the environment. In addition, the James Webb Space Telescope (JWST) is scheduled for the near future, and hence, the observational future for infrared PAH research is very bright. Today, the wealth of IR PAH emission bands and the large variability of the IR PAH spectra prompt more questions that can be answered with the current laboratory and theoretical data. Similarly, at optical wavelengths, there are now more observed unidentified DIBs than ever before. If we intend to make significant progress in our understanding of the PAHs, the observational effort needs to be balanced with dedicated laboratory and theoretical studies. Indeed, we can only fully exploit the treasure trove of information that is hidden in the PAH spectra by a joint effort of the observational, experimental, and theoretical tools.

See Also

- ▶ Acetylene
- ▶ Aliphatic Hydrocarbon
- ▶ Amorphous Carbon
- ▶ Aromatic Hydrocarbon
- ▶ Asteroid
- ▶ Benzene
- ▶ Cassini-Huygens Space Mission
- ▶ Comet (Nucleus)
- ▶ Cosmochemistry
- ▶ Diffuse Interstellar Bands
- ▶ Extended Red Emission
- ▶ Extinction, Interstellar or Atmospheric
- ▶ Fluorescence
- ▶ Fullerene
- ▶ Graphite
- ▶ Hydrocarbons
- ▶ Hydrogenated Amorphous Carbon
- ▶ Infrared Astronomy
- ▶ Infrared Spectroscopy
- ▶ Interstellar Chemical Processes
- ▶ Interstellar Dust
- ▶ Interstellar Ices
- ▶ Interstellar Medium
- ▶ Metallicity
- ▶ Meteorites
- ▶ Molecular Cloud
- ▶ Molecules in Space
- ▶ Nanodiamond
- ▶ Photochemistry
- ▶ Photodissociation Region
- ▶ Planetary Nebula
- ▶ Quenched Carbonaceous Composite
- ▶ Reflection Nebula
- ▶ Spitzer Space Telescope
- ▶ Stellar Evolution
- ▶ UV Absorption Bump

References and Further Reading

Allamandola LJ, Tielens AGGM, Barker JR (1989) Interstellar polycyclic aromatic hydrocarbons – the infrared emission bands, the excitation/emission mechanism, and the astrophysical implications. Astrophys J Suppl Ser 71:733–775

Bauschlicher CW Jr, Peeters E, Allamandola LJ (2008) The infrared spectra of very large, compact, highly symmetric, polycyclic aromatic hydrocarbons (PAHs). Astrophys J 678:316

Bauschlicher CW Jr, Peeters E, Allamandola LJ (2009) The infrared spectra of very large irregular polycyclic aromatic hydrocarbons (PAHs): Observational probes of astronomical PAH geometry, size, and charge. Astrophys J 697:311

Bauschlicher CW, Boersma C, Ricca A et al (2010) The NASA Ames polycyclic aromatic hydrocarbon infrared spectroscopic database: the computed spectra. Astrophys J Suppl Ser 189:341

Bellamy L (1958) The infra-red spectra of complex molecules, 2nd edn. Wiley, New York

Berné O, Fuente A, Goicoechea JR et al (2009) Mid-infrared polycyclic aromatic hydrocarbon and H_2 emission as a probe of physical conditions in extreme photodissociation regions. Astron Astrophys 706:L160

Bernstein MP, Sandford SA, Allamandola LJ, Gillette JS, Clemett SJ, Zare RN (1999) UV irradiation of polycyclic aromatic hydrocarbons in ices: production of alcohols, quinones, and ethers. Science 283:1135–1138

Boersma C (2009) PhD thesis, University of Groningen

Boersma C, Bouwman J, Lahuis F et al (2008) The characteristics of the IR emission features in the spectra of Herbig Ae stars: evidence for chemical evolution. Astron Astrophys 484:241

Calzetti D, Kennicutt RC, Engelbracht CW et al (2007) The calibration of mid-infrared star formation rate indicators. Astrophys J 666:870

Cami J, Bernard-Salas J, Peeters E, Malek SE (2010) Detection of C60 and C70 in a Young Planetary Nebula. Science 329(5996):1180

Cami J, Cox N (eds) (2013) In: Proceedings of IAU symposium 297: Diffuse Interstellar Bands, in press

Candian A, Kerr TH, Song I-O, McCombie J, Sarre PJ (2012) Spatial distribution and interpretation of the 3.3μm PAH emission band of the red rectangle. MNRAS 426:389

Charnley SB, Kuan Y-J, Huang H-C et al (2005) Astronomical searches for nitrogen heterocycles. Adv Space Res 36:137

Draine BT, Lazarian A (1998) Electric dipole radiation from spinning dust grains. Astrophys J 508:157

Duley WW, Williams DA (1981) The infrared spectrum of interstellar dust – surface functional groups on carbon. MNRAS 196:269

Engelbracht CW, Kundurthy KD, Gordon KD et al (2006) Extended mid-infrared aromatic feature emission in M82. Astrophys J 642:L127

Galliano F, Madden S, Tielens AGGM et al (2008) Variations of the mid-IR aromatic features inside and among galaxies. Astrophys J 679:310

Herbig GH (1995) The diffuse interstellar bands. Annu Rev Astron Astrophys 33:19

Hony S, Van Kerckhoven C, Peeters E et al (2001) The CH out-of-plane bending modes of PAH molecules in astrophysical environments. Astron Astrophys 370:1030

Hudgins DM, Bauschlicher CW Jr, Allamandola LJ (2005) Variations in the peak position of the 6.2 2 μm mu;m interstellar emission feature: a tracer of N in the interstellar polycyclic aromatic hydrocarbon population. Astrophys J 632:316

Jones AP, Tielens AGGM, Hollenbach DJ (1996) Grain shattering in shocks: the interstellar grain size distribution. Astrophys J 469:740

JTPAHs = Joblin C, Tielens AGGM (eds) (2011) In: Proceedings of symposium, PAHs and the universe: a symposium to celebrate the 25th anniversary of the PAH hypothesis, EAS Publications Series 46 http://www.eas-journal.org/action/displayIssue?jid=EAS&volumeId=46&seriesId=0&issueId=−1

Keller LD, Sloan GC, Forrest WJ et al (2008) PAH emission from Herbig Ae/Be stars. Astrophys J 684:411

Kwok S, Zhang Y (2011) Mixed aromatic-aliphatic organic nanoparticles as carriers of unidentified infrared emission features. Nature 479:80

Li A, Draine BT (2012) The carriers of the interstellar unidentified infrared emission features: aromatic or aliphatic? Astrophys J 760:L35

Micelotta (2009) Ph.D thesis, University of Leiden

Peeters E, Hony S, van Kerckhoven C et al (2002) The rich 6 to 9 micron spectrum of interstellar PAHs. Astron Astrophys 390:1089

Peeters E, Allamandola LJ, Hudgins DM, Hony S, Tielens AGGM (2004a) The unidentified Infrared features after ISO. In: Witt A, Draine BT, Clayton CC (eds) Astrophysics of dust. PASP, San Francisco, p 141

Peeters E, Spoon HWW, Tielens AGGM (2004b) Polycyclic aromatic hydrocarbons as a tracer of star formation? Astrophys J 613:986

Peeters E, Allamandola L, Bauschlicher CW Jr, Hudgins D, Sandford SA, Tielens A (2004c) Deuterated interstellar polycyclic aromatic hydrocarbons. ApJ 604:252

Pilleri P, Herberth D, Giesen TF (2009) Search for corannulene ($C_{20}H_{10}$) in the red rectangle. MNRAS 397:1053

Puget JL, Léger A (1989) A new component of the interstellar matter – small grains and large aromatic molecules. Annu Rev Astron Astrophys 27:161–198

Ricca A, Bauschlicher CW, Boersma C, Tielens AGGM, Allamandola LJ (2012) The infrared spectroscopy of compact polycyclic aromatic hydrocarbons containing up to 384 carbons. ApJ 754:75

Rosenberg MJF, Berne O, Boersma C, Allamandola LJ, Tielens AGGM (2011) Coupled blind signal separation and spectroscopic database fitting of the mid infrared PAH features. A&A 532:128

Sarre PJ (2006) The diffuse interstellar bands: a major problem in astronomical spectroscopy. J Mol Spectrosc 238:1

Schutte WA, Tielens AGGM, Allamandola LJ (1993) Theoretical modeling of the infrared fluorescence from interstellar polycyclic aromatic hydrocarbons. Astrophys J 415:397

Sellgren K (1984) The near-infrared continuum emission of visual reflection nebulae. Astrophys J 277:623

Sellgren K, Uchida KI, Werner MW (2007) The 15–20 20 μm mu;m spitzer spectra of interstellar emission features in NGC 7023. Astrophys J 659:1338

Sellgren K, Werner MW, Ingals J et al (2010) C_{60} in reflection nebulae. Astrophys J 722:L54

Sloan GC, Jura M, Duley WW et al (2007) The unusual hydrocarbon emission from the early carbon star HD

100764: the connection between aromatics and aliphatics. Astrophys J 664:1144
Tielens AGGM (2005) The physics and chemistry of the interstellar medium. Cambridge University Press, Cambridge. ISBN 0521826349
Tielens AGGM (2008) Interstellar polycyclic aromatic hydrocarbon molecules. Annu Rev Astron Astrophys 46(1):289–337
van den Ancker ME, Tielens AGGM, Wesselius PR (2000) ISO spectroscopy of the young bipolar nebulae S106 IR and Cep A East. Astron Astrophys 358:1035
van Diedenhoven B, Peeters E, van Kerckhoven C et al (2004) The profiles of the 3–12 micron polycyclic aromatic hydrocarbon features. Astrophys J 611:928
Yan L, Sajina A, Fadda D et al (2007) Spitzer mid-infrared spectroscopy of infrared luminous galaxies at $z \sim 2$. I. The spectra. Astrophys J 658:778
Ysard N, Miville-Deschênes MA, Verstraete L (2010) Probing the origin of the microwave anomalous foreground. Astron Astrophys 509:L1

Polydeoxyribonucleic Acid

▶ DNA

Polydeoxyribonucleotide

▶ Nucleic Acids

Polygenetic Breccia

▶ Polimictic Breccia

Polyhedral Bodies

▶ Carboxysomes, Structure and Function

Polylithologic Breccia

▶ Polimictic Breccia

Polymer

Koichiro Matsuno
Nagaoka University of Technology, Nagaoka, Japan

Keywords

Catalytic cycle; Formose reaction; Oligonucleotides; Oligopeptides; Peptide cycle; Template-directed polymerization

Definition

Polymers of prebiotic significance are those to be found on the verge of the evolutionary onset of various catalytic cycles of chemical reaction. One typical example is the ▶ formose reaction of polymerizing formaldehyde into glycolaldehyde. When one glycolaldehyde molecule enters the cycle in the presence of formaldehyde, two glycolaldehyde molecules come out of the cycle at the end. Significant to the operation of the reaction cycle is that the synthesis of glycolaldehyde is not due to the direct dimerization of formaldehyde. The initiation of the cycle presumes the prior presence of trace amounts of glycolaldehyde. This convoluted nature of the cycle requiring the prior presence of the intended products symbolizes a difficulty facing the emergence of polymers of prebiotic significance.

Overview

One specific case demonstrating a simple cyclic, though not yet autocatalytic, polymerization of small organic molecules is found in the acceleration of polymerizing hydrogen cyanide in the presence of formaldehyde (Schwartz and Goverde 1982). Under some fixed experimental conditions, the initial rate of polymerization of HCN monomers up to an HCN tetramer is increased almost 100-fold within a very short period of time. Although the present cyclic

polymerization up to HCN tetramer could be impressive especially in the respect of prebiotic synthesis of adenine, the reaction is also accompanied by a complex mixture of other products which might induce some deleterious effect on the focused reaction. The situation is almost similar to the formose reaction not yet sufficiently tailored enough to synthesize an adequate amount of ribose as the main ingredient of the backbone of RNA molecules. The difficulty comes from the interferences with other complex products available at the same time.

Destructive interferences between autocatalytic reactions in focus and the necessarily accompanied side-chain reactions can be conceivable even on a theoretical ground alone. A case in point is the peptide cycle (Kauffman 1986). It is one thing to expect an emergence of a set of autocatalytic peptides in a random mixture of amino acid molecules, while it is quite another to preserve the once appeared autocatalytic set for some indefinite period of time. If the random mixture is in thermal equilibrium, every forward reaction is counterbalanced by the reversed reaction as revealed in the principle of detailed balance. The appearance of a likely autocatalytic set, if any, is necessarily counterbalanced by its disappearance, with no net autocatalysis in the effect.

A rescue for saving the likelihood for the appearance of an autocatalytic set on an experimental ground may be sought in preparing specific initial conditions which are not in thermal equilibrium in themselves. If one can initially prepare appropriate peptides of 32-residue length that are carefully designed to self-associate to form stable coiled coils, they will facilitate the ligation of the accompanied N-terminal and C-terminal subsequences (Lee et al. 1996). The present ligation makes self-replication of peptides possible. An essence of the experimental operation of an autocatalytic peptide set is within the choice of uniquely designed initial conditions. This demonstration now invites us to face the issue of how the choice of the initial conditions can be naturalized.

One likely strategy for implementing the initial conditions is to update the experimental conditions frequently. A specific example for the present objective is the feeding experiment on the prebiotic synthesis of oligonucleotides and oligopeptides on mineral surfaces (Ferris et al. 1996). When the monomers activated by imidazole were fed successively onto the mineral surfaces (montmorillonite for nucleotides and elite or hydroxylapatite for amino acids), the formation of oligomers even up to 55 monomers long was confirmed.

Then the experimental endeavor for approaching polymers of prebiotic significance in a natural manner as much as possible will be found within how the experimental conditions could enhance their specificity as repeating their update without asking an intelligent help from the experimentalist every time in the process. Practicing this strategy exclusively on the theoretical ground is hardly conceivable because of the historical and evolutionary nature of the empirical or experimental counterpart. Even if molecular Darwinian process remains legitimate in its own light at least theoretically, one cannot rely upon the Darwinian process to figure out how self-replicating molecules could have got started. Some preliminary evolutionary process must have been in place so as to make the emergence of molecular Darwinian process tangible; otherwise the issue of the onset of self-replicating molecules would have to remain intangible.

One obvious clue for addressing how self-replicating molecules got started is sought within a reexamination of chemical reactions conceived in thermodynamics. Chemical reactions in thermal equilibrium certainly satisfy the principle of detailed balance, as implying that every forward reaction is counterbalanced by the reversed reaction as maintaining both the reactants and the products in equilibrium. No evolution could be in sight within the stipulation of detailed balance. However, once the condition of thermal equilibrium is lifted, the chemical reactions there may be set free from the theoretical stipulation of detailed balance.

Just for the sake of argument, let us imagine a reaction solution of monomers participating in their ligation and the resulting hydrolysis. If the reaction solution is in thermal equilibrium, the population distributions of the monomers and the possible oligomers, especially their ratios, depend only upon the equilibrium constants or

equivalently upon both the Gibbs free energies and temperatures, and not upon each rate constant. The situation would however be drastically changed if thermal equilibrium is not attainable. If the reaction solution happens to experience rapid decrease of its temperature as in the sudden transference from near hydrothermal vents in the ocean to the surrounding cold seawater, the likely products to remain must be the one that can survive the rapid quenching. The decisive factor for determining the likely product to survive is not the equilibrium constant, but is the rate constant measuring the extent of following the sudden temperature drops in the immediate neighborhood. Even if the material constituents remain the same, the most likely product to survive is the one whose internal configuration maximizes the rate constant for following rapid quenching. There is no chance of survival left for those products whose internal configurations fail in maximizing the rate constant for following rapid quenching. Only such an internal configuration that can be fastest in lowering its temperature as facing the rapid quenching while processing each of ligation and hydrolysis from within will win, and there is no chance left for the slower contenders.

Reaction kinetics is already selective internally in maximizing the rate constant for following rapid quenching, while the factor driving the internal selection is sudden temperature drops applied externally. Henceforth, once both the internal selection and the external driving factor are naturalized in an integrated manner, the outcome from the integration can be seen as a consequence of the selection of a natural origin even prior to the onset of Darwinian natural selection. A likely candidate for materializing pre-Darwinian natural selection on Earth could be chemical reactions riding on hydrothermal circulation of seawater through or near the hot vents in the ocean. Of course, the occurrence of hydrothermal circulation of seawater is exclusively of geological origin and totally external to biological processes and organizations. Nonetheless, chemical reactions riding on hydrothermal circulation of seawater, once happened to occur, could take advantage of pre-Darwinian natural selection.

What is specific to pre-Darwinian natural selection latent in chemical reactions riding on hydrothermal circulation of seawater is a frequent update of the reactants visiting the hot reaction spots. The reactants are only those products that could survive the rapid quenching to be experienced after visiting the hot spots the last time. It may look like a successive update of the reaction conditions in an increasingly specific manner progressively as repeating the visits, but no intelligence of external origin is involved. At the same time, how the surviving reaction products would manage the internal regulation of both ligation and hydrolysis could not be directly accessible to the external observer. Concrete factual aspects of pre-Darwinian natural selection associated with chemical reactions riding on hydrothermal circulation would have to be sought in the results of the corresponding experiments, while their actual objective and the likely target would also have to clearly be made as much as possible in advance.

One selective nature latent in the reaction solution of only monomers initially must be found in the selective scheme of the gradual buildup of oligomers through the internal regulation of both ligation and hydrolysis as repeating the cycle of heating and quenching. Further examination of the present conjecture on the selective elongation of oligomers requires consultation with a corresponding experiment. When a flow reactor simulating hydrothermal circulation of seawater equipped with rapid quenching from 250 °C down to 0 °C somewhere along the streamline was employed for studying elongation of glycine oligomers in the presence of copper ions, the elongation was found to proceed in the sequential order from ▶ diketopiperazine, diglycine, tetraglycine, to hexaglycine along the time course of development (Imai et al. 1999). Both triglycine and pentaglycine were not identified. The result reveals that the chain elongation could be due largely to aminolysis of diketopiperazine. The elongation was already selective in eliminating the cases of adding monomeric glycine one by one onto the then surviving oligoglycine.

Polymerization of monomers through elongation of oligomers proceeding under the influence

of rapid quenching can be history-dependent and evolutionary in demonstrating a pre-Darwinian natural selection. The hydrothermal environments on the seafloor in the ocean must have been pivotal in keeping the cradle for nurturing the operation of pre-Darwinian natural selection for synthesizing polymers of prebiotic significance.

See Also

- ▶ Darwin's Conception of the Origins of Life
- ▶ Diketopiperazine
- ▶ Formose Reaction
- ▶ Hydrothermal Reaction
- ▶ Natural Selection
- ▶ Nucleic Acids
- ▶ Protein

References and Further Reading

Ferris JP, Hill AR Jr, Liu R, Orgel LE (1996) Synthesis of long prebiotic oligomers on mineral surfaces. Nature 381:59–61

Imai E, Honda H, Hatori K, Brack A, Matsuno K (1999) Elongation of oligopeptides in a simulated submarine hydrothermal system. Science 283:831–833

Kauffman SA (1986) Autocatalytic sets of proteins. J Theor Biol 119:1–24

Lee DH, Granja JR, Martinez JA, Severin K, Ghadiri MR (1996) A self-replicating peptide. Nature 382:525–528

Schwartz AW, Goverde M (1982) Acceleration of HCN oligomerization by formaldehyde and related compounds: implications for prebiotic syntheses. J Mol Evol 18:351–353

Polymerase Chain Reaction

Carlos Briones
Centro de Astrobiología (CSIC/INTA),
Consejo Superior de Investigaciones Científicas,
Madrid, Spain

Keywords

Amplification; DNA; Replication; *Taq* polymerase; Thermostable DNA polymerase

Synonyms

PCR

Definition

Polymerase chain reaction or PCR is an artificial method for the amplification of double-stranded ▶ DNA – dsDNA – fragments based on the action of a thermostable DNA polymerase. It allows for the quick, reliable, and highly sensitive in vitro amplification of DNA from any source. The reaction consists of a series of replication cycles of three successive phases: (1) *denaturation* of the parental dsDNA into two complementary single-stranded – ssDNA – molecules; (2) *annealing* or hybridization of two short ssDNA primers with their respective complementary region in each ssDNA strain; and (3) *elongation* or DNA replication of each primer-bound ssDNA strain by the DNA polymerase, rendering two identical dsDNA molecules. Cycles of exponential amplification are repeated 30–40 times, resulting in over a million-fold amplification of the initial material.

Overview

Since its invention in the mid 1980s (Saiki et al. 1985; Mullis and Faloona 1987), PCR has revolutionized genetics and molecular biology by permitting rapid amplification of DNA of any length – up to 50,000 nucleotides, nt – and sequence. A general requirement for the target DNA is that the flanking sequences at both ends of the fragment to be amplified must be known, thus allowing the use of two short – usually 15–30 nt long – DNA primers complementary to them during the annealing phase of each cycle. Currently, PCR is a routine protocol that only requires the target DNA, forward and reverse primers, a thermostable DNA polymerase, triphosphate deoxynucleotides as monomers, and a buffer that provides the required pH and salts for the reaction.

Once the reaction mixture is prepared, PCR is performed automatically in equipment called thermocyclers or thermal cyclers, taking 2–3 h for completion. Alternatively, advances in microfluidics and microchip technology allow 20 cycles of PCR to be completed in only 90 s (Innis et al. 1990; Sambrook and Rusell 2001). The detection and characterization of the amplified product is done after the last cycle in traditional PCR. In turn, real-time quantitative PCR combines amplification and detection in a single tube, thus measuring the amount of amplified DNA at each cycle (Higuchi et al. 1992; Smith and Osborn 2009).

PCR amplification of DNA can be accomplished by DNA polymerases from different thermophilic microorganisms, able to withstand the high temperature – usually 90–94 °C – used during the denaturation phase of each cycle. The optimal DNA polymerization temperature of these enzymes – and thus the selected elongation temperature in PCR – is 68–74 °C. Different DNA polymerases show differences in efficiency (yield of DNA amplification per unit of the enzyme or per cycle), processivity (average length of the DNA amplified), and fidelity (frequency of polymerase-induced errors). These parameters also depend on the PCR conditions. The most widely used enzyme has been ▶ *Taq* polymerase, purified from the thermophilic bacterium *Thermus aquaticus*. Nevertheless, the high error rate associated with the DNA replication performed by this enzyme has encouraged the use of high fidelity DNA polymerases of some hyperthermophilic archaea such as: *Vent*, from *Thermococcus litoralis*; *Pfu*, from *Pyrococcus furiosus*; *Pwo*, from *Pyrococcus woesei*; and mixtures or genetically engineered versions of them (Pavlov et al. 2004; Lewin 2008).

Different experimental variants of PCR technology currently used include reverse transcription followed by PCR (also called RT-PCR), double or nested PCR, asymmetric PCR, multiplex PCR, mutagenic PCR, random PCR, inverse PCR, and ligation-mediated PCR (Innis et al. 1990; Lewin 2008). All of them enjoy an increasing applicability in different fields of biology and medicine.

See Also

- ▶ Amplification (Genetics)
- ▶ DNA
- ▶ Replication (Genetics)
- ▶ Taq Polymerase
- ▶ Thermophile

References and Further Reading

Higuchi R, Dollinger G, Walsh PS, Griffith R (1992) Simultaneous amplification and detection of specific DNA sequences. Biotechnology 10:413–417

Innis MA, Gelfand DH, Sninsky JJ, White TJ (eds) (1990) PCR protocols: a guide to methods and applications. Academic, San Diego

Lewin B (2008) Genes IX. Jones and Bartlett, Boston

Mullis KB, Faloona FA (1987) Specific synthesis of DNA in vitro via a polymerase-catalyzed chain reaction. Methods Enzymol 155:335–350

Pavlov AR, Pavlova NV, Kozyavkin SA, Slesarev AI (2004) Recent developments in the optimization of thermostable DNA polymerases for efficient applications. Trends Biotechnol 22:253–260

Saiki RK, Scharf S, Faloona F, Mullis KB, Horn GT, Erlich HA, Arnheim N (1985) Enzymatic amplification of β-globin genomic sequences and restriction site analysis for diagnosis of sickle cell anemia. Science 230:1350–1354

Sambrook J, Rusell D (2001) Molecular cloning: a laboratory manual. Cold Spring Harbor Laboratory Press, New York

Smith CJ, Osborn AM (2009) Advantages and limitations of quantitative PCR (Q-PCR)-based approaches in microbial ecology. FEMS Microbiol Ecol 67:6–20

Polynucleotide

Henderson James (Jim) Cleaves II
Earth–Life Science Institute (ELSI), Tokyo Institute of Technology, Meguro–ku, Tokyo, Japan
Institute for Advanced Study, Princeton, NJ, USA
Blue Marble Space Institute of Science, Washington, DC, USA
Center for Chemical Evolution, Georgia Institute of Technology, Atlanta, GA, USA

Definition

A polynucleotide is a repeating polymer composed of ▶ nucleotide monomers covalently

bonded via phosphodiester bonds. DNA and RNA are examples of polynucleotides. The chain length at which an oligonucleotide becomes a polynucleotide is somewhat arbitrary, but some biochemists define the transition as occurring at lengths of 13 or more nucleotide residues.

See Also

- ▶ Nucleic Acids
- ▶ Nucleotide

Polyoxymethylene

Hervé Cottin
Laboratoire Interuniversitaire des Systèmes Atmosphériques, Université Paris Est-Créteil, Créteil, France

Keywords

Comet; Distributed source; Formaldehyde; Polymer

Synonyms

Paraformaldehyde; POM

Definition

Polyoxymethylenes (POM) are polymers of formaldehyde. They can exist either in cyclic (trioxane $C_3O_3H_6$ and tetroxane $C_4O_4H_8$) or linear form. The latter includes a wide range of chain lengths with formula ($HO(CH_2O)_nH$). The low molecular weight polymers (typically ranging from 10 to 100 monomers units) are commonly known as paraformaldehyde and are readily thermally degraded into pure formaldehyde. They are used in chemistry as a source of pure H_2CO. High molecular weight polymers (a few hundreds to a few thousands monomer units) are extensively used in the plastics industry for their remarkable mechanical properties. POM could have had a key role in prebiotic chemistry as a source of concentrated formaldehyde for the ▶ formose reaction.

Overview

The presence of polyoxymethylene in comets has often been proposed to interpret various puzzling observations in their comae, although it has not been directly detected yet. The presence of polyoxymethylene in the interstellar medium has been discussed since the middle of the 1970s, but no clear observational evidence of its presence has ever been reported, either because it is not synthesized in such environments, or because its detection is compromised by the presence of silicates, the infrared signatures of which are similar to those of POM. In 1987, its detection was reported in the comet 1P/Halley by mass spectrometry. However, a few years later, it was demonstrated that the mass spectral characteristics attributed to POM could be also the signature of a complex mixture of organic compounds. This does not rule out the presence of POM, but makes its detection ambiguous. In the early twenty-first century it was demonstrated that the distribution of formaldehyde in the comae of comets 1P/Halley and C/1995 O1 (Hale Bopp), which could not be explained by a direct production of formaldehyde from the nucleus, could be explained by the presence of a few mass percent of POM in the nucleus of the comet, ejected on grains in the coma, and then slowly degraded into gaseous formaldehyde by photo and thermal degradation processes. POM would then be the parent compound of the so-called distributed source of formaldehyde in comets. Though this is not a direct detection, this demonstration strengthens the probability of the presence of this polymer in some comets, in the form of relatively small polymeric units similar to laboratory paraformaldehyde. This idea is backed by laboratory experiments showing that POM can be synthesized in cometary ice analogs under certain conditions.

The Rosetta mission's 2014 rendezvous with the comet Churyumov-Gerasimenko will provide an excellent opportunity to detect for the first

time this molecule using the satellite's powerful analytical capabilities. If POM is present, it could have played an important role in the synthesis of sugars on the primitive Earth bombarded by comets, being a source of concentrated formaldehyde for the formose reaction.

See Also

- ▶ Comet
- ▶ Formaldehyde
- ▶ Formose Reaction
- ▶ Rosetta Spacecraft

References and Further Reading

Cottin H, Bénilan Y, Gazeau M-C, Raulin F (2004) Origin of cometary extended sources from degradation of refractory organics on grains: polyoxymethylene as formaldehyde parent molecule. Icarus 167:397–416

Fray N, Bénilan Y, Biver N, Bockelée-Morvan D, Cottin H, Crovisier J, Gazeau M-C (2006) Heliocentric evolution of the degradation of polyoxylmethylene. Application to the origin of the formaldehyde (H2CO) extended source in comet C/1995 O1 (Hale-Bopp). Icarus 184:239–254

Huebner WF (1987) First polymer in space identified in comet Halley. Science 237:628–630

Schutte WA, Allamandola LJ, Sandford SA (1993) An experimental study of the organic molecules produced in cometary and interstellar ice analogs by thermal formaldehyde reactions. Icarus 104:118–137

Walker JF (1964) Formaldehyde. Reinhold, New York

Polypeptide

Shin Miyakawa
Ribomic Inc., Minato-ku, Tokyo, Japan

Definition

A polypeptide is a ▶ polymer formed by the covalent bonding of a certain number of amino acids. The exact lengths for peptides, oligopeptides, polypeptides, and ▶ proteins are not clearly defined, however: oligopeptides < polypeptides < proteins. Most naturally occurring polypeptides are composed of the 20 proteinogenic L-amino acids, although many microbial polypeptides contain unusual non-coded amino acids, such as ▶ sarcosine, β-amino acids, and D-amino acids. Some examples of biological peptides are calcitonin (32 amino acid long) and adrenocorticotropic hormone (39 amino acid long).

See Also

- ▶ Amino Acid
- ▶ Covalent Bonds
- ▶ D-Amino Acids
- ▶ L-Amino Acids
- ▶ Oligopeptide
- ▶ Polymer
- ▶ Protein
- ▶ Sarcosine

Polyribonucleotide

- ▶ Nucleic Acids

Polysaccharide

Shin Miyakawa
Ribomic Inc., Minato-ku, Tokyo, Japan

Definition

A polysaccharide is a polymeric ▶ carbohydrate composed of repeating ▶ monosaccharide or disaccharide units. Some of them contain uronic acids or ester sulfates. Examples are starches, cellulose, and heparin. Polysaccharides are constituents of plant and bacterial cell walls.

See Also

- ▶ Carbohydrate
- ▶ Monosaccharide

POM

► Polyoxymethylene

Population Genome

► Metagenome

Porphyrin

Henderson James (Jim) Cleaves II
Earth–Life Science Institute (ELSI), Tokyo Institute of Technology, Meguro–ku, Tokyo, Japan
Institute for Advanced Study, Princeton, NJ, USA
Blue Marble Space Institute of Science, Washington, DC, USA
Center for Chemical Evolution, Georgia Institute of Technology, Atlanta, GA, USA

Definition

Porphyrins are heterocyclic organic macrocycles composed of four modified pyrrole rings connected by their α-carbon atoms via methine [-CH=] linkages. Porphyrins are aromatic and thus obey Hückel's 4n + 2 π electron rule. Porphyrins are highly conjugated and have very intense absorption in the visible region and may be deeply colored. The name porphyrin derives from the Greek word for purple. Porphyrins are the conjugate acids of ligands that form complexes by binding metal ions, which are usually in the +2 or +3 oxidation state. Some porphyrins, such as ► heme, coordinate iron; other porphyrins chelate cobalt, magnesium, manganese, or nickel. Porphyrin-like compounds have been reported in meteorites, and a prebiotic synthesis has been proposed starting from pyrroles and aldehydes. Acidic conditions are required for this synthesis.

History

F. M. Johnson proposed in the 1970s that the porphyrins were the carriers of the ► diffuse interstellar bands. This proposal has not been supported by subsequent observations, although large organic molecules remain prime candidates for the still-unidentified carriers of these absorption features in stellar spectra.

See Also

► Aromatic Hydrocarbon
► Chlorophylls
► Diffuse Interstellar Bands
► Heme

Porpoise Cove Greenstone Belt

► Nuvvuagittuq (Porpoise Cove) Greenstone Belt

Positional Astronomy

► Astrometry

Postimpact Plume

Henderson James (Jim) Cleaves II[1,2,3,4] and Nicholas Arndt[5]
[1]Earth–Life Science Institute (ELSI), Tokyo Institute of Technology, Meguro–ku, Tokyo, Japan
[2]Institute for Advanced Study, Princeton, NJ, USA
[3]Blue Marble Space Institute of Science, Washington, DC, USA
[4]Center for Chemical Evolution, Georgia Institute of Technology, Atlanta, GA, USA
[5]ISTerre, Université Grenoble Alpes, France

A postimpact plume is the cloud of gas and fine debris ejected by the impacts of ► comets and

► meteorites on the surfaces or atmospheres of planetary bodies. One example is the plume released by impact of fragments of the comet Shoemaker-Levy on Jupiter; another is that produced by the impact of an artificial satellite and booster rocket on the moon. Spectral analysis of plumes provides information about the composition at the surface of the target and of the impacter. Such plumes could also be responsible for significant atmospheric chemical synthesis during the early formation of planets.

See Also

► Comet
► Meteorites

Power-Law Networks

► Scale-Free Networks

Poynting-Robertson Drag

William M. Irvine
University of Massachusetts, Amherst, MA, USA

Definition

A particle in orbit around a star absorbs stellar radiation and, assuming that it is rapidly rotating and hence has an isothermal surface, it reradiates energy isotropically in the particle's rest frame. Consequently, in the star's rest frame the particle radiates preferentially in the direction of its motion, so that it loses momentum, energy, and angular momentum, and thus spirals inward toward the star. This effect, the predominant perturbation on centimeter-sized particles in otherwise ► Keplerian orbits around a host star such as the Sun, is called Poynting-Robertson drag.

History

John Henry Poynting gave a classical physics description of this effect in 1903. In 1937, the more complete relativistic description was published by Howard Percy Robertson.

See Also

► Keplerian Orbits

References and Further Reading

Robertson HP (1937) Dynamical effects of radiation in the solar system. Mon Not R Astron Soc 97:423–438

P-P Chains

Nikos Prantzos
Institut d'Astrophysique de Paris, Paris, France

Definition

The p-p chain is the series of nuclear reactions converting four protons to one ^{4}He nucleus and releasing an energy of about 6.6 MeV/nucleon or 5×10^{18} erg/gr. This provides the main source of energy for Main sequence ► stars of less than 1.3 M. while in more massive stars the ► CNO cycle dominates. The first reaction of the series ($p + p \rightarrow D + e^+ + \nu_e + 0.42$ MeV) involves a slow, weak interaction (the conversion of a proton into a neutron), which is responsible for the long lifetimes (>10 Gyr) of the Sun and other low mass stars.

See Also

► CNO Cycle
► Nuclear Reaction
► Star

pppA

► ATP

Prasad-Tarafdar Mechanism

Steven B. Charnley
Solar System Exploration Division, Code 691, Astrochemistry Laboratory, NASA Goddard Space Flight Center, Greenbelt, MD, USA

Definition

The gas phase chemistry inside dark ► molecular clouds is driven by cosmic ray and ultraviolet ionization of atomic and molecular constituents. External UV radiation is largely blocked by dust grains, but a flux of UV photons is derived from the de-excitation of H_2 molecules following the impact of cosmic-ray-produced electrons. This is called the Prasad-Tarafdar mechanism.

History

First quantified by Prasad and Tarafdar (1983).

See Also

► Interstellar Chemical Processes
► Interstellar Dust
► Ion-Neutral Reaction
► Molecular Cloud

References and Further Reading

Prasad SS, Tarafdar SP (1983) UV radiation field inside dense clouds – its possible existence and chemical implications. Astrophys J 267:603–609

Prebiotic Chemistry

Henderson James (Jim) Cleaves II
Earth–Life Science Institute (ELSI), Tokyo Institute of Technology, Meguro–ku, Tokyo, Japan
Institute for Advanced Study, Princeton, NJ, USA
Blue Marble Space Institute of Science, Washington, DC, USA
Center for Chemical Evolution, Georgia Institute of Technology, Atlanta, GA, USA

Synonyms

Chemical evolution

Definition

Prebiotic chemistry is the study of the abiotic synthesis of organic compounds which may have been necessary for the origin of life. Although many syntheses which are now considered to be likely prebiotic processes, such as the Strecker synthesis, were demonstrated in the nineteenth century, few experiments were conducted with the express intent of demonstrating how organic compounds could have formed in primitive environments until the 1950s, beginning with the work of Calvin and coworkers, but more notably by Stanley Miller. This remains an ongoing area of investigation.

See Also

► Abiogenesis
► Evolution, Chemical

Prebiotic Photosynthesis

► Abiotic Photosynthesis

Prebiotic Soup

► Primordial Soup

Prebiotic Soup Hypothesis

► Heterotrophic Hypothesis

Precambrian

Nicholas Arndt
ISTerre, Université Grenoble Alpes, France

Definition

The *Precambrian* is the informal name given to the first part of Earth's history before the Cambrian Period of the Standard Global Chronostratigraphic Scale. It includes the (informal) ► Hadean eon, and the formal Archean and Proterozoic eons. It spans ca. 4 billion years, or 90 % of the lifespan or our planet. The Precambrian began with the formation of the Earth at about 4.56 Ga; it ended with the first appearance of a trace fossil (*Phycodes pedum*) at about 543 Ma ago, shortly after the proliferation of hard-shelled fossilizable organisms. The Precambrian was marked by a series of major events – the formation of the Moon and the ► Late Heavy Bombardment, the filling of the ocean basins, the emergence of ► life, the start of plate tectonics and growth of the ► continents, the ► great oxygenation event, and the ► "Snowball" Earth glaciations.

See Also

► Archaea
► Archean Eon
► Earth's Atmosphere, Origin and Evolution of
► Earth, Formation and Early Evolution
► Great Oxygenation Event
► Hadean
► Ocean, Chemical Evolution of
► Oceans, Origin of
► Proterozoic Eon
► Snowball Earth

Precambrian Oceans, Temperature of

François Robert
Laboratoire de Minéralogie et Cosmochimie du Muséum (LMCM), Muséum National d'Histoire Naturelle, UMR 7202 CNRS, Paris Cedex 05, France

Keywords

Ocean; Temperature; Stable isotopes; Oxygen isotopes; Silicon isotopes; Archean; Isotope paleothermometry

Synonyms

Ocean

Definition

The most ancient traces of life dated from about 3.8 Ga. At that time, Earth's surface was no longer the magma ocean that solidified 4.3 Ga ago or earlier. The primitive atmosphere inherited from the presolar nebula had disappeared, being replaced by a secondary atmosphere derived in part from the outgassing of the mantle and in part brought to the surface by extraterrestrial impactors and micrometeorites. This atmosphere was dominated not only by N_2 but also by several greenhouse gases such as carbon dioxide, methane, and water vapor. The

extent of surfaces covered by the oceans is unknown, but it can be postulated that – since the continents had not yet formed – the absence of the present-day bimodal distribution of elevations on Earth caused water to cover most of the surface of the Archean Earth. Undoubtedly, sedimentary rocks existed on Earth since at least 3.5 Ga ago as shown by unambiguous sedimentary structures recorded from rocks in South Africa and Greenland. The temperature of the first oceans, however, has always been a subject of debate.

Overview

Cherts: Surviving Witnesses of Early Oceans

In the early 1950s, geochemists showed that the isotopic compositions of sedimentary rocks could be used to reconstruct the temperature of the oceans provided (1) the isotopic composition of seawater from which these rocks precipitated was known and (2) the geological evolution of these rocks had not altered their pristine isotopic compositions. These two points are key issues in reconstructing paleotemperatures in all types of environments and samples. Siliceous sediments (▶ chert) are common in the Precambrian. Since microplankton (e.g., diatoms) able to fix soluble silica for building their skeleta did not exist in the Precambrian, it appears plausible that silica precipitated in Precambrian oceans in the form of amorphous silica deposited at the surface of the sediments. Today, this abiotic precipitation still exists in some rare terrestrial environments.

During burial of the marine sediments and subsequent diagenesis, the increase in pressure and temperature caused the progressive elimination of connate water along with mineralogical transformations of the silica. These transformations always involve the dissolution and reprecipitation of preexisting silica crystals. At the top of the sedimentary column, the first form of deposited silica is amorphous opal that is progressively transformed to microcrystalline silica ("opal-CT"), then to chalcedony and fibrous quartz. These transformations take place in situ, i.e., with almost no migration of silica; they are caused by the large amount of liquid water trapped in the rocks and that is progressively expelled during the compaction of the sediment (e.g., Knauth 1992, 1994). We shall see below that this diagenetic evolution has important consequences on the significance of the temperature recorded by silica.

Compaction yields a rock exceptionally resistant to weathering in which the diffusion of water is negligible. The cryptocrystalline nature of chert, combined with its average ability to resist weathering, recrystallization, and metamorphism, has made it an ideal rock for the preservation of indigenous geochemical tracers such as isotopic compositions or the chemical fossils of early life (e.g., Hayes et al. 1983; Beaumont and Robert 1999). During metamorphism, fluids may nevertheless circulate along cracks or veins that are still clearly visible at the spatial resolution of tens of micrometers. However, the spatial isotopic and chemical exchange between the matrix and these veins is restricted to a few hundred microns. Unless a chert is extensively crosscut by fluids during metamorphic events, their pristine geochemical compositions are preserved in their nanocrystalline silica matrix since deposition and crystallization. In this respect, cherts can be regarded as the best-preserved sedimentary rocks on Earth.

Early studies reported oxygen isotopic compositions of cherts with the aim of reconstructing the temperature of the Archean oceans (e.g., Knauth and Epstein 1976; Knauth and Lowe 1978).

Measuring the Temperature of the Early Oceans

The oxygen isotopic composition of cherts shows a systematic decrease with geological time: the older the sample, the lower the isotope ratio (e.g., Knauth and Lowe 1978, 2003). Assuming that the isotopic composition of seawater did not change with time, this trend was interpreted as resulting from the progressive cooling of the oceans since 3.5 Ga. The partition of oxygen isotopes between water and silica was determined in the laboratory, and accordingly, a temperature of up to 80 °C was derived for the Archean oceans (Knauth and

Lowe 1978). More quantitatively, there is 1.6 % more ^{18}O relative to ^{16}O at 20 °C than at 80 °C. The routine precision on the isotopic proportion being ±0.02 %, such a difference is easily detectable by modern isotope mass spectrometers. Precambrian cherts older than two billion years have oxygen isotopic compositions corresponding to crystallization temperatures higher than 40 °C. In contrast, Phanerozoic cherts have an isotopic composition corresponding to markedly cooler temperatures. It was thus concluded that the Precambrian oceans were hot (Knauth and Lowe 1978, 2003).

This interpretation has been challenged. First, it was argued that the isotopic composition of oxygen in seawater from which these rocks precipitated has changed with time (Perry 1967) and therefore that the isotopic trend observed as a function of time reflects this evolution of the ocean but not its temperature (Kasting et al. 2006). The progressive reset in ^{18}O would have taken place during the interaction of seawater with the mantle via the intense hydrothermal circulation at ▶ mid-ocean ridges (Kasting et al. 2006). The half-life for recycling the entire oceans through these ridges is less than ten million years, and oxygen isotopes should be quickly equilibrated with the mantle with respect to the three billion years of ^{18}O evolution observed in cherts. However, no evidence of such change appears in the geological record.

Several studies have shown that Precambrian pillow lavas – i.e., volcanic lavas cooled rapidly in contact with seawater – did not show any specific isotopic compositions at their interface with seawater compared with their modern counterparts. In addition, in some cases, the phosphates contained in cherts have provided an independent estimate of the seawater isotopic composition that appears constant through geological times. Although a few theoretical models have reopened the issue of a possible drift of ^{18}O with time (Kasting et al. 2006), the general consensus is that the seawater isotopic composition remained constant within reasonable uncertainties, corresponding to a precision of ±15 °C.

The second criticism of the thermometric interpretation deals with the problem of the preservation of the chert isotopic compositions, by arguing that the older the cherts, the more disturbed are their compositions. This second aspect is more difficult to circumvent on the basis of oxygen isotopes and the petrology of cherts. Silicon isotopes shed new light on this issue.

Measuring the Silicon Isotope Composition of the Early Oceans

Based on the analyses of more than 100 chert samples covering the whole Precambrian period, it was shown that silicon and oxygen isotopic compositions exhibit some covariation (Robert and Chaussidon 2006), a priori unexpected since silicon isotopes are – unlike oxygen – insensitive to temperature. The alteration processes for these two chemical elements – through which isotopic resets may take place – are completely decoupled. Indeed, during alteration, the carrier of silicon is the dissolved silica whose concentration rarely exceeds 200 ppm, while the carrier of oxygen is the water itself. In addition, once under the form of silica, the isotopic exchange of silicon could occur only in solution via the dissolution – reprecipitation of silica. Consequently, in order for the relation between the isotopic compositions of silicon and oxygen to be maintained, secondary effects postdating the chert formation must be limited. Some cherts, however, clearly show late disturbance in their oxygen isotopes with no counterpart for silicon.

These silicon and oxygen isotopic covariations are well accounted for by the solubility of silica in the oceans and hence are ultimately related to seawater temperature. The results of such a model are reported in Fig. 1 as variations in oceanic temperatures between 3.5 and 0.5 billion years. For samples younger than 0.5 billion years (arrow 1 on the Fig. 1), the silicon and oxygen isotopic covariation disappears, which indicates that silicon isotopes stop recording oceanic temperatures. This is attributed to the appearance of silica fixators in the oceans – siliceous plankton – that have maintained so far silica under saturation. In other terms, during the Phanerozoic, the concentration in silica dissolved in the ocean was no longer dictated by the

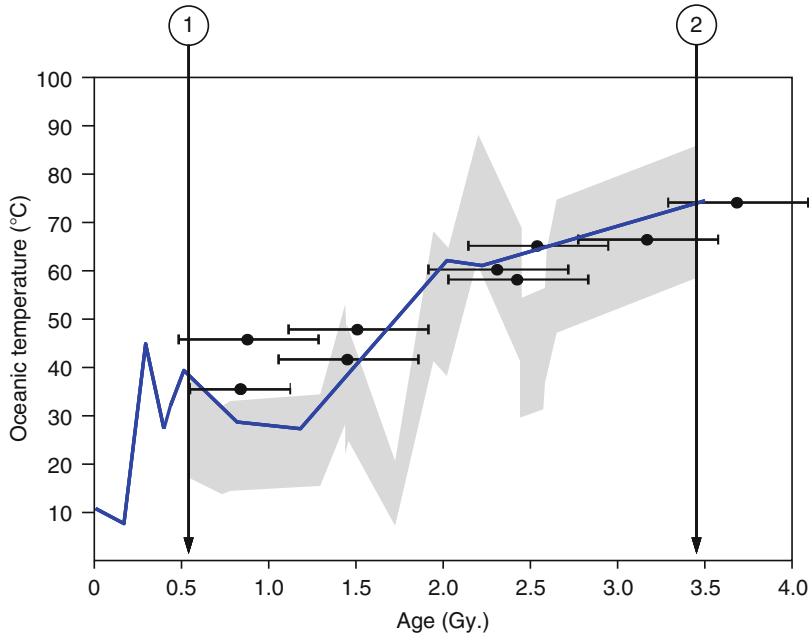

Precambrian Oceans, Temperature of, Fig. 1 The temperature of the oceans is reconstructed from three independent proxies: (1) the solid line stands for oxygen isotopes (After Knauth and Lowe 2003) (2) the gray area stands for silicon isotopes (After Robert and Chaussidon 2006) and (3) the data points with error bars stands for the elongation factors of a selection of proteins in microorganisms (After Gaucher et al. 2008). *Arrows* 1 and 2 designate (1) the emergence of silica-fixing organisms in oceans and (2) the oldest siliceous marine sediments found on Earth, respectively. Time is in Ga

temperature but by the metabolic activity of the plankton (De la Rocha et al. 1997). The oldest preserved cherts on Earth (dated at 3.5 Ga; cf. 2 on Fig. 1) exhibit the lowest silicon and oxygen isotope ratios, corresponding to the highest oceanic temperatures.

Robustness and Limits of the Secular Oceanic Temperature Evolution Model

Assuming that the temperature of crystallization of silica is registered by cherts with limited postdepositional alteration, the seawater thermometric variations account for the covariations in silicon and oxygen isotopes. Nevertheless, the exact significance of this temperature remains an open issue. Recent studies have demonstrated that isotopic compositions are highly heterogeneous at micrometric scale. Such ranges in oxygen isotopes reflect the progressive change in temperature during the sedimentary burial while the silica is successively dissolved and reprecipitated. Consequently, a correct thermometric interpretation of the chert oxygen isotopic compositions requires an assessment of the extent of diagenetic alteration. At present, such a detailed analysis has been performed for only one geological location on Earth; although the newly calculated seawater temperatures are 10–15 °C lower compared to the temperatures reported in Fig. 1, such an analysis confirms the high oceanic temperatures of the past.

Interestingly, this model was independently supported by biological studies on proteins in which the elongation factors can be scaled to estimate the age of the last mutation responsible for this elongation (Gaucher et al. 2008). The timescale of resurrected proteins provides a palaeotemperature proxy for the environments that hosted life from 3.5 to 0.5 billion years ago. The thermostability of several phylogenetically dispersed ancestral elongation factors suggests that these environments cooled progressively

during the last 3.5 billion years. It seems that ancient life has continually adapted to changes in environmental temperatures throughout its evolutionary history. The corresponding variations in temperature versus time are reported in Fig. 1 (data points with error bars) for comparison with isotopic temperatures. The resemblances in the trends are quite compelling.

From all these observations, the suggestion that early Precambrian oceans were several tens of degrees warmer than the modern ocean has definitively gained some acceptance.

See Also

- ▶ Chert
- ▶ Earth, Formation and Early Evolution
- ▶ Ocean, Chemical Evolution of
- ▶ Oxygen Isotopes

References and Further Reading

Beaumont V, Robert F (1999) Nitrogen isotope ratios of kerogens in Precambrian cherts: a record of the evolution of atmosphere chemistry? Precambrian Res 96:63–82

De La Rocha CL, Brzezinski MA, DeNiro M (1997) Fractionation of silicon isotopes by marine diatoms during biogenic silica formation. Geochim Cosmochim Acta 61:5051–5056

Gaucher EA, Govindarajan S, Ganesh OK (2008) Palaeotemperature trend for Precambrian life inferred from resurrected proteins. Nature 451(7179):704–707

Hayes JM, Kaplan IR, Wedeking KW (1983) Precambrian organic geochemistries, preservation of the record. In: Schopf WJ (ed) Earth's earliest biosphere. Cambridge University Press, Cambridge, pp 92–134

Kasting J, Howard M, Wallmann K, Veizer J, Shields G, Jaffres J (2006) Paleoclimates, ocean depth, and the oxygen isotopic composition of seawater. Earth Planet Sci Lett 252:82–93

Knauth PL (1992) Origin and diagenesis of cherts: an isotopic perspective. In: Clauer N, Chaudhuri S (eds) Isotopic signatures and sedimentary records, vol 43, Lecture notes in earth sciences, pp 123–152

Knauth PL (1994) Petrogenesis of chert. Rev Mineral Geochem 29(1):233–258

Knauth LP, Epstein S (1976) Hydrogen and oxygen isotope ratios in nodular and bedded cherts. Geochim Cosmochim Acta 40:1095–1108

Knauth LP, Lowe DR (1978) Oxygen isotope geochemistry of cherts from the Onverwatch Group (3.4 billion years), Transvaal Group, South Africa, with implications for secular variations in the isotopic composition of cherts. J Geol 41:209–222

Knauth LP, Lowe DR (2003) High Archean climatic temperature inferred from oxygen isotope geochemistry of cherts in the 3.5 Ga Swaziland Supergroup, South Africa. GSA Bull 115:566–580

Perry EC Jr (1967) The oxygen isotopic chemistry of ancient cherts. Earth Planet Sci Lett 3:62–66

Robert F, Chaussidon M (2006) A palaeotemperature curve for the Precambrian oceans based on silicon isotopes in cherts. Nature 443:969–972

Precession

Daniel Rouan
LESIA, Observatoire Paris-Site de Meudon, Meudon, France

Definition

Precession is the change in the orientation of the rotational axis of an astronomical body, such as a star or a planet, under the gravitational forces due to one or several nearby massive bodies. The change is slow and continuous and the axis, like in a wobbling top, describes a cone.

Earth's ▶ precession of the equinoxes is one of the best-studied effects of this kind: it results from the combined action of the Sun and the Moon on the equatorial bulge of the Earth, the bulge itself being created by the centrifugal force induced by the rotation. The Earth ▶ polar axis traces a cone of half-angle 23.4° in about 26,000 years.

Exoplanets as well are capable of precession, and it is not unlikely that the effect could be observed in some particular cases.

See Also

- ▶ Polar Axis
- ▶ Rotation Planet
- ▶ Rotational Velocity

Precursor

Kensei Kobayashi
Yokohama National University, Tokiwadai, Hodogaya-ku, Yokohama, Japan

Synonyms

Parent molecule (ion, species)

Definition

When a compound A gives rise to another compound B after some simple chemical reaction, A is called a precursor of B. For example, aminoacetonitrile is a precursor of glycine since hydrolysis of aminoacetonitrile gives glycine. This term is also used in astronomy (e.g., chemical species found in cometary nuclei are precursors of the species in cometary comae) and in biology (e.g., metabolic pathways).

See Also

► Amino Acid Precursors
► Parent Molecule, Comet

Predissociation

Stefanie N. Milam
Astrochemistry Laboratory, NASA Goddard Space Flight Center, Greenbelt, MD, USA

Definition

Predissociation is the break-up of a molecule in an excited state without the emission of radiation. Predissociation occurs when there is a radiationless transition from the excited energy level (electronic, vibrational, or rotational) to an overlapping dissociation continuum.

See Also

► Spectroscopy

Pre-main-sequence Star

Steven W. Stahler
Department of Astronomy, University of California, Berkeley, CA, USA

Keywords

Protostar; Star formation

Definition

A young star, which has reached its final mass by accreting material from its surrounding ► molecular cloud, but which is not yet fusing hydrogen into helium at its center, is called a pre-main-sequence star. Such a star is slowly contracting, and is actually larger and more luminous than a main-sequence (hydrogen fusing) star of the same mass. The relatively high luminosity stems from the conversion of gravitational potential energy during contraction. Our Sun spent 30 million years in this phase. Current pre-main-sequence stars of two solar masses and below are known observationally as ► T Tauri stars, while more massive ones are Herbig Ae/Be stars. Even younger objects, called protostars, are optically invisible and still gathering mass from their surrounding molecular clouds.

See Also

- ▶ Birthline
- ▶ Molecular Cloud
- ▶ T Association
- ▶ T Tauri Star

Pre-planetary Nebulae

- ▶ Protoplanetary Nebula

Primary Atmosphere

- ▶ Atmosphere, Primitive Envelope

Primary Eclipse

- ▶ Eclipse

Primary Kingdom

- ▶ Domain (Taxonomy)

Primary Producer

- ▶ Autotroph

Primary Production

- ▶ Autotrophy

Primer

Juli Peretó
Institut Cavanilles de Biodiversitat i Biologia Evolutiva, Universitat de València, València, Spain

Definition

Primer is a short oligonucleotide allowing the initiation of replication by a DNA polymerase. In vivo, usually the primer is a short RNA strand synthesized on the DNA strand and near the initiation site of replication. In vitro, primers are used in the PCR used for DNA amplification (or cloning).

See Also

- ▶ Amplification (Genetics)
- ▶ DNA
- ▶ Polymerase Chain Reaction
- ▶ Replication (Genetics)
- ▶ RNA

Primitive Atmosphere

- ▶ Atmosphere, Primitive Envelope

Primitive Broth

- ▶ Primordial Soup

Primitive Mantle Composition

- ▶ Bulk Silicate Earth

Primordial Heat

Doris Breuer
German Aerospace Center (DLR), Institute of Planetary Research, Berlin, Germany

Definition

Primordial heat is the internal heat energy accumulated by dissipation in a ▶ planet during its first few million years of evolution. The main contributions to the primordial heat are accretional energy – the energy deposited by infalling ▶ planetesimals – and ▶ differentiation energy. The latter is mainly released by core formation and is basically potential energy that is dissipated upon formation of a gravitationally stable layering of the planet. In addition to the primordial heat, the planet's internal heat source is mainly provided by the radioactive decay of long-lived unstable isotopes such as ^{238}U, ^{235}U, ^{232}Th, and ^{40}K and by latent heat.

See Also

- ▶ Core, Planetary
- ▶ Differentiation, Planetary
- ▶ Planet
- ▶ Planet Formation
- ▶ Planetesimals
- ▶ Radioactive Heating

Primordial Nucleosynthesis

- ▶ Big Bang Nucleosynthesis

Primordial Soup

Antonio Lazcano
Facultad de Ciencias, UNAM, Mexico, DF, Mexico

Keywords

Abiotic organic synthesis; Oparin-Haldane; Origin of life; Primordial heterotrophs

Synonyms

Prebiotic soup; Primitive broth

Definition

The primordial soup is a generic term that describes the aqueous solution of organic compounds that accumulated in primitive water bodies of the early Earth as a result of endogenous abiotic syntheses and the extraterrestrial delivery by cometary and meteoritic collisions, and from which some have assumed that the first living systems evolved.

Overview

The term "primordial soup" and its synonyms are linked to the proposal of the heterotrophic theory of the origin of life, which was suggested independently in the 1920s by Alexander I. Oparin, John B. S. Haldane, and few others. Based on the simplicity and ubiquity of fermentative reactions, Oparin and Haldane proposed that the first organisms must have been heterotrophic bacteria that could not make their own food but obtained organic material present in the primitive milieu. In order to support his proposal, Oparin appealed not only to astronomical observations that had

shown that hydrocarbons and other organic material were present in meteorites and cometary nuclei but also to the nineteenth-century experimental syntheses of organic molecules by Wohler, Butlerow, and Mendeleyeev, among others (Lazcano 2010a).

Similar ideas were being developed independently at the same time by other researchers. Like Oparin, the British biochemist and geneticist John B. S. Haldane argued in 1929 that the origin of life had been preceded by the synthesis of organic compounds. Based on experiments by E. C. C. Baly, an English chemist who had reported the formation of amino acids and sugars as a result of the UV irradiation of a solution of CO_2 in water, Haldane suggested that the absence of oxygen in a CO_2-rich primitive atmosphere led to the synthesis of organic compounds and their accumulation in the primitive waters of the Earth, which he wrote had "the consistency of hot dilute soup." The discovery of phages led Haldane to argue that viruses represented an intermediate step in the transition from the prebiotic broth to the first heterotrophic cells (Farley 1977; Lazcano 2010a).

A Darwinian Warm Little Pond

In 1871, Charles Darwin mailed a letter to his close friend Joseph Dalton Hooker in which he mentioned Pasteur's work on the absence of spontaneous generation and added that "It is often said that all the conditions for the first production of a living organism are now present, which could ever have been present. But if (and oh what a big if) we could conceive, in some warm little pond with all sorts of ammonia and phosphoric salts, light, heat, electricity, and c. present, that a protein compound was chemically formed, ready to undergo still more complex changes, at the present day such matter would be instantly devoured, or absorbed, which would not have been the case before living creatures were formed."

However, the "hot dilute soup" concept formulated by Haldane developed independently of Darwin's warm little pond. During the first part of the twentieth century, most authors assumed, at least implicitly, that the origin of life had taken place in an aqueous environment. When Winslow Herschel discussed the consistency of colloids, which by then were assumed to explain many of the properties of protoplasm (Podolsky 1996), he wrote that "How many factors determine consistency is a matter of controversy, but the colloquial meaning of the word is well understood and may be illustrated by the description, from a recent novel, of 'Flanders mud after a thaw'. As the flow increased, the side of the trenches began to fall in; the earth thus mixed with the water thickened it to a consistency which might be liked to a very rich soup" (Herschel 1926).

There is nothing that suggests that Herschel, Haldane, or Oparin had read Darwin's remarks about the origin of life and the warm little pond. Darwin's letter was included by his son Francis as a footnote in the 3rd volume of his father's book *Life and Letters* published in 1887, but it was not until 1969 that Melvin Calvin published it in his book on chemical evolution (Calvin 1969), calling it to the attention of the origins-of-life community (Peretó et al. 2009). By then, the concept of a prebiotic broth and a heterotrophic origin of life, which had been developed by Oparin and Haldane within the framework of an evolutionary perspective, had gained considerable support from the development of a multidisciplinary research program on the emergence of the first living systems.

Defining the Soup

The proposal that life was the outcome of prebiotic chemistry and the evolution of precellular systems was further elaborated and refined by Oparin in a more extensive book that was published in Russian in 1936 and translated 2 years later into English (Oparin 1938). In his new book, Oparin suggested that the primitive Earth was a highly reducing milieu in which iron carbides of geological origin would react with steam to form ▶ hydrocarbons. Their

oxidation would yield alcohols, ketones, aldehydes, etc., that would then react with ▶ ammonia to form amines, amides, and ammonium salts. The resulting protein-like compounds and other molecules would form a hot dilute soup, in which they would aggregate to form colloidal systems such as coacervates, from which the first heterotrophic microbes evolved. Others, like John D. Bernal, argued that the compounds were concentrated on the surfaces of minerals like clays, where the higher density would favor their chemical interaction (Bernal 1944).

Experimental evidence in support of Oparin's proposal came first from Harold C. Urey's laboratory, at the University of Chicago, who had considered the origin of life in the context of his proposal of a highly reducing terrestrial atmosphere (Urey 1952). The first successful prebiotic amino acid synthesis was carried out with an electric discharge and a strongly reducing model atmosphere of CH_4, NH_3, H_2O, and H_2 (Miller 1953). The result of this experiment was a significant yield of a racemic mixture of amino acids, together with hydroxy acids, short aliphatic acids, and urea. One of the surprising results of this experiment was that the products were not a random mixture of organic compounds; rather, a relatively small number of compounds, most of which were of biochemical significance, were produced in substantial yield. The Miller-Urey experiment marked not only a new epoch in the study of the origin of life but also led to surprisingly rapid acceptance by the public of both the heterotrophic theory and the idea of a primitive soup (Bada and Lazcano 2003).

Was There a Primitive Soup?

Although it is generally agreed that free oxygen was absent from the primitive Earth, there is no agreement on the composition of the primitive atmosphere; opinions vary from strongly reducing ($CH_4 + NH_3 + H_2O$, or $CO_2 + H_2 + N_2 + H_2O$) to neutral ($CO_2 + N_2 + H_2O$). In general, nonreducing atmospheric models were favored by planetary scientists, while prebiotic chemists leant toward more reducing conditions, under which the abiotic syntheses of amino acids, purines, pyrimidines, and other compounds are very efficient. Prior to the recognition that organic compounds can be synthesized under the neutral conditions of a CO_2-rich atmosphere (Cleaves et al. 2008), the difficulties involved with the endogenous synthesis of amino acids and nucleobases have led to the development of alternatives.

In the early 1990s, Chyba and Sagan reanalyzed Oró's 1961 proposal on the role of cometary nuclei as sources of volatiles to the primitive Earth and, based on the chemical composition of carbonaceous meteorites, proposed that the exogenous delivery of organic matter by asteroids, comets, and interplanetary dust particles could have played a significant role in forming the primitive soup, by seeding the early Earth with the compounds necessary for the origin of life (Chyba and Sagan 1992). On the other hand, proponents of an autotrophic theory of the origin of life (Wächtershäuser 1988) have dismissed the role of prebiotic synthesis and accumulation of organic compounds. However, since the FeS/H_2S combination is a strong reducing agent that has been shown to reduce nitrate and acetylene, induce the formation of peptide bonds between amino acids activated with carbon monoxide and (Ni, Fe)S (Maden 1995; Huber and Wächtershäuser 1998), and catalyze the synthesis of acetic acid and pyruvic acid from CO under simulated hydrothermal conditions (Huber and Wächtershäuser 1997; Cody et al. 2000), the role of Fe/S minerals is also compatible with a more general, modified model of the primitive soup in which pyrite formation is recognized as an important source of electrons for the reduction of organic compounds (Bada and Lazcano 2002).

There has been no shortage of discussion about how the formation of the primitive soup took place. However, it is likely that no single mechanism can account for the wide range of organic compounds that may have accumulated on the primitive Earth and that the prebiotic soup was formed by contributions from endogenous syntheses in a reducing atmosphere, metal sulfide-mediated synthesis in deep-sea vents, and exogenous sources such as comets, meteorites, and interplanetary dust. This eclectic view does not beg the issue of the relative significance

of the different sources of organic compounds, but it simply recognizes the wide variety of potential sources of organic compounds, the raw material required for the emergence of life (Bada and Lazcano 2009; Lazcano 2010b).

The Prebiotic Broth: A Risky Metaphor?

Synonymous terms like "primitive soup," "primordial broth," or "Darwin's warm little pond" have led in some cases to major misunderstandings, including the simplistic image of a worldwide ocean, rich in self-replicating molecules and accompanied by all sorts of biochemical monomers. However, nowadays, it refers to parts of the prebiotic environment where the accumulation and interaction of the products of abiotic synthesis may have taken place, including oceanic sediments, intertidal zones, shallow ponds, membrane-bound systems, freshwater lakes, and lagoons undergoing wet-and-dry cycles. The soup may have been semifrozen, and glacial ponds where evaporation, eutectic separations, or other physicochemical mechanisms, such as the adherence of biochemical monomers to active surfaces, could have raised local concentrations and promoted polymerization (Bada and Lazcano 2009).

Given adequate expertise and experimental conditions, it is possible to synthesize almost any organic molecule. However, the fact that a number of molecular components of contemporary cells can be formed nonenzymatically in the laboratory does not necessarily mean that they were also essential for the origin of life or that they were available in the prebiotic environment. The primitive soup must have been a bewildering organic chemical wonderland, but it could not include all the compounds or molecular structures found today in even the seemingly most primitive prokaryotes. It is possible that some compounds, including perhaps RNA itself, may not have been synthesized prebiotically, so their occurrence in living systems may have been the result of early metabolic syntheses.

During the past few years, laboratory simulations of prebiotic synthesis have been developing models of specific detailed environments, including those that may have been provided by the surface of clays, small volcanic ponds, and liposomes. Our ideas on the prebiotic synthesis of organic compounds are based largely on experiments in model system, and the evidence suggests that the remarkable coincidence between the molecular constituents of living organisms and those synthesized in prebiotic experiments is too striking to be fortuitous. The robustness of this type of chemistry is supported by the occurrence of many of these biochemical compounds in the 4.5-billion-year-old Murchison carbonaceous chondrite and other carbon-rich meteorites, suggesting that similar synthesis took place on the primitive Earth (Miller and Lazcano 2002).

Conclusions

How the first life evolved is not known, but analysis of carbonaceous chondrites and the laboratory simulations of the primitive Earth suggest that prior to the emergence of the first living systems, the prebiotic environment was endowed with (1) a large suite of organic compounds of biochemical significance; (2) many organic and inorganic catalysts (such as ▶ cyanamide, metallic ions, sulfur-rich minerals and clays); (3) purines and pyrimidines, that is, the potential for template-dependent polymerization reactions; (4) membrane-forming compounds; and (5) the availability of many possible sources of carbon and nitrogen for primordial heterotrophs. Once life appeared and biosynthetic pathways developed, the reservoir of organic material present on the Earth then shifted from one initially characterized by compounds of abiotic origin to one made up entirely of biologically derived components (Lazcano 2010b).

The existence of different abiotic mechanisms by which biochemical monomers can be synthesized under plausible prebiotic conditions is well established. Of course, not all prebiotic pathways are equally efficient, but the wide range of experimental conditions under which organic compounds can be synthesized demonstrates that prebiotic syntheses of the building blocks of life are robust, that is, the abiotic reactions leading to them do not take place under a narrow range

defined by highly selective reaction conditions, but rather under a wide variety of experimental settings. Like other scientific metaphors, the term "primitive soup" is risky but useful and has become a part of popular lore. For all the uncertainties surrounding the emergence of life, it appears that the formation of the prebiotic soup is one of the most firmly established events that took place in the primitive Earth.

See Also

- ▶ Aldehyde
- ▶ Amide
- ▶ Amine
- ▶ Amino Acid
- ▶ Ammonia
- ▶ Asteroid
- ▶ Clay
- ▶ Comet
- ▶ Cyanamide
- ▶ Haldane's Conception of Origins of Life
- ▶ Heterotrophic Hypothesis
- ▶ Hydrocarbons
- ▶ Meteorites
- ▶ Miller, Stanley
- ▶ Oparin's Conception of Origins of Life
- ▶ Pyrite
- ▶ RNA World

References and Further Reading

Bada J, Lazcano A (2002) Some like it hot, but not biomolecules. Science 296:1982–1983

Bada JL, Lazcano A (2003) Prebiotic soup: revisiting the Miller experiment. Science 300:745–746

Bada JL, Lazcano A (2009) The origin of life. In: Ruse M, Travis J (eds) The harvard companion of evolution. Belknap/Harvard University Press, Cambridge, pp 49–79

Bernal JD (1944) The physical basis of life. Routledge and Kegan Paul, London

Calvin M (1969) Chemical evolution: molecular evolution towards the origin of living systems on the earth and elsewhere. Oxford University Press, New York

Chyba CF, Sagan C (1992) Endogenous production, exogenous delivery, and impact-shock synthesis or organic compounds, an inventory for the origin of life. Nature 355:125–132

Cleaves JH, Chalmers JH, Lazcano A, Miller SL, Bada JL (2008) Prebiotic organic synthesis in neutral planetary atmospheres. Orig Life Evol Biosph 38:105–155

Cody GD, Boctor NZ, Filley TR, Hazen RM, Scott JH, Sharma A, Yoder HS Jr (2000) Primordial carbonylated iron-sulfur compounds and the synthesis of pyruvate. Science 289:1337–1340

Darwin F (ed) (1887) The life and letters of Charles Darwin, including an autobiographical chapter, vol 3. Murray, London

Farley J (1977) The spontaneous generation controversy from descartes to oparin. John Hopkins University Press, Baltimore/London

Haldane JBS (1929) The origin of life. Rationalist Annu 148:3–10

Herschel W (1926) Consistency. In: Alexander J (ed) Colloid chemistry, vol 1, Theoretical and Applied. Chemical Catalog, New York, pp 727–738

Huber C, Wächtershäuser G (1997) Activated acetic acid by carbon fixation on, Fe, Ni, S under primordial conditions. Science 276:245–247

Huber C, Wächtershäuser G (1998) Peptides by activation of amino acids with CO on Ni, Fe, S surfaces and implications for the origin of life. Science 281:670–672

Lazcano A (2010a) Historical development of origins of life. In: Deamer DW, Szostak J (eds) Cold spring harbor perspectives in biology: the origins of life. Cold Spring Harbor Press, Cold Spring Harbor, pp 1–16

Lazcano A (2010b) The origin and early evolution of life: did it all start in Darwin's warm little pond? In: Bell MA, Futuyma DJ, Eanes WF, Levinton JS (eds) Evolution since Darwin: the first 150 years. Sinauer, Sunderland, pp 353–375

Maden BEH (1995) No soup for starters? Autotrophy and origins of metabolism. Trends Biochem Sci 20:337–341

Miller SL (1953) A production of amino acids under possible primitive Earth conditions. Science 117:528

Miller SL, Lazcano A (2002) Formation of the building blocks of life. In: Schopf JW (ed) Life's origin: the beginnings of biological evolution. California University Press, Berkeley, pp 78–112

Oparin AI (1924) Proiskhozhedenie Zhizni. Mosckovskii Rabochii, Moscow. Reprinted and translated in Bernal JD (1967) The origin of life. Weidenfeld and Nicolson, London

Oparin AI (1938) The origin of life. McMillan, New York

Peretó J, Bada JL, Lazcano A (2009) Charles Darwin and the origins of life. Orig Life Evol Biosph 39:395–406

Podolsky S (1996) The role of the virus in origin-of-life theorizing. J Hist Biol 29:79–126

Urey HC (1952) On the early chemical history of the earth and the origin of life. Proc Natl Acad Sci U S A 38:351–363

Wächtershäuser G (1988) Before enzymes and templates, theory of surface metabolism. Microbiol Rev 52:452–484

Prion

María Gasset
Consejo Superior de Investigaciones Científicas, Instituto Química-Física Rocasolano, Madrid, Spain

Keywords

Infectious agent; Protein aggregation; Protein conformation multiplicity; Protein-encoded infectivity; Protein-encoded inheritance; Strains

Definition

Prions are ▶ protein-based elements of infection and inheritance. Prions are made by alternate protein conformations that by acting as templates propagate their conformations to the precursor proteins. In general, this propagative state is an insoluble polymer, rich in tightly packed β-sheets and displaying amyloid staining features. This state is not structurally unique but polymorphic allowing strains. The protein undergoing prion conversion loses its normal function and acquires the ability to transform the precursor into its like. This protein conformational code provides physiological switches for fast environmental adaptation and underlies the spread of the mammalian neurodegenerative diseases known as transmissible spongiform encephalopathies.

History

The unique inactivation pattern displayed by the infectious agent causing scrapie reported by Alper et al. (1967) prompted Griffith (1967) to propose the "protein-only" hypothesis to explain a nucleic acid-free information flow. This hypothesis considered mechanisms by which a protein could display replicative properties, as a catalyzed conformation and/or aggregation change. On the basis of the purification of the infectious agent causing scrapie, Prusiner (1982) coined the terms prion and PrP to refer to the proteinaceous infectious particle and the component protein, respectively. Since then, PrP prion properties have been ascribed to a conformational change from a normal cellular form (PrP^{C}) to a propagative form (PrP^{Sc}) that causes disease by converting the membrane-bound cellular form into its like. Whereas PrP^{C} is soluble and easily degraded by proteinase K, PrP^{Sc} is rich in β-sheets and aggregates into fibrils after proteinase K digestion (Prusiner 1998). While the essentiality of PrP^{C} for the prion infectivity, the propagative nature of PrP^{Sc} conformation, and its multiplicity have been demonstrated, the infectivity synthesized with pure protein polymers still provokes controversy by virtue of its low efficiency or by the requirement of effectors (Deleault et al. 2007; Aguzzi and Calella 2009; Colby et al. 2010; Makarava et al. 2010). Based on genetic observations, Wickner (1994) generalized the prion concept. Since then, an increasing number of yeast and fungi proteins exhibiting prion behaviors have been described. In fact, most of the compelling evidences for the prion concept have been established using these models. Of them, the direct demonstration of the infectious activity of a pure protein in its prion form was provided by [Het-s] prion (Maddelein et al. 2002). Establishment of the cell-to-cell transmissibility of some cytosolic self-aggregating proteins involved in distinct human disorders may allow soon their qualification as prions.

Overview

Despite being always viewed under the danger of their action and their heretical composition, prions are simply alternate structural states of proteins that, while perpetuating and transmitting, permit a fast and sustainable functional switch in response to a trigger (Aguzzi and Calella 2009; Halfmann et al. 2010). In yeast, fungi, and mollusks, prions represent a beneficial biological tool for adaptation to

environmental changes. For mammalian prions, the trigger remains unknown and is largely related to disease.

Proteins undergoing prion formation are structurally unrelated. However, according to the polypeptide chain, they can be classified into two groups. A first group is formed by those proteins containing a domain, generally featured by a high proportion of Q/N, which is indispensable for the function but hosts the prion formation capacity. The second group, exemplified by PrP, accounts for those chains in which the residues responsible for the prion function are scattered along the sequence.

Prion formation involves a conformational change in the precursor protein, which enables its polymerization. The resulting polymer is generally maintained by tightly packed intermolecular β-sheets that confer the assembly a peculiar resistance to degradation. Also, the feasibility of alternative packing arrangements makes possible a polymorphism in the assembly, which underlines the *strain* phenomena (Wiltzius et al. 2009).

Replication of prions occurs through the template-conversion of the precursor protein into its like. This reaction is a complex process involving steps of molecular recognition under the control of the protein sequence. Such recognition dependency sustains the *species-barrier* dependency of its transmissibility.

In addition to the previous traits, self-perpetuating protein aggregates become prions when they exhibit tractable cell-to-cell *transmission*. In prions from low organisms, transmission is linked to cell division and therefore follows an inheritable pattern, whereas in mammals, prions must travel from one cell to another (Aguzzi and Rajendran 2009).

See Also

- ▶ Protein
- ▶ Proteins, Secondary Structure
- ▶ Proteins, Tertiary Structure

References and Further Reading

Aguzzi A, Calella AM (2009) Prions: protein aggregation and infectious diseases. Physiol Rev 89:1105–1152

Aguzzi A, Rajendran L (2009) The transcellular spread of cytosolic amyloids, prions, and prionoids. Neuron 64:783–790

Alper T, Cramp WA, Haig DA, Clarke MC (1967) Does the agent of scrapie replicate without nucleic acid? Nature 214:764–766

Colby DW, Wain R, Baskakov IV, Legname G, Palmer CG, Nguyen HO, Lemus A, Cohen FE, DeArmond SJ, Prusiner SB (2010) Protease-sensitive synthetic prions. PLoS Pathog 6:e1000736

Deleault NR, Harris BT, Rees JR, Supattapone S (2007) Formation of native prions from minimal components in vitro. Proc Natl Acad Sci U S A 104:9741–9746

Griffith JS (1967) Self-replication and scrapie. Nature 215:1043–1044

Halfmann R, Alberti S, Lindquist S (2010) Prions, protein homeostasis, and phenotypic diversity. Trends Cell Biol 20:125–133

Maddelein ML, Dos Reis S, Duvezin-Caubet S, Coulary-Salin B, Saupe SJ (2002) Amyloid aggregates of the HET-s prion protein are infectious. Proc Natl Acad Sci U S A 99:7402–7407

Makarava N, Kovacs GG, Bocharova O, Savtchenko R, Alexeeva I, Budka H, Rohwer RG, Baskakov IV (2010) Recombinant prion protein induces a new transmissible prion disease in wild-type animals. Acta Neuropathol 119:177–187

Prusiner SB (1982) Novel proteinaceous infectious particle causing scrapie. Science 216:136–144

Prusiner SB (1998) Prions. Proc Natl Acad Sci U S A 95:13363–13383

Wickner RB (1994) [URE3] as an altered URE2 protein: evidence for a prion analog in Saccharomyces cerevisiae. Science 264:566–569

Wiltzius JJ, Landau M, Nelson R, Sawaya MR, Apostol MI, Goldschmidt L, Soriaga AB, Cascio D, Rajashankar K, Eisenberg D (2009) Molecular mechanisms for protein-encoded inheritance. Nat Struct Mol Biol 16:973–978

Priscoan

- ▶ Hadean

Prismatic Sodium Carbonate

- ▶ Thermonatrite

p-RNA

Ramanarayanan Krishnamurthy, Eun-Kyong Kim and Tammy Campbell
Chemistry, The Scripps Research Institute, La Jolla, CA, USA

Keywords

Watson-Crick; Pentopyranosyl; Oligonucleotides; Nucleic acids; Homochiral; Heterochiral; Base-pairing

Synonyms

Pentopyranosyl-RNA; Pyranosyl-RNA; Ribopyranosyl nucleic acid

Definition

Pyranosyl-RNA ("p-RNA") is an ▶ oligonucleotide in which the ribose units exist in the pyranose form and are linked together repetitively by phosphodiester groups between the hydroxyl groups at positions C-2′ and C-4′ (Fig. 1).

History

The systematic experimental study of nucleic acid alternatives has played an important role in understanding the chemical etiology of the structure of nucleic acids as functioning biomolecules (Eschenmoser 1993b). In 1992, Eschenmoser conceived the structure of p-RNA in context of the study toward the chemical etiology of the natural nucleic acid structure (Eschenmoser 1993a). The existence of p-RNA was predicted through a comprehensive and systematic qualitative conformational analysis of all possible hexo- and pentopyranosyl oligonucleotide systems that could be derived from the products of the aldol reaction of glycolaldehyde phosphate with itself and with formaldehyde (Pitsch et al. 1994).

Overview

Pyranosyl-RNA is a constitutional ▶ isomer of RNA, composed of the very same building blocks as natural RNA. p-RNA contains the D-ribose building unit in the pyranosyl (six-membered ring) form with the phosphodiester bonds linking the C(4′) atom of one pyranosyl unit with the C (2′) atom of the neighboring pyranosyl unit. Among the four possible pentopyranosyl (ribo-, arabino-, lyxo-, and xylo-) oligonucleotides, ribopyranosyl nucleic acid (p-RNA) has been studied extensively with respect to its base-pairing properties, structure, and function (Pitsch et al. 1993, 1995; Eschenmoser 1993b, 1997, 1999, 2011; Krishnamurthy et al. 1996; Schlönvogt et al. 1996; Micura et al. 1997; Bolli et al. 1997a, b; Beier et al. 1999; Jungmann et al. 1999; Pitsch et al 2003).

p-RNA oligomers form duplexes that are more selective (Watson-Crick mode, antiparallel orientation of strands) and stronger than the corresponding natural (furanosyl) RNA and DNA oligomers; the Hoogsteen or reverse Hoogsteen pairing modes seem not to be accessible (Pitsch et al. 1995; Eschenmoser 1993b, 1997). Watson-Crick purine-pyrimidine base-pairing in p-RNA is highly enantioselective; p-RNA duplexes comprised of strands of identical chirality were observed to be the strongest among the various possible combinations (Krishnamurthy et al. 1996). In spite of having a less flexible pyranose-unit containing backbone, p-RNA is capable of adopting secondary structures with similar ease as RNA, such as hairpin structures, containing three bases in the loop (Micura et al. 1997).

The overall base-pairing and nonenzymatic replicative properties of p-RNA (and other hexo- and pentopyranosyl-NA) have been discussed in the context of nature's choice of RNA (DNA) as the molecular basis for a genetic

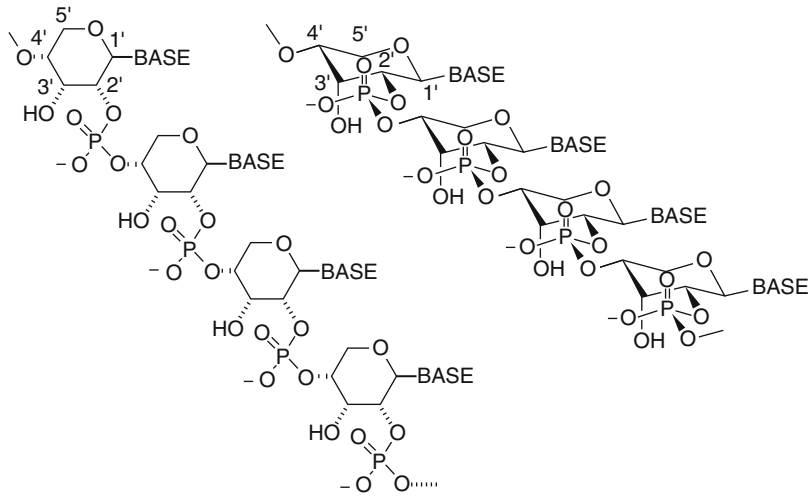

p-RNA, Fig. 1 A constitutional and an idealized conformational representation of pyranosyl-RNA (p-RNA); base = adenine, guanine, cytosine, uracil, thymine, as well as 2,4-diaminopurine, xanthine, iso-guanine, and iso-cytosine

system (Beier et al. 1999; Eschenmoser 1999). Two primary conclusions drawn from these studies are that (a) Watson-Crick base-pairing mode is not unique and specific to the double helix type of conformation characteristic of a ribofuranose system, but is widespread among potentially natural alternatives derived from the structural neighborhood of RNA, and (b) the selection of RNA (and DNA) seems not to be based on the criterion of maximizing base-pairing strength; rather, RNA and DNA seem to have optimal pairing capabilities with respect to achieving turnover in strand replication.

Basic Methodology

The basic methodology underlying the identification and investigation of p-RNA consisted of four parts:

(1) Identification of p-RNA: a qualitative conformational analysis of repetitive base-pairing arrangements of the four possible pentopyranosyl-NAs led to the selection of p-RNA as a candidate to be synthesized and further investigated.
(2) Synthesis of p-RNA: the required nucleoside building blocks of p-RNA were generated by synthetic organic chemistry, such as the reaction of a protected ribose with nucleobases by *Vorbrűggen* or *Hilbert-Johnson* nucleosidation, followed by synthetic manipulations to generate the phosphoramidites. The corresponding oligonucleotides were synthesized on a gene synthesizer using the phosphoramidites (automated solid-phase oligonucleotide synthesis) and isolated by ▶ HPLC techniques.
(3) Investigation of the physical and chemical properties of p-RNA: the base-pairing and structural properties were investigated by UV, CD, and NMR spectroscopy.
(4) Evaluation of the properties of p-RNA: the relevant base-pairing and structural properties of p-RNA were compared with those of natural RNA and DNA. The comparison of these properties and the capacity to replicate by (nonenzymatic) template-directed ligation were used to reason out why ribopyranose nucleic acid is probably not a biological functioning molecule in extant biology.

Key Research Findings

NMR investigations revealed that the p-RNA-(**CGAATTCG**) duplex adopts a quasi-linear (ladderlike) structure with a weak left-handed twist (Schlönvogt et al. 1996). There is a large inclination of the backbone relative to the base-pair axes. Such a marked inclination of the

backbone/base-pair-axes has a profound effect on the base-pairing properties of p-RNA such as (a) the highly sequence-dependent thermal stabilities, (b) the stronger and more selective base-pair formation, (c) the duplex stabilizing effect of the 2′-end dangling base, and (d) alternate or block sequences containing pyrimidine-purine arrangements forming more stable duplexes than the inverse series.

Remarkably, p-RNA undergoes extensive cross-pairing with oligonucleotides derived from the three other members of the (4′→2′)-pentopyranosyl family; extensive intersystem cross-pairing among the members was observed, in spite of the differences in the stereo-centers of the (4′→2′)-phosphodiester-linked oligonucleotides (Jungmann et al. 1999). However, no duplex formation was observed between the pentopyranosyl-derived oligonucleotides with RNA or DNA.

The distinctive chemical properties of p-RNA confer it with certain functional advantages when compared to the natural RNA and DNA oligomeric systems. For example, investigations of the (nonenzymatic) template-directed ligation of p-RNA sequences (via the 2′,3′-cyclophosphate activation) have demonstrated this process to be (a) very efficient (due to the absence of purine-purine self-pairing in Hoogsteen or reverse Hoogsteen mode), (b) highly regioselective (forming only the desired 4′→2′ linkage over the undesired 4′→3′, due to the large backbone/base-pair inclination. In contrast, the corresponding template-directed ligation of RNA forms exclusively the unnatural 5′→2′ linkage over the natural 5′→3′) (Bolli et al. 1997b), and (c) highly chiroselective (replacement of D-ribopyranosyl with L-ribopyranosyl nucleoside unit hampers the ligation reaction) (Bolli et al. 1997a, b). Hairpin-forming p-RNA sequences also act as templates for mediating the ligation reaction. However, product inhibition (as a consequence of high base-pairing strength) has impeded any prospects for catalytic "turnover." On the other hand, such strong base-pairing strength facilitates cooperative co-oligomerization of short hemi-self-complementary tetrameric sequences (activated as the 2′,3′-cyclophosphate) resulting in an efficient self-templating oligomerization process that leads to the formation of duplexes of higher oligomers (demonstrated up to 24-mers) starting from homochiral 4-mers (Pitsch et al. 2003).

Applications

In the field of biosensor technologies and molecular diagnostics, there have been a lot of efforts devoted toward developing methods for the detection and identification of target biological agents, e.g., nucleic acids. Typical methods for the analysis of DNA amplification products by PCR involve ▶ hybridization assays, such as DNA microarray, real-time PCR, and flow cytometry. p-RNA has been utilized for the development of methods and devices for immobilizing and detecting nucleic acid amplicons. Amplicons are comprised of a forward primer conjugated to a synthetic binding unit and a reverse primer conjugated to a detectable moiety that can hybridize to a complementary strand. This complementary strand serves as a synthetic capture unit localized at a predetermined location on the surface of the substrate. By binding the synthetic capture unit with the synthetic binding unit, the amplicon becomes immobilized under sufficient conditions, producing a complex in which the detectable moiety of the amplicon complex indicates the presence of the target nucleic acid in the sample. p-RNA can be incorporated into the synthetic binding and capture units due to its strong, selective, and reversible pairing properties (Huang et al. 2010).

DNA sequencing has also been useful for understanding the function of genes in human or other organisms and for applying many of the basic techniques of molecular biology by the control of genes. p-RNA molecules can be used as nucleic acid probes in sequencing by hybridization. The probes comprise predefined patterns of universal nucleotides (nucleic acid analogues including p-RNA) and designate nucleotides (canonical nucleic acids), the so-called gapped probes. In the process of sequencing, gapped probes allow each probe to operate in more than one way, requiring a smaller number of probes

than conventional probes composed entirely of natural nucleic acids. By the inclusion of p-RNA in the probes, efficient and rapid sequencing of longer nucleotide sequences can be realized compared to sequencing using traditional probes (Preparata et al. 2003).

Future Directions

p-RNA and other biomolecules, such as a peptides, proteins, or nucleic acids, conjugated through a covalent linkage may function as a sequence recognition unit since the conjugates contain two pairing systems which are orthogonal to one another. Specifically, coupling of the first oligonucleotide analog with the second oligonucleotide analog such as p-RNA may form antisense molecules capable of binding specifically to a target sequence of polynucleotides and also capable of activating a nuclease or catalyzing cleavage of the target polynucleotides.

Additionally, the inherent properties of p-RNA make it suitable for use in the field of nanotechnology, such as the production of novel supramolecular materials. For instance, p-RNA which contains a non-hydrogen-bonding tryptamine self-pair forms new supramolecular system exhibiting comparable stability to the natural pair due to strong interstrand stacking in the p-RNA duplex (Hamon et al. 1999). This model pairing system can be derivatized with a fluorescent probe without the necessity of additional labeling.

See Also

- Chirality
- Furanose
- Nucleic Acids
- Origin of Life
- RNA
- RNA World
- Watson-Crick Pairing

References and Further Reading

Beier F, Reck F, Wagner T, Krishnamurthy R, Eschenmoser A (1999) Chemical etiology of nucleic acid structure: comparing pentopyranosyl-(2′→4′) oligonucleotides with RNA. Science 283:699–703

Bolli M, Micura R, Eschenmoser A (1997a) Pyranosyl-RNA: chiroselective self-assembly of base sequences by ligative oligomerization of tetra nucleotide-2′,3′-cyclophosphates (with a commentary concerning the origin of biomolecular homochirality). Chem Biol 4:309–320

Bolli M, Micura R, Pitsch S, Eschenmoser A (1997b) Pyranosyl-RNA: further observations on replication. Helv Chim Acta 80:1901–1951

Eschenmoser A (1993a) Hexose nucleic acids. Pure Appl Chem 65:1179–1188, Lecture at the '18th IUPAC Symposium on the Chemistry of Natural Products', Strasbourg/F, August 1992

Eschenmoser A (1993b) Toward a chemical etiology of the natural nucleic acids' structure. In: Proc R. A. Welch Found, 37. Conf chem res 40 years of the DNA double Helix. R. A. Welch Foundation, Houston, p 201–235

Eschenmoser A (1997) Towards a chemical etiology of nucleic acid structure. Orig Life Evol Biosph 27:535–553

Eschenmoser A (1999) Chemical etiology of nucleic acid structure. Science 284:2118–2124

Eschenmoser A (2011) Etiology of potentially primordial biomolecular structures: from vitamin B12 to the nucleic acids and an inquiry into the chemistry of life's origin: a retrospective. Angew Chem Int Ed 50:12412–12472

Hamon C, Brandstetter T, Windhab N (1999) Pyranosyl-RNA supramolecules containing non-hydrogen bonding base-pairs. Synlett S1:940–944

Huang Y, Light J (II), Mather E, Weisburg W (2010) Methods for detecting nucleic acids in a sample. Patent No. US 2010/0167294 A1

Jungmann O, Wippo H, Stanek M, Huynh HK, Krishnamurthy R, Eschenmoser A (1999) Promiscuous Watson−Crick cross-pairing within the family of pentopyranosyl (4′→2′) oligonucleotides. Org Lett 1:1527–1530

Krishnamurthy R, Pitsch S, Minton M, Miculka C, Windhab N, Eschenmoser A (1996) Pyranosyl-RNA: base pairing between homochiral oligonucleotide strands of opposite sense of chirality. Angew Chem Int Ed 35:1537–1541

Micura R, Bolli M, Windhab N, Eschenmoser A (1997) Pyranosyl-RNA also forms hairpin structures. Angew Chem Int Ed 36:870–873

Pitsch S, Wendeborn S, Jaun B, Eschenmoser A (1993) Why pentose- and not hexose-nucleic acids? Pyranosyl-RNA ('p-RNA'). Helv Chim Acta 76:2161–2183

Pitsch S, Pombo-Villar E, Eschenmoser A (1994) Chemistry of alpha-aminonitriles. Formation of 2-oxoethyl

phosphates (glycolaldehyde phosphates) from rac-oxiranecarbonitrile and on (formal) constitutional relationships between 2-oxoethyl phosphates and oligo (hexo- and pentopyranosyl)nucleotide backbones. Helv Chim Acta 77:2251–2285
Pitsch S, Krishnamurthy R, Bolli M, Wendeborn S, Holzner A, Minton M, Lesueur C, Schlonvogt I, Jaun B, Eschenmoser A (1995) Pyranosyl-RNA ('p-RNA'): base-pairing selectivity and potential to replicate. Helv Chim Acta 78:1621–1635
Pitsch S, Wendeborn S, Krishnamurthy R, Holzner A, Minton M, Bolli M, Miculka C, Windhab N, Micura R, Stanek M, Jaun B, Eschenmoser A (2003) The β-D-ribopyranosyl-(4′→2′)-oligonucleotide system (pyranosyl-RNA): synthesis and resumé of base-pairing properties. Helv Chim Acta 86:4270–4363
Preparata F P, Upfal E, Oliver J S (2003) Systems and methods for sequencing by hybridization. Patent No. US 2003/0064382 A1
Schlönvogt I, Pitsch S, Lesueur C, Eschenmoser A (1996) Pyranosyl-RNA ('p-RNA'): NMR and molecular-dynamics study of the duplex formed by self-pairing of ribopyranosyl-(C-G-A-A-T-T-C-G). Helv Chim Acta 79:2316–2345

Pro

► Proline

Probing Lensing Anomalies Network

David W. Latham[1], B. Scott Gaudi[2] and Nader Haghighipour[3]
[1]Harvard-Smithsonian Center for Astrophysics, Cambridge, MA, USA
[2]Department of Astronomy, Ohio State University, Columbus, OH, USA
[3]Institute for Astronomy, University of Hawaii-Manoa, Honolulu, Hawaii, HI, USA

Synonyms

PLANET

Definition

The PLANET (Probing Lensing Anomalies NETwork) was a worldwide collaboration of astronomers that used telescopes spread throughout the Southern Hemisphere to follow up microlensing events discovered by other teams such as OGLE and MOA, in order to search for the short-lived signatures of exoplanets. In 2006, PLANET (along with the RoboNet, OGLE, and MOA collaborations) announced the discovery of the first cool ► super-Earth planet ► OGLE-2005-BLG-390Lb. The PLANET collaboration ended in 2007. In 2009, a new collaboration, μFUN-PLANET, was initiated.

See Also

► Exoplanets, Discovery
► Microlensing Observations in Astrophysics
► Microlensing Planets
► OGLE-2005-BLG-390Lb
► Optical Gravitational Lensing Experiment
► Super-Earths

Prokaryote

Ramon Rosselló-Móra
IMEDEA (CSIC-UIB), Esporles, Mallorca, Balearic Islands, Spain

Keywords

Archaea; Bacteria; Microorganism

Synonyms

Bacteria

Definition

Prokaryote (from Greek *pro* [before] and *karyon* [nucleus]) denotes organisms that lack a membrane-enclosed nucleus, as well as other ► organelles.

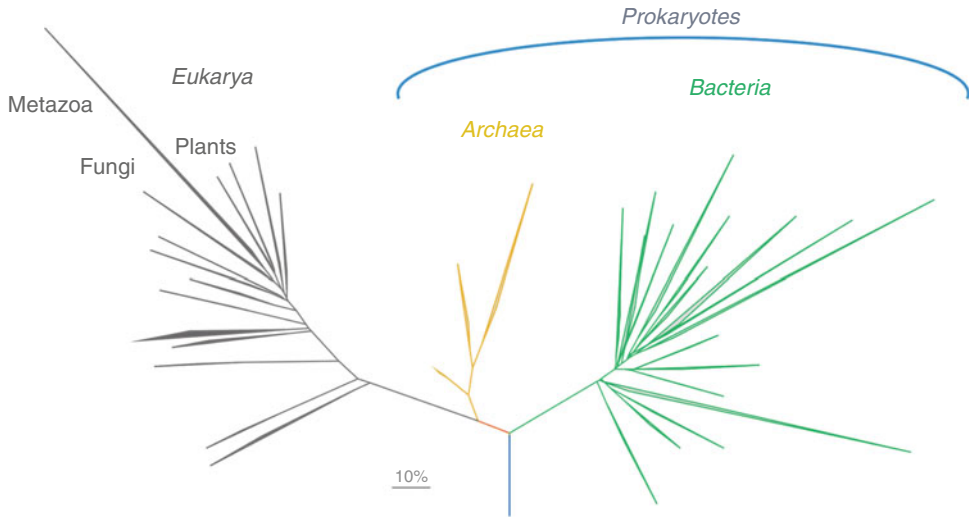

Prokaryote, Fig. 1 Phylogenetic reconstruction based on 16S rRNA gene sequence analyzes of the three domains of life. The figure shows that the Prokaryotes appear to be a paraphyletic group embracing Archaea and Bacteria

Overview

Cellular life is represented by three lines of descent: the domains ▶ *Bacteria*, ▶ *Archaea*, and ▶ *Eukarya*. Two of them (*Bacteria* and *Archaea*) are embraced by the term "prokaryote," a term that has no standing in the taxonomic hierarchy. From the phylogenetic reconstructions based on the analysis of the ribosomal small subunit gene sequences, it seems that both domains differ dramatically in their evolutionary history (see Fig. 1). In this regard, *Archaea* and *Eukarya* seem to share a common ancestor, whereas *Bacteria* seem to be an independent line of descent. In contrast to eukaryotic cells, prokaryotes have a simpler internal structure, lacking membrane-enclosed organelles. Prokaryotes do not develop or differentiate into multicellular forms. Some grow in filaments, or masses of cells, but each cell in the colony is identical and capable of independent existence, they never form specialized tissues. It is generally accepted that the first living cells on the earth were prokaryotes that might have appeared about 3.5 billion years ago or before, and remained alone for about 1.5 billion years until the eukaryotes developed (2.0 billion years ago).

Prokaryotes are considered to be the most abundant living cells in the biosphere, with numbers that range from 4×10^{30} to 6×10^{30}, and that produce a biomass equivalent to that of the vegetal material. They colonize almost every place on the earth where life is possible, and show the widest range of extreme life habitats. They colonize any available surface and cavity, and their abundance depends on the habitat. For example, 1 cm^3 may contain about 10^6 cells in seawater, 10^9 in sediments, 10^{12} in soils, 10^{10} in animal gut. Their metabolism is very diverse and can obtain energy from light (phototrophy), inorganic chemicals (chemolithotrophy), or organic chemicals (chemoorganotrophy). Some can fix inorganic carbon (autotrophy), but others depend on the assimilation of organic carbon (heterotrophy). Respiratory metabolism can occur aerobically (by reducing oxygen as a terminal electron acceptor), or anaerobically (by reducing a wide range of molecules such as sulfate, nitrate, iron, manganese, among others). On the other hand, some organisms ferment (reducing organic products of their own metabolism), or generate methane as a product of their anaerobic oxidative metabolism. In the prokaryotic world all these combinations are possible,

and many of them can switch their metabolism depending on environmental conditions and the availability of different carbon and energy sources. The endosymbiosis of prokaryotes with eukaryotic cells had been essential for the development of the latter in the biosphere. Mitochondria seem to have originated from the symbiosis of an alphaproteobacterium, and gave eukaryotes the ability to respire oxygen. Chloroplasts seem to have their origin from a symbiosis with a cyanobacterium that gave algae and plants their photoautotrophic metabolism. Some animals show additional symbiosis with chemolithotrophs that provided them with an autotrophic metabolism. Prokaryotes are essential for the development of the biogeochemical cycles in the biosphere, and finally are responsible for recycling the basic elements that maintain life.

See Also

- ▶ Archaea
- ▶ Biogeochemical Cycles
- ▶ Cyanobacteria
- ▶ Electron Acceptor
- ▶ Endosymbiosis
- ▶ Eukarya
- ▶ Fermentation
- ▶ Microorganism
- ▶ Organelle
- ▶ Prokaryotes, Origin of

References and Further Reading

Cavicchioli R (2007) Archaea molecular and cellular biology. ASM Press, Herndon
Garrity GM (2001) Bergey's manual of systematic bacteriology, 2nd edn. Springer, New York
Lengeler JW, Drews G, Schlegel HG (1999) Biology of the prokaryotes. Blackwell Science, Stuttgart
Madigan MT, Martinko JM, Parker J (2003) Brock biology of microorganisms, 10th edn. Pearson Education, Upper Saddle River
Wheelis ML, Kandler O, Woese CR (1992) On the nature of global classification. Proc Natl Acad Sci USA 89:2930–2934
Whitman WB, Coleman DC, Wiebe WJ (1998) Prokaryotes: the unseen majority. Proc Natl Acad Sci USA 95:6578–6583
Woese CR (1987) Bacterial evolution. Microbiol Rev 51:221–271
Woese CR (1998) The universal ancestor. Proc Natl Acad Sci USA 95:6854–6859

Prokaryotes, Origin of

Purificación López-García
Unité d'Ecologie, Systématique et Evolution, CNRS UMR8079 Université Paris-Sud 11, Paris, Orsay Cedex, France

Keywords

Archaea; Bacteria; Cenancestor; Early diversification of life domains; Last universal common ancestor

Definition

Prokaryotes are organisms constituted by cells lacking a nuclear membrane that separates the genetic material from the rest of the cytoplasm and, consequently, where transcription from DNA to mRNA and translation from mRNA to proteins are coupled. As soon as mRNA begins to be synthesized, ribosomes begin to attach to it and translate it into protein on one end while transcription proceeds at the other end. There are two groups of organisms having a prokaryotic cell structure: ▶ archaea and ▶ bacteria. The origin of prokaryotes refers to the origin and evolution of their shared common ancestor.

History

The terms *prokaryote* and *eukaryote* were introduced with their actual meaning in biology by microbiologists R. Stanier and C.B. van Niel in 1962. At that time, however, the third domain of

► life, the archaea, had not yet been discovered, and prokaryotes were synonymous to bacteria. With the discovery of the archaea as a phylogenetically distinct domain of organisms, as distant from bacteria as from eukaryotes, it became clear that the term *prokaryote* should refer exclusively to a structural kind of cell but had no phylogenetic sense, since it grouped organisms from two far-distant groups.

Overview

The origin of prokaryotes can be viewed in two different ways, either as the origin of the ancestor from which archaea and bacteria diverged but also as the origin (specialization and/or diversification) of archaea and bacteria from that ancestor. The problem of the origin of prokaryotes is therefore intimately linked to that of the root of the tree of life and the evolution of the three phylogenetic domains of organisms. This is a highly debated and far-from-solved issue. Several theoretical possibilities have been proposed to explain the major splits in the three organismal domains, archaea, bacteria, and eukaryotes. One proposes that the last cenancestor (last universal common ancestor) was eukaryotic like and that prokaryotes derived from that ancestor by a reduction process, perhaps linked to the adaptation to high temperatures. This hypothesis is the least favored by mainstream science, owing to the difficulties of explaining the origin of a rather complex eukaryotic cell early in evolutionary times from scratch. All the other hypotheses sustain the idea that prokaryotes emerged before eukaryotes and, hence, that the origin of prokaryotes is coincident with that of the last cenancestor. There are two major models for the evolution of the three domains of life from such a prokaryotic ancestor. The first proposes that the cenancestor splits in one branch leading to the bacteria and another branch that subdivided later into two branches corresponding to that of the archaea and to a third hypothetical protoeukaryotic branch in which the nucleus and several eukaryotic features such as phagocytosis evolved. This model, supported by C.R. Woese, is the most popular and the one explained in most textbooks. A related, though quite minoritary, model proposing the existence of a protoeukaryotic lineage sister to the archaea is that by T. Cavalier-Smith, who proposes that archaea and eukaryotes derive from within Gram-positive bacteria, sharing with them the possession of only one cell membrane. The second, increasingly expanding, set of models proposes that the last cenancestor simply split into two major branches leading to, respectively, archaea and bacteria. Eukaryotes would be the evolutionary outcome of one (or two) symbiotic event(s) between archaea and bacteria. The bifurcation between the archaeal and bacterial lineages would have been accompanied by a specialization of their membrane lipids and the replication machinery of DNA, which are very different in both lineages, as well as the fine-tuning of transcription and translation. The last cenancestor from which archaea and bacteria evolved was certainly a rather complex organism, but how and when it evolved from earlier life forms remain obscure at present.

See Also

- ► Archaea
- ► Bacteria
- ► Cyanobacteria
- ► Eukaryote
- ► Eukaryotes, Appearance and Early Evolution of
- ► Life
- ► LUCA
- ► Prokaryote

References and Further Reading

Cavalier-Smith T (1987) The origin of eukaryotic and archaebacterial cells. Ann N Y Acad Sci 503:17–54

Madigan MT, Martinko JM, Parker J (2003) Brock biology of microorganisms. Prentice Hall, Upper Saddle River

Martin W, Koonin E (2006) A positive definition of prokaryotes. Nature 442:24

Moreira D, López-García P (2006) The last common ancestor (in 5. prebiotic chemistry-biochemistry-emergence of life, 4.2-2 Ga). Earth Moon Planet 98:187–197
Sapp J (2005) The prokaryote-eukaryote dichotomy: meanings and mythology. Microbiol Mol Biol Rev 69:292–305
Sapp J (2009) The new foundations of evolution. Oxford University Press, New York, p 425
Stanier R, van Niel CB (1962) The concept of a bacterium. Archives für Mikrobiologie 42:17–35
Woese C, Fox GE (1977) Phylogenetic structure of the prokaryotic domain: the primary kingdoms. Proc Natl Acad Sci U S A 74:83–86
Woese CR, Kandler O, Wheelis ML (1990) Towards a natural system of organisms. Proposal for the domains archaea, bacteria and eucarya. Proc Natl Acad Sci U S A 87:4576–4579

Proline

Kensei Kobayashi
Yokohama National University, Tokiwadai, Hodogaya-ku, Yokohama, Japan

Synonyms

Pro; Pyrrolidine-2-carboxylic acid

Definition

Proline, $C_5H_9NO_2$, is one of the 20 protein amino acids. The amine in proline is a secondary amine (Fig. 1), whereas the other 19 coded amino acids all contain primary ($-NH_2$) amino groups. Its three-letter symbol is Pro, and its one-letter symbol is P. It has a molecular weight of 115.13, and its isoelectric point is 6.30. Proline is a hydrophobic ▶ amino acid. Since it contains a secondary amino group, its reactivity is different from that of the other amino acids, and special care is needed for its determination. For example, the reaction product of proline with ninhydrin is of a different color from that of the other coded amino acids.

Proline, Fig. 1 Structure of proline

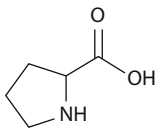

See Also

▶ Amino Acid
▶ Protein

Propanal

▶ Propionaldehyde

Propanenitrile (IUPAC Name)

▶ Ethyl Cyanide

Propanone

▶ Acetone

1, 2, 3-Propantriol

▶ Glycerol

Propene

▶ Propylene

2-Propenenitrile (IUPAC Name)

▶ Vinyl Cyanide

Proper Motion

Daniel Rouan
LESIA, Observatoire Paris-Site de Meudon, Meudon, France

Synonyms

Apparent motion

Definition

The proper motion is the apparent angular motion of a star or any celestial object on the celestial sphere, as measured from the position of the Sun. Proper motion is given in arc seconds per year for each component of the equatorial coordinates (▶ right ascension and ▶ declination). Proper motion should not be confused with ▶ parallax, which is the apparent motion of a star on the sky in 1 year, caused by the motion of the Earth as it travels along its orbit around the Sun.

Since the apparent motion is due to the star's velocity with respect to the Sun, the proper motion is proportional to the ratio of transverse velocity to distance; it is consequently larger when the star is nearby (Fig. 1). For instance, Barnard's star, one of the closest stars to the solar system (6 light-years), has the largest proper motion of all stars, moving at 10.3 s of arc per year (Fig. 2).

Until recently, proper motions of stars were obtained by comparing photographic sky survey images taken many years apart. The European ▶ Hipparcos satellite brought a revolution in the 1990s by providing much more accurate proper motion measurements for several millions of stars. The Gaia space mission launched in fall 2013 will extend the catalog to a billion stars with another very big step in accuracy.

Since stars with large proper motions tend to be nearby, this is a way to select targets for exoplanet searches, either for direct detection or when the astrometric technique is used.

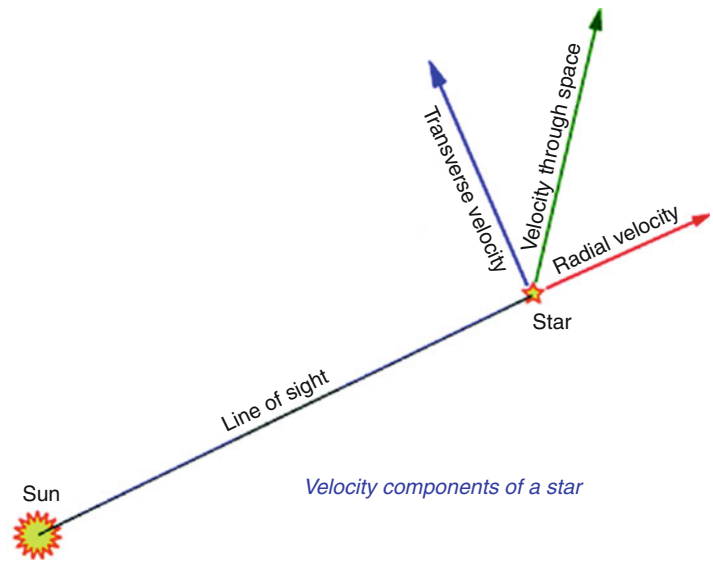

Proper Motion, Fig. 1 A star has a certain velocity through space with respect to the Sun, and the transverse component of this velocity corresponds to the proper motion

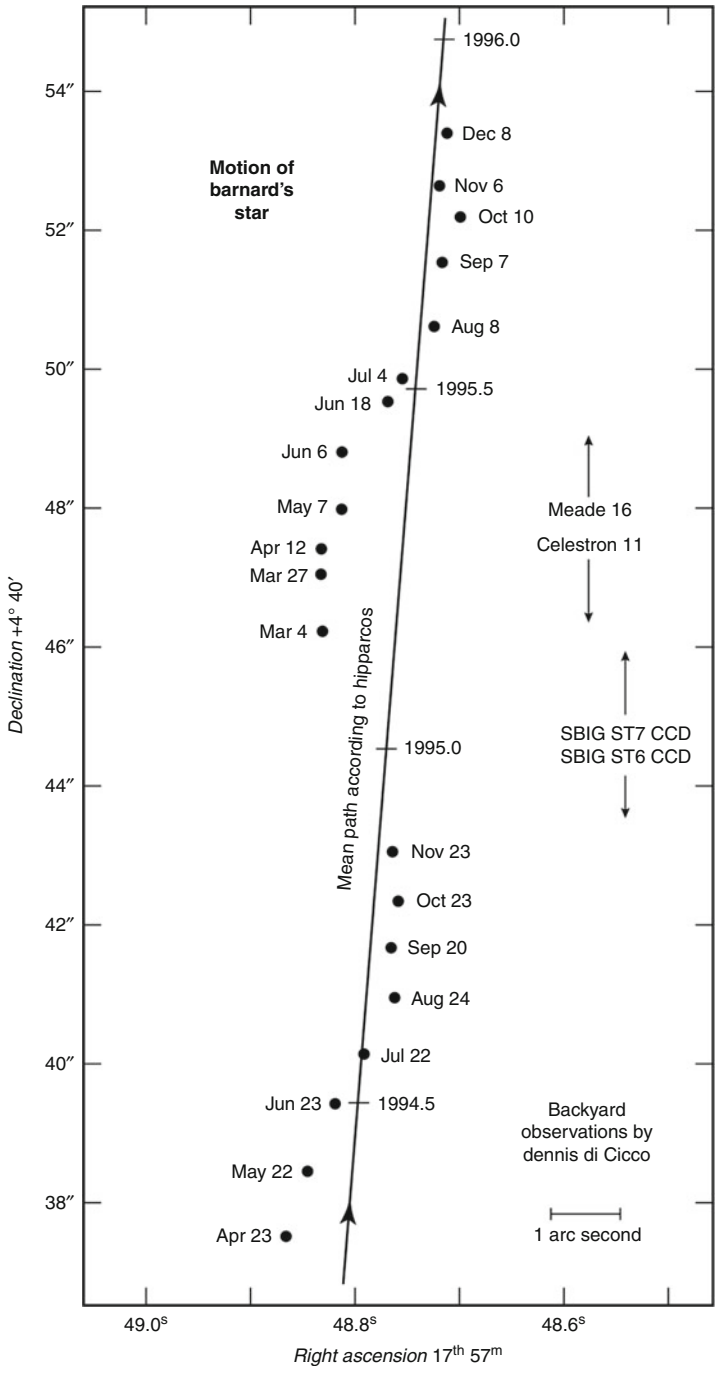

Proper Motion, Fig. 2 The nearby Barnard's star exhibits a very large proper motion, as illustrated by the measurements obtained by the European satellite Hipparcos

P

See Also

► Coordinate Systems
► Parallax

Propionaldehyde

Henderson James (Jim) Cleaves II
Earth–Life Science Institute (ELSI), Tokyo Institute of Technology, Meguro–ku, Tokyo, Japan
Institute for Advanced Study, Princeton, NJ, USA
Blue Marble Space Institute of Science, Washington, DC, USA
Center for Chemical Evolution, Georgia Institute of Technology, Atlanta, GA, USA

Synonyms

CH_3CH_2CHO; Propanal

Definition

Propionaldehyde is an organic compound with the formula CH_3CH_2CHO. It is a colorless liquid at room temperature and pressure. Propionaldehyde has been discovered in the interstellar medium. Propionaldehyde is could be a Strecker synthesis precursor to α-amino-n-butyric acid, which has been detected in several carbonaceous chondrites.

See Also

► Aminobutyric Acid
► Molecules in Space

Propionitrile

► Ethyl Cyanide

Proplyd

► Protoplanetary Disk

Propyl Cyanide

William M. Irvine
University of Massachusetts, Amherst, MA, USA

Synonyms

Butanenitrile; Butyronitrile; C_3H_7CN

Definition

The IUPAC name of this organic molecule is butanenitrile. Under standard laboratory conditions it is a colorless liquid that is miscible with most polar organic solvents.

History

Propyl cyanide is among the largest organic molecules unambiguously detected by radio astronomers in the ► interstellar medium (Belloche et al. 2009). These authors suggest that it may be produced by surface reactions on ► interstellar dust grains, perhaps by sequential addition of CH_2 or CH_3 radicals to known interstellar species such as CN and CH_2CN. It is the third member of the series that includes methyl cyanide (CH_3CN) and ► ethyl cyanide (CH_3CH_2CN).

See Also

► Ethyl Cyanide
► Interstellar Dust
► Molecules in Space

References and Further Reading

Belloche A, Garrod RT, Müller HSP, Menten KM, Comito C, Schilke P (2009) Increased complexity in interstellar chemistry: detection and chemical modeling of ethyl formate and *n*-propyl cyanide in Sagittarius B2(N). Astron Astrophys 499:215–232

Propylene

Didier Despois
Laboratoire d'Astrophysique de Bordeaux, CNRS-Universite de Bordeaux, France

Synonyms

CH_3CHCH_2; Methylethylene; Propene

Definition

Propylene (IUPAC name propene) is an unsaturated hydrocarbon with a double bond, the second alkene after ethylene. It is a gas at standard ambient temperature and pressure. It can polymerize (polypropylene). It has been detected in the interstellar medium.

History

Propylene was not specifically searched for in the interstellar medium, as its rotational lines were expected to be weak, due to its low electric dipole moment. It has, however, been detected serendipitously in a spectral survey toward the dark cloud TMC-1 (Marcelino et al. 2007).

See Also

▶ Molecules in Space

References and Further Reading

Marcelino N, Cernicharo J, Agúndez M, Roueff E, Gerin M, Martín-Pintado J, Mauersberger R, Thum C (2007) Discovery of interstellar propylene (CH_2CHCH_3): missing links in interstellar gas-phase chemistry. Astrophys J 665:L127–L130

Propynyl Radical

▶ Propynylidyne

Propynylidyne

William M. Irvine
University of Massachusetts, Amherst, MA, USA

Synonyms

C_3H; Propynyl radical

Definition

The ▶ radical C_3H can exist in either a linear form (l-C_3H) or as a tricarbon ring with the attached hydrogen atom (c-C_3H). Both isomers have been detected at millimeter wavelengths in the ▶ interstellar medium and in the envelopes of evolved stars. C_3H is an important intermediary in the production of heavier species of the form C_nH ($n > 3$), which have been detected astronomically for $n = 4$–8. The linear propynylidynium ion, ▶ C_3H^+, has recently been reported in the interstellar medium (Pety et al. 2012).

See Also

- ▶ Interstellar Medium
- ▶ Molecules in Space
- ▶ Radical

References and Further Reading

Pety J, Gratier P, Guzmán V, Roueff E, Gerin M, Goicoechea JR, Bardeau S, Sievers A, Le Petit F, Le Bourlot J, Belloche A, Talbi D (2012) The IRAM-30 m line survey of the Horsehead PDR. II. First detection of the l-C_3H^+ hydrocarbon cation. Astron Astrophys 548: A68

Thaddeus P, Gottlieb CA, Hjalmarson A, Johansson LEB, Irvine WM, Friberg P, Linke RA (1985) Astronomical identification of the C3H radical. Astrophys J 294: L49–L53

Yamamoto S, Saito S, Ohishi M, Suzuki H, Ishikawa S, Kaifu N, Murakami A (1987) Laboratory and astronomical detection of the cyclic C3H radical. Astrophys J 322:L55–L58

Propynylidynium, *l*-C_3H^+

- ▶ C_3H^+

Protein

Eric Gaucher[1] and Vanessa Cox[2]
[1]School of Biology, Georgia Institute of Technology, Atlanta, GA, USA
[2]Georgia Institute of Technology, Atlanta, GA, USA

Keywords

Amino acid; Enzyme; Translation

Synonyms

Peptide; Polypeptide

Definition

A protein is a biopolymer comprised of a linear chain of amino acids. Proteins not only act as the main catalytic molecules of life in the form of enzymes, they also serve structural, mechanical, and signaling roles, as well as other cellular functions. The chemical properties of amino acids and their sequential organization determine how a protein folds into a three-dimensional structure. This structure, in turn, dictates the function of the protein molecule. Instructions for the amino acid sequence of a protein are stored in the genetic material of a cell in the form of a gene.

History

According to the "RNA World" hypothesis, prior to the evolution of protein synthesis, RNA oligonucleotides acted as both the information carrier and the catalytic molecule of life. If true, proteins eventually replaced these oligonucleotides as superior catalytic molecules. Today, proteins are largely responsible for a cell's metabolism and play a key role in most cellular processes. Although proteins are most noted for their catalytic capabilities, they also act as key structural components of cells, having important roles in the cytoskeleton and transport of small molecules through the cellular membrane. Researchers are able to study ancient life through a process termed ancestral sequence reconstruction to gain insight into ancient proteins, ancient organisms, and the environments in which ancient organisms may have lived. Across the domains of life, all proteins are made up of a canonical set of 20 different amino acids. However, evidence suggests that early proteins were likely synthesized from a reduced set of amino acids and that this set evolved over time to incorporate additional amino acids which have expanded chemical functionalities. Some interesting questions astrobiologists attempt to address include why nature selected these particular 20 amino acids, what was the function of early proteins, and how did the protein synthesis machinery evolve.

Overview

Proteins are linear biopolymers composed of a non-branching chain of amino acid monomers. All amino acids consist of a hydrogen atom, an amino group, a carboxyl group, and an R-group attached to a central alpha carbon. The R-group varies among amino acids and is the distinguishing feature between one amino acid and another. The various R-groups allow amino acids to exhibit a range of solubilities, hydrophobicities, and reactivities while maintaining a basic structure. Although dozens of different amino acid species can be observed in meteorites or as products in prebiotic synthesis experiments, all known life uses the same set of 20 (or, in some cases, 22) amino acids for protein synthesis. This conservation of proteinogenic amino acid species, along with their uniform chirality (L) and central alpha carbon, led to one of the first hypotheses that all life on Earth evolved from a common ancestor (Fig. 1).

The sequence of amino acids comprising a protein is specified by its corresponding gene in the cell's genetic material and determines the structure and function of the protein. The sequence of amino acids is known as the primary structure of a protein. As a protein is synthesized (i.e., translated), the various chemical properties of the amino acid R-groups (such as size, charge and polarity) lead to chemical interactions that cause the growing chain of amino acids to adopt a three-dimensional structure. Local regions of a protein generally form alpha-helix or beta-sheet conformations, which can then fold to bring distal regions of the protein into close proximity.

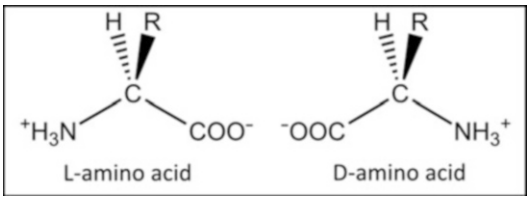

Protein, Fig. 1 L and D amino acids. Biotically synthesized amino acids are found in the L configuration. However, abiotic amino acids, including those synthesized in labs or identified in meteors, can exhibit either chirality

Alpha-helices and beta-sheets are classified as types of secondary structure. The three-dimensional arrangements of alpha-helices and beta-sheets in relation to each other create the protein's tertiary structure. Some proteins also have quaternary structure when multiple three-dimensional proteins associate as subunits to form a larger protein complex (Fig. 2). Chemical modifications of proteins (post-translational modifications) are often used to stabilize or modify protein structures (i.e., disulfide bonds) or to change their chemical and functional properties (i.e., methylation).

To assemble a protein's primary structure, individual amino acids are linked by a peptide bond between the carboxyl group of one amino acid and the amino group of the next amino acid via a condensation reaction. Due to resonance structures, the peptide bond has some double-bond characteristics that make it much more rigid and slightly shorter than a true single-bond. Additionally, the six atoms comprising the peptide group are planar in spatial organization, which imparts rigidity to the peptide backbone (Fig. 3). These restrictions severely limit the number of conformations a protein's backbone can adopt. Such rigidity provides the peptide chain with a constrained shape and limited flexibility, and, thus, explains the prevalence of the secondary structural elements discussed above.

The alpha-helix and beta-sheet conformations allow hydrogen bonding between the positively charged amino groups and the negatively charged carboxylate groups along the backbone of a protein. Since the amino and carboxyl groups are charged at physiological pH, the result of these associations is the hydrophobicity of the protein is controlled by the amino acid R-groups, the side chains which differ among amino acids and lend them specific functionality, as opposed to the protein backbone, which is common to all proteins. Thus, not only can proteins demonstrate a wide range of hydrophobicities, but even within a single protein, different regions can have different hydrophobicities. A random coil (also called a beta-turn or a reverse turn) is another class of secondary structure identified by the absence of a regular secondary structure. These are amino

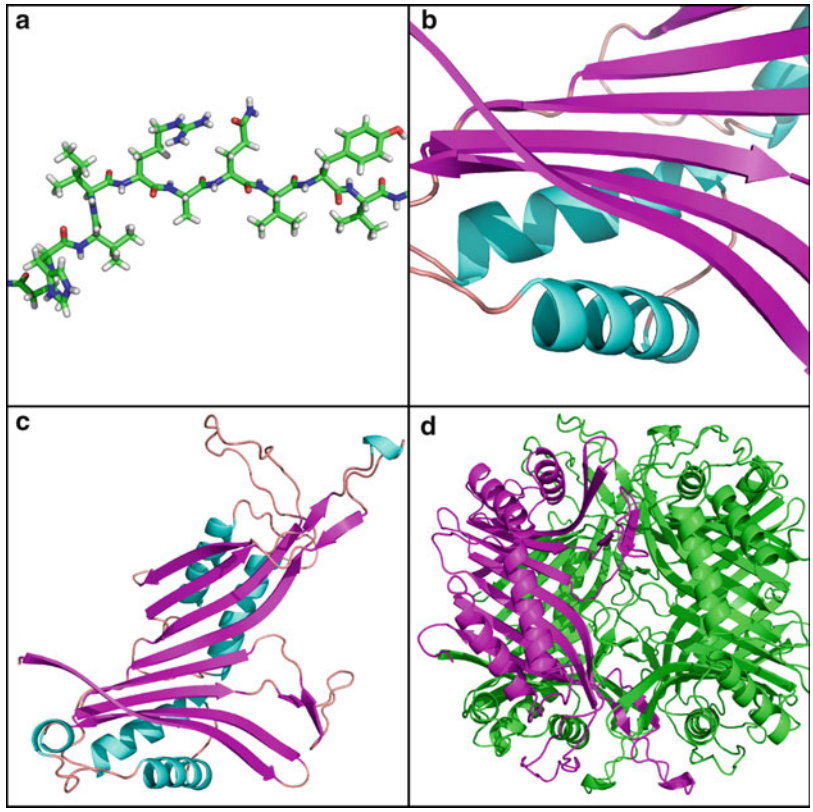

Protein, Fig. 2 Ancient uricase structure. Above are cartoon depictions of the crystal structure of an ancient uricase. Frame (**a**) shows the primary structure of a beta-strand, part of a beta-sheet, whose sequence is histidine, valine, isoleucine, arginine, alanine, glutamine, valine, tyrosine, and valine *left* to *right*. Carbon atoms are *green*, nitrogen are *blue*, oxygen are *red*, hydrogen are *white*. The peptide backbone bisects the frame with the amino acids' R-groups protruding above and below the backbone. Frame (**b**) depicts alpha-helix (*blue*) and beta-sheet (*magenta*) structures with the remaining portions colored salmon. Frame (**c**) illustrates the protein's tertiary structure. The *magenta* beta-sheets and *blue* alpha-helices make up the peptide strand's three-dimensional structure. In Frame (**d**), four monomers associate as a tetramer forming the proteins' quaternary structure. One monomer is highlighted in *magenta*; the other three are *green*. To make a functional uricase enzyme, 11 of these tetramers would associate to make the full protein complex

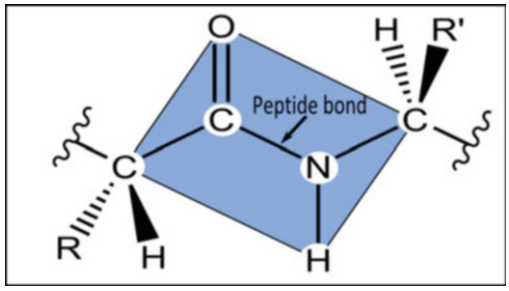

Protein, Fig. 3 Planar peptide group. The six planar atoms surrounding the peptide bond, highlighted by the *blue* polygon, impart rigidity to the peptide's primary structure, leading to the formation of the most common secondary structures, alpha-helices and beta-sheets

acid sequences which are not part of an alpha-helix or beta-sheet but often connect these more common secondary structures.

The design of the secondary structure participates in the formation of the tertiary and quaternary structure of the protein. Proteins must balance hydrophobic and hydrophilic properties in order to fold properly and fulfill their prescribed cellular function. For example, proteins active in the cytoplasm must be water-soluble. Additionally, the exterior of the protein and the interior of the protein may have different hydrophobicities. For example, a transport protein in a

cell's membrane would have a hydrophobic exterior so it can span the lipid bilayer, while the interior core of the protein might be hydrophilic to allow water-soluble molecules passage between the interior and exterior of a cell, a passage not otherwise possible with a lipid bilayer.

See Also

- ▶ Alpha Helix
- ▶ Amino Acid
- ▶ Chirality
- ▶ Enzyme
- ▶ Genetic Code
- ▶ Hydrophobic Effect
- ▶ Meteorites
- ▶ Miller, Stanley
- ▶ Peptide
- ▶ Polypeptide
- ▶ Proteins, Primary Structure
- ▶ Proteins, Quaternary Structure
- ▶ Proteins, Secondary Structure
- ▶ Proteins, Tertiary Structure
- ▶ Ribosome
- ▶ Translation

References and Further Reading

Crick F (1970) Central dogma of molecular biology. Nature 227:561–563

Crick FHC, Barnett L, Brenner S, Watts-Tobin RJ (1961) General natural of the genetic code for proteins. Nature 192:1227–1232

Gilbert W (1986) Origin of life: the RNA world. Nature 319:618

Kvenvolden K, Lawless J, Pering K, Peterson E, Flores J, Ponnamperuma C, Kaplan IR, Moore C (1970) Evidence for extraterrestrial amino-acids and hydrocarbons in the Murchison meteorite. Nature 228:923–926

Miller SL (1953) A production of amino acids under possible primitive earth conditions. Science 117:528–529

Pauling L, Corey RB (1951) Configurations of polypeptide chains with favored orientations around single bonds: two new pleated sheets. Proc Natl Acad Sci U S A 37:729740

Pauling L, Corey RB, Branson HR (1951) The structure of proteins: two hydrogen-bonded helical configurations of the polypeptide chain. Proc Natl Acad Sci U S A 37:205–211

Sanger F, Tuppy H (1951) The amino-acid sequence in the phenylalanyl chain of insulin 1. The identification of lower peptides from partial hydrolysates. Biochem J 49:463–481

Voet D, Voet JG, Pratt CW (2008) Fundamentals of biochemistry: life at the molecular level, 3rd edn. Wiley, New York

Protein Synthesis

- ▶ Translation

Proteinoid Microsphere

Koichiro Matsuno
Nagaoka University of Technology, Nagaoka, Japan

Keywords

Amino acids; Microspherules; Protocells

Synonyms

Thermal copolymers of amino acids

Definition

Proteinoid microspheres are spherical structures to be formed when a heated mixture of amino acid molecules in the dry conditions is dissolved in water. The diameter of a typical microsphere is about a few micrometers.

Overview

The first experimental observation of proteinoid microsphere was made by Sidney W. Fox, Kaoru Harada and their colleague in 1959

(Fox et al. 1959). The term proteinoid coined by Fox is for a thermal copolymer of amino acid molecules. Proteinoids maintain within themselves side-chain bonds in addition to peptide bonds.

Proteinoids readily form microspherules in water. This is due to the fact that they are amphiphilic, consisting of molecules having a polar water-soluble group attached to a water-insoluble group. The presence of a polar water-soluble group which can easily be ionized has indirectly been confirmed in a dynamic manner by observing the oscillation of electrical potential of the surface of proteinoid microspheres. In addition, when the proteinoids are rich in basic amino acids such as arginine and lysine, the surface of the resulting microsphere can have local areas where naked positive charges are exposed directly to the immediate surroundings. These naked positive charges can attract some types of molecule having negatively charged locales. A typical example of molecule having negatively charged locales includes both amino acids and nucleic acids. The surface of proteinoid microspheres may provide a reaction site for further chemical synthesis to follow. Furthermore, proteinoid microspheres can exhibit some forms of dynamic structural flexibility including an instance of giving birth to daughter microspheres through budding when the ionic strength or the pH of the aqueous milieu is changed.

Then, it would seem to follow that proteinoid microspheres may serve as a model of proto-cell in prebiotic evolution as championed by Fox. However, the subtle part in the claim of proteinoid microspheres as a model of protocell is in the difficulty of refuting the claim itself. A reliable model must be explicit in drawing the demarcation line beyond which it is not applicable. Although the model of proteinoid microspheres does not meet the requirement yet, this does not mean that it is irrelevant. The future fate of the proteinoid model remains to be seen.

See Also

► Protocell

References and Further Reading

Fox SW, Harada K, Kendrick J (1959) Production of spherules from synthetic proteinoid and hot water. Science 129:1221–1223

Protein-Protein Interaction Networks

► Biological Networks

Proteins, Primary Structure

Henderson James (Jim) Cleaves II
Earth–Life Science Institute (ELSI), Tokyo Institute of Technology, Meguro–ku, Tokyo, Japan
Institute for Advanced Study, Princeton, NJ, USA
Blue Marble Space Institute of Science, Washington, DC, USA
Center for Chemical Evolution, Georgia Institute of Technology, Atlanta, GA, USA

Definition

The primary structure of a peptide or a ► protein describes the linear sequence of its amino acid units. By convention, the sequence of a protein or peptide is reported starting from the amino-terminal (NH_2) end. Proteins also often contain disulfide cross-linkages, and the primary structure also specifies the cross-linking ► cystine residues. The primary structure also describes other post-translational and interstrand linkages.

See Also

► Cysteine
► Cystine

- ▶ Disulfide Bond
- ▶ Protein
- ▶ Proteins, Secondary Structure
- ▶ Proteins, Tertiary Structure

Proteins, Quaternary Structure

Henderson James (Jim) Cleaves II
Earth–Life Science Institute (ELSI), Tokyo Institute of Technology, Meguro–ku, Tokyo, Japan
Institute for Advanced Study, Princeton, NJ, USA
Blue Marble Space Institute of Science, Washington, DC, USA
Center for Chemical Evolution, Georgia Institute of Technology, Atlanta, GA, USA

Definition

Many proteins are composed of more than one folded polypeptide chain, which are known as ▶ protein subunits. Quaternary structure describes the organization of multiple subunits into a complex. Some examples of proteins with quaternary structure include hemoglobin and many ion channel proteins. Changes in quaternary structure can occur through conformational changes within individual subunits or through reorientation of the subunits relative to each other. These conformational changes, which may be cooperative or allosterically (induced by binding of other molecule) effected, often govern the mechanism by which proteins are regulated or perform their catalytic functions.

See Also

- ▶ Protein
- ▶ Proteins, Primary Structure
- ▶ Proteins, Secondary Structure
- ▶ Proteins, Tertiary Structure

Proteins, Secondary Structure

Henderson James (Jim) Cleaves II
Earth–Life Science Institute (ELSI), Tokyo Institute of Technology, Meguro–ku, Tokyo, Japan
Institute for Advanced Study, Princeton, NJ, USA
Blue Marble Space Institute of Science, Washington, DC, USA
Center for Chemical Evolution, Georgia Institute of Technology, Atlanta, GA, USA

Definition

In biochemistry, ▶ protein secondary structure describes common three-dimensional structural motifs found in proteins. Secondary structure is determined by inter-residue interactions mediated most often by hydrogen bonding occurring between backbone amide nitrogen and carbonyl groups of a polypeptide. The most common secondary structural motifs are ▶ alpha helices and beta sheets. Tight turns and flexible loops link the regular secondary structural elements.

Amino acids in a polypeptide vary in their tendency to form secondary structure elements. Proline and glycine are sometimes called "helix breakers" because they tend to disrupt the regularity of α-helical backbone conformations; however, both of these amino acids have unusual conformational abilities and are often found in turns. Amino acids that prefer to adopt helical conformations in proteins include methionine, alanine, leucine, glutamic acid, and lysine. In contrast, large aromatic amino acids such as tryptophan, tyrosine, and phenylalanine, and branched amino acids such as isoleucine, valine, and threonine generally prefer to adopt β-strand conformations.

See Also

- ▶ Alpha Helix
- ▶ Protein
- ▶ Proteins, Primary Structure
- ▶ Proteins, Tertiary Structure

Proteins, Tertiary Structure

Henderson James (Jim) Cleaves II
Earth–Life Science Institute (ELSI), Tokyo Institute of Technology, Meguro–ku, Tokyo, Japan
Institute for Advanced Study, Princeton, NJ, USA
Blue Marble Space Institute of Science, Washington, DC, USA
Center for Chemical Evolution, Georgia Institute of Technology, Atlanta, GA, USA

Definition

In biochemistry, the tertiary structure of a ▶ protein is its three-dimensional structure, as defined by the atomic coordinates. Tertiary structure is largely determined by the protein's primary structure. The environment in which a protein is synthesized and allowed to fold is a significant determinant of a polypeptides final folded conformation. In globular proteins, tertiary structure is often stabilized by the sequestration of hydrophobic amino acid residues in the protein's interior, from which water is excluded, and by the exposure of charged or hydrophilic residues on the protein's cytosol-exposed surface.

See Also

▶ Disulfide Bond
▶ Protein

Proteobacteria

Irma Marín
Departamento de Biología Molecular, Universidad Autónoma de Madrid, Madrid, Spain

Keywords

Alphaproteobacteria; Betaproteobacteria; Deltaproteobacteria; Epsilonproteobacteria; Gammaproteobacteria

Definition

Proteobacteria is the largest and most diverse phylum of the domain Bacteria.

Overview

Proteobacteria is an evolutionarily, geologically, and environmentally important group of microorganisms. All proteobacteria are ▶ Gram-negative bacteria, with an outer membrane mainly composed of lipopolysaccharides. Members of this phylum show extreme ▶ metabolic diversity, including chemoautotrophic, chemoorganotrophic, and phototrophic microorganisms, which represent most of the known bacteria of medical, industrial, and agricultural significance. Photosynthetic proteobacteria are called purple bacteria, referring to their reddish pigmentation. Most members of the phylum are facultative or obligate anaerobes, with gas vesicles, flagella, or the ability to move by gliding. Morphologically, they show a variety of cellular forms including rods, curved rods, ovoids, and spirals, and some have stalks or other appendages. There is evidence that eukaryotic mitochondria originated from an endosymbiotic relationship with a member of this group of bacteria. Phylogenetically, the group is defined on the basis of sequence of the small ribosomal subunit RNA gene (16S rRNA) and is divided into five classes: *Alphaproteobacteria*, *Betaproteobacteria*, *Gammaproteobacteria*, *Deltaproteobacteria*, and *Epsilonproteobacteria*.

The *Alphaproteobacteria* comprise numerous phototrophs, chemolithotrophs, and chemoorganotrophs. Some members of this group are symbionts of plants and animals, and others have adopted intracellular life styles and constitute important human and animal pathogens.

Betaproteobacteria consist of several groups of aerobic or facultative bacteria, which are often highly versatile in their degradation capacities. Many of the species of this class play a role in ▶ nitrogen fixation in various types of plants or are able to use ammonium, hydrogen, or methane as a source of energy.

Gammaproteobacteria are the largest subgroup of proteobacteria. Many pathogens belong to this class. Many genera are chemoorganotrophs and facultative anaerobes, while others are chemolithotrophs. Some members of this group are photosynthetic using hydrogen sulfide as environmental reducing power.

Deltaproteobacteria is comprised of chemoorganotrophic microorganisms. This class can be divided into two branches. Aerobic predators and fruiting-body-forming bacteria have been found among one, while most of the known sulfate- and sulfur-reducing bacteria, an activity associated to the sulfur cycle, belong to the other.

Epsilonproteobacteria consist of few known genera with symbionts or pathogens species for humans or animals. Some environmental sequences have been recovered from cold and hydrothermal environments.

See Also

- ▶ Aerobic Respiration
- ▶ Anaerobic Respiration
- ▶ Anoxygenic Photosynthesis
- ▶ Bacteria
- ▶ Biogeochemical Cycles
- ▶ Chemolithotroph
- ▶ Chemoorganotroph
- ▶ Chemotroph
- ▶ Endosymbiosis
- ▶ Gram-Negative Bacteria
- ▶ Metabolic Diversity
- ▶ Nitrogen Fixation
- ▶ Photosynthesis
- ▶ Photosynthetic Pigments
- ▶ Phototroph

References and Further Reading

Brenner DJ, Krieg NR, Garrity GM, Staley JT, Boone DR, Vos P, Goodfellow M, Rainey FA, Schleifer KH (2005) Bergey's manual of systematic bacteriology. The proteobacteria, vol 2. Brenner, Springer, New York

Emelyanov VV (2003) Mitochondrial connection to the origin of the eukaryotic cell. Eur J Biochem 270(8):1599–1618. doi10.1046/j.1432-1033.2003.03499.xDOI:dx.doi.org

Futuyma DJ (2005) On Darwin's shoulders. J Nat Hist 114:64–68

Gray MW, Burger G, Lang BF (1999) Mitochondrial evolution. Science 283(5407):1476–1481

Madigan MT, Martinko JM, Dunlap PV, Clark DP (2008) Brock biology of microorganisms, 12 e. Benjamin Cumming, San Francisco

Stackebrandt E (ed) (2006) Molecular identification, systematics, and population structure of prokaryotes. XIV, 320 p 56 illus, ISBN: 978-3-540-23155-4

Willey J, Sherwood L, Woolverton C (2007) Prescott/Harley/Klein's microbiology, 7th edn. McGraw-Hill Science, New York

Proteome, Proteomics

Carlos Briones
Centro de Astrobiología (CSIC/INTA), Consejo Superior de Investigaciones Científicas, Madrid, Spain

Definition

A proteome is the complete set of ▶ proteins encoded by a ▶ genome. It is also defined as the ▶ protein complement of the genome. Whereas the proteome of a species is the whole set of potentially expressed proteins, the proteome of an individual organism displays variations according to the cell cycle, metabolic status, and environment-dependent variables. In multicellular organisms, the proteome is the subset of all encoded proteins which is expressed in a cell or tissue, also affected by the developmental stage and health of the organism. Proteomics is the field of molecular biology which studies the entire proteome for determining the structures and functions of the expressed proteins, as well as the relationships among them. Technologies widely used in proteomics include two-dimensional gel electrophoresis, mass spectrometry, techniques for structural characterization of proteins, and proteome-focused bioinformatic tools. In parallel to proteomics,

other global and high-throughput "omic" fields have been developed including transcriptomics, interactomics, and metabolomics, where each of these fields involves the study of the entire set of transcribed mRNAs, protein-protein interaction networks, and metabolites within the cell, respectively. The basic and technological advances in the current "post-genomic era" have profound consequences in biology, medicine, and environmental sciences.

See Also

- ▶ Bioinformatics
- ▶ Biological Networks
- ▶ Gene
- ▶ Genome
- ▶ Genomics
- ▶ Phenotype
- ▶ Protein

Proterozoic Eon

Felix M. Gradstein
University of Oslo, Blindem, Oslo, Norway

Keywords

Banded iron formation; Eukaryotes; Geological timescale; Great oxygenation event; Precambrian

Definition

The Proterozoic is the youngest of the two great divisions of the Precambrian and ranges from 2,500 to 542 Ma.

Overview

The Proterozoic Eon begins at 2.5 Ga, which approximately marks the time when oxygen from cyanobacteria began to dramatically change the composition of the Earth's atmosphere and oceans and when complex one-celled life (eukaryotes) evolved from simple cells (prokaryotes). The Proterozoic is subdivided into ten periods, generally of 200-Myr duration, grouped into three eras. The poetic names for these periods (see International Stratigraphic Chart: www.stratigraphy.org) are derived from the larger-scale tectonic or sedimentary features that occurred within each period. For example, the Siderian Period (2.5–2.3 Ga) is named from the banded iron deposits (sideros = iron) that peaked within that interval. The lack of a diverse and well-preserved fossil record, the sparse volume of supracrustal rocks, a variable degree of metamorphism and tectonic disturbance, and the uncertainties in the configuration of the continents all contribute to making the establishment of a chronostratigraphic timescale beyond the Phanerozoic Eon problematical. Therefore, the main method for correlation of Precambrian strata requires radiometric ages of interbedded volcanic rocks. The Precambrian Subcommission of the International Commission on Stratigraphy (www.stratigraphy.org; see also Ogg et al. 2008) is striving to establish a more "natural" set of subdivisions that incorporates major tectonic, biologic, atmospheric, and geochemical events.

See Also

- ▶ Archaea
- ▶ Banded Iron Formation
- ▶ Cyanobacteria, Diversity and Evolution of
- ▶ Eukaryotes, Appearance and Early Evolution of
- ▶ Geological Timescale
- ▶ Great Oxygenation Event
- ▶ Oxygenation of the Earth's Atmosphere

References and Further Reading

Ogg JG, Ogg G, Felix M (2008) Gradstein. The concise geologic time scale. Cambridge University Press, Cambridge, p 177

Protists

Ricardo Amils
Departamento de Biologia Molecular, Universidad Autónoma de Madrid, Madrid, Spain

Definition

Protists are a diverse group of eukaryotic microorganisms that encompass mostly unicellular and some ▶ multicellular organisms that do not fit phylogenetically into the well-defined kingdoms: Animalia, Plantae, and Fungi. Historically, protists were treated as the kingdom Protista, but this group has been contested in modern taxonomy. Protists do not have much in common besides a relatively simple organization, either unicellular or multicellular, with no specialized tissues. The term protista was first used by Ernst Haeckel in 1866. Protists live in almost any environment that contains liquid water. Most protists, such as ▶ algae, are photosynthetic and are fundamental primary producers in many ecosystems, making up a large part of the plankton of the oceans.

See Also

- ▶ Algae
- ▶ Eukarya
- ▶ Multicellular Organisms
- ▶ Photosynthesis
- ▶ Phylogeny
- ▶ Unicellular Organisms

Protists with Chloroplasts

- ▶ Algae

Protobinary Star

Steven W. Stahler
Department of Astronomy, University of California, Berkeley, CA, USA

Keywords

Binary star, young; Protostar

Definition

Binaries are pairs of stars locked into orbit around each other by their mutual gravitational attraction. When both stars are too young to undergo hydrogen fusion, the system is called a protobinary. In the very youngest protobinaries, neither star is optically visible, since both are still heavily embedded in the dust and gas that formed them. Several hundred protobinaries are known. In a few cases, the actual orbits of the component stars have been partially traced. Most protobinaries, however, are detected as close pairs of stars that share a common space motion within a young stellar cluster.

Overview

Most stars are not isolated objects, but have an orbiting companion. This fundamental fact was first established in the 1960s through surveys of main-sequence G-type stars, i.e., objects similar to the Sun. Over the last two decades, it has emerged that pairing is also common among much younger stars. The term protobinary refers to a pair of stars in which the components are either ▶ protostar or ▶ pre-main-sequence star. In the former case, each star is still accreting gas from its parent molecular cloud. A pre-main-sequence star, on the other hand, has reached its final mass, but is still too young to undergo hydrogen fusion at its center.

Both protostars and the youngest pre-main-sequence stars are still heavily obscured by surrounding dusty gas. Protobinaries are therefore

only seen at infrared and longer wavelengths. The actual radiation detected comes from dust grains that are being heated by the stars within. Thus, the emitted spectrum depends more sensitively on properties of the dust than on properties of the star itself. It is therefore not surprising that the true evolutionary state of the many known protobinaries is uncertain.

In principle, one could identify a protobinary by seeing each star trace an orbit around the other. In practice, the spatial resolution at longer wavelengths makes such observations difficult, although they have been achieved using interferometers. Most of the known protobinaries were found, instead, as close pairs of infrared or millimeter point sources that share a common space motion within a young stellar cluster. Here, the physical separations range from several 100 to 1,000 AU. Assuming both stars to be of roughly solar mass, the corresponding periods are 1,000–30,000 years.

In some cases, optically visible, pre-main-sequence stars are accompanied by others that are still deeply embedded. The nature of these infrared companions is still unknown. It is doubtful that they are truly younger than the visible star for the following reason. When *both* stars in a binary are optically visible, pre-main-sequence stars, it is possible to measure their ages individually. These ages, typically a few million years, usually match fairly well. This finding also indicates that the components of protobinaries were born together, presumably out of a common molecular cloud core.

See Also

- ▶ Binary Stars, Young
- ▶ Pre-main-sequence Star
- ▶ Protostars
- ▶ T Tauri Star

References and Further Reading

Ghez AM, Weinberger AJ, Neugebauer G, Matthews K, McCarthy DW (1995) Speckle imaging measurements of the relative tangential velocities of the components of T Tauri binary stars. Astron J 110:753–765

Koresko CD, Herbst TM, Leinert C (1997) The infrared companions of T Tauri stars. Astrophys J 480:741–753

Palla F, Stahler SW (2001) Binary masses as a test for pre-main-sequence tracks. Astrophys J 553:299–306

Zinnecker H, Mathieu RD (eds) (2001) The formation of binary stars. Astronomical Society of the Pacific, San Francisco

Protocell

Kepa Ruiz-Mirazo
Department of Logic and Philosophy of Science, FICE, UPV-EHU, Biophysics Research Unit (CSIC – UPV/EHU), Donostia, San Sebastián, Spain

Keywords

Compartmented reaction systems; Lipid self-assembly; Prebiotic membranes; Protometabolism; Vesicles

Synonyms

Artificial cells; Cell models; Synthetic cells

Definition

A protocell is any experimental or theoretical model that involves a self-assembled compartment (typically a supramolecular structure, like a lipid vesicle) linked to chemical processes taking place around or within it, aimed at explaining how more complex biological cells or alternative forms of cellular organization may come about.

Overview

Terrestrial biology is based on cells – systems that produce their own boundaries and carry out various transformation and replication processes within those boundaries. This includes processes

leading to cell growth, cell division, and evolution of interacting cell populations. Furthermore, there are several good reasons to believe that the generation of any living entity, terrestrial or not, requires cellular compartmentalization (Morowitz 1992; Harold 1986). However, the level of molecular and organizational complexity shown by even the simplest known ▶ prokaryotes is so high that their origin remains a mystery. Different ideas to tackle this problem scientifically have been proposed. In some of them, compartmentalization through membranes is considered a late (or even the last) major event in the process, under the assumption that all the necessary prebiotic chemistry leading to biopolymer chemistry could have taken place in bulk (aqueous) solution, perhaps with the help of mineral surfaces. For approaches that, instead, consider that membrane compartments or colloidal organic interfaces must play an important role at an earlier prebiological stage, the idea of "protocell" becomes central. A protocell would be any chemically reacting system organized around or within a self-assembled, supramolecular boundary, which mimics – without fully reproducing – the behavior of biological cells. This is an important concept not only for the traditional research program in the origins of life, but also for related emerging fields of synthetic biology, artificial life, and astrobiology.

Early ideas on protocellularity involved quite diverse systems (Hanczyc 2009), which did not always resemble modern cells topologically nor in the molecular composition and structure of the boundary (e.g., Oparin's "coacervates" or Fox's "proteinoid microspheres"). Nevertheless, the development of liposome technologies in the last few decades has made it possible to elaborate and implement model systems in the laboratory using lipid or amphiphilic bilayers, which contain – and are contained in – aqueous solutions, sharing many properties with biological membranes. Depending on the types of compounds making up the protocells (i.e., their boundary and their internal microenvironment), different models have been put forward over the years. For instance, due to their higher prebiotic plausibility, fatty acid vesicles have recently attracted attention of many researchers in the area, even if they are less stable and much more permeable, in general, than phospholipid membranes (Morigaki and Walde 2007; Deamer 2008). Regarding internal components and their dynamics, there is presently great interest in coupling vesicle growth and reproduction with polynucleotide replication taking place within the compartment (e.g., Mansy et al. 2008). Although the chemical logic of a minimum protocell would not necessarily involve complex macromolecules, like nucleic acid chains or other biopolymers (Morowitz et al. 1988), it seems that the search is currently focused on finding a protocell that can evolve – or be evolved – in a "Darwinian" way (i.e., with a mechanism for reliable heredity of molecular sequences), perhaps expecting that other relevant features of the system (robustness, internal lipid production, autonomous energetic viability, membrane functionalization, etc.) will derive from there. In the next years, it will become clearer whether this type of experimental shortcut proves successful, whether some other semisynthetic alternative (Luisi et al. 2006; Chen and Walde 2010) provides more solid results, or whether the bottom-up construction of functional protocells actually requires a longer, more winding pathway.

See Also

- ▶ Cell Models
- ▶ Cell, Minimal
- ▶ Genome, Minimal
- ▶ Lipid Bilayer
- ▶ Permeability
- ▶ Self-Assembly

References and Further Reading

Chen I, Walde P (2010) From self-assembled vesicles to protocells cold spring harb. Perspect Biol 2:a002170

Deamer DW (2008) Origins of life: how leaky were primitive cells? Nature 454:37–38

Hanczyc M (2009) The early history of protocells. In: Rasmussen S (ed) Protocells: bridging nonliving and living matter. MIT Press, Cambridge, pp 3–17

Harold FM (1986) The vital force: a study of bioenergetics. W. H Freeman, New York
Luisi PL, Ferri F, Stano P (2006) Approaches to semi-synthetic minimal cells: a review. Naturwissenschaften 93:1–13
Mansy SS, Schrum JP, Krishnamurthy M, Tobé S, Treco DA, Szostak JW (2008) Template directed synthesis of a genetic polymer in a model protocell. Nature 454:122–126
Morigaki K, Walde P (2007) Fatty acid vesicles. Curr Opin Colloid Interface Sci 12:75–80
Morowitz HJ (1992) Beginnings of cellular life. Yale University Press, Binghamton
Morowitz HJ, Heinz B, Deamer DW (1988) The chemical logic of a minimum protocell. Orig Life Evol Biosph 18:281–287
Rasmussen S, Bedau MA, Chen L, Deamer D, Krakauer C, Packard NH, Stadler PF (eds) (2009) Protocells: bridging nonliving and living matter. MIT Press, Cambridge
Walde P (ed) (2005) Prebiotic chemistry from simple amphiphiles to model protocells. Topics in current chemistry. Springer, Berlin

Proton Irradiation

Kensei Kobayashi
Yokohama National University, Tokiwadai, Hodogaya-ku, Yokohama, Japan

Definition

Irradiation of a medium by high-energy protons (hydrogen ions) by using accelerators such as Van de Graaff accelerators and synchrotrons is called proton irradiation. Cosmic rays are one of the possible energy sources for ▶ prebiotic chemistry, and protons are predominant in cosmic rays. Thus, a number of proton irradiation experiments have been performed. The energy of the protons used in these experiments is usually a few MeV (mega electron volt; 10^6 eV) or higher. Not only the high-energy protons but also secondary electrons (electrons formed by the interaction of initial protons and target molecules) are effective for dissociation and ionization of molecules. Proton irradiation causes less specific chemical reactions than UV irradiation.

Proton irradiation of gas mixtures containing carbon species like methane or carbon monoxide and nitrogen species like nitrogen and ammonia produces a wide variety of organic compounds including precursors to amino acids (Kobayashi et al. 1998) and nucleic acid bases. In addition to irradiation of gas mixtures, proton irradiation of ice mixtures simulating ice mantles of ▶ interstellar dust particles has often been performed, to examine the possible role of cosmic rays in interstellar space (particularly in ▶ molecular clouds) (Kasamatsu et al. 1997). In these experiments, major targets have included carbon monoxide, methane, methanol, ammonia, and water ices. ▶ Amino acids were also detected after hydrolysis of the resulting irradiation products.

Proton irradiation is also used to determine the tolerance of organisms to cosmic radiation.

See Also

▶ Amino Acid

References and Further Reading

Kasamatsu T, Kaneko T, Saito T, Kobayashi K (1997) Formation of organic compounds in simulated interestellar media with high energy particles. Bull Chem Soc Jpn 70:1021–1026
Koyabashi K, Kaneko T, Saito T, Oshima T (1998) Amino acid formation in gas mixture by high energy particles irradiation. Orig Life Evol Biosph 28:155–165

Proton Motive Force

José Pascual Abad
Facultad de Ciencias, Departamento de Biología Molecular, Universidad Autónoma de Madrid, Cantoblanco, Madrid, Spain

Keywords

ATP synthase; LUCA; Proton gradient; Sodium motive force

Synonyms

Chemiosmotic potential; Electrochemical potential

Definition

Proton motive force (PMF) is the force that promotes the movement of protons across membranes downhill the ▶ electrochemical potential.

Overview

A difference of solute concentration between two compartments separated by a biological membrane generates a tendency to equilibrium, which, in the case of protons, is called proton motive force (PMF). This is measured in terms of the potential energy resulting from the difference in concentration between the two compartments. With a charged solute, the potential has two components: the chemical (concentration) and the electrical potentials (Fig. 1); thus, it is named electrochemical potential.

$$PMF = \Delta\Psi - 2.3RT/F(pH_{in} - pH_{out}) = \Delta\Psi - 2.3RT/F\Delta pH$$

($\Delta\Psi$ is the transmembrane difference of electrical potential).

This energy can be used in different ways, particularly in the synthesis of ATP by ATP synthases, promoting different types of secondary transport, for example, fueling flagellar movement and, in some cases, generating heat (Fig. 2).

Proton gradients can originate in different ways and are an energy source for cells. In animal and plant cells, proton gradients are generated in mitochondria by means of the vectorial transport of protons driven by components of the respiratory chain. In plants, photosynthetic electronic transport also generates proton gradients in chloroplasts.

In most bacteria and archaea, the electronic transport chain generates proton, and/or Na^+, gradients, but fermenting bacteria use membrane-linked ATPases to hydrolyze ATP for uphill transport of protons. *Halobacteria*, a group of *Archaea* living at high salt concentrations, use bacteriorhodopsin, a light-driven membrane protein to generate a proton gradient.

Most extant organisms use PMF; however, the use of proton gradients might not have been the first gradient used by life systems. There is evidence to suggest that this may be a mechanism that evolved from a more ancestral one based on

Proton Motive Force, Fig. 1 Proton gradients and proton motive force

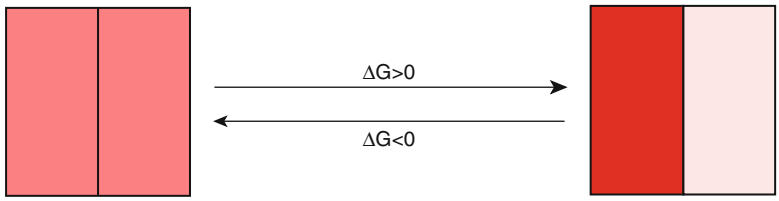

Proton gradients require energy to be formed (G>0) and generate the proton-motive force, which favours re-establishing the equilibrium (G<0)

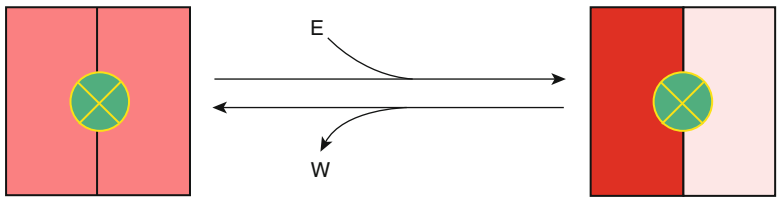

Certain membrane-associated proteins can use energy to generate proton gradients (E) and/or use the generated proton-motive force to make different types of work (W)

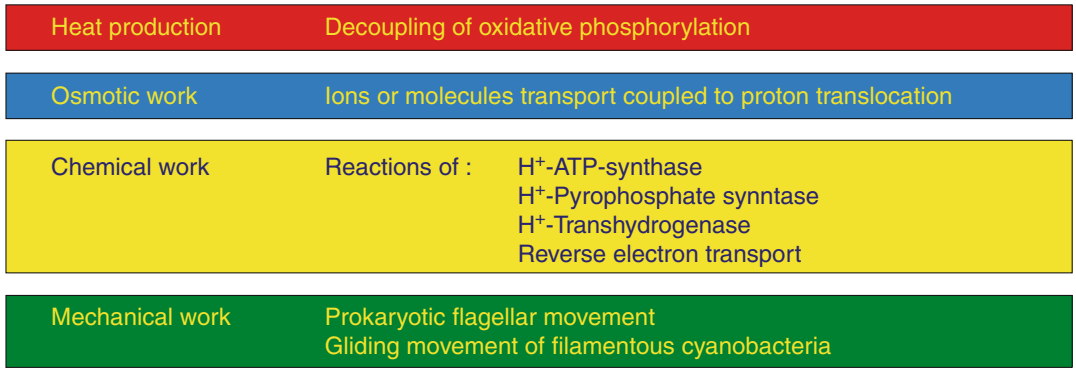

Proton Motive Force, Fig. 2 Proton motive force (PMF) can be used to perform different types of work

Na^+ gradients, used by organisms when membranes were quite proton leaky. The persistence of the use of a sodium motive force (SMF) by some obligate anaerobes, thermophiles, and alkaliphiles may be due to their low energy budgets that do not allow them to cope with the energy losses due to the proton leakiness of the modern membranes (10^5–10^7 times that of Na+ ions). However, some authors claim that the last universal common ancestor (▶ LUCA) used natural proton gradients. The evolutive origin of the use of ion gradients for bioenergetics purposes is still a very controversial issue.

See Also

- ▶ ATPase
- ▶ ATP Synthase
- ▶ Concentration Gradients
- ▶ Last Universal Common Ancestor
- ▶ Membrane Potential
- ▶ Proton Pump
- ▶ Proton Transfer

References and Further Reading

Baker-Austin C, Dopson M (2007) Life in acid: pH homeostasis in acidophiles. Trends Microbiol 15:165–171

Daniel H, Spanier B, Kottra G, Weitz D (2006) From bacteria to man: archaic proton-dependent peptide transporters at work. Physiology (Bethesda) 21:93–102

Harris DA (1995) Bioenergetics at a glance: an illustrated introduction. Wiley-Blackwell, Oxford

Lane N, Allen JF, Martin W (2010) How did LUCA make a living? Chemiosmosis in the origin of life. Bioessays. doi:10.1002/bies.200900131

Nicholls DG, Ferguson SJ (2002) Bioenergetics 3. Academic, London

Papa S, Lorusso M, Di Paola M (2006) Cooperativity and flexibility of the protonmotive activity of mitochondrial respiratory chain. Biochim Biophys Acta 1757:428–436

Proton Pump

Felipe Gomez
Centro de Astrobiología (CSIC/INTA), Instituto Nacional de Técnica Aeroespacial, Torrejón de Ardoz, Madrid, Spain

Definition

The proton pump is a membrane-integrated enzymatic complex which is able to mobilize protons to generate a proton gradient across the cell ▶ membrane. This proton gradient constitutes a fundamental energy reservoir. The proton pump plays an important role in cell ▶ respiration and ▶ photosynthesis. The ▶ electron transport chain in cell respiration generates an ▶ electrochemical potential which is coupled to the proton pumps located in the membrane. This proton gradient is an energy reservoir because it is the driver for the

generation of chemical energy (ATP), or any secondary transport system associated to it, such as the transport of nutrients, the maintenance of the ionic homeostasis of cells, or the movement of bacterial flagellum.

See Also

- ▶ ATP Synthase
- ▶ ATPase
- ▶ Bioenergetics
- ▶ Electrochemical Potential
- ▶ Electron Transport
- ▶ Energy Conservation
- ▶ Membrane
- ▶ Mitochondrion
- ▶ Photosynthesis
- ▶ Proton Motive Force
- ▶ Respiration

Proton Transfer

Steven B. Charnley
Solar System Exploration Division, Code 691, Astrochemistry Laboratory, NASA Goddard Space Flight Center, Greenbelt, MD, USA

Definition

In astrochemistry, proton transfer is a chemical process in which a positive ion reacts with a neutral molecule to add a proton to the neutral, e.g., $XH^+ + Y \rightarrow X + YH^+$.

For issues related to proton transfer in biology, see the entries on ▶ Bioenergetics and on ▶ Proton Motive Force.

Proton-Induced X-ray Emission

- ▶ PIXE

Protoplanetary Disk

Michiel R. Hogerheijde
Leiden Observatory, Leiden University, Leiden, The Netherlands

Keywords

Accretion; Dust coagulation; Solar nebula; Nebular hypothesis; Planet formation; Spectral energy distribution; Star formation; T Tauri star

Synonyms

Planet-forming disk; Proplyd

Definition

A protoplanetary disk is a disk of gas (99 % by mass) and dust (1 %), orbiting a newly formed star, from which planets are (hypothesized to be) formed. Disks are common by-products of star formation and range in mass from 0.001 to 0.3 solar masses (10^{27}–10^{29} kg) and in size from several tens to almost 1,000 AU (10^{12}–10^{14} m). Inside the disk, matter slowly moves inward, and dust particles grow to centimeter-sized pebbles: the first steps toward the formation of kilometer-sized planetesimals. Protoplanetary disks typically disperse after two to three million years through the coalescence of their matter into ▶ planets and photoevaporation by the stellar radiation.

History

As a hypothesis, the concept of protoplanetary disks dates back to the eighteenth century, inspired by the motions of the planets in the Solar System. Already in the antique world, astronomers had realized that all planets move in the same direction around the Sun, in approximately the same plane and in almost circular

orbits. This led to the hypothesis that the planets originated from a rotating disk of material that, at some point in the past, encircled the Sun. This *nebular hypothesis* was first put forward by Swedenborg in 1734 and further developed by Kant in 1755 and Laplace in 1796. In essence, the theory still holds today. While the origin of such a disk was beyond scientific investigation in the eighteenth century, the twentieth century has shown that there is a continuum of composition between the Sun, the planets, and the asteroids and meteorites. These bodies also are all nearly coeval, strongly suggesting a common origin for the Solar System from a disk formed as a by-product of the formation of the Sun. By extension, similar disks should exist around other newly formed stars, and these were found in the late twentieth century.

Overview

Protoplanetary disks are the birth sites of planets and are commonly found around newly formed stars (Williams and Cieza 2011). The Sun was likely surrounded by a protoplanetary disk shortly after its formation, and the planets, asteroids, and comets we observe today are the remainders of this disk. Modern astronomical observations provide mass estimates for typical protoplanetary disks in the range of 0.001–0.3 solar masses (1 solar mass = 1.989×10^{30} kg) and sizes of up to several hundred to a thousand astronomical units (1 AU = the mean distance between the Earth and the Sun = 1.496×10^{11} m). The material in the disks is thought to consist mainly of gas (99 % by mass), predominantly molecular hydrogen and helium with trace amounts of CO and other molecules, and small dust particles (1 % by mass). There is evidence that the dust particles are significantly larger in disks than in the overall ▶ interstellar medium and have grown from micrometers to centimeters in size. The gas motions, which can be tracked through Doppler techniques, reveal that the material is in orbit around the central star. For stars less than one million years old, >80 % are surrounded by heated dust, presumably a disk. In contrast, less than 10 % of stars with ages of about ten million years have disks. Fifty percent of disks disappear in two to three million years after the formation of the star-disk system. Disks can disappear because their material has coalesced into asteroids and planets and/or because the molecular gas has been dissociated by the star's ultraviolet radiation and blown away by the stellar wind. Recent observations have revealed a small but distinct population of stars with disks with evacuated inner zones, which may represent a short-lived but pivotal stage in the disks' evolution.

The next section ("Basic Methodology") places protoplanetary disk within the wider context of star formation and introduces the main diagnostic tools used in their study. It also describes three cases which can claim to be the first "direct" evidence of circumstellar disks. The following section ("Key Research Findings") discusses the observational statistics of basic disk properties such as mass, size, and incidence; the major constituents of the disk, dust particles and gas; the dynamics of disks; and our current knowledge of disk evolution. The final section ("Future Directions") lists the most important open questions, in which telescopes currently under construction will address.

This contribution focuses entirely on disks around low- to intermediate-mass stars, up to approximately 8 solar masses. Although there is mounting evidence that more massive young stars also are surrounded by disks, these are currently much less well understood and are not discussed here.

Basic Methodology

Protoplanetary disks are the by-product of the formation of a star and are often found around young ▶ pre-main-sequence stars (so-called T Tauri stars). Disks are commonly studied through excess infrared emission, through their full spectral energy distribution from infrared to millimeter wavelengths and through resolved imaging at near-infrared wavelengths (predominantly scattered light) and (sub)

millimeter wavelengths, either thermal emission from dust or spectral lines from (molecular) gas.

Star Formation

In the general picture of star formation, which has emerged since the mid-1980s, interstellar molecular clouds slowly contract to form dense cores. Initially, these clouds are thought to be supported against self-gravity by (magneto) hydrodynamic turbulence. Once the condensations become sufficiently dense, they decouple from this supporting field. At this point, the cloud cores collapse and form stars. Each of these cores is likely to have a net amount of angular momentum, inherited from the (turbulent) velocity field of their parent cloud. During their collapse, conservation of angular momentum will inevitably lead to the formation of a circumstellar disk around the newly formed star; some of the angular momentum may also be stored in a binary or multiple systems. Only once a disk has been formed are physical processes capable for transporting angular momentum outward, causing a small amount of matter at the disk's outer radius to spread and most other matter to accrete inward onto the star.

The above scenario strictly applies to the formation of single stars or perhaps narrow binaries. Many young stars are formed as a part of (bound) multiple systems with a few members or in large (unbound) clusters of tens or hundreds of stars. This should have a profound impact on the formation of stars and their disks. For example, in binaries, dynamical interactions limit the size of a disk to one-third of the binary separation, while a circumbinary disk can surround the entire system. In clusters, frequent stellar flybys can perturb disks. If sufficiently massive stars are also present, intense radiation fields can efficiently photo-evaporate disks.

Observational Probes

Although dust particles make up only 1 % of the mass of protoplanetary disks, their thermal emission offers powerful observational probes of the presence of disks and their structure. Inside a disk, dust particles have temperatures between 10 and 20 K at the outer edges, to 1,000–1,500 K near the inner disk edge close to the star. In fact, the location where this temperature is reached defines the disk's inner edge, as dust particles will evaporate at higher temperatures closer to the star. At these temperatures, dust particles emit detectable thermal radiation at wavelengths between a centimeter (the radio regime) and a micron (the infrared regime), which can be observed with ground-based telescopes. At intermediate frequencies of 20–300 μm (the far infrared), the Earth's atmosphere is bright, and space telescopes need to be used. In addition to thermal emission, dust particles also scatter the stellar light, which dominates the emission around 1 μm and shorter and which can be imaged to derive the extent and structure of the disk (Fig. 1).

The 99 % of the disk that consists of gas is more difficult to observe: throughout the bulk of the disk, the main gas constituents, molecular hydrogen and helium, are too cold to emit emission lines. Only the upper disk layers where very warm gas resides can be probed through molecular hydrogen lines in the near infrared and ultraviolet. Instead, trace molecules are used, like CO that has easily excited and observable lines at millimeter wavelengths. The observations then need to be extrapolated to deduce information about the full gas content.

The Spectral Energy Distribution

One of the most powerful tools in determining the structure of a circumstellar disk is its spectral energy distribution (SED), which logarithmically plots the observed energy at a given wavelength or frequency, $\log(\nu F_\nu)$ vs. $\log(\nu)$, where F_ν is the observed specific flux in a narrow frequency band around the observing frequency ν. By plotting $\log(\nu F_\nu)$ instead of simply $\log(F_\nu)$, which would be more appropriately called the broadband spectrum, peaks of similar height provide similar contributions to the total radiated energy. Other ways to plot the SED are $\log(\lambda F_\lambda)$ vs. $\log(\lambda)$, which is the equivalent expression in terms of observing wavelength λ or $\log \log(\nu L_\nu)$ vs. $\log(\nu)$, where L_ν is the specific luminosity or flux corrected for the source distance.

Using the slope of the SED between 2 and 25 μm, three classes of young stellar objects

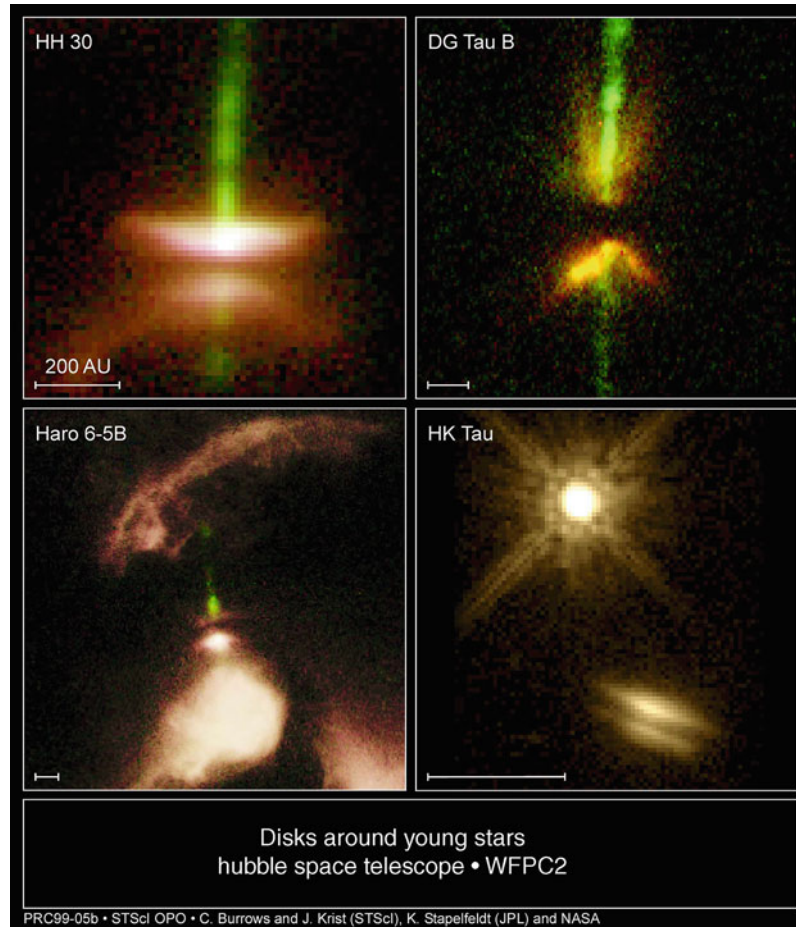

Protoplanetary Disk, Fig. 1 Four protoplanetary disks imaged in scattered light with the Hubble Space Telescope: HH 30 (*top left*), DG Tau B (*top right*), Hare 6-5B (*lower left*, object at the *center* of the image), and around one of the members of the HK Tau binary system (*lower right*). The flared surfaces of the disks can easily be seen, as well as the full obscuration caused by the dense disk midplanes. All objects except HK Tau also power jets where they expel material from their poles at velocities of several hundred kilometers per second. Such bipolar jets are common side effects of ongoing mass accretion from disks onto stars (Credit: C. Burrows (STScI), J.Krist (STScI), K. Stapelfeldt (JPL) and colleagues, the WFPC2 science team, and NASA)

(YSOs) have been defined: (1) Class I sources have SEDs that are broader than a single blackbody and are rising in the infrared; (2) Class II objects have SEDs that are also broader than a single-temperature blackbody, but have SEDs that are falling in the infrared; (3) Class III objects have little excess emission, and their SEDs are closely approximated by a single-temperature blackbody, although in the Hertzsprung-Russell diagram, they fall above the main sequence. These classes of YSOs can be equated with three distinct stages in the formation of a star: Class I objects are deeply embedded in an accreting envelope of gas and dust, Class II objects are optically visible stars surrounded by an accretion disk, and Class III sources are pre-main-sequence stars without any appreciable excess emission. Later work added a fourth class, Class 0, representing the earliest stages of star formation where the object is so deeply embedded that only far-infrared and (sub) millimeter wave emissions can escape (and formally no 2–25 μm slope can be defined).

T Tauri Stars

Well before the YSO classes were defined in the 1980s, a group of young stars had drawn the attention of astronomers: T Tauri stars. The class of T Tauri stars was first identified by Joy in 1945 as variable stars with prominent, wide optical emission lines (especially those of hydrogen, the Hα line at 6,563 Å) attributed to the accretion of matter. Modern classification also takes into account association with star-forming interstellar clouds and the presence of youth-indicating lithium lines. T Tauri stars occur in

two subclasses: (1) classical T Tauri stars, with strong Hα lines and therefore significant ongoing mass accretion, are likely surrounded by accretion disks; (2) weak-lined or naked T Tauri stars, with weak Hα lines and little or no accretion, likely have no disks (anymore).

T Tauri stars often exhibit excess emission at near-infrared wavelengths over their stellar emission and show far-infrared and submillimeter emission attributed to the presence of circumstellar dust. A simple argument shows that the material needs to be distributed in a disk (or at least a flat distribution) rather than a spherical shell: the inferred dust masses are sufficient to completely obscure the stars at optical wavelengths if the matter would be distributed in a shell. Indeed, the SEDs of (classical) T Tauri stars are well fit by simple accretion disk models, and their SED slopes classify them as Class II objects.

T Tauri stars have masses up to 2 solar masses. Pre-main-sequence stars between 2 solar masses and 8 solar masses are known as Herbig Ae/Be stars, which often are surrounded by accretion disks as well. In the remainder of the text, little distinction is made between T Tauri stars and Herbig Ae/Be stars, and they are treated simply as young stars with disks. Stars more massive than about 8 solar masses reach the main sequence (i.e., they start hydrogen fusion) before accretion stops. Although there is increasing evidence that at least some of these massive stars also have accretion disks, they are not further discussed here.

First Evidence for Disks

The infrared and millimeter emission from T Tauri stars provide *indirect* evidence that newly formed stars are surrounded by accretion disks. As first *direct* evidence for a circumstellar disk, one could count the disk around the star β Pic, although this is a debris disk with too little mass to form a planetary system (Smith and Terrile 1984). The Hubble Space Telescope provided some of the first direct images of disks in silhouette against the gas of the Orion Nebula (O'Dell et al. 1993; Fig. 2). These so-called proplyds have the size and mass to form a planetary system, but are located in a hostile environment perhaps untypical of that where the average planetary system forms. Another candidate for the first direct detection is formed by early millimeter-interferometric observations of HL Tau, showing an elongated CO gas structure surrounding the star with clear velocity gradients consistent with rotation (Sargent and Beckwith 1987); however, later observations have shown this gas structure to be more extended than previously thought, and it is likely not a disk. In the years following these exploratory observations of the 1980s and early 1990s, circumstellar disks have been studied in great detail using a variety of observational tools.

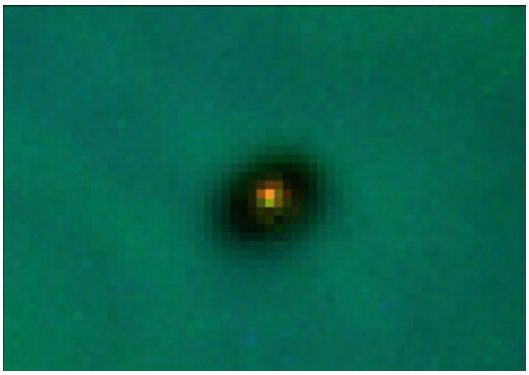

Protoplanetary Disk, Fig. 2 A protoplanetary disk, or "proplyd," seen in silhouette against the background of the Orion Nebula. Observed with the Hubble Space Telescope, the disk measures 600 AU across and contains at least seven Earth masses of dust (Credit: C.R. O'Dell (Rice University) and NASA)

Key Research Findings

Basic Properties

Incidence of Disks – The most sensitive method to determine whether circumstellar material is present around a young star is to measure its infrared excess. Even very small amounts of dust, one Earth mass or less, will emit detectable amounts of emission in the near- or mid-infrared bands. Because only hot dust emits at these wavelengths, this method is only sensitive to dust close to the star. For a solar-type star, measurements at 1–2 μm trace as little as 3.5 Earth masses (1 Earth mass = 5.976×10^{24} kg) in the 0.03–0.1 AU

range where dust temperatures reach 1,000 K; ground- and space-based observations at 3–20 μm probe down to an Earth mass around 0.2–10 AU with dust temperature of 100 K. To accurately determine the presence and amount of dust, the contribution from the stellar photosphere needs to be subtracted and corrections for (interstellar) reddening made. This method works for individual stars, but finds its true power when observing young clusters of stars. In color-color diagrams, the locus of stars with excess infrared emission is immediately apparent and well separated from either field (main sequence) stars or pre-main-sequence stars without excess. This way, the fraction of stars surrounded by disk material can be derived.

Lifetime of Disks – Since the age of a cluster can also be estimated much better than the age of individual stars, infrared excess measurements can be used to answer the question of how long disk material persists. It is found that the disk fraction (relative number of stars with detected dust emission) decreases from more than 80 % for clusters less than a few million years old to less than 10 % for clusters older than 10 million years. For the inner disk, which is what the near-infrared excess is sensitive to, the typical life expectancy is two to three million years, meaning that roughly 50 % of stars will no longer show infrared excess after this period. This statistic is not to be confused with a single disk loosing half its mass over this period; instead, for a sample of disks, half of the objects will have lost *all* (inner) disk material in two to three million years.

If we want to trace material further out in the disk, at temperatures of about 100 K, we need to go to longer wavelengths only accessible from space. Spitzer Space Telescope measurements show that in general objects that lack near-infrared excess also do not show excess emission at 24 μm. This suggests that material from 0.1 AU and out to 20 AU disappears nearly simultaneously. For weak-lined T Tauri stars, it was already known that they do not show near-infrared excess and do not have an inner disk, consistent with their apparent lack of accretion. The Spitzer Space Telescope showed that the disk fraction deduced from 24 μm observations decreases monotonically with Hα line strength. Of weak-lined T Tauri stars less than one to two million years old, more than half have less than 10^{-4} Earth mass within 10 AU. This shows that weak-lined T Tauri stars are not physically older than classical T Tauri stars (many of those still have disks around one to two million years), but have either lost their disk earlier or did not have a disk to start with. The small number of object without an inner disk but with an outer disk (see below) argues that the timescale for disk clearing, once started, is short, $<$0.5 million years.

Finally, only submillimeter observations can trace the cold dust out at 50–100 AU, which emits mainly at these longer wavelengths. Observations from the Submillimeter Array show that of stars without inner disks, at most 10 % have an outer disk of 10^{-3}–10^{-4} solar masses. This supports the idea that the inner and outer disks disappear simultaneously and that the disk dispersal mechanism, once started, is fast compared to the typical time before dispersal kicks in. Note, however, the much less stringent mass limit obtained from submillimeter observations compared to the infrared.

Disk Masses – Unlike infrared wavelengths, at (sub)millimeter wavelengths, the thermal emission from dust in disks is thought to be optically thin and can therefore be used to deduce the mass. This requires an estimate of the (average) dust temperature and the emissivity per unit mass. Typical masses in the range of 0.001–0.3 solar masses are obtained, with a systematic uncertainty of a factor 2–3 due to the ill-constrained emissivity. Especially if dust grains have grown to centimeter size or more, their emissivity drops significantly, and reported disk masses may underestimate the true values. In this determination, a gas-to-dust mass ratio of 100 (the interstellar value) is used. There is no a priori reason why a disk cannot be enriched in either gas or dust if both components evolve differently, and this caveat needs to be kept in mind.

Disk Structure – As mentioned above, the SED provides a powerful tool to determine the disk's structure. The shape of the SED reflects the temperature distribution of the dust (since the emission from hotter material peaks at shorter

wavelengths), which in turn depends on the location of the dust. If the disk is in vertical hydrostatic equilibrium as is commonly assumed, the location and the temperature of the gas and dust are closely linked. In this picture, the gas provides the pressure, while the dust is largely responsible for the energy balance through the intercepted stellar radiation and its own continuum emission. To a lesser extent, other heating mechanisms (e.g., through the photoelectric effect or cosmic rays) and molecular or atomic line cooling may be relevant in some regions of the disk. With detailed measurements of the SED, a self-consistent model for the disk can be fit, and the underlying disk structure obtained.

Pringle (1981) reviews the theory of steady-state accretion disks. Such disks are governed by a small number of conservations laws: conservation of mass dictates that, at every radius, the rate at which mass flows inward (or outward) is balanced by the amount of mass moving in from larger (or smaller) radii. At the same time, conservation of angular momentum dictates that the rate of change of the angular momentum at a given radius is balanced by the amount of angular momentum carried in (or out) of that radius by matter flow *plus* the amount of angular momentum that is *transferred* to material at adjacent radii by *viscosity*. The latter quantity relates the amount of torque that two adjacent radii exert on each other due to the velocity shear (=difference in angular velocity) between them. In the absence of viscosity, matter at adjacent radii can slide past each other without exerting any torque. Matter at all radii will orbit the star at the angular velocity dictated by the laws of Kepler (a so-called Keplerian velocity pattern). In reality, the material will move at slightly lower speeds, because gas pressure provides a small counterbalancing force against the star's gravity. In the presence of viscosity, the faster moving matter at the smaller radius is slowed down by matter at the larger radius (which, in turn, is accelerated). The net result is that matter from the smaller radius will move inward, while angular momentum is carried outward by material in the larger radius.

In the foregoing description, no assumptions are made about the source of the viscosity. Ordinary molecular viscosity is too small to explain existing accretion disks. Shakura and Sunyaev (1973) suggested that turbulence could be an efficient source of viscosity by radially mixing material and exchanging angular momentum. Magnetic fields can offer another mechanism through the so-called magneto-hydrodynamic instability (Balbus and Hawley 1991). Whatever its nature, dimensional analysis shows that viscosity has the units of length times velocity. Locally, the typical length scale would be the hydrostatic scale height H and the typical velocity locally the sound speed c_s. Shakura and Sunyaev parameterized the viscosity as $\nu = \alpha H c_s$, where α is an unknown parameter less than unity. Typically, $\alpha = 0.01$ results in radial density profiles and mass accretion rates that are comparable to observed values. Of course, a single value for α is unlikely to be an accurate description for the full spatial extent of the disk and its temporal evolution.

This simple "α-formulation" produces an accretion disk with matter flowing inward and the outer edge of the disk spreading outward, carrying with it the excess angular momentum. From the conservation of mass and angular momentum, and taking into account the disk's gas temperature as function of radius (which sets the hydrostatic scale height as well as the local sound speed and therefore determines the viscosity in the α-disk description), one finds that the surface density (mass per unit surface area) drops off inversely proportional to radius, $\Sigma(R) \propto R^{-1}$. Another common profile is $\Sigma(R) \propto R^{-1.5}$, which is the density slope inferred for the so-called minimum mass solar nebula (Weidenschilling 1977; Hayashi 1981). This is the density distribution one obtains by taking the current distribution of mass in the Solar System and accounting for the H_2 and He lost from the inner Solar System (evident since the composition of the terrestrial planets differs from that of the Sun) and not bound to the smaller bodies. As such, it represents the distribution of the material that was accreted into planets, but there is no a priori reason why a $R^{-1.5}$ should apply to a disk before planet formation has occurred. With a value of $\alpha = 0.01$, both density distributions

roughly reproduce the observed range of mass accretion rates of 10^{-6}–10^{-12} solar mass per year and the crude correlation between accretion rate and stellar mass.

The vertical structure of disks follows from the radial density distribution and the assumption of vertical hydrostatic equilibrium, resulting in an exponential drop off of density with height above the midplane. For a geometrically thin disk, the temperature decreases with distance from the star as both the distance and the angle of incidence of the stellar radiation increase. However, the stellar gravity also decreases with distance, and the result is a scale height that increases linearly with radius and a disk that is no longer perfectly thin. This raised surface intercepts more light, causing the temperature to drop off less steeply with radius. This in turn causes the scale height to increase faster than the radius, and the disk starts to *flare*. Disk flaring naturally accounts for the flatter temperature profiles and correspondingly flatter SEDs commonly observed.

Flaring disks can be described with varying levels of sophistication. The first attempts approximated the disk as a two-layer structure with a warm surface layer on top of a cooler midplane (Chiang and Goldreich 1997; D'Alessio et al. 1998). Subsequent treatments include more sophisticated radiative transfer and more detailed vertical temperature structure. Such models also include what happens at the inner edge of the disk, where the disk is either truncated by accretion processes or where the dust starts to sublimate (around 1,000–1,500 K). Here, the stellar radiation illuminates the full height of the disk directly, increases the temperature, and raises the scale height. Behind this "puffed-up inner rim," material can only be heated by radiation obliquely entering the surface, and much lower temperatures and scale heights are found. Under some conditions, parts of the disk can be entirely shadowed, receiving no stellar radiation and having a small scale height.

Composition: Gas and Dust

Dust – By mass, roughly 1 % of interstellar material consists of dust particles of sizes 0.01–1 μm. Initially, the gas-to-dust ratio of the disk material will also be 100:1, but this may subsequently evolve throughout the disk's lifetime. The dust particles consist of silicate and graphite cores, as well as some other minerals. They originate in the mass outflows of evolved stars. During their time in the interstellar medium, their minerals become amorphous, and in the cold and dense clouds, preceding star formation is covered by ice mantles of frozen out water, carbon monoxide, and other species. A recent review of our knowledge of ▶ interstellar dust can be found in Draine (2003).

Infrared spectroscopy has shown that dust particles in disks contain olivine, pyroxene, and forsterite. These species show up as broad spectral features in the 8–12 μm region. From the detailed shape of the feature, one can derive the relative fraction of amorphous and crystalline material; the latter has more peaked emission features. Disks show a variation in shapes of 10 μm silicate features, hinting at dust evolution. Infrared interferometry can resolve the emission from disks, and observations have shown that the inner disk (<1–2 AU) is enriched in crystalline material compared to the outer disk. Both crystalline material and ices are observed to be present in comets, indicating that radial mixing of material takes place.

In addition to their composition, dust particles also undergo evolution of their size distribution. The slope of the SED in the (sub)millimeter range, where the dust emission is generally optically thin, is sensitive to the size of the particles. For an interstellar dust size distribution, optically thin continuum emission in the Rayleigh-Jeans regime is expected to follow a flux vs. frequency relation $F_\nu \propto \nu^{2+\beta}$ with $\beta = 2$ (the other factor of 2 originates from the slope of the Planck curve). For particles that have grown in size to about 3 mm, β decreases to approximately 1. The composition of the material, its temperature, and the shape of the dust agglomerates (spherical, linear, or "fractal") also determine the exact value of β and the corresponding mass emissivity. Observations have shown that the slope of the SED in the (sub)millimeter and centimeter regime indicates β values smaller than 1 (Beckwith and Sargent 1991). This suggests that particles have grown to at least a few cm in size. The β-index has been

found to decrease radially toward the star, suggesting faster grain growth closer to the star or inward drift of particles.

An interesting question is whether the dust particles segregate as they grow to larger sizes, with the largest particles settling toward the midplane as they decouple from the gas pressure. In addition, larger dust particles could also drift inward with respect to the gas, as they experience a "head wind" of the sub-Keplerian gas on their Keplerian orbit. Dust settling affects the disk shape and SED, decreasing the far-infrared and submillimeter fluxes. The concentration of larger dust agglomerates in the disk midplane may be an important first step toward planet formation.

Gas – The 99 % of the disk mass that consists of gas is predominantly made up of hydrogen (80 %) and helium (20 %). Only trace amounts of C, O, N, and other elements are present. At the low temperatures and high densities of disks, the gas is predominantly molecular, although the upper layers and the material close to the star may be photodissociated or photo-ionized. The dominant species, molecular hydrogen, is very difficult to detect. Because it lacks a permanent dipole moment, it has no allowed rotational dipole transitions. Its rotational quadrupole transitions are intrinsically weak and fall in the difficult to observe 12–28 μm range for its first few energy levels. These levels also require relative high temperatures of 100 K and more to be excited. Nevertheless, a number of tentative detections have been made. The vibrational and electronic transition of H_2 can be more easily detected, but is generally fluorescently excited by the stellar ultraviolet or X-ray radiation. While they probe the presence of H_2, they cannot generally be used as an accurate mass tracer.

Although only present in trace amounts, molecules like CO offer much easier means to probe the gas content. In the molecular interstellar medium, CO is thought to have a stable abundance with respect to H_2 of approximately 10^{-4}. Its first few rotational levels are easy to excite, lying only several K above the ground level, and its emission lines are strong and occur at easily accessible millimeter wavelengths. Interferometric observations of T Tauri stars in CO with typical resolutions of a few arcseconds (several 100 AU at the typical distance of nearby star-forming regions) reveal flattened structures with clear velocity patterns consistent with the gas orbiting the star.

The disk size inferred from CO observations is often larger than that found from the continuum dust emission, even when accounting for the different surface density sensitivity levels. Although the different sensitivity limits to gas and dust combined with an exponentially tapered outer disk may explain these observations, in at least several cases, millimeter-sized grains have drifted inward leaving only gas and micron-sized grains in the outer disk.

The amount of molecular gas deduced from CO observations is generally lower by factors 10–100 compared to the mass obtained from dust continuum measurements. Although these comparisons include an assumed value of 100 for the, unknown, gas-to-dust mass ratio, the mass discrepancy is usually inferred to imply a reduced CO/H_2 fraction. Some CO may be photodissociated in the upper layers of the disk, and most importantly, significant amounts of CO may be frozen out onto dust particles in the dense and cold ($<$20 K) disk interior. Other species are also detected in disks, such as HCO^+, HCN, CN, CH_3OH, N_2H^+, and H_2CO, and follow similar abundance patterns. Theoretical models predict that molecules (other than H_2 which does not freeze out) are present predominantly at intermediate heights in the disk, where the temperature is high enough for them to be present in the gas phase and the ultraviolet radiation field sufficiently weak for them not to be photodissociated. These models are complicated by the level of radial and vertical mixing that is included. Some species, such as CN, are photodissociation products and are expected to be present at larger heights. Recent observations show strong evidence for the existence of a water snow line where the disk temperature drops to 100 K. Mixing of material across this line traps significant amounts of water ice just outside this snow line. Only small amounts of water vapor exist across the surface of the outer disk, where ultraviolet radiation from the star can photodesorb

some of the ice material. Observations of chemical species that increase in abundance when CO freezes out have indicated the existence of a similar CO snow line when the temperature drops to 20 K. Future observations with large (sub)millimeter interferometers will test these models directly and will offer powerful probes of the disk structure and dynamics.

With so many molecular species frozen out in the disk midplane, little opportunity exists to trace the gas kinematics through spectral line observations. A promising avenue is offered by H_2D^+. This species has its ground state transition in the submillimeter range and can be observed from a good site like Mauna Kea in Hawaii or Chajnantor in Chile. Although the cosmic abundance of deuterium is only about 10^{-5} relative to H, in cold molecular gas, the abundance of deuterated molecules can be enhanced by several orders of magnitude. The formation of H_2D^+ starts with the cosmic-ray ionization of molecular hydrogen, H_2 + cosmic ray $\rightarrow$ H_2^+ + e. H_2^+ then reacts swiftly with another H_2 molecule to form H_3^+ and H. This is followed by the proton-exchange reaction H_3^+ + HD $\leftrightarrow$ H_2D^+ + H_2 which, at temperatures below approximately 20 K, strongly favors the forward reaction because of the lower vibrational ground state energy of H_2D^+ compared to H_3^+. This leads to a strong enhancement of the H_2D^+ abundance and detectable line emission. Another, direct measurement of the gas mass was obtained by the Herschel Space Observatory through detection of the HD molecule in the TW Hya disk (Bergin et al. 2013).

Dynamics

Millimeter-interferometric observations of the CO line have shown that many disks exhibit clear Keplerian velocity patterns, confirming that the flattened structures are indeed rotationally supported and not, e.g., by magnetic fields (so-called *pseudo disks*). From the Keplerian rotation velocities, the mass of the central star can be derived and pre-main-sequence tracks calibrated.

In an accretion disk, material slowly (subsonically) streams inward,, while the outer disk edge spreads. Such low speeds and deviations from Keplerian motion are not easily detected when taking into account possible contributions of (micro)turbulent motions and thermal line broadening (both of the order of 0.1 km s^{-1}). Such observations potentially provide important limits on the levels of disk turbulence and mixing, but require detailed modeling of the line profile to extract the information. Recent work shows that levels of turbulence in the disk interior may be very small (<40 m/s), but increase to 300 m/s well above the midplane.

Evolution

Disk Clearing – As discussed above, roughly half of the disks disperse after 2–3 million years, in a relatively short time of <0.5 million years. The inner disk and the outer disk disappear roughly simultaneously, although there are a small but significant number of so-called transitional disks where the outer disks persist, while the inner disk has dispersed. The Spitzer Space Telescope has proven instrumental in uncovering this class of *cold* or *transitional* disks, through their SEDs which rise sharply in the mid-infrared wavelength regime. One of the first examples is CoKu Tau/4, which has an inner hole of 10 AU devoid of dust (<7–13 *lunar* masses, 1 lunar mass = 7.3×10^{22} kg) inside a 0.001 solar mass disk (D'Alessio et al. 2005). Other examples include MWC 480, LkCa 15, TW Hya, and LkHα 330, all of which have resolved disk clearings using millimeter interferometry (Piétu et al. 2007; Hughes et al. 2007; Brown et al. 2008). Infrared molecular line observations have shown, however, that some "holes" are not entirely devoid of material, e.g., the inner disk around TW Hya is filled with 0.07 Earth masses of warm gas.

Theoretical models suggest two different ways in which protoplanetary disks can develop holes or gaps and enter a phase of rapid dispersal. Theories propose that photo-ionization of the disk surface erodes the disk to the point where at some radius, a gap opens. Once a gap has opened, material interior to the gap quickly drains onto the star; material outside the gap cannot flow inward and over time disperses through photoevaporation as well. The formation of a planet of sufficient mass also opens a gap in the disk, leading to the same draining of the inner

disk. Recent studies suggest that most disk gaps are consistent with being opened by a companion, either stellar or planetary.

Not every disk with an inner hole is necessarily transitional. A close binary will inhibit disk formation within roughly three times its separation. A famous example of such circumbinary disks is GG Tau, where a 45 AU separation binary is surrounded by a 180–800 AU radius circumbinary disk. Each of the binary components individually is surrounded by a small circumstellar disk. Close binaries can explain an unknown fraction of disk gaps. Recent observations of the prototypical transitional disk, CoKu Tau/4, show that it is in fact an 8 AU separation binary, and its disk is therefore circumbinary and not (necessarily) in the process of dispersal.

Disk Formation – Disk evolution starts with disk formation, and surprisingly little is known about this phase. Theoretical models predict that the disks grow gradually throughout the collapse of the prestellar core and protostellar phase. The details depend critically on the original distribution of angular momentum. The formation and growth of a rotating disk from a collapsing core are not amenable to the semi-analytical approaches that have proven so powerful to describe collapse itself. Material spirals inward onto the nascent disk, where it undergoes an accretion shock. The increased temperatures associated with such a shock may have observational consequences in the form of molecular emission lines and have been tentatively identified in observations.

Resolved millimeter-continuum observations are powerful probes of the density in collapsing cloud cores and with difficulty can separate the densest part of the collapsing core from any disk that has already formed. More detailed observations of larger source samples are required to answer important questions such as whether disks form early or late during collapse; whether they form gradually or reach their final mass fast and subsequently transport infalling material efficiently onto the star; how often they go through phases of increased accretion, possibly caused by gravitational instabilities and leading to so-called FU Orionis outbursts; and whether grain growth receives a head start during these early phases.

Planet Formation – The observational evidence for planet formation in disks is indirect: there are clear indications of the growth of dust particles to centimeter sizes, and there is a class of disks with cleared-out inner regions that *could* be explained by the presence of planets around these stars. Recently, strong indication has been found for embedded (proto)planets in at least two disks (LkCa 15 and HD100546).

A close interaction between observational studies of disks and theoretical modeling of planet formation is essential. The former provide the essential initial conditions for planet formation, while the latter may produce testable predictions of the effect that planet formation has on the appearance of disks.

Future Directions

In spite of the rapid progress in the study of circumstellar disks, many important questions remain to be answered in the coming years. Do all stars form with disks, even around massive stars? Do some disks disappear already well within 1 million years, or was a disk never formed? What determines the (final) mass and size range of disks? What are the radial, vertical, and turbulent motions in disks? What is the connection between disk dissipation and planet formation? What fraction of disks disperses as a consequence of planet formation? How fast, and when in its development, do km-size bodies grow in disks? How do disks form? How much grain growth happens early on? Are the disks that survive to several million years the ones that form rich planetary systems, or have these already disappeared to form a planetary system by 1 million years?

Finding answers to these questions will be helped by existing and upcoming facilities such as the Submillimeter Array (SMA), the IRAM Plateau de Bure interferometer, the Combined Array for Millimeter Astronomy, the Atacama Large Millimeter/Submillimeter Array, the Herschel Space Observatory, and the James Webb Space Telescope.

See Also

- ▶ Debris Disk
- ▶ Interstellar Chemical Processes
- ▶ Interstellar Dust
- ▶ Interstellar Medium
- ▶ Pre-Main-Sequence Star
- ▶ Protoplanetary Disk, Chemistry
- ▶ Protoplanetary Disk Instability
- ▶ Protostars
- ▶ Solar Nebula
- ▶ Star Formation, Observations
- ▶ T Tauri Star

References and Further Reading

Adams FC, Lada CJ, Shu FH (1987) Spectral evolution of young stellar objects. Astrophys J 312:788–806

Balbus SA, Hawley JF (1991) A powerful local shear instability in weakly magnetized disks. Astrophys J 376:214–233

Beckwith SVW, Sargent AI (1991) Particle emissivity in circumstellar disks. Astrophys J 381:250–258

Bergin EA, Cleeves LI, Gorti U, Zhang K, Blake GA, Green JD, Andrews SM, Evans NJ, Henning T, Öberg K, Pontoppidan K, Qi C, Salyk C, van Dishoeck EF (2013) An old disk still capable of forming a planetary system. Nature 493:644–646

Brown JM, Blake GA, Dullemond CP, Merín B, Augereau JC, Boogert ACA, Evans NJ II, Geers VC, Lahuis F, Kessler-Silacci JE, Pontoppidan KM, van Dishoeck EF (2007) Cold disks: Spitzer spectroscopy of disks around stars with large gaps. Astrophys J 664: L107–L110

Brown JM, Blake GA, Qi C, Dullemond CP, Wilner DJ (2008) LkHalpha330: evidence for dust clearing through resolved submillimeter imaging. Astrophys J 675:L109–L112

Chiang EI, Goldreich P (1997) Spectral energy distributions of T Tauri stars with passive circumstellar disks. Astrophys J 490:368–376

D'Alessio P, Calvet N, Hartmann L (1998) Accretion disks around young objects I. The detailed vertical structure. Astrophys J 500:411–427

D'Alessio P, Hartmann L, Calvet N, Franco-Hernández R, Forrest WJ, Sargent B, Furlan E, Uchida K, Green JD, Watson DM, Chen CH, Kemper F, Sloan GC, Najita J (2005) The truncated disk of CoKu Tau/4. Astrophys J 621:461–472

O'Dell CR, Zheng W, Hu X (1993) Discovery of new objects in the Orion nebula on HST images – shocks, compact sources, and protoplanetary disks. Astrophys J 410:696–700

Draine BT (2003) Interstellar dust grains. Annu Rev Astron Astrophys 41:241–289

Hayashi C (1981) Structure of the solar nebula, growth and decay of magnetic fields and effects of magnetic and turbulent viscosities on the nebula. Prog Theor Phys Suppl 70:35–53

Hughes AM, Wilner DJ, Calvet N, D'Alessio P, Claussen MJ, Hogerheijde MR (2007) An inner hole in the disk around TW Hya resolved at 7 mm dust emission. Astrophys J 664:536–542

Lada CJ (1987) Star formation – from OB associations to protostars. In: Peimbert M, Jugaku J (eds) Proceedings of the IAU symposium 115, Astronomical Society of the Pacific, San Francisco, pp 1–18

Lada CJ (1999) The formation of low-mass stars – an overview. In: Lada CJ, Kylafis ND (eds) The origin of stars and planetary systems. Kluwer, Dordrecht, pp 143–191

Lada CJ, Wilking BA (1984) The nature of the embedded population in the ρ Ophiuchi dark cloud – mid-infrared observations. Astrophys J 287:610–621

Piétu V, Dutrey A, Guilloteau S (2007) Probing the structure of protoplanetary disks: a comparative study of DM Tau, LkCa 15, and MWC 480. Astron Astrophys 467:163–178

Pringle JE (1981) Accretion disks in astrophysics. Annu Rev Astron Astrophys 19:137–162

Sargent AI, Beckwith S (1987) Kinematics of the circumstellar gas of HL Tauri and R Monocerotis. Astrophys J 323:294–305

Shakura NI, Sunyaev RA (1973) Black holes in binary systems: observational appearance. Astron Astrophys 24:337–355

Smith BA, Terrile RJ (1984) A circumstellar disk around β pictoris. Science 226:1421–1424

Weidenschilling SJ (1977) The distribution of mass in the planetary system and the solar nebula. Astrophys Space Sci 51:153–158

Williams JP, Cieza LA (2011) Protoplanetary disks and their evolution. Annu Rev Astron Astrophys 49:67–117

Protoplanetary Disk Dead Zone

Avi M. Mandell
NASA Goddard Space Flight Center, Greenbelt, MD, USA

Definition

A dead zone is an annular region of a circumstellar disk where the local ▶ viscosity is essentially zero, leading to a negligible infall of disk material toward the central star. Viscosity is needed to

remove the orbital energy and angular momentum from gas and dust in the disk, allowing material to spiral inward and accrete onto the central star (as observed in young stellar systems with known circumstellar material). The source of this disk viscosity is uncertain, but the most likely source is electromagnetic interactions between ionized species, known as the magnetorotational instability (MRI). Dead zones may be created when the local gas is insufficiently ionized to support the MRI. They can occur, for example, when the gas column density is large enough to protect the inner zones of the disk from ionization by cosmic rays.

See Also

- ▶ Planetary Migration
- ▶ Protoplanetary Disk
- ▶ Turbulence (Planetary Disks)
- ▶ Viscosity

Protoplanetary Disk Instability

Avi M. Mandell
NASA Goddard Space Flight Center, Greenbelt, MD, USA

Synonyms

Gravitational instability

Definition

Disk instability refers to a model for giant planet formation in which a region of a circumstellar disk becomes dense and cool enough to be unstable to gravitational collapse, resulting in the formation of a gaseous protoplanet. The disk instability mechanism for giant planet formation has been postulated as a mechanism for forming massive ▶ giant planets on short timescales (1 Ky–1 My), which may be required to form gas giant planets in short-lived disks and disks with a low metal abundance. However, it is unclear whether real circumstellar disks can cool sufficiently quickly to initiate gravitational disk instabilities before the gaseous disk dissipates. The quantitative measure of a disk's ability to become gravitationally unstable is the Toomre Q value.

See Also

- ▶ Core Accretion, Model for Giant Planet Formation
- ▶ Giant Planets
- ▶ Gravitational Collapse, Planetary
- ▶ Protoplanetary Disk
- ▶ Q (Toomre Parameter)

Protoplanetary Disk Midplane

Avi M. Mandell
NASA Goddard Space Flight Center, Greenbelt, MD, USA

Definition

The disk midplane corresponds to the region of a circumstellar disk where the vertical density distribution peaks. The midplane is thought to be the coldest region of the disk, due to the inability of stellar radiation to penetrate deeply. The low temperatures and high densities lead to the fastest growth timescales for ▶ planetesimals and result in planets with coplanar orbits (if no scattering or inclination pumping occurs).

See Also

- ▶ Planetary Migration
- ▶ Planetesimals
- ▶ Protoplanetary Disk
- ▶ Turbulence (Planetary Disks)

Protoplanetary Disk of Second Generation

Avi M. Mandell
NASA Goddard Space Flight Center, Greenbelt, MD, USA

Synonyms

Debris disk

Definition

A second-generation ▶ protoplanetary disk is a disk of circumstellar material created by the destruction of young planetary bodies during the late stages of planetary formation. Such disks are commonly called "▶ debris disks." Debris disks have been detected around stars with ages from 10 My up to billions of years, and they usually contain approximately a lunar mass of material in small grains. The presence of planets is usually unknown, though several giant planets have now been directly imaged in debris disks.

See Also

▶ Debris Disk

Protoplanetary Disk, Chemistry

Dmitry Semenov
Max Planck Institute of Astronomy, Heidelberg, Germany

Keywords

Accretion; Chemical reactions; Circumstellar disks; Depletion; Dissociation; Dust grains; Freeze out; High-energy radiation; Ices; Ionization; Isotopic fractionation; Molecular lines; Molecules; Photochemistry; Radio-interferometers; Solar nebula; (Sub)millimeter observations; Turbulence; Young stellar objects

Definition

▶ Protoplanetary disks (PPDs) surrounding young stars are short-lived (∼1–10 Myr), compact (∼10–1,000 AU) rotating reservoirs of gas and dust. Disks are believed to be the birthplaces of planetary systems, where tiny grains are assembled into pebbles, ▶ planetesimals, and eventually planets, asteroids, and comets. The evolution of gas and grain growth in disks is related to the redistribution and transport of angular momentum, which is thought to be governed by magnetohydrodynamical turbulence. The intense high-energy radiation from one or more young stars and strong spatial and temporal variations in the physical conditions (accretion rate, temperature, density, grain sizes) make a variety of chemical processes active in protoplanetary disks. In PPDs, simple molecules are rapidly produced in the gas phase via ▶ ion-molecule and ▶ neutral-neutral reactions. The more complex (organic) species in disks are slowly synthesized on and in the icy mantles of dust grains and later are either released to the gas phase or become trapped inside growing dust aggregates.

Overview

It is particularly important to understand under what conditions prebiotic molecules and their simpler "building-block" precursor species could be produced and how they evolve during the star- and planet-formation process. Powerful ground-based and airborne observational facilities and robotic space missions have recently become available, which have permitted the chemical composition of nearby star-forming regions to be sensed remotely and pristine Solar System materials to be collected in situ. In addition, increasing computer power makes sophisticated simulations of the interstellar chemistry

feasible. The progress is particularly rapid in understanding the physics and chemistry of protoplanetary disks around young stars – analogs of our Solar System at the age of several million years.

Many protoplanetary disks surrounding young Sun-like stars possess sufficient material, of order several Jupiter masses, to assemble planetary systems(e.g., Lin and Papaloizou 1980; Payne and Lodato 2007; Williams and Ciesza 2011). According to the modern paradigm of star formation, the collapse of a cold ▶ molecular cloud of several solar masses leads to formation of (a) protostar(s) surrounded by a compact, rotating, flattened structure, the protoplanetary disk. The protostar is initially still enshrouded by an envelope of cloud material. During a few million years of dynamical evolution, much of the prenatal cloud material accretes on to the protostar, with some material ejected as a ▶ bipolar outflow. After that, the outflow ceases and the newly born central star becomes visible.

Photospheric activity of the star drives intense, variable ultraviolet (UV) and X-ray radiation, leading to steady photo-evaporation and, after taking account of ongoing accretion, to dispersal of remaining disk matter (e.g., Gorti et al. 2009). The dense disk interior conditions are favorable for rapid agglomeration of submicron-sized dust grains into larger cm-/m-sized pebbles and rocks. During formation, they sediment toward the disk equatorial plane ("▶ Protoplanetary Disk Midplane"), eventually forming ▶ planetesimals and planets as well as ▶ comets, or move inward due to gas friction and are accreted onto the star. The forming planets interact gravitationally with the surrounding gas, inducing asymmetric spiral waves and other substructures, and may even open gaps or clear central holes in disks (e.g., Fukagawa et al. 2004; Grady et al. 2013).

Molecules are important diagnostics of physical conditions in disks. Also, molecules are key heating and cooling agents of the gas, especially in the disk atmospheres. Dust grains determine the opacity of the disk medium to the stellar radiation and so shape the disk thermal and density structure. Ionization chemistry induced by high-energy radiation from (a) central star(s) or interstellar space and cosmic ray particles (CRPs) determines the strength of the coupling between the gas and magnetic fields, thus controlling the global disk dynamics via ▶ turbulence.

Consequently, a strong time-dependent variation of temperature, density, and dissociating radiation intensity across a disk induces pronounced spatial gradients and leads to a rich chemistry in the gas phase and on the surfaces of dust grains. In this entry, we summarize *the major modern observational methods and theoretical paradigms* used to investigate disk chemical composition and evolution and present the most important results. Future research directions that will become possible with the advent of the Atacama Large Millimeter Array (▶ ALMA) and other forthcoming observational facilities are also discussed.

Basic Methodology

In the table and in the text that follows, we use the standard spectroscopic notation that specifies the ionization state by Roman numerals: I for a neutral atom (e.g., NeI for Ne), II for singly ionized (e.g., NeII for Ne+), etc. So far, astronomers have discovered about 160 molecular species (230 including isotopomers) in space (▶ Molecules in Space). These vary from simple radicals (e.g., CH^+) to complex molecules like cyanopolyynes (e.g., $HC_{11}N$), ▶ polycyclic aromatic hydrocarbons (PAHs; up to C_{60} and C_{70}), and organic molecules (e.g., CH_3OH, HNCO, $HCOOCH_3$, $HOCH_2CHO$) as well as positive (e.g., HCO^+) and negative (e.g., C_8H^-) ions. Among these interstellar species, only a handful of molecules have been identified in disks through infrared (IR) and (sub)millimeter spectroscopy: H_2, HD, CII, NeII, FeI, OH, H_2O, CO (and isotopologs), CN, HCN, DCN, HNC, HC_3N, C_2H, C_2H_2, c-C_3H_2, CS, HCO^+, H_2CO, DCO^+, NH_3, and N_2H^+ (Dutrey et al. 1997, 2007b; Kastner et al. 1997; Aikawa et al. 2003; Qi et al. 2008, 2013; Chapillion et al. 2012).

Solid materials detected in nearby PPDs via infrared spectroscopy include aliphatic and aromatic carbon-based materials (in unknown form),

polyaromatic hydrocarbons (PAHs), amorphous and crystalline silicates of olivine and pyroxene stoichiometry, and molecular ices (like CO, CO_2, H_2O). The presence of various other organic compounds has also been inferred (e.g., Terada et al. 2007; Acke et al. 2010; Min and Flynn 2010; Henning and Meeus 2011; Teske et al. 2011; Aikawa et al. 2012; Bergin et al. 2013).

Another vital source of information about the pristine composition of solids at the verge of planet formation in the young Solar System are the studies of meteoritic materials and cometary samples and remote observations of active comets passing near the Sun (Ehrenfreund and Charnley 2000). An isotopic analysis of various primitive refractory materials allows us to discern the time of their condensation (▶ radiogenic dating). In addition, petrological, mineralogical, and texture analyses constrain the timescales of the cooling of the freshly formed minerals and the physical conditions (temperature, density) at which they have condensed out.

Unfortunately, a vast majority of volatiles have either vaporized during the formation and evolution of solids or have been lost due to further thermal processing in the meteorite parent bodies or during the sample preparation in the laboratory. A direct access to the composition of pristine ices and organics in cometary dust is possible via robotic missions, like the *Stardust* mission that collected and delivered to Earth the first dust samples from the comet *Wild* 2 (Elsila et al. 2009; Wozniakiewicz et al. 2012). The Rosetta mission of the European Space Agency will deposit by November 2014 a lander and an orbiter on the comet 67P/Churyumov-Gerasimenko for detailed in situ analysis of the comet surface (http://www.esa.int/Our_Activities/Space_Science/Rosetta/Europe_s_comet_chaser).

(Sub)millimeter Observations

Dusty PPDs are transparent only when observed at wavelengths longer than ~100 μm (far-infrared/(sub)millimeter wavelengths). Since the dominant molecular component of the gas, H_2, does not emit observable radiation at (sub)millimeter wavelengths apart from high-temperature regions around the star (e.g., Bitner et al. 2007), other trace species and dust are used to study physical conditions in disks (Table 1). A unique tracer of the total gas mass is deuterated molecular hydrogen, HD, whose fundamental rotational transition at 112 μm has been recently detected with the ▶ *Herschel* satellite toward the nearest protoplanetary disk around TW Hya (Bergin et al. 2013).

At (sub)millimeter wavelengths, there are no prominent solid-state features, but the observed continuum emission allows us to estimate dust disk mass and infer the presence of large, millimeter-sized grains. Since dust opacities at these wavelengths and the dust/gas mass ratio are poorly known, the constrained disk mass is subjected to large uncertainties.

By contrast, the (sub)millimeter spectral window is rich in molecular rotational lines. It is not fully accessible from the ground due to atmospheric absorption, primarily by water and hydroxyl (OH). Single-dish telescopes like the IRAM 30-m antenna (ESO, Spain), the APEX 12-m antenna (ESO, Chile), and the 15-m James Clerk Maxwell Telescope (UK, Hawaii) are used to survey PPDs in lines of potentially detectable species. Although lacking the spatial resolution to resolve the disks, single-dish molecular spectra allow astronomers to constrain disk-averaged amounts of emitting molecules (column densities) and roughly estimate disk orientation and temperature.

The sub-arc-second imaging required to resolve PPDs is provided by antenna arrays such as the Plateau de Bure Interferometer (France), the Submillimeter Array (USA), and the Combined Array for Research in Millimeter-wave Astronomy (USA). Since 2013, observations have begun with the much more powerful Atacama Large Millimeter Array (▶ ALMA, Chile), a joint project of Europe (ESA), the USA, and Japan. Until the advent of ALMA, such studies were scarce and restricted to outer disk regions ($r > 30$ AU). The objects best studied thus far included DM Tau, LkCa 15, AB Aur, TW Hya, MWC 480, HD 163296, and HD 100546. In PPDs, most molecular lines are optically thin and so their observed spectral line shapes result from a combination of molecular spatial distribution, excitation conditions, and transport of the line radiation

Protoplanetary Disk, Chemistry, Table 1 Diagnostic molecules used to study disk physics and chemistry and wavelength ranges of observations (e.g., millimeter, centimeter, and infrared (IR)). In the three columns giving the wavelength range of the observations for a particular portion of the disk, 0 indicates that the molecule is not present and a dash (–) indicates that the molecule is either not excited or not present; in the Probe column, a dash indicates the same property as in the row above

Species	Probe	Midplane	Molecular layer	Atmosphere	Inner zone
^{12}CO, ^{13}CO, $C^{18}O$	Temperature, density	mm	mm	sub-mm	IR
H_2	Temperature	–	–	–	IR
HD	Density	IR	IR	IR	–
NH_3	–	cm	cm	0	0
CS, H_2CO, HC_3N	Density	0	mm	0	IR
C_2H, HCN, CN, OH, H_2O, C_2H_2, c-C_3H_2	Photoprocesses	0	mm	0	IR
HCO^+	Ionization	mm	mm	0	0
N_2H^+, H_2D^+	–	mm	0	0	0
C^+	–	mm	0	IR	IR
Metal ions (e.g., NeII)	–	0	0	0	IR
Complex organics (e.g., H_2CO)	Surface chemistry	IR	IR, mm	0	IR, mm
DCO^+, DCN, H_2D^+	Deuterium fractionation	mm	mm	0	0
CO, CS, HC_3N	▶ Turbulence	mm	mm	mm	0

through the disk. The molecular spectra yield unique information on disk kinematics and geometry, temperature and density structure, and the intensity of dissociating and ionizing radiation.

The disk size and orientation can be constrained directly by the geometry of dust emission and integrated line intensity maps (e.g., ^{13}CO 1-0); see Fig. 1. Next, the PPD kinematics can be recovered by analyzing the velocity at various points in the disk from the Doppler shift of molecular lines. By high-resolution observations of heavy molecules like CS and HC_3N, which have narrow intrinsic and thermal broadening of the line profiles, one can constrain the levels of gas turbulence in outer disk regions (Guilloteau et al. 2012, see also Hughes et al. 2011). For molecules with high dipole moments and regular energy-level structure (e.g., CS, H_2CO, HC_3N, HCO^+), multi-transition observations constrain the gas density distribution, since higher energy transitions require higher densities for excitation. The thermal disk structure is derived from the strength of optically thick CO lines (e.g., ^{12}CO 1-0, ^{12}CO 2-1, etc.), which trace different disk heights. The line shapes of CO ▶ isotopologs carry information about both temperature and molecular density distribution, and these can be used to derive the disk surface density profile. Ratios of line intensities for a parent molecule and its photodissociation product (like HCN and CN) reflect the strength of the disk irradiation by high-energy UV photons. However, for larger molecules, the population is divided over many energy levels, leading to lower line intensities and making it harder to detect and resolve the spectra of such species. Furthermore, the spectra of molecules with a complex level structure, like water, are particularly difficult to analyze. Therefore, to fully interpret interferometric spectra of a given molecule, one has to construct computational models which take into account many disk properties, kinematics and geometry, density and thermal structure, and radial and vertical molecular distributions, and employ a line radiation transport model to fit the observed data iteratively.

Infrared Observations

At IR wavelengths, spectral features associated with various components of solid dust particles

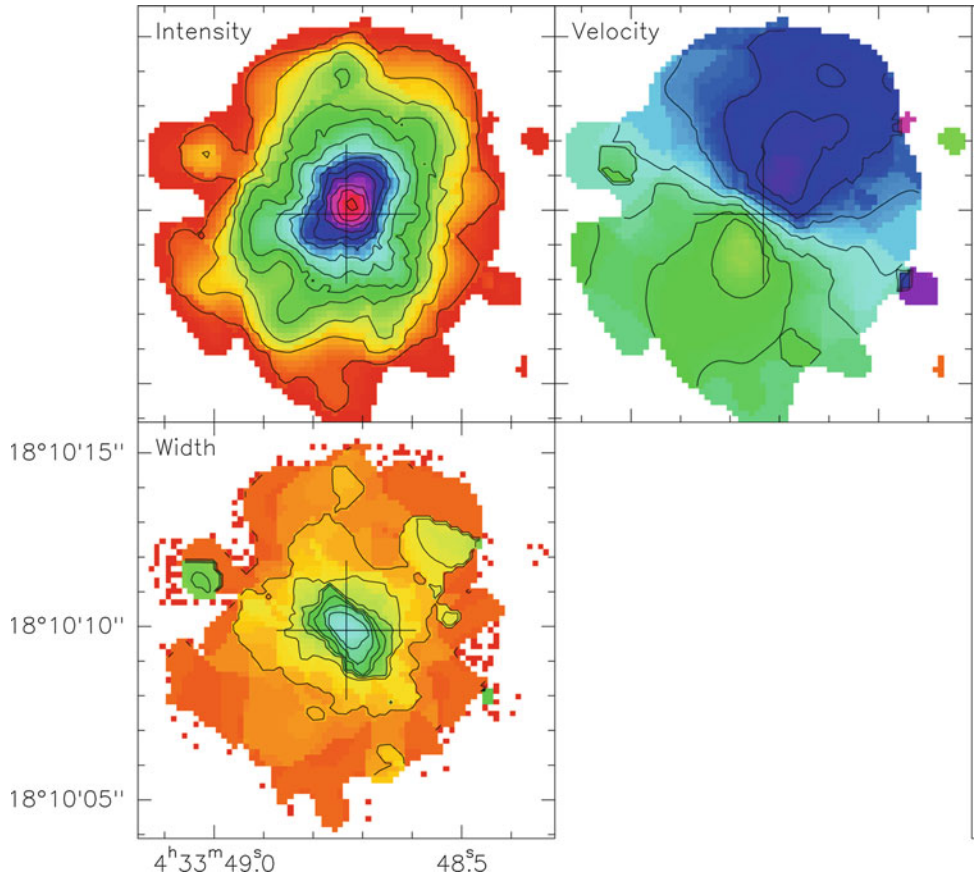

Protoplanetary Disk, Chemistry, Fig. 1 The DM Tau disk imaged with the Plateau de Bure Interferometer in the HCO^+ 1–0 line with 1.5″ resolution. Shown are the integrated line intensity (*top left*) that increases toward the central star (indicated by cross), the velocity map (*right top*) that reveals a "butterfly"-like symmetric pattern typical of rotating disks (*bluer* side approaching, *greener* side receding), and the line width distribution (*bottom left*), where velocity increases toward the disk center due to Keplerian rotation ($V(r) \propto r^{-1/2}$)

are evident, as are the rotational-vibrational and vibrational bands of gas-phase species (e.g., due to stretching and bending of molecular bonds). Atmospheric transparency windows permit limited observations from the ground, and so spaceborne telescopes are essential for full spectral coverage. From analysis of these data, we can constrain the local temperature and amount of absorbing/emitting material on the line of sight. The ratio between near-IR and far-IR dust emission is used to indicate an evolutionary phase of a disk, because in an old system, dust grains may grow so big in the dense inner region that the near-IR flux disappears, while the far-IR excess emission is still characteristic of cold, submicron-sized grains (Bouwman et al. 2008).

The inner, ∼1–20 AU planet-forming disk regions only recently became accessible, with the advent of near- and mid-IR ground-based interferometers (such as those at the Palomar Observatory, W.M. Keck Observatory, and Very Large Telescope Observatory) and the launch of space observatories (the ▶ Infrared Space Observatory, ▶ Spitzer Space Telescope, and ▶ Herschel Mission). IR interferometers do not retain the phase information of the detected signal and thus require sophisticated analysis of the acquired data based on template disk models to constrain the geometry and mass of the hot dust region. The (ro-)vibrational emission/absorption molecular lines and solid-state emission bands of ices as well as a variety of silicates and polyaromatic

hydrocarbons (▶ PAHs) and simple organics have been detected in disks (van Dishoeck 2004; Pontoppidan et al. 2005; Lahuis et al. 2006; Pascucci et al. 2007; Bouwman et al. 2008; Zasowski et al. 2009; Acke et al. 2010; Salyk et al. 2011; Teske et al. 2011; Fedele et al. 2012). Identified species include H_2O, C_2H_2, HCN, OH, NeII, and some others; from their spectra local temperature, FUV intensity and molecular concentrations can be derived.

The major components of dust grains in disks are amorphous and crystalline silicates (e.g., $MgSiO_3$ and Mg_2SiO_4), troilite (FeS), metals and oxides, quartz, C-containing compounds, and water/CO ices (Pollack et al. 1994). Metals do not have any distinct spectroscopic signatures, while only certain carbon-bearing compounds show generic aliphatic and aromatic features, making it difficult to identify their exact composition (which is likely a mixture of ▶ hydrogenated amorphous carbon, diamonds, ▶ PAHs, and polymerized organic materials). Studies of chemical and petrological compositions of meteorites and samples of cometary materials seem to be the only possibility to try to understand the properties and composition of the pristine organics that can be present at the planet-formation stage of the disk evolution (Ehernfreund and Charnley 2000).

Key Research Findings

Outer Disk: (Sub)millimeter and Far-Infrared Observations

High-resolution interferometric observations at submillimeter and millimeter wavelengths have allowed the chemical composition and physics of the outer regions (beyond 30–50 AU) to be examined in several nearby PPDs. Observations at the Plateau de Bure Interferometer (PdBI; France), the Very Large Array (USA), and the Australia Telescope Compact Array (ATCA) at millimeter and centimeter wavelengths show evidence for significant grain growth up to cm sizes in disks (e.g., Rodmann et al. 2006; Cortes et al. 2009; Guilloteau et al. 2011). The IR spectroscopic surveys of young stars in stellar clusters of various ages have placed tight constraints on typical dispersal times of dense ▶ protoplanetary disks of ~5 Myr, while their inner, planet-forming zones (<10–100 AU) are cleared of submicron-sized dust grains within only ~1 Myr (Fedele et al. 2010).

Prominent low- and high-energy CO rotational lines are readily excited by collisions at densities of $\sim 10^3$–10^5 cm^{-3}. The ^{12}CO lines are ▶ optically thick, and their intensities measure kinetic temperature in the disk upper layer. The lines of less abundant ^{13}CO and C^{18}O are typically optically thin or partially optically thick and are sensitive to both temperature and the CO column densities through the disk. Strong CO lines are suitable for accurate determination of disk kinematics, orientation and geometry, and hence the mass of the central star. From interferometric observations, it has been found that measured disks radii appear the smallest for the dust continuum and progressively larger in the C^{18}O, ^{13}CO, and ^{12}CO lines, with typical values of ~100–1,000 AU. Multi-line CO studies have revealed a clear sign of vertical temperature gradients in several disks, increasing from ~10 K at the midplane to ~50 K in the atmosphere region (e.g., Dartois et al. 2003; Qi et al. 2006; Piétu et al. 2007). The high surface temperature of the TW Hya disk as measured by the ^{12}CO ($J = 6-5$) line cannot be solely caused by the black body stellar radiation and requires an additional heating source, likely stellar X-rays (Qi et al. 2006). A number of protoplanetary disks with large inner "dust" holes, such as LkCa15, do not show temperature variation in the vertical direction and thus must have a peculiar structure. Dartois et al. (2003) and Piétu et al. (2007) have reported that a large amount of CO and other gas-phase molecules exist at ~10–15 K in the DM Tau disk, which contradicts the expectation that most of these molecules should reside on grains at such low temperatures. The recent interferometric observations of water vapor in the closest disk around TW Hya by (Zhang et al. 2013) determined the location of the "snow line" (the location where water ices is thermally evaporated, T ~120–160 K) and thus constrain the disk's radial temperature distribution. In a similar study, (Qi et al. 2013) have

observed the TW Hya and HD 163296 disks in lines of N_2H^+ and H_2CO and inferred the location of the "snow line" for CO, which is located far away from the central stars, where dust temperatures are below 20 K.

Molecules with larger electric dipole moments than CO require higher gas densities to excite emission, since collisional excitation must overcome radiative de-excitation in order for higher energy levels to be populated. An easily observable molecular species in disks is HCO^+, which does have a larger dipole moment (3.92 D = Debye). The lower energy $J = 1$-0, 2-1, and 3-2 transitions of this ion (J is the rotational quantum number) are excited at densities of $\gtrsim 10^5$ cm^{-3} and are (partially) optically thin. This is one of the most abundant charged species in PPDs, the other being C^+, which is not observable at millimeter wavelengths. Due to its large dipole moment, HCO^+ is a good density probe, in addition to being a tracer of ionization degree (see Table 1). Another, less abundant observable ion in disks is N_2H^+ (3.37 D). The 1-0 N_2H^+ line exhibits hyperfine splitting, and so from relative intensities of its individual components, one can reliably determine the ▶ optical depth of the line and constrain the N_2H^+ column density. Using these ions as probes, it has been found that the degree of ionization in disk interiors is $\sim 10^{-9}$ (one charged species per billion), in agreement with the derived cosmic ray ionization rate and predictions from disk chemical models (Qi et al. 2003).

The distribution and total amount of HCN and its dissociation product, CN, depend on the intensity and spectral shape of the high-energy UV radiation impinging into the disk (Bergin et al. 2003). The stronger the FUV flux, the higher the CN-to-HCN line ratio due to higher concentrations of CN and lower abundances of HCN. The observationally inferred elevated ratio of CN to HCN abundances indicates that the chemistry in PPDs is indeed affected by the stellar FUV radiation. Another radical observed in disks, C_2H, is sensitive to the X-ray luminosity of the central star, as higher flux of X-ray photons replenishes more of the elemental carbon locked in CO back into the gas phase, where it is quickly converted to light hydrocarbons (Henning et al. 2010). The recently detected cyclopropenylidene (c-C_3H_2) in the disk of TW Hya with the ALMA interferometer by Qi et al. (2013) seems to be another excellent tracer of the UV radiation intensity penetrating through disk upper layers.

Rotational lines of the less abundant CS and H_2CO are difficult to observe even in bright disks. The CS lines, excited at densities $n \sim 10^5$–10^7 cm^{-3}, have very narrow intrinsic widths and as such can be utilized to measure turbulent gas velocities in disks through the Doppler effect, as well as to discern disk density structure. The measured turbulent broadening is subsonic, with a typical microturbulent velocity of $\sim$0.05–0.2 km s^{-1} (Hughes et al. 2011; Guilloteau et al. 2012). The simplest organic molecule, H_2CO, has a slightly asymmetric top structure and serves as both a densitometer and a thermometer. It is partly produced on surfaces of dust grains and can also be used as a probe of the efficiency of surface chemical processes. Recently detected DCO^+ and DCN in TW Hya have abundances comparable to the abundances of their main isotopologs, HCO^+ and HCN (Qi et al. 2008), while the cosmic abundance ratio of D/H is only 10^{-5}. Their radial distributions in the TW Hya disk have been derived by Oberg et al. (2012) using the Science Verification ALMA data. While DCO^+ column density increases with radius in the disk, the DCN emission is more centrally peaked, indicating different pathways to deuterium fractionation in disks. It remains to be verified though whether such a large degree of deuterium fractionation is a heritage of pre-disk cold evolutionary phases in the parent ▶ molecular cloud or if these large D/H ratios can be produced in situ in PPDs.

A remarkably consistent finding is that gas-phase molecular abundances relative to molecular hydrogen are lower by factors of 5–100 compared to the values in the cold interstellar Taurus Molecular Cloud (Dutrey et al. 2007). This has been interpreted as a combination of intense UV and X-ray dissociation of molecules at elevated disk heights by the young central stars and proficient sticking of gas-phase molecules to dust grains in cold disk interiors, forming thick icy mantles.

The observations at far-infrared wavelengths with the ▶ *Herschel* space telescope probe molecular emission lines and solid-state bands of ices and silicates arising at distances of ~1–100 AU in disks. The data are still being reduced and analyzed; here we report on major recent discoveries that have been published.

In a number of protoplanetary disk orbiting around Sun-like and more massive, hotter intermediate-mass Herbig stars, emission from hydroxyl (OH) has been detected. Combined with ▶ *Spitzer* observations of warm water, there is an apparent lack of water in the more heavily irradiated disks around Herbig stars, suggesting that H_2O in their upper inner disk regions can be severely dissociated (Fedele et al. 2013).

The non-detection of cold H_2O in DM Tau provided stringent upper limits to the amount of water vapor in the outer disk region. The low amount of water vapor cannot be explained by modern astrochemical models. A plausible scenario is that a substantial fraction of water ice (the major reservoir of water) can be already locked in big grains that settled toward the midplane, unable to be photo-evaporated (Bergin et al. 2010). A higher amount of water vapor in the disk around another star, DG Tau, was inferred by Podio et al. (2013). Using an advanced disk physical and chemical model, they derived that the water emission stems from a hot region of ~600 K in the upper disk region, with a total amount of water vapor of $\sim 10^2$–10^3 Earth oceans (and 100 times more in the solid form).

(Hogerheijde et al. 2011) have successfully detected emission lines from both the ortho- and para-spin isomers of water in the disk around TW Hya. This ratio cannot be changed by radiative or collisionally induced transitions and can only be modified by chemical processes involving proton exchange. The ortho-para ratio (OPR) of water is thought to be determined by the temperature at which water ice formed on dust grains via hydrogenation of surface O and OH. Hogerheijde et al. have found that the ortho-para ratio for H_2O in TW Hya is 0.77, indicating low temperatures of the H_2O ice formation, ~15–20 K. Interestingly, this temperature seems to be lower than the temperatures derived from various OPR ratios measured in Solar System comets (~30–50 K; see Woodwart et al. 2007; Bockelee-Morvan et al. 2009; Bonev et al. 2013).

A detection of pure HD rotational lines in the TW Hya disk allowed probing for the first time the total gas disk mass, as the HD/H_2 ratio should not change much even in warm protoplanetary disks (Bergin et al. 2013). The inferred disk mass was larger than previously suggested, 0.05 solar masses, which is somewhat surprising for a ~5 million-year-old system.

Inner Disk: Infrared Spectroscopy

Results from the ▶ Infrared Space Observatory and the ▶ Spitzer Space Observatory have revealed the presence of a large amount of ice, ▶ polycyclic aromatic hydrocarbons (PAHs), and both amorphous and crystalline silicates in disks (e.g., Bouwman et al. 2008; van Dishoeck 2004; Pontoppidan et al. 2005; Lahuis et al. 2006; Pascucci et al. 2007). The PAH features at ~3–12-μm probe the intensity and shape of the incident radiation field and the density distribution in the disk. Only ~10 % of PPDs around young Sun-like stars show aliphatic (C-H) and aromatic (C-C) PAH bands, and often these bands appear only in the outer disk zone (beyond ~30–100 AU). The small PAHs with unbound geometry (<50 C atoms) are destroyed by the intense FUV and, in particular, X-ray stellar radiation, while bigger and compact PAHs do survive in PPDs. The PAHs remain in the gas phase only in dilute, ice-free upper disk regions and are frozen out in disk interiors. It is interesting to note that the 3-μm diamond emission tends to be centrally peaked in PPDs, which may indicate a high-temperature conversion of H-poor large PAHs into ▶ nanodiamonds.

A multitude of amorphous and crystalline silicates with varying Fe/Mg ratios and grain topology/sizes have also been detected (Bouwman et al. 2008). A striking result is that both the crystallinity fraction and the abundance ratio of forsterite/enstatite ($Mg_2SiO_4/MgSiO_3$) change across a disk. The fact that mid-IR features are characteristic of mostly iron-poor silicates implies their rapid condensation from the gas

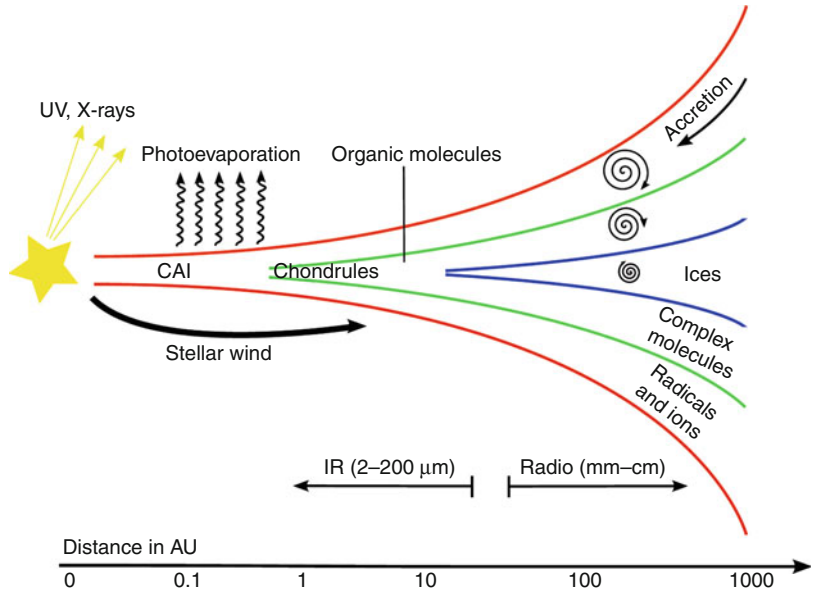

Protoplanetary Disk, Chemistry, Fig. 2 A sketch of the vertical structure of a protoplanetary disk

phase during transformation of a ▶ molecular cloud into a disk. Other metals like Fe and Ca are found as a component (often as sulfides) of glassy inclusions inside a silicate matrix in meteorites (see ▶ GEMS). The variety of observed silicate band profiles is due to various average sizes of emitting grains, implying that small submicron-sized particles and bigger, several micron-sized grains exist in PPDs.

Ices are present in the cold, outer disk region beyond the "snow line," at temperatures below $\sim$120 K ($r \gtrsim 20$ AU). These features are easier to detect in highly inclined systems. The major mantle component is water ice, with an abundance of about 10^{-4} (relative to the total particle density). Water ice is intermixed with other, more volatile ices of, e.g., CO, CO_2, NH_3, CH_4, H_2CO, and HCOOH (Zasowski et al. 2009). Typical abundances of these minor constituents are about 0.5–10 % with respect to water. As it has been revealed from the complex shape of icy features with substructures, a substantial part of these volatile ices can be chemically bound to grain surface sites ("chemisorbed") and thus will remain frozen even at elevated grain temperatures and UV irradiation.

The detection of NeII line emission from several disks, as well lines from iron, sulfur, and argon, has confirmed theoretical predictions that the disk atmosphere is heavily ionized and superheated by the energetic photons. Detected rotational H_2 and (ro-)vibrational CO, CO_2, C_2H_2, and HCN as well as H_2O and OH lines trace a hot gas in the inner, planet-forming disk zone with $T \sim 300$ K (Lahuis et al. 2006; Salyk et al. 2008). The HCN-to-C_2H_2 ratio is a sensitive tracer of the UV/X-ray intensity or accretion rate inside an inner disk, while the easily populated CO lines allow us to constrain kinetic temperature. The rich chemical composition inside planet-forming disk zones suggests that many endothermic reactions with barriers become active there.

Theoretical Picture of Chemical Structure of a Disk

We present a general scheme of a PPD structure based on observational results and theoretical predictions in Fig. 2 (see, e.g., Aikawa and Herbst (1999), Willacy and Langer (2000), Bergin et al. (2003), van Zadelhoff et al. (2003), and Semenov et al. (2004); for a discussion of ▶ CAIs and ▶ chondrules, see the links). The viscous evolution of the disk gas is driven by the angular momentum transport due to turbulent torques. This leads to inward transport of the bulk

of the disk matter (~80 %), while a minor fraction of the disk gas carries the angular momentum outward (mostly along the midplane). This leads to a steady-state power-law surface density profile that has a radial dependence that is roughly proportional to $r^{-3/2}$ (surface density ~1,700 g cm^{-2} at 1 AU for the model ▶ solar nebula). In the vertical direction, the gas density drops exponentially away from the midplane. The average temperature in disks decreases radially outward and, for a given distance, increases from the disk midplane to disk atmosphere. The stellar radiation heats the upper layers such that the disk develops a flared structure. The upper disk atmosphere has a low density, resulting in higher gas temperatures compared to those of the dust. Closer to the star, the gas temperature in the disk atmosphere rises so high ($T \sim$ 1,000–5,000 K) that the matter starts to evaporate. As one moves below the upper atmosphere, the disk density increases and the gas and dust temperatures reach an equilibrium value. In the very inner part, the disk midplane is again warmed up by the viscous accretion heating.

The intensity of ionizing and dissociating UV radiation is determined by the dust opacities, while penetration of the stellar X-ray radiation into the disk is controlled by the gas density structure. The larger the energy of a photon or a particle, the deeper disk regions it can reach. The stellar X-ray emitting source is often located high above the star's photosphere, at distances of several stellar radii (~0.01 AU), and thus X-ray photons reach the disk atmosphere at an oblique angle and are able to penetrate deeper into the disk interior compared to the UV photons. The stellar UV intensity drops in the disk with radius as r^{-2}, while the X-ray intensity decreases even faster, and the interstellar UV radiation starts to prevail in the outer disk region ($r \gtrsim$ 100 AU). The FUV continuum radiation is blocked by a gas column of <0.01 g cm^{-2}, hard X-ray photons (~1–5 keV) are stopped at a gas column of 0.1–1 g cm^{-2}, and ~GeV cosmic ray particles penetrate gas columns as large as ~100 g cm^{-2}.

Consequently, the disk structure can be divided into four chemically distinct regions: the warm "inner zone" where a planetary system is built (observable currently only at IR and optical wavelengths) and the differing layers in the outer disk region observed by modern radio-interferometric facilities. The inner region is at thermodynamical equilibrium, and chemical abundances there can be calculated as a function of temperature, pressure, and elemental abundances by ▶ condensation sequence modeling. The major problem here is to obtain reliable equilibrium coefficients for all species of interest. Chemical kinetics controls the evolution of the outer disk region ($r >$ 20–50 AU). It is divided into a cold, dense disk midplane where dust grains are coated with ices, a slightly UV-/X-ray-irradiated warm layer above the midplane with a rich chemical composition, and a heavily ionized, hot, and dilute disk atmosphere.

The key reactions for disk chemistry are summarized in Table 2. Modern astrochemical databases include up to 600 species involved in 6,000 gas-phase, gas-grain, and surface reactions. Only ~10 % of the reaction rates have been accurately measured in the laboratory or calculated theoretically, making calculated molecular concentrations uncertain by factor of ~3–5 (see, e.g., Wakelam et al. 2006; Vasyunin et al. 2008). The most widely utilized astrochemical networks are those of the University of Manchester (UMIST) (Woodall et al. 2007), the Ohio State University (OSU) (Smith et al. 2004), Kinetic Database for Astrochemistry (KIDA; Wakelam et al. 2011), and a network incorporated in the Meudon code (Le Petit et al. 2006). Several datasets of surface reactions have also been compiled (e.g., Tielens and Hagen 1982; Hasegawa et al. 1992; Garrod and Herbst 2006).

The formation and destruction of polyatomic molecules in a ▶ protoplanetary disk continue from preceding dense core phase and are controlled by various chemical processes (Table 2). In the dense inner zone, three-body gas-phase processes become competitive at densities above ~10^{10}–10^{13} cm^{-3} (Aikawa et al. 1999); otherwise all gas-phase reactions in PPDs are one- and two-body processes. As majority of key species such as H_2, H_2O, and CO have been formed in cold prestellar cores or even at earlier evolutionary stages, radiative association

Protoplanetary Disk, Chemistry, Table 2 Key chemical processes in protoplanetary disks

Name	Representation	Example	Rate[a]
Radiative association	$A + B \rightarrow AB + h\nu$	$C^+ + H_2 \rightarrow CH_2^+$	$\sim 10^{-10}$–10^{-17} cm^3 s^{-1}
Ion-molecule	$A^+ + B \rightarrow C^+ + D$	$CO + H_3^+ \rightarrow HCO^+ + H_2$	$\sim 10^{-7}$–10^{-10} cm^3 s^{-1}
Neutral-neutral	$A + B \rightarrow C + D$	$O + CH_3 \rightarrow H_2CO + H$	$\sim 10^{-10}$–10^{-16} cm^3 s^{-1}
Charge transfer	$A^+ + B \rightarrow B^+ + C$	$C^+ + Mg \rightarrow C + Mg^+$	$\sim 10^{-9}$ cm^3 s^{-1}
Radiative recombination	$A^+ + e^- \rightarrow A + h\nu$	$Mg^+ + e^- \rightarrow Mg + h\nu$	$\sim 10^{-12}$ cm^3 s^{-1}
Dissociative recombination	$AB^+ + e^- \rightarrow A + B$	$HCO^+ + e^- \rightarrow CO + H$	$\sim 10^{-7}$ cm^3 s^{-1}
Ionization	$A + h\nu \rightarrow A^+ + e^-$	$C + h\nu \rightarrow C^+ + e^-$	$\sim 10^{-10} \times$ RF[b] cm^3 s^{-1}
Dissociation	$AB + h\nu \rightarrow A + B$	$CO + h\nu \rightarrow C + O$	$\sim 10^{-10} \times$ RF cm^3 s^{-1}
Accretion	$A + g \rightarrow A(g)$	$H_2O + g \rightarrow H_2O(g)$	$\gtrsim 4\ 10^{-6}$ cm^3 s^{-1}
Surface reaction	$A(g) + B(g) \rightarrow AB(g)$	$H + H \rightarrow H_2$	$\gtrsim 10^{-9}$ cm^3 s^{-1}
Desorption	$A(g) \rightarrow A$ (hν or T)	$H_2CO(g) \rightarrow H_2CO$	$\sim$0–10^5 s^{-1}

[a]Chemical reaction rates vary widely in disks due to strong gradients of physical conditions
[b]RF designates the local UV radiation field in the disk; hν represents a photon

reactions like $C^+ + H_2 \rightarrow CH_2^+$ (Herbst 1985) creating new molecular bonds are of less significance.

The reactions between neutral and charged molecules in the gas phase and on the surfaces of dust grains dominate the synthesis of new species in disks. The ion-molecule reactions dominate the gas-phase chemistry, especially at low temperature in the outer disk region. Most of these reactions are exothermic, with high rate coefficients, $\sim 10^{-7}$ cm^3 s^{-1} that often increase toward low temperatures, and low (if any) reaction barriers (e.g., Dalgarno and Black 1976). The long-distance Coulomb attraction of an ion and a molecule with a high dipole moment is what makes the ion-molecule rates increase when temperature decreases. ▶ Ion-neutral reactions lead to the restructuring of molecular bonds. One of the most important classes of reactions in disks is proton transfer reactions involving a key H_3^+ ion, such as $H_3^+ + CO \rightarrow HCO^+ + H_2$. A number of ▶ neutral-neutral reactions between radicals and radicals, radicals and open-shell atoms, and radicals and unsaturated molecules are competitive in disks even at low temperatures (van Dishoeck 1988), with a typical rate coefficient that is only about an order of magnitude lower than for the ion-molecule processes (e.g., Smith et al. 2004). These reactions usually have barriers and as such become more active within the warm inner zone of a disk. One of the most interesting reactions of this type is the formation of formaldehyde: $CH_3 + O \rightarrow H_2CO + H$ (Woodall et al. 2007). The reaction rates of ion-molecule reactions are usually accurate within 50 %, while those for neutral-neutral reactions are harder to constrain due to reaction barriers.

The rapid neutralization of polyatomic molecular ions by dissociative recombination with electrons and negative ions leads to the production of smaller neutral molecules in disks. These processes are fast at low temperatures, with typical rates of about 10^{-7} cm^3 s^{-1} (Woodall et al. 2007). For nearly all observed molecules, dissociative recombination is an important formation pathway. Often, at late evolutionary phase, $\sim$0.1 Myr, dissociative recombination balances protonation reactions, e.g., $H_3^+ + CO \rightarrow HCO^+ + H_2$ followed by $HCO^+ + e^- \rightarrow CO + H$.

Additional energy is brought to reacting gas species by cosmic ray particles (CRPs), X-rays, and UV photons, which dissociate and ionize species, destroying molecular bonds. The cosmic rays dominate ionization at disk interiors (unless surface density does not exceed $\sim$100 g cm^{-2}), whereas X-rays and FUV photons are important at upper disk regions (surface density $\lesssim$1 g cm^{-2}). The cosmic ray- and X-ray-driven ionization is mainly caused by secondary energetic electrons upon primal ionization of H_2. The respective reaction rates are uncertain, since the CRP and X-ray spectra cannot be directly derived from disk observations (e.g., due to local absorption of low-energy CRPs and X-rays). The key

ionization reactions in PPDs are CRP/X-ray ionizations of H_2 and He.

The ionization and dissociation of some chemical species proceed by absorption of the UV continuum radiation, while other molecules are destroyed by absorbing UV photons of particular energies. For example, H_2 and CO dissociate via absorptions of FUV photons in discrete lines, whereas other molecules are dissociated either by the continuum (e.g., CH_4) or by the continuum and lines (e.g., C_2; see van Dishoeck et al. 2006). Atmospheres of young Sun-like stars generate nonthermal UV radiation, with an intensity at 100 AU from the star that can be as high as 1,000 (in units of the interstellar UV field, see Bergin et al. 2003). In some stars like TW Hya, a significant fraction of the total UV luminosity of the star is emitted in the ▶ Ly alpha line. Stellar and interstellar UV photons are able to penetrate deep into flaring disks by scattering on dust grains (van Zadelhoff et al. 2003). By dissociating and ionizing molecules, mild UV radiation drives active chemistry involving these ions and radicals, increasing the chemical complexity of the disk. For example, the high ratio of CN to HCN abundance observed in some disks (Dutrey et al. 1997) is attributed to the intense photodissociation of HCN when part of the stellar UV flux comes as Ly alpha photons (121.6 nm; Bergin et al. 2003).

The key photodissociation reaction in disks is that for CO – a molecule that otherwise locks up almost all the elemental carbon see (Table 2). Since the dissociation of the H_2 and CO molecules involves absorption of FUV at discrete wavelengths shortward of ~115 nm, ▶ self-shielding and isotope-selective photodissociation effects are possible. In the disks, H_2 and CO are so abundant that dissociating FUV lines saturate, shielding the rest of molecules from being destroyed (Draine and Bertoldi 1996; Lee et al. 1996). In contrast, rare, less abundant ▶ isotopologs of CO absorb FUV photons at shifted wavelengths compared to $^{12}C^{16}O$, making self-shielding unimportant and enriching the gas with rare O and C isotopes (Thiemens and Heidenreich 1983).

The observed overabundance of deuterated species in disks compared to the measured interstellar D/H ratio of $\sim 10^{-5}$ is well established. Deuterium enrichment operates at low temperatures of 10–20 K via a key fractionation reaction: $H_3^+ + HD \leftrightarrow H_2D^+ + H_2 + 232$ K (Gerlich et al. 2002). A reactive H_2D^+ ion acts similar to H_3^+, donating D to neutral radicals via a "protonation" reaction. For example, a predominant reaction pathway to produce DCO^+ is via the ion-molecule reaction of CO with H_2D^+. Two other key fractionation reactions are active till higher temperatures (up to 70 K): $CH_3^+ + HD \leftrightarrow CH_2D + H_2 + 390$ K (Asvany et al. 2004) and $C_2H_2^+ + HD \leftrightarrow C_2HD^+ + H_2 + 550$ K. Both reactions lead to, e.g., DCN by the ion-molecule reaction, $N + CH_2D^+ \rightarrow DCN^+ + H_2$, followed by protonation reaction and then dissociative recombination. The mass-dependent fractionation for heavier elements like C and O is not that effective, due to the much lower mass difference between isotopologs, and other mechanisms, like mass-independent isotope-selective dissociation and surface processes, have to be considered.

In cold disk regions, where $T \sim 10$–120 K, volatile species can condense out on dust grains. The rate of this freeze-out process depends on grain sizes and concentration and is effective in the outer disk midplane where grains do not grow significantly beyond ~1 μm. At ~10–20 K, many gas-phase molecules stick to a grain with a nearly 100 % probability by ▶ weak van der Waals forces, while some may form a much stronger chemical bond with the surface. Consequently, desorption of chemisorbed species requires higher temperatures/UV irradiation than that of physisorbed molecules and thus allows limited surface chemistry to occur even under harsh conditions.

Frozen species are released back to the gas by thermal evaporation, CRP heating, and UV desorption. A molecule evaporates thermally when it has energy to overcome binding to the surface (e.g., Leger et al. 1985). Typical binding energies are about 1,000 K for light molecules such as CO and N_2 (Bisschop et al. 2006) and larger for heavier ▶ cyanopolyynes and carbon chains (~5,000 K). CRP-induced desorption is a transient heating event when a relativistic Fe atom hits a grain and raises T to 70 K

(e.g., Leger et al. 1985). Also, UV photons can kick off surface molecules with a probability which has been roughly measured to be $\sim 10^{-6}$–10^{-3} (e.g., Öberg et al. 2007).

The dust grain surfaces serve as a catalyst for many reactions with slow gas-phase rates (such as endothermic reactions with barriers). The most notable example is the formation of molecular hydrogen that proceeds entirely on dust at $T < 15$–20 K (e.g., Hollenbach and Salpeter 1971). A reaction may occur when an accreted atom or light radical, if it is not chemisorbed or desorbed back to the gas, hops over the surface sites and finds a radical. At low temperatures, surface hydrogenation of radicals is a key mechanism, leading to the formation of saturated products like water, methane, ammonia, and methanol (e.g., Tielens and Hagen 1982). At higher temperatures of ∼50 K, heavier reactants become mobile (such as O, C, OH, HCO, etc.), and complex molecules are produced. So far, this is the only viable route to form complex organic matter in protoplanetary disks.

Applications

Nonexistent for this topic apart from similar fields of astronomy such as chemistry in (exo) planetary atmospheres, chemistry of primordial prebiotic molecules (in astrobiology), and isotopic fractionation in the early solar nebula.

Future Directions

The ▶ ALMA interferometer in northern Chile is becoming fully operational in 2014. It will revolutionize our understanding of protoplanetary disks by providing high spatial resolution (up to 0.01″), large collecting area (5,000 m^2) and thus high sensitivity, and a broad frequency coverage (86–950 GHz or ∼0.2–3 mm). This is a gain by a factor of 50 in resolving power and orders of magnitude in sensitivity in comparison with earlier observational facilities. First, this will allow us to observe high-lying rotational transitions of simple abundant species like CO, CN, HCN, and HCO^+ and to discover more complex molecules with weaker lines at low frequencies. With this information, we can better constrain disk chemical composition and physical conditions. Second, with much higher spatial resolution, we will be able to image planet-forming regions around nearby PPDs in detail and thus determine the distribution of and properties of dust there. Third, molecular layers in protoplanetary disks may become directly observable for the first time, allowing us to better tune theoretical disk chemical models and laboratory measurements of photodissociation and freeze-out processes. Fourth, data acquisition will be rapid with ALMA, and many protoplanetary disks around various young stars will be surveyed, enabling their proper statistical analysis. Other future instruments, like the Square Kilometer Array (SKA) at cm wavelengths, may allow the detection of low-energy lines from highly complex (organic) species in cold disk regions. Future progress in our understanding of disk physics and chemistry will not be achieved without development of more advanced chemical disk models, in particular, including disk dynamics, grain evolution, and transport of UV and X-ray radiation. The chemical models will strongly benefit from ongoing activities of laboratory/theoretical chemists to derive the rates and products of astrophysically relevant processes, binding energies and photodesorption yields of surface species, and high-precision IR/microwave spectra of potentially detectable, chemically interesting species.

See Also

- ▶ ALMA
- ▶ Bipolar Flow
- ▶ Chemisorption
- ▶ Chondrite
- ▶ Electron Dissociative Recombination
- ▶ Infrared Space Observatory
- ▶ Interstellar Chemical Processes
- ▶ Ion-Neutral Reaction
- ▶ Isotopic Fractionation (Interstellar Medium)
- ▶ JWST
- ▶ Molecular Cloud

- ▶ Molecules in Space
- ▶ Neutral-Neutral Reaction
- ▶ Optical Depth
- ▶ Physisorption
- ▶ Polycyclic Aromatic Hydrocarbon
- ▶ Protoplanetary Disk
- ▶ Protostars
- ▶ Solar Nebula
- ▶ Spitzer Space Telescope

References and Further Reading

Acke B et al (2010) Spitzer's view on aromatic and aliphatic hydrocarbon emission in Herbig Ae stars. Astrophys J 718:558

Aikawa Y, Herbst E (1999) Molecular evolution in protoplanetary disks. Two-dimensional distributions and column densities of gaseous molecules. Astron Astrophys 351:233

Aikawa Y, Umebayashi T, Nakano T, Miyama SM (1999) Evolution of molecular abundances in protoplanetary disks with accretion flow. Astrophys J 519:705–725. doi:10.1086/307400

Aikawa Y, Momose M, Thi W-F et al (2003) Interferometric observations of formaldehyde in the protoplanetary disk around LkCa 15. Publ Astron Soc Jpn 55:11

Aikawa Y et al (2012) AKARI observations of ice absorption bands towards edge-on young stellar objects. Astron Astrophys 38:57

Asvany O, Schlemmer S, Gerlich D (2004) Deuteration of CH_n^+ ($n = 3$–5) in collisions with HD measured in a low-temperature ion trap. Astrophys J 617:685

Bergin E, Calvet N, D'Alessio P, Herczeg GJ (2003) The effects of UV continuum and Lyα radiation on the chemical equilibrium of T Tauri disks. Astrophys J 591:L159–L162

Bergin EA, Aikawa Y, Blake GA, van Dishoeck EF (2007) The chemical evolution of protoplanetary disks. In: Reipurth B, Jewitt D, Keil K (eds) Protostars and planets V. University of Arizona Press, Tucson, pp 751–766, 951

Bergin E et al (2010) Sensitive limits on the abundance of cold water vapor in the DM Tauri protoplanetary disk. Astron Astrophys 521:L33

Bergin E et al (2013) An old disk still capable of forming a planetary system. Nature 493:644

Bisschop SE, Fraser HJ, Öberg KI, van Dishoeck EF, Schlemmer S (2006) Desorption rates and sticking coefficients for CO and N_2 interstellar ices. Astron Astrophys 449:1297

Bitner MA, Richter MJ, Lacy JH et al (2007) TEXES observations of pure rotational H2 emission from AB Aurigae. Astrophys J 661:L69

Bockelee-Morvan D, Woodwart CE, Kelley MS, Wooden DH (2009) Water in comets 71P/Clark and C/2004 B1 (linear) with Spitzer. Astrophys J 696:1075

Bonev BP et al (2013) Evidence for two modes of water release in comet 103P/Hartley 2: distributions of column density, rotational temperature, and ortho-para ratio. Icarus 222:740

Bouwman J, Henning T, Hillenbrand LA et al (2008) The formation and evolution of planetary systems: grain growth and chemical processing of dust in T Tauri systems. Astrophys J 683:479–498

Chapillion E, Dutrey A, Guilloteau S et al (2012) Chemistry in disks. VII. First detection of HC_3N in protoplanetary disks. Astrophys J 756:58

Cortes SR, Meyer MR, Carpenter JM et al (2009) Grain growth and global structure of the protoplanetary disk associated with the mature classical T Tauri star, PDS 66. Astrophys J 697:1305–1315

Dalgarno A, Black JH (1976) Molecule formation in the interstellar gas. Rep Prog Phys 39:573

Dartois E, Dutrey A, Guilloteau S (2003) Structure of the DM Tau outer disk: probing the vertical kinetic temperature gradient. Astron Astrophys 399:773–787

Day JMD, Ash RD, Liu Y et al (2009) Early formation of evolved asteroidal crust. Nature 457(7226):179–182

Draine BT, Bertoldi F (1996) Structure of stationary photodissociation fronts. Astrophys J 468:269

Dutrey A, Guilloteau S, Guelin M (1997) Chemistry of protosolar-like nebulae: the molecular content of the DM Tau and GG Tau disks. Astron Astrophys 317:L55

Dutrey A, Guilloteau S, Ho P (2007a) Interferometric spectroimaging of molecular gas in protoplanetary disks. In: Reipurth B, Jewitt D, Keil K (eds) Protostars and planets V. University of Arizona Press, Tucson, p 495

Dutrey A, Henning T, Guilloteau S et al (2007b) Chemistry in disks. I. Deep search for N_2H^+ in the protoplanetary disks around LkCa 15, MWC 480, and DM Tauri. Astron Astrophys 464:615–623

Ehrenfreund, Charnley (2000) Annual Reviews in Astronomy & Astrophysics 38:427

Elsila JE, Glavin DP, Dworkin JP (2009) Cometary glycine detected in samples returned by Stardust. Meteorit Planet Sci 44:1323

Fedele D, van den Acker ME, Henning T, Jayawardhana R, Oliveira JM (2010) Timescale of mass accretion in pre-main-sequence stars. Astron Astrophys 510:72

Fedele D et al (2012) Warm H_2O and OH in the disk around the Herbig star HD 163296. Astron Astrophys 544:L9

Fedele D et al (2013) DIGIT survey of far-infrared lines from protoplanetary disks. II. [OI], [CII], OH, H_2O and CH^+. Astron Astrophys 559:77–99

Fukagawa M et al (2004) Spiral structure in the circumstellar disk around AB Aurigae. Astrophys J 605:L53

Garrod RT, Herbst E (2006) Formation of methyl formate and other organic species in the warm-up phase of hot molecular cores. Astron Astrophys 457:927

Gerlich D, Herbst E, Roueff E (2002) H^{3+}+HD $\leftrightarrow$ H_2D^++H_2: low-temperature laboratory measurements and interstellar implications. Planet Space Sci 50:1275

Gorti U, Dullemond CP, Hollenbach D (2009) Time evolution of viscous circumstellar disks due to photoevaporation by far-ultraviolet, extreme-ultraviolet, and X-ray radiation from the central star. Astrophys J 705:1237

Grady CA et al (2013) Spiral arms in the asymmetrically illuminated disk of MWC 758 and constraints on giant planets. Astrophys J 762:48

Guilloteau St, Dutrey A, Pietu V, Boehler Y (2011) A dual-frequency sub-arcsecond study of protoplanetary disks at mm wavelengths: first evidence for radial variations of the dust properties. Astron Astrophys 529:105

Guilloteau St et al (2012) Chemistry in disks. VIII. The CS molecule as an analytic tracer of turbulence in disks. Astron Astrophys 548:70

Hasegawa TI, Herbst E, Leung CM (1992) Models of gas-grain chemistry in dense interstellar clouds with complex organic molecules. Astrophys J Suppl Ser 82:167

Henning T, Meeus G (2011) Dust processing and mineralogy in protoplanetary accretion disks. In: Garcia PJV (ed) Physical processes in circumstellar disks around young stars. Chicago University Press, p 114

Henning T et al (2010) Chemistry in disks. III. Photochemistry and x-ray driven chemistry probed by the ethynyl radical (CCH) in DM Tau, LkCa 15, and MWC 480. Astrophys J 714:1511

Herbst E (1985) An update of and suggested increase in calculated radiative association rate coefficients. Astrophys J 291:226

Herbst E, Klemperer W (1973) The formation and depletion of molecules in dense interstellar clouds. Astrophys J 185:505

Hogerheijde M et al (2011) Detection of the water reservoir in a forming planetary system. Science 334:338

Hollenbach D, Salpeter EE (1971) Surface recombination of hydrogen molecules. Astrophys J 163:155, http://astrochemistry.net

Hughes AM et al (2011) Empirical constraints on turbulence in protoplanetary accretion disks. Astrophys J 727:85

Kastner JH, Zuckerman B, Weintraub DA, Forveille T (1997) X-ray and molecular emission from the nearest region of recent star formation. Science 277:67

Lahuis F, van Dishoeck EF, Boogert ACA et al (2006) Hot organic molecules toward a young low-mass star: a look at inner disk chemistry. Astrophys J 636:L145

Le Petit F, Nehmé C, Le Bourlot J, Roueff E (2006) A model for atomic and molecular interstellar gas: the meudon PDR code. Astrophys J Suppl Ser 164:506

Lee H-H, Herbst E, des Forets GP, Roueff E, Le Bourlot J (1996) Photodissociation of H2 and CO and time dependent chemistry in inhomogeneous interstellar clouds. Astron Astrophys 311:690

Leger A, Jura M, Omont A (1985) Desorption from interstellar grains. Astron Astrophys 144:147

Lin DNC, Papaloizou J (1980) On the structure and evolution of the primordial solar nebula. MNRAS 191:37

Min M, Flynn G (2010) Dust composition in protoplanetary disks. In: Apai D, Lauretta D (eds) Protoplanetary dust: astrophysical and cosmochemical perspectives. Cambridge University Press, Cambridge, pp 160–191

Öberg KI, Fuchs GW, Awad Z et al (2007) Photodesorption of CO ice. Astrophys J 662:L23

Oberg KI, Qi C, Wilner DJ, Hogerheijde MR (2012) Evidence for multiple pathways to deuterium enhancements in protoplanetary disks. Astrophys J 749:162. doi:10.1088/0004-637X/749/2/162

Pascucci I, Hollenbach D, Najita J et al (2007) Detection of [Ne II] emission from young circumstellar disks. Astrophys J 663:383

Payne MJ, Lodato G (2007) The potential for Earth-mass planet formation around brown dwarfs. MNRAS 381:1597

Piétu V, Dutrey A, Guilloteau S (2007) Probing the structure of protoplanetary disks: a comparative study of DM Tau, LkCa 15, and MWC 480. Astron Astrophys 467:163–178

Podio L et al (2013) Water vapor in the protoplanetary disk of DG Tau. Astrophys J 766:L5

Pollack JB, Hollenbach D, Beckwith S, Simonelli DP, Roush T, Fong W (1994) Composition and radiative properties of grains in molecular clouds and accretion disks. Astrophys J 421:615

Pontoppidan KM, Dullemond CP, van Dishoeck EF et al (2005) Ices in the edge-on disk CRBR 2422.8-3423: Spitzer spectroscopy and Monte Carlo radiative transfer modeling. Astrophys J 622:463

Qi C, Kessler JE, Koerner DW, Sargent AI, Blake GA (2003) Continuum and CO/HCO^+ emission from the disk around the T Tauri star LkCa 15. Astrophys J 597:986

Qi C et al (2006) CO $J = 6$–5 observations of TW Hya with the SMA. Astrophys J L636:L157

Qi C, Wilner DJ, Aikawa Y, Blake GA, Hogerheijde MR (2008) Resolving the chemistry in the disk of TW Hydrae. I. Deuterated species. Astrophys J 681:1396–1407

Qi C et al (2013) First detection of c-C_3H_2 in a circumstellar disk. Astrophys J L765:L14

Rodmann J, Henning T, Chandler CJ, Mundy LG, Wilner DJ (2006) Large dust particles in disks around T Tauri stars. Astron Astrophys 446:211–221

Salyk C, Pontoppidan KM, Blake GA et al (2008) H_2O and OH gas in the terrestrial planet-forming zones of protoplanetary disks. Astrophys J 676:L49–L52

Salyk C et al (2011) A Spitzer survey of mid-infrared molecular emission from protoplanetary disks. II. Correlations and local thermal equilibrium models. Astrophys J 731:130

Semenov D, Wiebe D, Henning T (2004) Reduction of chemical networks. II. Analysis of the fractional ionisation in protoplanetary discs. Astron Astrophys 417:93

Semenov D, Pavlyuchenkov Y, Henning T, Wolf S, Launhardt R (2008) Chemical and thermal structure

of protoplanetary disks as observed with ALMA. Astrophys J 673:L195–L198
Smith IWM, Herbst E, Chang Q (2004) Rapid neutral-neutral reactions at low temperatures: a new network and first results for TMC-1. MNRAS 350:323
Terada H et al (2007) Detection of water ice in edge-on protoplanetary disks: HK Tauri B and HV Tauri C. Astrophys J 667:303
Teske JK et al (2011) Measuring organic molecular emission in disks with low-resolution Spitzer spectroscopy. Astrophys J 734:27
Thiemens MH, Heidenreich JE III (1983) The mass-independent fractionation of oxygen: a novel isotope effect and its possible cosmo-chemical implications. Science 219:1073
Tielens AGGM, Hagen W (1982) Model calculations of the molecular composition of interstellar grain mantles. Astron Astrophys 114:245
van Dishoeck EF (1988) Photodissociation and photoionization processes. In: Millar T, Williams D (eds) ASSL, rate coefficients in astrochemistry. Kluwer, Dordrecht, pp 49–72
van Dishoeck EF (2004) ISO spectroscopy of gas and dust: from molecular clouds to protoplanetary disks. Annu Rev Astron Astrophys 42:119
van Dishoeck EF, Jonkheid B, van Hemert MC (2006) Photoprocesses in protoplanetary disks. In: Sims IR, Williams DA (eds) Chemical evolution of the Universe, Faraday discussion, Royal Society of Chemistry, Cambridge, UK, vol 133. pp 231–244
van Dishoeck EF, Bergin EA, Lis DC, Lunine JI (2014) Water: from clouds to planets. In: Beuther H, Klessen R, Dullemond C, HenningTh (eds) Protostars and planets VI. University of Arizona Press, Tucson (in press)
van Zadelhoff G-J, Aikawa Y, Hogerheijde MR, van Dishoeck EF (2003) Axi-symmetric models of ultraviolet radiative transfer with applications to circumstellar disk chemistry. Astron Astrophys 397:789
Vasyunin AI, Semenov D, Henning T et al (2008) Chemistry in protoplanetary disks: a sensitivity analysis. Astrophys J 672:629
Wakelam V, Herbst E, Selsis F (2006) The effect of uncertainties on chemical models of dark clouds. Astron Astrophys 451:551
Wakelam V et al (2011) A KInetic database for astrochemistry (KIDA). Astrophys J Suppl Ser 199:21
Willacy K, Langer WD (2000) The importance of photoprocessing in protoplanetary disks. Annu Rev Astron Astrophys 49:67
Willams JP, Ciesza LA (2011) Protoplanetary disks and their evolution. Astrophys J 544:903
Woodall J, Agúndez M, Markwick-Kemper AJ, Millar TJ (2007) The UMIST database for astrochemistry. Astron Astrophys 466:1197
Woodwart CE, Kelley MS, Bockelee-Morvan D, Gehrz RD (2007) Water in comet C/2003 K4 (LINEAR) with Spitzer. Astrophys J 671:1065
Wozniakiewicz PJ, Kearsley AT, Ishii HA et al (2012) The origin of crystalline residues in Stardust Al foils: surviving cometary dust or crystallized impact melts? Meteorit Planet Sci 47:660
Zasowski G, Kemper F, Watson DM et al (2009) Spitzer infrared spectrograph observations of class I/II objects in Taurus: composition and thermal history of the circumstellar ices. Astrophys J 694:459–478
Zhang K, Pontoppidan KM, Salyk C, Blake GA (2013) Evidence for a snow line beyond the transitional radius in the TW Hya protoplanetary disk. Astrophys J 766:82

Protoplanetary Nebula

Sun Kwok
Faculty of Science, The University of Hong Kong, Hong Kong, China

Keywords

Planetary nebulae; Reflection nebulae; Stellar evolution

Synonyms

Pre-planetary nebulae

Definition

Protoplanetary nebulae (PPN) are objects in transition between the ▶ asymptotic giant branch (AGB) and the ▶ planetary nebulae (PN) phases of stellar evolution. The optical nebulosity of PPN is due to scattered light from the central star, not emission lines as in the case of PN. Observationally, PPN are defined as gaseous nebulae surrounding stars in a post-AGB phase of evolution showing no emission lines in their optical spectra.

History

Since the 1970s, PN have been known to be descendants of AGB stars, and the nebulae

represent remnants of ejecta from AGB stars. The visual brightness of PN is the result of ▶ line emission from gas photoionized by a hot central star. From models of stellar evolution, it was known that the central stars of PN need a few thousand years to evolve from the end of the AGB to a temperature hot enough to emit a significant amount of ultraviolet radiation capable of photoionizing the circumstellar gas (Schönberner 1983). However, for a long time, no such transition object was known and the phase linking AGB stars and PN represented a missing link in the late stages of stellar evolution.

The emission mechanisms responsible for the brightness of PN are primarily recombination lines and collisionally excited lines. Both are extremely efficient, making PN bright optical objects (Kwok 2000). Without ionized gas, PPN have to rely on scattered light from the central stars, making the nebulosity very faint in the visible. However, since AGB stars are known to be strong infrared sources due to dust emission, it was suspected some infrared sources discovered in the Air Force Infrared Sky Survey could be PPN (e.g., AFGL 618, Westbrook et al. 1975; AFGL 2688, Ney et al. 1975). After the Infrared Astronomical Satellite (IRAS) sky survey observed a large number of AGB stars and planetary nebulae, it was realized that PPN could be identified as objects having infrared colors intermediate between those of AGB stars and planetary nebulae (Volk and Kwok 1989). A systematic search of IRAS sources matching such color criteria has resulted in the discovery of ∼30 PPN (Kwok 1993), one of which is shown in Fig. 1.

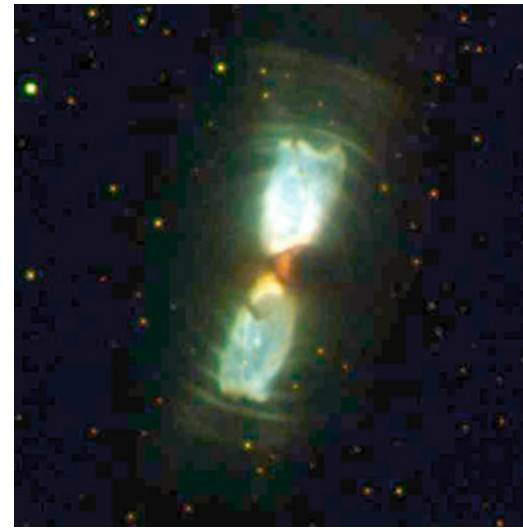

Protoplanetary Nebula, Fig. 1 Hubble Space Telescope Wide-Field Planetary Camera 2 image of the protoplanetary nebula IRAS 17150-3224 (the Cotton Candy Nebula). The visual brightness of the object is entirely due to scattered light. In addition to its bipolar morphology, multiple concentric arcs can also be seen

Overview

PPN have the following observational characteristics: (i) their central stars have spectral types intermediate between those of AGB stars and PN, usually of spectral types F, G, and K; (ii) their central stars have low surface gravity, often classified as luminosity class I or Ia; (iii) their infrared spectra are dominated by thermal continuum emission from warm dust; (iv) molecular emission lines can be seen in their mm/submm spectra; (v) their spectral energy distributions show evidence of detached dust envelopes; and (vi) their optical nebulosity is due to scattered light.

Imaging observations by the *Hubble Space Telescope* have shown that many PPN show bipolar morphology, suggesting that the transformation from spherical to bipolar morphology has already taken place during the post-AGB phase of evolution (Balick and Frank 2002). Some PPN have binary central stars (Van Winckel 2003), which may play a role in the creation of the nebular bipolar morphology.

Most interestingly, spectral signatures of aromatic and aliphatic organics first appear during the PPN stage, suggesting that the synthesis of complex organics can occur in the circumstellar environment (Kwok et al. 1999).

See Also

- ▶ Asymptotic Giant Branch Star
- ▶ Stellar Evolution
- ▶ Unidentified Infrared Emission Bands

References and Further Reading

Balick B, Frank A (2002) Shapes and shaping of planetary nebulae. Annu Rev Astron Astrophys 40:439–486
Kwok S (1993) Proto-planetary nebulae. Annu Rev Astron Astrophys 31:63–92
Kwok S (2000) The Origin and evolution of planetary nebulae. CUP, Cambridge
Kwok S, Volk K, Hrivnak BJ (1999) Chemical evolution of carbonaceous materials in the last stages of stellar evolution. Astron Astrophys 350:L35–L38
Ney EP, Merrill KM, Becklin EE, Neugebauer G, Wynn-Williams CG (1975) Studies of the infrared source CRL 2688. Astrophys J 198:L129–L131
Schönberner D (1983) Late stages of stellar evolution. II – mass loss and the transition of asymptotic giant branch stars into hot remnants. Astrophys J 272:708–714
Van Winckel H (2003) Post-AGB stars. Annu Rev Astron Astrophys 41:391–427
Volk KM, Kwok S (1989) Evolution of proto-planetary nebulae. Astrophys J 342:345–363
Westbrook WE, Willner SP, Merrill KM, Schmidt M, Becklin EE, Neugebauer G, Wynn-Williams CG (1975) Observations of an isolated compact infrared source in Perseus. Astrophys J 202:407–409

Protoplasmic Theory of Life

Stéphane Tirard
Centre François Viète d'Histoire des Sciences et des Techniques EA 1161, Faculté des Sciences et des Techniques de Nantes, Nantes, France

Definition

During the second part of the nineteenth century, the British biologist, Thomas Huxley (1825–1895), claimed that, inside the cell, the protoplasm was essentially composed of albuminoidal bodies and would be the place of the physical basis of life. This theory led some biologists, as the German Ernst Haeckel (1834–1919), to assume that origin of life could correspond to the formation of free protoplasm.

See Also

▶ Abiogenesis
▶ Cellular Theory, History of
▶ Huxley's Conception on Origins of Life

Protoplast

Ricardo Amils
Departamento de Biologia Molecular, Universidad Autónoma de Madrid, Madrid, Spain

Synonyms

Spheroplast

Definition

A protoplast is a bacterial, fungal, or plant cell that has had its cell wall completely or partially removed using either enzymatic or mechanical means. ▶ Cell walls are made of a variety of polysaccharides (▶ peptidoglycan, chitin, cellulose). Protoplasts are generally prepared by degrading cell walls with a mixture of appropriate polysaccharide-degrading enzymes. In the case of gram-positive ▶ bacteria, lysozyme, an enzyme that breaks the bonds that maintain the structure of the peptidoglycan, is used. To prepare plant cell protoplasts, a mixture of hydrolyzing enzymes (cellulose, proteinase, and xylanase) is required. In the case of fungal protoplast, chitinase is the enzyme of choice. During and subsequent to digestion of the cell wall, the protoplast becomes very sensitive to osmotic stress. This means that cell wall digestion and protoplast storage must be carried out in an isotonic solution to prevent the disruption of the plasma membrane. Protoplasts are useful for genetic recombination experiments, because the absence of a cell wall facilitates the transport of DNA molecules to the cytoplasm. Protoplasts are normal cells, their growth allows the generation of cells with cell walls. Although most prokaryotes

cannot survive in nature without a cell wall, some are able to do so. These include the mycoplasma, gram-positive bacteria, and *Thermoplasma*, an acidophilic and thermophilic *Euryarchaea*.

See Also

- ▶ Acidophile
- ▶ Bacteria
- ▶ Cell Wall
- ▶ Euryarchaeota
- ▶ Fungi
- ▶ Gram-Positive Bacteria
- ▶ Peptidoglycan
- ▶ Thermophile

Protosolar Nebula, Minimum Mass

Avi M. Mandell
NASA Goddard Space Flight Center, Greenbelt, MD, USA

Synonyms

Solar nebula

Definition

The minimum-mass ▶ solar nebula is the theoretical minimum amount of mass required to have formed the Solar System. The amount is calculated based on the known quantity of refractory elements in the planets and adjusting for the original composition of the pre-solar nebula (i.e., adjusting for the failure of most of the planets to completely incorporate the more volatile elements from the nebula). The minimum-mass solar nebula model typically assumes a surface density that decreases with orbital distance r as $r^{(-3/2)}$, with a total mass between 0.01 and 0.1 solar masses. This is comparable to the masses of some disks observed around young stars. More recent observations of disks suggest that the radial distribution of mass is flatter than the $-3/2$ power law, probably much closer to a -1 slope.

See Also

- ▶ Protoplanetary Disk
- ▶ System Solar Formation, Chronology of

Protostars

Steven W. Stahler
Department of Astronomy, University of California, Berkeley, CA, USA

Keywords

Accretion; T Tauri star

Definition

Stellar evolution begins when a diffuse interstellar cloud undergoes gravitational collapse. Toward the cloud's center, a primitive star forms and continues to build up its mass from the surrounding gas. This object, called a protostar, is unique in that most of its luminosity stems from the kinetic energy of infalling matter crashing onto its surface and surrounding disk. The infalling envelope of gas contains dust grains, which absorb and reemit stellar photons into the infrared. The fusion of deuterium inside protostars determines the location of the stellar ▶ birthline in the ▶ Hertzsprung-Russell diagram. In the most massive protostars, ordinary hydrogen ignites while cloud infall is still occurring.

Overview

Stellar Life Cycle

All stars are born through the gravitational collapse of diffuse, interstellar clouds. During its

initial, protostar phase, the star is optically invisible, as it is completely embedded in its parent cloud. Indeed, it is still gathering mass from that body. The protostar phase is unique in that the star's luminosity arises mostly from the kinetic energy of infalling gas. Following infall, the star then contracts slowly. During this longer, pre-main-sequence phase, energy is released by the increasing gravitational binding of the star.

Stars achieve maturity once they begin to fuse hydrogen into helium at their centers. This main-sequence phase comprises the longest period, by far, in the star's life. As hydrogen is consumed, the central regions of the star contract and heat up, so that successively heavier elements (helium, carbon, oxygen, etc.) begin to fuse. The process is an accelerating one. During this relatively brief post-main-sequence phase, the outer layers of the star swell, and the object brightens enormously, as a consequence of both the increased fusion and the further gravitational contraction of its central region.

The final fate of a star depends on its initial mass. Our Sun, after shedding a large amount of gas during the post-main-sequence epoch, will become a white dwarf, an object with the diameter of the Earth. Lacking nuclear reserves, the white dwarf will gradually cool over billions of years. In more massive stars, the remnant, condensed object at the center is a ▶ neutron star, with a diameter of a few kilometers or a ▶ black hole, an object so dense that not even light can escape it.

Taking a larger, galactic perspective, star formation represents the conversion of interstellar gas into the much more condensed objects we call stars. But the process does not just operate in one direction. Stars themselves spew back matter into space, in the form of winds, novae, and supernovae. This matter, enriched in heavy elements by previous fusion, cools and eventually becomes new interstellar clouds which in turn produce more stars. White dwarfs, neutron stars, and black holes constitute a sink that slowly drains mass away from this cyclical process.

Parent Clouds

The interstellar medium consists of both ionized and neutral gas. The specific interstellar clouds that form stars are those composed of molecular hydrogen and are thus known as molecular clouds. Of all the clouds in interstellar space, only these are dense and cold enough so that self-gravity plays an important role in their overall force balance. Since stars form through gravitational collapse, molecular clouds are strongly implicated in the process.

Molecular clouds have a range of sizes and masses. At the top end of the spectrum are the giant complexes. With typical sizes of 50 parsecs, these are the largest coherent entities in the Galaxy. We can also see giant molecular complexes in other, nearby spiral galaxies. All complexes are highly clumpy. A single clump can have a mass of hundreds to thousands of solar masses. The clumps are also found individually, outside of a giant complex, where they are more commonly known as dark clouds. The term refers to the fact that these objects obscure background starlight, giving the sky a patchy appearance.

Stars do not form uniformly throughout a giant complex, but only in its interior clumps. They also form within the more isolated dark clouds. But again, it is only the very densest gas that can produce stars. Both the clumps within complexes and dark clouds contain numerous patches of especially dense gas. These regions, typically 0.1 parsecs in size, are known as dense cores. They are the objects which collapse to form stars. We know this critical fact because a large fraction of dense cores contain embedded stars. The latter appear as point sources of infrared or submillimeter radiation.

Dense cores, like their surrounding molecular gas in the clump or dark cloud, have temperatures of 10–20 K. Even this very low temperature provides some thermal pressure. Prior to its collapse, a dense core is supported against self-gravity by this outward force. The parent clump has a similarly low temperature. However, its higher mass also implies a stronger force of self-gravity. Support of the larger object comes from the pressure associated with internal, turbulent motion. Dense cores are special locations within the clump where the turbulent motion has, for some reason, died down.

Not all dense cores are currently forming stars. Barren objects called starless cores appear rather

similar to those containing infrared point sources. However, the densest of the starless cores appear to be undergoing a slow, inward contraction. This motion may be the prelude to the full-scale collapse that gives rise to a star.

We know all of these facts because of the emission of radio and millimeter waves by the dense cores. The chief constituent of these objects is molecular hydrogen, which unfortunately is a very poor emitter at the extremely cold, ambient temperatures. We must therefore turn to other molecules which, despite their rarity, emit more strongly. Carbon monoxide is a convenient choice, especially for the larger clumps and dark clouds. In dense cores, the millimeter radiation from carbon monoxide becomes trapped, and other molecules must be used. Ammonia is one such species, emitting a strong spectral line at 1.3 cm.

Careful analysis of the spectral line emission, often from a variety of molecules, has yielded the densities and temperatures of all types of molecular clouds, including dense cores. Furthermore, the detailed shape of the line gives information about the gas motions. We know, for example, that larger clouds are turbulent because their carbon monoxide lines are much too broad to arise solely from thermal motion of the molecule. Conversely, it is the relative narrowness of the ammonia lines in dense cores that indicates their quiescence.

Inside-Out Collapse

It is still unclear whether we have observed dense cores in the act of collapse. As mentioned previously, a large fraction of starless cores do show signs of inward motion. The signature is an asymmetric line profile in an optically thick, i.e., relatively opaque, molecular line. The blueward component of the line is stronger than the red, and there is often a strong absorption dip near line center. Such a profile is also seen in YY Orionis stars, older, pre-main-sequence objects that are surrounded by infalling gas. In the case of dense cores, the asymmetric line is observed over a broad area and indicates slow, subsonic infall velocities. Lacking a detailed explanation for these observations, we must rely on theory to tell us how collapse proceeds.

A clear advance in our understanding of cloud collapse came in the 1960s, through computer simulations and accompanying analytical models. Prior to that time, the assumption was that clouds collapse as a whole. Moreover, collapse could lead to fragmentation and further collapse of the fragments. Theorists came to realize that this picture does not hold when the original cloud is close to a state of force balance. In that case, the density rises sharply toward the center of the object. The local ▶ free-fall time is correspondingly brief in that region. As a result, the center of the cloud collapses first, while the outer regions lag behind.

This inside-out mode of collapse undoubtedly applies to dense cores. Observations show that their internal temperatures are sufficiently high that the objects as a whole are indeed in force balance between thermal pressure and self-gravity. Moreover, the spatial rise in density toward the cloud center can be seen directly in molecular line observations. Since the strongest, highly supersonic collapse is concentrated in the central region, that motion is more difficult to observe.

Both analytic theory and numerical simulations predict that the boundary of infall spreads outward through the cloud. In effect, the collapse and infall to the central protostar has lowered the gas pressure. A rarefaction wave of collapse propagates at the local speed of sound. Given typical dense core sizes and temperatures, the wave reaches the cloud edge in a time of 100,000 to a million years. This time span measures the lifetime of protostars.

The most detailed models assume a perfectly spherical cloud. Observations show, however, that real cores are aspherical, with aspect ratios of about 2–1. This fact alone demonstrates that there are more supporting forces than simply thermal pressure, which is intrinsically isotropic. One obvious candidate is the interstellar magnetic field, which exerts a force that is comparable to that from thermal pressure. The direction of the magnetic force depends on that of the field lines. Observers have recently begun to obtain images of bent magnetic field lines penetrating dense cores. These images were achieved by mapping the polarization direction of light

emitted by dust grains. Clearly, detailing the collapse in a magnetized cloud is a more daunting proposition, and no complete models exist. Nevertheless, the general picture of inside-out collapse should hold.

What precedes collapse? To first approximation, starless cores are in a state of hydrostatic (or, more correctly, magnetostatic) equilibrium. However, the object is actually evolving. Most theorists agree that this evolution occurs through the slippage of neutral matter past the internal magnetic field, the process known as ► ambipolar diffusion. This slippage is possible because it is only the charged species in the cloud (ions and electrons) that directly feel the magnetic force. These species then transfer their momentum to the neutral gas via collisions. In a dense core, however, the level of ionization is so low that such collisions are rare. Hence, gravity can pull the neutral gas inward, past the magnetic field.

While there is a good theoretical understanding of ambipolar diffusion, the applicability of the concept to dense cores is not yet secure. The difficulty is that ambipolar diffusion is relatively slow. For typical conditions, a dense core will not begin collapse for about 10 million years. However, we see young clusters in which stars were born over an interval of just a few million years. Some other process, operating on a larger scale, must be synchronizing dense core contraction and collapse. One possibility is that the larger, parent body (clump or dark cloud) is also slowly contracting and somehow stimulating the growth and collapse of its internal dense cores.

A second difficulty is that most models of collapsing, magnetized clouds find that the object flattens in a plane perpendicular to the main field direction. This finding runs counter to observations. Both starless cores and those containing central stars exhibit similar aspect ratios. One must de-project this shape to obtain the object's true, three-dimensional configuration. It appears that dense cores of both types are prolate. That is, they are elongated, rather than flattened. Clearly, there is some important ingredient missing in our understanding of the role magnetic fields play in dense core formation and collapse.

Main Accretion Phase

As the dense core collapses, the first stable object to form at its center is not a star, but a more compact cloud composed of molecular hydrogen. This short-lived entity is traditionally (and rather confusingly) known as the first core. It reaches a mass of less than 0.1 times the solar value and a radius of about 5 AU before it too collapses on itself. This second collapse is triggered by dissociation of the hydrogen molecules. Such dissociation effectively absorbs energy. Since the internal pressure is not rising appreciably during the process, gravity overwhelms it, and the first core collapses.

Following the demise of the first core, a much smaller and denser object arises at the center of infalling gas. This is a protostar. Its internal gas is ionized, and so the object will not suffer the destabilization that doomed the first core. The protostar is a genuine star, although one that is deeply buried in the infalling gas of the surrounding dense core. The period during which the dense core gas falls onto the protostar is known as the main accretion phase. As previously estimated, this phase lasts from 100,000 to a million years for a solar-type star. Figure 1 depicts schematically a protostar during its main accretion phase.

The outer boundary of an ordinary star is a photosphere, a thin surface layer through which radiation can escape. In contrast, the outer boundary of a protostar is a shock front, where infalling gas impacts the star itself. This gas is moving at hypersonic speed. Consequently, post-shock gas has a very high temperature, of order one million Kelvin. This heated gas radiates X-rays, both into the outside flow and back into the body of the protostar.

Remember that a protostar, by definition, derives most of its luminosity from infall. This luminosity is that generated just behind the accretion shock front. However, the X-ray photons themselves never leave the dense core. They are quickly absorbed by infalling gas just outside the star. This gas reradiates the energy into optical wavelengths. Thus, while the total energy output in radiation is conserved outward, the character of that radiation changes markedly.

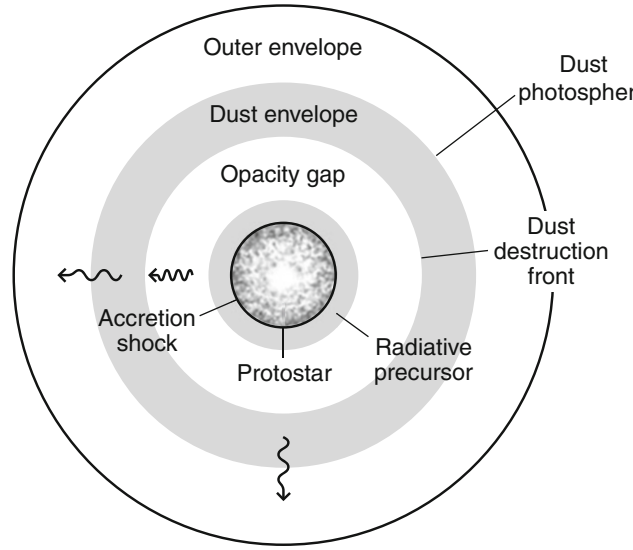

Protostars,
Fig. 1 Structure of a spherical protostar and its infalling envelope. The relative dimensions of the outer regions are greatly reduced for clarity. Note the convection induced by deuterium burning in the central protostar. Note also the conversion of optical (short-wavelength) to infrared (long-wavelength) photons in the dust envelope

Indeed, even the optical radiation does not escape. Infalling dust grains, present in the original dense core, absorb these photons. Heated dust grains radiate in the infrared region of the spectrum. As this infrared flux travels outward through the dust, it is continually degraded through multiple absorption and reemission to yet longer wavelengths. Eventually, the photons have such long wavelengths that they break free of the infalling, dusty gas. The dust photosphere, located some 10 AU from the central protostar, is the surface which emits the bulk of the luminosity.

The radius of the dust photosphere is still tiny compared to that of the dense core itself, which is larger by a factor of 1,000. It makes sense, therefore, that protostars are observed as unresolved point sources of infrared and submillimeter radiation inside dense cores. The energy emitted by these sources is relatively high. For a protostar of solar mass, the luminosity is about ten times the solar value, and the radiation peaks in the mid- to far-infrared regime.

The dust grains responsible for degrading the protostar's radiation into the infrared do not survive close to the central object. As they fall inward, they are heated by the outgoing flux of energy. At a distance of about 1 AU from the star, the grains reach a temperature of 1,500 K and sublimate. There is thus a zone surrounding the protostar through which the shock-generated radiation can propagate freely. This region is known as the opacity gap. The inner boundary of the opacity gap is the layer of infalling gas that is absorbing the shock-generated X-rays and converting them into optical photons. The outer boundary of the gap is known as the dust destruction front.

Deuterium Fusion

Protostars, as we have emphasized, are too young and cold to fuse hydrogen into helium. Indeed, they are younger than pre-main-sequence stars, which derive their luminosity from gravitational contraction rather than fusion. Nevertheless, both protostars and pre-main-sequence stars do ignite deuterium. This hydrogen isotope, whose nucleus consists of a proton and neutron, fuses with protons at a temperature of only 1,000,000 K, an order of magnitude lower than the ignition temperature of ordinary hydrogen.

The luminosity generated by deuterium fusion represents a minor fraction of the protostar's total energy budget. Furthermore, this luminosity does not escape the star, but is absorbed in gas overlying the central region of active fusion. However, this very heating does aid in swelling the

protostar as it continues gathering mass from its infalling cloud envelope. The net result is that protostars of a given mass all have nearly the same radius while burning deuterium, regardless of their detailed accretion history. This fact, in turn, means that the youngest pre-main-sequence stars have a nearly unique mass-radius relationship. These are the optically visible objects that lie along the birthline in the Hertzsprung-Russell diagram. In summary, the location of the birthline is largely determined by the phenomenon of deuterium fusion in protostars.

Deuterium fusion has another interesting consequence. The intense heat generated near the protostar's center creates thermal convection. This motion of buoyant, heated fluid elements, rather than the diffusion of photons, carries outward the protostar's luminosity. In protostars more massive than a few tenths of the solar mass, the region of convective instability extends to the surface, just below the accretion shock. This property, too, is bequeathed to the youngest pre-main-sequence stars, which are fully convective. In the present-day Sun, the convection zone extends inward from the photosphere for about the outer third of the solar radius.

Disk Formation

Our description of the main accretion phase has omitted two key ingredients – magnetic fields and rotation. We know that dense cores are penetrated by the interstellar magnetic field. If the ionization fraction in the gas is sufficiently high, this field is dragged down toward the protostar during collapse. Two circumstances prevent the buildup of very strong fields. First, field lines of opposite direction reconnect, releasing energy and lowering the field strength. Second, in regions of very low ionization, such as those found deep inside the ▶ protostellar envelope, the neutral matter slips past the field, in the process known as ambipolar diffusion. Since this slippage already occurred in the parent dense core prior to collapse, it must be amplified here. In any case, detailed calculations of protostellar collapse incorporating both magnetic reconnection and ambipolar diffusion are not yet available.

Rotation, the second missing ingredient, is key to the formation of circumstellar disks. Many pre-main-sequence stars are believed to have such disks. In a few cases, they have been imaged directly. In many other objects, the classical T Tauri stars, the presence of a disk is inferred from the excess emission at infrared wavelengths. It is these disk structures that ultimately form planets. Their presence in even the youngest pre-main-sequence stars implies that they were created earlier, during the protostar phase. If the collapse were spherically symmetric, no disk would arise. However, dense cores are observed to rotate, so a purely spherical picture of infall cannot be correct.

The rotation of dense cores is too slow to affect their gross structure. For example, the observed departure of these clouds from spherical symmetry cannot be attributed to rotational distortion. On the other hand, angular momentum is conserved during collapse. As each fluid element carries inward its initial angular momentum, the associated centrifugal force rises. If this force reaches or exceeds the gravity of the central protostar, the fluid element is effectively repelled. Rather than falling onto the star, it goes into orbit within the equatorial plane perpendicular to the cloud rotation axis. Thus are born circumstellar disks.

While the birth of disks is thus understood generally, our description is again a simplification. As the collapse proceeds, an increasing amount of gas is diverted to the disk, at the expense of the central star. Eventually, the mass of the disk would rival or exceed that of the protostar. But such massive disks are unstable to fragmentation. We observe intact disks, and these contain typically a few percent of the stellar mass. Some process must limit their growth. The consensus is that matter within the disk spirals inward toward the star, a process known generically as disk accretion. The spiraling process must occur even as more matter is impacting the disk from the protostellar envelope. For many stars, the bulk of their mass may be acquired by this route, rather than by direct infall from the protostellar envelope.

What causes the spiraling? There is no generally accepted answer to this question. One widely discussed possibility is that magnetic fields become trapped in the disk and are tangled up by its rotation. In effect, the disk material becomes turbulent. As is well known in fluid dynamics, turbulence can create an effective viscosity. In principle, such internal friction causes the more rapidly orbiting disk material to transfer its angular momentum outward and to drift inward. Another possibility is that spiral arms develop in the disk, analogous to those in galaxies. Such a perturbation of the density also creates internal torques that might result in the desired effect. Yet a third possibility is that the disk sheds angular momentum in the form of a rotating, magnetized wind.

Whatever its cause, the outcome of the process is clear enough. At least half of known pre-main-sequence stars of solar-type mass, the classical T Tauri stars, are born with disks. Another portion, dubbed weak-lined stars, have little or no disk material surrounding them. Apparently, the spiraling process operated more efficiently in the latter group.

Massive Protostars

We have described how the fusion of deuterium near the center of a protostar drives convection throughout the interior. Parcels of gas, heated by the nuclear reactions, rise upward toward the surface. There, in the layers behind the accretion shock, they mix with infalling gas containing fresh deuterium. After radiating their energy, these cooler, denser parcels drift back down, to start the cycle anew. In this manner, the concentration of deuterium throughout the protostar is kept spatially uniform.

The situation changes for protostars that achieve a mass of from two to three times the solar value. The opacity of stellar gas to radiation is a decreasing function of temperature. Since more massive protostars tend to be hotter on the inside, they are in effect more transparent to radiation. Convection ceases, first in the deep interior and then further out.

In these radiatively stable protostars, deuterium cannot be resupplied continually from the outside. Once the isotope fuses, it vanishes from the star's interior (see Fig. 2). The fuel only remains in a thin layer below the accretion shock. The fusion reactions now occur, not at the star's center, but at the bottom of this mantle. Although this mantle contains little mass and is geometrically thin, its heating has a dramatic effect. Protostars undergoing deuterium shell burning quickly swell.

These swollen protostars are the ancestors not of T Tauri stars, but of the more massive Herbig Ae and Be stars. The very youngest stars in this class indeed have observed radii that are larger than one would expect by extrapolation from their lower-mass counterparts. The theory of protostar evolution has successfully explained this fact.

Another puzzling fact is also neatly explained. Some close binary stars seem to be *twins*. That is, the masses of the two stars orbiting each other are essentially identical, to within the errors of measurement. However binary stars form in detail, it is unreasonable to expect that two dense cores (or two regions within a single dense core) would happen to produce the same stellar masses. Clearly, the two young stars must have been in contact, trading mass as they evolved. Just such a picture applies if one of the stars is swollen because of deuterium shell burning. Gas can overflow this swollen envelope and fall onto the close, companion star.

As we consider protostars with masses exceeding about ten times the solar mass, there is a new development. Interior temperatures are now so high that ordinary hydrogen, and not just the deuterium isotope, begins to fuse. The subsequent release of energy quickly overwhelms that from infall. The star essentially joins the main sequence while it is still acquiring gas from its parent dense core. Such nuclear burning protostars are the precursors to all the most massive and luminous stars we see in our Galaxy and others, those of spectral type O and B.

In summary, O and B stars have no pre-main-sequence phase, but go directly from the protostar

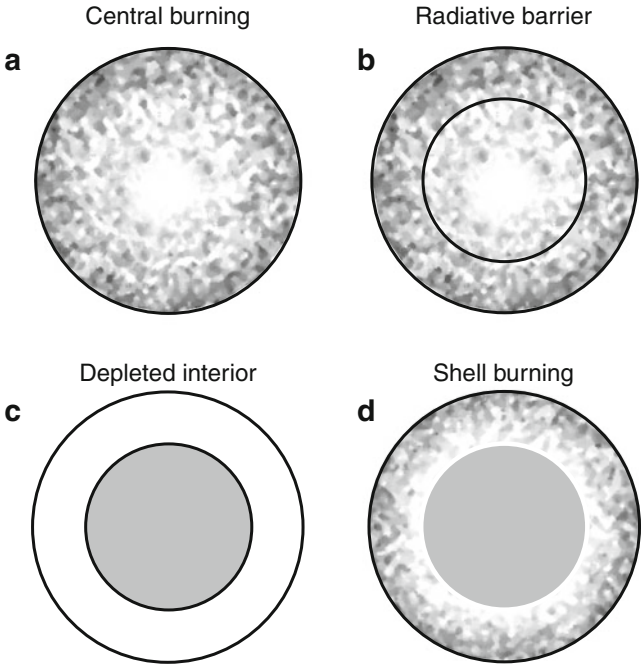

Protostars, Fig. 2 The four stages of deuterium burning in protostars. Active burning begins at the center and continues until a radiative barrier appears. The entire protostar is then stable against convection, and its interior depleted of deuterium. The fuel later ignites in a thick shell, driving convection in the outermost region

to the main-sequence stage of evolution. Moreover, it is not at all clear that the main accretion phase, as we have described it, applies here. The harsh ultraviolet radiation from O stars, together with their vigorous winds, tends to drive back the cloud envelope. Some researchers believe that the formation of an O star can only proceed through the coalescence of lower-mass objects. Others think that the traditional ideas concerning protostar formation continue to apply in this regime.

End of Infall

The far more common stars of solar-type mass and below do not have copious ultraviolet emission. The single biggest shortcoming in the current theory of protostars is that it gives no indication how the main accretion phase ends in general. Since the mass of the star is built up during this period, theorists cannot account for the fact that these masses have a well-documented distribution, known as the initial mass function. Explaining the initial mass function has been a goal for many years, as yet unrealized.

In general, there are two processes that might end cloud infall. First, all of the dense core may collapse onto the star, either directly or through the circumstellar disk. This possibility was implicitly assumed in the early computer calculations of cloud collapse and protostar formation. It faces the obvious objection that there is no rigid wall separating the dense core from its surroundings. Indeed, we know little about the real transition region, beyond the fact that gas outside the dense core seems to be more turbulent than gas inside.

The second broad possibility is that the dense core is dispersed by the star itself during the infall phase. This picture gains credence from the observation that most, if not all, embedded young stars drive jets and molecular outflows. The jets are fast-moving winds expelled by the star and channeled into narrow,

bipolar flows. Molecular outflows trace cloud gas that has been entrained by the jet and also driven outward in a bipolar pattern. There is no question that stellar winds do disperse molecular clouds.

A question that arises is the scale over which cloud dispersion occurs. Stellar jets extend several parsecs from their driving stars, well beyond the size of their parent dense cores. It is plausible that the larger clouds spawning entire clusters of stars are dispersed by these flows, but what of dense cores themselves? There are several images of jets erupting from seemingly intact cores. If future observations show that these clouds are more turbulent than those without internal stars, then the case for wind dispersal will be stronger.

In the last decade, several groups have documented the mass distribution of dense cores within larger molecular clouds. Dense core masses were obtained either by the observed thermal emission from heated dust grains or else by these objects' extinction of near-infrared light from background field stars. An intriguing result has emerged. The mass distribution of dense cores is very similar in shape to the initial mass function for stars. Specifically, it appears that each dense core produces, on average, a star containing about one third of the core mass.

This result, if upheld by future work, has at least two implications. First, the idea that all of dense cores collapse onto its protostar will have been disproved definitively. We are left with the wind dispersal picture. Within this context, the new results imply that each star successfully disperses its parent dense core once it reaches a fixed fraction of the core mass. Our present, admittedly limited, understanding of protostellar winds gives no clue as to why such a universal relationship should hold.

Observational Prospects

Infrared point sources are commonly seen in T associations, loose groups containing primarily T Tauri stars. The latter are optically visible objects that often have excess infrared radiation, indicating the presence of circumstellar disks. However, the very fact that they are visible means that T Tauri stars are *not* surrounded by infalling dense cores. Hence, they are in the pre-main-sequence, rather than the protostar, phase of evolution. Some of the nearby objects that are only seen at infrared and longer wavelengths must be true protostars. Others could be pre-main-sequence stars that still possess a residual envelope of dusty gas, perhaps trapped in the star's strong magnetic field.

In principle, there is a clear distinction between these two kinds of objects. Protostars, we recall, derive most of their energy from the accretion of an infalling gaseous envelope. Pre-main-sequence stars are releasing internal energy through slow gravitational contraction, with only minor residual disk accretion. As already indicated, it has proved difficult to verify the presence of infalling motion directly. Moreover, stars of both types appear similar when cloaked in a sufficient quantity of dusty gas. Under these circumstances, the emergent spectrum largely reflects the absorption and emission properties of the dust grains and is rather insensitive to characteristics of the underlying star other than its total luminosity.

Nevertheless, there is an intriguing pattern to the spectra. For visible T Tauri stars that have an infrared excess, the observed flux declines between 2 and 10 μm. In the so-called Class I infrared sources, the flux rises in this range. Finally, there exists an even more embedded set of objects designated as Class 0. Here, there is no flux at near- or mid-infrared wavelengths. The observed emission peaks in the far infrared and continues to be strong into the submillimeter regime.

Class I sources are often loosely called "protostars." However, there is serious doubt as to whether the term applies. Relative to the pre-main-sequence phase of slow contraction, the phase of true infall is quite brief. Hence, the fraction of protostars in any T association should be correspondingly small. Class I sources, on the other hand, comprise a large fraction of the stars in the best-studied, nearby groups, typically 30 % of the total membership. Moreover, a protostar should be brighter on average than a pre-main-sequence star, since it is deriving extra energy

from infall. Class I sources are observed to have the same luminosities as T Tauri stars. This fact constitutes the "luminosity problem" of star formation theory.

The problem goes away if Class I sources are actually older, pre-main-sequence stars that are still embedded in surrounding dust. Indeed, both Class I and Class 0 sources are always associated with dense cores of molecular gas. It seems that the main infall phase has ended for the former, but still might be ongoing for the latter. This supposition is supported by the lower ratio of submillimeter luminosity (tracing the envelope mass) to total luminosity in Class I sources. It is also true that Class 0 sources are brighter on average than T Tauri stars, and there are relatively few of them. This scarcity, however, hampers any attempt to draw quantitative conclusions.

It is encouraging that the dense cores surrounding both types of sources often show asymmetric profiles in molecular line emission. Such emission, we have noted, is thought to arise from inward motion of the molecular gas. The associated velocities are subsonic, far below those of gas elements entering the accretion shock of a protostar. A primary goal for the future is to obtain more direct evidence for both supersonically infalling gas and for the emission expected from the accretion shock itself.

See Also

- ▶ Ambipolar Diffusion
- ▶ Bipolar Flow
- ▶ Birthline
- ▶ Convection, Stellar
- ▶ Dense Core
- ▶ Gravitational Collapse, Stellar
- ▶ Fragmentation of Interstellar Clouds
- ▶ Free-Fall Time
- ▶ Hertzsprung-Russell Diagram
- ▶ Molecular Cloud
- ▶ Pre-Main-Sequence Star
- ▶ Protoplanetary Disk
- ▶ Protostellar Envelope

References and Further Reading

Krumholz MR, Thompson TA (2007) Mass transfer in close, rapidly accreting protobinaries: an origin for massive twins? Astrophys J 661:1034

Meyer MR, Adams FC, Hillenbrand LA, Carpenter JM, Larson RB (2000) Protostars and planets IV. University of Arizona Press, Tucson, p 121

Stahler SW, Palla F (2004) The formation of stars. Wiley-VCH, Weinheim, Chapter 11

Ward-Thompson D, Andre P, Crutcher R, Johnstone D, Onishi T, Wilson C (eds) (2007) Protostars and planets V. University of Arizona Press, Tucson, p 33

Protostellar Envelope

Steven W. Stahler
Department of Astronomy, University of California, Berkeley, CA, USA

Definition

The mantle of gas surrounding a protostar is called the protostellar envelope. This material is freely collapsing onto the central star and its surrounding disk. The envelope is the densest portion of a ▶ molecular cloud core that went into gravitational collapse. Infalling, envelope material impacts the ▶ protostar and disk, creating a radiating shock front. The envelope gas contains solid dust grains, which absorb all optical and ultraviolet radiation from the star and accretion shock, reradiating it at infrared and longer wavelengths. Within about 1 AU from the star, the dust grains are thermally destroyed by sublimation. The dust photosphere (10 AU) is the radius at which the grains are so sparse that radiation streams passed them unimpeded. The emergent spectrum resembles a cold blackbody.

See Also

- ▶ Birthline
- ▶ Free-Fall Time
- ▶ Gravitational Collapse, Planetary
- ▶ Molecular Cloud
- ▶ Protostars

Protosun Composition

Yann Alibert[1] and Ravit Helled[2]
[1]Space Research and Planetary Sciences, Physics Institute, University of Bern, Bern, Swiss
[2]Geophysical, Atmospheric and Planetary Sciences, Raymond and Beverly Sackler Faculty of Exact Sciences, Tel Aviv University, Tel Aviv, Israel

Keywords

Solar Nebula

Definition

The protosun composition is the initial composition of the giant ▶ molecular cloud, from which the solar system has formed (sun and protoplanetary disk). This composition consists of about 70.5 % hydrogen, 27.5 % helium, and 2 % of heavier elements.

See Also

- ▶ Molecular Cloud
- ▶ Protoplanetary Disk
- ▶ Solar Nebula

Pseudofossil

Emmanuelle J. Javaux
Palaeobiogeology-Palaeobotany-Palaeopalynology, Geology Department, Université de Liège, Liège, Belgium

Definition

A pseudofossil is a nonbiological structure, impression, or trace resembling a biological structure. Several natural physical and chemical processes may produce objects or patterns resembling biological structures. Pseudofossils can also be made artificially in the laboratory. Pseudofossils are unambiguously abiotic, in contrast to ▶ dubiofossil. Knowledge of nonbiological processes and structures mimicking life is crucial when looking for early traces of life on Earth or for extraterrestrial life.

See Also

- ▶ Archean Traces of Life
- ▶ Biogenicity
- ▶ Biomarkers, Morphological
- ▶ Biomarkers
- ▶ Dubiofossil
- ▶ Fossil
- ▶ Microfossils

16 Psyche

- ▶ Psyche

Psyche

Line Drube
DLR Institute of Planetary Research, German Aerospace Center (DLR), Berlin-Adlershof, Germany

Synonyms

16 Psyche

Definition

Psyche is considered the tenth most massive main-belt asteroid and contains about 1 % of all the mass in the main-belt. Its mass has been estimated based on its gravitational effect on asteroids 94 Aurora and 13,206 Baer during close flybys. Over the last 10 years, the diameter has been estimated to range

from 186 to 288 km, which makes the bulk density difficult to estimate, and everything from 1.8 to 7 g/cm^3 has been published.

Psyche has a featureless spectrum and a surface reflecting 12 % in the visual light and an exceptionally 42 % in radar, making it a metallic-rich M-type and an Xk-type. If the density turns out to be close to the 7 g/cm^3, then it points toward the composition of Psyche being almost pure iron-nickel. In that case Psyche would once have been part of the metallic core of a differentiated body, which experienced a catastrophic collision, leaving the core exposed. The high metallicity makes Psyche a promising site for planetary mining companies.

Psyche orbits the Sun about three times farther out than Earth with a Psyche year being equal to 5 Earth years and a day just 4.196 h long. From radar and light-curve measurements, the shape seems to be ellipsoidal. Some postulate that Psyche might have a strong remnant magnetic field.

History

Italian astronomer Annibale de Gasparis discovered Psyche in 1852 as his fifth asteroid discovery and as the sixteenth asteroid discovered in all of history.

See Also

► Main Asteroid Belt

Psychrophile

Laura Kelly
Ecogenomics of Interactions Lab, Nancy, France

Keywords

Archaea; Bacteria; Enzymes; Eukaryote; Barophilic; Extremophiles; Halophilic; Low temperature; Prokaryote

Synonyms

Cryophile

Definition

Psychrophiles (adj. psychrophilic), literally meaning cold-loving, are organisms adapted to growth at low temperatures, having an optimum growth temperature of <15 °C and a maximum growth temperature of <20 °C. Psychrophiles are not to be confused with psychrotrophs (adj. psychrotrophic), also referred to as psychrotolerants, which are capable of growth at low temperature but grow optimally above 15 °C.

History

The term "psychrophile" was first used in 1902 to refer to bacteria which could multiply at 0 °C. The exact definition of a psychrophile has been disputed over time, with the definition suggested by Morita (Morita 1975) receiving general widespread acceptance. The exact parameters for classifying an organism as psychrophilic, however, are constantly under scrutiny (Feller and Gerday 2003).

Overview

Psychrophiles, also known as cryophiles, are considered to be extremophiles, flourishing in the coldest habitats on Earth and regarded as astrobiological models (Margesin and Miteva 2011). As >80 % of Earth's biosphere is permanently below 5 °C (Russell et al. 1990), suitable environments for psychrophiles are widespread and include, among others, ocean waters, permafrost, glaciers, Antarctic rocks, snowfields, and polar ice caps. Although eukaryotic psychrophiles have been identified among algae (the snow algae *Chlamydomonas nivalis* being a well-studied example), yeast, fungi and protozoa, and some higher eukaryotes are considered to be psychrophilic, the prokaryotic domain (both

► bacteria and ► archaea) receives greater attention, containing the majority of known psychrophiles. Among the prokaryotes, psychrophiles are found in very diverse lineages that represent a wide variety of photosynthetic, heterotrophic, and autotrophic nutritional abilities (Scherer and Neuhaus 2006). Psychrophiles are particularly important to the ecology of permanently cold environments where they may be present in diverse bacterial assemblages. Prokaryotic psychrophiles vary in their requirement and indeed tolerance to oxygen and include (strictly) aerobic, (strictly) anaerobic, and facultative species. In addition to extremes of cold, many psychrophiles tolerate or in some cases require other extreme environmental conditions for growth and survival. Deep-sea psychrophiles, for example, may require high pressures for growth, thus making them barophilic psychrophiles (baro-psychrophiles). Furthermore, salt-loving (halophilic) psychrophiles or halo-psychrophiles have been identified inhabiting liquid brine within sea ice. Psychrophilic bacteria and archaea possess various adaptations, which allow them to thrive in cold environments (D'Amico et al. 2006; Casanueva et al. 2010). Cell integrity in many psychrophiles is maintained through increased flexibility of membranes by the inclusion of polyunsaturated fatty acids or the production of cryoprotectants such as exopolysaccharides (Methé et al. 2005). Furthermore, cell integrity may be maintained through the production of antifreeze proteins, which protect the cells from destructive effects of ice crystals. Other psychrophile adaptations include enhanced protection against reactive oxygen species, a greater risk in cold environments due to the greater solubility of oxygen at low temperature. Psychrophile enzymes receive great industrial interest due to their high catalytic efficiency at low temperatures. Psychrophile enzymes are cold-adapted, having improved flexibility of the structural components involved in catalysis and a high specific activity at low temperatures (Feller and Gerday 1997; D'Amico et al. 2006; Scherer and Neuhaus 2006). These enzymes, however, have a low thermal stability, a factor that contributes to the heat sensitivity of psychrophiles, where exposure to even moderate temperature (e.g., room temperature) for even brief periods can result in death.

See Also

- ► Barophile
- ► Extremophiles
- ► Halophile
- ► Prokaryote

References and Further Reading

Casanueva A, Tuffin M, Cary C, Cowan D (2010) Molecular adaptations to psychrophily: the impact of 'omic' technologies. Trends Microbiol 10:374–381

D'Amico S, Collins T, Marx JC, Feller G, Gerday C (2006) Psychrophilic microorganisms: challenges for life. EMBO Rep 7(4):385–389

Feller G, Gerday C (1997) Psychrophilic enzymes: molecular basis of cold adaptation. Cell Mol Life Sci 53:830–841

Feller G, Gerday C (2003) Psychrophilic enzymes: hot topics in cold adaptation. Nat Rev Microbiol 1(3):200–208

Margesin R, Miteva V (2011) Diversity and ecology of psychrophilic microorganisms. Res Microbiol 161:346–361

Methé BA, Nelson KE, Deming JW et al (2005) The psychrophilic lifestyle as revealed by the genomic sequence of *Colwellia psychrerythraea* 34H through genomic and proteomic analyses. Proc Natl Acad Sci U S A 102(31):10913–10918

Morita RY (1975) Psychrophilic bacteria. Bacteriol Rev 39(2):144–167

Russell NJ, Harrisson P, Johnston IA et al (1990) Cold adaptation of microorganisms (and discussion). Phil Trans R Soc B Biol Sci 326:595–611

Scherer S, Neuhaus K (2006) Life at low temperatures. In: The prokaryotes. Springer, New York, pp 210–262

Pulsar

Nikos Prantzos
Institut d'Astrophysique de Paris, Paris, France

Definition

A pulsar is a rapidly rotating and strongly magnetized ► neutron star that emits a (rotating)

beam of electromagnetic radiation, observable when it points toward the Earth. The gravitational collapse of the neutron star's precursor (the iron core of a massive star) produces magnetic fields of $>10^{12}$ Gauss and rotational periods of down to a few ms (as precise as an atomic clock), due to conservation of magnetic flux and angular momentum, respectively. Pulsars decelerate because of radiation losses, but accretion from a companion star may spin them up. A few pulsars are known to have planets orbiting them. While the origin of such planets is still unknown, they probably form after the supernova explosion and, in all probability, they are uninhabitable because of the intense high-energy radiation emitted by the neutron star.

See Also

- ▶ Neutron Star
- ▶ Pulsar Planets

Pulsar Planets

Alexander Wolszczan
Department of Astronomy & Astrophysics and
Center for Exoplanets & Habitable Worlds,
The Pennsylvania State University,
University Park, PA, USA

Keywords

Millisecond pulsar; Neutron star; PSR B1257+12; Pulse arrival times

Definition

Planets that orbit ▶ pulsars have been detected by detecting the changes in the times of the arrival of the radio pulses from the spinning host ▶ neutron stars, which serve as ultraprecise celestial clocks.

History

At a meeting of the International Astronomical Union in Buenos Aires in 1991, Andrew G. Lyne announced the discovery of a planet orbiting the ▶ pulsar PSR B1829-10, based on periodic changes in the times of the arrival of pulses from the host ▶ neutron star, measured with the radio telescope at Jodrell Bank (Bailes et al. 1991). Regrettably, the 6-month periodic signal was due to a subtle error in the treatment of the motion of the one real planet involved, namely the Earth. Nevertheless, the intense interest in PSR B1829-10 motivated theoretical work on the survival and/or formation of planets in systems involving ▶ supernova events, which produce pulsars. This set the stage for the dramatic discovery of a system of three planets orbiting the 6.2-millisecond (ms) pulsar PSR B1257+12, based on observations with the giant radio telescope at Arecibo (Wolszczan and Frail 1992). The planets were soon confirmed by the detection of their mutual gravitational perturbations (Wolszczan 1994). Extensive searches for additional pulsar planets have yielded one convincing example, in the globular cluster M4. That planet orbits a close pair of stars consisting of a ▶ white dwarf together with the neutron star PSR B1620-26.

Overview

The discovery in 1992 and confirmation in 1994 of three planets around a neutron star, the 6.2-ms pulsar PSR B1257+12, provided the first convincing evidence for a system of ▶ exoplanets. Although these pulsar planets are definitely not hospitable to life as we know it, their very existence led to optimistic speculations about the occurrence of exoplanets in general. First, the extreme nature of the host neutron star and its evolutionary history did suggest that planets might indeed be common around various types of stars and that their diversity could not be easily foreseen from extrapolations of our knowledge of the Solar System. This view was dramatically reinforced by the celebrated discovery of the

first planet around a normal star – a "► hot Jupiter" in the surprisingly tight 4.2-day orbit around 51 Pegasi (Mayor and Queloz 1995). Second, the existence of a system of three terrestrial-mass planets around the pulsar PSR B1257+12, dynamically strikingly similar to the inner Solar System, and with a clear signature of a disk origin, supported the speculation that the frequency of occurrence of small rocky exoplanets might also be quite high. Recent evidence from surveys both for ► radial-velocity planets and for ► transiting planets is revealing that such systems are indeed common.

Basic Methodology

Observations of a newly discovered pulsar involve precise pulse timing measurements, which provide a means to model the neutron star's rotational, astrometric, and dynamical parameters. In the case of millisecond pulsars, which are extremely stable rotators, the arrival of their clock-like pulses can be measured and predicted with an unprecedented, microsecond (μs) precision. This property has made the timing of pulsar clocks a very efficient tool to study a variety of phenomena in physics and astrophysics, including detection and characterization of their possible planet-mass companions, all the way down to masses of large asteroids.

The topocentric time-of-arrival (TOA) measurements are made at the telescope, which takes part in the Earth's rotation and in its motion within the Solar System. The TOAs are determined in terms of the local time, usually with the observatory's hydrogen maser clock. To account for the effects of the Earth's motion in an inertial reference frame and to express the TOAs in the standard units of time, the initially measured TOAs are corrected to the Terrestrial Time (TT) and then referred to the Solar System ► barycenter to give the final arrival times in units of the Barycentric Dynamical Time (TDB). Practical translation of the topocentric TOAs to the barycentric pulse arrival times is accomplished with the aid of a Solar System ► ephemeris, which is used to determine the exact position and motion of the telescope at the time of observation. These data are usually extracted from the Jet Propulsion Laboratory DE200 or DE405 ephemerides. All other effects influencing the pulse arrival time, which include classical and relativistic delays in the Solar System, a dispersive delay of the signal as it propagates through the ionized ► interstellar medium, and errors in the pulsar position and proper motion, are corrected for in the process of calculating the barycentric TOAs (for details, see Lorimer and Kramer 2004).

In the analysis process, the number of pulses received over a time interval between some initial epoch and the barycentric arrival time is a measure of the accumulated pulse phase. Since for most of the millisecond and binary pulsars there is no evidence that processes other than the deterministic spin down caused by a gradual loss of the neutron star's rotational energy have a significant effect on their rotational stability (this is generally not true for young pulsars with large spin-down rates), the pulsar spin behavior can be modeled in terms of the rotation frequency and its time derivatives as a mathematical Taylor series. The parameters of the timing model are then determined as corrections to their initial values computed by means of a linearized least-square fit of the model to the pulse arrival time data.

If the pulsar has a binary companion or orbiting planets, its reflex motion translates into ► Doppler shifts of the apparent pulsar period and the equivalent, varying time delay of pulse arrival times. In the case of a single Keplerian (elliptical) orbit, the delay is modeled in terms of the five standard orbital parameters: the orbital period, the eccentricity, the argument of periastron, the projected semi-major axis, and the time of periastron passage. For a circular orbit and planet mass, m_{pl}, assumed to be much smaller than the pulsar mass, M_{psr}, the maximum TOA amplitude, Δt, can be approximated as $\Delta t \sim 0.5\ a_{pl}\ (m_{pl}/m_{Jup})\ (M_{psr}/M_{Sun}),^{-1}$ where a_{pl} is the orbital radius, m_{Jup} is the mass of Jupiter, M_{Sun} is the mass of the Sun, and Δt and a_{pl} are expressed in seconds and astronomical units, respectively. An Earth-mass planet orbiting a pulsar with a typical mass of $\sim$1.35 M_{Sun} would generate a $\sim$1 ms TOA variation, which would be easily detectable given the typical

~1 μs timing precision achievable with millisecond pulsars. In principle, because of its extraordinary precision, the millisecond pulsar timing is capable of detecting large asteroids on sufficiently wide orbits.

Key Research Findings

The 6.2-ms radio pulsar, PSR B1257+12, has three terrestrial-mass planets forming a compact system that is not much larger than the orbit of Mercury (Wolszczan 1994). The relative sizes of the orbits and the distribution of masses of planets b, c, and d are strikingly similar to those of the three inner planets in the Solar System (Mazeh and Goldman 1995).

The near 3:2 ▶ mean motion resonance between the orbits of planets c and d in the PSR B1257+12 system and the existence of detectable gravitational perturbations between the two planets (Rasio et al. 1992; Wolszczan 1994) provide the mechanism to derive their masses without a priori knowledge of the orbital inclinations. A semi-analytical model, in which perturbations between the two planets are parametrized in terms of the two planetary masses and the mutual orientation of their orbits, has been applied to the PSR B1257+12 timing data by Konacki and Wolszczan (2003). A least-square fit of this model to the data yielded the true masses and orbital inclinations of planets b and c, assuming the canonical pulsar mass $M_{psr} = 1.35\ M_{Sun}$. The near 3:2 mean motion resonance between planets c and d and the fact that their orbits are nearly coplanar imply that this pulsar's planetary system has been created as the result of a disk evolution similar to that invoked to describe planet formation around normal stars (e.g., Papaloizou and Terquem 2006). Together with the true mass measurements, these results offer a fairly complete dynamical characterization of the first known exoplanetary system shown to contain terrestrial-mass planets. Its existence provides evidance that ▶ protoplanetary disks beyond the Sun can evolve low-mass planets to a dynamical configuration that is similar to that of the planets in the inner Solar System.

Pulsar Planets, Table 1 Observed and derived parameters for the planets orbiting PSR B1257+12 (numbers in parentheses give standard error in last displayed digit)

Parameter	Planet b	Planet c	Planet d
Projected semi-major axis (ms)	0.0031 (2)	1.3097 (2)	1.4136 (1)
Eccentricity	0.0	0.0195 (3)	0.0259 (3)
Epoch of periastron (MJD)	49764.1 (8)	49768.7 (2)	49766.0 (2)
Orbital period (d)	25.274 (8)	66.5292 (8)	98.2408 (9)
Longitude of periastron (deg)	0.0	250.5 (9)	110.1 (7)
Mass (Earth masses)	0.020 (2)	4.3 (2)	3.4 (2)
Orbital inclination, solution 1 (deg)	–	52 (4)	57 (6)
Orbital inclination, solution 2 (deg)	–	128 (4)	123 (6)
Semi-major axis, AU	0.19	0.36	0.46

The most recent update of the parameters of the PSR B1257+12 planets has been published by Wolszczan (2008) and is summarized in Table 1. Continuing observations of the pulsar have not changed this model in any substantial way.

The early theories of the PSR B1257+12-type planet formation have been summarized by Podsiadlowski (1993) and further discussed by Phinney and Hansen (1993). More recently, Miller and Hamilton (2001) and Hansen et al. (2009) have examined the conditions of survival and evolution of pulsar protoplanetary disks. They have concluded that an initially sufficiently massive ($>10^{28}$ g) disk would be able to resist evaporation by the pulsar accretion flux and create planets on a typical, 10^7-year timescale. Quick formation of a sufficiently massive disk around a pulsar could, for instance, be accomplished by tidal disruption of a stellar companion (e.g., Phinney and Hansen 1993), a supernova fallback (e.g., Currie and Hansen 2007), or, possibly, in the process of a white dwarf merger (e.g., Livio et al. 1992). The possible detection of a dust disk around the X-ray pulsar, 4U 0142+61 (Wang et al. 2006), if confirmed, may present the first direct evidence for a disk formed by the

supernova fallback mechanism. These processes, although entirely feasible, cannot be very common. In fact, with the exception of PSR B1257 +12, no planetary companions have emerged from precise timing observations of the known Galactic millisecond pulsars (Lorimer 2008), suggesting their rarity, independently of the specific formation mechanism.

See Also

- Barycenter
- Doppler Shift
- Ephemeris
- Extrasolar Planets
- Interstellar Medium
- Mean Motion Resonance
- Neutron Star
- Pulsar
- Radial-Velocity Planets
- Transiting Planets
- White Dwarf

References and Further Reading

Bailes M, Lyne AG, Shemar SL (1991) A planet orbiting the neutron star p SR1829–10. Nature 352:311
Currie T, Hansen BMS (2007) The evolution of protoplanetary disks around millisecond pulsars: the SR 1257 +12 system. Astrophys J 666:1232
Hansen BMS, Shih H-Y, Currie T (2009) The pulsar planets: a test case of terrestrial planet assembly. Astrophys J 691:382
Konacki M, Wolszczan A (2003) Masses and orbital inclinations of planets in the PSR B1257+12 system. Astrophys J 591:147
Livio M, Pringle JE, Saffer RA (1992) Planets around massive white dwarfs. Mon Not R Astron Soc 257:15
Lorimer DR (2008) Binary and millisecond pulsars. Living Rev Relat. http://relativity.livingreviews.org/Articles/lrr-2008-8
Lorimer DR, Kramer M (2004) Handbook of pulsar astronomy. Cambridge University Press, Cambridge
Mayor M, Queloz D (1995) A Jupiter-mass companion to a solar-type star. Nature 378:355
Mazeh T, Goldman I (1995) Similarities between the inner solar system and the planetary system of the PSR B1257+12. Publ Astron Soc Pac 107:250
Miller MC, Hamilton DP (2001) Implications of the PSR 1257+12 planetary system for isolated millisecond pulsars. Astrophys J 550:863
Papaloizou JCB, Terquem C (2006) Planet formation and migration. Rep Prog Phys 69:119
Phinney ES, Hansen BMS (1993) The pulsar planet production process. Astron Soc Pac Conf Ser 36:371
Podsiadlowski P (1993) Planet formation scenarios. Astron Soc Pac Conf Ser 36:149
Rasio FA et al (1992) An observational test for the existence of a planetary system orbiting PSR1257+12. Nature 355:325
Wang Z, Chakrabarty D, Kaplan D (2006) A debris disk around an isolated young neutron star. Nature 440:772
Wolszczan A (1994) Confirmation of Earth-mass planets orbiting the millisecond pulsar PSR B1257+12. Science 264:538
Wolszczan A (2008) Fifteen years of the neutron star planet research. Phys Scr 130:4005
Wolszczan A, Frail DA (1992) A planetary system around the millisecond pulsar PSR1257+12. Nature 355:145

Purine Bases

Michael P. Callahan
Astrochemistry Laboratory, Code 691, NASA Goddard Space Flight Center, Greenbelt, MD, USA

Keywords

Adenine; Guanine; Hypoxanthine; Nitrogen heterocycle; Xanthine

Definition

A purine is an aromatic heterocyclic nitrogen compound, composed of a pyrimidine ring system fused to an imidazole ring system, with the core molecular formula $C_5H_4N_4$. Purines are weakly basic compounds. Purines are stabilized by resonance among the atoms in the ring structure, which gives most of the bonds a partial double-bond character. As a result, purines are nearly planar molecules with a slight pucker and are characterized by a strong UV absorption typically near 260 nm. Purine bases may exist in different tautomeric forms depending on the pH. At neutral pH, purines are hydrophobic and therefore relatively insoluble. Substituted purines

are components of ribonucleic acids (RNA), deoxyribonucleic acids (DNA), and ▶ coenzymes and are broadly distributed in nature.

Overview

Purines consist of a six-membered pyrimidine ring fused to a five-membered imidazole ring. Purines (along with pyrimidines) serve as the informational monomers of RNA and DNA, the molecular carriers of genetic information. ▶ Hydrogen bonding and base-stacking interactions of substituted purines are important for stabilizing the three-dimensional structure of ▶ nucleic acids. The most important biological substituted purines are ▶ adenine and guanine, which are the major purine bases found in RNA and DNA. In DNA, ▶ guanine and adenine ▶ base pair (see "▶ Watson-Crick pairing") with cytosine and thymine (see "▶ Pyrimidine Base"), respectively. Adenine is also found in adenosine triphosphate (see "▶ ATP") and other coenzymes. Two other important biological purines are hypoxanthine and xanthine. While hypoxanthine and xanthine are not incorporated into nucleic acids, they are important intermediates in purine metabolism.

A plausible prebiotic synthesis of adenine was first demonstrated by Oró (1960) using a mixture of ▶ hydrogen cyanide (HCN) and ammonia in an aqueous solution. HCN undergoes self-condensation to form diaminomaleonitrile (DAMN), a tetramer of HCN. DAMN then reacts with formamidine (formed in situ) or by photochemical rearrangement to form 4-aminoimidazole-5-carbonitrile (AICN). Finally, AICN reacts with HCN to form the purine adenine. Other purines such as guanine, hypoxanthine, and xanthine can be formed by the addition of small molecules (e.g., ▶ cyanogen or cyanate) to AICN or its amide, aminoimidazole carboxamide (AICA), followed by various ▶ hydrolysis steps. However, one drawback to this synthesis is that relatively high concentrations of HCN are required. The likelihood of such high concentrations of HCN is unclear on the early Earth especially since HCN cannot be concentrated by simple evaporation because it is more volatile than water. Miller and Orgel proposed that eutectic freezing provides a plausible concentration mechanism. In the temperature range of 0 °C to −20 °C, HCN remains in the liquid phase and can concentrate in the voids between ice crystals.

Purines (and also pyrimidines) are formed as condensation products of formamide heated at 110–160 °C in the presence of metal oxides and minerals. Under these conditions, the diversity and yield of purine synthesis can be enhanced by UV light (even in the absence of inorganic catalysts). Purines are unlikely to form and survive in most interstellar and circumstellar environments since they are unstable against UV radiation. Purines may be able to survive if located in a dense ▶ interstellar cloud, although no positive detection has been made yet. Purines have also been reported in carbonaceous meteorites suggesting their formation in space is possible. Martins et al. (2008) have reported that xanthine (along with the pyrimidine uracil) has an extraterrestrial origin in the Murchison meteorite based on compound-specific carbon isotopic measurements.

See Also

- ▶ Adenine
- ▶ Base Pair
- ▶ Carbonaceous Chondrite
- ▶ Codon
- ▶ Coenzyme
- ▶ Cyanogen
- ▶ Genetic Code
- ▶ Guanine
- ▶ HCN Polymer
- ▶ Hydrogen Cyanide
- ▶ Hydrolysis
- ▶ Hypoxanthine
- ▶ Interstellar Medium
- ▶ Miller, Stanley
- ▶ Nucleic Acid Base
- ▶ Nucleotide
- ▶ Prebiotic Chemistry
- ▶ Pyrimidine Base

- ▶ Ribonucleoside
- ▶ Ribonucleotide
- ▶ Watson-Crick Pairing

References and Further Reading

Barks HL, Buckley R, Grieves GA, Di Mauro E, Hud NV, Orlando TM (2010) Guanine, adenine, and hypoxanthine production in UV-irradiated formamide solutions: relaxation of the prebiotic purine nucleobase formation. Chembiochem 11:1240–1243

Costanzo G, Saladino R, Crestini C, Ciciriello F, Di Mauro E (2007) Formamide as the main building block in the origin of nucleic acids. BMC Evol Biol 7:S1

Martins Z, Botta O, Fogel ML, Sephton MA, Glavin DP, Watson JS, Dworkin JP, Schwartz AW, Ehrenfreund P (2008) Extraterrestrial nucleobases in the Murchison meteorite. Earth Planet Sci Lett 270:130–136

Miller SL, Orgel LE (1974) The origins of life on the earth. Prentice-Hall, Englewood Cliffs, p 229

Nelson DL, Cox MM (2000) Lehninger principles of biochemistry, 3rd edn. Worth Publishers, New York, p 1255

Oró J (1960) Synthesis of adenine from ammonium cyanide. Biochem Biophys Res Commun 2:407–412

Peeters Z, Botta O, Charnley SB, Kisiel Z, Kuan Y-J, Ehrenfreund P (2005) Formation and photostability of N-heterocycles in space: I. The effect of nitrogen on the photostability of small aromatic molecules. Astron Astrophys 433:583–590

Plaxco KW, Gross M (2006) Astrobiology: a brief introduction. The John Hopkins University Press, Baltimore, p 259

Saenger W (1984) Principles of nucleic acid structure. Springer, New York, p 556

Stoks PG, Schwartz AW (1981) Nitrogen-heterocyclic compounds in meteorites: significance and mechanisms of formation. Geochim Cosmochim Acta 45:563–569

PVED

Jun-Ichi Takahashi
NTT Microsystem Integration Laboratories, Atsugi, Japan

Synonyms

Parity nonconservative energy difference; Parity violation energy difference

Definition

The effect of intrinsic differences in energy between biomolecular ▶ enantiomers due to the weak interactions mediated by neutral Z particles is known as parity-violating energy difference (PVED). Asymmetric enantiomer distribution in terrestrial biomolecules, with L-amino acids and D-sugars dominant, has been suggested to be the result of this effect. Calculations of the PVED between enantiomers of α-amino acids have suggested that the L-enantiomers are more stable than the D-enantiomers by an amount equivalent to 10^{-17}–10^{-14} kT at room temperature. More recent calculations, however, have suggested that such conclusions may be ambiguous or erroneous, currently leaving both the direction and magnitude of the PVED an open question.

See Also

- ▶ Chirality
- ▶ Enantiomers
- ▶ Parity Violation Energy Difference

Pyranose

Henderson James Jim Cleaves II
Earth–Life Science Institute (ELSI), Tokyo Institute of Technology, Meguro–ku, Tokyo, Japan
Institute for Advanced Study, Princeton, NJ, USA
Blue Marble Space Institute of Science, Washington, DC, USA
Center for Chemical Evolution, Georgia Institute of Technology, Atlanta, GA, USA

Definition

A pyranose is a cyclic six-membered ring form of a monosaccharide, formed as an intramolecular hemiacetal and containing an oxygen atom in the

ring. Monosaccharides smaller than pentoses are incapable of forming pyranoses. Important biological pyranoses include glucose and mannose. ▶ Ribose in solution also adopts a pyranose form to a minor extent.

See Also

- ▶ Aldose
- ▶ Carbohydrate
- ▶ Ketose
- ▶ Ribose

Pyranosyl-RNA

- ▶ p-RNA

Pyrimidine Base

Michael P. Callahan
Astrochemistry Laboratory, Code 691,
NASA Goddard Space Flight Center, Greenbelt, MD, USA

Keywords

Cytosine; Nitrogen heterocycle; Thymine; Uracil

Definition

Pyrimidine is a six-membered nitrogen heterocyclic compound with the molecular formula $C_4H_4N_2$. Pyrimidine bases are weakly basic. Pyrimidines are stabilized by resonance among atoms in the ring, which gives most of the bonds a partial double-bond character. As a result, pyrimidines are planar molecules and are characterized by strong UV absorption generally near 260 nm. Pyrimidine bases may exist in different ▶ tautomeric forms depending on the pH. At neutral pH, pyrimidines are hydrophobic and therefore relatively insoluble. Substituted pyrimidines are components of ribonucleic acids (RNA), deoxyribonucleic acids (DNA), and ▶ coenzymes and are broadly distributed in nature.

Overview

Pyrimidines are aromatic nitrogen heterocycles with a structure similar to benzene but containing two nitrogen atoms at the 1 and 3 positions of the ring. Pyrimidines (along with purines) serve as the informational monomers of RNA and DNA, the molecular carriers of genetic information. ▶ Hydrogen bonding and base-stacking interactions of pyrimidines are important for stabilizing the three-dimensional structure in ▶ nucleic acids. The most important biological substituted pyrimidines are ▶ cytosine, ▶ thymine, and ▶ uracil. Cytosine and thymine are the two major pyrimidine bases in DNA and ▶ base pair (see ▶ Watson-Crick Pairing) with guanine and adenine (see ▶ Purine Bases), respectively. In RNA, uracil replaces thymine and base pairs with adenine.

The prebiotic synthesis of cytosine may have started with the precursor ▶ cyanoacetylene, which is produced in spark discharge experiments of methane-nitrogen gas mixtures. The reaction of cyanoacetylene with cyanate produces cytosine. An alternative route uses cyanoacetaldehyde, which can be formed by the hydration of cyanoacetylene. Cyanoacetaldehyde reacts with urea, which is considered a common prebiotic molecule and is produced via Miller-Urey chemistry, to produce cytosine in excellent yields. Furthermore, cytosine is readily hydrolyzed to uracil. However, since cytosine is rather unstable, it raises the question if cytosine was used in the first genetic material.

A number of plausible prebiotic syntheses of uracil and thymine have been demonstrated in the laboratory. For example, uracil is liberated from ▶ HCN polymers upon acid hydrolysis. Schwartz and coworkers also produced uracil by UV irradiation of a mixture of urea and alanine in the

presence of clay minerals. Thymine is produced via the methylation of uracil with formaldehyde and hydrazine. Thymine is also obtained from formamide in the presence of titanium dioxide heated at 160 °C.

Uracil has been identified in carbonaceous meteorites. Both pyrimidines and purines have been reported in ▶ meteorites, which presents the tantalizing suggestion that some of the building blocks of genetic materials were delivered by meteorites (assuming these molecules do not originate from terrestrial contamination). Martins et al. (2008) have reported that uracil (along with the purine xanthine) has an extraterrestrial origin in the ▶ Murchison meteorite based on compound-specific carbon isotopic measurements.

See Also

- ▶ Anticodon
- ▶ Base Pair
- ▶ Carbonaceous Chondrite
- ▶ Codon
- ▶ Coenzyme
- ▶ Cyanoacetylene
- ▶ Cytosine
- ▶ Genetic Code
- ▶ HCN Polymer
- ▶ Hydrolysis
- ▶ Miller, Stanley
- ▶ Nucleic Acids
- ▶ Nucleotide
- ▶ Prebiotic Chemistry
- ▶ Purine Bases
- ▶ Ribonucleoside
- ▶ Ribonucleotide
- ▶ Spark Discharge
- ▶ Thymine (T)
- ▶ Uracil (Ura)
- ▶ Watson-Crick Pairing

References and Further Reading

Chittenden GJF, Schwartz AW (1976) Possible pathway for prebiotic uracil synthesis by photodehydrogenation. Nature 263:350–351

Martins Z, Botta O, Fogel ML, Sephton MA, Glavin DP, Watson JS, Dworkin JP, Schwartz AW, Ehrenfreund P (2008) Extraterrestrial nucleobases in the Murchison meteorite. Earth Planet Sci Lett 270:130–136

Miller SL, Orgel LE (1974) The origins of life on the earth. Prentice-Hall, Englewood Cliffs, p 229

Nelson DL, Cox MM (2000) Lehninger principles of biochemistry, 3rd edn. Worth Publishers, New York, p 1255

Plaxco KW, Gross M (2006) Astrobiology: a brief introduction. The John Hopkins University Press, Baltimore, p 259

Saenger W (1984) Principles of nucleic acid structure. Springer, New York, p 556

Saladino R, Ciambecchini U, Crestini C, Costanzo G, Negri R, Di Mauro E (2003) One-pot TiO_2-catalyzed synthesis of nucleic bases and acyclonucleosides from formamide: implications for the origin of life. Chembiochem 4:514–521

Stephen-Sherwood E, Oró J, Kimball AP (1971) Thymine: a possible prebiotic synthesis. Science 173:446–447

Stoks PG, Schwartz AW (1979) Uracil in carbonaceous meteorites. Nature 282:709–710

Voet AB, Schwartz AW (1982) Uracil synthesis *via* HCN oligomerization. Orig Life Evol Biosph 12:45–49

Pyrite

Nicholas Arndt
ISTerre, Université Grenoble Alpes, France

Definition

Pyrite is an iron sulfide with the formula FeS_2. It has a metallic luster and a pale yellow color (hence the name "fool's gold"). It is relatively hard and commonly forms cubic crystals. It is the most common sulfide mineral and forms under a wide variety of conditions: in relatively oxidized magmas, from hydrothermal fluids, in metamorphic rocks, and in sediments. It is rarely a primary mineral in high-temperature rocks, and usually forms by replacement of high-temperature minerals under oxidizing conditions. It is also a common mineral in many types of sulfide ore and is present in most gold deposits. It grows or recrystallizes during the diagenesis of sediments, commonly through the action of bacteria: framboidal pyrite in sediments is commonly biogenic. Oxidation of pyrite provides an energy source for microbes in anaerobic settings. It is an

important mineral for understanding the redox changes at the surface of the Earth, particularly during the ▶ Great Oxygenation Event. Pyrite also figures prominently in many models in which the origin of life is related to hydrothermal vents and has been shown to be an effective reducing agent for compounds including nitrogen species and CO.

See Also

▶ Black Smoker
▶ Great Oxygenation Event
▶ Oxygenation of the Earth's Atmosphere
▶ Sulfur

Pyroclastics (in Volcanology)

▶ Ejecta

Pyrolysis

Mark Dörr
University of Southern Denmark, Odense M, Denmark

Synonyms

Carbonization; Thermal decomposition

Definition

Pyrolysis (from Greek πυρ (pyr) = "fire" and λυσις (lysis) = "decomposition") is a chemical process in which bonds of a compound are spontaneously broken by high temperatures (500–900 °C). Extreme *pyrolysis* of carbon-containing substances, which leaves mostly ▶ carbon as the residue, is called *carbonization*. The production of charcoal from wood is an example of *pyrolysis* and *carbonization*.

See Also

▶ Carbon
▶ Combustion

Pyrolysis Gas Chromatography Mass Spectrometry

▶ Pyrolysis GC/MS

Pyrolysis GC/MS

Henderson James (Jim) Cleaves II
Earth–Life Science Institute (ELSI), Tokyo Institute of Technology, Meguro–ku, Tokyo, Japan
Institute for Advanced Study, Princeton, NJ, USA
Blue Marble Space Institute of Science, Washington, DC, USA
Center for Chemical Evolution, Georgia Institute of Technology, Atlanta, GA, USA

Synonyms

Pyrolysis gas chromatography mass spectrometry

Definition

▶ Pyrolysis gas chromatography mass spectrometry (abbreviated as Pyr-▶ GC/MS) is a method of chemical analysis. In Pyr-GC/MS, the sample is decomposed by heating at high temperatures under an inert atmosphere or under vacuum to produce smaller molecules that are separated by gas chromatography and detected using a mass spectrometer. Pyr-GC/MS is widely used to characterize polymers and complex organic molecules such as ▶ tholins.

See Also

- ▶ GC/MS
- ▶ Pyrolysis
- ▶ Tholins

Pyrometer

- ▶ Bolometer

Pyrophosphate

Matthew A. Pasek
University of South Florida, Tampa, FL, USA

Synonyms

Diphosphate

Definition

Pyrophosphate is a dimer of orthophosphate (PO_4^{3-}), linked by a single oxygen via a dehydration reaction. Pyrophosphate hydrolyzes in water to give two molecules of orthophosphate with the release of about 20 kJ/mol at standard state. Pyrophosphate is a potential precursor to ATP as the main metabolic energy carrier of life, as it is formed by transmembrane protein proton pumping using a much simpler mechanism. Pyrophosphate may have been synthesized on the early Earth either by dehydration reactions; by the phosphorylation of phosphate by high-energy phosphate precursors, such as reduced forms of phosphorus; or by radical-driven reactions.

See Also

- ▶ ATP
- ▶ Phosphates

Pyrrolidine-2-carboxylic Acid

- ▶ Proline

Pyruvate

Henderson James (Jim) Cleaves II
Earth–Life Science Institute (ELSI), Tokyo Institute of Technology, Meguro–ku, Tokyo, Japan
Institute for Advanced Study, Princeton, NJ, USA
Blue Marble Space Institute of Science, Washington, DC, USA
Center for Chemical Evolution, Georgia Institute of Technology, Atlanta, GA, USA

Definition

Pyruvate is the conjugate base of pyruvic acid (2-oxopropanoic acid), the simplest keto acid. It is a key component of intermediary metabolism in all extant organisms. It is derived principally from glycolysis of glucose in many organisms and serves as a major precursor of fatty acids via the synthesis of acetyl-CoA. It is also a feedstock for the citric acid cycle in which it is carboxylated to yield oxaloacetate. It can also be shunted into amino acid metabolism by reductive amination to yield alanine and is a transient species in alcoholic fermentation, in which it is decarboxylated to yield acetaldehyde, which is ultimately reduced to yield ethanol.

See Also

- ▶ Acetaldehyde
- ▶ Alanine
- ▶ Amino Acid
- ▶ Citric Acid Cycle
- ▶ Ethanol
- ▶ Fatty Acids, Geological Record of
- ▶ Fermentation
- ▶ Glycolysis
- ▶ Metabolism